# University of Southampton

Faculty of Medicine

Clinical and Experimental Sciences

**Investigation into the immunomodulatory activity of XPO1 inhibitors**

Volume 1 of 1

by

**Jack Graham Fisher**

MBiol, MRes

ORCID ID 0000-0002-5090-7503

Thesis for the degree of Doctor of Philosophy in Biomedical Sciences

April 2025

# University of Southampton

## Abstract

Faculty of Medicine

Clinical and Experimental Sciences

Doctor of Philosophy in Biomedical Sciences

Investigation into the immunomodulatory activity of XPO1 inhibitors

by

Jack Graham Fisher

Nuclear export is an important process for regulating transcription and translation by spatial distribution of transcription factors, RNA and signalling components. Exportin-1 (XPO1) is a nuclear export protein that transports key tumour suppressor proteins, oncogenic mRNA and ribosomal constituents into the cytoplasm and its function is often dysregulated in haematological malignancies to promote cancer cell survival and proliferation.

Selinexor is a first-in-class inhibitor of XPO1 and is approved for the treatment of relapsed and refractory multiple myeloma and diffuse large B cell lymphoma. Selinexor induces the accumulation of tumour suppressor proteins in the nucleus and inhibits oncogene translation to impair cell proliferation and induce apoptosis. It is beginning to be appreciated that small molecule drugs which target tumourigenic pathways also possess immunomodulatory activity. Understanding the mechanism behind these immunomodulatory effects can improve the design of rational combination strategies with immunotherapies. Selinexor has been shown to enhance T cell function, increase NK cell abundance in tumours and promote tumour regression in combination with PD-1 blockade. But how XPO1 inhibition impacts NK cell-mediated immunity is unknown, which this project aimed to address, with the hypothesis that XPO1 inhibition sensitises cancer cells to NK cell immunosurveillance via modulation of NK cell ligand expression.

XPO1 inhibition in B-cell lymphoma and multiple myeloma cell lines and primary chronic lymphocytic leukaemia cells sensitised cancer cells to NK cell cytotoxicity. Increased sensitivity to NK cell activation was due to decreased surface expression of HLA-E, the ligand for the inhibitory NK cell receptor NKG2A. As such, XPO1 inhibition led to preferential activation of NKG2A+ NK cells and potentiated the effects of expanded allogeneic NK cells, anti-CD19 CAR NK cells and promoted antibody-dependent cellular cytotoxicity in combination with clinically relevant monoclonal antibodies. This research project also identified that lymph node-associated signals IL-4 and CD40L confer resistance of malignant B cells to NK cell activation through upregulation of HLA-E, and this can be reversed by XPO1 inhibition.

Overall, this research project revealed a novel immunomodulatory mechanism of XPO1 inhibition in haematological malignancies by sensitising cancer cells to NK cell anti-tumour functions via disruption of NKG2A:HLA-E interactions. Future work could investigate the combination of selinexor with NK cell therapeutic strategies *in vivo* to assess the potential for translation of these findings to clinical trials.

# Table of Contents

**Table of Contents** ..... **7**

**Table of Tables** ..... **15**

**Table of Figures** ..... **16**

**List of Accompanying Materials** ..... **23**

**Research Thesis: Declaration of Authorship** ..... **24**

**Acknowledgements** ..... **25**

**Definitions and Abbreviations** ..... **26**

**Chapter 1 Introduction** ..... **29**

**1.1 Overview of the immune system** ..... **29**

1.1.1 The innate immune system ..... 29

1.1.2 T lymphocytes ..... 30

1.1.3 B lymphocytes ..... 31

**1.2 Human Leukocyte Antigens (HLA).** ..... **33**

1.2.1 HLA class I proteins ..... 33

1.2.2 The non-classical HLA class I molecule HLA-E ..... 35

1.2.3 The role of HLA-E in cancer ..... 38

**1.3 Human NK cell development, maturation, education and function** ..... **41**

1.3.1 The development and maturation of NK cells ..... 41

1.3.2 NK cell education and licensing ..... 42

1.3.3 The immunological synapse and the cytotoxic functions of NK cells ..... 44

1.3.4 Secretion of cytokines and chemokines ..... 49

1.3.5 ADCC ..... 50

1.3.6 Adaptive/memory NK cells ..... 50

**1.4 Receptors regulating NK cell activity.** ..... **51**

1.4.1 Killer cell immunoglobulin-like receptors (KIR) ..... 51

1.4.1.1 Inhibitory KIR ..... 51

1.4.1.2 Activating KIR ..... 52

1.4.2 NK cell inhibitory receptors ..... 53
1.4.3 NK cell activating receptors ..... 54
1.4.4 NKG2A and NKG2C receptors ..... 55
**1.5 Roles of NK cells in disease ..... 58**
1.5.1 Role in infection ..... 58
1.5.2 Role in cancer ..... 59
1.5.2.1 Historical perspective of NK cells and the role of NKG2A expression in cancer ..... 59
1.5.2.2 Expression of KIR2DS2 in cancer ..... 60
**1.6 Exploiting NK cells in cancer therapy ..... 61**
1.6.1 Direct targeting monoclonal antibody therapy ..... 61
1.6.2 Immunomodulatory mAb therapy ..... 62
1.6.2.1 Immune checkpoint inhibitors ..... 62
1.6.2.2 Stimulatory antibodies and NK cell engagers ..... 64
1.6.3 NK cell adoptive transfer therapy ..... 65
1.6.4 Chimeric antigen receptor (CAR) NK cells ..... 66
**1.7 B-cell and plasma cell malignancies ..... 68**
1.7.1 Development of B cell lymphoma/leukaemia and multiple myeloma ..... 68
1.7.2 Treatment of B-cell lymphoma/leukaemia and multiple myeloma ..... 71
1.7.3 NK cells in B-cell lymphoma/leukaemia and multiple myeloma ..... 72
**1.8 Immunomodulation by anti-cancer agents ..... 74**
**1.9 Exportin-1 and selective inhibitors of nuclear export (SINE) ..... 76**
1.9.1 The function of Exportin-1 ..... 76
1.9.2 Exportin-1 in cancer ..... 79
1.9.3 SINE compounds ..... 79
1.9.4 The effects of XPO1 inhibition on immune cell functions ..... 82
**1.10 Study hypothesis, aims and objectives ..... 84**
**Chapter 2 Materials and Methods ..... 87**
**2.1 Cell culture ..... 87**

2.1.1 Peripheral blood mononuclear cell (PBMC) isolation ..... 87
2.1.2 Culture of cancer cell lines and NK cell lines ..... 87
2.1.3 Purification of NK cells ..... 87
2.1.4 Allogeneic NK cell expansion ..... 88
2.1.5 Isolation of chronic lymphocytic leukaemia (CLL) cells from patient PBMC ..... 88
**2.2 Drug treatments ..... 88**
2.2.1 SINE treatment and Q-VD-OPh (Q-VD) incubation ..... 88
2.2.2 Selinexor in combination with BTK inhibitors ..... 89
**2.3 Phenotyping experiments of NK cell lines and primary NK cells and cancer cells post XPO1 inhibition ..... 89**
2.3.1 Surface expression of NK cell ligands on SINE-treated cancer cells ..... 89
2.3.2 Surface expression of activating and inhibitory receptors on NK cells ..... 89
2.3.3 Acid strip experiments to measure the recovery of HLA proteins at the plasma membrane ..... 90
**2.4 Co-culture experiments to examine NK cell activation and cytotoxicity ..... 90**
2.4.1 NK cell specific lysis (cytotoxicity) assay ..... 90
2.4.2 Degranulation (CD107a/LAMP) assay and measuring IFNγ production ..... 90
2.4.3 Assessing XPO1 inhibition on ADCC ..... 91
2.4.4 Selinexor in expanded NK-cancer co-cultures ..... 91
2.4.5 TRAIL blockade experiments ..... 92
2.4.6 NKG2A blockade experiments ..... 92
2.4.7 Autologous NK cell activation against CLL cells ..... 92
**2.5 Microenvironmental support experiments ..... 92**
2.5.1 CD40L and IL-4 lymph node support mimic ..... 92
2.5.2 Treatment of tumour cells with recombinant human IFNγ or supernatant from NK-cancer co-cultures ..... 93
2.5.3 HLA expression on intact and permeabilised cancer cells ..... 93
**2.6 Chimeric antigen receptor (CAR) NK cell experiments ..... 94**
2.6.1 CAR NK cell generation and measurement of transduction efficacy ..... 94

2.6.2 Assessment of CAR NK cell cytotoxicity ..... 95

**2.7 IFNγ ELISA.....95**

**2.8 Western blotting.....96**

**2.9 *In vivo* experiments .....96**

2.9.1 Selinexor treatment of NSG mice..... 96

2.9.2 Raji *in vivo* growth kinetics..... 97

**2.10 Anti-CD19 CAR T cell experiments .....97**

2.10.1 Anti-CD19 CAR T cell lysis of B-cell lymphoma cell lines..... 97

2.10.2 T cell stimulation experiments to assess NKG2A expression on activated T cells 97

**2.11 Macrophage phagocytosis experiments .....98**

2.11.1 Generation of monocyte-derived macrophages..... 98

2.11.2 Assessing the effect of XPO1 inhibition on macrophage phagocytosis ..... 98

**2.12 Statistical analysis.....99**

**Chapter 3 NK cell immunomodulatory properties of XPO1 inhibitors in malignant B cell lines .....103**

**3.1 NK cell cytotoxicity against malignant B cell lines treated with XPO1 inhibitors ...103**

**3.2 Effect of XPO1 inhibition in cancer cell lines on NK cell activation .....107**

**3.3 Mechanism for increased sensitivity of malignant B cell lines to NK cell cytotoxicity after XPO1 inhibition .....110**

3.3.1 Effect of XPO1 inhibition on the activation of KIR2DS2+ NK cells..... 110

3.3.2 Expression of NK cell activating ligands and HLA proteins on malignant B cell lines post XPO1 inhibition ..... 114

**3.4 Mechanism for HLA-E downregulation with XPO1 inhibitors.....118**

3.4.1 Examining total proteins levels of HLA-E ..... 118

3.4.2 Investigating the induction of ER stress upon XPO1 inhibition..... 118

3.4.3 HLA-E trafficking to the plasma membrane in the presence of XPO1 inhibitors 120

**3.5 XPO1 inhibition with selinexor or leptomycin B preferentially activates NKG2A+ NK cells against malignant B cell lines.....126**

**3.6 The effect of selinexor on ADCC ..... 130**

3.6.1 Combining selinexor with anti-CD20 monoclonal antibodies ..... 130

**3.7 Discussion ..... 134**

3.7.1 XPO1 inhibition sensitises B-cell lymphoma cells to NKG2A+ NK cell activation 134

3.7.2 Mechanism for HLA-E downregulation by XPO1 inhibitors ..... 137

3.7.3 Combining XPO1 inhibitors with monoclonal antibody therapy ..... 138

**Chapter 4 The effect of XPO1 inhibition in primary human Chronic Lymphocytic Leukaemia cells on NK cell activation ..... 141**

**4.1 XPO1 inhibition sensitises patient derived Chronic Lymphocytic Leukaemia (CLL) cells to NK cell cytotoxicity ..... 141**

**4.2 Mechanism for increased sensitivity of selinexor-treated CLL cells to NK cell cytotoxicity ..... 145**

**4.3 Combining XPO1 inhibition with approved treatments for CLL ..... 156**

**4.4 Lymph node microenvironmental support ..... 162**

**4.5 HLA-E expression on healthy immune cell populations treated with selinexor ..... 168**

**4.6 Autologous NK cell activation with selinexor ..... 169**

**4.7 Discussion ..... 170**

4.7.1 XPO1 inhibition downregulates HLA-E and increases the surface expression of DR5 on CLL cells ..... 170

4.7.2 XPO1 inhibitors potentiate ADCC by anti-CD20 and anti-CD38 mAbs ..... 171

4.7.3 Lymph node-derived signals IL-4 and CD40L protect CLL cells from NK cell activation ..... 172

4.7.4 Second generation BTK inhibitors do not impair enhanced NK cell function with XPO1 inhibition ..... 173

4.7.5 XPO1 inhibition did not enhance autologous NK cell function against CLL cells 173

**Chapter 5 *In vitro* analysis of expanded NK cell and CAR NK cell therapies combined with XPO1 inhibition ..... 177**

**5.1 Receptor expression on NK cell lines and primary IL-2 expanded NK cells ..... 177**

**5.2 Cytotoxicity of NK cell lines and primary IL-2 expanded NK cells against B cell lymphoma cells treated with XPO1 inhibitors ..... 180**

**5.3 Assessing expanded NK cell cytotoxicity in a 2D lymph node support model ..... 186**

5.3.1 IL-4 and CD40L increase HLA-E expression on B cell lymphoma cells, which is reversed by XPO1 inhibition ..... 186

5.3.2 IL-4 and CD40L protects B cell lymphoma cells from NK cell anti-tumour functions, which is reversed by XPO1 inhibition ..... 188

**5.4 The immunomodulatory effect of XPO1 inhibition in B-cell cell lines with impaired HLA-E expression ..... 191**

**5.5 The effect of a pro-inflammatory tumour microenvironment on B-cell lymphoma cell sensitivity to expanded NK cells ..... 195**

5.5.1 IFNγ production by expanded NK cells co-cultured with selinexor-treated B-cell lymphoma cells ..... 195

5.5.2 A pro-inflammatory TME modelled by IFNγ induces the expression of HLA-E on B cell lymphoma cells ..... 197

5.5.3 Mechanism for HLA-E downregulation with XPO1 inhibitors in the presence of IFNγ ..... 199

5.5.4 IFNγ protects B cell lymphoma cells from NK cell anti-tumour functions via HLA-E:NKG2A interactions that is overcome by XPO1 inhibition ..... 202

**5.6 Investigating selinexor-expanded NK cell treatment approaches for future *in vivo* studies ..... 205**

**5.7 Examining CAR NK cell function against selinexor-treated B-cell lymphoma cells . 208**

5.7.1 Generation of anti-CD19 CAR NK cells ..... 208

5.7.2 Selinexor promotes anti-CD19 CAR NK cell function ..... 213

**5.8 The effect of XPO1 inhibition in malignant B cells on T cell, CAR T cell and macrophage activation ..... 219**

5.8.1 XPO1 inhibition sensitises malignant B cells to CAR T cell lysis ..... 219

5.8.2 NKG2A expression on stimulated T cells ..... 222

5.8.3 Macrophage phagocytosis of malignant B-cells is enhanced by selinexor ..... 225

**5.9 Discussion ..... 228**

5.9.1 XPO1 inhibition sensitises malignant B cells to primary, expanded NK cells but not NKL or NK-92 cell lines ..... 228

5.9.2 Functional HLA-E expression is required for the immunomodulatory activity of selinexor ..... 229

5.9.3 Increased HLA-E expression by the lymph node support molecules IL-4+CD40L protect B-cell lymphoma cells from NK cell cytotoxicity, which is reversed by selinexor ..... 230

5.9.4 IFNγ protects B-cell lymphoma cells from NK cytotoxicity via the NKG2A:HLA-E axis, which is overcome by XPO1 inhibition ..... 232

5.9.5 Future *in vivo* experiments ..... 236

5.9.6 XPO1 inhibition and IFNγ modulate the function of anti-CD19 CAR NK cells ..... 237

5.9.7 Future studies investigating the consequences of selinexor-induced HLA-E downregulation on macrophage and NKG2A+ T cell function ..... 239

**Chapter 6 The NK cell immunomodulatory effect of XPO1 inhibition in multiple myeloma cell lines ..... 241**

**6.1 HLA-E expression on multiple myeloma cell lines treated with selinexor ..... 241**

**6.2 NK cell function against multiple myeloma cells treated with selinexor ..... 242**

**6.3 IFNγ treatment of multiple myeloma cells and the effects on HLA-E expression and NK cell function ..... 244**

6.3.1 The effect of IFNγ and XPO1 inhibition on the expression of HLA-E in multiple myeloma cell lines ..... 244

6.3.2 Expanded NK cell function against multiple myeloma cells incubated with IFNγ in the presence of XPO1 inhibitors ..... 247

6.3.3 The effect of XPO1 inhibition on the expression of receptors targeted by monoclonal antibody therapy and CAR immune cells in multiple myeloma ..... 248

**6.4 Discussion ..... 250**

6.4.1 HLA-E downregulation by XPO1 inhibition on multiple myeloma cell lines ..... 250

6.4.2 HLA-E downregulation on multiple myeloma cell lines by XPO1 inhibition in the presence of IFNγ ..... 251

6.4.3 Future experiments investigating the immunomodulatory effect of XPO1 inhibition in multiple myeloma cells and the consequences for NK cell immunotherapy combinations ..... 252

**Chapter 7 Discussion ..... 254**

**7.1 Limitations of study and future work ..... 259**

**7.2 Conclusion ..... 260**

**List of References ..... 261**

# Table of Tables

**Table 1-1: Selection of HLA-E stabilising peptides at homeostasis and stressed states** ..... 56

**Table 1-2: Clinical trials assessing the combination of selinexor with immunotherapy in haematological malignancies.**..... 81

**Table 1-3: Clinical trials assessing the combination of selinexor with immunotherapy in solid malignancies.** ..... 82

**Table 2-1: Concentration of plasmids used to generate lentiviruses for CAR NK cell production.** ..... 94

**Table 2-2: CLL patient characteristics**..... 100

**Table 2-3: Antibodies and recombinant proteins used in flow cytometry experiments** ..... 101

**Table 2-4: Western blot antibody information**..... 102

# Table of Figures

**Figure 1-1: HLA surface expression dynamics.** ..... 35

**Figure 1-2: Regulation of HLA-E gene expression by inflammatory signals.** ..... 37

**Figure 1-3: The missing self-hypothesis of NK cells activation.** ..... 39

**Figure 1-4: NK cell activating and inhibitory receptor signalling cascades.** ..... 46

**Figure 1-5: General immune functions of NK cells and death receptor pathways in target cells.** ..... 47

**Figure 1-6: Non-KIR inhibitory and activating NK cell receptors.** ..... 54

**Figure 1-7: Mechanisms of action of monoclonal antibodies which promote NK cell activation against tumours.** ..... 61

**Figure 1-8: Generations of chimeric antigen receptor constructs.** ..... 66

**Figure 1-9: Cellular origin of B-cell malignancies and multiple myeloma.** ..... 69

**Figure 1-10: XPO1 structure and SINE interactions with XPO1.** ..... 77

**Figure 1-11: The function of XPO1 and the mechanism of action of SINE compounds.** ..... 78

**Figure 3-1: Sensitivity of B cell lymphoma cell lines to selinexor treatment.** ..... 104

**Figure 3-2: NK cell specific lysis assay workflow.** ..... 105

**Figure 3-3: Selinexor sensitises B-cell lymphoma cell lines to NK cell specific lysis.** ..... 106

**Figure 3-4: LAMP and IFNγ assay workflow to assess NK cell activation against selinexor-treated cancer cells.** ..... 108

**Figure 3-5: Selinexor pre-treatment of malignant B cell lines enhances NK cell degranulation.** 109

**Figure 3-6: Selinexor pre-treatment of SUDHL4 cells enhances IFNγ production by NK cells.** 110

**Figure 3-7: Gating strategy used to identify KIR2DS2+ NK cells.** ..... 112

**Figure 3-8: Selinexor pre-treatment of SUDHL4 cells enhances KIR2DS2+ and KIR2DS2- NK cell degranulation.** ..... 113

**Figure 3-9: Impact of selinexor treatment on the expression of NK cell activating ligands on B-cell lymphoma cell lines.** ..... 115

**Figure 3-10: XPO1 inhibition decreases HLA-E surface expression on malignant B cell lines.** 117

**Figure 3-11: Total HLA-E protein abundance is unaffected by selinexor.** ..... 118

**Figure 3-12: Western blot of ER stress markers in B-cell lymphoma cell lines treated with XPO1 inhibitors.** ..... 119

**Figure 3-13: Acid strip experiment workflow.** ..... 120

**Figure 3-14: HLA acid strip optimisation of Raji and Ramos cell lines.** ..... 122

**Figure 3-15: HLA recovery at the plasma membrane in the presence of selinexor.** ..... 123

**Figure 3-16: Selinexor impairs HLA-E and HLA-A/B/C trafficking to the plasma membrane.** 125

**Figure 3-17: XPO1 inhibition in SUDHL4 cells with selinexor preferentially activates NKG2A+ NK cells.** ..... 127

**Figure 3-18: XPO1 inhibition with leptomycin B in SUDHL4 cells reduces surface HLA-E expression and enhances the activation of NKG2A+ NK cells.** ..... 129

**Figure 3-19: LAMP and NK cell specific lysis assay workflows to assess the effect of XPO1 inhibition on ADCC *in vitro.*** ..... 130

**Figure 3-20: Selinexor combined with anti-CD20 mAbs further enhance the activation of NKG2A+ NK cells.** ..... 132

**Figure 3-21: Selinexor enhances NK cell specific lysis of anti-CD20 coated SUDHL4 cells.** .... 133

**Figure 4-1: *Ex vivo* selinexor treatment induces XPO1 degradation in patient CLL cells.** ..... 141

**Figure 4-2: Flow cytometry gating strategy used to measure lysis of patient derived CLL cells.** 142

**Figure 4-3: XPO1 inhibitors sensitise CLL cells to NK specific lysis.** ..... 143

**Figure 4-4: Selinexor pre-treatment of CLL cells enhances NK cell activation.** ..... 144

**Figure 4-5: Flow cytometry gating strategy to identify CD5+CD19+ CLL cells.** ..... 145

**Figure 4-6: XPO1 inhibitors downregulate HLA-E surface expression on CLL cells.** ..... 146

**Figure 4-7: HLA expression on CLL patient cells after *ex vivo* selinexor treatment stratified on IGHV mutational status and IgM surface expression level.** ..... 147

**Figure 4-8: HLA-E is downregulated after 16 hour-selinexor treatment and remains lowly expressed after selinexor removal.** ..... 148

**Figure 4-9: NKG2A+ and NKG2A- NK cell degranulation against patient CLL cells pre-treated with selinexor *ex vivo*.** ..... 149

**Figure 4-10: IFNγ production in NKG2A+ and NKG2A- NK cells after co-culture with patient derived CLL cells pre-treated with selinexor *ex vivo*.** ..... 150

**Figure 4-11: NKG2A+ and NKG2A- NK cell activation against LMB-treated CLL cells.** ..... 150

**Figure 4-12: IFNγ is expressed in degranulating CD107a+ NK cells after co-culture with CLL cells pre-treated with XPO1 inhibitors.** ..... 151

**Figure 4-13: NKG2D ligand expression on CLL cells treated with selinexor.** ..... 152

**Figure 4-14: Expression of NK cell activating ligands on CLL cells treated with selinexor.** .... 153

**Figure 4-15: Selinexor increases the expression of death receptor 5 on CLL cells.** ..... 153

**Figure 4-16: TRAIL blockade protects CLL cells from NK cell specific lysis with selinexor.** .... 154

**Figure 4-17: TRAIL blockade slightly impairs NKG2A+ NK cell degranulation with selinexor.** 155

**Figure 4-18: CD20 is stably expressed on CLL cells after selinexor treatment.** ..... 156

**Figure 4-19: Selinexor enhances NK cell activation in the presence anti-CD20 mAbs.** ..... 157

**Figure 4-20: CD38 is stably expressed on CLL cells treated with selinexor.** ..... 158

**Figure 4-21: Selinexor enhances NK cell activation in the presence of the anti-CD38 mAb daratumumab.** ..... 159

**Figure 4-22: XPO1 inhibition induces HLA-E downregulation in the presence of BTK inhibitors.** 160

**Figure 4-23: Selinexor sensitises CLL cells to NK specific lysis in the presence of BTK inhibitors.** ..... 161

**Figure 4-24: The second generation BTK inhibitor acalabrutinib does not impair increased NK cell activation with selinexor.** ..... 162

**Figure 4-25: Lymph node-associated signals IL-4 and CD40L increase HLA-E expression on CLL cells.** ..... 163

**Figure 4-26: Selinexor reduces HLA-E expression on CLL cells incubated with IL-4 + CD40L.** 164

**Figure 4-27: IL-4 + CD40L protect CLL cells from on NK cell degranulation, which is reversed by selinexor treatment.** ..... 165

**Figure 4-28: IL-4 + CD40L dampens IFNγ production by NK cells, which is reversed by selinexor treatment.** ..... 166

**Figure 4-29: Gating strategy to measure HLA expression on CLL cell populations based on CXCR4 and CD5 expression.** ..... 167

**Figure 4-30: CXCR4lowCD5hi CLL cells have increased HLA-E expression.** ..... 167

**Figure 4-31: Selinexor decreases HLA-E surface expression on healthy donor B cells and monocytes.** ..... 168

**Figure 4-32: Selinexor does not enhance autologous NK cell activation against CLL cells.** ... 169

**Figure 5-1: Expansion of primary NK cells expanded with 500 IU/mL IL-2.** ..... 178

**Figure 5-2: Expression of activating receptors and the inhibitory receptor CD96 on NK cell lines and primary NK cells.** ..... 179

**Figure 5-3: Expression of NKG2x receptors on NK cell lines and primary NK cells.** ..... 180

**Figure 5-4: XPO1 inhibition does not enhance NK-92 and NKL cytotoxicity of B cell lymphoma cells.** ..... 181

**Figure 5-5: Anti-NKG2A blocking antibodies do not promote NK-92 and NKL cytotoxicity.** . 182

**Figure 5-6: NKG2A expression on IL-2 expanded NK cells.** ..... 183

**Figure 5-7: Proliferation of NKG2A+ and NKG2A- NK cells during 14-day expansion.** ..... 184

**Figure 5-8: XPO1 inhibition enhances expanded NK cell cytotoxicity of B cell lymphoma cells.** 184

**Figure 5-9: The next generation XPO1 inhibitor eltanexor downregulates HLA-E expression which sensitises B cell lymphoma cells to expanded NK cell cytotoxicity.** ..... 185

**Figure 5-10: Anti-NKG2A blocking antibodies enhance expanded NK cell cytotoxicity.** ..... 186

**Figure 5-11: HLA and CD19 expression on lymphoma cell lines incubated with lymph node-associated molecules IL-4 and CD40L.** ..... 187

**Figure 5-12: HLA and CD19 expression on lymphoma cell lines treated with selinexor in the presence of IL-4 + CD40L.** ..... 188

**Figure 5-13: Lymph node-associated molecules IL-4 and CD40L protect B cell lymphoma cells from expanded NK cell cytotoxicity.** ..... 189

**Figure 5-14: Anti-NKG2A antibodies reverse the NK-protective effect of IL-4 + CD40L in B cell lymphoma cells.** ..... 190

**Figure 5-15: XPO1 inhibition reverses the NK-protective effect of IL-4 + CD40L in B cell lymphoma cells.** ..... 191

**Figure 5-16: Flow cytometry histograms of HLA proteins on B lymphoblastoid cell lines 721.174 and 721.221.** ..... 192

**Figure 5-17: Selinexor does not affect the expression of HLA proteins and CD19 on 721.174 and 721.221 cell lines.** ..... 193

**Figure 5-18: Selinexor degrades XPO1 and induces p53 in 721 cell lines.** ..... 193

**Figure 5-19: Selinexor or anti-NKG2A mAbs do not sensitise 721 cell lines to NK cell cytotoxicity.** ..... 194

**Figure 5-20: IFNγ production and secretion by expanded NK cells co-culture with selinexor-treated B cell lymphoma cells.** ..... 196

**Figure 5-21: Workflow to examine HLA expression on cancer cells that were resuspended in expanded NK:cancer cell co-culture supernatant.** ..... 197

**Figure 5-22: NK-cancer cell co-culture supernatants enhance HLA-E expression, which is reversed by XPO1 inhibition.** ..... 198

**Figure 5-23: Selinexor impairs IFNγ signalling in B-cell lymphoma cell lines.** ..... 199

**Figure 5-24: IFNγ signalling is functional in 721 cell lines but does not induce HLA-E expression.** ..... 200

**Figure 5-25: Selinexor impairs total HLA-E expression in the presence of IFNγ.** ..... 201

**Figure 5-26: HLA-E is trapped internally in 721.221 cells.** ..... 202

**Figure 5-27: IFNγ protects B-cell lymphoma cells from expanded NK cell lysis via HLA-E:NKG2A interactions.** ..... 203

**Figure 5-28: IFNγ impairs NKG2A+ NK cell activation, which is overcome by XPO1 inhibition.** 204

**Figure 5-29: IFNγ does not protect 721 cell lines from expanded NK cell cytotoxicity.** ..... 205

**Figure 5-30: Sequential vs concurrent selinexor-expanded NK cell treatments *in vitro*.** ..... 206

**Figure 5-31: Toxicity of twice weekly selinexor in NSG mice administered for two weeks.** . 207

**Figure 5-32: Raji tumour growth kinetics in NSG mice.** ..... 208

**Figure 5-33: Generation of anti-CD19 CAR NK cells using lentivirus transduction.** ..... 210

**Figure 5-34: Optimisation of NK cell numbers required for transduction.** ..... 211

**Figure 5-35: Anti-CD19 CAR expression is unstable on NK cells.** ..... 212

**Figure 5-36: Anti-CD19 CAR transduction efficacy in primary NK cells.** ..... 212

**Figure 5-37: XPO1 inhibition promotes anti-CD19 CAR NK cell cytotoxicity.** ..... 213

**Figure 5-38: CAR expression on NKG2A+ and NKG2A- NK cells.** ..... 214

**Figure 5-39: Selinexor and anti-NKG2A mAbs promote anti-CD19 CAR NK cell cytotoxicity.** 215

**Figure 5-40: Selinexor downregulates CD19 surface expression.** ..... 216

**Figure 5-41: IFNγ protects Raji cells from anti-CD19 CAR NK cell cytotoxicity, which is reversed by selinexor.** ..... 217

**Figure 5-42: NKG2A+/- CAR NK cell activation against Raji cells incubated with IFNγ ± selinexor.** ..... 218

**Figure 5-43: CAR T cell transduction efficacy.** ..... 220

**Figure 5-44: Selinexor promotes CAR T cell lysis of Raji cells.** ..... 220

**Figure 5-45: NKG2A expression on anti-CD19 CAR T cells.** ..... 221

**Figure 5-46: NKG2A expression on T cells after multiple rounds of stimulation.** ..... 223

**Figure 5-47: Expression of activation markers on T cells after repeated rounds of stimulation.** 224

**Figure 5-48: Gating strategy to measure macrophage phagocytosis.** ..... 226

**Figure 5-49: Selinexor enhances macrophage phagocytosis or Raji cells.** ..... 227

**Figure 5-50: Macrophage phagocytosis of Raji cells pre-treated with IFNγ.** ..... 227

**Figure 6-1: Total HLA-E expression and PARP cleavage in MM.1S cells treated with selinexor in the presence of the apoptotic inhibitor Q-VD.** ..... 241

**Figure 6-2: Selinexor downregulates HLA-E on multiple myeloma cells with high basal levels of HLA-E.** ..... 242

**Figure 6-3: Selinexor sensitises MM1S cells to NKG2A+ NK cell activation and cytotoxicity.** 243

Table of Figures

**Figure 6-4: IFNγ enhances HLA-E expression on L363 cells, which is overcome by selinexor.** 245

**Figure 6-5: Surface and total expression levels of HLA-E in L363 cells treated with selinexor in the presence of IFNγ.** ..... 246

**Figure 6-6: Selinexor impairs IFNγ signalling in L363 cells.** ..... 247

**Figure 6-7: IFNγ protects L363 cells from expanded NK cell cytotoxicity, which is reversed by selinexor.** ..... 248

**Figure 6-8: CD38 and BCMA expression on selinexor-treated multiple myeloma cell lines.** . 249

**Figure 7-1: Mechanism for HLA-E downregulation by SINE compounds.** ..... 256

**Figure 7-2: The NK-stimulating immunotherapies promoted by XPO1 inhibition.** ..... 258

# List of Accompanying Materials

The data presented in this thesis has been published in the following research articles:

- **Fisher, J.G**., Doyle, A.D.P., Graham, L. V., Sonar, S., Sale, B., Henderson, Isla., Del Rio, Luis., Johnson, P.W., Landesman, Y., Cragg, M.S., Forconi, F., Walker, C. J., Khakoo, S.I., and Blunt, M.D. (2023). XPO1 inhibition sensitises CLL cells to NK cell mediated cytotoxicity and overcomes HLA-E expression. *Leukaemia*. *37*, 2036-2049.
- **Fisher, J.G**., Walker, C.J., Doyle, A.D., Johnson, P.W., Forconi, F., Cragg, M.S., Landesman, Y., Khakoo, S.I., and Blunt, M.D. (2021). Selinexor Enhances NK Cell Activation Against Malignant B Cells via Downregulation of HLA-E. *Frontiers in Oncology*. *11*, 1–12.

First-author reviews written whilst conducting the PhD:

- **Fisher J.G**, Graham L.V, Blunt M.D. (2024). Strategies to disrupt NKG2A:HLA-E interactions for improved anti-cancer immunity. *Oncotarget*. *15*, 501-503.
- **Fisher, J.G**., Doyle, A.D.P., Graham, L. V., Khakoo, S.I., and Blunt, M.D. (2022). Disruption of the NKG2A:HLA-E Immune Checkpoint Axis to Enhance NK Cell Activation against Cancer. *Vaccines*. *10*, 1993.

Research articles and reviews involved with whilst conducting the PhD:

- Graham L.V., **Fisher J.G**, Doyle A.D.P., Sale B., Del Rio L., French A.J.E., Mayor N.P., Turner T.R., Marsh S.G.E., Cragg M.S., Forconi F., Khakoo S.I. and Blunt M.D. (2024) KIR2DS2+ NK cells in cancer patients demonstrate high activation in response to tumour-targeting antibodies. *Frontiers in Oncology*. 14:1404051.
- Graham, L.V., **Fisher, J.G.,** Khakoo, S.I., and Blunt, M.D. (2023). Targeting KIR as a novel approach to improve CAR-NK cell function. Journal of Translational Genetics and Genomics. 7, 230-5.
- Blunt, M.D., Vallejo Pulido, A., **Fisher, J.G**., Graham, L. V., Doyle, A.D.P., Fulton, R., Carter, M.J., Polak, M., Johnson, P.W.M., Cragg, M.S., et al. (2022). KIR2DS2 Expression Identifies NK Cells With Enhanced Anticancer Activity. *Journal of Immunology*. *209*, 379–390.

# Research Thesis: Declaration of Authorship

Print name: Jack Graham Fisher

Title of thesis: Investigation into the immunomodulatory activity of XPO1 inhibitors

I declare that this thesis and the work presented in it are my own and has been generated by me as the result of my own original research.

I confirm that:

1. This work was done wholly or mainly while in candidature for a research degree at this University;
2. Where any part of this thesis has previously been submitted for a degree or any other qualification at this University or any other institution, this has been clearly stated;
3. Where I have consulted the published work of others, this is always clearly attributed;
4. Where I have quoted from the work of others, the source is always given. With the exception of such quotations, this thesis is entirely my own work;
5. I have acknowledged all main sources of help;
6. Where the thesis is based on work done by myself jointly with others, I have made clear exactly what was done by others and what I have contributed myself;
7. Parts of this work have been published as:

- **Fisher, J.G**., Doyle, A.D.P., Graham, L. V., Sonar, S., Sale, B., Henderson, Isla., Del Rio, Luis., Johnson, P.W., Landesman, Y., Cragg, M.S., Forconi, F., Walker, C. J., Khakoo, S.I., and Blunt, M.D. (2023). XPO1 inhibition sensitises CLL cells to NK cell mediated cytotoxicity and overcomes HLA-E expression. *Leukaemia*. *37*, 2036-2049.
- **Fisher, J.G**., Walker, C.J., Doyle, A.D., Johnson, P.W., Forconi, F., Cragg, M.S., Landesman, Y., Khakoo, S.I., and Blunt, M.D. (2021). Selinexor Enhances NK Cell Activation Against Malignant B Cells via Downregulation of HLA-E. *Frontiers in Oncology*. *11*, 1–12.

Signature: ..... Date: .....

# Acknowledgements

Firstly, huge thank you to my supervisors Matt and Salim. Being Matt's first PhD student, I hope that I have set a good standard! But you're only as good as your trainer and I think I've been blessed to have one of the best. So, thank you Matt for transferring your laboratory expertise, guiding experiments, reviewing my written work and for encouraging me to attend conferences and to submit my work for awards. The main highlights include 7 combined publications, winning the PGR publication award and receiving the UK CLL Forum Catovsky prize, all of which would not have been possible without your mentorship! I hope to keep up to date with the future successes of the Blunt lab, although few will be achieved in FPL if Pep is still around.

Huge thank you to Salim for project guidance at NK lab meetings. I'm very grateful for all the contributions of the wider NK cell team at Southampton, in particular Amber Doyle and Lara Graham the founding members of the Blunt group who collectively we have supported each other's experiments and drafted manuscripts. Thank you also to Rosalba for answering all my questions on CAR NK cells and to Becky and Laura ES for their expertise in molecular biology. The whole NK group have been amazing to work alongside, I couldn't have imagined working with so many great people during my PhD research.

I'd also like to thank the Cancer Sciences department at the university for their assistance, especially Nurdan, Vici and Michael for their advice and reagents which have greatly helped me with my work on CAR immune cells. Special thanks to the CLL team in the Somer's, especially Luis and Isla, for collecting CLL patient samples which were used throughout chapter 4 and of course to the patients who agreed to donate their cells. Finally, thanks to the PCU staff and Kerry for their help and training with *in vivo* experiments.

Thank you to the flow cytometry team, Carolann McGuire and Sarah Pearson for all their help and support in the flow cytometry facility. Thanks to the wider Level E community, the skilled phlebotomists (Anju, Bonnie and Matt M) and the kind blood donors, who without, this thesis would not be possible. I've made many great friends on Level E, through the LSPS society and from football on Thursday, all of whom have made my time in Southampton a delight. Special mentions go to Timo, Alex L, Alex R, Natasha P, Lara B, Anna and Victor. I'll always cherish the office banter, the BBQs and football and F1 chat.

My family have also been a great support throughout. Especially my parents for helping me move to the South of England and for visiting me during holidays. My brothers and my niece and nephew, Keeva and Elliot, thank you for visiting me to help maintain my momentum and for calling me for updates, especially during the writing-up period.

Finally, I'd like to thank my fiancée Alba for keeping me focussed during the PhD - like you have always done throughout my studies and career to date. Thank you for the after-work discussions on antibodies and T cell biology which have helped me draft up experiments and contributed to the write up. I will miss starting and ending the working day together and seeing you occasionally around the lab and at lunchtime. We have made many happy memories together over the course of doing our PhDs together in Southampton including, exploring the South coast, moving into our first flat and of course getting engaged! May the future bring many more happy memories like those we've made here.

# Definitions and Abbreviations

ADCC..... Antibody dependent cellular cytotoxicity

ALL ..... Acute lymphoblastic leukaemia

AML ..... Acute myeloid leukaemia

AML ..... Acute myeloid leukaemia

APC ..... Antigen presenting cell

BaLV..... Baboon lentivirus

BCMA..... B cell maturation antigen

BCR ..... B cell receptor

BiKE..... Bi-specific killer cell engager

BTK..... Bruton's tyrosine kinase

BTKi..... Bruton's tyrosine kinase inhibitor

CAR ..... Chimeric antigen receptor

CIML..... Cytokine-induced memory-like

CLL ..... Chronic lymphocytic leukaemia

CLP ..... Common lymphoid progenitor

CML..... Chronic myeloid leukaemia

cPARP..... Cleaved poly (ADP-ribose) polymerase

CRS..... Cytokine release syndrome

cSMAC ..... Central supramolecular activation complex

DAMPs ..... Danger-associated molecular patterns

DC ..... Dendritic cell

DLBCL..... Diffuse large B cell lymphoma

ER..... Endoplasmic reticulum

GAS ..... Interferon-gamma activated site

GZMB..... Granzyme B

HCV ..... Hepatitis C virus

HDAC ..... Histone de-acetylase

Definitions and Abbreviations

HIV ..... Human immunodeficiency virus

HLA ..... Human leukocyte antigen

HSC ..... Hematopoietic stem cell

ICI..... Immune checkpoint inhibitor

IGHV..... Immunoglobulin variable heavy chain

IRF ..... Interferon response factor

ITAM ..... Immunoreceptor tyrosine-based activation motif

ITIM ..... Immunoreceptor tyrosine-based inhibitory motif

ITK..... IL-2 inducible kinase

KIR..... Killer cell immunoglobulin-like receptor

LAMP/CD107a ..... Lysosomal-associated membrane protein/cluster of differentiation 107a

LCMV ..... Lymphocytic choriomeningitis mammarenavirus

LILRB ..... Leukocyte immunoglobulin-like receptor subfamily B

LMB..... Leptomycin B

mAb ..... Monoclonal antibody

MCL..... Mantle cell lymphoma

MHC..... Major histocompatibility complex

NHL ..... Non-hodgkin lymphoma

NK cells ..... Natural killer cells

NKE ..... Natural killer cell engager

NKP ..... Natural killer progenitor cell

NLRC5 ..... NOD-like receptor family CARD domain containing 5

NSP13 ..... Non-structural protein 13

PAMPs ..... Pathogen-associated molecular patterns

PEBL..... Protein expression blocker

PM ..... Plasma membrane

pSMAC..... Peripheral supramolecular activation complex

RanGTP ..... Ras-related nuclear protein-GTP

rRNA ..... Ribosomal RNA

Definitions and Abbreviations

SARS-CoV-2..... Severe acute respiratory syndrome coronavirus 2

SASP..... Senescence-associated secretory phenotype

SHIP-1/2..... Src homology 2 domain-containing inositol 5-phosphatase-1/2

SHM..... Somatic hypermutation

SHP-1/2..... Src homology 2 domain-containing phosphatase-1/2

SINE..... Selective inhibitor of nuclear export

SMIC..... Supramolecular inhibitory complex

STAT..... Signal transducer and activator of transcription 1

TCR..... T cell receptor

TriKE..... Tri-specific killer cell engager

XPO1..... Exportin-1

# Chapter 1 Introduction

## 1.1 Overview of the immune system

To fight infections and remove neoplastic cells animals have evolved to have an immune system consisting of a variety of cells that work together to maintain an animal's healthy state. The immune system comprises of two arms: the innate and adaptive immune system. Both work in unison to resolve damage inside the body and respond to vaccination to protect from future disease.

The immune system develops from CD34+ haematopoietic stem cells (HSC) which reside in the bone marrow throughout life. HSCs continuously re-populate the immune system by differential expression of transcription factors that determine the fate of HSCs and progenitor cells. There are two main differentiation trajectories of HSCs. The first is the myeloid lineage in which a common myeloid progenitor produces most innate immune cell populations. The second is the lymphoid lineage in which a common lymphoid progenitor (CLP) produces T and B lymphocytes, Natural Killer (NK) cells and some populations of dendritic cells (DCs).

### 1.1.1 The innate immune system

The innate immune system, named because of its natural capacity to quickly respond non-specifically to a plethora of danger signals, consists of eight main cell types. Neutrophils, eosinophils, basophils and mast cells are collectively referred to as granulocytes because of the toxic granules found inside the cytoplasm. These cells have similar, but non-redundant roles within the innate immune system. Neutrophils are important regulators of anti-bacterial immunity, eosinophils and basophils play crucial roles in clearing parasitic infections and mast cells along with basophils are regulators of allergic responses.

Other cells of the innate immune system include NK cells, which play roles in the killing of virus-infected cells and cancer cells, monocytes, macrophages and DCs. The latter three are hugely important in cross talk between the innate and adaptive immune systems. Similar to granulocytes, macrophages and dendritic cells have similar, but non-redundant roles. Macrophages are main regulators of phagocytosis. Phagocytosis is the process by which a cell engulfs another cell. Once a macrophage engulfs a bacterium, infected or damaged cell, danger signals, also referred to as DAMPs (danger-associated molecular patterns) or PAMPs (pathogen-associated molecular patterns), are transmitted which lead to macrophage activation. The activated macrophage then differentiates into a type of macrophage best adapted to clearing the assault. For example, M1 macrophages are best equipped for dealing with intracellular pathogens and cancer cells and M2 macrophages are best

adapted to resolve infections of extracellular pathogens. This consequently leads to inflammation which is characterised by the invasion of multiple immune cells leading to clinical features of heat, redness, itching and swelling. The resultant immune response is more complex than described due to the involvement of other immune populations which secrete inflammatory mediators that also contribute to skewing the immune response to optimally resolve the type of infection/inflammation.

DCs also have roles in phagocytosis, but once activated differentiate into professional antigen presenting cells (APC). Macrophages also carry out APC functions, but to a lesser extent compared to DCs. Antigen presentation involves the presentation of pathogen or cancer-associated peptides to induce an antigen-specific adaptive immune response. More specifically, once an APC is activated by DAMPs or MAMPs, these cells transit to secondary lymphoid organs where they interact with immature adaptive immune cells to prime their effector functions. Antigen presentation involves the loading of peptides on to major histocompatibility complex I or II (MHC-I and MHC-II) which interact with T cell receptors (TCR) on CD8+ and CD4+ T cells, respectively, and with killer cell immunoglobulin-like receptors (KIR) on NK cells. T cell activation not only requires TCR-MHC interactions, but also a secondary signal derived from the CD28 receptor which interacts with CD80/86 on activated macrophages and mature DCs. CD80/86 is only expressed on activated APCs and therefore avoids initiating an adaptive immune response unnecessarily. This is referred to as peripheral tolerance which avoids damage to self-tissue. Once activated, T cells then transit to the site of infection to carry out their effector functions such as directly killing of infected and cancer target cells and releasing inflammatory cytokines and chemokines to promote the activity of other immune cells.

### 1.1.2 T lymphocytes

T lymphocytes express a TCR that is activated against a specific peptide that is presented on MHC-I and MHC-II for CD8+ and CD4+ T cells, respectively. CD4 and CD8 are co-receptors that stabilise that MHC:TCR complex. T cells start their development in the bone marrow and transit to the thymus in a naïve state to undergo a process of education, in which T cells adapt to the host. Autoreactive T cells are deleted in a process of negative selection. T cells leaving the thymus possess TCRs specific for foreign peptides and these T cells survey peptides presented by APCs at secondary lymphoid organs and become activated once the peptide is recognised. The complexity of TCRs is due to the expression of RAG1/2 enzymes that rearrange VDJ genes encoding the variable regions of TCRs, and the specific rearrangements of these are not inherited. Because of the education process, T cells are MHC-restricted within individuals such that T cell infusions have to be MHC matched otherwise graft-versus host or host-versus graft disease will surmount.

Similar to M1 and M2 macrophages, T cell populations exist that are better equipped at dealing with different types of pathogens. Depending on the inflammatory environment, CD4+ T cells differentiate into either $T_h1$ (intracellular-specific), $T_h2$ (extracellular-specific) or $T_h17$ (parasite-specific) T cells. The differentiation process is regulated by a set of transcription factors ($T_h1$ = t-bet, $T_h2$ = GATA-3, $T_h17$ = RORγt) which are induced by the stimulation of cytokines in the microenvironment (t-bet = IFNγ + IL-12, GATA-3 = IL-4, RORγt = TGFβ + IL-6). These differentiated CD4+ T cells then secrete inflammatory modulators ($T_h1$ = IFNγ + IL-2, Th2 = IL-4 + IL-5, Th17 = IL-6 + IL-17) to orchestrate the most effective immune response to deal with the type of infection. Whilst CD4+ T cells orchestrate the immune response, CD8+ T cells have roles in direct cytotoxicity of target cells that present specific peptides at the plasma membrane. Another important population of T cells are T regulatory T cells ($T_{reg}$) which possess TCRs specific for autoantigens. $T_{reg}$ cells are derived from T cells with high affinity TCRs and these cells play important roles in circumventing autoimmunity and dampening inflammation. $T_{reg}$ cells mediate their anti-inflammatory functions via expression of the transcription factor FOXP3 and secretion of anti-inflammatory cytokines IL-10 and TGFβ.

Of equal importance is switching off an on-going T cell immune response. This is because once pathogens or neoplastic cells are removed an on-going immune response would lead to destruction of healthy tissues and the development of autoimmunity. Dampening of the immune response is done through a variety of mechanisms such as via $T_{reg}$ activation but also through the downregulation of MHC-II and upregulation of CTLA-4 on APCs (CTLA-4 inhibits the interaction of MHC-II with CD28). Equally important is the ligation of inhibitory T cell receptors (e.g. PD-1) and NK-mediated clearance of T cells and DCs (1).

Once the inflammation is cleared, T cells produce immunological memory unlike innate cells. Therefore, when they encounter the same pathogen, they can respond much faster and clear the infection before disease ensues. This is the basis of vaccination. Vaccines involve the exploitation of pathogen antigens without the need for inoculation with the real agent. The antigen initiates an immune response which culminates in inducing immunological memory so that when the host encounters the real pathogen disease is avoided. Memory T cells arise from activated T cells once the inflammatory insult has been resolved. These exist in the body throughout a person's life circulating through the body in search of the specific antigen.

### 1.1.3 B lymphocytes

B lymphocytes are another type of lymphoid cell that is a part of the adaptive immune system. These cells produce antibodies which are mediators of humoral immunity. Antibodies, like TCRs, are specific to antigens on target cells but antibodies activate innate immune cells to perform effector functions against opsonised targets. Similar to T cells, B cells undergo a process of selection whereby

autoreactive cells are destroyed and after B cell activation, long-lived memory B cells develop to clear repeat infections.

In addition to stimulation of the B cell receptor (BCR), B cells require a secondary signal derived from MHC-II which interacts with the TCR of follicular T helper CD4+ T cells ($T_{fh}$). $T_{fh}$ cells differentiate using the transcription factor Bcl6 which responds to IL-6. These $T_{fh}$ cells create a supportive microenvironment for B cell activation through the secretion of IL-4 and IL-21 and via the expression of surface receptors for example CD40L. IL-21 facilitates the creation of germinal centers, important for B cell maturation and CD40 and IL-4 potentiate BCR signalling and promote cell survival and proliferation (2). Within germinal centers B cells interact with $T_{fh}$ cells, macrophages and follicular DCs which aid somatic hypermutation (SHM), a process of affinity maturation whereby antibody variable fragment genes of heavy (IGHV) and light chains mutate to produce high affinity antibodies against specific antigens. SHM takes place in the dark zone of germinal centers after which B cells progress into the light zone. Within the light zone, mutations that induce low affinity BCRs or BCRs against autoantigens induce apoptosis of B cells. Cells with mutations that confer improved affinity for antigens are selected for and these undergo proliferation and antibody class switching, a process essential for the production of antibody isotypes with the correct properties to deal with the inflammatory insult. Following B cell maturation in germinal centers, B cells develop into terminally differentiated plasma cells or memory B cells and leave germinal centers (3). Plasma cells secrete large quantities of a specific antibody and memory B cells once activated quickly differentiate into antibody-secreting plasma cells.

Antibodies in tissues bind to target cells which result in various downstream events partaken by different immune cells that express Fc receptors (FcR). FcRs bind to the Fc constant region of antibodies and upon ligation induce activating signals via adapter proteins containing immunoreceptor tyrosine-based activation motif (ITAM) domains. One FcR, FcγRIIb, transduces inhibitory signals via immunoreceptor tyrosine-based inhibitory motif (ITIM) domains. FcRs selectively bind antibody isotypes: FcαRs bind IgA antibodies, FcγRs bind IgG, FcεR bind IgE and FcμRs bind IgM. For example, NK cells solely express FcγRIIIa (CD16a) which binds to IgG1 antibodies to induce antibody-dependent cellular cytotoxicity (ADCC). Phagocytic cells express multiple FcRs which enable them to perform antibody-dependent phagocytosis (ADCP). However, FcγRIIb (CD32b) transduces signals to inhibit phagocytosis and to inhibit B cell activation which is important for shutting down the immune response, clearing antibodies and inhibiting further production of antibodies by B cells (4). Another function of antibodies is the activation of complement-dependent cytotoxicity. At opsonised sites, a membrane attack complex is formed which induces pores in target cell membranes which leads to apoptosis of the cell (5).

## 1.2 Human Leukocyte Antigens (HLA).

### 1.2.1 HLA class I proteins

MHC in humans is referred to as human leukocyte antigen (HLA). These are proteins expressed by all individuals that enable self-recognition by T cells through the presentation of self-peptides to the TCR and by NK cells through engagement of inhibitory killer cell immunoglobulin-like receptors (KIR). Upon oncogenesis or infection, non-self-peptides are presented on HLA molecules that enable activation of the immune system through the activation of CD8+ T cell TCRs and impairment of KIR interactions.

HLAs consist of two major classes: HLA class I and HLA class II. HLA class II is only expressed on professional APCs and is upregulated on APCs and B cells during inflammation. HLA class II presents peptides to the TCR of CD4+ T cells. HLA class I is constitutively expressed on all nucleated cells and is responsible for presenting peptides to CD8+ T cell TCRs and to KIR on NK cells. There are three classical HLA class I proteins: HLA-A, HLA-B and HLA-C and each gene contains thousands of different alleles making these the most highly polymorphic proteins in the human genome. As well as classical HLA protein presentation to TCRs, the non-classical HLA class I protein HLA-E also presents peptides to HLA-E-restricted TCRs (6). At homeostasis, HLA-E presents peptides derived from the leader sequences of HLA class I proteins that are trimmed by signal peptidases in the endoplasmic reticulum (ER) (7). During inflammation, non-canonical peptides derived from pathogens or stress-related conditions can be presented by HLA-E and recognised by these HLA-E-restricted TCRs on CD8+ T cells. Most research on peptide presentation to HLA-E-restricted TCRs has been in the context of mycobacterium tuberculosis, HCV and CMV infections (6).

Classical HLAs have a uniform structure made from two polypeptides: α and β2-microglobulin. The α chain consists of three domains, two at the most extracellular portion of the protein (α1 and α2) which bind to and present amino acid chains of 8-10 amino acids in length and a third domain (α3) which spans the plasma membrane. β2-microglobulin is essential for HLA expression at the plasma membrane and for stabilisation of the peptide binding groove (8). Endogenous peptides derived from the proteasome are loaded onto HLA proteins in the ER by the peptide loading complex consisting of the proteins TAP1, TAP2, calreticulin, ERAP1/2, ERp57 and tapasin. These proteins are important for maintaining the stability of unloaded HLA proteins and the trimming of peptides by ERAP allows for the appropriate binding of peptides in the binding groove. The abundance of HLA molecules at the plasma membrane is regulated at multiple levels including the rate of transcription, the availability of peptides that initiate HLA exit from the ER, the stability of HLA molecules at the plasma membrane and the internalisation rate (**Figure 1-1**). HLA class I genes are mainly regulated by NOD-like receptor family CARD domain containing 5 (NLRC5), but other factors including signal transducer and activator

of transcription (STAT), nuclear factor kappa-light-chain-enhancer of activated B cells (NF-kB), interferon response factors (IRF) and CIITA can enhance the transcription of HLA class I genes to promote peptide presentation to T cells under inflammatory conditions. Proteasome function is crucial for supplying peptides to stabilise HLA proteins and promote their export from the ER (9). When peptides are low in abundance, for example with proteasome inhibitors, HLA proteins become trapped in the ER which reduces the replenishment of HLA molecules at the plasma membrane resulting in decreased surface expression. Once at the plasma membrane, HLA stability is affected by the affinity of the peptide in the binding groove and by internalisation via the endocytosis pathway (9). A low affinity peptide will become detached from the binding groove resulting in an empty HLA protein which will quickly become internalised into the cell (10,11). Endocytosis is a natural process to survey the extracellular environment which is regulated by clathrin that binds to the intracellular tails of receptors. HLA molecules contain clathrin-binding domains on their intracellular tails (12) and differences in sequence between HLA tails result in different rates of internalisation (9). If one of these processes is disrupted or enhanced, such as during tumour transformation, viral infection or targeted agents, HLA expression levels change enabling recognition or protection from the immune system (11).

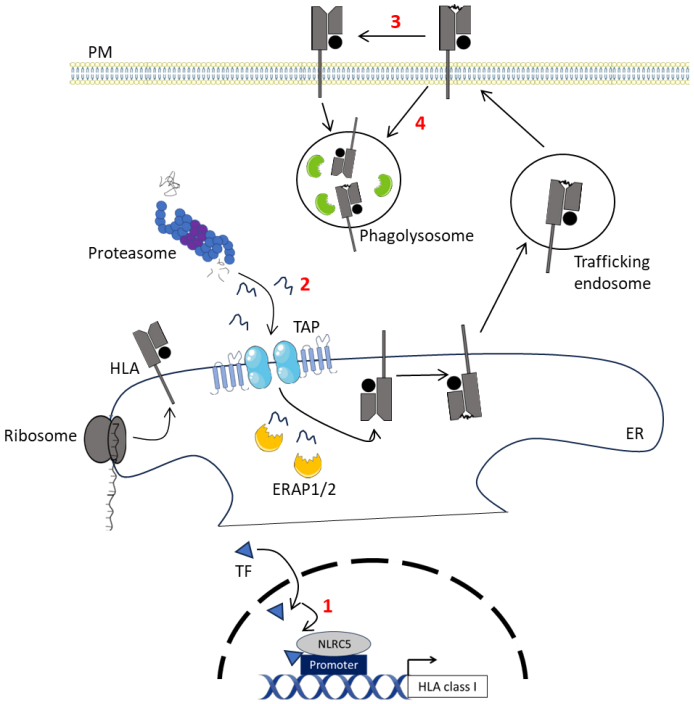


**Figure 1-1: HLA surface expression dynamics.**

HLA class I expression at the plasma membrane is regulated by multiple cellular process. (1) HLA class I gene transcription is governed by multiple transcription factors (TF) which become activated downstream of receptor activation during inflammation and these bind to enhancer regions of HLA class I genes for example interferon response elements. The main transcription factor complex for all HLA class I genes is the NLRC5 complex. (2) HLA mRNA is translated in the endoplasmic reticulum (ER) where peptides from the proteasome derived from endogenous proteins are loaded onto HLA molecules by the TAP peptide loading complex and ERAP enzymes. Once peptides are loaded on to HLA molecules, HLAs can exit from the ER and transit to the plasma membrane (PM). (3) The stability of peptides within the binding groove determines the surface stability of HLA molecules at the PM. Once peptides become unbound HLA molecules are internalised. (4) Internalisation rates of HLA proteins are also determined by their cytoplasmic tails which have different affinities for clathrin. Part of this figure was made using SmartArt.

### 1.2.2 The non-classical HLA class I molecule HLA-E

There are three non-classical HLA class I proteins: HLA-E, HLA-F and HLA-G. The major similarity between non-classical HLA class I and classical HLA class I proteins is their structure with the α polypeptide chain and β2-microglobulin (13). On the other hand, there are numerous dissimilarities. Firstly, non-classical HLA are much less polymorphic, for example HLA-E has two known allelic variants (HLA-E*0101 and HLA-E*0103) compared to classical HLA class I molecules of which there are thousands of alleles (13). The two allelic variants of HLA-E stem from differences in the amino acid at position 107 outside of the peptide binding groove: HLA-E*0101 has an arginine and HLA-E*0103 has a glycine (13,14). As a result, the peptide repertoires are overlapping (13,14). Secondly, they do not solely act as ligands for TCRs, but as ligands for KIRs on NK cells and other receptors

found on NK, T and NKT cells. For example, HLA-E binds to NKG2A and NKG2C receptors which are expressed on NK cells, NKT cells and T cells (15). However, because of the low polymorphism of HLA-E, its primary function during evolution must have been to interact with non-rearranging receptors on NK cells. Thirdly, although HLA-E is ubiquitously expressed like classical HLA-A/B/C, the expression level of non-classical HLA is much lower and HLA-G and HLA-F are expressed differentially among cell types (16,17).

All HLA proteins differ in their ability to present certain peptides because of differences in the peptide binding groove which discriminate peptide size and anchor different residue of the peptide chain (18). At homeostasis, HLA-E primarily presents peptides derived from the leader sequences of HLA-A/B/C (VMAPRTLIL) and HLA-G (VMAPRTLFL) and therefore HLA-E expression usually correlates with expression of HLA-A/B/C (7,19). The leader sequence is important in trafficking HLA class I to the ER (20). Once there this is trimmed by signal peptidase and signal peptide peptidase and the leader peptide is loaded on to HLA-E in the ER where it then transits to the plasma membrane (7,21). The peptide binding groove of HLA-E supports peptides of 9-11 amino acids in length and primary anchor residues are located at positions 2 (methionine) and 9 (Leucine) (7).

At the surface HLA-E acts to inhibit NK cell activation via engagement with the NKG2A-CD94 heterodimer and signal peptide polymorphisms in HLA class I can determine the level of NK cell inhibition (15,22,23). Under non-homeostatic conditions, HLA-E can present non-canonical peptides, which abrogate NKG2A interactions and stimulate the activating receptor NKG2C-CD94, consequently activating NK cells (23–26). During physiological processes, HLA-E has been shown to protect activated B and T lymphocytes and activated macrophages from NK-mediated clearance (27–30) and HLA-E enables NK-DC crosstalk to prevent off-target effects of an on-going immune response (1).

HLA-E can also act as a ligand for TCRs on CD8+ T cells, particularly in the context of viral infection (31,32). Virus-associated peptides are less stable when bound to HLA-E than canonical HLA-E-binding peptides (26), but during viral infection the large abundance of viral peptides enable loading on to HLA-E, altering the binding motif to enable interactions with TCRs to stimulate a CD8+ anti-viral immune response (33).

The low surface expression of HLA-E is attributable to the limited peptide pool able to stabilise HLA-E in the ER and initiate its transit to the plasma membrane, therefore HLA-E is trapped intracellularly (9). This low surface expression of HLA-E has evolved to enable HLA-E to sense changes in the function of the antigen processing and presentation machinery, for example during inflammation to modulate innate immune responses quickly (34). HLA-E expression is highly influenced by the inflammatory microenvironment. As such, HLA-E has the ability to act as a sensor of the inflammatory environment at levels of signalling cascades and peptide availability resulting in the

modulation of NK cell immune response. For example, IL-27 increases HLA-E expression through STAT1 signalling and this is particularly important on monocytes which subsequently inhibit autologous NK cell function via NKG2A (35) (**Figure 1-2**). In a pro-inflammatory microenvironment enriched with IFNγ as within immunologically 'hot' tumours and during viral infection, activation of the IFNγ receptor leads to STAT1 activation and downstream HLA-E transcription (36). Within the nucleus, STAT1 is dephosphorylated by the TC45 phosphatase (37), enabling its export into the cytoplasm via the nuclear export protein exportin-1 (XPO1) to re-initiate the IL-27 and IFNγ signalling cascades (38). In addition to STAT1 recycling, STAT1 autoregulates its transcription (39), increasing total STAT1 levels by 16-24 hours post IFNγ treatment as shown by western blot (40). Therefore, the translation of de novo STAT1 protein in the cytoplasm may contribute to perpetuating inflammatory signals alongside STAT1 nuclear-cytoplasmic shuttling.

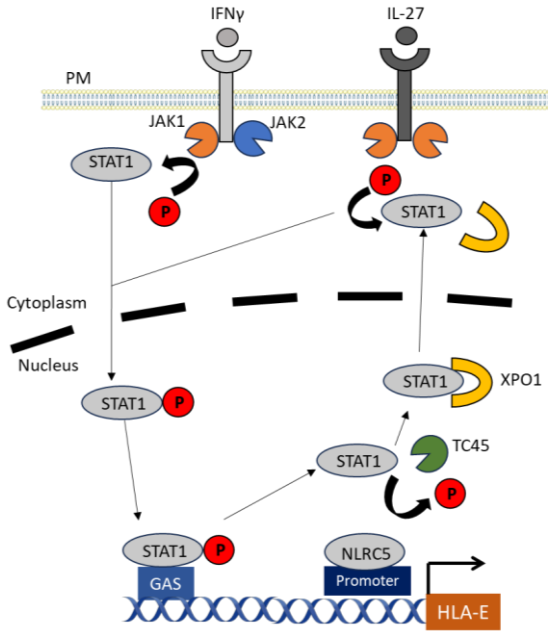


**Figure 1-2: Regulation of HLA-E gene expression by inflammatory signals.**

Activation of the IFNγ and IL-27 receptors activate STAT1 via phosphorylation by JAK1/2 leading to its nuclear translocation. There it binds to the gamma-activated site (GAS) enhancer sequences upstream of HLA-E to enhance HLA-E transcription. STAT1 is then dephosphorylated by the TC45 phosphatase in the nucleus and transported back to the cytoplasm via exportin-1 (XPO1) to re-start the STAT1 activation cycle enabling chronic IL-27 and IFNγ signalling.

### 1.2.3 The role of HLA-E in cancer

Cancer develops from the disruption of multiple cellular processes in healthy cells. As a brief overview, cells acquire genetic abnormalities overtime that induces genetic instability, enhances proliferation, increases resistance to apoptosis and protects from immune destruction. Collectively this is referred to as the hallmarks of cancer (41). Immune evasion can occur via many mechanisms such as cancer cell secretion of anti-inflammatory molecules such as IL-10 and TGFβ, through the upregulation of inhibitory immune cell ligands (such as PD-L1) and via the downregulation of classical HLA class I to avoid T cell activation (42).

Although HLA class I downregulation enables cancer cells to evade CD8+ T cell immunity, NK cells are activated by loss of inhibitory HLA class I on target cells as explained by the missing-self hypothesis (**Figure 1-3**). Therefore, evasion from T cells renders cancer cells susceptible to NK cell activation. In order to escape NK cell-mediated immunity, cancer cells develop further mechanisms such as shedding of NK cell activating ligands and upregulation of non-classical HLA class I molecules, for example HLA-E (43,44). The presence of IFNγ in the TME is a well described mechanism for HLA-E upregulation (**Figure 1-2**). Even when classical HLA class I is downregulated, HLA-E can still be overexpressed as shown with immunohistochemistry of ovarian carcinoma samples (45,46). However, this study did not identify the mechanism for HLA-E expression in the absence/reduced pool of class I leader sequences, most likely stress-associated peptides are being presented by HLA-E in this context (24,26). In a recent *in vivo* CRISPR screen to investigate the mechanisms of immune resistance in tumours, loss of IFNγ signalling sensitised tumours to immune destruction, and indeed in melanoma and renal cell carcinoma patients, IFNγ signature correlated with worse response to checkpoint therapy and correlated with HLA-E expression (47).

Through the upregulation of HLA-E, cancer cells inhibit NK cell function via NKG2A and multiple reports have noted HLA-E and NKG2A upregulation across many haematological cancers including chronic lymphocytic leukaemia (48,49), multiple myeloma (50,51), acute myeloid leukaemia (52) and many solid tumours: renal carcinoma (53), glioblastoma (54), sarcomas (55), non-small cell lung cancer (56) and bladder cancer (57). This upregulation correlates with worse outcome and in acute lymphoblastic leukaemia (ALL), HLA-E is a determinant for disease monitoring after HSC transplantation such that low, but tolerogenic levels on ALL cells protect them from NK cell deletion (58).

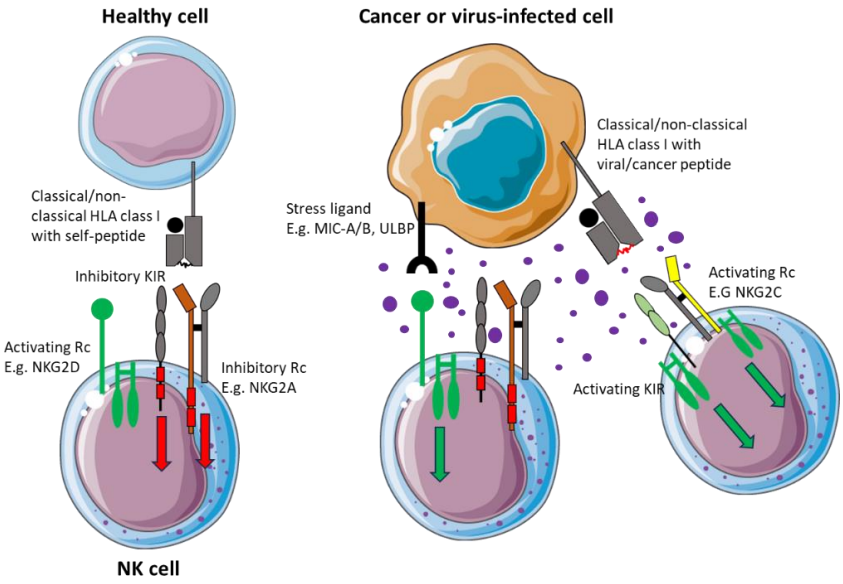


**Figure 1-3: The missing self-hypothesis of NK cells activation.**

Healthy cells present self-peptides on classical HLA class I molecules (HLA-A/B/C) to inhibitory KIR and on non-classical HLA class I (e.g. HLA-E) to inhibitory NK cell receptors (e.g. NKG2A-CD94 heterodimer). These NK cell receptors signal via ITIM domains (red boxes) to inhibit NK cell activation (red arrows) and protect healthy cells from NK-mediated lysis. During oncogenic transformation or viral infection, HLA class I protein expression is downregulated preventing the activation of inhibitory KIR and inhibitory NK cell receptors. Alongside this, expression of stress-associated ligands stimulates activating NK receptors (e.g. NKG2D) culminating in NK cell activation via signalling of adapter proteins FcγR, CD3ζ and DAP10/12 (green). HLA class I can also present virus/stress-derived peptides to activating KIR and activating receptors (e.g. NKG2C-CD94 heterodimer) to activate NK cell release of cytotoxic granules and inflammatory cytokines and chemokines.

The two allelic variants of HLA-E also hold prognostic value and this is independent of their structure and the peptides that are presented by both allotypes since their structure and peptide repertoires are the same (14,59). The difference lies in their peptide binding groove affinity for peptides. The HLA-E*0103 variant has a higher affinity for peptides (14,59) which, as described in **Figure 1-1**, results in increased plasma membrane stability and improved intracellular transport efficiency. As a result, it is more highly expressed on cells compared to the HLA-E*0101 variant (14,59) and this has consequences on signalling downstream of NKG2A and NKG2C (23). As such, patients with aggressive B-cell lymphoma either homozygous or heterozygous for the HLA-E*0103 allele have a less favourable treatment outcome compared to HLA-E*0101 homozygous patients (60). For solid cancer few studies have investigated HLA-E variants and outcome, but research in head and neck cancer and ovarian cancer revealed a higher representation of the HLA-E*01:03 variant in patients, suggesting a role for HLA-E:NKG2A interaction in the development of these cancers (61,62). Interestingly, allelic

variants of the HLA-B leader sequence presented by HLA-E have been found to correlate with improved survival in bladder cancer, such that the 21-MT variant improves patient outcomes (63). This is potentially due to enhanced NK cell education via NKG2A of HLA-B 21-MT patients and these individuals also had improved outcome in AML (64).

Furthermore, the HLA-E hold prognostic value in the susceptibility to and resolution of COVID-19 infection. HLA-E*0101 homozygosity confers protection from COVID-19 infection and HLA-E*0103 homozygous individuals are more susceptible to severe disease (65). Therefore, not only in cancer but also viral infection HLA-E alleles determine disease and treatment outcomes. It could be speculated that this association of the HLA-E*0103 variant in B-cell lymphoma and COVID-19 infection is due to increased resistance from NK-mediated immunity via increased HLA-E:NKG2A interactions given that higher HLA-E expression inhibits NK cell activation more potently (17).

During oncogenesis in which cells are stressed from tonic oncogenic signalling and DNA damage, cellular senescence can be induced (66). The process of cellular senescence involves cell cycle arrest and activation and recruitment of the immune system via IL-6 and IL-8 to clear senescent cells by macrophage phagocytosis and NK cell-mediated lysis (67). However, senescent cells can escape immune activation and HLA-E:NKG2A interactions play an important role in this immune escape process. Senescent cells upregulate HLA-E via pro-inflammatory cytokines as a result of the senescence-associated secretory phenotype (SASP) and this facilitates protection from NK and CD8+ T cell immune destruction (68). The SASP has also been shown to induce HLA-E expression on senescent hepatocytes in mice which impair NKG2A+ NK cell function (69). As a result, the SASP phenotype can confer protection of tumour cells and senescent cells during oncogenesis from NKG2A+ immune cells via HLA-E upregulation.

## 1.3 Human NK cell development, maturation, education and function

### 1.3.1 The development and maturation of NK cells

Common lymphoid progenitors (CLP) have the potential to commit to the B cell, T cell or NK cell lineage. Commitment to the NK cell lineage is defined by CD122 (IL-2Rβ) surface expression, giving rise to NK cell progenitors (NKP) (70). The final step from immature NK cell to mature NK cell is the appearance of CD56, which is initially expressed at a high-level allowing identification of a $CD56^{bright}$ NK cell population. The majority of $CD56^{bright}$ NK cells (>90%) downregulate CD56 producing another major NK cell population found in the circulation, $CD56^{dim}$ NK cells (70). Within tissues however, the proportion of $CD56^{bright}$ and $CD56^{dim}$ NK cells differ for example in the liver >50% of NK cells are $CD56^{bright}$ (71).

Multiple cytokines are essential for orchestrating NK cell maturation. IL-7, stem cell factor (SCF) and FLT-3L are crucial for differentiation of HSCs and CLPs to early NKP (72). Lymphotoxin then contributes to early-stage NK cell development as mice knockout for lymphotoxin receptors do not support NK cell differentiation (73). IL-15 can partially rescue NK cell numbers in lymphotoxin knockout mice, but ablation of the IL-15, the IL-15 receptor or the common γ chain receptor abolish NK cell differentiation, highlighting the crucial role of IL-15 to NK cell development (73,74). From NKPs to terminally differentiated CD57+ NK cells, IL-15 plays a crucial role and in addition to this, IL-15 enables continued NK cell expansion *in vivo* and *in vitro* and supports cell survival via activation of STAT3 and STAT5 (72).

There are also cytokines that impede NK cell maturation and function. TGFβ is the best described cytokine which signals to phosphorylate smad2/3 which then binds to smad4 to inhibit NK cell maturation by reducing levels of granzyme B and IFNγ and impairing IL-15 signalling reducing NK cell proliferation (75,76).

Multiple transcription factors work sequentially and in unison during the NK cell maturation process in concert with the cytokine milieu. NK cell lineage commitment is regulated by E4BP4, TOX and ID2 and NK cell maturation is governed by ID-2, T-bet and Eomes (72). E4BP4 is crucially important for CLP to NKP differentiation as knockout in mice accumulate CLPs in the bone marrow and lack NKP cells (77,78). The latter group of transcription factors are important for expression of effector molecules, chemokine receptors and maturation markers in maturing NK cells.

$CD56^{dim}$ and $CD56^{bright}$ NK cells generally have opposite, but not mutually exclusive, immune functions. $CD56^{dim}$ NK cells are highly cytotoxic and are positive for CD16a (FcγRIIIa) endowing these cells with ADCC capabilities (79). In contrast, $CD56^{bright}$ NK cells are considered more immunoregulatory with high expression of inhibitory receptor NKG2A; able to produce and secrete

large quantities of cytokines and proliferate strongly (80). NKG2A is the first HLA-specific receptor expressed during maturation with the acquisition of KIRs at the latter stages of differentiation (81). The acquisition of multiple KIRs correlates with loss of NKG2A such that mature NK cells express KIR or NKG2A, although a small circulating population express both (82,83). Complete maturation is marked by expression of CD57 and these terminally differentiated NK cells have the highest cytotoxic capacity with high CD16a expression, but limited proliferative capabilities (84).

Circulating NK cells comprise ~5-20% of total peripheral blood mononuclear cells (PBMC), and of these NK cells, >90% are $CD56^{dim}$ (85). $CD56^{bright}$ NK cells mainly reside in secondary lymphoid tissue, and there are mounting observations of tissue-resident NK cells, which display unique tissue-specific markers and are developmentally less mature as a result of the local tissue microenvironment (86). Many unknowns remain about tissue-resident NK cells such as their transcriptional control, differentiation and plasticity (86).

Mounting evidence suggests that NK cells possess memory-like traits of long-term persistence and a trained response to repeat stimulation (87). Memory NK cells have been mostly studied in setting of CMV infection in which activated and expanded NK cells in infected mice lyse after the infection has cleared, but some NK cells develop into memory cells (87,88). Upon re-infection, these memory NK cells are capable of being activated again more quickly, producing a stronger immune response and protecting mice from infection and cancer. In humans, memory NK cells are marked by NKG2C expression and these cells are expanded and persist after CMV infection and show stronger immune responses and increased maturation upon CMV re-inoculation (89,90). A key area of current research is investigating which transcription factors regulate memory NK cell formation (91), but it is known that memory NK cells exist in a primed state possessing a more open chromatin and an epigenetic profile at key activation genes that enable a fast immune response (92,93).

Additionally, a recent paper describing NK cells in terms of gene expression and chromatin landscape rather than surface marker expression unravelled the existence of three major NK cell populations: NK1, NK2 and NK3 in human blood (94). The significance of this study could pave the way for re-evaluating the nomenclature of NK cells away from the current $CD56^{dim}$ and $CD56^{bright}$ description. NK1 cells were shown to be primed for cytotoxic functions and NK2 and NK3 cells possessed an immunoregulatory phenotype with tissue remodelling and chemotaxis properties.

### 1.3.2 NK cell education and licensing

Before NK cells become functionally competent and tolerant of self-tissue, NK cells undergo a process of education/licensing whereby NK cells adapt to the host. NK licensing/education and maturation/differentiation described above act in parallel, but their effects on NK cell function are mutually exclusive (81).

The process of NK cell education involves engagement of self-MHC class I with specific inhibitory receptors on NK cells, but education can also involve non-classical MHC class I-dependent and MHC class I-independent mechanisms (95). There are multiple theories of NK cell education/licensing. One is the arming model in which the engagement of inhibitory receptors with MHC ligands arms NK cells with effector functions (96). Another is the disarming theory in which activating signals in a developing NK cell result in NK cell hypo-responsiveness unless inhibitory signals are integrated into the cascade (97). Both types of education may contribute to NK cell licensing, which is not an all-or-nothing outcome, but a fine-tuning process. It was shown that increases in inhibitory receptor engagement results in NK cells with more potent effector functions (98), giving rise to a rheostat model of NK cell education. As such, a poorly educated NK cell will still possess effector functions, but it will need a greater stimulus in order to carry out target cell killing (81).

As described above, failure to educate NK cells does not result in autoreactivity (there is no evidence of NK-dependent autoimmunity), but in hypo-responsiveness towards infected and malignant cells and activating stimuli. Mice which are deficient in MHC expression possess NK cells that are unresponsive to self-tissue and not alloreactive (96,99,100). The same is true when inhibitory NK cell receptors Ly49 (mouse KIR equivalent) and NKG2A are deleted, NK cell degranulation and production of IFNγ are greatly impaired (101). NKG2A is particularly important in the education of uterine NK cells. Genetic ablation of NKG2A results in birth abnormalities in mice and dimorphisms in the HLA-B leader peptide in women results in poor NKG2A licensing and increased risk of pregnancy-related problems including pre-eclampsia (102). Furthermore, impairing ITIMs on mouse inhibitory NK cell receptors (103) and deleting downstream inhibitory phosphatases SHP-1 and SHP-2 (Src homology region 2 domain-containing phosphatase) (104) specifically in NK cells results in NK cell hypo-responsiveness, demonstrating that inhibitory receptor signalling during NK cell licensing is crucial for generating functional NK cells. Recently, it was shown that SHP-1 acts as a rheostat to fine tune the NK cell immune response. SHP-1 protein levels may be determined during the education process such that educated NK cells develop low levels of SHP-1 through KIR and NKG2A interactions with self-ligands which then endows educated NK cells with high cytotoxic potential (105). Therefore, in order to generate functionally competent NK cells, developing NK cells require a process of licensing to fine-tune inhibitory and activating receptor signalling to orchestrate effective immune responses when required.

To summarise NK cell maturation and education, maturation produces NK cells with different functional capacities and can be described by maturation marker expression. For example, CD57 marks mature NK cells with high cytotoxic capacity and low proliferative potential, whereas NKG2A marks immature NK cells with cytokine secreting phenotypes and high proliferative potential, and this is consistent across individuals (81,84). Education, however, produces functionally competent NK cells such that an uneducated NK cell or an NK cell without expression of KIR or NKG2A is functionally

incompetent (101,104). Mature NK cells possess at least one self-reactive receptor so that autoreactive immune responses are avoided (96). Between human individuals and murine specimens, the level of NK cell education differs resulting in donors with variable NK cell functionality (105).

One important aspect to consider with cancer treatment targeting NK cell receptors, in particular anti-KIR and anti-NKG2A antibodies, is the impact on NK cell education. Education is a continuous process in tissues, including tumours, and it has been shown in mice that NK cell infiltrates into MHC-I deficient tumours become anergic as opposed to cytotoxic (106,107). This highlights that protection from NK cells can be conferred through loss of MHC-I expression such that an NK cell undergoing licensing in the tumour becomes anergic to cancer cells. Through using anti-KIR and anti-NKG2A antibodies, there is the potential of inducing NK cell anergy towards tumours through impairing the NK cell education process, therefore treatment regimens may have to account for this for example through low dose administration or drug holidays to allow for NK cells to be educated in the TME.

### 1.3.3 The immunological synapse and the cytotoxic functions of NK cells

Immunosurveillance is one of the main functions of NK cells in which NK cells survey the environment to identify transformed tumour cells or cells infected with intracellular pathogens (108–110). This process is well described by the missing self-hypothesis (**Figure 1-3**) (111,112). On encountering a healthy cell the engagement of HLA class I and HLA-E with inhibitory KIRs and NKG2A, respectively, in addition to the absence of activating ligands on healthy cells results in immune tolerance. During oncogenic transformation, for example, the downregulation of HLA class I (to evade T cell immunity) and increase in stress ligand expression result in NK cell activation leading to lysis of the target cell (**Figure 1-3**). In parallel, HLA class I can present peptides which are recognised by activating KIRs (113) (**Figure 1-3**). This is also true for HLA-E in which stress-derived peptides bound to HLA-E abrogate NKG2A interactions and stimulate NKG2C activation (26).

NK cells induce lysis of target cells via two main mechanisms: the release of cytotoxic granules in a process called degranulation and by activation of death receptor signalling in target cells. During degranulation toxic granules containing perforin and granzyme B are released at the immunological synapse. The NK cell cytotoxic immunological synapse is divided into three stages: initiation, effector and termination. Initiation involves tethering and increasing strength of adhesion to enable effective receptor clustering and signalling (114). NK cells are sensitive to tension and the stiffness of target cells, potentially due to the stabilisation of the immunological synapse (115). The effector stage is marked by microtubule polarisation and actin accumulation at the synaptic membrane to form the supramolecular activation cluster (SMAC) which consists of peripheral (pSMAC) and central (cSMAC) zones, and these allow for strong adhesion and directed granule release, respectively (114) (**Figure**

**1-4**). At activating receptor clusters, the adaptor proteins DAP10/12 are recruited which subsequently recruit downstream effector proteins including SRC family kinases, ZAP70, SYK and VAV1. These proteins are activated by phosphorylation and potentiate the signalling cascade ultimately activating the transcription factors ERK, NK-κB and NFAT to stimulate the expression of effector NK cell molecules including perforin, granzyme B and IFNγ (116). ERK also enhances NK cell survival and proliferation through the activation of IL-2 transcription and Myc and cyclin activation (117). The activating signalling cascades also increase the cytosolic concentration of calcium which stimulates the release of cytotoxic granules which are directed along actin filaments to the SMAC. The directed granule release ensures efficient target cell killing and negation of bystander cell death and autolysis of NK cells (118). Finally, termination involves the downregulation of activating receptors at the synapse and detachment from the target cell via actin destabilisation. After termination NK cells re-stock cytotoxic granules and re-express activating receptors to enable serial killing (114).

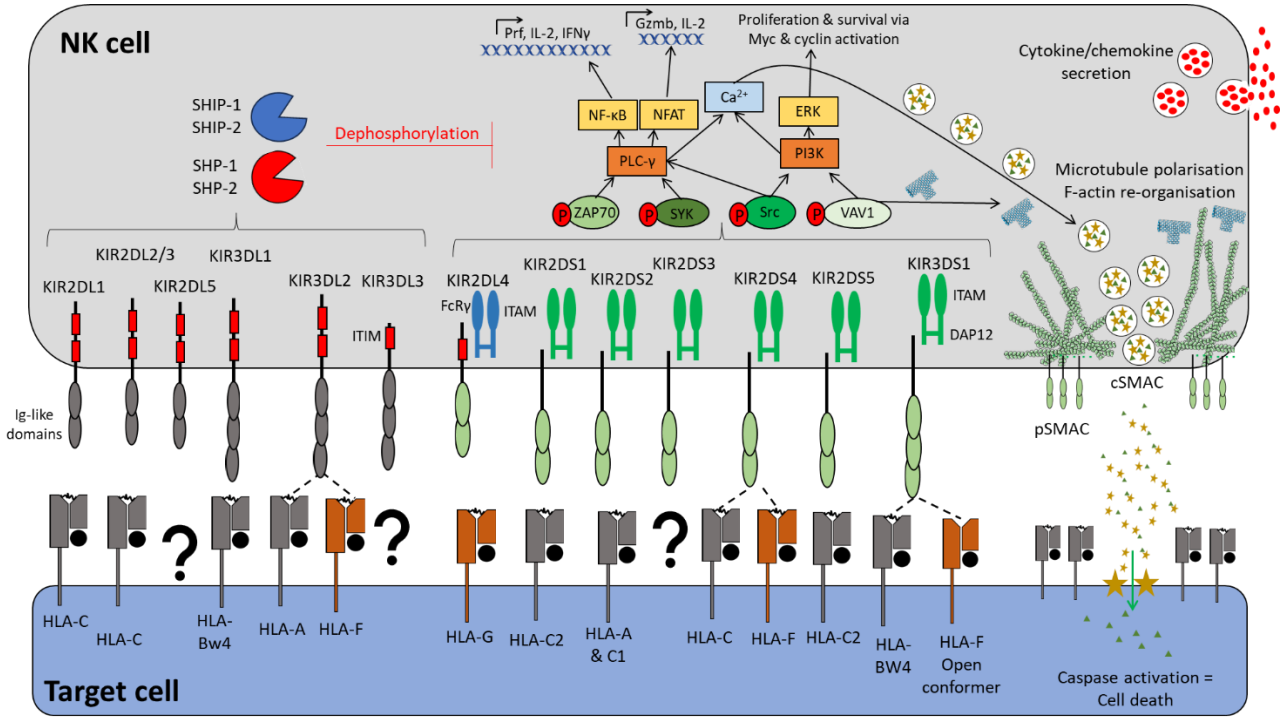


**Figure 1-4: NK cell activating and inhibitory receptor signalling cascades.**

Killer cell immunoglobulin-like receptors (KIR) contain either two or three Ig-like domains that interact with HLA class I proteins loaded with peptides. The intracellular domains of inhibitor KIR possess ITIM domains which activate SHP-1/-2 and SHIP-1/-2 phosphatases that dephosphorylate, and therefore deactivate, signalling proteins downstream of activating KIR. Upon ligation of activating KIR with HLA class I, DAP12 (or FcRγ for KIR2DL4) is recruited which contains ITAM domains which are phosphorylated in order to recruit downstream activating proteins for example SRC family kinases, ZAP70, SYK and VAV1 which are themselves phosphorylated. These proteins propagate signalling cascades via MAPK, PLC-γ and PI3K to activate transcription factors such as NF-κB, NFAT and ERK which stimulate the expression of NK cell effector molecules such as perforin, granzyme B (Gzmb) and IFNγ. Proteins involved in NK cell survival and proliferation also become activated. The GTP exchange factor VAV1 is also involved in the polarisation of microtubules and the reorganisation and accumulation of F-actin to form and stabilise the NK cell immunological synapse referred to as the SMAC. The SMAC is made up of peripheral (pSMAC) and central zones (cSMAC) and this is the site of activating receptor clustering, adapter protein activation and cytotoxic granule recruitment and release. Activated NK cells also secrete pro-inflammatory cytokines and chemokines to orchestrate innate and adaptive immunity and these molecules are secreted away from the immunological synapse to enable diffusion into the microenvironment. Broad HLA ligands for KIRs are shown with HLA-C allotype 1 and 2 marked as HLA-C1 and HLA-C2, respectively.

Within granules the acidic pH inactivates perforin, but once released into the neutral environment of the immunological synapse, perforin monomers oligomerise and form pores in the plasma membrane of target cells. These pores allow granzyme B, which is also released from cytotoxic granules, to transit into targets and induce lysis via cleavage of multiple targets including the effector caspase-3 and mitochondrial apoptotic regulators such as Bid which results in cytochrome C leakage and apoptosome formation (119,120) (**Figure 1-5**). Executioner caspase-3 and the apoptosome lead to cell lysis via cleavage of enzymes involved in DNA fragmentation such as ICAD and degradation of the proteasome and transcription factors involved in cell survival and differentiation (121).

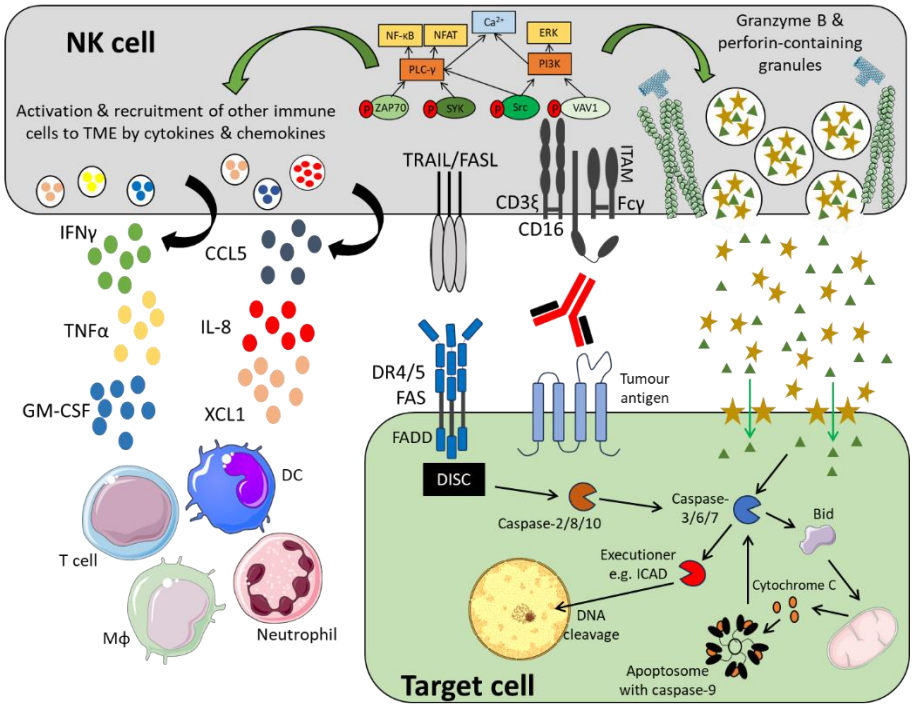


**Figure 1-5: General immune functions of NK cells and death receptor pathways in target cells.**

NK cells can induce direct lysis of target cells (cancer or infected cells) via death receptor activation and release of cytotoxic granules which contain perforin and granzyme B. Perforin forms pores in the membrane of targets to enable transit of granzyme B into target cells to initiate apoptosis via cleavage of executioner caspases-3/6/7. These caspases cleave bid which initiates cytochrome c release from mitochondria and subsequent apoptosome formation with caspase-9 which cleaves further executioner caspases. Apoptotic executioner proteins are cleaved by capsase-3/6/7 such as ICAD which transits to the nucleus to digest chromatin. Upon engagement of TRAIL and FASL on NK cells with DR4/5 and FAS on target cells, respectively, the Fas-associated death domain (FADD) recruits adapter proteins to form the death-inducing signalling complex (DISC). The DISC then activates adapter caspases-2/8/10 which cleave the executioner caspases-3/6/7. CD16a (FcRγIIIa) expression on NK cells enables antibody-dependent cellular cytotoxicity (ADCC) when target cells are opsonised with antibodies. CD16a signals via the ITAM-containing adapter proteins FcγR and CD3ζ to activate NK cells. Upon activation, NK cells recruit and activate innate and adaptive immune cells through the secretion of pro-inflammatory cytokines and chemokines.

NK cells are protected from granzymes and perforin-mediated autolysis by numerous other mechanisms. The fusion of exosomes with the plasma membrane during granule release temporarily places lysosome-associated membrane protein-1 (LAMP-1/CD107a) at the plasma membrane which offers protection from degranulation-suicide due to the heavy, negatively charged glycosylation of LAMP-1 which inhibits perforin (122). A high density of lipids at the synapse along with the negatively charged lipid phosphatidylserine on the outer surface of the lipid bilayer also inactivate perforin to shield NK cells from autolysis (123). High levels of the granzyme B inhibitor serpin B9 is expressed by NK cells which protects from autolysis (124).

Equally important is the establishment of an inhibitory NK cell synapse. Inhibitory receptors on NK cells bind to MHC class I ligands to activate SHP-1/2 and SHIP-1/2 (Src homology 2 domain containing inositol polyphosphate 5-phosphatase 1) phosphatases and this complex is called the supramolecular inhibitory cluster (SMIC) (114). Phosphatases from the SMIC de-phosphorylate proteins downstream of activating receptors and impede F-actin formation at the SMAC via de-phosphorylation of F-actin re-modellers including VAV1 (125,126) (**Figure 1-4**). To activate an NK cell, SMIC formation is impaired alongside the formation of the SMAC. To disrupt the SMIC, peptides on MHC class I with low affinity for inhibitory NK cell receptors stall SMIC formation by impeding strong, stable interactions resulting in reduced levels of SHP activation (127). Additionally, the colocalisation of inhibitory and activating receptors that are engaged with their cognate ligands can determine the activation status of NK cells, such that the closer the receptors the greater the level of inhibition (128). In addition to this, the size of receptor-ligand interactions also plays a crucial role in regulating NK cell activation, such that increased length of ligand-receptor pairs reduces the activating/inhibitory effect of receptors (129,130). This aligns with the kinetic-segregation model where molecules with large ectodomains are excluded from the immunological synapse in favour of small ligand-receptor interactions to promote receptor signal integration to either induce immune activation or inhibition. How NKG2A:HLA-E interactions impact synapse integrity, size and shape remains to be investigated, but NKG2A engagement is known to abolish actin polymerisation and exclude lipid raft formation at the synapse (site of activating receptor clustering) (125,131).

The second method of killing involves the ligation of TRAIL and FASL on NK cells with death receptors DR4 and DR5, and FAS on targets, respectively (**Figure 1-5**). Death receptor activation results in the formation of a death-inducing signalling complex (DISC) and the Fas-associated death domain (FADD) on the intracellular tails of death receptors. The recruitment and activation of initiator caspase-8 leads to the activation of executioner caspases including casapase-3 to mediate apoptosis (132).

Degranulation and death-receptor signalling work in unison to lyse target cells (133), although a single degranulation event has been shown to be sufficient to lyse a target cell (134). During serial killing, NK cells switch between killing methods using degranulation for early events and death

receptor-mediated killing at later stages (135). CD107a expression, the marker for cytotoxic granule release, correlates with TRAIL and FAS expression, which enable NK cells to switch killing methods from granzyme B to death receptor pathways (135). The production of IFNs also induce TRAIL expression which my contribute to the switch in killing methods (136). Interestingly, cancers can express decoy receptors (Dc1 and Dc2) which engage with TRAIL to prevent apoptosis as these do not contain a FADD. A mechanism by which NK cells circumvent decoy receptors is by TRAIL potentially facilitating activating signals in NK cells leading to enhanced production of granzyme B and increased degranulation and IFNγ production (137,138), although the mechanism behind this remains to be determined since TRAIL possesses no signalling capacity. Together, both granzyme-B mediated and death receptor-mediated killing mechanisms work in unison to ensure efficient killing of target cells.

### 1.3.4 Secretion of cytokines and chemokines

As well as direct lysis of target cells, NK cells produce a plethora of chemokines and cytokines to stimulate the recruitment of and activation of innate and adaptive immune cells. As quick responders of inflammation NK cells are readily poised to transcribe cytokines quickly due to the open configuration of chromatin (139). Key proinflammatory cytokines include IFNγ, TNFα and GM-CSF and well-studied chemokines include CCL1-5 and CXCL8 (140) (**Figure 1-5**). These cytokines skew the CD4+ T helper cell response towards a Th1 phenotype, polarise macrophages towards an M1 phenotype and aid DC maturation to enhance antigen presentation to T cells (140). IFNγ-producing NK cells have been recently identified as a key orchestrator of anti-tumour T cell immunity through remodelling of the TME (141).

Similar to perforin and granzymes, cytokines are stored in secretory granules which are readily released after NK cell stimulation (142). However, the secretion of cytokines and chemokines is different to cytotoxic granule release which takes place at the immunological synapse close to the plasma membrane of target cells. Cytokines and chemokines are secreted away from the immunological synapse to enable efficient release into the microenvironment to modulate the function of and recruit further immune cells into the inflamed site (142) (**Figure 1-4**) For example, NK cell secretion of CCL5, XCL1 and XCL2 recruit DCs to the tumour microenvironment and induce DC differentiation and this has been shown to promote tumour regression in mouse models of melanoma (143). As well as IFNγ playing important roles in promoting macrophage phagocytosis and T cell polarisation, IFNγ enhances HLA class I expression on antigen presenting cells and target cells, including tumours, to promote antigen presentation to CD8+ T cells. The increase in HLA class I expression however, dampens NK cell function via inhibitory KIR and NKG2A activation (144,145).

Another function of NK cells which is becoming increasingly understood is their role in dampening inflammation. This is important when inflammation is not further needed once infections and

transformed cells are cleared. This is achieved via the secretion of immunomodulatory cytokines such as IL-10 and direct cytotoxicity towards effector T cells, mature macrophages and DCs (28–30,146–148).

### 1.3.5 ADCC

Another important activating receptor expressed by NK cells is CD16a (FcγRIIIa) which enables NK cells to partake in humoral immunity (**Figure 1-5**). This provides NK cells with an antigen-specific modality whereby NK cells are activated against a specific antigen. CD16a binds IgG1 antibodies (149), therefore IgG1 antibodies that opsonise a cell can activate NK cells via CD16a engagement to the Fc region of IgG1. CD16a signals via the adapter proteins CD3ζ and Fcγ which possess ITAMs to recruit downstream signal transducers as outlined in **Figure 1-5** to induce degranulation of cytotoxic granules and secretion of cytokines and chemokines. There are two alleles of CD16a with a single amino acid substitution at position 158 of phenylalanine (F158) to valine (V158) (150). The valine allele confers stronger binding to IgG1 (and IgG3) and transduces stronger activating signals into NK cells leading to enhanced ADCC (150). Compared to other Fc receptors such as CD16b, CD32a/b and CD64, CD16a has a low-intermediate affinity for IgG1 (151). Compared to other IgG isotypes IgG3 has the highest affinity for CD16a followed by IgG1 > IgG4 > IgG2 (151). Besides ADCC, NK cells can indirectly boost other forms of antibody-mediated immune responses such as antibody-dependent cellular phagocytosis (ADCP). NK cell secretion of CCL3/4/5 and IFNγ promote macrophage infiltration and activation and in the presence of anti-CD20 mAbs enhance macrophage phagocytosis of B-cell lymphomas (152).

### 1.3.6 Adaptive/memory NK cells

Although NK cells are classically described as innate effector cells of the innate immune system, evidence is emerging of an adaptive, memory-like NK cell population (153). These possess phenotypic, functional and epigenetic differences compared to other NK cell populations and can persist after hantavirus infection in humans for more than two months (154). In viral experiments in mice, re-exposure to the infectious agents induces a rapid response by adaptive NK cells which are able to produce larger quantities of cytokines, are highly cytotoxic and are able to protect naïve mice from primary infection (87,155). The promoter region of IFNγ is hypomethylated in adaptive NK, endowing them with a high capacity to produce IFNγ (156). In humans, a similar adaptive NK cell population has been reported in HCMV-infected individuals marked by high NKG2C expression (153). Cytokine-induced memory (CIML) NK cells can be induced by incubation with IL-12, IL-15 and IL-18 and these NK cells have shown increased persistence, expansion and activation in *in vitro* and *in vivo* models of cancer (157,158).

## 1.4 Receptors regulating NK cell activity.

As depicted in **Figure 1-4**, NK cell activation is governed by the integration of signals derived from inhibitory and activating receptors. NK cell receptors are germ-line-encoded and do not undergo gene rearrangement like TCRs and BCRs. As such NK cell receptors are not antigen specific and this allows for a rapid NK cell immune response. Not all receptors are expressed by any one NK cell, therefore NK cell subpopulations exist with differentially expressed receptor profiles (159).

Studying NK receptor functions and signalling usually involves the use of the B-cell leukemic cell line 721 which was derived from the PBMC of a healthy individual and transformed with Epstein-Barr virus (160). From the parental 721 cell line generations of cells were generated including 721.221 which is knock out for HLA class I genes and 721.174 which is deficient in the peptide protein exporter TAP (161). As such 721.221 and 721.174 cell lines do not express HLA class I proteins. By transduction of specific HLA genes or delivery of peptides in the cell media and subsequent co-culture with NK cells, ligand-receptor interactions can be examined.

### 1.4.1 Killer cell immunoglobulin-like receptors (KIR)

#### 1.4.1.1 Inhibitory KIR

KIRs represent a major family of inhibitory receptors which recognise peptide-loaded HLA class I molecules. KIRs do not undergo rearrangement unlike TCRs and BCRs, thus are germline encoded. Similar to CD8+ TCRs which bind the top of HLA class I molecules on the α1 and α2 domains, KIRs bind the top of HLA molecules making contact with the presented peptide at the C-terminus end (162) and KIR specificity for HLA is determined by polymorphisms in the α1 domain (163). Although KIR contact the presented peptide on HLA molecules, KIR recognise HLA-peptide complexes by a motif-based mechanism, in contrast to the restricted peptide specificity of TCR:HLA class I interactions, enabling the recognition of multiple peptides by KIR (164). In terms of peptide recognition, slight changes in the amino acid sequence can alter the recognition motif and therefore modulate KIR binding (165). As such, the peptide repertoire contains peptides that strongly inhibit and weakly inhibit NK cell functions through differences in KIR affinity for the peptide MHC complex (165). As a result of this, KIR genes that are differentially expressed among the population can confer protection to infectious diseases based on engagement of KIR with the peptide repertoire presented by HLA class I.

In humans, inhibitory KIRs contain long cytoplasmic tails, four with two Ig-like extracellular domains (KIR2DL1-3 and KIR2DL5) and three with three Ig-like extracellular domains (KIR3DL1-3) (166) (**Figure 1-4**). ITIM motifs on the intracellular domain of KIRs transduce inhibitory signals via SHP-1/-2 and SHIP-1/-2 phosphatases that target effector proteins downstream of activating NK cell receptors to

inhibit NK cell activation (**Figure 1-4**) (167,168). Mechanistically, SHP-1/-2 and SHIP-1/-2 contain Src homology 2 (SH2) domains that recognise phosphorylated tyrosine on target proteins including activators of NK cells such as SYK and VAV1 (**Figure 1-4**). Inhibitory receptors binding non-classical HLA class I molecules (HLA-F/G) have also been identified, such as KIR2DL4:HLA-G and KIR3DL2:HLA-F (**Figure 1-4**).

#### 1.4.1.2 Activating KIR

Alongside inhibitory KIRs NK cell express activating KIRs. Like inhibitory KIRs, activating KIRs contain either two (KIR2DS1-5 and KIR2DL4) or three (KIR3DS1) Ig-like domains. However, activating KIRs contain a short cytoplasmic tail and possess positively charged amino acids in their transmembrane domains (lysine or arginine) that facilitate interactions with DAP12 (or FcRγ for KIR2DL4) (169). These adapter proteins contain ITAM motifs to transmit activating signals via phosphorylation of ZAP70, Syk and Vav1 (**Figure 1-4**). Similar to inhibitory KIRs, activating KIRs recognise HLA class I proteins, but with lower affinity due to amino acid differences in the HLA-binding domain which has evolved for inflammatory settings in which HLA class I is highly expressed (113). Activating KIR recognise HLA by self-altered or non-self-peptides loaded onto the HLA binding groove and by open HLA conformers lacking peptides within the binding groove (170). The peptides recognised by KIR include self-peptides for self-tolerance and NK cell education, viral-associated peptides and tumour-associated peptides. Most work has addressed KIR recognition in the context of viral infection (17), but increasing evidence suggests a role for KIR recognition of cancer-associated antigens (171–173).

However, the difficulty identifying peptide ligands for activating KIR is the high sequence homology between different KIR and the dominating affinity of inhibitory KIR for HLA-peptide loaded complexes. For example, in the ligand binding domain there is a 98% amino acid sequence homology between KIR2DS2 and KIR2DL2/3 all of which bind to HLA-C group 1 allotypes, however KIR2DS2 does not recognise HLA-C group 2 allotypes (174,175). This high sequence homology also makes it difficult to raise antibody clones against specific KIR. Usually, multiple antibody clones are used together to allow identification of specific KIR NK cell populations. This is illustrated by the combination of the antibody clones REA147 (KIR2DL3 and KIR2DL2 specific) and CH-L (KIR2DL3, KIR2DL2 and KIR2DS2 specific) to identify KIR2DS2+ NK cells enabling research into KIR2DS2 receptor function (176). Through using these antibody clones, it is thought that KIR2DS2+ NK cells are primed for activation, even in the absence of a cognate HLA-C ligand (172). In terms of peptides that activate the KIR2DS2 receptor, peptides derived from flaviviruses and hepatitis C virus (HCV) with an AT (alanine-threonine) motif at positions 1 and 2 at the C-terminus end are recognised by KIR2DS2 leading to Vav1 phosphorylation and NK cell activation (174). Recently, it was demonstrated that a cancer-derived peptide from the nuclear export protein exportin-1 (XPO1), which also has an AT motif, can

be recognised by KIR2DS2, demonstrating that KIR2DS2 may have a role in anti-cancer immunity alongside anti-viral immunity (171).

As mentioned earlier, KIRs are germline encoded and KIR genes are organised into two main haplotypes. Group A is characterised by inhibitory KIRs plus KIR2DS4 and group B consists of more activating KIRs (including KIR2DS1-3, KIR2DS5 and KIR3DS1). Because of this variation in gene content, the frequency of activating KIRs between populations vary. This adds additional complexity in the study of activating KIRs since donors possess different KIR NK cell populations. For example KIR2DS2 is present in approximately 50% of Caucasians and therefore specific donors are required to investigate KIR2DS2 function (113). As a result, NK cell subsets with differential activating receptor expression possess different thresholds of activation. For example, KIR2DS2+ NK cells are more readily activated against tumour targets and have enhanced ADCC functions (172,177) which perhaps reflects their association with improved overall survival following cord blood transplantation in acute myeloid leukaemia (178) and with improved outcomes of anti-GD2 mAb therapy in neuroblastoma (179). As such selectively activating specific NK cell populations with antibodies or peptides (173) and exploiting specific KIR NK cell populations in adoptive transfer therapy may improve the efficacy of immunotherapy aimed at promoting NK cell function.

### 1.4.2 NK cell inhibitory receptors

NK cell subsets also express non-HLA-specific inhibitory receptors. Examples include PD-1, CD96 and TIGIT (**Figure 1-6**) (166). These receptors, in particular PD-1, are expressed at a very low levels on resting NK cells, but upon cytokine stimulation are highly expressed (180). Therefore, these receptors are only expressed under specific inflammatory conditions and are important in switching off the NK cell immune response.

HLA class I bind to other receptors expressed by immune cells such as the LILRB(1-5) receptor family, although LILRBs have other non-HLA ligands, expressed on a plethora of immune cell types including NK cells (181). LILRB1 and LILRB5 on NK cells recognise HLA class I and transduce inhibitory signals to prevent NK cell activation. In the context of cancer, NK cells from multiple myeloma and prostate cancer patients express high levels of LILRB1 (182). Recently LILRB1 and 2 have been reported to recognise murine MHC-E irrespective of peptide cargo (34) and this engagement impedes macrophage phagocytosis.

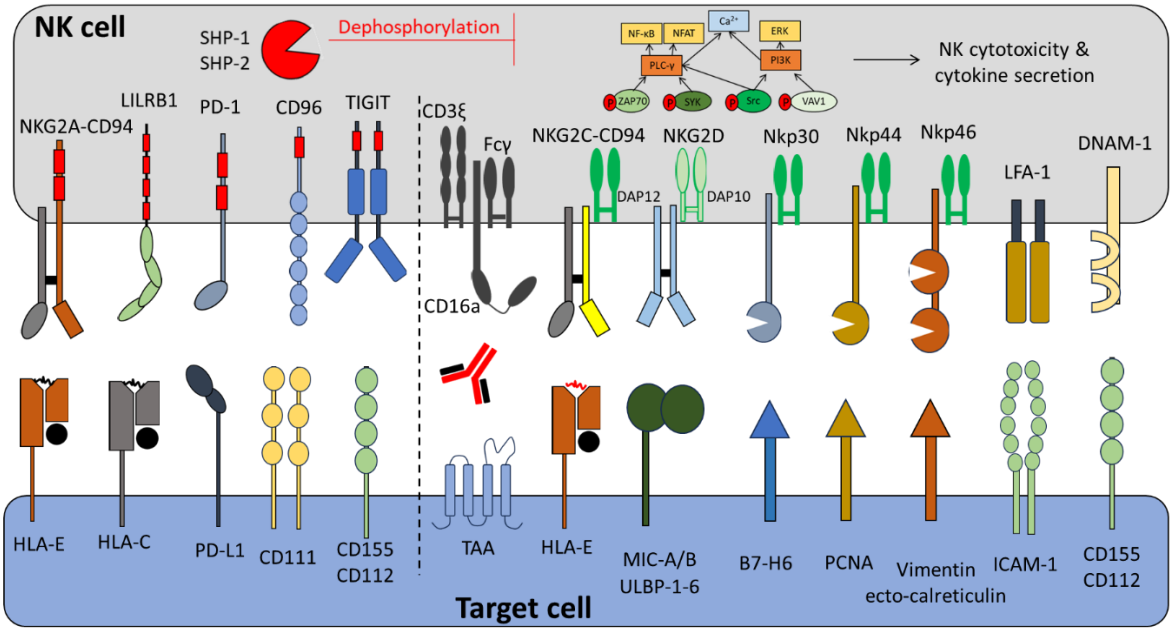


**Figure 1-6: Non-KIR inhibitory and activating NK cell receptors.**

Major NK cell inhibitory and activating receptors expressed by NK cells and their ligands on target cells. Activating receptors associate with ITAM-bearing DAP12 and PI3K-binding DAP10 and upon ligand engagement recruit phosphatases and activating signalling components. CD16a signals via Fcγ and CD3ζ which has multiple ITAM domains to transduce potent activating signals. Red boxes on inhibitory receptors represent ITIM domains.

### 1.4.3 NK cell activating receptors

As described above the activating receptor CD16a (FcγRIIIa) enables NK cells to contribute to humoral immunity by binding to antibody-coated target cells. CD16a engagement with IgG antibodies recruits the ITAM-bearing Fcγ and CD3ζ adapter proteins (149,183). CD3ζ possesses multiple ITAM domains and can therefore transduce strong activating signals and indeed CD16 engagement alone is sufficient to activate NK cells (184) (**Figure 1-6**). Other activating receptors act in parallel to activate NK cells (185). ITAM-bearing DAP-10-associated activating receptors include NKp30, NKp44 are NKp46 which are referred to as natural cytotoxicity receptors that are activated by a plethora of ligands usually expressed by virus-infected and cancerous cells (186). DNAM-1 (CD155 and CD112 binding) and LFA-1 (CD54/ICAM-1 binding) enable strong immunological synapse formation to stabilise the SMAC and can recruit activating proteins via the phosphorylation of the DNAM-1 cytoplasmic tail (187,188). Natural killer Group 2 member D (NKG2D) is another important activating NK cell receptor that has important immunosurveillance functions by recognising MHC-like ligands such as MHC class I-related protein-A/B (MIC-A/B) and UL16-binding proteins (ULBP1-6) that

are upregulated during stress (110). NKG2D associates with the adapter protein DAP10, which does not have an ITAM domain and does not signal via SRC-family kinases, but instead signals via the recruitment of PI3K and VAV1 (189,190). The crucial immunosurveillance role of NKG2D is highlighted by the fact that lymphoma cells deficient in NKG2D ligands promote more aggressive disease in mice (191) and the shedding of these ligands on human CLL cells are important in dampening NK tumour immunosurveillance (49).

TRAIL and FASL expression by NK enable target cell apoptosis through binding to DR4/DR5 and FAS on target cells, respectively. In addition to inducing apoptotic signalling in cancer cells, TRAIL also transmits activating signals into NK cells leading to NK degranulation and production of IFNγ (137,138). TRAIL activation has been shown to promote expression of granzyme B via modulation of the IL-15 signalling pathway (138) and potential activation of the MAPK pathway (137).

### 1.4.4 NKG2A and NKG2C receptors

NKG2A and NKG2C receptors form a heterodimer with CD94 which predominantly acts as a scaffold to interact with the ligand HLA-E (**Figure 1-6**) (15). The signalling component of the heterodimer is determined by NKG2A/C. NKG2A contains two ITIM domains to activate SHP-1/2 to inhibit NK cell activation (**Figure 1-6**) (192), whereas NKG2C associates with the ITAM-containing DAP12 adapter protein to activate NK cell functions (**Figure 1-6**). NKG2A/C expression on NK cells is mutually exclusive (193) and therefore there is no competition for HLA-E on the same cell. NKG2A is encoded by the *Klrc1* gene and NKG2C by *Klrc2*. NKG2A/C not only differ by their intracellular tails, but they also differ in their extracellular domains such that they associate with HLA-E bound to different peptides, being highly selective such that one amino acid change in the presented peptide alters NKG2A/C interactions (194,195). When HLA-E presents canonical HLA class I signal peptides, NKG2C has a much lower affinity for HLA-E (6-fold lower) and therefore NKG2A interactions dominate (195).

The functions of NKG2A/C receptors are very well described because of homologues found in mice that possess the same functions and have the same receptor ligand as humans. In mice HLA-E is referred to as Qa-$1^b$ and Qa-$1^b$ also presents signal peptides derived from MHC class I proteins (196). NKG2A is also highly expressed in the human circulation (~30-60% of peripheral blood NK cells) making it easy to obtain samples and study human NKG2A functions. Besides regulating NK cell activation and inhibition, NKG2A is also important for HLA class I-independent NK cell education as described in section 1.3.2. Loss of NKG2A in mice during NK cell development results in NK cell hypo-responsiveness towards targets such as cancer cells or virally-infected cells both i*n vivo* and *in vitro* (101,104).

In addition to the canonical HLA class I signal peptides presented by HLA-E, non-canonical peptides which modulate NKG2A/C activity are being elucidated, particularly in the context of viral and

bacterial infection (26) (**Table 1-1**). No tumour-associated HLA-E stabilising peptides have been identified to date, although stress-associated peptides such as those derived from heat shock proteins (HSPs) are well known to stabilise HLA-E and regulate NK cell activity and these may be expressed by stressed cancer cells (24,197). For example, HSP60 peptides are presented by HLA-E which abrogate NKG2A/C interactions (24). NKG2A binds a wide range of peptides presented on HLA-E compared to the restricted pool for NKG2C (197). Single nucleotide polymorphisms in HLA class I signal peptides induce different levels of HLA-E expression and engage NKG2A/C receptors with varying affinity (23), leading to varying signal strength and activating/inhibitory responses. Therefore, the level of NKG2A/C signalling depends on the peptides presented by HLA-E and as a result different levels of education could be conferred via NKG2A. The varying affinities for peptides by NKG2A/C receptors in different disease contexts and the levels of NKG2A+ and NKG2C+ NK cell infiltrates will also determine the magnitude of an NK cell activating response.

**Table 1-1: Selection of HLA-E stabilising peptides at homeostasis and stressed states**

| Peptide | Protein | Reference |
|---|---|---|
| **Homeostatic conditions** | | |
| VMAPRTLVL | HLA-A | (26)(194)(198)(15)(19) |
| VMAPRTVLL | HLA-B | (26)(194)(198)(15)(19) |
| VMAPRTLIL | HLA-C | (26)(194)(198)(15)(19) |
| VMAPRTVFL | HLA-G | (26)(194)(198)(15)(19) |
| VMAPRTLFL | HLA-G | (199)(200) |
| VNPGRSLFL | BFR (bifunctional apoptosis regulator) | (26) |
| **Viral and bacterial infection** | | |
| VMPLSAPTL | SARS-CoV-2 – Nsp13 | (201) |
| AISPRTLNA | HIV | (202) |
| VMAPRTLIL | HCMV – UL40 | (203)(204) |
| VMAPRTLFL | HCMV – UL40 | (203) |
| RLPAKAPLL | TB – enoyl reductase | (205) |
| **Stress** | | |
| QMRPVSRVL | HSP60 | (24) |

Alongside regulating NK cell activation, NKG2A maintains the expansion capacity of NK cells (82) and enhances NK cell survival (206). It was shown *in vitro* with human NK cells that NKG2A marks highly proliferative NK cells and that NKG2A+ NK cells are more resistant to apoptosis (82). But whether NKG2A plays a critical role in maintaining NK cell expansion or is a passive marker on proliferative NK cells remains to be determined. The study by Kaulfuss (82) did not look into the function of NKG2A during NK cell expansion, and the K562 feeder cell line is negative for functional HLA-E expression (26,207) and therefore NKG2A would not have been engaged during expansion. It would have been interesting to decipher whether re-introducing NKG2A into sorted NKG2A- NK cells would recapitulate a highly proliferative NKG2A+ NK cell phenotype. Furthermore, it will be interesting to uncover whether these findings hold true *in vivo*, such as do NKG2A+ NK cells outcompete NKG2A- NK cells when introduced into mice at a 1:1 ratio?

The activation kinetics of NKG2A, unlike KIR, follows saturation kinetics such that when HLA-E is lowly expressed changes in surface expression leads to potent changes in NKG2A signalling, perhaps reflecting the evolution of NKG2A with the lowly expressed HLA-E protein (17,208). When HLA-E is highly expressed, further increases in expression have limited consequences on NK cell function. In this manner, NKG2A can respond quickly and potently to slight changes in HLA-E expression levels which may be disrupted during oncogenesis and viral infection when antigen processing and peptide presentation is disrupted, acting as a sensor for antigen processing machinery (34).

Besides being expressed on NK cells, NKG2A is also found on activated CD8+ T cells (209). NKG2A is a late checkpoint receptor being expressed after three rounds of stimulation on CD8+ T cells and is a marker of clonal expansion (209–212). Because of this upregulation of NKG2A upon activation, NKG2A increases the survival capability of T cells which allows clone-specific proliferation (206,213). Interestingly, anti-CD19 chimeric antigen receptor (CAR) T cells used to treat patients with diffuse large B-cell lymphoma (DLBCL) had increased NKG2A expression after 28 days compared to the pre-infused product (214), suggesting that repeated CAR T cell activation also induces the expression of the late checkpoint receptor NKG2A. Hence, in the context of cancer NKG2A can mark disease-specific exhausted T cells within the tumour microenvironment.

Because of the important cytotoxic functions of NK cells and their role in modulating adaptive immune responses via the secretion of inflammatory molecules, NK cells are critical to the onset and resolution of multiple diseases including infections and cancer. There have been many investigations into the role of activating and inhibitory NK cell receptors during disease and discussed briefly below are the key studies into KIR2DS2 and NKG2A in infection and cancer.

## 1.5 Roles of NK cells in disease

### 1.5.1 Role in infection

NK cells are critically important in the resolution of viral infection as demonstrated by specific KIR NK cell populations providing protection from infections and contributing to the resolution of disease (113). For example, higher levels of KIR3DS1 expression correlate with lower HIV viral loads (215) and KIR2DS2 has been shown to protect from HCV (174) and COVID-19 (216) infections. This is perhaps reflected by the virus-associated peptides presented on HLA proteins that activate these KIR which confers protection to individuals with specific HLA allotypes and KIR haplotypes.

NKG2A is also associated with virus infection outcomes. Individuals with late-stage HIV infection were found to have increased NKG2A expression on cytotoxic NK cells and this may impede HIV clearance (217). HIV infection in *in vitro* models demonstrated that increased HLA-E expression on CD4-expressing 721.221 cells promoted escape from NKG2A+ NK-mediated immunity (218) and high viral load is associated with higher HLA-E expression in individuals (219). Additionally, HCV peptides released from infected hepatocytes stabilise HLA-E at the plasma membrane inhibiting NKG2A+ NK cell function (220). Blockade of this interaction with antibodies against NKG2A or Qa-$1^b$ in infected mice promoted HCV clearance, illustrating that NKG2A is an important checkpoint in HCV infection (221). HLA-E overexpression was also found in cervical cancer biopsies of HPV-infected women (222). Together, these studies demonstrate the importance of HLA-E:NKG2A interactions in limiting the anti-viral NK cell immune response.

On the other hand, HLA-E expression has been linked to improved NK cell-mediated immunity. HLA-E presentation of non-structural protein 13 (Nsp13) from SARS-CoV-2 abrogates interactions with NKG2A to stimulate NK cell activation, but its physiological relevance needs to be determined (201), but overrepresentation of NKG2A+ NK cells has been observed in COVID-19 patients compared to healthy controls (223–225). This suggests that modulation of NKG2A:HLA-E interactions may improve COVID-19 resolution or that an on-going immune response by NKG2A+ NK cells due to Nsp13 presentation by HLA-E is promoting immunopathology in COVID-19.

NKG2A+ NK cells are also important in the identification of and lysis of vaccinia virus-infected cells (226). Specific downregulation of HLA-E after vaccina virus infection of 721.221 cells activate NKG2A+ NK cells. In mice, LCMV infection induces Qa-$1^b$ expression on B and T lymphocytes which inhibits NKG2A+ NK cell killing of anti-viral T cells allowing clearance LCMV (27). This study demonstrates the opposing functions of NK cells in anti-viral immunity. In certain settings NK cells directly lyse infected targets thereby facilitating viral clearance. In other settings, NK cells limit anti-viral T cell responses

which enable viral replication and immunopathology. Understanding the interplay between immune cell populations in specific viral infections will aide therapeutic intervention strategies.

### 1.5.2 Role in cancer

#### 1.5.2.1 Historical perspective of NK cells and the role of NKG2A expression in cancer

Since their initial discovery, NK cells have been shown to possess potent anti-cancer functions from cancer onset to metastasis. Early studies revealed that perforin-deficient (227) and TRAIL-deficient (228) mice develop lymphoma with age and NK cell production of perforin is crucial to control tumours *in vivo* (229). An important 11-year follow up study into NK cell activity and cancer incidence in humans revealed that high activity of NK cells reduced cancer incidence across >3000 individuals (230). Numerous studies have looked at NK cell tumour infiltrates and found that increased NK cell number correlates with better prognosis, highlighting the positive role NK cells play in anti-tumour immunity (231–233).

During cancer onset, NK cells identify transformed cells by the decreased surface expression of MHC proteins and by upregulation of stress ligands (B7H6, MIC-A/B and ULBPs) as outlined previously (234). Oncogenic stress, which is associated with increased DNA damage and enhanced cell proliferation, can induce upregulation of stress ligands and therefore enhance NK cell immunosurveillance (110). In terms of MHC expression, murine lymphoma cells expressing Qa-$1^b$ are able to establish tumours, whereas lymphoma cells knockout for Qa-$1^b$ are able to establish tumours and this was shown to be dependent on NK cells (43). In addition, NK cells have been shown to inhibit metastasis in murine models of ovarian cancer, highlighting a role of NK cells in late-stage cancer progression (235). Recently, it was illustrated that high HLA-E and HLA-C expression on circulating pancreatic tumour cells can protect from NKG2A+ and KIR2DL1+ NK cell-mediated clearance, respectively, and therefore promote metastasis to the lung, demonstrating that NK cells participate in cancer elimination during tumour migration (236,237).

In cancer patients, it is evident that NK cell function is impaired intrinsically alongside tumour promoting an immunosuppressive environment. For example, in haematological malignancies NK cells have decreased cytotoxic granule number, have impaired ADCC capability and patients have reduced NK cell numbers (238–240). In addition, NK cell subsets are skewed towards an inhibitory phenotype through differential expression of activating and inhibitory receptors. For example, in paediatric leukaemia NKG2A associates with NK cell dysfunction (241) and in chronic lymphocytic leukaemia (CLL) the activating receptor NKp30 is severely downregulated (49) and in conjunction with reduced total NK cell number correlates with worse survival (242).

An in-depth RNA-seq analysis of 33 tumour types revealed that HLA-E is upregulated in cancer and this correlates with NKG2A expression in tumours (243) and in mice intratumoral NK cells upregulates NKG2A (244). Upon entry into an immune-suppressive TME, NK cells become rapidly dysfunctional, losing expression of effector molecules and having increased expression of inhibitory receptors including NKG2A (245). This loss of NK function may involve increased expression of HLA-E on tumours, since HLA-E expression is known to be regulated by inflammatory conditions (34,144,246). Overall, these studies demonstrate that an opportunity exists to disrupt HLA-E:NKG2A interactions in cancer to induce an NK cell immune response given the important of HLA-E expression in cancer onset and progression.

#### 1.5.2.2 Expression of KIR2DS2 in cancer

As for specific KIR NK cell subsets certain KIR NK cell populations are correlated with cancer development and treatment outcomes. For example, KIR2DS2 is associated with decreased risk of developing childhood B-cell acute lymphoblastic leukaemia (178,247). In terms of treatments, KIR2DS2 is associated with lower risk of relapse in haematological malignancies after cord blood transplantation and is correlated with improved progression-free survival of patients with non-Hodgkin lymphoma after transplantation (248). Furthermore, improved clinical outcome in multiple cancer types including breast (249), lung (250), liver (251) and colorectal (252) cancer is correlated with KIR2DS2 expression. This may be due to the high anti-tumour activity of KIR2DS2+ NK cells as compared to other KIR NK cells; KIR2DS2 expression marks those with enhanced degranulation and increased IFNγ production (172). By targeting KIR2DS2+ NK cells with viral peptide vaccines containing the AT motif, an anti-tumour NK cell immune response can be generated to augment tumour regression in mice (173). Interestingly, CD16a expression is higher on KIR2DS2+ NK cells (172,253) and this promotes enhanced ADCC as shown with anti-GD2 (179) and CD20 antibodies (172). Moreover, KIR2DS2-expressing neuroblastoma patients who received anti-GD2 treatment had superior event-free survival (179).

As a result of their potent anti-cancer function and detailed knowledge of the molecular mechanisms governing NK cell activation, therapies have been designed to promote NK cell activation. These include peptide vaccination strategies, NK cell adoptive transfer approaches using allogeneic and CAR NK cells and monoclonal antibody therapy that induce ADCC or impede inhibitory signalling.

## 1.6 Exploiting NK cells in cancer therapy

### 1.6.1 Direct targeting monoclonal antibody therapy

Monoclonal antibody (mAb) therapy has revolutionised cancer treatment being used to treat a wide variety of cancer types with great success. There are two main types of mAb therapy classified by antigen specificity: direct targeting and immunomodulatory mAb therapy. Direct targeting mAbs bind to specific receptors on cancer cells and act by opsonising tumours to the immune system. These work by inducing ADCP by macrophages and enhancing complement-dependent immunity. NK cells also contribute to the efficacy of direct targeting mAbs through their ADCC capabilities (254) (**Figure 1-7**). On the other hand, immunomodulatory mAbs recognise receptors expressed by tumours or immune cells, including NK cells, to either potentiate immune cell activation (immune stimulatory mAbs) or prevent their inhibition (immune checkpoint inhibitors) (**Figure 1-7**).

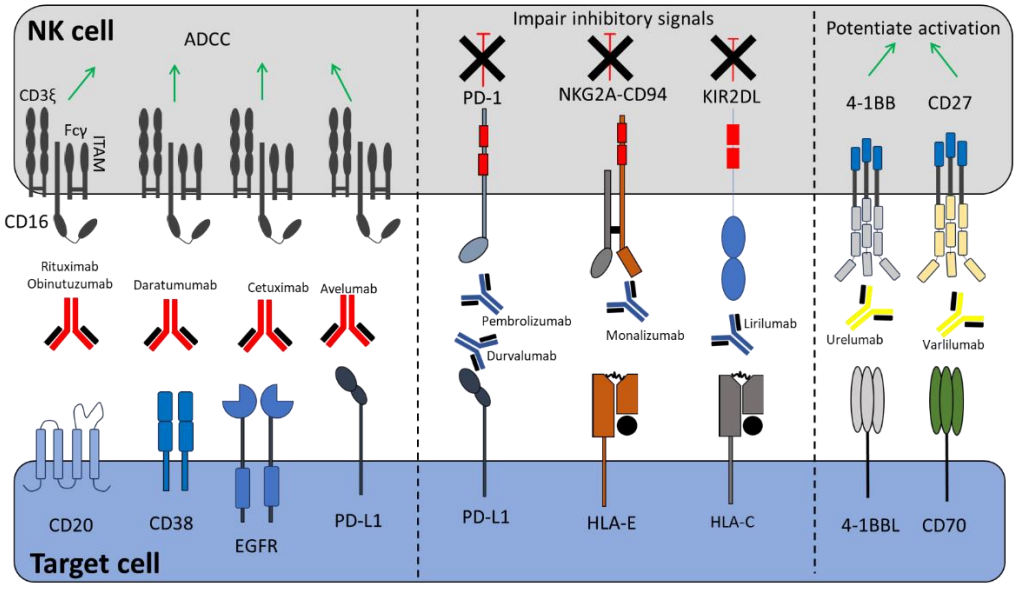


**Figure 1-7: Mechanisms of action of monoclonal antibodies which promote NK cell activation against tumours.**

Direct targeting monoclonal antibodies (left) which target tumour antigens enhance NK cell ADCC via engagement with CD16a. Immune checkpoint inhibitors block inhibitory NK cell receptor interactions with ligands on tumour cells to impair inhibitory NK cell signalling. Stimulatory antibodies which are undergoing clinical assessment potentiate activating signalling by NK cells.

The first and one of the most successful direct targeting mAbs are those targeting CD20 in B cell malignancies. Rituximab was the first anti-CD20 IgG1 mAb approved in 1997 (255). Although IgG3 has increased affinity for CD16a, IgG1 isotypes are preferred due to the numerous allotypes of IgG3 making it incompatible for clinical use due to increased immunogenicity and reduced half-life (256). A cascade of next generation anti-CD20 mAbs followed rituximab to improve ADCC and ADCP (257). Obinutuzumab is a next-generation anti-CD20 mAb with a glycoengineered Fc domain that is non-core-fucosylated enabling it to bind more strongly to CD16a (258). Obinutuzumab has shown increased efficacy over rituximab in chronic lymphocytic leukaemia (CLL), enhancing the progression free survival of patients (259). In terms of NK cells, an association between fewer circulating NK with shorter progression free survival with anti-CD20 chemoimmunotherapy in non-Hodgkin lymphoma was observed (260) and patients bearing the high affinity CD16 allele (V158) had improved response and survival to rituximab (261,262), highlighting the potential importance of NK cells to contributing to anti-CD20 mAb therapy.

Some direct targeting mAbs, such as daratumumab (anti-CD38) used to treat multiple myeloma, bind tumour antigens that overlap with receptors expressed on effector immune cells. NK cells express CD38, albeit at a lower level compared to myeloma cells, thus daratumumab opsonises NK cells to NK cell-mediated lysis (263). Although NK cell counts reduced in patients treated with daratumumab, clinical response was not affected. The remaining NK cells in Daratumumab-treated patients were still able to lyse opsonised tumour cells highlighting the importance of NK cells in anti-CD38 efficacy and suggesting that improved efficacy may be observed by shielding CD38+ NK cells from daratumumab binding (264).

Inhibitory receptors on NK cells can impede ADCC (265) including the NKG2A receptor (266) and inhibitory KIR (267) and the activity of these receptors can be inhibited to augment the anti-tumour functions of NK cells. This class of antibody therapy is referred to as immune checkpoint therapy.

### 1.6.2 Immunomodulatory mAb therapy

#### 1.6.2.1 Immune checkpoint inhibitors

The current approved immunomodulatory mAbs target either CTLA-4 or the PD-1/PD-L1 interaction and more recently the anti-LAG-3 mAb relatlimab was approved for melanoma (268). In terms of NK cells, the PD-1/PD-L1 axis plays an important role in myeloma escape from NK cell activation and the use of anti-PD-1 mAbs demonstrated enhanced NK cell activation against patient myeloma cells (269). Interestingly, tumours can induce PD-L1 expression on NK cells and anti-PD-L1 therapy has been shown to stimulate NK cells which may explain anti-PD-L1 efficacy in PD-L1 negative tumours (270). Building upon this, it was recently demonstrated that PD-L1+ NK cells were efficacious in combination with the anti-PD-L1 monoclonal antibody atezolizumab in *in vivo* models of lung cancer

(271). Despite the success of immunomodulatory mAbs in treating many cancer types, not all patients respond, and new targets are warranted.

Novel checkpoint inhibitors are being clinically investigated to unleash the anti-tumour capacity of T cells and NK cells. TIGIT has been described as an important NK cell checkpoint, being expressed on activated NK cells and promoting exhaustion (272). Knockout of TIGIT can improve NK cell cytotoxicity and promote metabolic fitness (273). TIGIT expression correlates with anti-tumour activity, and blocking TIGIT promotes a potent activating NK cell response and improves tumour regression in mice (272,274). As described above in sections 1.4.4 and 1.5.2.1, NKG2A is an important immune checkpoint on NK cells and CD8+ cytotoxic T cells. The fact that NKG2A is not expressed on regulatory T cells (209) makes it an attractive target to enhance an anti-tumour T cell immune response. Furthermore, NKG2A identifies highly anti-tumorigenic γδ T cells (275) and antigen experienced, clonal CD8+ T cells (211,212) and in contrast to PD-1, NKG2A is a late checkpoint on T cells, appearing at the plasma membrane after three rounds of TCR stimulation (210). Therefore, alongside activating a potent NK cell immune response, specific T cell populations with high anti-tumour activity will be activated.

Monalizumab is an anti-NKG2A mAb that promotes NKG2A+ NK cell and NKG2A+ T cell function by disrupting NKG2A engagement with the inhibitory ligand HLA-E (43). This checkpoint inhibitor has shown great promise in pre-clinical trials of B-cell lymphoma (43) and is currently in phase III clinical trials in combination with cetuximab (anti-EGFR) for the treatment of head and neck squamous cell carcinoma (276,277) (NCT04590963) and in phase III clinical trials with durvalumab for non-small cell lung cancer (NCT05221840). Additionally blockade of NKG2A function can promote anti-tumour vaccine strategies (278). However, the problem with impairing NKG2A signalling with mAbs is the potential to impede NK cell education which is important for producing functional NK cells (101,102,104) and the fact that that different peptides presented on HLA-E can modulate the activity of anti-NKG2A mAbs (279). For example, HLA-G leader peptide presentation on HLA-E reduces the potency of monalizumab-induced NK cell activation and therefore patient stratification may be required. Considering these points, targeting HLA-E with mAbs may be a more viable option that may provide a tumour-specific approach through peptide targeting and avoiding the negative effects of negating NKG2A-mediated education and targeting HLA-E may also promote ADCC alongside reducing inhibitory signalling as with targeting PD-L1 (**Figure 1-7**) (280,281).

On the reverse, high HLA-E expression may offer the opportunity to promote anti-tumour immune responses via NKG2A. Overexpression of HLA-E on adoptively transferred stem cells evade rejection by NK cells (282) and multiple studies have shown that high expression of HLA-E improves persistence of CAR T cells and CAR NK cells *in vivo* which could potentially be used as a universal source of CAR immune cells (283–285). An interesting study also showed that swapping the

extracellular domain of NKG2C with NKG2A can augment NK cell and T cell function against HLA-E-expressing tumours and control glioblastoma in xenograft murine models (286). Overall, these studies demonstrate the powerful immunosuppressive nature of HLA-E which can be capitalised upon in adoptive transfer settings.

Further NK cell immune checkpoints are being investigated for their potential to stimulate an anti-tumour immune response. LILRB1, known for its inhibitory functions in macrophages (287), is a novel target that through blocking its interaction with HLA class I may promote an NK cell immune response and increased LILRB1 expression on NK cells has been reported in prostate cancer patients (182,288). Further targets include blocking inhibitory KIR on NK cells (289). Lirilumab is an anti-KIR2DL mAb which increases NK cell cytotoxicity and shows synergy with anti-CD20 mAbs in mouse models of B-cell lymphoma (290). Combined with IL-2, lirilumab can reverse NK cell hypo-activity in glioblastoma (291). However, the challenge with targeting KIR is the high homology between KIR which may impede activating KIR activation and block other inhibitory KIR leading to overactive NK cells. Indeed, in a phase II clinical trial for AML, lirilumab impaired T cell activation and reduced NK cell counts, and did not improve survival outcomes for patients (292). Potentially, lirilumab impairs NK cell licensing to tumour cells. Hence, it is important to determine the optimal treatment regimen when targeting key receptors involved in NK cell education, such as KIR and NKG2A, such that transient blockade will promote an anti-tumour immune response but negate deleterious effects on NK cell education.

#### 1.6.2.2 Stimulatory antibodies and NK cell engagers

Besides discovering novel immune checkpoint inhibitors, stimulatory antibodies may provide increased response rates in cancer patients to mAb therapy. These work by binding to activating receptors on T cells and NK cells to stimulate receptor signalling to promote an anti-tumour immune response. Examples include antibodies targeting 4-1BB, OX40 and CD27 and these are being pre-clinically and clinically tested (293–295). These molecules are found on activated T cells and NK cells, therefore utilising these antibodies would potentiate an on-going immune response. Designing antibodies against NK cell activating KIRs could be another strategy to enhance NK cell activation against tumours. However, the major problem with this strategy is the genetic similarity between KIRs such that an antibody raised against an activating receptor may also bind inhibitory KIRs (113). Identifying which KIR to target is an additional challenge because assays comparing KIR NK cell populations are difficult to conduct since there are no commercially available antibodies to specifically detect certain KIRs. As such, novel approaches are required to activate KIR on NK cells.

Similar to antibodies, next generation multifunction molecules that co-target tumour antigens and NK cell activating receptors are aimed at improving engagement and activation of NK cells against tumours (296,297). These molecules are termed killer cell engages (NKEs) and are being developed in

multiple formats: bi-specific killer cell engagers (biKEs) and tri-specific killer engagers (TriKEs). These induce stronger activating signals via the simultaneous engagement of more than one activating receptor (298).

A CD16axCD33 biKE has shown to be an effective activator of autologous NK cells in AML and ALL in *ex vivo* experiments (299). A TriKE designed against CD16a on NK cells, CD19 on tumour targets and linked to the IL-15 cytokine to promote NK cell proliferation and survival promoted a potent NK immune response against B-cell lymphoma cell lines and CLL patient targets (300). NK production of IFNγ was superior compared to rituximab treatment, highlighting that these next generation NK engagers boost NK anti-tumour functions more potently than mAbs. Other NK receptor targets of NKEs include NKG2D and NCRs, which in certain contexts may promote a more effective NK cell immune response (298).

### 1.6.3 NK cell adoptive transfer therapy

Adoptive NK cell therapy involves the transfer of *ex vivo* expanded autologous or allogeneic NK cells into patients (301). Compared to T cell adoptive transfer therapy, NK cells have the potential of providing an off-the-shelf, universal product using allogeneic NK cell sources. To date no evidence of graft-versus host disease (GvHD) nor cytokine release syndrome (CRS) have been observed (302–305). The lack of CRS may be due to the reduced abundance of cytokines that drive CRS such as IL-6 (303). Sources of NK cells include cell lines (NK-92 and YT), primary NK cells derived from peripheral blood and umbilical cord blood and the differentiation of NK cells from pluripotent stem cells. The concept of using alloreactive NK cells stems from the observation that NK cell infusion of KIR ligand mismatch grafts induce better responses in AML patients (306). This complements the missing self-hypothesis such that KIRs on infused NK cells are not inhibited by HLA in patients.

Expanded NK and CIML NK cells are known to be highly cytotoxic towards cancer cells (157,307) including primary patient CLL cells (308) and so exploiting their use in patients is of particular interest. One major challenge with NK adoptive transfer therapy is the production of clinically relevant NK cell numbers. How to effectively culture and grow NK cells requires optimisation and knowledge of how culture methods regulate NK cell receptors is important for predicting efficacy. Common culture methods use IL-2, IL-15, IL-21 cytokines and feeder cells and recently, it was illustrated that IL-21 produces high yields and highly cytotoxic NK cells (309,310). All culture methods upregulate the inhibitory receptor NKG2A (243,311–313) hence, the efficacy of NK cell adoptive transfer therapy may be reduced in cancer settings with high HLA-E expression. To overcome this NK cells could be genetically manipulated to downregulate NKG2A expression and this was shown to be more effective at promoting NK cell anti-tumour functions compared to antibody blockade (314). Preclinical work has shown that knockdown of NKG2A with siRNA boost NK cell effector functions

against HLA-E+ tumours *in vitro* and *in vivo* (315–317). Use of protein expression blockers (PEBLs) against NKG2A which sequester NKG2A in the Golgi enhance NK cell anti-tumour functions against AML cell lines and primary tumours (243). CIML NK cells may provide improved benefit as these have enhanced anti-tumour functions and increased persistence and have induced remission in paediatric AML patients (157,318,319). Improving the efficacy of memory-like NK adoptive transfer could involve targeting the NKG2A:HLA-E axis as memory NK cells also upregulate NKG2A expression (318).

### 1.6.4 Chimeric antigen receptor (CAR) NK cells

CAR NK cells are designed to improve the activation, tumour-specificity and persistence of adoptively transferred NK cells. As with CAR T cells, NK cells can be engineered to express a receptor specific for a tumour antigen using retroviral or lentiviral delivery methods into NK cell lines or primary NK cells. The intracellular signalling domain of CAR constructs varies depending on NK cell source and consists of combinations of CD3ξ, CD28, 4-1BB, DAP10 and DAP12 (**Figure 1-8**) (320). Many CAR NK constructs are undergoing pre-clinical investigation with multiple studies now in clinical trials primarily for haematological malignancies (304), in particular using anti-CD19 CAR NK against B-cell malignancies (321). Anti-CD19 CAR NK cells have provided promising results in phase I and II clinical trials for non-Hodgkin lymphoma and CLL (303) and in a recent trial (NCT03056339) of relapsed/refractory patients with CD19+ tumours responders to anti-CD19 CAR NK cells had a 1-year overall survival of 94% with no observations of toxicities (cytokine release syndrome, neurotoxicity nor GvHD) (305).

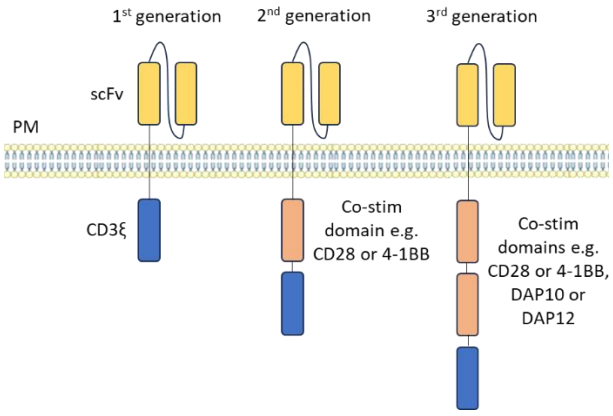


**Figure 1-8: Generations of chimeric antigen receptor constructs.**

CAR NK cells express a construct consisting of an antibody short chain variable fragment (scFv) specific for a cell surface antigen and signalling domains to promote activating signalling. The intracellular domain of the first-generation construct consists only of a CD3ξ signalling domain. Subsequent generations of CARs include co-stimulatory domains from the intracellular domains of CD28, 4-1BB, DAP10 or DAP12.

It could be imagined that specific NK cell populations with high anti-tumour activity such as KIR2DS2+ NK cells transduced with a CAR construct will boost the efficacy of CAR NK cell therapy (172). Additionally, it could be speculated that KIR2DS2+ CAR NK cells could be further bolstered by strategies activating KIR2DS2 via presentation of peptides on HLA molecules such as with peptide vaccine strategies (173). Boosting CAR NK cell efficacy could also be achieved using NK receptors with a wide range of ligands such as NKG2D. NKG2D-tranduced CAR NK cells enhance the survival of mice engrafted with multiple myeloma cell lines (313). In addition to CAR expression, NK cells could be engineered with multiple receptors to improve tumour targeting. This has been demonstrated with a quadruple gene-engineering approach in which NK cells target B cell maturation antigen (BCMA), express non-cleavable CD16a, possess membrane-bound IL-15 and are knockout for CD38 to avoid NK cell fratricide with anti-CD38 mAbs (322). These quadruple-gene engineered NK cells are extremely cytotoxic towards multiple myeloma cells in combination with anti-CD38 mAbs.

Another mechanism by which to improve CAR NK cell approaches could be through modulation of inhibitory receptors that become highly expressed on NK cells during expansion (after ~1 week) and activation (43,243). The increased expression of inhibitory receptors may skew CAR NK cells into an inhibitory state, since there exists a fine balance between activating and inhibitory NK cell signalling (105). Levels of the inhibitory SHP-1 phosphatase is a biomarker for enhanced NK cell activity in donors, such that low levels (induced through productive education via KIR and NKG2A) enhance NK cell activity (105). Therefore, exploiting donors with low SHP-1 expression or targeting SHP-1 expression via genetic engineering approaches may overcome inhibitory receptor signalling in CAR NK cells.

As described above, NKG2A is upregulated across multiple expansion protocols and indeed NKG2A can limit anti-BCMA and anti-CD33 CAR NK cell anti-tumour functions and this can be overcome with antibody blockade or CRISPR/Cas9, respectively (323,324). Besides combining NK cell immunotherapy with knockout or antibody approaches, small molecules that induce intrinsic cancer cell toxicity whilst mediating anti-cancer immunity through the modulation of NK cell ligand expression could be an effective method of improving tumour regression in patients. Moreover, preclinical models have shown increased tumour regression using NK cell immunotherapy in combination with anti-cancer agents (325,326). Using CLL murine models allogeneic and autologous membrane-bound IL-21-expanded NK cells in combination with venetoclax or obinutuzumab showed improved mouse survival compared to monotherapy (327). Additionally, this study illustrated that the bruton's tyrosine kinase inhibitor (BTKi) ibrutinib was less effective in combination with NK cells compared to venetoclax or obinutuzumab, most likely due to the off-target effect of ibrutinib inhibiting IL-2-inducible kinase (ITK) which is important for NK cell function (328). The use of the next-generation BTKi orelabrutinib with reduced ITK inhibition improved mouse survival in combination with rituximab compared to ibrutinib (329). Thus, understanding which small molecule

drugs best combine with immunotherapies will enable the most optimal anti-cancer responses in patients. The most promising results to date corroborating the use for NK cell immunotherapy have been observed for haematological malignancies, particularly of B cell origin and the multiple compounds used to treat B-cell malignancies offer a potential opportunity to combine small molecules with NK-stimulating immunotherapies.

## 1.7 B-cell and plasma cell malignancies

### 1.7.1 Development of B cell lymphoma/leukaemia and multiple myeloma

Haematological malignancies arise from the cells of the blood, including NK cells, B and T lymphocytes, myeloid cells and megakaryocytes. Oncogenic transformation is a result of healthy cells acquiring genetic abnormalities overtime which induces genetic instability, enhances cell proliferation, increases resistance to apoptosis and protects from immune destruction as in the hallmarks of cancer (41). There are two main types of lymphoma: Hodgkin lymphoma and non-Hodgkin lymphoma (NHL), the latter account for 90% lymphoma cases (330). Hodgkin lymphoma is characterised by Reed-Sternburg cells at diagnosis and a key risk factor is Epstein-Barr virus infection in childhood (330). Focussing on B-cell NHL which account for 90% of NHL, this is separated into 19 subtypes of which there are two major groups of disease: aggressive disease and indolent disease.

The cellular origin of B-cell lymphomas was deciphered from gene expression studies comparing expression profiles between malignant cells and normal B cells (331,332) and the subtypes studied in this thesis are highlighted in **Figure 1-9**. Diffuse large B cell lymphoma (DLBCL) is the most common and most aggressive NHL accounting for 31% of cases in adults, mantle cell lymphoma (MCL) accounts for 6% of cases and Burkitt lymphoma 2% of cases (333).

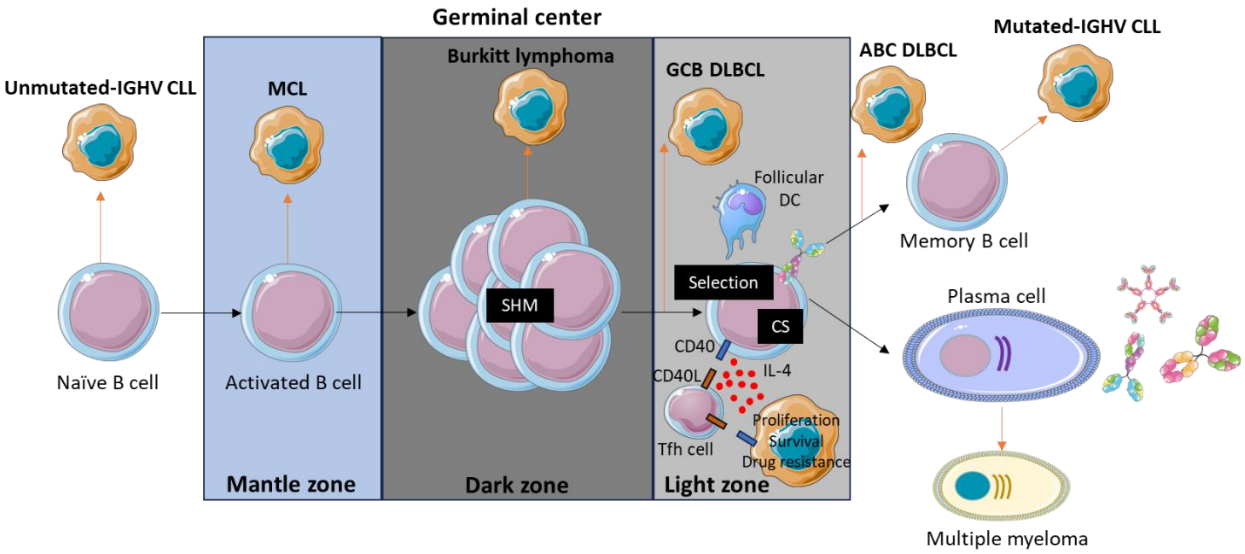


**Figure 1-9: Cellular origin of B-cell malignancies and multiple myeloma.**

Chronic lymphocytic leukaemia (CLL) with unmutated IGHV (immunoglobulin heavy chain) develops from naïve B cells. Upon B cell activation such as TLR stimulation or encountering BCR-specific antigen, activated B cells enter the germinal center to begin the process of somatic hypermutation (SHM) in the dark zone and selection and class switching (CS) which takes place in the light zone with help from follicular dendritic cells (which present antigens to assess BCR affinity) and T helper cells (through CD40:CD40L interactions and cytokine secretion e.g. IL-4), respectively. IL-4 and CD40L signalling in malignant B cells facilitates cell proliferation, survival and drug resistance. At different stages of B cell development through the germinal center different malignancies arise. Early after activation and progression into the mantle zone, mantle cell lymphoma (MCL) originates. Burkitt lymphoma develops from clonal expansion in the dark zone and germinal center B-cell diffuse large B cell lymphoma (GCB-DLBCL) originates from centrocytes. At the end of B cell maturation, B cells differentiate into either a memory B-cell or an antibody-secreting plasma cell. Another form of DLBCL, activated B-cell lymphoma (ABC-DLBCL), stems from B cells leaving the germinal center after B cell maturation. CLL cells with mutated IGHV due to SHM develop from memory B cells. Malignancies of plasma cells is referred to as multiple myeloma.

There are common genetic lesions associated with driving malignant transformation of B cells as per the hallmarks of cancer (334). In terms of cell proliferation, a gain-of-function in MYC through, for example, through chromosome translocation in Burkitt lymphoma leads to overexpression of *Myc* (335,336). MYC acts as a transcription factor for genes involved in cell proliferation, therefore MYC overexpression leads to enhanced cell multiplication (337). p53 is an important tumour suppressor protein that becomes activated via multiple mechanisms including upon DNA damage and oncogenic signalling to halt cell division and if necessary, induce apoptosis (338). Mutations in p53 induce genomic instability, allow for oncogenic signalling and promote cell survival and p53 mutations are common across all cancers including B-cell neoplasms. Translocation of the *BCL2* gene (339,340) in

DLBCL promotes resistance to apoptosis via increased BCL2-mediated inhibition of pro-apoptotic proteins that induce mitochondrial leakage and caspase activation. One mechanism to evade immune-mediated clearance is through silencing of β2-microglobulin via gene deletion or mutation which has been recorded in 29% of DLBCL (341).

In addition to the many genetic lesions of B-cell malignancies, the multiple developmental stages of maturing B cells in germinal centers also contribute to disease heterogeneity (**Figure 1-9**). MCL is derived from naïve B cells in the mantle zone of germinal centers, hence its name. The mantle zone surrounds the dark and light zones and develops because proliferating B cells in the dark and light zones push naïve B cells to the periphery of the germinal center. Therefore, MCL develops from B cells that have not undergone B cell differentiation. Burkitt lymphoma is derived from B cells undergoing SHM within the dark zone. DLBCL is separated into two main types depending on the origin of the B cell: germinal center B cell-DLBCL (GCB-DLBCL) and activated B cell-DLBCL (ABC-DLBCL). GCB-DLBCL develops from B cells within the dark zone undergoing SHM, and ABC-DLBCL is derived from B cells at the final stage of differentiation. Compared to GCB-DLBCL, ABC-DLBCL is correlated with poorer outcomes with standard treatments (342). Lastly, multiple myeloma develops from plasma cells which are terminally differentiated, antibody-producing cells that have lost expression of classic B cell marker CD19 and CD20.

Chronic lymphocytic leukaemia (CLL), on the other hand, is the most common adult leukaemia in the western world and is associated with the expansion of immature B lymphocytes in the blood, spleen and lymph node. Malignant cells are characterised by the positive expression of both CD5 and CD19 (343) and patients present with various subtypes of the disease which hold prognostic value. The major subtype of CLL is based on the mutational status of the immunoglobulin heavy chain variable region (*IGHV*) (344). The genetic differences arise from malignant cells originating from B cells post- or pre-somatic hypermutation (SHM), a process of B cell receptor (BCR) affinity maturation towards antigens. Unmutated *IGHV* (U-*IGHV*) CLL develops from naïve B cells, therefore the *IGHV* gene resembles the germline reference sequence. Mutated-*IGHV* (M-*IGHV*) CLL originates from mature B cells after SHM and is described as the dominant clonal population having >2% genetic differences in the *IGHV* sequence from the germline reference sequence (345). M-*IGHV* CLL is usually an indolent disease, but the U-*IGHV* subtype is more aggressive and patients have poorer clinical outcome due to the immaturity and proliferative potential of naïve B cells (344,346). In 2-10% of CLL patients, particularly those with M-*IGHV* CLL, Richter's transformation can occur which is an aggressive B-cell malignancy with similar histopathology to DLBCL and is associated with poor prognosis (347).

In addition to unmutated and mutated forms of CLL, patients present with different expression levels of surface proteins which also provide prognostic value. For example high surface expression of IgM (the BCR) is associated with poorer clinical outcome as too is high expression of CD49 and patients

positive for CD38 have lower survival probability compared to CD38 negative patients (348–351). High expression of these proteins allows for enhanced survival signalling. CD49 mediates interactions between CLL cells and aids migration to lymphoid tissue in which CLL cells are immersed in a protective, proliferative environment where drug resistance can develop (352,353).

### 1.7.2 Treatment of B-cell lymphoma/leukaemia and multiple myeloma

The survival of CLL cells largely depends on BCR signalling, which upon activation a complex signalling cascade ensues which terminates in NFAT, ERK and NF-κB activation which promotes CLL cell survival and proliferation (354). Therefore, targeting BCR signalling has demonstrated long-term efficacy, both as first-line treatments and in the chemoimmunotherapy relapsed/refractory setting. The treatments include PI3-kinase inhibitors (E.g. Idelalisib) and bruton's tyrosine kinase inhibitors (BTKi, such as ibrutinib). Ibrutinib achieved a 70% 5-year progression free survival rate as a front-line treatment (355) and in relapsed/refractory settings to immunotherapy showed a progression free survival of 44 months (356). As mentioned previously, BCL2 overexpression enhances the survival of malignant B cells (339,340) and the anti-BCL2 drug venetoclax is approved for use in CLL (357).

Immunotherapy regimens are also successfully used to treat CLL as well as NHL including anti-CD20 mAbs rituximab and obinutuzumab. Rituximab was the first immunotherapy to be approved for CLL (358) and the efficacy of anti-CD20 mAbs has greatly improved with antibody engineering approaches, such as the development of obinutuzumab which has increased glyocsylation of its Fc domain to augment ADCC and ADCP (359,360). For CLL anti-CD20 mAbs are combined with BTKi and BCL2 inhibitors described above. For DLBCL anti-CD20 mAbs are used in combination with chemotherapy, referred to as R-CHOP therapy and chemotherapy regimens and radiation therapy are standard treatments for other types of NHL.

The anti-CD38 mAb daratumumab is used for the treatment of multiple myeloma as well as the anti-SLAMF7 mAb elotuzumab, both are used as front-line treatments in combination with chemotherapy and the proteasome inhibitor bortezomib. In terms of cellular therapies, the FDA have approved anti-BCMA CAR T cell therapy for relapsed multiple myeloma patients who have received four rounds of therapy and astonishing results have been reported with overall response rates of >90% and progression free survival of 2-3 years to date (361).

Despite the success of these treatment options, they are not able to successfully treat all individuals. For example, 60% of DLBCL patients are cured with R-CHOP, but for patients who relapsed prognosis is dismal (362). Relapsed DLBCL patients have a median overall survival of 6.6 months on high intensity chemotherapy regimens and stem cell transplantation (363). Anti-CD19 CAR T cell therapy which is now used as a second line therapy for DLBCL has shown an event-free survival benefit of 6 months (NCT03391466) (364). For relapsed CLL patients with Richter's transformation, prognosis is

extremely poor with an overall survival of 5.9-8 months (365,366). Therefore, new approaches are required for the treatment of relapsed and refractory individuals with B-cell lymphoma/leukaemia.

Approaches to improve CAR T cell therapy include combinations with mAbs or small molecules (367). One challenge with CAR T cell therapy is the use of autologous T cells which have encountered rounds chemotherapy treatment and have been immersed in an immunosuppressive environment. Another challenge is the period between apheresis and CAR T cell generation which could take up to one month and therefore bridging therapies are required to maintain a patient with advanced disease in a state capable of receiving CAR T cells (368). Hence, another approach could involve the adoptive transfer of allogeneic NK cells which have the potential as an off-the-shelf product, reducing the time from intention to treat to NK cell adoptive transfer. As outlined above in section 1.6.4, clinical trials (NCT03056339) using anti-CD19 CAR NK cells are showing great promise for the treatment of advanced CLL and relapsed/refractory NHL (303,305). But understanding how best to promote NK cell function in patients requires knowledge of the extent of patient NK cell dysfunction and the mechanisms behind immune evasion of malignant B cells and multiple myeloma cells.

### 1.7.3 NK cells in B-cell lymphoma/leukaemia and multiple myeloma

In newly diagnosed CLL, NK cell number is predictive of disease progression, such that higher NK cell frequency induces longer time to treatment in individuals, but compared to healthy controls, NK cell abundance is diminished (49,369,370). Although NK cell abundance may be important in CLL, CLL cells are immunosuppressive towards NK cells (49,371,372). For example the upregulation of surface HLA-E on CLL cells avoids NKG2A+ NK cell recognition and the use of anti-NKG2A blocking antibodies revives NKG2A+ NK cell activity (48,372). Additionally ligands for activating NK cell receptors are shed from the plasma membrane of CLL cells to escape NK cell immunosurveillance (49,372).

In addition to the immunosuppressive mechanisms of CLL cells, patient NK cells are partially dysfunctional, suggesting impairment of intracellular processes (49,370). Patient-derived NK cells are hyporesponsive, being less cytotoxic (373), having decreased degranulation capabilities (374) and producing inferior levels of IFNγ (300). NKG2D levels are downregulated in CLL patients compared to healthy controls and this downregulation is greater in advanced disease (375) and in DLBCL NKG2A is highly expressed on patient NK cells compared to healthy NK (376). The ADCC capacity of patient NK is also severely impaired compared to healthy controls (377) and increased expression of HLA class I molecules through engagement of inhibitory KIR can mediate escape from ADCC by anti-CD20 mAbs (267). Therefore, strategies to replenish NK cell numbers and sensitise CLL cells to NK are required and indeed NK hyporesponsiveness can be reversed in CLL patients by providing adequate activating signals (374).

Malignant B cells besides being in circulation, which are the main cells used in laboratory experiments, are also found in secondary lymphoid organs and the bone marrow. Within secondary lymphoid organs, malignant B cells are submersed in a microenvironment enriched with molecules which can promote proliferation, enhance survival and facilitate drug resistance (2) For example, IL-4 and CD40L stimulate the expresion of MCL-1, an anti-apoptotic protein, which enhances CLL survival and protects from venetoclax treatment (378). In CLL, T cells produce IL-4 (379) and express CD40L (380) and in progressive CLL the abundance of T cell-producing IL-4 cells is increased in addition to increased IL-4 receptor expression on CLL cells (381) (**Figure 1-9**). The IL-4 receptor signals via JAK1 and JAK3 leading to STAT6 phosphorylation and IL-4 is known to increase surface IgM levels (2) and inhibit the expression of miRNAs that impair BCR signalling (382) and therefore IL-4 augments proliferative and survival BCR signals. As such, IL-4 can impede the effects of BTK and PI3-K inhibition (2). With regards to CD40 signaling, NF-κB and mTOR become activate which support CLL survival and drug resistance via the expression of Bcl-2 family of anti-apoptotic proteins including MCL-1 (378,383). As such, IL-4 and CD40L together provide a model of lymph node signalling in B-cell lymphoma/leukaemia to mimic the tissue microenvironment. Besides the intrisic survival properties conferred by IL-4 and CD40L lymph node support molecules, how they modulate NK cell immune responses and impact NK-stimulating immunotherapies is largely unknown (384).

In multiple myeloma NK cell function is severely impaired with NK cell adhesion abnormalities and reduced cytotoxic capacity, and these correlates with poor prognosis (385). In advanced disease HLA class I molecules are highly expressed on myeloma cells to further impede NK cell function (240). Higher HLA expression is also correlated with shorter survival and poor prognosis (386). Other soluble factors expressed by myeloma cells are known to suppress NK cell function such as cyclooxygenase-2 and expression of inhibitory NK cell ligands HLA-E and HLA-G (50,371,387). As a result of the immunosuppressive mechanisms of malignant B cells and multiple myeloma cells and the dysfunction of patient NK cells, strategies to promote NK cell anti-tumour functions have been established inlcuding monoclonal antibody therapy to promote ADCC and block inhibitory NK cell signalling and the adoptive transfer of allogeneic NK cells or CAR NK.

However, cancer treatments are often used in combinations to avoid drug resistance and reduce doseage to negate adverse events. Nevertheless, combinations could be tailored to maximise anti-tumour effects by complementing each other's modes of action. Small molecules induce intrinisic toxicities in cancer cells and immunotherapies promote immune responses, therefore combining these drugs may induce potent anti-cancer responses. Indeed, combining T cell immunotherapy with small molecules is being considered, especially small molecules that actively enhance immune function (367). The same could be considered for NK cell immunotherapies and interestingly, anti-cancer agents have been shown to possess NK cell immunomodulatory activity. Therefore, understanding the mechanisms of small molecule modulation of cancer cell immunogeneicity will

enable the design of tailored combination therapies to induce potent anti-cancer responses in patients.

## 1.8 Immunomodulation by anti-cancer agents

It is beginning to be appreciated that cancer targeted drugs (and radiotherapy) possess immunomodulatory activity alongside tumour-intrinsic toxicity (388–390). This is thought to be due to increased stress induced in cancer cells and stress signals are known to enhance the immunosurveillance properties of NK cells (110). But understanding the specific immunomodulatory mechanisms of cancer treatments will aid the design of potent combinations with immunotherapies. For example, mitochondrial apoptosis acts as a facilitator of NK-mediated immunotherapy (391). Priming of cancer cells with apoptotic agents, such as through inhibition of the pro-survival molecule BCL-2, enhances NK cell cytotoxicity *in vitro* and *in vivo* (391). Based on these findings, a reasonable treatment regimen may involve sensitising cancer cells with anti-cancer agents followed by adoptive NK cell therapy or a therapy which stimulates NK cell function. But to select the most optimal NK cell population or the most appropriate immunotherapy combination, further studies investigating the mechanisms behind sensitisation of anti-cancer agents are required.

Cancer targeted drugs are designed against specific proteins to re-establish tumour suppressor function, inhibit the action of oncogenic proteins, and impede survival and proliferative signals. The histone deacetylase inhibitor (HDAC), Panobinostat, approved for the treatment of multiple myeloma promotes NK cell lysis of myeloma cell lines and enhances NK cell activation *in vivo* (392). This was due to increased expression of adhesion molecules and tight junctions which are important for NK cell immunological synapse formation (393). Furthermore, in malignant B cells HDACs can increase CD20 antigen density and thereby augment anti-CD20-based therapeutics including mAbs and anti-CD20 CAR T and CAR NK cells (394–396).

MDM2 negatively regulates the expression and function of the important tumour suppressor protein p53 (397). Nutlin-3a is a small molecule designed to inhibit MDM2 action and therefore restores p53 expression and function (398). Interestingly, nutlin-3a re-activation of p53 increases the expression of the NK cell activating ligand PVR (CD155) on neuroblastoma cells, sensitising these to NK-mediated lysis both *in vitro* and *in vivo* (326). PVR is the ligand for the DNAM-1 receptor, therefore as a proof-of-concept, Nutlin-3a treatment has subsequently been shown to improve DNAM-1 CAR NK cell cytotoxicity against neuroblastoma cell lines (325). This proof-of-concept study provides justification for sensitising cancer cells to NK with anti-cancer agents followed by specific immunotherapy treatments.

How anti-cancer therapies effect cellular processes in different cancer types requires consideration and this is particularly true with ionising radiation which has been shown to differentially effect the expression of NK cell ligands in different malignancies (399). Irradiation of melanoma cells lines downregulates HLA-E expression (400) while HLA-E expression is enhanced in glioblastoma (54). Irradiation has also been shown to impact the expression of NKG2D ligands and death receptors to promote an NK cell immune response against tumours (399).

Another important aspect to investigate with anti-cancer agents and radiation therapy is the effect on intrinsic NK cell function and viability. Although cancer cells are more vulnerable to the disruption of biological processes due to their dependency on particular pathways, anti-cancer treatments are not cancer-specific, they target proteins and pathways that overlap with healthy cells. As such, it is important to consider the effect on NK cell function and indeed irradiation has been shown to facilitate and impede NK cell function (54,400). The drug lenalidomide, which inhibits the transcription factors IKZF1 and IKZF3 that are important for B cell function, potentiates NK cell function and proliferation alongside inducing intrinsic toxicity in CLL cells (401). Moreover, CD20 expression on CLL cells increases with lenalidomide and therefore can potentiate ADCC by rituximab (401).

Besides enhancing activating ligand expression, anti-cancer agents can downregulate inhibitory ligands to promote NK cell activation. Bortezomib, a proteasome inhibitor approved for multiple myeloma, is able to sensitise tumour cells to NK cell cytotoxicity through increased death receptor expression and bortezomib treatment combined with NK cell adoptive transfer improves survival of leukemic mice (402). But recently it was shown that proteasome inhibition downregulates HLA-E expression as an additional mechanism to activate NK cells (403). The cyclin-dependent kinase inhibitor dinaciclib approved for acute myeloid leukaemia also downregulates HLA-E promoting an NKG2A+ NK cell immune response against cell lines *in vitro*, *in vivo* and against primary patient samples (404). In an opposite but similar manner, dasatinib, a tyrosine kinase inhibitor used in chronic myeloid leukaemia, potentiates NK cell activation due to downregulation of NKG2A on patient NK cells enabling NK cells to evade HLA-E-mediated suppression (405). This study also highlights the importance of understanding how anti-cancer agents impact NK cells, not only in terms of function but also in terms of receptor expression.

It is clear from these studies that small molecule cancer therapies can possess NK cell immunomodulatory activity. Knowledge of how the immune system is sensitised by these agents will enable the design of potent immunotherapy combination strategies. A plethora of other compounds may also possess NK cell immunomodulatory activity. Studies describing changes in the tumour immune landscape with anti-cancer agents are suggestive of immunomodulatory activity, but detailed functional and mechanistic studies are required to understand how anti-cancer agents

promote specific immune cell responses. For example, the exportin-1 (XPO1) inhibitor selinexor increases the abundance of NK cells in the TME in murine models of melanoma (406,407) and in human studies, it has been suggested that XPO1 inhibition can modulate the immunogenicity of multiple myeloma cells to NK-stimulating immunotherapy (408). However, how XPO1 inhibition regulates the interactions of immune cells with cancer cells remains to be determined.

## 1.9 Exportin-1 and selective inhibitors of nuclear export (SINE)

### 1.9.1 The function of Exportin-1

Nuclear export is a physiologically important process for the control of gene expression, protein translation and signalling cascades by the spatial distribution of transcription factors, RNA, ribosomal constituents and signalling proteins (409). Transfer of material between the cytoplasm and nucleus is controlled by karyopherins, a GTPase family of proteins consisting of importins, exportins and biportins that recognise specific motifs within cargo (410).

The primary structure of XPO1 consists of 21 tandem HEAT domain repeats that possess two hairpin alpha helices (A and B) which fold XPO1 into a ring shape with A helices forming the outer ring and B the inner (**Figure 1-10A**). The specific function of XPO1 is to transport cargo that contain a leucine-rich nuclear export signal sequence (NES) in its hydrophobic pocket which is located in HEAT domains 11 and 12 (411) (**Figure 1-10A**). XPO1 cargo shuttling is controlled by ras-related nuclear protein GTP (RanGTP) (**Figure 1-10**) in which a gradient is established between the nucleus and cytoplasm regulated by nuclear Ran GTPase-activating protein which catalyses RanGTP from RanGDP. A higher concentration of RanGTP in the nucleus enables XPO1:cargo to transit to the cytoplasm through the nuclear pore complex. Hydrolysis of RanGTP to RanGDP by Ran guanine nucleotide exchange factor dissociates cargo from XPO1.

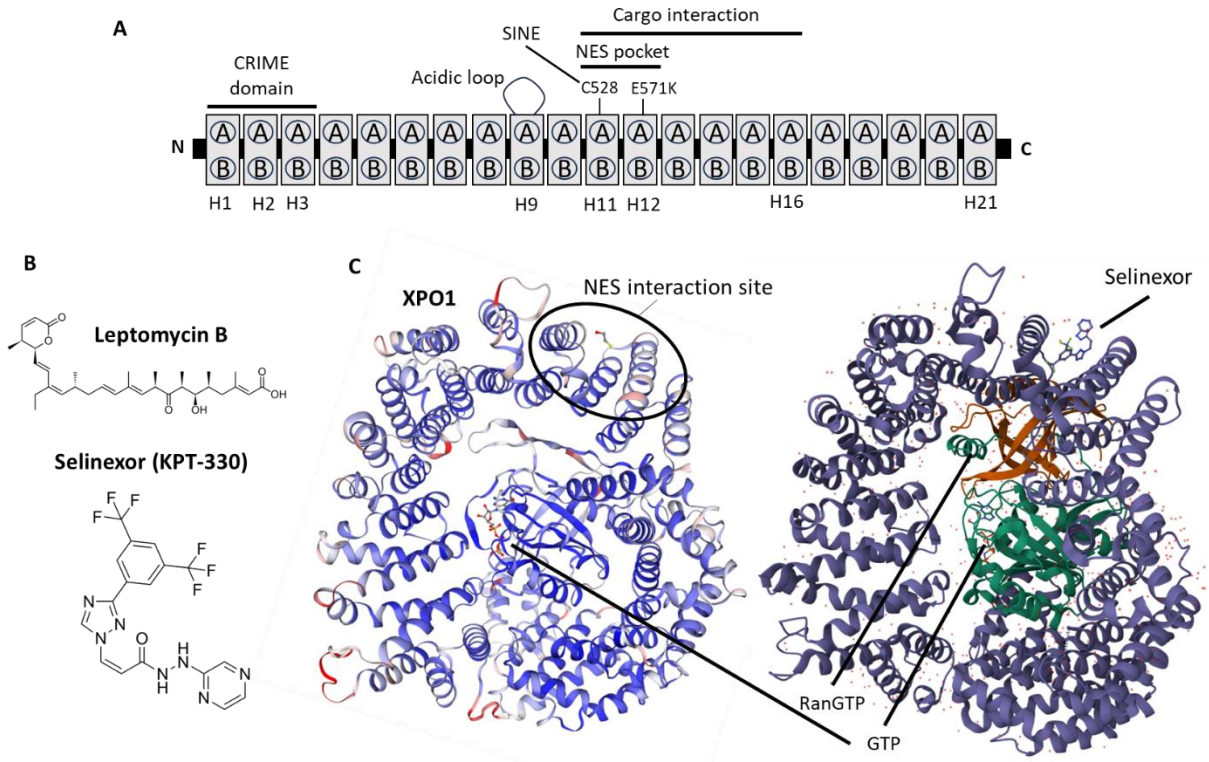


**Figure 1-10: XPO1 structure and SINE interactions with XPO1.**

(**A**) Primary protein structure of XPO1 which consists of 21 tandem repeat HEAT domains which each produce two alpha-helix structures A and B. At the N-terminus end is a CRIME domain which interacts with RanGTP, in H9 there is an acidic loop which also aids RanGTP interactions and inhibits cargo binding in the absence of RanGTP. The nuclear export signal (NES) interaction pocket resides in H11-H12 where cargo proteins containing an NES sequence are recognised and the interface of cargo interactions span H11-H16 domains. SINE compounds interact with the cysteine residue 528 to inhibit cargo recognition and the frequent cancer driver mutation E571K (glutamate to lysine substitution) is located within the NES pocket to aid stronger interactions with cargo, but critically it does not impede SINE action. (**B**) Shown is the structure of SINE molecules Leptomycin B and selinexor (KPT-330) adapted from Crochiere et al., (2015) and Ferreira et al., (2020). (**C**) Crystal structures of XPO1 with the NES interaction site displayed in the absence (left) and presence (right) of selinexor. Also shown is the interaction of XPO1 with RanGTP. Crystal structures of XPO1 in contact with selinexor are derived from Walker et al., (2021) and were created with NGL (415).

Over 200 proteins have been identified to interact with XPO1. These include key tumour suppressor proteins p53, Rb, p21, FOXO and I-κB (416–419). XPO1 has also been shown to transport ribosomal RNA (rRNA) to aid protein translation (420) (**Figure 1-11**). Reports also indicate that XPO1 regulates the expression of oncogenes including *Myc* and *cyclin D1* through the indirect shuttling of mRNA into the cytoplasm which promotes cell proliferation (421). Additionally, XPO1 aides the amplification of cell signalling including NF-κB via the export of the NF-κB inhibitor I-κB (422) and IFNγ signalling by

the export of dephosphorylated STAT-1 (38) into the cytoplasm to enable re-activation of STAT-1 by JAK1/2 downstream of the IFNγ receptor (**Figure 1-2**).

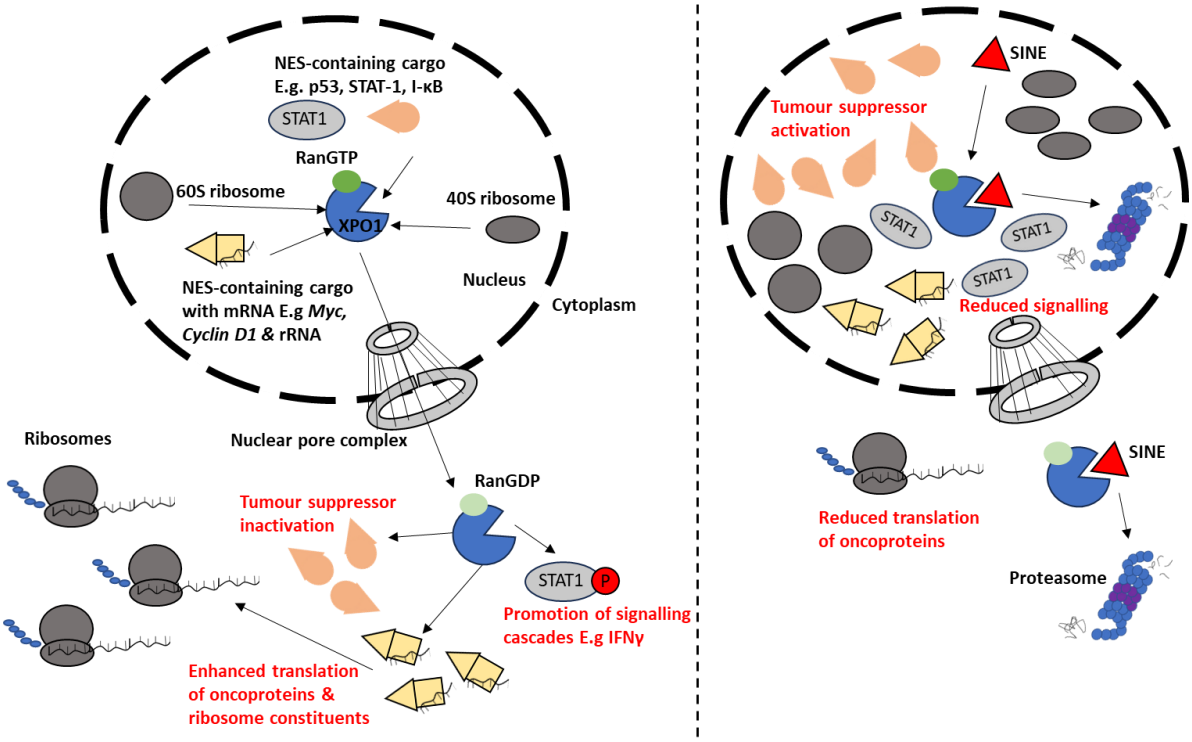


**Figure 1-11: The function of XPO1 and the mechanism of action of SINE compounds.**

(Left) XPO1 transports protein cargo with a nuclear export signal sequence (NES) in a GTP-dependent mechanism from the nucleus into the cytoplasm which includes tumour suppressor proteins such as p53. XPO1 also exports ribosome constituents and RNAs indirectly via binding to NES-containing protein cargo including oncogenic mRNA such as *Myc*. Once in the cytoplasm, the transcription factor function of tumour suppressor proteins is inhibited, and protein translation of oncogenic mRNA is enhanced resulting in increased cancer cell survival and enhanced proliferation. XPO1 also exports proteins involved in signalling cascades and can therefore perpetuate inflammatory signalling such as with IFNγ via STAT-1 cytoplasmic shuttling. (Right) Through using SINE compounds, tumour suppressors accumulate in the nucleus and the translation of oncoproteins is inhibited resulting in cancer cell apoptosis and reduced proliferation. Signalling cascades can be impaired for example through the nuclear accumulation of unphosphorylated STAT-1. Depending on the SINE compound, XPO1 can be degraded by the proteasome.

### 1.9.2 Exportin-1 in cancer

XPO1 expression can become dysregulated during oncogenesis through amplification of the *XPO1* gene (423,424), and via mutations in the cargo-binding domain which promote stronger interactions with cargo and alters the XPO1 interactome (425,426). As a consequence, tumour suppressor proteins become inactivated through enhanced export from the nucleus which promotes cancer cell survival. Additionally, cell proliferation is enhanced via the export of cell cycle regulator mRNA and via the export of ribosomal constituents to enable sufficient protein production for cell growth.

Mutations within the NES-interacting cleft of XPO1, such as the frequently observed E571K mutation in B-cell malignancies (414), can act as a driver of oncogenesis (427). Injection of CLL cells expressing the E571K *XPO1* mutation in mice result in increased tumour burden and reduced survival (427). Within CLL patients, the mutation was responsible for increasing mutational and epigenetic burden in cancer cells so that tumours acquire further DNA changes and modifications to drive cancer phenotypes (414) and recently *XPO1* mutations were reported in the late stages of CLL enabling expansion of CLL clones highlighting a clonal advantage conferred by *XPO1* mutation (428). Moreover, XPO1 expression is linked to the survival and treatment outcomes of cancer patients. High XPO1 expression is an unfavourable prognostic factor in CLL (429) and is often upregulated in DLBCL and multiple myeloma and is associated with poor prognosis and drug resistance (430). In GCB-DLBCL, high expression of *XPO1* is associated with shorter progression-free survival and overexpression of XPO1 was found to be overrepresented in the resistant/relapsed subgroup of DLBCL patients (431). XPO1 overexpression is also associated with worse outcome across solid malignancies including pancreatic adenocarcinoma (432) and hepatocellular carcinoma (433). Furthermore, XPO1 has also been linked to resistance across multiple cancer types including multiple myeloma resistance to the proteasome inhibitor bortezomib (434) and resistance to ibrutinib treatment in MCL and CLL (424). *XPO1* knockout by CRISPR in DLBCL is lethal, highlighting the importance of XPO1 function to malignant B cell survival (435,436). Therefore, molecules to suppress XPO1 function were designed to restore tumour suppressor protein function and inhibit translation of oncogenic proteins.

### 1.9.3 SINE compounds

The hydrophobic pocket of XPO1 makes an ideal druggable target, hence small molecules were designed to block the interaction of XPO1 with the NES of cargo. Collectively these drugs are referred to as selective inhibitors of nuclear export (SINE). Naturally occurring compounds that block XPO1 function assisted the design of XPO1 inhibitors and the incubation of B-cell lymphoma cell lines, multiple myeloma cells and primary CLL cells with SINEs induce apoptosis of cancer cells (437,438). Leptomycin B (LMB) is an anti-fungal antibiotic from *Streptomyces* that targets XPO1 to cause cell

cycle arrest and induce anti-tumour effects in murine tumour models (439). However, LMB is not advised for human use due to potent toxicity observed in phase I clinical trials (440). As a result, synthetic SINEs were designed to improve *in vivo* tolerance (441) (**Figure 1-10B**). SINEs covalently bind to the Cysteine 528 residue in the hydrophobic pocket of XPO1 (**Figure 1-10A and C**), however in a slower and reversible manner unlike LMB (442–444). Another dissimilarity between LMB and synthetic SINEs is that synthetic SINEs induce the degradation of XPO1 via the proteasome (445). One SINE, selinexor, produced favourable anti-tumour responses with fewer toxic side effects compared to LMB (446). Selinexor is a first-in-class SINE compound that is licenced for the treatment of relapsed and refractory DLBCL (FDA-approved) and relapsed and refractory multiple myeloma. Currently, selinexor is in clinical trials as a single agent and in combination with approved treatments in many solid and haematological malignancies (447). Of specific interest, XPO1 inhibition is undergoing clinical investigation for CLL in combination with ibrutinib (NCT02303392) which has shown improved tumour regression in patients (448). This combination was based on data illustrating that XPO1 inhibition successfully overcomes ibrutinib resistance in mouse models of CLL (449).

As with many anti-cancer agents selinexor induces adverse side effects, most frequently gastrointestinal toxicities (409,450). As a result, next generation XPO1 inhibitors are in development to circumvent these adverse events. Eltanexor is a second generation SINE compound which has shown reduced toxicity in pre-clinical mouse models compared to selinexor (451). As a result, eltanexor is in phase I clinical trials for multiple relapsed and refractory cancers including multiple myeloma and AML (NCT02649790). Another strategy to reduce selinexor side effects is through combination with immunotherapies to enable a reduction in selinexor dosage and dosing schedule and currently selinexor is in clinical trials with immunotherapies in haematological (**Table 1-2**) and solid cancer indications (**Table 1-3**). Additionally, combination therapy may help to avoid the development of tumour resistance to selinexor.

**Table 1-2: Clinical trials assessing the combination of selinexor with immunotherapy in haematological malignancies.**

| Disease | Immunotherapy combination | NCT number | Status | Phase |
|---|---|---|---|---|
| Double hit & triple hit Lymphoma | Rituximab + CHOP | NCT05974085 | Recruiting | II |
| B cell lymphoma | Rituximab | NCT02741388 | Completed | I |
| DLBCL | Rituximab | NCT02471911 | Completed | I |
| EBV+ DLBCL | Rituximab + CHOP | NCT05577364 | Recruiting | I/II |
| DLBCL & indolent NHL | Rituximab | NCT05265975 | Recruiting | I/II |
| RR B-NHL | Anti-CD19 CAR T | NCT05322330 | Unknown | II |
| RR-DLBCL | Rituximab | NCT04442022 | Recruiting | II/III |
| GCB-DLBCL | Rituximab | NCT05422066 | Recruiting | II |
| R/RCLL NHL | Ibrutinib | NCT02303392 | Completed | I |
| Multiple myeloma (MM) | Daratumumab | NCT04661137 | Recruiting | II |
| | Lenalidomide | NCT05422027<br>NCT04941937 | Recruiting<br>Recruiting | I/II<br>II |
| | Elotuzumab | NCT05028348 | Recruiting | III |
| | Lenalidomide<br>Daratumumab<br>Elotuzumab<br>Belantamab Mafodotin | NCT02343042 | Active, not recruiting | I/II |
| Refractory MM | Daratumumab | NCT03589222<br>NCT04756401 | Unknown<br>Recruiting | II<br>II |
| | Lenalidomide | NCT04519476 | Recruiting | I |
| Relapsed MM | Daratumumab | NCT04925193 | Recruiting | II |
| Newly diagnosed MM | Lenalidomide | NCT04717700 | Recruiting | II |
| High risk, newly diagnosed MM | Daratumumab | NCT06169215 | Recruiting | II |
| MM with extramedullary disease | Lenalidomide | NCT05900882 | Recruiting | II |
| RR extramedullary MM | Anti-BCMA CAR T | NCT05201118 | Recruiting | I/II |
| MM & myeloma-associated amyloidosis | Lenalidomide | NCT05820763 | Recruiting | II |
| Advanced malignancy | Ipilimumab<br>Nivolumab<br>Pembrolizumab | NCT02419495 | Active, not recruiting | I |

**Table 1-3: Clinical trials assessing the combination of selinexor with immunotherapy in solid malignancies.**

| Disease | Immunotherapy combination | NCT number | Status | Phase |
|---|---|---|---|---|
| Solid tumours | Pembrolizumab | NCT04256707 | Recruiting | I/II |
| HCC | Bevacizumab & Atezolizumab | NCT05093608 | Terminated | I |
| Metastatic solid malignancy | Nivolumab + ipilimumab | NCT04850755 | Recruiting | I |
| Urothelial carcinoma | Pembrolizumab | NCT04856189 | Ongoing | I/II |
| Recurrent advanced melanoma | Pembrolizumab | NCT04768881 | Ongoing | II |

### 1.9.4 The effects of XPO1 inhibition on immune cell functions

Alongside the role of XPO1 in driving oncogenesis and being negatively associated with cancer outcomes and drug resistance, XPO1 expression has been linked to an anti-inflammatory tumour microenvironment (TME). RNA-seq analysis of 4,665 DLBCL patient tumours revealed a negative correlation between *XPO1* expression and IFNγ signalling which suggests either a disruption in the number of immune cells in the TME or impaired immune responses and indeed high *XPO1* expression was associated with immune deficiency (431). A lympho-depleted TME was also observed for gain-of-function mutations of *XPO1* in GCB-DLBCL patients (452). An in-depth analysis of *XPO1* expression across multiple tumours also revealed negative associations between *XPO1* expression and immune responses. Decreased activated NK cells and decreased CD8+ T cell abundance was noted with increased expression of *XPO1,* alongside increased expression of inhibitory checkpoints suggesting that XPO1 permits an immunosuppressive TME (453). The E571K *XPO1* driver mutation which is present in approximately 5% of CLL cases and 30% of CLL cases progressing to Richter's syndrome, is associated with impaired IFNγ, granzyme B and CD28 expression and this may contribute to the impaired immune function in CLL patients (414,454). Together, these studies indicate that XPO1 expression and function may contribute to generating an immunosuppressive TME and thus by impeding XPO1 function an anti-tumour immune response may be restored.

As with many anti-cancer agents outlined in section 1.8, emerging evidence suggests that XPO1 inhibition induces an anti-tumour immune response alongside producing intrinsic anti-tumour effects. Selinexor has been shown to polarise macrophages from pro-tumourigenic M2-like macrophages to anti-tumourigenic M1-like macrophages (455) in addition to selective depletion of lymphoma-associated macrophages (456). Neutrophil extracellular trap formation has been

illustrated to promote metastasis and XPO1 inhibition was shown to impede trap production (457). Modulation of the adaptive immune system by XPO1 inhibition has been shown for B-cell malignancies. Selinexor has been shown to sensitise breast cancer cells to T cell activation in combination with TRAIL-R2xCD3 bispecific antibodies (458). In terms of adoptive transfer therapies, pre-treatment of malignant B cell lines with selinexor enhance the activation of anti-CD19 CAR T cells *in vitro* (459) and sequential administration of selinexor and CAR T cells enhance tumour regression in mice (460). Because of these results, selinexor is gaining traction as a bridging therapy for CAR T infusion during the weeks-long process of apheresis and autologous CAR T cell generation. Indeed, sequential selinexor administration followed by anti-CD19 CAR T cell (461) or anti-BCMA CAR T cell (462) infusion led to responses in 4/6 NHL patients and deep-remission in two multiple myeloma patients, respectively. The mechanism behind sensitisation of malignant B cells and plasma cells to CAR T cells remains undefined.

In contrast, the effect of XPO1 inhibition on the immunogenicity of cancer cells to NK cells remains largely unknown. In melanoma-bearing mice, selinexor increases the abundance of NK cells in the tumour microenvironment (406). NK cell infiltration in the bone marrow has been reported to be an indicator of myeloma patient response to selinexor treatment which through combination with NK cell immunotherapy approaches may bolster tumour regression (463). But whether XPO1 inhibition modulates NK cell function is unknown. This research project therefore sought to uncover the functional consequences of XPO1 inhibition on NK cell activation against multiple myeloma and malignant B cells, including DLBCL, for which selinexor is approved. Ultimately, this research project will provide evidence that through understanding of how small molecules such as XPO1 inhibitors promote immune responses, tailored anti-cancer combinations can be designed to promote the most potent anti-tumour responses.

## 1.10 Study hypothesis, aims and objectives

It was hypothesised that XPO1 inhibition sensitises malignant B cells and multiple myeloma cells to NK cell activation via modulation of surface proteins that engage NK cell activating and inhibitory receptors. As such, it was further hypothesised that the first-in-class, FDA-approved XPO1 inhibitor selinexor would augment the effects of NK-stimulating immunotherapies including direct targeting monoclonal antibodies, allogeneic, expanded NK cells and CAR NK cells. This research project has the following aims and objectives:

1. Determine whether XPO1 inhibition modifies NK cell anti-tumour functions against malignant B cells and multiple myeloma cells.
    - To evaluate the sensitivity of malignant B cells and multiple myeloma cells to NK cell activation and NK cell cytotoxicity with XPO1 inhibition, DLBCL, mantle cell lymphoma, Burkett's lymphoma and multiple myeloma cell lines will be treated with XPO1 inhibitors and co-cultured with NK cells. The expression of NK cell activation markers CD107a/LAMP and IFNγ will be assessed as well as cancer cell death via propidium iodide staining.
    - Malignant B cells derived from patients with CLL will also be used in co-culture experiments as a primary human cancer model to determine whether XPO1 inhibition sensitises primary leukemic cells to NK cell anti-tumour functions.

2. Underpin the mechanism for changes in NK cell function following co-culture with selinexor-treated cancer cells.
    - An XPO1-derived peptide presented on HLA-C has been shown by the research group to selectively activate the KIR2DS2 receptor expressed by NK cells (171). Therefore, to explore whether XPO1 degradation by selinexor selectively activates KIR2DS2+ NK cells, NK cells from donors with the KIR2DS2 gene will be co-cultured with selinexor-treated cancer cells to compare activation between KIR2DS2+ and KIR2DS2- NK cells.
    - To identify other NK-stimulating/inhibitory mechanisms of XPO1 inhibition, cancer cells will be screened for changes in the surface expression of activating and inhibitory NK cell ligands by flow cytometry post XPO1 inhibition. Additionally, leptomycin B which inhibits XPO1 function but does not cause XPO1 degradation (442) will be used to investigate XPO1 peptide-independent mechanisms for changes in NK cell function.

3. Assess the combination of selinexor with immunotherapies that promote NK cell function.
    - ADCC against selinexor-treated cancer cells will be assessed by using the clinically approved direct targeting anti-CD20 mAbs rituximab and obinutuzumab and the anti-CD38 mAb daratumumab.

- To mimic allogeneic NK cells that are used for adoptive transfer therapy, NK cells will be expanded for two weeks with IL-2 and the activation, cytotoxicity and IFNγ production of these cells in combination with selinexor will be assessed.
- To assess the function of CAR NK cells against selinexor-treated cancer cells, anti-CD19 CAR NK cells derived from the peripheral blood of healthy donors will be generated using the third-generation lentiviral transduction system. Anti-CD19 CAR NK cell activation and cytotoxicity against selinexor-treated CD19+ cancer cells will then be investigated.

4. Examine the effect of microenvironmental support on the immunomodulatory function of XPO1 inhibitors in 2D cancer models.
    - To mimic the lymph node microenvironment, B cell lymphoma cell lines and primary CLL cells will be incubated with IL-4 and CD40L in the presence of selinexor and assessed for the expression of NK cell ligands. Co-culture assays will be used to measure NK cell activation and cytotoxicity in this setting.
    - To mimic a pro-inflammatory tumour microenvironment, lymphoma and myeloma cell lines will be incubated with recombinant IFNγ in the presence of selinexor and assessed for changes in NK ligand expression and co-cultured with NK cells to measure NK cell activation and cytotoxicity.

# Chapter 2 Materials and Methods

## 2.1 Cell culture

### 2.1.1 Peripheral blood mononuclear cell (PBMC) isolation

Ethical approval for the use of healthy donor peripheral blood mononuclear cells (PBMC) was obtained from the National Research Ethics Committee (ERGO ID: 86319.A1, reference 06/Q1701/120). To extract PBMC, fresh blood from healthy volunteers or blood cones (from University Hospital Southampton blood bank) was layered over 15 mL of ficoll (GE Healthcare) and centrifuged at 2000 rpm for 20 min with accelerator and brake off. The buffy coat layer containing PBMC was extracted and washed three times in phosphate buffer saline (PBS, Lonza) and centrifuged at 1500 rpm for 5 min with accelerator and brake on after each wash. PBMC were then cryopreserved in heat inactivated foetal bovine serum (FBS) with 10% DMSO (Sigma) for use in future experiments outlined below.

### 2.1.2 Culture of cancer cell lines and NK cell lines

All B cell lymphoma cell lines representing diffuse large B cell lymphoma (SUDHL4, SUDHL6), Burkitt's lymphoma (JeKo-1) and mantle cell lymphoma (Raji, Ramos) and multiple myeloma cells L363, JJN3 and AMO were cultured in R10 medium (RPMI 1640 [Gibco] plus 1% penicillin-streptomycin [Life Technologies] and 10% heat inactivated FBS) and split to $0.5x10^6$ cells/mL every ~2/3 days when cells reached confluency ~$2x10^6$ cells/mL. Semi-adherent multiple myeloma cell lines MM.1S, RPMI-8226 and U266 were also cultured in R10 and split every ~2/3 days, but these cells required light scraping to detach loosely adhered cells. Confluency was based on appearance under the microscope.

The variants of the 721 B lymphoblastoid cell line 721.221 (HLA-A/B/C negative) and 721.174 (TAP deficient) were cultured in R10 medium and split to $0.3x10^6$ cells/mL every ~2/3 days including complete replenishment of fresh medium once per week.

NK cell lines NK92 and NKL were cultured in R10 supplemented with 1X sodium pyruvate (Invitrogen), 1X non-essential amino acids (Invitrogen) and 100 IU/mL IL-2 and split every ~2/3 days.

### 2.1.3 Purification of NK cells

CD3-CD56+ NK cells were purified from fresh or cryopreserved PBMC using the Miltenyi human NK cell isolation kit following the manufacturer's instructions. Briefly, PBMC were resuspended in MACS buffer (1X PBS, 2 mM EDTA [Invitrogen], 0.5% bovine serum albumin [BSA, Sigma]) and negatively

selected for using LS columns (Miltenyi) after antibody cocktail and magnetic bead incubation. NK cells were subsequently cultured in R10 medium at a density of $2x10^6$ cells/mL and incubated with 1 ng/mL IL-15 (R&D Systems) over night before use in the NK cell specific lysis assay the next day.

### 2.1.4 Allogeneic NK cell expansion

NK cells were isolated from healthy donor PBMC as described above using magnetic bead isolation on day 0 followed by resuspension in NK MACS medium supplemented with 1% MACS supplement, 5% human serum and 500 IU/mL IL-2 at a cell concentration of $10^6$/mL in 700 µL and plated in a 24 well plate. On day 5, 300 µL medium was added to wells. On day 7, 10, 12 and 14 NK cells were counted and split to $0.5x10^6$ cells/mL. From day 14-21, NK cells were split every 2/3 days to $0.5x10^6$ cells/mL and used in experiments outlined in this section.

### 2.1.5 Isolation of chronic lymphocytic leukaemia (CLL) cells from patient PBMC

PBMC from CLL donors were collected from patients attending the clinic at Southampton General Hospital. Patients were recruited to the "real-world" observational study at the University of Southampton (NIHR/UKCRN ID: 31076, CI F. Forconi) and the characteristics of the patients used in the study can be found in **Table 2-2**. Cancer Research UK staff processed the PBMC and performed phenotype analysis to obtain information on CD5+CD19+ CLL cell frequency, *IGHV* mutational status and expression level of surface markers including IgM, CD38 and CD49. Phenotype information was inputted into an online database for cross referencing. If the percentage of CLL cells (CD19+CD5+) < 90% of total PBMC as detailed on the online database, CLL cells were isolated by magnetic bead extraction using the Miltenyi human B-CLL cell isolation kit (catalogue number 130-103-466) following the manufacturer's instructions. CLL cells were cultured at $10x10^6$ cells/mL in R10 medium for at least 1 hour before treatment with selinexor described below.

## 2.2 Drug treatments

### 2.2.1 SINE treatment and Q-VD-OPh (Q-VD) incubation

Malignant B cell lines and multiple myeloma cells were plated at $10^6$ cells/mL and incubated with 50, 500 or 2000 nM selinexor (KPT-330, gift from Karyopharm® Therapeutics), eltanexor (KPT-8602) or 50 nM Leptomycin B (Sigma) to inhibit exportin-1 (XPO1). Cell lines were treated with DMSO as a control and cells were incubated at 37°C for 24 hours. CLL cells were treated with selinexor as described, but CLL cells were seeded at $10x10^6$ cells/mL. To inhibit SINE-induced apoptosis, cancer cells were co-

incubated with Q-VD-OPh (QVD, Sigma), a pan-caspase inhibitor, at the concentrations stated in figure legends.

### 2.2.2 Selinexor in combination with BTK inhibitors

CLL cells were treated with selinexor as above in combination with 1 μM BTK inhibitors (BTKi) ibrutinib or acalabrutinib (Selleckchem) for 24 hours at 37°C. After, CLL cells were examined for expression of NK cell ligands and used in the NK specific lysis assay. To measure NK cell activation in the presence of BTKi, after 24-hour drug treatments CLL cells were co-cultured with healthy donor PBMC in the presence of selinexor and/or BTKi and used in the LAMP assay.

## 2.3 Phenotyping experiments of NK cell lines and primary NK cells and cancer cells post XPO1 inhibition

### 2.3.1 Surface expression of NK cell ligands on SINE-treated cancer cells

Cancer cell lines and CLL cells were incubated with Q-VD plus selinexor or leptomycin B or DMSO control as above. The following day FcRs were blocked using 10% human serum (15 minutes, 4°C) after which cells were surface stained for 30 minutes in the dark at 4°C with antibodies against activating NK cell ligands: Vimentin-A488 (clone 280618, R&D Systems), ULBP-1-PE (170818, R&D Systems), ULBP-2/5/6-PerCP (165903, R&D Systems), CD54-PB (HCD54), B7H6-APC (875001, R&D Systems) and MICA/B-PE/Cy7 (6D4) or with antibodies against HLA proteins: HLA-E-PE/Cy7 (3D12) and HLA class I molecules (anti-HLA-A/B/C [W6/32], referred throughout at pan-HLA/total HLA/HLA-A/B/C). Antibodies were purchased from Biolegend, unless stated otherwise and antibody concentrations can be found in supplementary table 1. Cell events were acquired on an Aria II (BD Biosciences) flow cytometry machine using FACSDiva software (BD Biosciences) and NK cell ligand expression was analysed on FlowJo™ v10 (Treestar).

### 2.3.2 Surface expression of activating and inhibitory receptors on NK cells

To phenotype primary NK cells and NK cell lines NK92 and NKL, cells were incubated with 10% human serum for 15 minutes at 4°C to block FcRs after which cells were stained with antibodies against CD56-PE/Cy7 (clone HCD56), NKG2A-FITC (REA110), NKG2C (REA205), NKG2D (1D11), CD16-APC (3G8) and CD96 (NK92.39) for 30 minutes in the dark at 4°C after which cells were resuspended in FACS wash before being run on a FACS Aria II.

### 2.3.3 Acid strip experiments to measure the recovery of HLA proteins at the plasma membrane

Cancer cell lines were treated with selinexor and QVD as previously described for 24 hours. Cells were then washed in strip wash buffer (10% FBS in PBS), spun at 1500 rpm for 3 minutes before being resuspended in 0.1M citrate buffer (pH 3.0, distilled water with 0.131M citric acid, 0.066M sodium phosphate and 1% BSA) at 1 mL per $10^6$ cells to strip HLA molecules from the surface of cells. After 1.5 minutes in citrate buffer, cells were washed with 5x volume of strip wash buffer and spun at 1500 rpm for 3 minutes. Cells were washed once more in strip wash buffer (1 mL per $10^6$ cells) before being resuspended in R10 medium at $10^6$ cells/mL. Some cells were taken for BFA treatment (10 µg/mL) as a positive control for no HLA recovery at the plasma membrane. HLA-stripped cells were incubated at 37°C and cells were taken for HLA FACS staining at the following timepoints: 0 hrs, 0.5, 1, 2, 4 and 6. At these timepoints, FcRs were blocked with 10% human serum for 15 minutes at 4°C followed by surface staining with antibodies against HLA-E-PE/Cy7 (clone 3D12), HLA-A/B/C-A488 (pan-HLA, W6/32) and CD19-PB (HIB19) for 30 minutes at 4°C.

## 2.4 Co-culture experiments to examine NK cell activation and cytotoxicity

### 2.4.1 NK cell specific lysis (cytotoxicity) assay

Immediately before Q-VD and selinexor treatment, cancer cells were labelled with CellTrace™ Violet/FarRed Cell Proliferation Kit (Invitrogen™) following the manufacturer's instructions. Briefly, CellTrace was resuspended in 20 uL of DMSO which was then diluted 1:5000 in 1X PBS. Cancer cells were then resuspended in this diluted solution as 1 mL per $1x10^6$ cells and placed at 37°C for 15 minutes. After, 2x volume of R10 medium was added to inhibit the labelling reaction for 5 minutes at RT before being resuspended in R10 medium at $1x10^6$ cells/mL and treated with anti-cancer agents as above. The day after cancer cell treatment, NK cells (cell lines, IL-15 overnight or day 14-21 IL-2 expanded NK cells) were co-cultured with tumour targets at an effector: target ratio (E:T) of 5:1, 1:1 or 1:10 for 4 or 24 hours at 37°C as stated in figure legends. After co-culture, cells were washed in 1X PBS and stained with 1.6 µg/mL propidium iodide (Invitrogen™) to identify lysed, violet/FarRed-labelled cancer cells by flow cytometry using the FACS Aria II or BD Accuri c6 machines.

### 2.4.2 Degranulation (CD107a/LAMP) assay and measuring IFNγ production

When using healthy donor PBMC, these cells were incubated overnight with 1 ng/mL IL-15 at a cell density of $2x10^6$ cells/mL. When using IL-2 expanded NK cells, these were used at day 5 or from day

14-21 during expansion as stated in figure legends. PBMC were subsequently co-cultured for 4 hours at 37°C with selinexor- or leptomycin B-treated cancer cell lines at an E:T of 5:1, unless otherwise stated in figure legends, or at an E:T of 1:1 with CLL cells. Expanded NK cells were co-cultured with cancer cells at an E:T of 1:1 or 1:10 for 4 or 24 hours as stated in figure legends. Immediately before co-culture, 0.17 µg/mL anti-CD107a (LAMP)-eFluor660 (clone eBioH4A3, Invitrogen) was added to PBMC/expanded NK cells. After 1-hour of co-culture, GolgiStop™ (1:2000 final dilution, Fisher Scientific) was added to allow measurement of surface CD107a by flow cytometry. Following 4-hour incubation, FcRs were blocked with 10% human serum at 4°C for 15 mins before surface staining with combinations of anti-CD3-PerCP (clone UCHT1), anti-CD56-PE/Cy7 (HCD56), anti-NKG2A-FITC (REA110, Miltenyi), anti-CD158ba (KIR2DL3)-FITC (REA147, Miltenyi) and anti-CD158b-PE (CH-L, BD Pharmingen) in FACS buffer (1X PBS, 1% BSA, 0.5% sodium azide) at 4°C for 30 min.

If continuing with analysis of IFNγ production, cells were permeabilised and fixed with BD Cytofix/Cytoperm (BD Biosciences) at 4°C for 20 min, washed with 1X Perm/Wash buffer (BD Biosciences) and stained with α-IFNγ-BV421/PE (RUO, BD Biosciences) at 4°C for 30 min. Cells were washed again with 1X Perm/Wash buffer and resuspended in FACS buffer or 1% paraformaldehyde (Alfa Aesar) in PBS for acquisition on an Aria II (BD Bioscience) machine. Antibodies were purchased from Biolegend unless otherwise stated and the concentrations of which are specified in **Table 2-3**.

### 2.4.3 Assessing XPO1 inhibition on ADCC

NK cell mediated ADCC was examined via the LAMP and cytotoxicity assays. For both experiments, immediately before co-culture of PBMC/NK cells with selinexor-treated cancer cells, cancer cells were incubated with 0.1 or 1 µg/mL anti-CD20 monoclonal antibodies (mAb) Rituximab or Obinutuzumab or 0.1 µg/mL Daratumumab (anti-CD38) or with an isotype control (anti-EGFR cetuximab) for 20 min at 37°C as stated in the figure legends. PBMCs/NK cells were added to cancer cells following the protocols outlined above.

To remove unbound anti-CD20 and anti-CD38 antibodies, after 20 minutes incubation of cancer cells with mAbs, cells were centrifuged at 1500 rpm for 5 minutes followed by resuspension with PBMC/NK cells.

### 2.4.4 Selinexor in expanded NK-cancer co-cultures

B-cell lymphoma cell lines were labelled with CellTrace™ and treated with selinexor (50-2000 nM) for 24 hours in the presence of Q-VD (30 µM). The next day these were co-cultured with IL-2 (500 IU/mL) expanded NK cells (14-21 days) at an E:T = 1:1 for 24 hours in the absence or presence of selinexor (50-2000 nM). B cell lines that were not pre-treated with selinexor for 24 hours were also co-cultured with IL-2 (500 IU/mL) expanded NK cells (14-21 days) at an E:T = 1:1 for 24 hours in the

presence of selinexor (50-2000 nM), resulting in three types of co-culture: 1) Selinexor pre-treated lymphoma cells + NK cells 2) selinexor pre-treated lymphoma cells + NK cells + selinexor and 3) lymphoma cells + NK cells + selinexor. After co-culture, cells were stained with propidium iodide to identify lysed CellTrace™ positive cancer cells in co-culture and NK specific lysis was then calculated. Dead expanded NK cells in co-cultures was also recorded via propidium iodide staining.

### 2.4.5 TRAIL blockade experiments

Prior to co-culture of healthy donor PBMC or purified NK cells with selinexor-treated CLL cells, NK cells were incubated with anti-TRAIL (RIK-2, Biolegend, 10 µg/mL) antibodies or isotype control for 20 minutes at 37°C. NK specific lysis of CLL target cells was then assessed using the cytotoxicity assay and NK activation via the LAMP assay.

### 2.4.6 NKG2A blockade experiments

Before the co-culture of expanded NK cells with selinexor-treated cancer cells in cytotoxicity experiments, NK cells were incubated with anti-NKG2A (Z199, Biolegend, 10 µg/mL) antibodies or isotype control for 20 minutes at 37°C. NK specific lysis of cancer target cells was then assessed using the cytotoxicity assay.

### 2.4.7 Autologous NK cell activation against CLL cells

CLL patients with low CD5+CD19+ CLL cell burden (<60%) within the lymphocyte PBMC population were treated with selinexor as above for 24 hours. The cultures contained all cells within the PBMC of CLL patients, including NK cells, allowing the activation status of NK cells to be assessed using the LAMP assay. To optimise CLL cells within the PBMC to NK cells, rituximab (1 µg/mL) or isotype control (cetuximab, 10 µg/mL) was added to cultures for 20 minutes prior to addition of selinexor.

## 2.5 Microenvironmental support experiments

### 2.5.1 CD40L and IL-4 lymph node support mimic

CD40L (300 ng/mL, R&D Systems) and IL-4 (10 ng/mL, R&D Systems) were added to CLL cells 1 hour prior to the addition of selinexor (0-2000nM) for a further 24 hours in the presence of 30 µM Q-VD. CLL cells were then either assessed for expression of surface ligands or co-cultured with PBMC and NK cell activation assessed by IFNγ production as described above.

Assessment of CLL cells that have recently egressed from the lymph nodes was performed by analysis of CXCR4 and CD5 expression. Patient CLL cells were thawed and rested for 1 hour at 37°C, then incubated with human serum for 15 minutes at 4°C and subsequently stained with antibodies for CD19-BV510 (clone HIB19), CD5-APC (UCHT2), HLA-E-PE/Cy7 (3D12), pan-HLA (W6/32) and CXCR4-PE (12G5) before acquisition on a BD FACS Aria II (BD Biosciences) flow cytometer.

### 2.5.2 Treatment of tumour cells with recombinant human IFNγ or supernatant from NK-cancer co-cultures

If necessary, cancer cell lines were treated with selinexor and QVD as previously described. 30 minutes after addition of selinexor, 10 ng/mL recombinant human IFNγ (R&D Systems, cat #285-IF-100) was added to cells plated at $10^6$ cells/mL. Cells were then incubated for 24 hrs at 37°C before use in NK cytotoxicity, activation, NK ligand expression experiments or western blot analysis. For treatment with supernatants from NK-cancer co-cultures, 200,000 IU/mL IL-2 expanded NK cells were co-cultured with 200,000 cancer cells (E:T = 1:1) for 24 hrs at 37°C. The next day, co-cultures were centrifuged at 1500 rpm for 5 minutes and the supernatants were taken and used to resuspend corresponding cancer cells which were pelleted by centrifugation. Selinexor was then added to cancer cells and cells were incubated for 24 hrs at 37°C after which HLA-E and HLA-A/B/C surface expression was assessed on cancer cells. Tumour cells were then screened for expression of HLA molecules and/or used in NK cytotoxicity/activation experiments as above in addition to being lysed for western blot analysis of XPO1, STAT, pSTAT and HLA-E.

### 2.5.3 HLA expression on intact and permeabilised cancer cells

Cancer cell lines were treated with QVD, selinexor and recombinant IFNγ as previously described. After treatment, some cancer cells were taken for permeabilization using the BD Cytofix/Cytoperm (BD Biosciences) kit. Briefly, cells were first incubated with 10% human serum to block FcRs, centrifuged at 1500 rpm at 4°C for 5 minutes followed by resuspension in Cytofix/Cytoperm buffer for 20 minutes at 4°C. Cells were then washed with 1X Perm/Wash buffer (BD Biosciences) and stained with antibodies against HLA-E-PE/Cy7 (clone 3D12), HLA-A/B/C-A488 (pan-HLA, W6/32) and CD19-PB (HIB19) for 30 minutes at 4°C in 1X Perm/Wash buffer. Cells being assessed for surface expression of HLA molecules were incubated with 10% human serum, pelleted and resuspended in HLA-E-PE/Cy7 (clone 3D12), HLA-A/B/C-A488 (pan-HLA, W6/32) and CD19-PB (HIB19) for 30 minutes at 4°C in FACS wash buffer. Finally, all cells were washed again with 1X Perm/Wash buffer or FACS wash and resuspended in 1% paraformaldehyde (Alfa Aesar) in PBS for acquisition on an Aria II (BD Bioscience) machine.

## 2.6 Chimeric antigen receptor (CAR) NK cell experiments

### 2.6.1 CAR NK cell generation and measurement of transduction efficacy

Generation of anti-CD19 CAR NK cells from healthy donors was approved by the national ethics review committee (24/PR/0245).

Lentiviral vectors for CAR NK cell generation were produced using the third-generation lentiviral system. In brief, *E. coli* were transformed separately with the plasmid constructs containing lentiviral components VSV-G (envelope protein), RSV-rev (facilitates nuclear export of transcripts), pMDLg/pRRE (encodes gag and pol enzymes for structural capsid proteins and reverse transcriptase and integrase components) and the CAR construct consisting of the anti-CD19 short chain variable fragment (scFv) mouse antibody clone FMC63 joined to a CD8 transmembrane domain and CD3ζ and 4-1BB intracellular signalling domains and these four transformed *E. coli* were a kind gift from Nurdan Askoy (University of Southampton). To grow *E. coli*, cells were half thawed and 10 µL of the frozen mix was added to 5 mL broth and put shaking at 37°C for 6 hours. This culture was then added to 200 mL LB broth in conical flasks overnight at 37°C. The next day, the culture was transferred into 50 mL falcon tubes and centrifuged at 4500 rpm for 15 minutes. The supernatant was decanted into waste and the pellets were frozen down until required for plasmid isolation. To isolate plasmids, maxi preps were performed following the manufacturer's instructions (Qiagen).

293FT (human endothelial kidney cell lines) cells were used as the packaging cell line. These cells were cultured in DMEM supplemented with 10% FBS, sodium pyruvate and L-glutamine. For transfection 293FT cells were plated in 6 well plates as $0.25x10^6$ cells in 2 mL. After two days, per well, 5 uL GeneJuice was added to 95 µL plain DMEM along with the DNA constructs below at the given concentrations:

**Table 2-1: Concentration of plasmids used to generate lentiviruses for CAR NK cell production.**

| Plasmid construct | Concentration (µg/well of a 6 well plate) |
|---|---|
| VSV-G | 0.352 |
| RSV-rev | 0.5 |
| pMDLg/pRRE | 0.65 |
| FMC63-CD3ζ-41BB | 0.372 |

Once DNA was added, liposomes were left to form by incubation for 15 minutes at RT, inverting the tube every 5 minutes. After, 100 uL of DNA-GeneJuice mix was added to a well of a 6wp. 293FT wells were left without addition of DNA to use in untransduced NK cells. 293FT cells were placed at 37°C for 48 hours until transduction of NK cells.

NK cells were isolated from healthy donor PBMC as described previously and resuspended in NK MACS medium supplemented with 1% MACS supplement, 5% human serum, 500 IU/mL IL-2 and 140 U/mL IL-15 at a cell concentration of $10^6$/mL. After 3-5 days of expansion, NK cells were transduced with fresh viral supernatant from 293FT supernatants. NK cells were plated in a 24 well plate as $10^6$ cells in 1mL in NK MACS medium containing 1% MACS supernatant (no human serum). The supernatant from transfected 293FT was carefully collected into a 50 mL falcon tube and centrifuged at 4°C, 1250 rpm for 5 minutes. The supernatant containing the lentivirus vector was filtered with a 0.22 µm filter. Per well of a 24 wp, 200 µL of lentivirus supernatant was mixed with 300 µL plain NK MACS medium. This mix was then added to 500 µL vectofusin-1-plain NK MACS medium mix at a vectofusin-1 concentration of 20 µg/mL. For untransduced NK cells, the same process was performed using supernatant from 293FT cells transfected with no DNA. Finally, 1 mL of lentivirus-vectofusin-1 mix was added to 1 mL NK cells with vectofusin-1 final concentration of 10 µg/mL. The plate was spintransfected for 2 hours at 400g. 24 hours later, 80% of the medium was removed and 80% fresh NK MACS medium supplemented with 1% MACS supplement, 5% human serum, 500 IU/mL IL-2 and 140 U/mL IL-15 was added back to cells. 48 hours later, NK cells were tested for CAR expression using antibodies against the idiotype of the FMC63 scFv clone made in-house at the University of Southampton, Cancer Sciences.

### 2.6.2 Assessment of CAR NK cell cytotoxicity

The cytotoxicity assay described in 2.4 was followed but with untransduced NK cells and anti-CD19 CAR NK cell co-cultures with selinexor-treated cancer cells at E:T ratios of 1:1 and 1:2. This was to ensure that the number of CAR NK cells in co-cultures did not exceed the total number of NK cells in untransduced NK-cancer co-cultures.

## 2.7 IFNγ ELISA

Co-cultures from expanded NK cell cytotoxicity experiments using at least 100,000 NK cells per well at an E:T = 1:1, were pelleted and the supernatant collected and frozen at -80°C. For ELISA experiments the IFNγ ELISA kit from Invitrogen was used (catalogue #88-7316) following the manufacturer's instructions. Briefly, ELISA plates were coated with a 1:10 dilution of the capture

antibody overnight at 4°C. The next day, supernatants were thawed, the plate was washed with 1X PBS (x3 by flicking plate and tapping on a paper towel) and wells were blocked with ELISA diluent for 1 hour at RT. After wells were washed again (x3) and supernatant samples were loaded into wells along with the standard curve and incubated at 4°C overnight. On the last day, wells were washed (x3) and the detection antibody was added for 1 hour at RT. After washing (x3), streptavidin-HRP (horseradish peroxidase) was added to wells for 30 minutes at RT. After washing (x3), TMB substrate was added to wells for 15 minutes at RT after which STOP solution (Fisher Scientific) was added. The plate was then immediately read at a wavelength of 450 nm on an ELISA plate reader and values read at 570 nm were subtracted.

## 2.8 Western blotting

B-cell lymphoma and multiple cell lines and CLL patient cells that were treated with Q-VD plus selinexor or leptomycin and IFNγ as described were lysed in whole cell lysis buffer (Cell Signalling Technology) supplemented with PMSF (Sigma, 174 µg/mL), protease inhibitor (Sigma, 1:100 final dilution) and phosphatase inhibitor (1:100 final dilution) for 30 min on ice. Cells were then centrifuged at 13,000 rpm for 10 min at 4°C and proteins in supernatants were denatured with 80 mM DTT (Sigma) at 95°C for 5 min. Proteins were then separated on 10% polyacrylamide gels (Thermo Fisher Scientific), transferred to nitrocellulose membranes (Amersham) and blocked in 5% BSA before being probed with antibodies against those in and antibody dilutions are stated in **Table 2-4**.Protein bands were detected following incubation with HRP-linked secondary antibodies (Dako) and chemiluminescence reagents (Thermo Scientific) and visualized using the ChemiDoc-It imaging system (UVP). Secondary antibodies were used at concentrations recommended by the manufacturer.

## 2.9 *In vivo* experiments

### 2.9.1 Selinexor treatment of NSG mice

Animal experiments were conducted under the project license number (PPL) PP2322487 and PIL number I91978372 and experiments were approved by the pre-clinical unit at University of Southampton. Nod-SCID-gamma chain deficient (NSG) male mice (3 months old) were administered 10 mg/kg selinexor or vehicle control (0.6% Plasdone PVP K-29/32 and 0.6% Poloxamer Pluronic F-68 in water) in 250 µL by oral gavage twice per week (Monday and Thursday) for two weeks. Prior to the

first dose, mice were weighed to record a pre-treatment weight. After the first dose, mice were subsequently weighed every 2-3 days or every day once a mouse lost 10% of its original weight. At a weight loss of 15% of the original weight, mice were humanely sacrificed. After the last dose, the experiment continued for one more week to assess any side effects of twice weekly selinexor administered over two weeks. Every day fresh food pellets were soaked in water and provided in cages to aid food intake.

### 2.9.2 Raji *in vivo* growth kinetics

Raji cells were resuspended in sterile, endotoxin-free PBS at $50x10^6$ cells/mL and NSG mice were injected subcutaneously with $5x10^6$ cells in 100 µL by members of the Pre-clinical Unit at the University of Southampton. Tumours were measured by animal technicians and tumour volume was calculated as 0.5*width*length*length. The end point was set at a tumour diameter of 12 mm or volume of 1500 $mm^3$ whichever came first.

## 2.10 Anti-CD19 CAR T cell experiments

### 2.10.1 Anti-CD19 CAR T cell lysis of B-cell lymphoma cell lines

Anti-CD19 CAR T cells were generated using the third-generation lentiviral packaging system with the FMC63-CD3ζ-41BB construct and these cells were a kind gift from Nurdan Askoy and Michael Spurway (University of Southampton). The Raji cells used as target cells were labelled with CellTrace™ and treated with selinexor as in the cytotoxicity assays described in 2.4. The day after Raji cell treatment, anti-CD19 CAR T cells or untransduced T cells were co-cultured with tumour targets at an effector: target ratio (E:T) of 5:1 and 1:1 for 4 at 37°C. After co-culture, cells were washed in 1X PBS and stained with 1.6 µg/mL propidium iodide (Invitrogen™) to identify lysed, CellTrace™-labelled cancer cells by flow cytometry using the FACS Aria II or BD Accuri c6 machines.

### 2.10.2 T cell stimulation experiments to assess NKG2A expression on activated T cells

Anti-CD19 CAR T and untransduced T cells gifted by Nurdan Askoy and Michael Spurway (University of Southampton), were stimulated for three days at a concentration of $1x10^6$ cells/mL with T cell TransAct™ (polymer matrix containing recombinant CD3 and CD28 agonists) used at a 1:100 final dilution in the T cell culture in TexMACS medium. After three days, T cells were washed by addition of TexMACS medium and centrifuged at 1500 rpm for 5 minutes. T cells were replated at $1x10^6$ cells/mL in fresh TexMACS medium supplemented with IL-7 (500 U/mL) and IL-15 (290 U/mL) and left at 37°C for four days. This was referred to as a ‘rest/recovery’ period. After the rest period, T cells

were counted and diluted to $1x10^6$ cells/mL accordingly and re-stimulated for three days with TransAct™ followed by another rest period. A third stimulation and rest period. After each 3-day stimulation and 4-day rest period, T cells were stained with antibodies against CD3-PerCP (clone UCHT1), NKG2A-BV421 (REA147), PD-1-APC (EH12.2H7), CD137-PE (4-1BB, 4B4-1), CD25-PE/Cy7 (BC96), CD69-APC (FN50) and FMC63 idiotype to identify CAR+ T cells.

## 2.11 Macrophage phagocytosis experiments

### 2.11.1 Generation of monocyte-derived macrophages

Monocytes were isolated from healthy donor PBMC by plating $20x10^6$ PBMC in 2 mL in 6-well plates in RPMI medium supplemented with 1% human serum overnight at 37°C. Lymphocytes in suspension were removed from wells and adhered monocytes were washed by gentle swirling with 1X PBS to obtain a monolayer ~80% confluent. 2mL R10 medium supplemented with 100 ng/mL macrophage-colony-stimulating factor (M-CSF) was added to monocytes and left for 48 hours at 37°C to allow for macrophage differentiation. After, 800 µL of medium was removed from cultures and 1 mL medium containing 100 ng/mL M-CSF was added back to cultures. Cells were put at 37°C for 72 hours after which macrophages were harvested by removal of medium and incubation with 5 mM EDTA in 1X PBS at 37°C for 15 minutes followed by scraping the bottom of wells with a syringe plunger. Macrophages in suspension were then centrifuged at 300g for 5 minutes and resuspended at $1x10^6$ cells/mL in R10 supplemented with 100 ng/mL M-CSF for used in experiments.

### 2.11.2 Assessing the effect of XPO1 inhibition on macrophage phagocytosis

Macrophages generated above were plated in a flat 96-well plate as $1x10^5$ cells in 100 uL and macrophages were allowed to adhere to the bottom of the plate overnight at 37°C. Meanwhile Raji target cells were labelled with CellTrace™ and treated with selinexor as previously described in 2.4.

The next day, Raji cells were washed in R10 medium by centrifugation (1500 rpm, 5 minutes) and resuspended in R10 and added into macrophage-containing wells as $1x10^5$ (E:T = 1:1) in 100 uL. Co-cultures were placed at 37°C for 2 hours after which co-cultures were stained with anti-CD14-PE (clone M5E2) for 15 minutes in the dark at room temperature. The supernatant containing cells in suspension and unbound anti-CD14-PE was removed and adhered cells were washed in 1X PBS for 30 seconds. PBS was removed and FACS wash was added to wells and the plate was put on ice. Wells were scraped with a P200 pipette tip to detach adhered cells which were then ran through a flow cytometer (FACS Aria II or Accuri c6) and phagocytosis was measured as the proportion of double positive CD14+CellTrace+ cells.

## 2.12 Statistical analysis

Statistical analyses were performed, and graphs produced, using GraphPad Prism V.10.0 (GraphPad). The Shapiro-Wilk test was performed to test normality of the data and statistical significance of differences between the means of two groups was calculated with t-test and the differences between the mean of multiple groups with one- or two-way ANOVA followed by the recommended post-hoc test for multiple group comparison. Paired-sample statistical tests were carried out where necessary and this is stated within figure legends. Significance scores are defined as: *P<0.05, **P<0.01, ***P<0.005 and ****P<0.001.

**Table 2-2: CLL patient characteristics**

| Patient number | Age at Diagnosis | Binet Stage | Rai Stage | IGHV |
|---|---|---|---|---|
| 135 | 55 | A | 0 | M-CLL |
| 139 | 73 | A | 0 | M-CLL |
| 572 | 60 | A | 0 | M-CLL |
| 644 | 49 | A | 1 | U-CLL |
| 727 | 72 | C | 4 | M-CLL |
| 809 | 70 | A | 1 | U-CLL |
| 883 | 89 | A | 0 | U-CLL |
| 888 | 75 | B | 2 | M-CLL |
| 1346 | 61 | A | 0 | M-CLL |
| 1373 | 60 | NA | NA | M-CLL |
| 1050 | 50 | A | 1 | M-CLL |
| 1259 | 52 | A | NA | M-CLL |
| 911 | 63 | A | 0 | U-CLL |
| 1003 | 51 | A | 1 | U-CLL |
| 1270 | 57 | A | 0 | NA |
| 1204 | 82 | A | 0 | U-CLL |
| 1352 | 67 | B | 1 | M-CLL |
| 1358 | 74 | A | 2 | M-CLL |
| 1220 | 56 | A | NA | M-CLL |
| 1225 | 65 | A | NA | U-CLL |
| 1423 | 37 | B | 1 | U-CLL |
| 1321 | 61 | A | NA | U-CLL |
| 1414 | 67 | A | 0 | U-CLL |
| 1348 | 60 | A | NA | M-CLL |
| 1436 | 56 | A | 0 | M-CLL |
| 1438 | 73 | A | 2 | U-CLL |
| 1445 | 43 | A | 1 | M-CLL |
| 1446 | 77 | A | 0 | M-CLL |
| 1447 | 74 | A | 1 | M-CLL |
| 252 | 70 | A | 1 | M-CLL |
| 1454 | 61 | C | 4 | U-CLL |
| 1341 | 53 | B | 2 | M-CLL |

**Table 2-3: Antibodies and recombinant proteins used in flow cytometry experiments**

| Specificity | Fluorochrome | Clone | Manufacturer | Concentration (µg/mL) |
|---|---|---|---|---|
| CD3 | PerCP | UCHT1 | Biolegend | 1 |
| CD56 | PE/Cy7 | HCD56 | Biolegend | 4 |
| NKG2A | FITC/APC | REA110 | Miltenyi | 1 |
| CD158b | PE | CH-L | BD Pharmingen | 20 |
| CD158b2 (KIR2DL3) | FITC | REA147 | Miltenyi | 1:25 dilution |
| CD107a (LAMP) | eFluor660 | eBioH4A3 | Invitrogen | 0.17 |
| IFNγ | PE | B27 | biolegend | 2 |
| HLA-E | PE/Cy7 | 3D12 | Biolegend | 9 |
| HLA-A/B/C | A488 | W6/32 | Biolegend | 1.2 |
| PD-L1 | APC | 29E.2A3 | Biolegend | 16 |
| Vimentin | A488 | 280618 | R&D Systems | 1:25 dilution |
| ULBP-1 | PE | 170818 | R&D Systems | 1:25 dilution |
| ULBP-2/5/6 | PerCP | 165903 | R&D Systems | 1:25 dilution |
| CD54 | PB | HCD54 | Biolegend | 20 |
| CD19 | PE | UCHT2 | Biolegend | 1 |
| CD5 | PerCP | UCHT2 | Biolegend | 1 |
| CD20 | APC | 2H7 | Biolegend | 2 |
| CD38 | FITC | HIT2 | Biolegend | 1 |
| B7H6 | APC | 875001 | R&D Systems | 1:25 dilution |
| MIC-A/B | PE/Cy7 | 6D4 | Biolegend | 2 |
| CXCR4 | PE | QA18A64 | Biolegend | 10 |
| FAS | FITC | DX2 | Biolegend | 10 |
| DR4 | PE | L243 | Biolegend | 10 |
| DR5 | APC | DJR2-4 | Biolegend | 10 |

| | | | | |
|---|---|---|---|---|
| Ecto-calreticulin | A488 | ERP3924 | Abcam | 10 |
| Recombinant CD19 | FITC | N/A | AcroBIO | 2.5 |
| Anti-FMC63 idiotype | Unconjugated | N/A | In-house | 1 |
| Anti-mouse secondary | PE | | Biolegend | 0.5 |
| CD14 | PE | M5E2 | Biolegend | 1 |
| BCMA | APC | 19F2 | Biolegend | 1 |

**Table 2-4: Western blot antibody information**

| Specificity | Clone | Manufacturer | Dilution factor |
|---|---|---|---|
| XPO1 | D6V7N | Cell Signalling Technology | 1000 |
| PARP | 4C10-5 (RUO) | BD Pharmingen | 1000 |
| β-ACTIN | 8H10D10 | Cell Signalling Technology | 1750 |
| p53 | 1C12 | Cell Signalling Technology | 1400 |
| HLA-E | SAB1401182 | Sigma | 500 |
| CHOP | L63F7 | Cell Signalling Technology | 1000 |
| p-eIF2 | Polyclonal | Cell Signalling Technology | 500 |
| BIP | C50B12 | Cell Signalling Technology | 1000 |
| PERK | D11A8 | Cell Signalling Technology | 1000 |
| IRE-1a | 14C10 | Cell Signalling Technology | 1000 |
| LC3A/B | D3U4C | Cell Signalling Technology | 1000 |
| STAT1 | Polyclonal | Cell Signalling Technology | 1000 |
| pSTAT1 | D3A4 | Cell Signalling Technology | 1000 |

# Chapter 3 NK cell immunomodulatory properties of XPO1 inhibitors in malignant B cell lines

## 3.1 NK cell cytotoxicity against malignant B cell lines treated with XPO1 inhibitors

Selinexor is an approved anti-cancer therapy for the treatment of relapsed and refractory multiple myeloma and DLBCL. Selinexor acts by inhibiting and degrading exportin-1 (XPO1) which leads to the suppression of cell growth and induction of cancer cell apoptosis via the accumulation of tumour suppressor proteins in the nucleus and reduced translation of oncogenic mRNA (409). To confirm the pharmacological activity of selinexor in B cell lymphoma cell lines, XPO1 protein abundance post selinexor treatment was measured by western blot. Three B-cell lymphoma cell lines representing three B-cell lymphoma subtypes were examined: RAMOS (Burkitt's lymphoma), JeKo-1 (MCL) and SUDHL4 (DLBCL). All cell lines were sensitive to selinexor treatment as demonstrated by XPO1 degradation (**Figure 3-1**) and indeed increased apoptosis was observed with increasing selinexor concentration as shown by the increased abundance of cleaved PARP (cPARP) (**Figure 3-1A**). In order to differentiate between NK cell specific lysis and selinexor-induced apoptosis of cancer cells and to mimic selinexor drug resistance in future experiments, cancer cells were treated with selinexor in the presence of the apoptotic inhibitor Q-VD-OPh (referred to as Q-VD) which inhibits the function of apoptotic effector caspases (464). Co-incubation of selinexor and Q-VD resulted in successful inhibition of selinexor-induced apoptosis across all cell lines as shown by the absence of cPARP (**Figure 3-1B**).

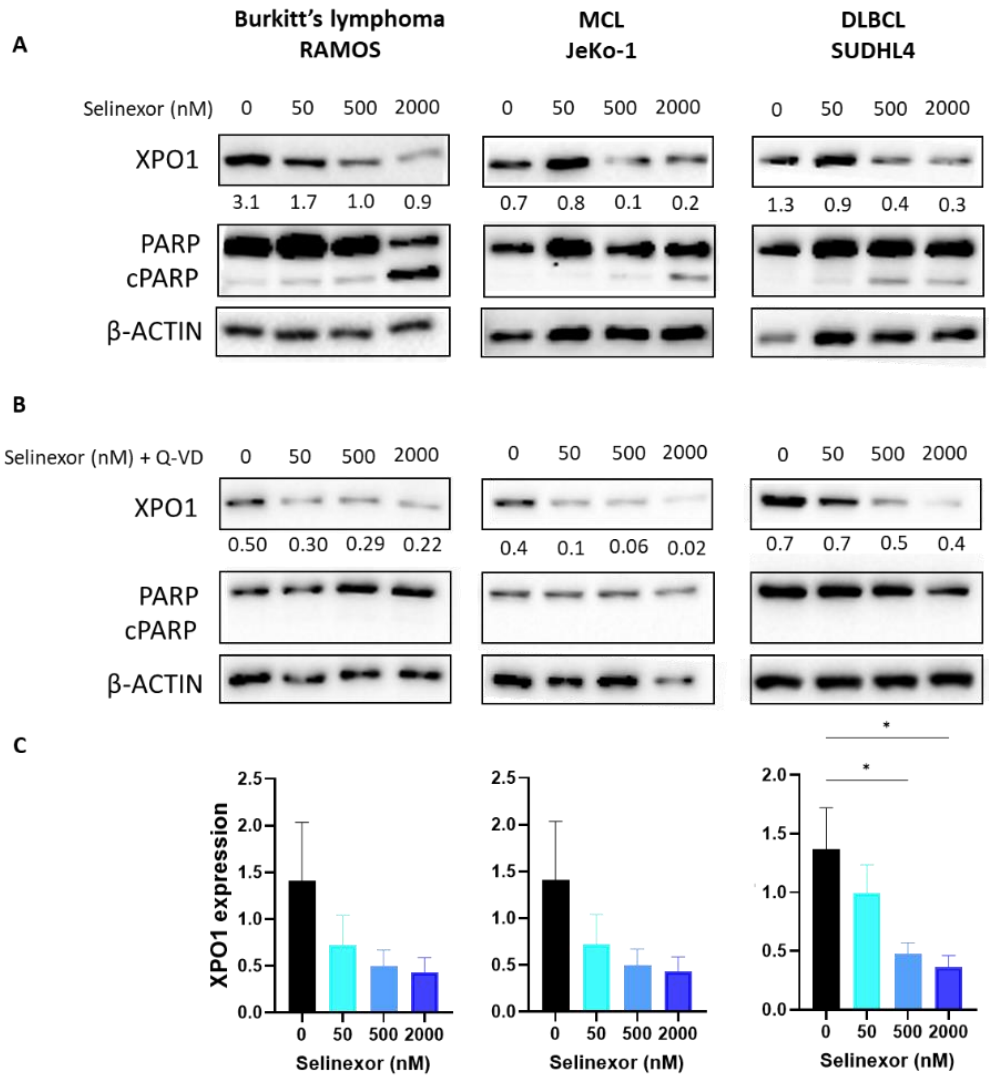


**Figure 3-1: Sensitivity of B cell lymphoma cell lines to selinexor treatment.**

XPO1 protein abundance in B-cell lymphoma cell lines RAMOS, SUDHL4 and JeKo-1 after 24-hour treatment with selinexor at the indicated concentrations without (**A**) and in the presence of the apoptotic inhibitor Q-VD (**B**). Number represents the XPO1 band intensity relative to the actin loading control. SINE-induced apoptosis is depicted by the abundance of cleaved PARP (cPARP). Shown is one representative experiment of three separate experiments. MCL = Mantle cell lymphoma; DLBCL = Diffuse large B cell lymphoma. (**C**) Quantified XPO1 band intensity with increasing selinexor concentration (n=3). One-way ANOVA: *P<0.05.

Co-incubation of selinexor and Q-VD was used in subsequent experiments to determine whether XPO1 inhibition sensitises cancer cell lines to NK-mediated lysis. CellTrace™-labelled, selinexor-treated cancer cell lines were co-cultured with purified NK cells and lysis of cancer targets was measured with propidium iodide (**Figure 3-2**). In accordance with absent cPARP using Q-VD, in the absence of NK cells, cell lines remained viable across all selinexor concentrations as shown in **Figure 3-3A** using RAMOS as an example. After co-culture with NK cells, the proportion of lysed lymphoma cells increased with increasing selinexor concentration across all cell lines tested (**Figure 3-3B**). This implies that XPO1 inhibition sensitises malignant B cell lines to NK-mediated lysis.

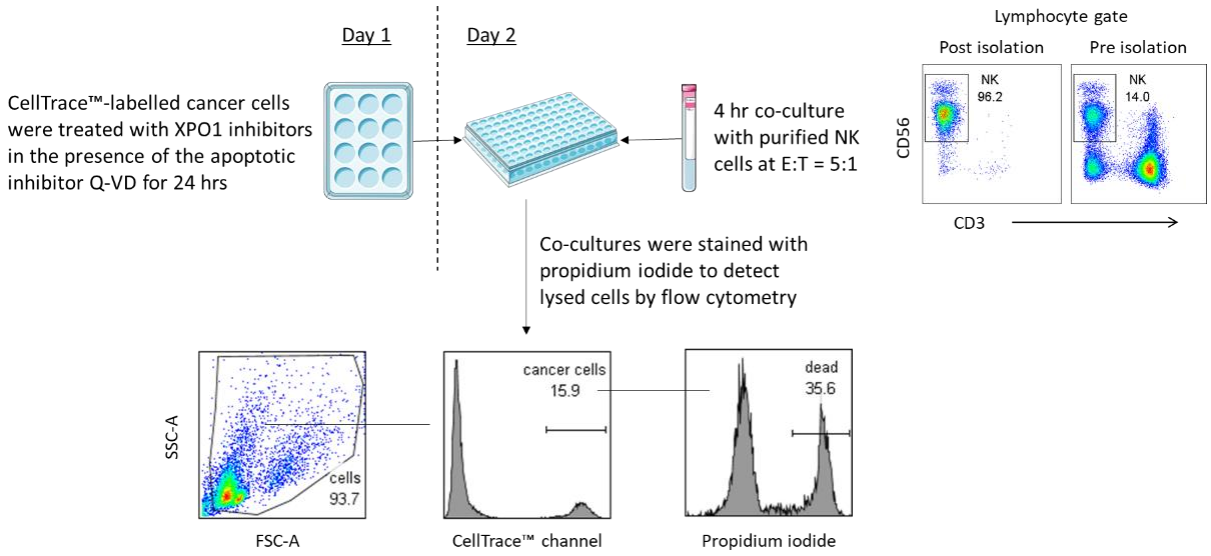


**Figure 3-2: NK cell specific lysis assay workflow.**

Cancer cells were stained with Cell Trace™ Cell Proliferation Kit (Invitrogen™) and pre-treated with selinexor at concentrations of 50, 500 and 2000 nM or DMSO control for 24 hours in the presence of the apoptotic inhibitor Q-VD (20 uM for SUDHL4 and JeKo-1, 40 uM for RAMOS). After, selinexor was washed out and cancer cells were co-cultured with purified NK cells at an effector:target (E:T) ratio of 5:1 for 4 hours after which cells were stained with propidium iodide to enable quantification of dead, CellTrace™ positive cancer cells by flow cytometry. NK cell specific lysis was calculated as *(% target lysis - % spontaneous lysis) * 100 / (100 - % spontaneous lysis).* Spontaneous lysis of cancer cells was measured for each selinexor concentration in the absence of NK cells in the culture.

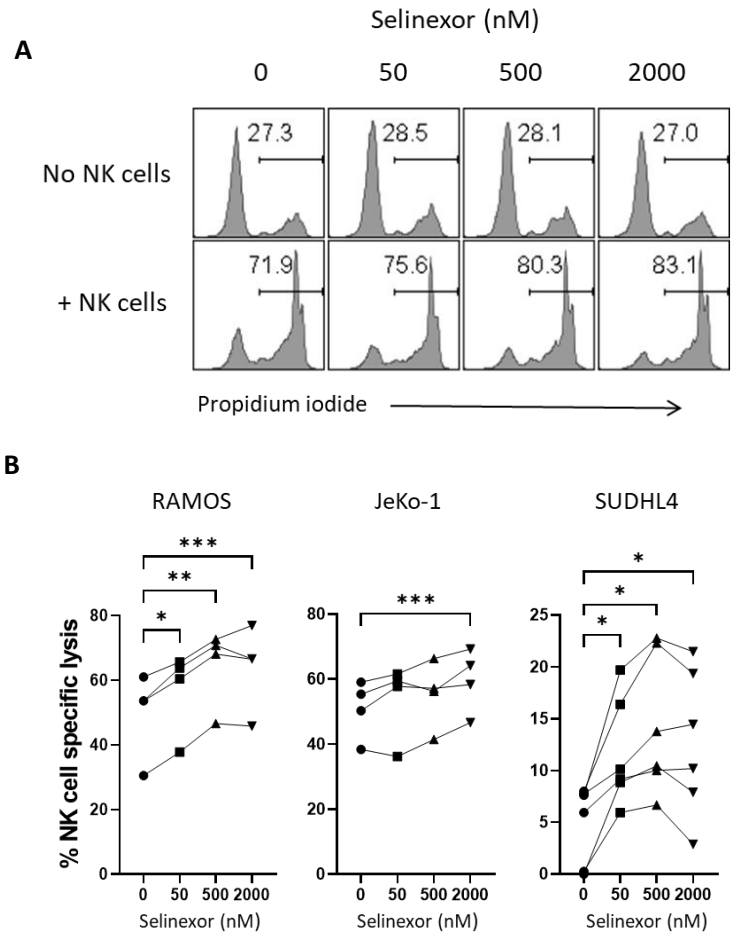


**Figure 3-3: Selinexor sensitises B-cell lymphoma cell lines to NK cell specific lysis.**

(**A**) Representative example of RAMOS cell lysis in the absence and presence of purified NK cells after 24-hour treatment with selinexor plus Q-VD. Number on graphs indicate the percentage of lysed RAMOS cells positive for propidium iodide. (**B**) NK cell specific lysis of selinexor-treated B-cell lymphoma cell lines RAMOS (n=4), JeKo-1 (n=4) and SUDHL4 (n=6). Cancer cells were pre-treated with selinexor at the indicated concentrations in the presence of Q-VD for 24 hours. Each line represents NK cells from a single donor and NK cell specific lysis at each selinexor concentration was normalised to 'no NK' controls using the formula in **Figure 3-2**. Significant differences in NK specific lysis between the 0 nM control and selinexor concentrations were calculated by repeated measure one-way ANOVA followed by Tukey's post-hoc test: ***P<0.005, **P<0.01, *P<0.05.

## 3.2 Effect of XPO1 inhibition in cancer cell lines on NK cell activation

In addition to measuring NK specific lysis of cancer cells treated with XPO1 inhibitors, the activation status of NK cells was assessed as measured by expression of CD107a (also referred to as LAMP - lysosomal-associated membrane protein) and IFNγ when PBMC were co-cultured with selinexor-treated cancer cell lines (**Figure 3-4**). First, how selinexor pre-treatment of cancer cells affected the degranulation ability of the highly cytotoxic CD3-CD56$^{dim}$ NK cell population and of the more immunoregulatory CD3-CD56$^{bright}$ NK cell population was examined (**Figure 3-5**). The level of degranulation can be assessed using the LAMP assay which measures surface expression of LAMP/CD107a as an indicator of cytotoxic granule release (**Figure 3-4**) (465). CD107a marks cytotoxic granules inside NK cells, therefore as NK cells degranulate upon activation, CD107a appears at the plasma membrane. By using Golgi-ER trafficking inhibitors, CD107a expression at the plasma membrane can be retained which can then be detected in flow cytometry to approximate the proportion of activated NK cells. Through performing the LAMP assay, NK cell degranulation increased after co-culture with selinexor-treated cancer cell lines in both the CD56$^{dim}$ and CD56$^{bright}$ NK cell populations compared to the untreated controls (**Figure 3-5A and B**). With the apoptotic inhibitor Q-VD, a clearer dose-dependent response was observed for SUDHL4 cells (**Figure 3-5C**). Because selinexor-treated SUDHL4 induced the greatest degranulation response by NK cells, IFNγ production by NK cells was examined when PBMC were co-cultured with SUDHL4. Enhanced production of IFNγ was observed in the CD56$^{dim}$ NK cell population (**Figure 3-6**). For CD56$^{bright}$ NK cells, two of the five donors had to be removed due to a very small percentage of CD56$^{bright}$ NK cells within the PBMC. This then affected the analysis such that one event within the positive gate resulted in a large change in percentage. Overall, these experiments demonstrate that selinexor sensitises lymphoma cell lines to NK cell activation which results in increased NK cell-mediated lysis of cancer targets as demonstrated in **Figure 3-3**.

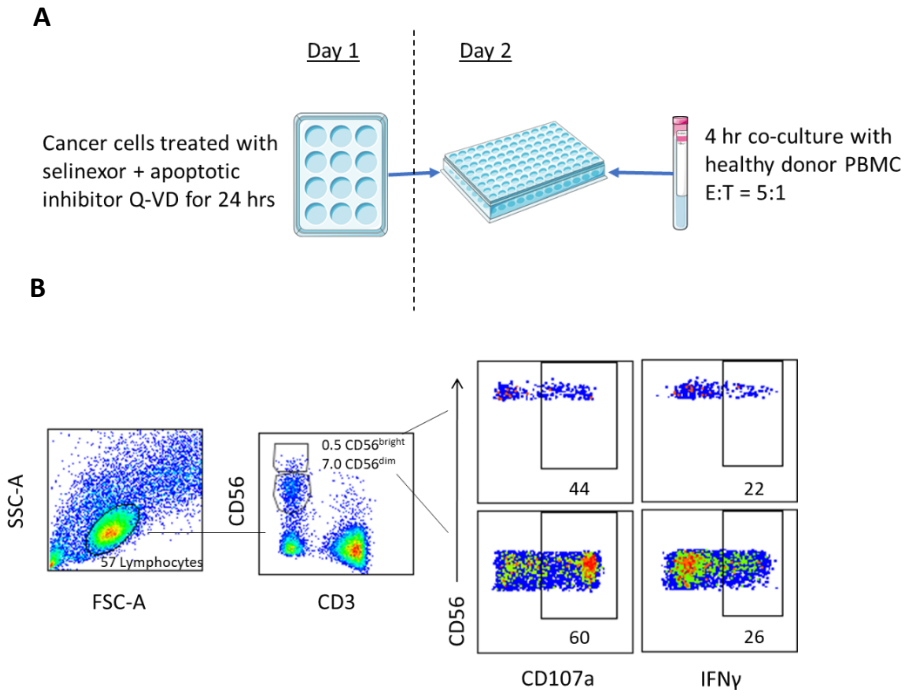


**Figure 3-4: LAMP and IFNγ assay workflow to assess NK cell activation against selinexor-treated cancer cells.**

(**A**) Cancer cells were pre-treated with selinexor at concentrations of 50, 500 and 2000 nM or DMSO control for 24 hours in the presence of the apoptotic inhibitor Q-VD (20 µM for SUDHL4 and JeKo-1, 40 µM for RAMOS). After, selinexor was washed out and cancer cells were co-cultured with healthy donor PBMC at an effector:target (E:T) ratio of 5:1 for 4 hours after which NK cell activation in co-cultures was assessed by measuring CD107a and IFNγ expression on CD56+CD3- NK cells. (**B**) Flow cytometry gating strategy to examine NK cell activation against selinexor-treated cancer cells. Activation was measured as percent CD107a+ and IFNγ+ cells in CD3-CD56$^{dim}$ and CD3-CD56$^{bright}$ NK cells. Shown is a representative example of a healthy donor PBMC co-cultured with SUDHL4 cells. Number on plots represent the percentage of cells inside gates.

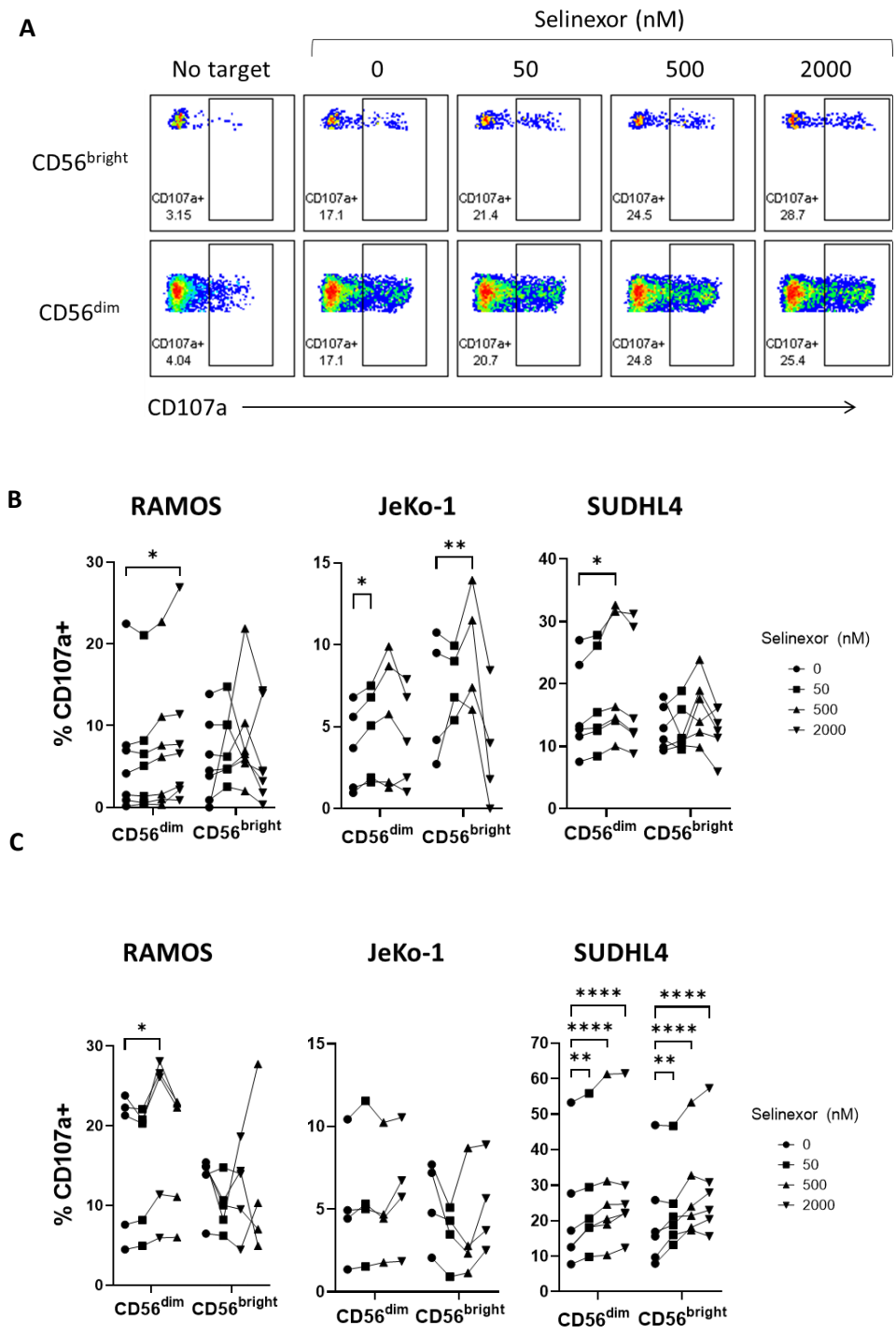


**Figure 3-5: Selinexor pre-treatment of malignant B cell lines enhances NK cell degranulation.**

(**A**) Representative example of CD107a staining in CD3-CD56$^{bright}$ and CD3-CD56$^{dim}$ NK cells when PBMC were co-cultured with selinexor-treated SUDHL4 cells at the indicated selinexor concentrations. Number on plots represent the percentage of CD107a+ NK cells within gates. Percent CD107a+ NK cells across multiple donor PBMC when PBMC were co-cultured with selinexor-treated cancer cells (E:T = 5:1) at the indicated selinexor concentrations without (**B**) and in the presence (**C**) of the apoptotic inhibitor Q-VD. Percentage of CD107a+ NK cells was normalised to the no target control for each donor. Each line represents a single donor (n=4-7). Significant differences in NK cell activation between the 0 nM control and selinexor concentrations were calculated with repeated measure two-way ANOVA followed by Tukey's post-hoc test: *P<0.05, **P<0.01, ****P<0.001.

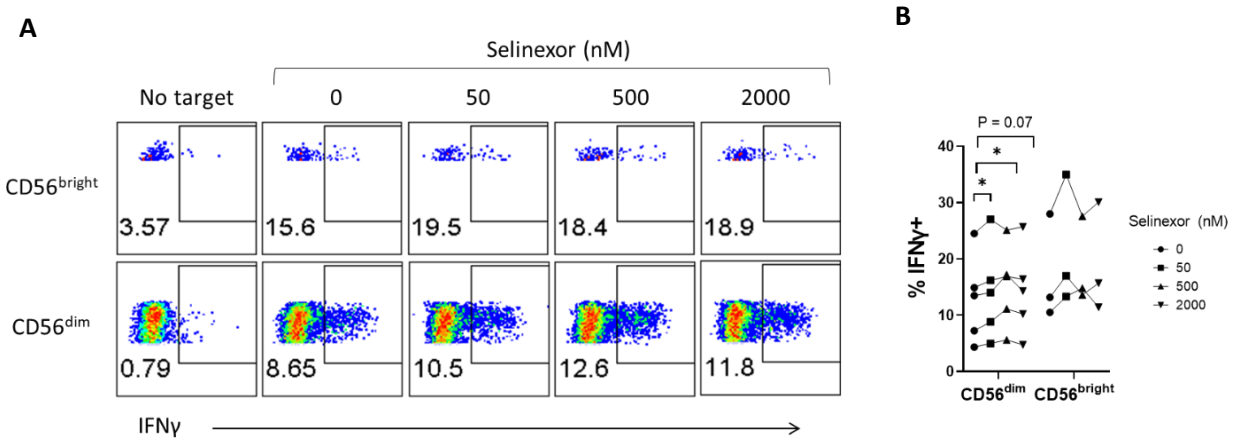


**Figure 3-6: Selinexor pre-treatment of SUDHL4 cells enhances IFNγ production by NK cells.**

(**A**) Representative example of IFNγ staining in CD3-CD56$^{bright}$ and CD3-CD56$^{dim}$ NK cells when PBMC were co-cultured with selinexor-treated SUDHL4 cells at the indicated selinexor concentrations. Number on plots represent the percentage of IFNγ+ NK cells within gates. (**B**) Percentage of IFNγ+ NK cells across multiple donor PBMC when PBMC were co-cultured with selinexor-treated SUDHL4 cells at the indicated selinexor concentrations in the presence of 20 µM Q-VD. Percentage of IFNγ+ NK cells was normalised to the no target control for each donor. Each line represents a single donor (n=5 for CD56$^{dim}$ and n=3 for CD56$^{bright}$ NK cells). Significant differences in NK cell activation between the 0 nM control and selinexor concentrations were calculated with repeated measure two-way ANOVA followed by Tukey's post-hoc test: *P<0.05.

## 3.3 Mechanism for increased sensitivity of malignant B cell lines to NK cell cytotoxicity after XPO1 inhibition

### 3.3.1 Effect of XPO1 inhibition on the activation of KIR2DS2+ NK cells.

NK cells are a heterogenous immune cell population largely due to the differential expression of activating and inhibitory receptors. One important family of receptors governing NK cell activation are the killer cell immunoglobulin-like receptors (KIR). KIRs are stimulated by peptides presented by HLA class I molecules which subsequently transduce inhibitory or activating signals into NK cells (113). It was shown by the research group that a peptide derived from XPO1 (NAPLVHATL) stimulates the activating KIR2DS2 receptor (171). As a result, it was hypothesised that the selinexor-induced degradation of XPO1 in B-cell lymphoma cells would specifically enhance the activation of KIR2DS2+ NK cells due to increased abundance of XPO1-derived peptides.

The KIR2DS2 gene is not present in all individuals therefore to assess KIR2DS2+ NK cell activation, PBMC from KIR2DS2+ donors were used in the LAMP assay and KIR2DS2+ NK cells were identified using the antibody clones REA147 and CH-L as previously described (176) (**Figure 3-7**). By using these antibody clones, two KIR2DS2+ NK cell populations can be identified. One that expresses high levels of KIR2DS2 (labelled KIR2DS2$^{high}$) and one that expresses high levels of the inhibitory KIRs KIR2DL3 and KIR2DL2 as well as KIR2DS2 (labelled KIR2DL3/L2$^{high}$) (**Figure 3-7**). An NK cell population that does not express KIR2DS2, KIR2DL3 or KIR2DL2 (labelled KIR2DL3/L3/S2-) is also present. Each of these NK cell populations was gated on in the LAMP assay to assess degranulation against selinexor-treated SUDHL4 cells. SUDHL4 was chosen not only because it stimulated NK cells the most post XPO1 inhibition, but because SUDHL4 expresses the group 1 allotype HLA-C molecule HLA-C*03:04 and KIR2DS2 is known to engage group 1 HLA-C allotypes and not group 2 allotypes (175). After co-culture, the degranulation of all NK cell populations was enhanced with selinexor, but significance between selinexor concentrations was only achieved in KIR2DS2+ NK cell populations (KIR2DS2$^{high}$ and KIR2DL3/L2$^{high}$) (**Figure 3-8**). To understand the magnitude of enhanced NK cell activation between KIR2DS2 NK cell populations relative to untreated samples, relative change of CD107a expression was calculated. Across all selinexor concentrations, an increased fold change in CD107a expression was observed in KIR2DS2-expressing NK cells compared to KIR2DS2 negative NK cells (1.6x compared to 1.3x at 500 nM) (**Figure 3-8**). However, two-way ANOVA interaction analysis revealed no significant difference between the activation status of NK cell populations with increasing selinexor concentration. This suggests that selinexor is not selectively activating KIR2DS2+ NK cells (KIR2DS2$^{high}$ and KIR2DL3/L2$^{high}$). This was further evidenced by increased NK cell activation against selinexor-treated SUDHL4 cells using KIR2DS2- donors (KIR2DL3 homozygotes) (**Figure 3-8**). Therefore, an XPO1 peptide-independent mechanism must be occurring to activate NK cells with selinexor. However, these data do not disprove the contribution of XPO1-derived peptides induced by selinexor in activating the KIR2DS2 receptor.

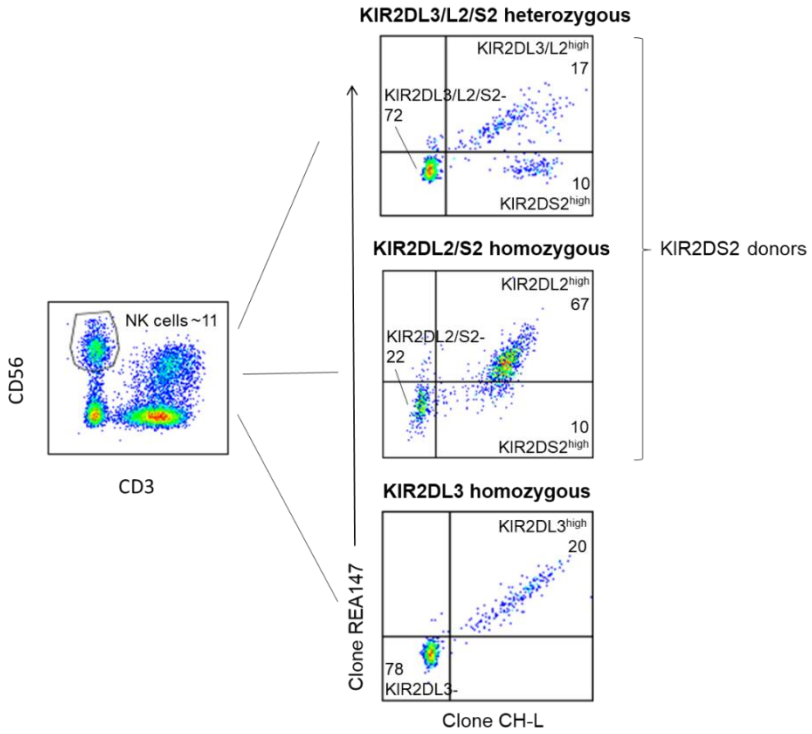


**Figure 3-7: Gating strategy used to identify KIR2DS2+ NK cells.**

By gating on CD3-CD56+ NK cells, three donor genotypes can be distinguished using REA147 and CH-L antibody clones as described in Blunt et al. (2019). The REA147 antibody clone binds to KIR2DL3 and KIR2DL2 and the antibody clone CH-L binds to KIR2DL3, KIR2DL2 and KIR2DS2. Used together, NK cells with higher levels of KIR2DS2 expression (KIR2DS2$^{high}$ = CH-L positive, REA147 negative) can be identified. To study the effect of selinexor on KIR2DS2$^{high}$ NK cell populations, we used PBMC derived from KIR2DL3/L2/S2 heterozygous and KIR2DL2/S2 homozygous donors. The 'KIR2DL3/L2/S2-' and 'KIR2DL2/S2-' NK cell populations from KIR2DL3/L2/S2 heterozygous and KIR2DL2/S2 homozygous donors, respectively, were grouped together in the LAMP assay analysis and labelled 'KIR2DL3/L2/S2-'. The 'KIR2DL3/L2$^{high}$' and 'KIR2DL2$^{high}$' NK cell populations from KIR2DL3/L2/S2 heterozygous and KIR2DL2/S2 homozygous donors, respectively, were also grouped and analysed together and labelled

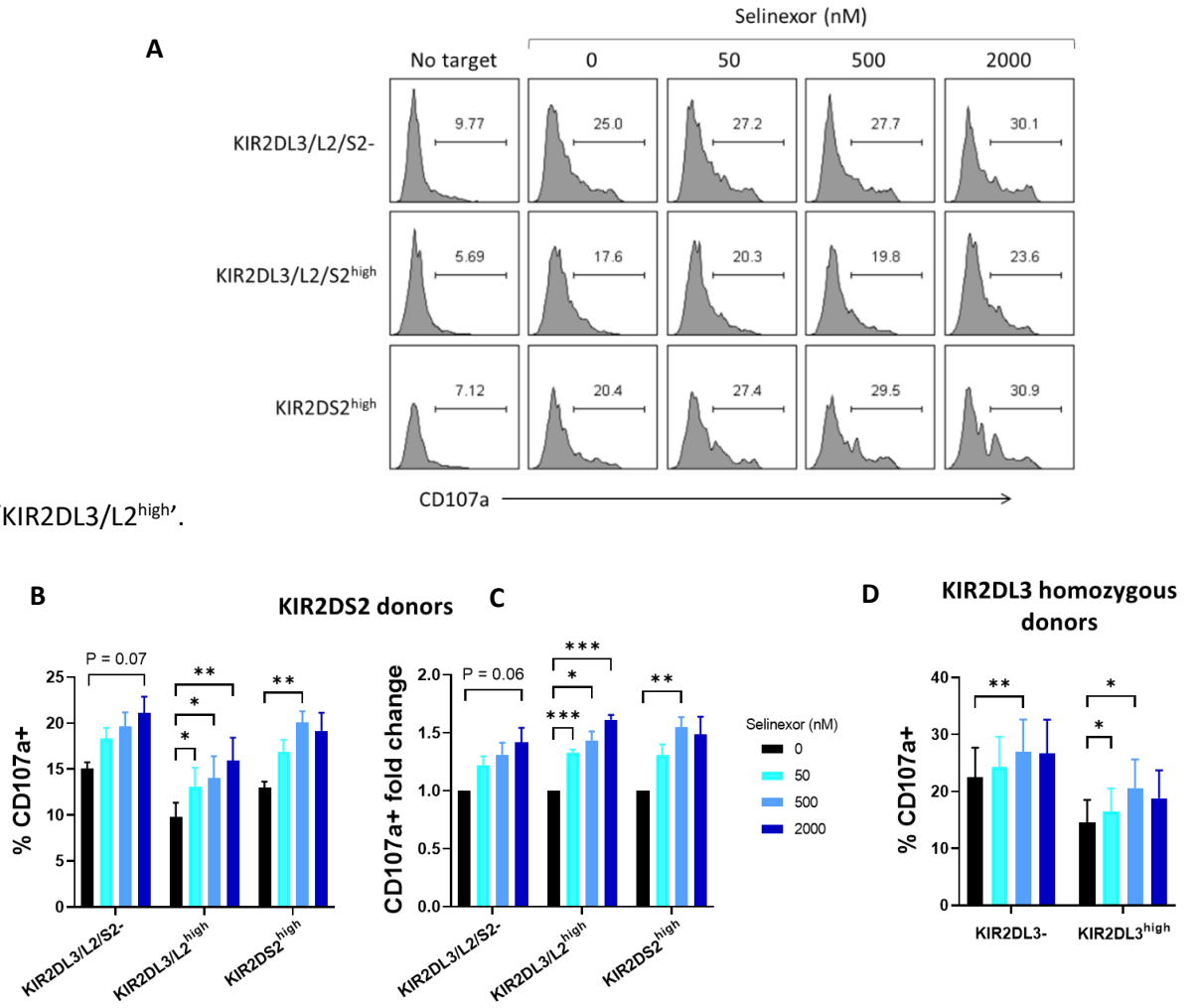


'KIR2DL3/L2$^{high}$'.

**Figure 3-8: Selinexor pre-treatment of SUDHL4 cells enhances KIR2DS2+ and KIR2DS2- NK cell degranulation.**

(**A**) Representative example of CD107a staining in KIR2DS2$^{high}$, KIR2DL3/L2$^{high}$ and KIR2DL3/L2/S2- NK cells when PBMC derived from KIR2DS2 donors were co-cultured with selinexor-treated SUDHL4 cells at the indicated selinexor concentrations. Number on plots represent the percentage of CD107a+ NK cells within gates. (**B**) Percentage of CD107a+ and (**C**) CD107a+ fold change relative to the untreated control in KIR2DS2$^{high}$, KIR2DL3/L2$^{high}$ and KIR2DL3/L2/S2- NK cells when PBMC derived from KIR2DS2 donors were co-cultured for 4 hours with selinexor-treated SUDHL4 cells (E:T = 5:1). SUDHL4 cells were treated with 50-2000 nM selinexor for 16 hours in the presence of the apoptotic inhibitor Q-VD. Percentage of CD107a+ KIR NK cells was normalised to the no target control for each donor. Shown is mean ± SEM (n=5). Repeated measure two-way ANOVA: *P<0.05, **P<0.01, ***P<0.005. (**D**) Percentage of CD107a+ KIR2DL3$^{high}$ and KIR2DL3- NK cells when PBMC derived from KIR2DL3 homozygous donors were co-cultured for 4 hours with selinexor-treated SUDHL4 cells (E:T = 5:1). Percentage of CD107a+ KIR NK cells was normalised to the no target control for each donor. Shown is mean ± SEM (n=8) and significant differences in NK cell activation between the 0 nM control and selinexor concentrations were calculated with repeated measure two-way ANOVA followed by Tukey's post-hoc test: *P<0.05, **P<0.01, ***P<0.005.

### 3.3.2 Expression of NK cell activating ligands and HLA proteins on malignant B cell lines post XPO1 inhibition

To uncover an alternative explanation for enhanced activation of NK cells against selinexor-treated tumour targets, changes in the cell surface expression of ligands for a range of important NK cell receptors involved in tumour immunosurveillance (110) was assessed on B-cell lymphoma cell lines post selinexor treatment. Expression of the activating ligands (with their corresponding NK cell receptor, **Figure 1-6**) vimentin (NKp46), ULBP-1 (NKG2D), ULBP-2/5/6 (NKG2D), MIC-A/B (NKG2D), CD54/ICAM-1 (LFA-1) and B7H6 (NKp30) on SUDHL4 and JeKo-1 cells was assessed after 24-hour selinexor treatment. Vimentin was not expressed on either cell line and ULBP-1, ULBP-2/5/6 and MIC-A/B were lowly expressed across all selinexor concentrations (**Figure 3-9**). CD54 and B7H6 were moderately expressed by both cell lines (**Figure 3-9**). For these activating ligands to explain increased NK cell activation with increasing selinexor concentration, their surface expression level would be hypothesised to increase. However, no clear increase in all activating ligands examined was observed (**Figure 3-9**). For CD54 which was moderately expressed on SUDHL4 and JeKo-1 cells, a slight increase on JeKo-1 cells was observed with selinexor. For B7H6, a slight increase was also seen at 50 nM selinexor, but B7H6 expression decreased at high selinexor concentrations. Similarly, ULBPs also increased at the plasma membrane at 50 nM selinexor, however the contribution of ULBPs to activate NK cells at such low expression levels is unlikely. MIC-A/B decreased on both cell lines with increasing selinexor concentration. In summary, the direction and magnitude of expression changes of activating ligands post selinexor treatment cannot explain increased NK cell activation against selinexor-treated tumour targets.

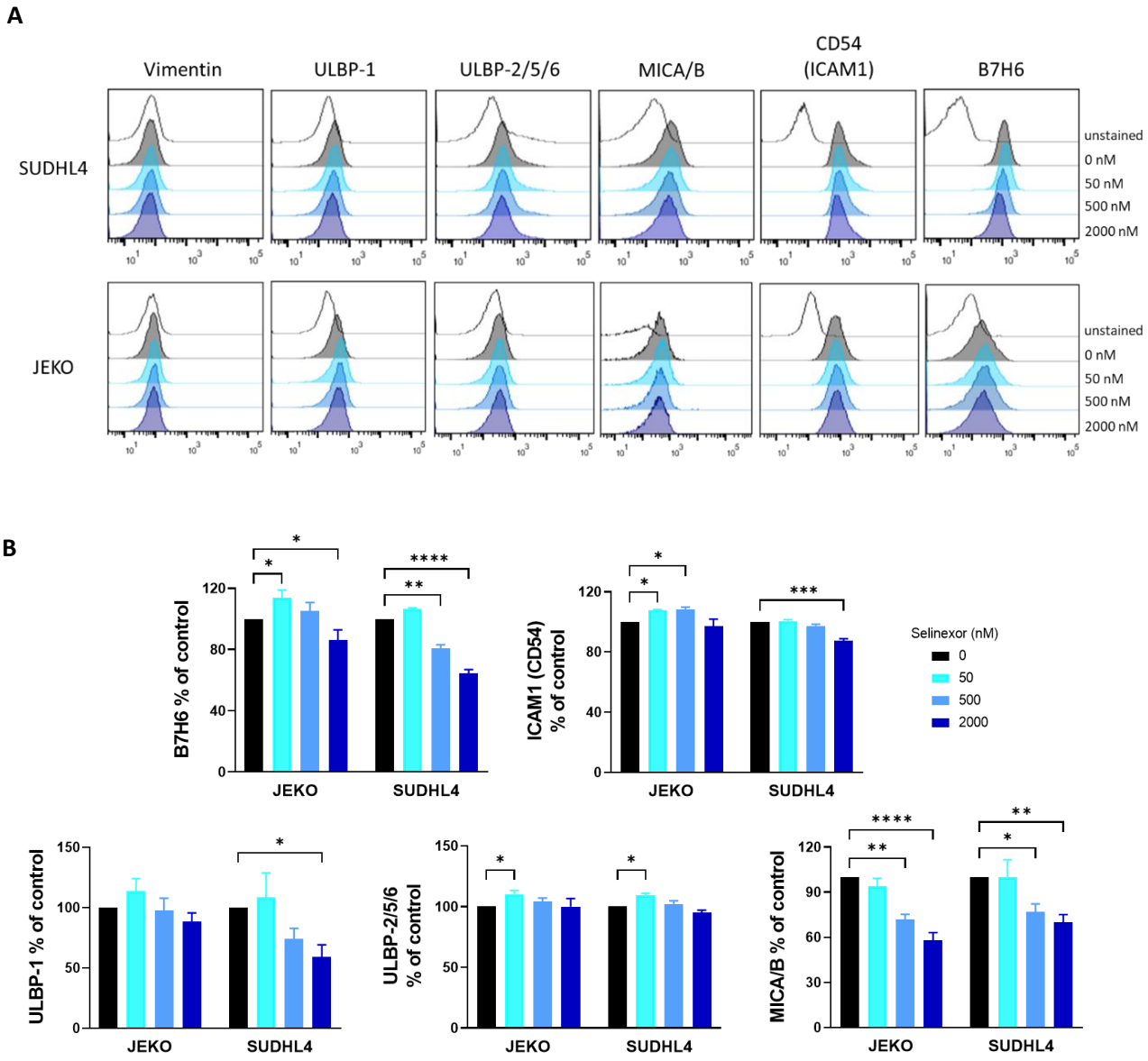


**Figure 3-9: Impact of selinexor treatment on the expression of NK cell activating ligands on B-cell lymphoma cell lines.**

(**A**) Representative example of the cell surface expression of vimentin, ULBP-1, ULBP-2/5/6, MICA/B, CD54 (ICAM1) and B7H6 on SUDHL4 and JEKO-1 cells treated with selinexor for 24 hours at the concentrations shown. (**B**) Cell surface expression relative to the untreated control of ULBP-1, ULBP-2/5/6, MICA/B, CD54 ICAM1) and B7H6 on SUDHL4 (n=5) and JEKO-1 (n=5) cell lines after treatment with selinexor for 16 hours at the concentrations shown. Shown is mean ± SEM and significant differences in protein expression between the 0 nM control and selinexor concentrations were calculated with repeated measure one-way ANOVA followed by Tukey's post-hoc test: *P<0.05, **P<0.01, ***P<0.005, **** P<0.0001.

Another potential mechanism for enhanced NK cell activation against selinexor-treated cancer cells is decreased expression of HLA proteins that bind NK cell inhibitory receptors as described by the 'missing-self hypothesis' (**Figure 1-3**). Expression of total HLA class I proteins (HLA-A/B/C) with the antibody clone W6/32 and HLA-E using the antibody clone 3D12 was assessed post XPO1 inhibition (**Figure 3-10**). For all B-cell lymphoma cell lines (RAMOS, JeKo-1 and SUDHL4) selinexor decreased surface levels of HLA-E, with a greater decrease observed on RAMOS and SUDHL4 cells compared to JeKo-1 (**Figure 3-10**). A slight, but significant increase in the expression of total HLA molecules was noted at 50 nM selinexor and a significant but slight decrease was observed at high selinexor concentrations (**Figure 3-10**). To ensure selinexor was affecting surface protein expression and not impacting cell morphology, cell size was measured using the FSC-A flow cytometry parameter (**Figure 3-10**). SUDHL4 and JeKo-1 cell size remained consistent at all selinexor concentrations and a slight decrease was observed for RAMOS.

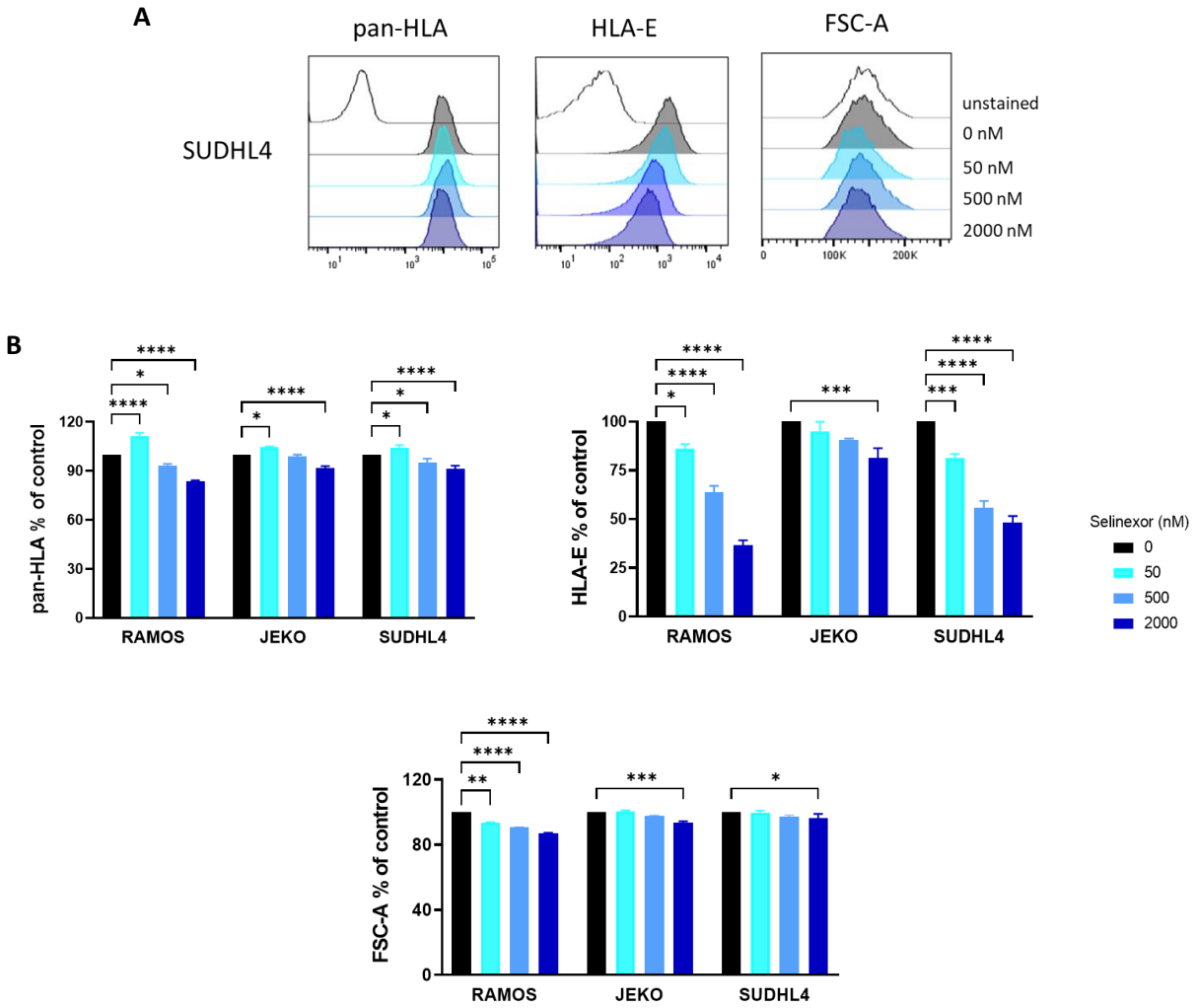


**Figure 3-10: XPO1 inhibition decreases HLA-E surface expression on malignant B cell lines.**

(**A**) Representative example of the cell surface expression of HLA class I (total HLA) and HLA-E on SUDHL4 cells treated with selinexor for 24 hours at the concentrations shown. FSC-A represents the size of SUDHL4 cells post selinexor treatment. (**B**) Cell surface expression relative to the untreated control of HLA class I (total HLA) and HLA-E on RAMOS (n=3), JeKo-1 (n=5) and SUDHL4 (n=5) cell lines after treatment with selinexor for 24 hours at the concentrations shown. Cell size after treatment with selinexor is described by the FSC-A parameter. One-way ANOVA analysis followed by Dunnett's post-hoc test was used to compare expression between the 0 nM control and selinexor concentrations: *P<0.05, **P<0.01, ***P<0.005, ****P<0.0001.

## 3.4 Mechanism for HLA-E downregulation with XPO1 inhibitors

### 3.4.1 Examining total proteins levels of HLA-E

Downregulation of surface HLA-E with selinexor could be explained by decreased levels of total HLA-E protein, either by increased HLA-E degradation or reduced transcription/translation. To assess total levels of HLA-E protein with selinexor, western blot experiments were performed with SUDHL4 (**Figure 3-11**). With increasing selinexor concentration, the abundance of total HLA-E remained constant suggesting that XPO1 inhibition impairs HLA-E plasma membrane stability rather than regulating HLA-E transcription or translation.

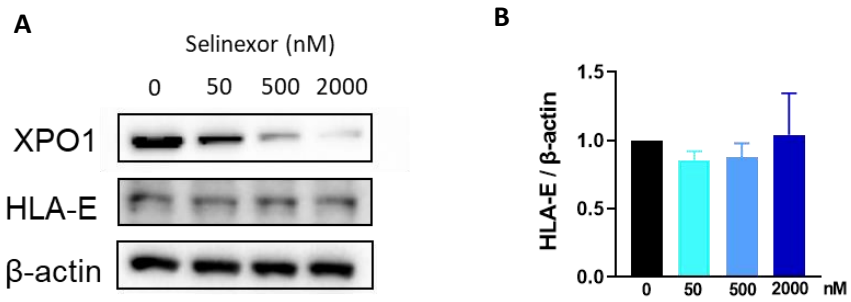


**Figure 3-11: Total HLA-E protein abundance is unaffected by selinexor.**

(**A**) Total HLA-E protein abundance assessed by western blot on SUDHL4 cells treated with selinexor (50-2000 nM) for 24 hours. (**B**) HLA-E protein band intensity calculated on ImageJ was normalised to the β-ACTIN loading control for each selinexor concentration and HLA-E expression relative to the 0 nM control was examined. Shown is mean ± SD across three separate experiments.

### 3.4.2 Investigating the induction of ER stress upon XPO1 inhibition

HLA-E surface expression has been shown to be sensitive to endoplasmic reticulum (ER) stress due to dysregulated production of peptides able to stabilise HLA-E at the plasma membrane (403). Treatment of multiple myeloma cell lines with bortezomib induced the expression of ER stress markers BiP and CHOP which correlated with HLA-E downregulation (403). Therefore, to determine whether XPO1 inhibition induces ER stress, selinexor-treated and leptomycin B (LMB)-treated B-cell lymphoma cells were assessed for the expression of multiple ER stress markers by western blot (466) (**Figure 3-12**). Brefeldin A (BFA) was used as a positive control to inhibit Golgi-ER membrane traffic and induce ER stress (403). With BFA, ER stress was successfully induced, with all markers increasing in abundance besides p-PERK which instead showed decreased mobility on the gel and reduced

levels of total PERK, perhaps reflecting complete phosphorylation with BFA (**Figure 3-12**). After treatment with selinexor or LMB, induction of ER stress proteins varied between cell lines, between ER stress proteins and between different concentrations of selinexor (**Figure 3-12**). For example, CALNEXIN was clearly induced with 50 nM selinexor, but then the band intensity reduced at higher selinexor concentrations, which was also seen for IRE-1α in SUDHL4 cells. In contrast, JeKo-1 displayed a dose-dependent response in IRE-1α expression, which was also strongly induced in both cell lines with LMB and BFA treatment. ERO-Lα was also induced with selinexor and LMB. Besides these increases in ER stress marker expression similar to the BFA positive control, the majority of markers (PDI, p-eIF2α, PERK, CHOP and BIP) showed either no change or decreased expression with increasing selinexor or LMB treatment. Across all cell lines increasing selinexor concentration had no effect on total HLA-E protein levels (**Figure 3-12**). Overall, these western blots demonstrate that XPO1 inhibition results in specific induction of ER stress markers in B-cell lymphoma cell lines, which may have consequences on HLA expression at plasma membrane and subsequent modulation of the on NK cell immune response.

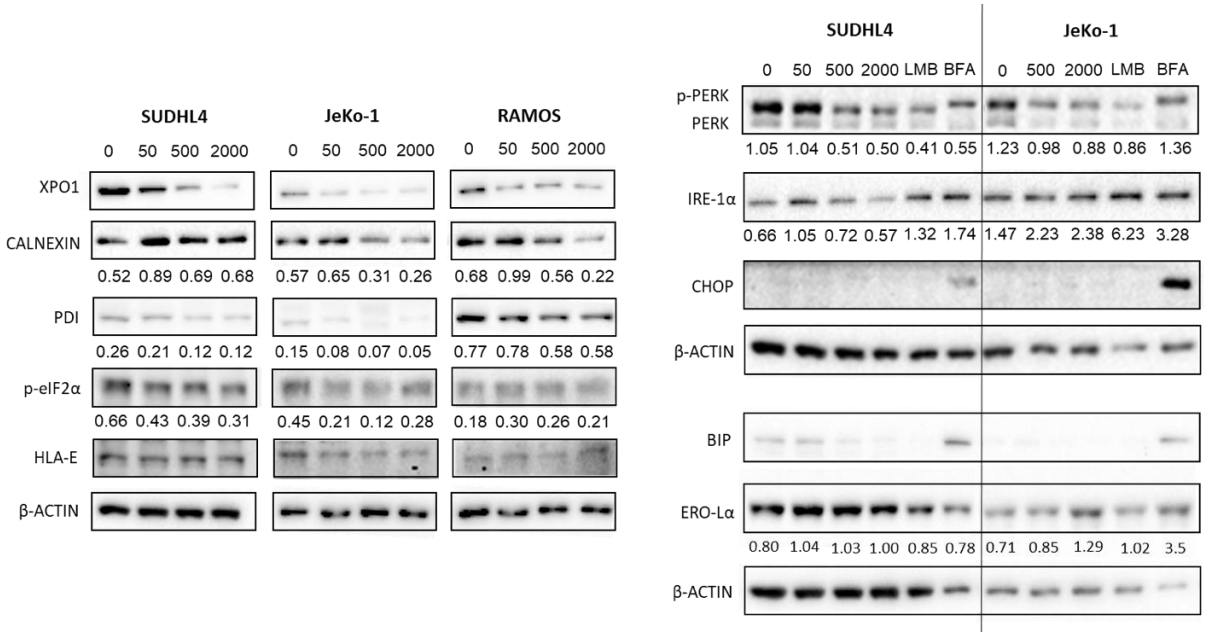


**Figure 3-12: Western blot of ER stress markers in B-cell lymphoma cell lines treated with XPO1 inhibitors.**

Abundance of ER stress markers in SUDHL4, JeKo-1 and Ramos cells after 24-hour treatment with XPO1 inhibitors selinexor (50-2000 nM) or leptomycin B (LMB, 50 nM). Cells were treated with 2 µg/mL brefeldin A (BFA) as a positive control for ER stress induction. Top band with anti-PERK represents phosphorylated PERK which signifies ER stress induction. Shown is one experiment of two and numbers on blot represent the relative band intensity relative to the β-ACTIN loading control calculated using ImageJ.

### 3.4.3 HLA-E trafficking to the plasma membrane in the presence of XPO1 inhibitors

Compared to classical HLA class I molecules, HLA-E is known to have a short half-life ($T_{1/2}$) at the plasma membrane with a $T_{1/2}$ of 4 hours ($T_{1/2}$ 24 hours for HLA-A/B/C) (9). This is due to a higher turnover of HLA-E molecules at the plasma membrane and because of the limited availability of peptides able to stabilise HLA-E and initiate translocation of HLA-E to the plasma membrane from the ER (9). Considering this, it was hypothesised that XPO1 inhibition further limits HLA-E-binding peptide availability resulting in reduced trafficking of HLA-E to the plasma membrane. To test this, B-cell lymphoma cell lines were stripped of HLA molecules at the plasma membrane with citric acid and recovery of HLA-E and total HLA molecules at the plasma membrane was measured over time in the presence of selinexor (**Figure 3-13**).

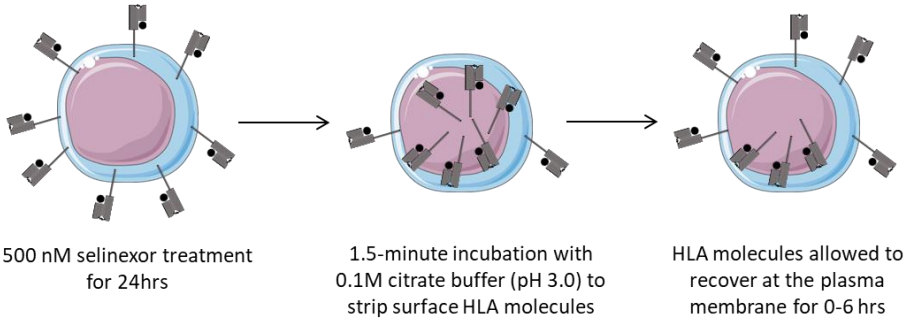


**Figure 3-13: Acid strip experiment workflow.**

Cancer cell lines were initially treated with selinexor (500 nM) or DMSO control for 24 hrs after which cells were resuspended in 0.1M citrate buffer (pH 3.0) to strip HLA molecules off the plasma membrane. Cells were placed back into medium and surface recovery of HLA molecules was assessed over a 6-hour period.

First, the duration of citrate buffer incubation required optimisation for cancer cell lines. With excess time cells would die due to the low pH of the citrate buffer and too little time would result in insufficient stripping of HLA molecules at the surface. Raji and Ramos cells were therefore incubated in citrate buffer for 0.5, 1, 2, 3 and 5 minutes and assessed for expression of surface HLA-E and HLA-A/B/C using the antibody clones 3D12 and W6/32, respectively, by flow cytometry (**Figure 3-14**). Compared to the 0-minute control in which cells were not incubated with citrate buffer, HLA-E and HLA-A/B/C molecules were stripped from the plasma membrane across all timepoints. After 1 minute, Ramos cells were mostly stripped of all HLA molecules and further timepoints did not further increase HLA stripping, but it did reduce the viability of cells. For Raji cells, HLA-A/B/C molecules were progressively stripped with increasing duration in acid up to 3 minutes. HLA-E on the other hand was fully stripped at 1 minute and Raji cell viability suffered greatly from 2 minutes. After 2 minutes for both cell lines, HLA-E expression increased slightly, most likely due to non-specific binding to dead cells. As such, the optimal time in acid was determined to be 1.5 minutes for both cells lines as cells were mostly viable at this time point and HLA-E was fully stripped in addition to HLA-A/B/C full stripping for Ramos. 1.5 minutes was decided as opposed to 1 minute to ensure optimal stripping of HLA molecules as this step is crucial to obtaining robust results from the experiment.

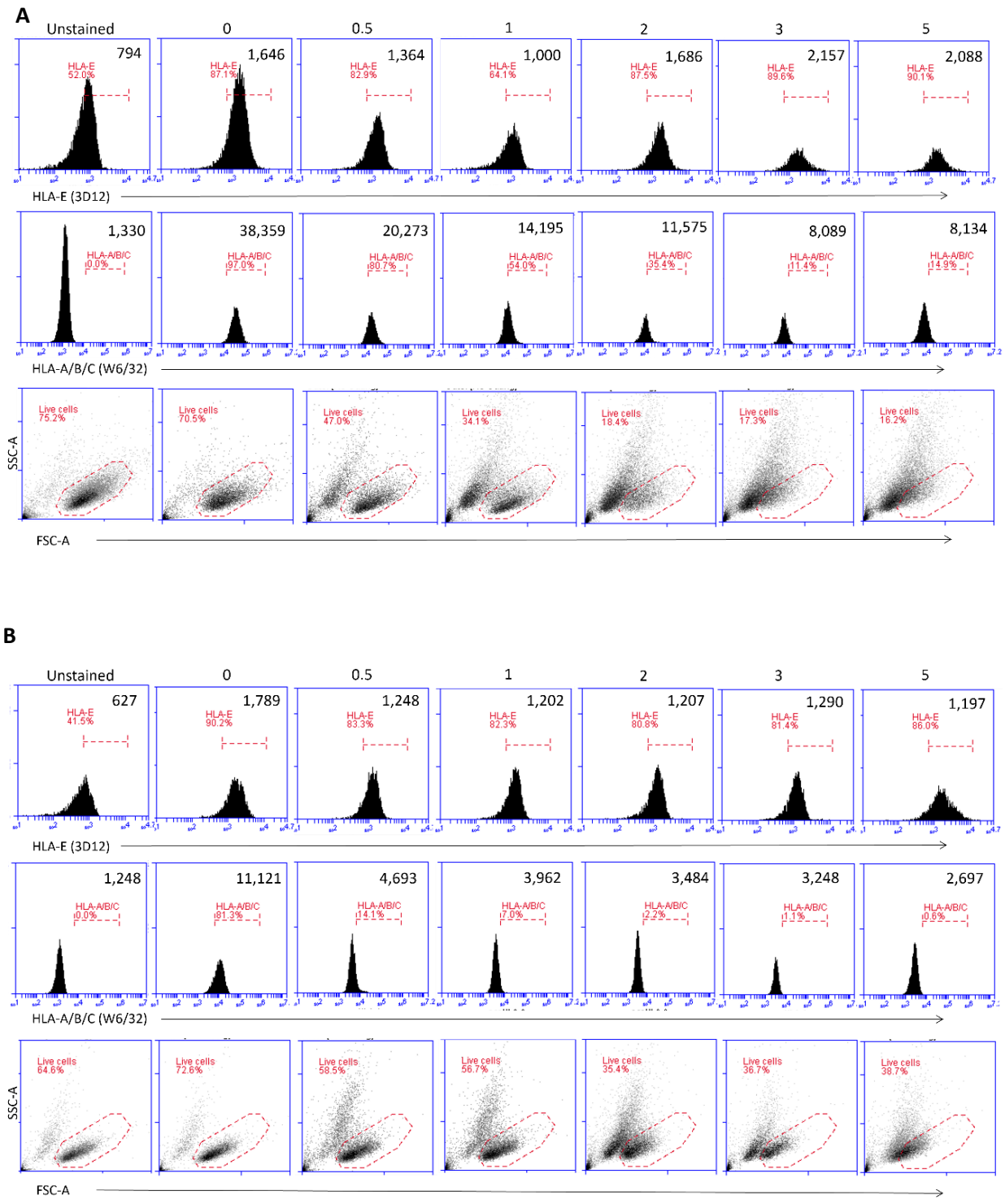


**Figure 3-14: HLA acid strip optimisation of Raji and Ramos cell lines.**

Raji cells (**A**) and Ramos cells (**B**) were incubated in citrate buffer (0.1 M, pH 3.0) for 0.5, 1, 2, 3 and 5 minutes and assessed for surface expression of HLA-E (antibody clone 3D12) and HLA-A/B/C (W6/32). Percentage of live cells within the SSC-A vs FSC-A gate for each timepoint is shown. Red numbers on histograms represent the proportion of cells within arbitrary gates that help illustrate shifts in histograms and the black numbers represent the MFI at each timepoint.

Following optimisation, Raji and Ramos cells were examined for HLA surface recovery in the presence of selinexor to determine HLA trafficking dynamics with XPO1 inhibition. Initially, cells were treated with selinexor during the HLA recover period only. During this period, cells were also treated with brefeldin A, an ER-Golgi transport inhibitor which impedes the recovery of HLA molecules at the plasma membrane (9). The rate of HLA recovery at the surface was similar in selinexor-treated and DMSO-treated Raji and Ramos cells (**Figure 3-15**). Brefeldin A successfully inhibited HLA surface recovery across the whole time period.

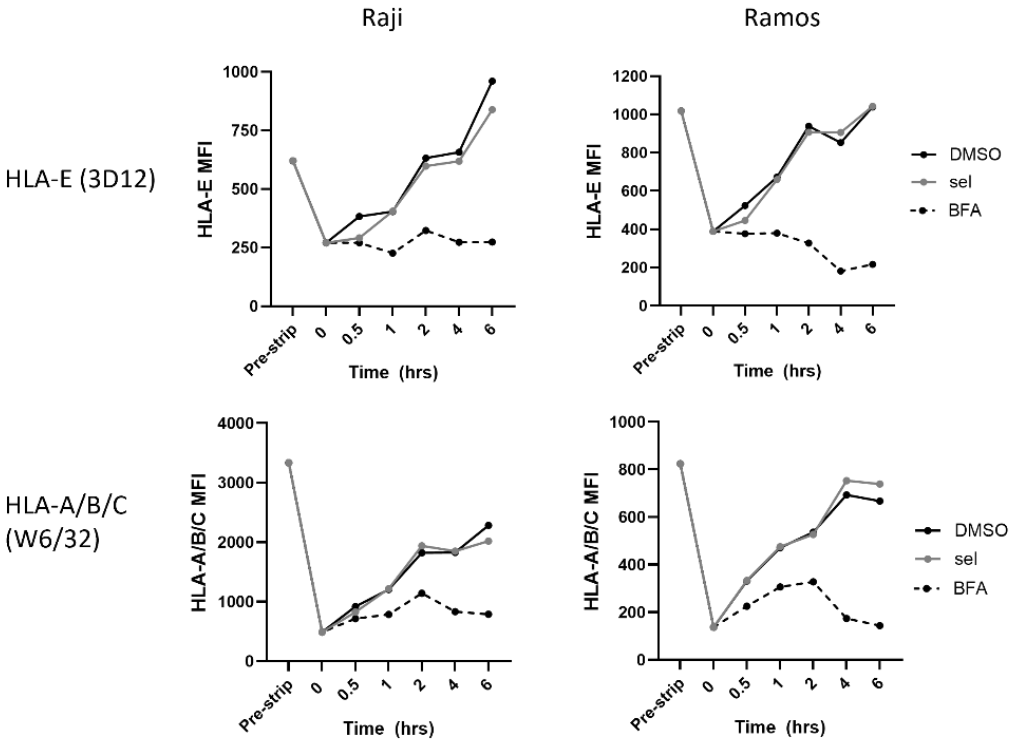


**Figure 3-15: HLA recovery at the plasma membrane in the presence of selinexor.**

Raji and Ramos cells were stripped of HLA molecules at the plasma membrane with citrate buffer (0.1 M, pH 3.0) for 1.5 minutes. Cells were then replated in fresh medium in the presence of selinexor (500 nM), brefeldin A (GolgiPlug, 2 µg/mL) or DMSO. Cells were then harvested at the given timepoints and assessed for surface expression of HLA-E and HLA-A/B/C with the antibody clones 3D12 and W6/32, respectively. Shown is the MFI from one experiment.

In previous cytotoxicity and NK cell activation assays, cell lines were treated with selinexor for 24 hours prior to co-culture with immune cells. As such, to allow for sufficient time for XPO1 inhibition and degradation by selinexor, Ramos cells were treated with selinexor for 24 hours prior to the start of the acid strip experiment. Ramos was selected because it expresses HLA-E at a higher level compared to Raji. In this scenario, Ramos cells treated with selinexor had a slower rate of HLA-E and HLA-A/B/C surface recovery compared to DMSO control cells (**Figure 3-16**). Selinexor did not impair HLA surface recovery at the same magnitude as the brefeldin A control. As shown in previous experiments (**Figure 3-10**), 24-hour selinexor treatment decreased HLA-E surface expression, hence selinexor pre-strip samples had an initial lower HLA-E surface expression level compared to the DMSO control. In **Figure 3-16A**, it took ~6 hours for HLA-E to recover at the plasma membrane in the presence of selinexor compared to ~3 hours for the DMSO control. This held true for $t_{1/2}$ (time taken to recover 50% of stripped molecules) shown in **Figure 3-16B**, as it took selinexor-treated Ramos ~3 hours and DMSO controls ~1 hour. For HLA-A/B/C plasma membrane recovery, $t_{1/2}$ for selinexor was ~4 hours and DMSO control 1.5 hours. Therefore, these experiments suggest that XPO1 inhibition impairs HLA plasma membrane trafficking but does not completely abolish this process like Brefeldin A (positive control). Further replicates are required to inform on statistical differences between selinexor and DMSO control, however one-way ANOVA analysis revealed no statistical difference between selinexor and BFA positive control at each timepoint reflecting that selinexor impairs HLA plasma membrane trafficking. Although HLA-A/B/C trafficking is also affected by XPO1 inhibition, the plasma membrane stability of HLA-A/B/C compared to HLA-E is much greater (9), as such the inefficient plasma membrane trafficking with selinexor only reduces HLA-E surface expression in non-strip conditions.

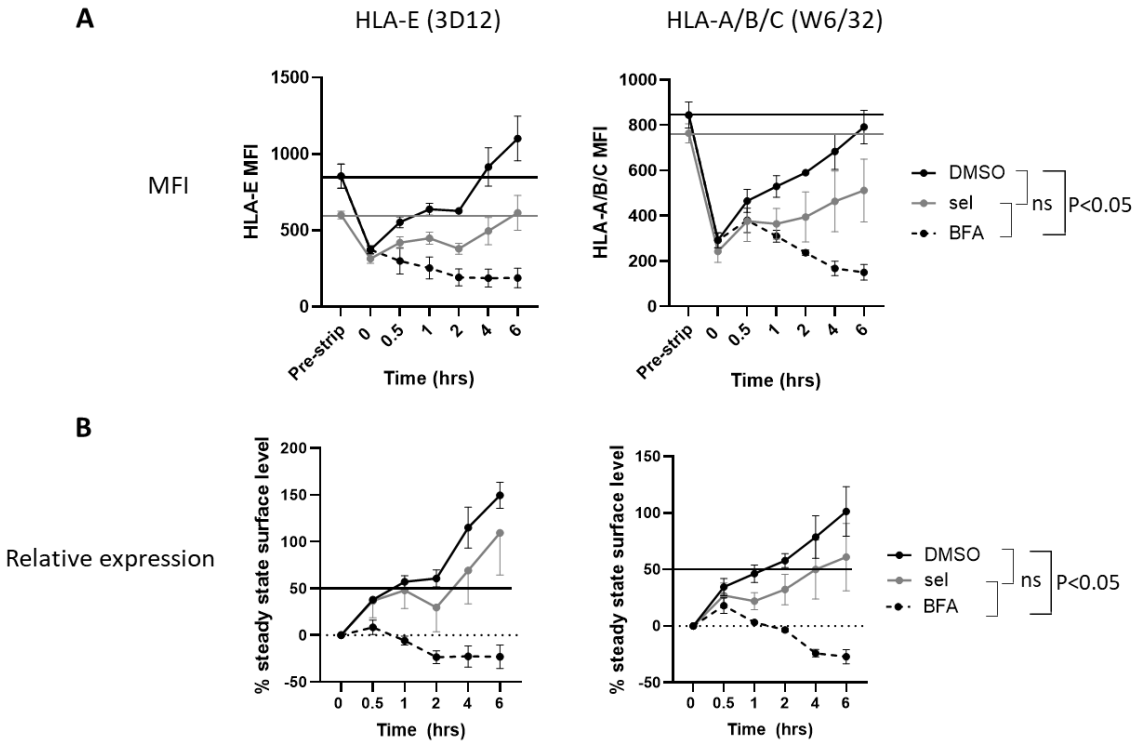


**Figure 3-16: Selinexor impairs HLA-E and HLA-A/B/C trafficking to the plasma membrane.**

Ramos cells were treated with selinexor (500 nM) or DMSO control for 24 hrs before being stripped of HLA molecules at the plasma membrane with citrate buffer (0.1 M, pH 3.0) for 1.5 minutes. Cells were then replated in fresh medium to allow for HLA recovery at the plasma membrane. A proportion of DMSO control cells were treated with brefeldin A (GolgiPlug, 2 µg/mL) during the 6-hour recovery period as a positive control for impaired HLA recovery. Cells were then harvested at the given timepoints and assessed for surface expression of HLA-E and HLA-A/B/C with the antibody clones 3D12 and W6/32 respectively. (**A**) Shown is the mean MFI ± SEM (n=4) with the black and grey horizontal bars representing the MFI of the pre-stripped DMSO control and selinexor samples, respectively. (**B**) Mean relative expression ± SEM (n=4) of HLA molecules at the given timepoints. Pre-strip values was set to 100% and 0 timepoint was set to 0%. One-way ANOVA was performed between all three treatments at each time point: ns = not significant, P<0.05 between DMSO negative control and BFA positive control for 1hr+ timepoints.

## 3.5 XPO1 inhibition with selinexor or leptomycin B preferentially activates NKG2A+ NK cells against malignant B cell lines

HLA-E is the ligand for the activating, heterodimeric NK cell receptor NKG2C-CD94 and the ligand for the inhibitory receptor NKG2A-CD94 (7). Because surface HLA-E expression decreased on selinexor-treated cancer cells, the lead hypothesis is that selinexor increases the activation of NKG2A+ NK cells. To test this in the LAMP assay, the degranulation and IFNγ production of NKG2A+ and NKG2A- NK cells were assessed and compared after PBMC co-culture with selinexor-treated SUDHL4 cells (**Figure 3-17**). As hypothesised, selinexor specifically enhanced the activation of NKG2A+ NK cells (**Figure 3-17**). Two-way ANOVA analysis revealed a significant effect of NKG2A expression on the degranulation of NK cells with increasing selinexor concentration ($F = 5.0$, $DF = 3, 27$, $P<0.01$).

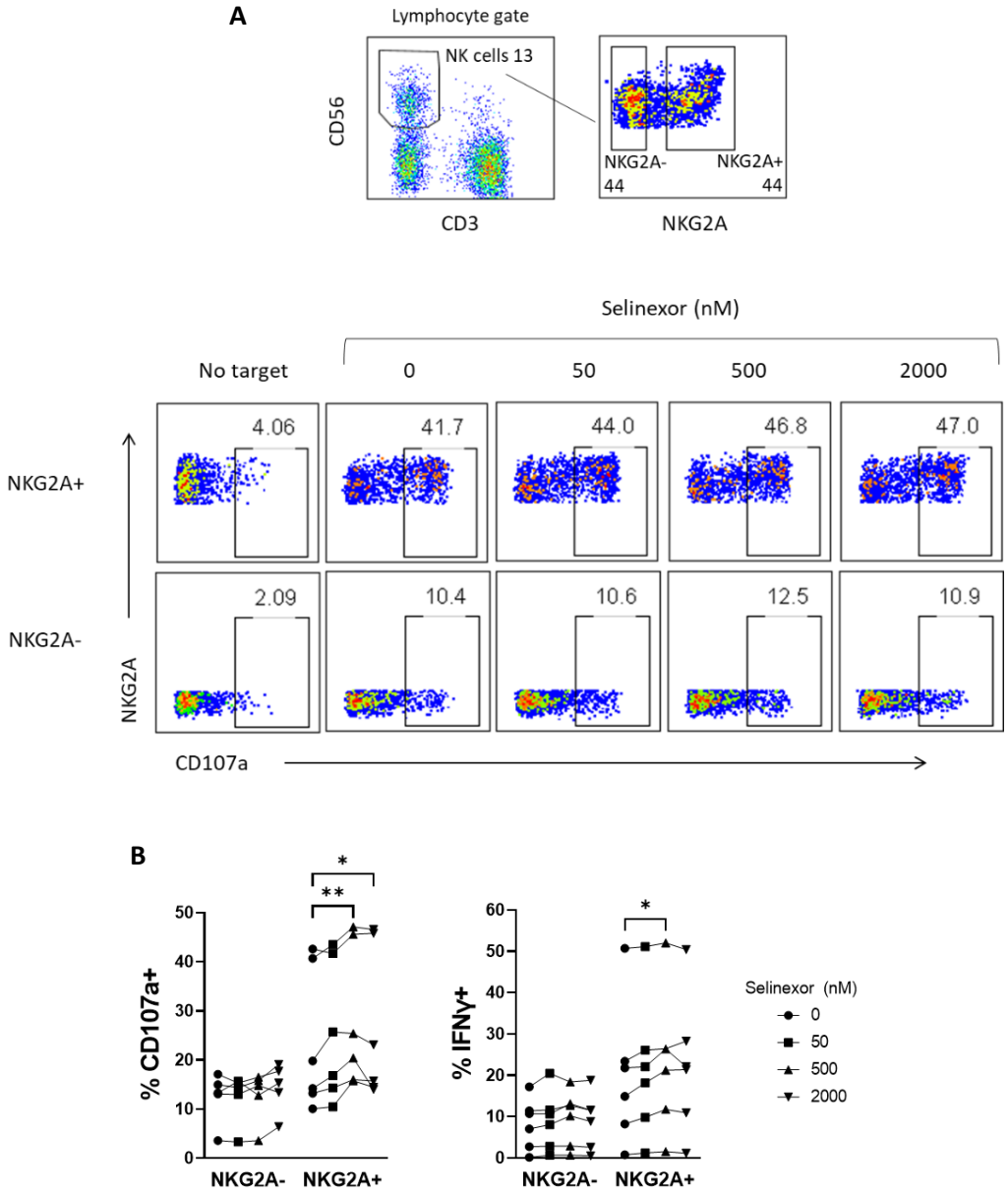


**Figure 3-17: XPO1 inhibition in SUDHL4 cells with selinexor preferentially activates NKG2A+ NK cells.**

(**A**) The degranulation of NKG2A+ and NKG2A- NK cells, measured by CD107a expression, was compared when healthy donor PBMC were co-cultured for 4 hours with selinexor pre-treated SUDHL4 cells at the concentrations shown. Numbers on flow cytometry plots represent the percentage of cells within gates. (**B**) Activation of NKG2A+ and NKG2A- NK cells measured by CD107a (left) and IFNγ (right) when healthy donor PBMC (n=6) were co-cultured with selinexor-treated SUDHL4 cells at an E:T of 5:1. The percentage of CD107a+ and IFNγ+ cells was normalised to no target controls for each donor. Significant differences in NK cell activation between 0 nM control and selinexor concentrations were calculated with repeated-measure two-way ANOVA followed by Tukey's post-hoc test: **P<0.01, *P<0.05.

Finally, to confirm that XPO1 inhibition results in downregulation of HLA-E and subsequent NKG2A+ NK cell activation, SUDHL4 cells were treated with an alternative XPO1 inhibitor leptomycin B (LMB). In contrast to selinexor, LMB does not induce the degradation of XPO1 (418), but like selinexor, LMB activates an intrinsic anti-cancer response as highlighted by increased abundance of p53 measured by western blot (**Figure 3-18A**). 24-hour LMB incubation at 50 nM led to surface HLA-E downregulation with no impact on cell morphology similar to 2000 nM selinexor treatment (**Figure 3-18B and C**). By co-incubating PBMC with LMB-treated SUDHL4 cells increased degranulation in the NKG2A+ NK cell population compared to the untreated control was observed (**Figure 3-18C and D**). As with selinexor, two-way ANOVA analysis revealed a significant effect of NKG2A expression on the degranulation of NK cells with LMB treatment ($F = 13.2$, $DF = 1, 8$, $P<0.05$). Through utilising another inhibitor of XPO1 function, SINEs sensitise B cell malignancies to NK cell lysis by activating NKG2A+ NK cells via downregulation of HLA-E. LMB also confirms an XPO1 peptide-independent mechanism for increased NK cell activation against SINE-treated cancer cells as LMB does not induce the degradation of XPO1. However, it does not discount an XPO1 peptide-dependent mechanism with selinexor by presentation of XPO1 peptides to KIR2DS2+ NK cells.

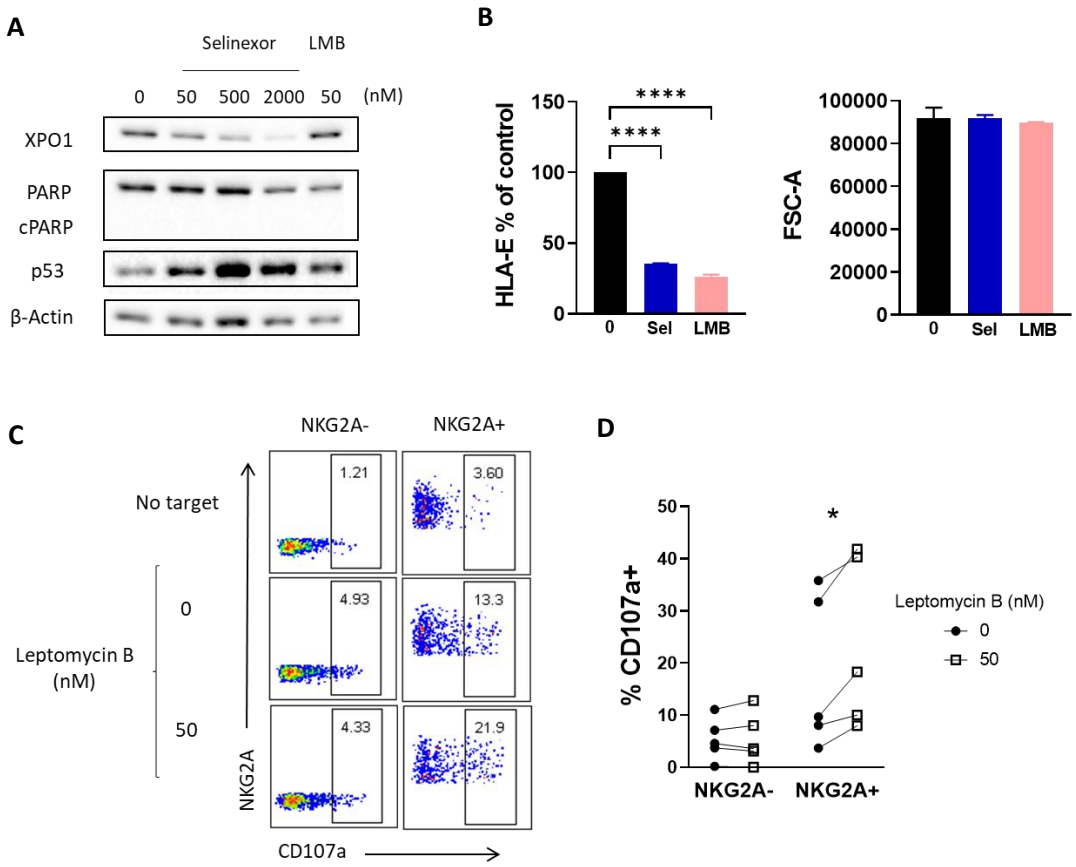


**Figure 3-18: XPO1 inhibition with leptomycin B in SUDHL4 cells reduces surface HLA-E expression and enhances the activation of NKG2A+ NK cells.**

(**A**) Abundance of XPO1 and p53 in SUDHL4 cells after 24-hour treatment with selinexor or leptomycin B (LMB) at the indicated concentrations in the presence of the apoptotic inhibitor Q-VD. SINE-induced apoptosis is depicted by the abundance of cleaved PARP (cPARP). (**B**) Cell surface expression relative to the untreated control of HLA-E on SUDHL4 cells (n=3) after treatment with 2000 nM selinexor or 50 nM LMB for 24 hours. Cell size after SINE treatment is described by the FSC-A parameter. One-way ANOVA: ****P<0.0001. (**C and D**) The degranulation of NKG2A+ and NKG2A- NK cells, measured by CD107a expression, was assessed when healthy donor PBMC were co-cultured with SUDHL4 cells pre-treated with 50 nM leptomycin B. Numbers on flow cytometry plots represent the percentage of cells within gates (**C**). Each line represents an individual donor (n=5) and the percentage of CD107a+ cells was normalised to no target control. Paired-sample t-test: *P<0.05 (**D**).

## 3.6 The effect of selinexor on ADCC

### 3.6.1 Combining selinexor with anti-CD20 monoclonal antibodies

NK cells express the activating Fc-binding receptor CD16a (FcγRIIIa) which enables them to perform ADCC. ADCC contributes to anti-CD20 mAb therapy as shown by the association of low NK cell number with shorter progression free survival in patients receiving anti-CD20 chemoimmunotherapy (260) and illustrated by NHL patients with the low affinity CD16a receptor (F158) having worse response to and overall survival of rituximab therapy (261,262). Currently, selinexor is in multiple clinical trials in combination with anti-CD20 mAbs for the treatment of advanced non-Hodgkin lymphoma (**Table 1-2**), however it is not known whether selinexor impacts ADCC. Therefore, it was assessed whether selinexor could synergise with the clinically relevant anti-CD20 mAbs rituximab and obinutuzumab *in vitro*. SUDHL4 cells were pre-treated with 500 nM selinexor for 24 hours followed by incubation with anti-CD20 mAbs for 20 minutes. PBMC or NK cells were subsequently added to opsonised cancer targets and NKG2A+ NK cell activation or NK cell specific lysis, respectively, was measured (**Figure 3-19**).

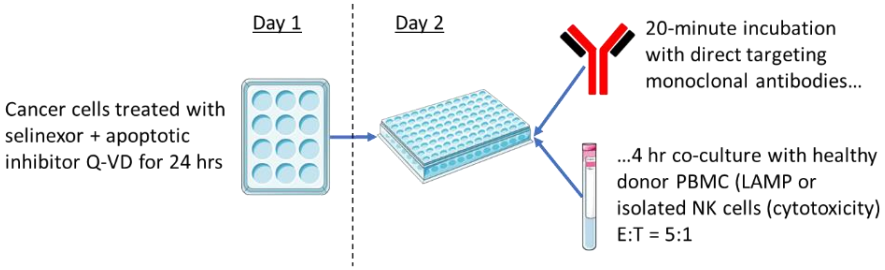


**Figure 3-19: LAMP and NK cell specific lysis assay workflows to assess the effect of XPO1 inhibition on ADCC *in vitro.***

Cancer cells were pre-treated with 500 nM selinexor or DMSO control for 24 hours in the presence of the apoptotic inhibitor Q-VD. After, selinexor was washed out and cancer cells were incubated for 20 minutes with direct targeting mAbs. Opsonised targets were then co-cultured with healthy donor PBMC to compare NKG2A+ and NKG2A- NK cell activation in the LAMP assay or co-cultured with purified NK cells to measure NK cell specific lysis at an effector:target (E:T) ratio of 5:1 for 4 hours.

In the LAMP assay, after addition of anti-CD20 mAbs to untreated controls, enhanced degranulation was observed in both NKG2A+ and NKG2A- NK cells with greater stimulation using obinutuzumab (**Figure 3-20,** black circles in **B**). As previously observed, in media and isotype controls, pre-treatment of SUDHL4 cells with selinexor increased the activation of NKG2A+ NK cells but not NKG2A- NK cells (**Figure 3-20**). When anti-CD20 mAbs were incubated with selinexor-treated SUDHL4 cells, NKG2A+ NK cells were further activated compared to anti-CD20 treatment alone, however only very slightly with a mean increase of 3.4% (**Figure 3-20**). In contrast, although NKG2A- NK cells were activated by opsonised SUDHL4 cells, pre-treatment with selinexor did not further enhance their activation. These data indicate that selinexor-treated cancer cells with downregulated HLA-E can be opsonised with anti-CD20 mAbs to further augment NKG2A+ NK cell activation compared to single agent treatments.

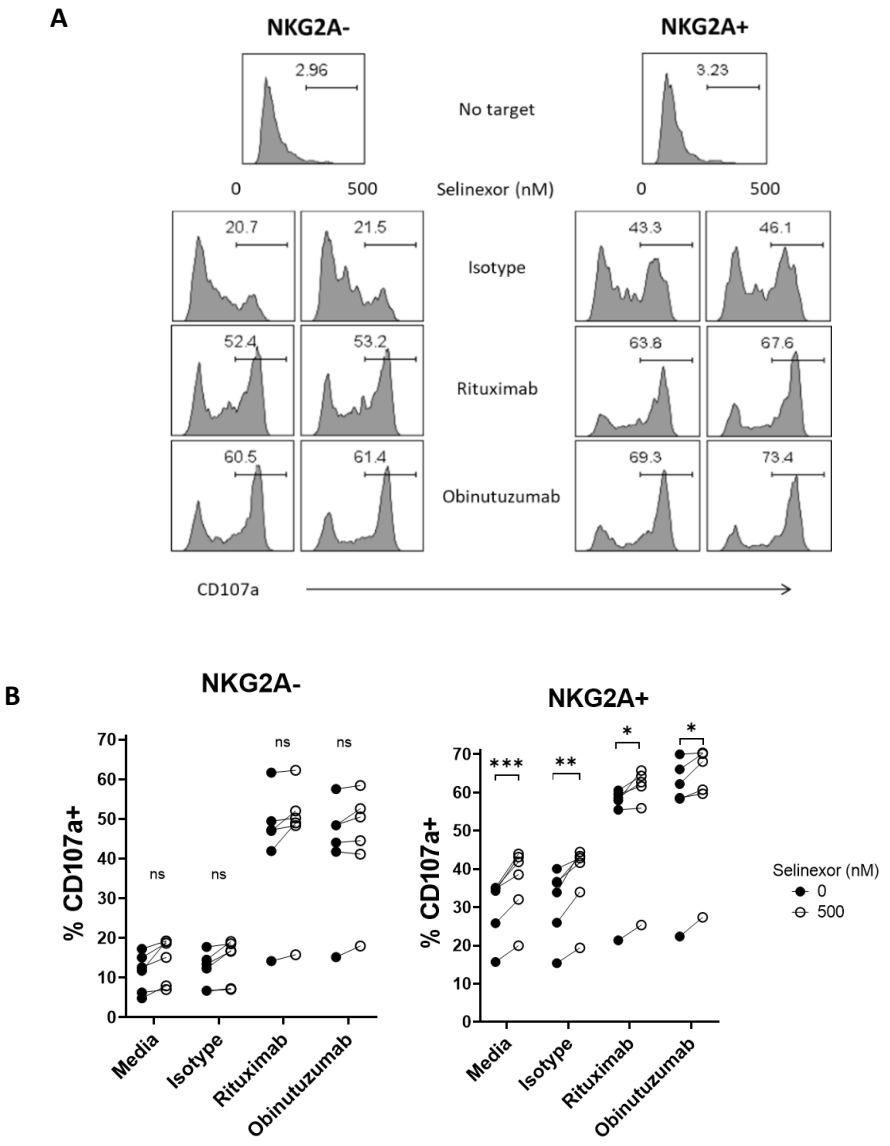


**Figure 3-20: Selinexor combined with anti-CD20 mAbs further enhance the activation of NKG2A+ NK cells.**

(**A**) Representative example of NKG2A- and NKG2A+ NK cell degranulation when PBMC were co-cultured with selinexor-treated SUDHL4 cells that were opsonised with 1 µg/mL anti-CD20 mAbs rituximab or obinutuzumab. Cetuximab (anti-EGFR) was used as the isotype control. Number on plots represent the percentage of CD107a+ NK cells within gates. (**B**) Percentage of CD107a+ NKG2A- and NKG2A+ NK cells when PBMC were co-cultured with SUDHL4 cells that were pre-treated with 500 nM selinexor for 24 hours and opsonised with 1 µg/mL anti-CD20 mAbs rituximab or Obinutuzumab. Each line represents one healthy donor PBMC (n=6). Paired sample t-test: ***P<0.005, **P<0.01, *P<0.05, ns = not significant.

Next, NK cell specific lysis of selinexor-treated SUDHL4 cells opsonised with anti-CD20 mAbs was assessed. In the 'no NK' control samples that were not treated with selinexor, addition of anti-CD20 mAbs induced cancer cell apoptosis (**Figure 3-21A**). When these cells were pre-treated with selinexor, there was no change in cancer cell viability in isotype and Rituximab sample (**Figure 3-21**). As expected, considering the results from the LAMP assay, NK cell specific lysis of SUDHL4 targets was enhanced by the combination of selinexor and anti-CD20 mAbs compared to single agent treatments (**Figure 3-21B**).

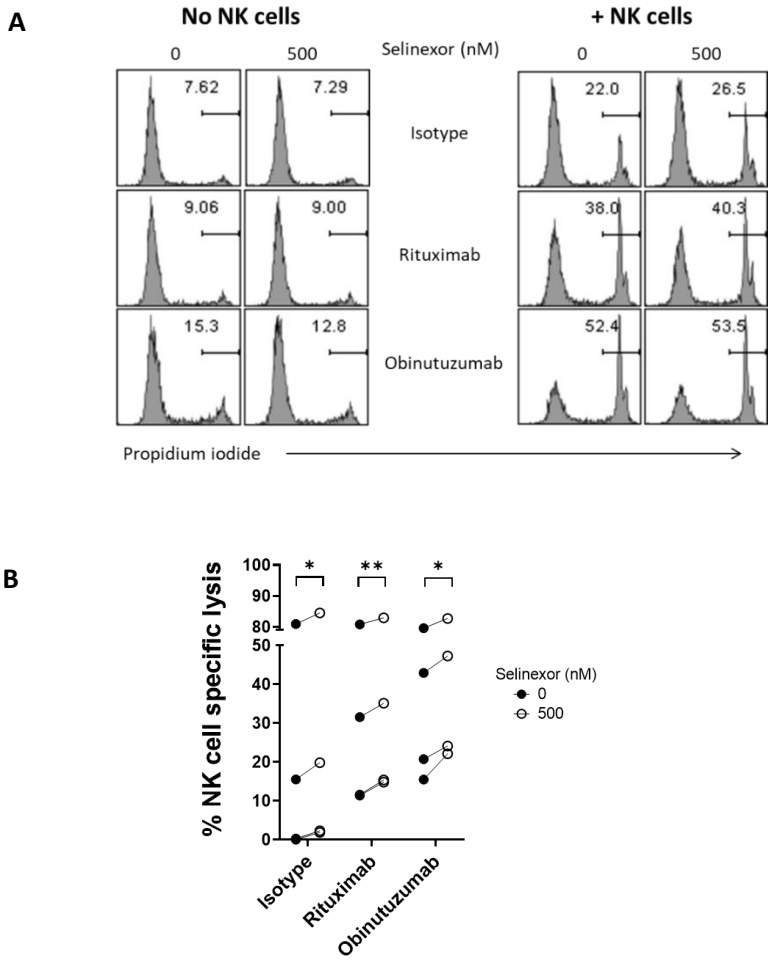


**Figure 3-21: Selinexor enhances NK cell specific lysis of anti-CD20 coated SUDHL4 cells.**

(**A**) Representative example of the percentage of lysed (propidium iodide positive), CellTrace™-labelled SUDHL4 cells. SUDHL4 cells were treated with 500 nM selinexor for 24 hours and coated with 1 µg/mL anti-CD20 mAbs rituximab and obinutuzumab or isotype control (cetuximab) for 20 minutes before co-culture with purified NK cells (right). Corresponding 'no NK' controls (left) were used to calculate % NK cell specific lysis as follows: *(% '+ NK cell' lysis - % 'no NK' lysis) * 100 / (100 - % 'no NK' lysis).* (**B**) % NK cell specific lysis of selinexor-treated SUDHL4 cells that were opsonised by anti-CD20 mAbs rituximab or obinutuzumab or isotype control (cetuximab). Each line represents one healthy donor PBMC (n=4). Paired sample t-test: **P<0.01, *P<0.05.

## 3.7 Discussion

### 3.7.1 XPO1 inhibition sensitises B-cell lymphoma cells to NKG2A+ NK cell activation

In this chapter, cell lines representing B-cell lymphomas (Burkitt's Lymphoma, MCL and DLBCL) were sensitised to NK cell activation and cytotoxicity following XPO1 inhibition. Since an XPO1-derived peptide (NAPLVHATL) described by the research group has been reported to stimulate KIR2DS2 (171), it was initially hypothesised that the selinexor-induced degradation of XPO1 would preferentially activate KIR2DS2+ NK cells via the increased abundance of the NAPLVHATL peptide. This hypothesis was then discarded by the data illustrating that KIR2DS2 negative NK cells and KIR2DS2 deficient donor NK cells were stimulated by XPO1 inhibition (**Figure 3-8**). Additionally, leptomycin B which does not induce the degradation of XPO1 was able to enhance NK cell activation and cytotoxicity, further indicating a peptide-independent mechanism for SINE-induced activation of NK cells (**Figure 3-18**). Although, an XPO1 NAPLVHATL peptide-dependent mechanism cannot be discounted. It must be considered that SUDHL4 cells used in KIR2DS2 experiments express the HLA-C*03:04 allele and NAPLVHATL peptide presentation to KIR2DS2 was shown in the context of HLA-C*01:02 expression (171). Therefore, although KIR2DS2 binds to HLA-C group 1 alleles such as HLA-C*03:04 (175) analysing the peptides presented on HLA class I molecules after XPO1 inhibition with selinexor will determine whether NAPLVHATL is being presented on SUDHL4 cells which may potentially contribute to enhanced KIR2DS2+ NK cell activation.

Interestingly, the SUDHL4 cell line which is derived from a patient with DLBCL activated NK cells the most after selinexor treatment. Importantly, DLBCL tumours have a high infiltration of NK cells (467) and NKG2A is highly expressed on patient NK compared to healthy controls (376). Selinexor is approved for the treatment of relapsed/refractory DLBCL, thus it could be speculated that enhanced NKG2A+ NK cell activation by selinexor may contribute to the positive anti-tumour effects in DLBCL, although this remains to be tested in patients.

HLA-E downregulation by selinexor and LMB enhanced NKG2A+ NK cell degranulation and IFNγ production. The NKG2A receptor is highly sensitive to changes in HLA-E surface levels on target cells and this is because of the low expression level of HLA-E, thus NKG2A has evolved to be sensitive to slight changes in HLA-E surface expression (17,208). NKG2A:HLA-E interactions exhibit saturation kinetics compared to HLA class I and KIR which follow linear kinetics (17,208). As such slight changes in HLA-E expression result in potent NKG2A+ NK cell immune responses. On the other hand, KIRs have evolved in cooperation with high HLA class I expression resulting in linear activation/inhibitory kinetics such that large changes in HLA class I expression are required to induce a response by KIR+ NK cells. Therefore, although HLA-A/B/C was slightly downregulated on Ramos after XPO1 inhibition (**Figure 3-10**), it is likely that the changes in HLA-E expression are responsible for enhancing NK cell

cytotoxicity with selinexor. Building on this, it will be important to dissect the activating receptors that are signalling in competition with NKG2A. Adding antibodies against activating NK cell receptors such as NKG2D and DNAM-1 to the flow panel in co-culture experiments will address this and the level of expression of these receptors between donors may explain donor variability in enhanced NK cell activity with XPO1 inhibition. Additionally, it has to be taken into consideration the effect of other immune cells in NK cell PBMC activation assays including T cells which will be activated against cancer cell lines and release inflammatory modulators to control NK cell functions and phenotypes. Interestingly, induction of HLA-E expression on activated T cells protects them from NK cell lysis, as such, in PBMC assays XPO1-induced NK cell activation may be impeded by T cell activation (29,468).

Ligands for NK cell activating receptors have been reported to increase with small molecules that induce p53 activation including nutlin-3a and doxorubicin (326,469,470). Although XPO1 inhibition was shown to induce a p53 response (**Figure 3-18**), no change in the expression of NK cell activating ligands were observed (**Figure 3-9**). This might reflect cell-specific responses to p53 activation. It was recently shown that induction of oxidative phosphorylation in B-cell lymphoma cells and multiple myeloma cells increase the expression of stress ligands MIC-A/B, ULBPs and ICAM-1 in a p53-dependent manner (471). This perhaps suggests that the p53-induced increase in NK cell activating ligand expression may require disruption to metabolic pathways and p53 activation alone does not increase NK cell activating ligand expression. XPO1 inhibition has been shown to disrupt metabolic-associated genes and reduce oxygen consumption rate in AML cells as measured by Seahorse and these experiments could be performed with B-cell lymphoma cells to affirm the link between p53, metabolism and activating ligand expression (472–474). NKG2D ligand shedding is a critical mechanism employed by leukaemia cells to evade NK cell immunity (475). The lack of NKG2D ligand expression after XPO1 treatment may be due to ligand shedding with selinexor. Conducting ELISA experiments with cell supernatants to measure soluble NKG2D ligands would address this.

Calreticulin, a marker of ER stress and also a ligand for NKp46 (476), also did not change with XPO1 inhibition. Interestingly, calreticulin can be used as a marker to distinguish between immunogenic cell death and apoptosis (477). Therefore, conducting co-culture experiments and measuring calreticulin surface expression on dying cancer cells will inform on the proportion of selinexor-induced death versus NK-mediated cell death (**Figure 3-9**). If calreticulin increases on tumour cells after co-culture with NK cells, this could provide a feedback loop via NKp46 to further promote NK-mediated lysis of tumour targets and thus, this warrants investigation as this may contribute to enhanced NK cell activation in co-cultures.

HLA-E overexpression is a well described mechanism employed by tumours to evade NK cell-mediated immunity (372). For HLA-E to become stably expressed at the plasma membrane, peptides are loaded on to HLA-E in the endoplasmic reticulum (ER) followed by transport to the plasma

membrane (9). As such, peptide availability and the loading on to HLA-E is a crucial step in determining HLA-E surface expression levels (9,34). Interestingly, the variant HLA-E*0103, which has a higher affinity for peptides resulting in increased surface expression compared to HLA-E*0101 (14,194), is associated with less favourable treatment outcome in non-Hodgkin lymphoma (60). Furthermore, RNA-seq analysis of tumours from 33 tumour types identified heterogeneity in the level of *HLA-E* expression, with particularly high expression in DLBCL samples (243). *HLA-E* expression was found to correlate with *KLRC1* (NKG2A) expression suggesting that the HLA-E:NKG2A immunosuppressive mechanism exists in patients and that interfering with this interaction may unleash an anti-tumour immune response by NK cells. Additionally, NKG2A+ NK cells have been reported in the lymph nodes of follicular lymphoma patients, therefore NKG2A may be a promising target to promote NK cell immune responses in patient lymph nodes (478). Through the use of selinexor, patient NKG2A+ NK cells may become greatly activated and stratification of patients based on HLA-E variants may provide some interesting insights on selinexor efficacy and NK cell contribution to tumour regression.

Because of the importance of HLA-E in protecting cancer cells from NKG2A+ NK cells, multiple strategies are undergoing intense research to disrupt NKG2A:HLA-E interactions. These include antibody blockade of which monalizumab, an anti-NKG2A mAb, is in phase 3 clinical trials for non-small cell lung cancer in combination with durvalumab (anti-PD-L1) (NCT05221840) and for head and neck squamous cell carcinoma in combination with cetuximab (NCT04590963) (276,277). Antibodies have also been raised against HLA-E and the mouse homolog Qa-$1^b$ which in addition to blocking inhibitory NKG2A:HLA-E interactions also promote ADCC because these antibodies can be IgG1 isotype (280,281). An interesting approach using a bispecific antibody exploiting HLA-E-restricted TCRs to improve specificity has also shown improved immune responses by NK cells and T cells (479). Adoptive transfer approaches using NK cells deficient in NKG2A expression by means of CRISPR-Cas9 (480), siRNA (315,316) and the use of protein expression blockers (243) to retain NKG2A in the Golgi have also shown enhanced NK cell responses *in vitro* and *in vivo*. Targeting signals downstream of NKG2A may also prove a viable option including the use of nanoparticles to direct siRNA against SHP-1, the inhibitory phosphatase downstream of NKG2A (481). The tyrosine kinase inhibitor dasatinib, used for the treatment of AML, also pertains immunomodulatory properties via the downregulation of NKG2A in patient NK cells (405). Interestingly, a recent study demonstrated that selinexor and dasatinib combine to enhance apoptosis of chronic myeloid leukaemia cells (473). Building on this, it would be interesting to investigate whether these two compounds combine to further enhance NK cell function against myeloid leukaemia. Overall, these studies demonstrate the importance of the NKG2A:HLA-E axis in oncology research and the data presented here illustrate that XPO1 inhibitors modulate this critical NK cell immune checkpoint.

The variation between donor NK cell activation (**Figure 3-5** and **Figure 3-6**) and cytotoxicity (**Figure 3-3**) may be due to different levels of education within individuals (101,104). Indeed, the varying levels of SHP-1 expression between NK cell donors, the adapter phosphatase recruited by NKG2A to inhibit NK cell activation signals, determines the level of response by NK cells (105). Even in scenarios of MHC downregulation, as with XPO1 inhibition, the magnitude of the NK cell response is determined by the basal levels of SHP-1 such that low levels of SHP-1 expression correlate with high NK cell cytotoxicity (105). Thus SHP-1 acts as a rheostat to fine tune the NK cell immune response and could be targeted with immunotherapy in addition to the targeting of surface receptors. This approach may be more effective at inducing potent anti-tumour immune responses given that many inhibitory receptors signal via SHP-1. In fact, intracellular immune checkpoints are the target of immunotherapy approaches including knockout of SHP-1 (482) and CISH (483), an inhibitory signalling protein in NK cells, in adoptively transferred NK cells and these have shown promising pre-clinical tumour regression data. CISH also negatively regulates TCR signalling and its deletion by CRIPSR in autologous T cells is being clinically tested in metastatic gastrointestinal indications (NCT04426669).

### 3.7.2 Mechanism for HLA-E downregulation by XPO1 inhibitors

The mechanism for downregulation of HLA-E with XPO1 inhibition was not due to reduced nuclear export of HLA-E because it is not present within the nucleus and has not been described as an interacting partner with XPO1. Equally, neither decreased transcription nor translation explained decreased surface expression of HLA-E as total protein analysis by western blot did not change with selinexor treatment (**Figure 3-11**). HLA-E is known to have low plasma membrane stability as inhibiting Golgi-ER traffic with brefeldin A quickly reduces HLA-E surface expression compared to classical HLA class I proteins (9,403). The cytoplasmic tail contributes to low surface stability of HLA-E because it induces rapid internalisation and when HLA class I cytoplasmic tails are expressed on HLA-E, surface stability is enhanced (9). The major contributing factor for HLA-E surface instability and low surface expression is the low availability of HLA-E-binding peptides. Peptide loading enables exit of HLA-E from the ER and the low availability of peptides at homeostasis results in HLA-E accumulation in the ER (9). This coupled with high internalisation rates result in low HLA-E surface expression compared to HLA-A/B/C proteins.

Modulating the abundance of HLA-E-binding peptides leads to significant changes in HLA-E surface expression, for example increasing peptide abundance results in increased HLA-E surface expression (9). XPO1 is known to transport ribosomal proteins and ribosomal RNA into the cytoplasm, hence XPO1 indirectly affects global protein translation rate (484,485). Additionally, XPO1 exports the translation initiation factor eIF4 and selinexor treatment therefore reduces protein translation rates (486). As such, XPO1 inhibition may reduce the abundance of peptides able to induce exit of HLA-E

from the ER and stabilise HLA-E at the plasma membrane. Experiments using puromycin to measure global protein translation rate would confirm whether XPO1 inhibition inhibits translation. In acid strip experiments, XPO1 inhibition impaired HLA-E and classical HLA class I protein recovery at the plasma membrane, indicating disruption to trafficking processes (**Figure 3-16**). One mechanism may be reduced abundance of peptides able to initiate exit from the ER. Although trafficking of classical HLA proteins was affected by XPO1 inhibition, under non-strip conditions these proteins were not massively downregulated after 24-hour selinexor treatment (**Figure 3-10** and **Figure 3-16**). This can be explained by their increased plasma membrane stability compared to HLA-E such that the slow rate of HLA-A/B/C replenishment at the surface is not apparent with XPO1 inhibition. The half-life ($T_{1/2}$) of HLA-A/B/C is 24 hours compared to HLA-E $T_{1/2}$ of 4 hours (9), therefore 24-hour selinexor treatment resulting in impaired HLA trafficking to the plasma membrane will mainly impact HLA-E surface expression. This is in accordance with a recent article showing that HLA-E is a real-time sensor of functional antigen processing and presentation machinery, such that any disruption to antigen processing because of infection or oncogenesis will lead to an NK cell activating response (34).

Carlsten et al., (2019) deduced by western blot of CHOP and BIP that ER stress was associated with HLA-E downregulation after bortezomib treatment in multiple myeloma cells. However, ER stress has also been linked to NK cell activation via stimulation of NKp46 binding to calreticulin (476) which may also contribute to the sensitisation of multiple myeloma cells to NK cells with bortezomib treatment. With XPO1 inhibition levels of CHOP and BIP did not change, neither did stress markers PERK, p-eIF2α, CALNEXIN nor PDI however, ERO-Lα and IRE-1α levels did increase with XPO1 inhibition (**Figure 3-12**). BIP binding to IRE-1α inhibits IRE-1α dimerization, therefore the decrease in BIP expression with XPO1 inhibition may have activated IRE-1α, which could be tested by western blot against phosphorylated IRE-1α, and downstream IRE-1α gene expression (487). In a recent publication, IRE-1α was shown to fine tune the magnitude of the ER stress response, enhancing PERK expression under chronic ER stress conditions after 24-36 hours (487). This suggests that XPO1 inhibition may induce low levels of ER stress which results in IRE-1α activation but not PERK. Furthermore, downregulation of surface HLA-E has also been described by increased oxidative stress in various cancer cell lines including multiple myeloma (488). Intracellular free thiol levels are indicative of oxidative stress which could be measured in cancer cells post selinexor treatment, to determine whether oxidative stress contributes to HLA-E downregulation.

### 3.7.3 Combining XPO1 inhibitors with monoclonal antibody therapy

CD16a (FcγRIIIa) on NK cells acts as a strong activating receptor due to its association with the CD3ζ adapter protein which contain multiples ITAM domains (149,183). There is evidence to suggest that NK cells play important roles in contributing to the efficacy of direct targeting monoclonal antibody

therapy. DLBCL patients with low numbers of circulating NK cells have worse prognosis when treated with anti-CD20 immunochemotherapy (260) and the expression of the high affinity CD16a receptor in CLL patients induces stronger ADCC responses by rituximab (489). High expression of HLA class I can impede ADCC induced by anti-CD20 mAbs via engagement with inhibitory KIR on NK cells (267). As such approaches to promote ADCC such as through combination treatments with small molecules that modulate inhibitory ligands on tumour cells, such as selinexor, may improve monoclonal antibody efficacy in patients and indeed anti-CD20 mAbs are in clinical trials with selinexor for non-Hodgkin lymphoma (**Table 1-2**). The results of these trials are eagerly anticipated to determine whether XPO1 inhibition can promote direct targeting mAb therapy in NHL.

As illustrated in section 3.6, selinexor potentiated ADCC of NK cells *in vitro* by the clinically relevant anti-CD20 mAbs rituximab and obinutuzumab. This enhanced ADCC with selinexor was due to modulation of the NKG2A:HLA-E inhibitory axis because only the NKG2A+ NK cell population was further activated by combination treatment (**Figure 3-20**). Past research has demonstrated *in vitro* that NKG2A signalling is important in dampening ADCC by NK cells with anti-CD20 mAbs (43,265,267,490). Anti-CD20 mAbs were combined with anti-NKG2A mAbs and enhanced NK cell activation and cytotoxicity was observed similar to the results collected here combining anti-CD20 mAbs with selinexor. NKG2A+ and NKG2A- NK cells express CD16a (CD16a is expressed on ~90% of circulating NK cells) and this can be seen by enhanced activation of NKG2A+ and NKG2A- NK cells with anti-CD20 mAbs (**Figure 3-20**). But when lymphoma cells were pre-treated with selinexor, only NKG2A+ NK cell activation was further enhanced because the imbalance of inhibitory and activating signals in these cells was further skewed towards activation compared to NKG2A- NK cells which are regulated by other inhibitory receptors for example KIRs. Whether NK cell ADCC *in vivo* can be enhanced by modulation of the NKG2A:HLA-E axis remains to be determined. Similar *in vivo* experiments using SCID mice inoculated with lymphoma cells as performed with BTK inhibitors in combination with rituximab could be used to assess the *in vivo* applicability of combined selinexor-anti-CD20 treatment (329).

# Chapter 4 The effect of XPO1 inhibition in primary human Chronic Lymphocytic Leukaemia cells on NK cell activation

## 4.1 XPO1 inhibition sensitises patient derived Chronic Lymphocytic Leukaemia (CLL) cells to NK cell cytotoxicity

CLL is a good primary patient model for studying B-cell malignancies primarily for the abundance of malignant cells in the circulation which is easily accessible for collection. Although variable, the lymphocyte population within the PBMC of CLL patients consist primarily of CD5+CD19+ CLL cells (90-99%) (491). Additionally, CLL was used a primary cancer model here because selinexor is in clinical trials for the treatment of CLL in combination with ibrutinib (NCT02303392) (448), as too are allogeneic and CAR NK cell therapies (NCT03056339) (305,492). Therefore, determining *in vitro* whether XPO1 inhibition can promote NK cell immune responses against CLL may warrant pre-clinical and clinical studies exploring selinexor-NK cell immunotherapy for CLL.

In the first instance, PBMC from patients with CLL were assessed for sensitivity to the XPO1 inhibitors selinexor and leptomycin B (LMB). The CLL patient characteristics used in this study can be found in **Table 2-2**. XPO1 inhibition was confirmed by western blot analysis showing that increasing selinexor concentration induced XPO1 degradation (**Figure 4-1**). LMB was used as a different mechanism by which to inhibit XPO1 and as with cell lines, XPO1 degradation was not seen in CLL samples after treatment with LMB (**Figure 4-1**).

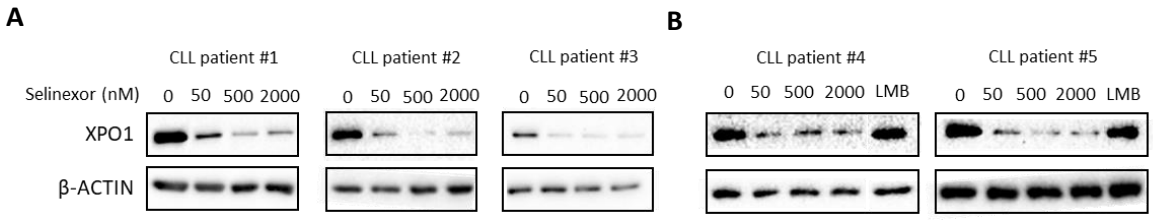


**Figure 4-1: *Ex vivo* selinexor treatment induces XPO1 degradation in patient CLL cells.**

XPO1 protein abundance measured by western blot in five representative CLL patient samples after treatment with selinexor (50-2000 nM, **A** and **B**) or leptomycin B (LMB, 50 nM, **B**) for 24 hrs.

To assess the sensitisation of CLL cells to NK cell cytotoxicity after treatment with XPO1 inhibitors, CLL cells were pre-treated with selinexor or LMB and co-cultured for 4 hours with purified, healthy donor NK cells. For CLL donors which harbour <90% CLL cells of total lymphocytes, CD19+CD5+ CLL cells were first purified by magnetic bead purification before use in assays. To inhibit drug-induced apoptosis, CLL cells were co-incubated with 30 µM Q-VD. Propidium iodide was used to measure CLL cell lysis and NK cell specific lysis was calculated taking into account background, drug-induced apoptosis of CLL cells (**Figure 4-2**).

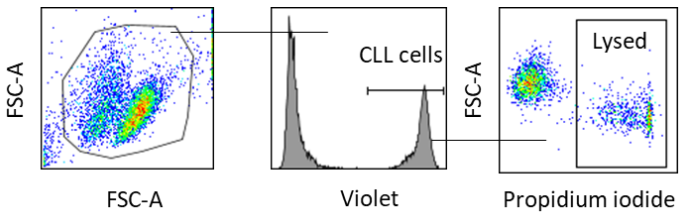


**Figure 4-2: Flow cytometry gating strategy used to measure lysis of patient derived CLL cells.**

CLL cells were stained with CellTrace™ Violet Cell Proliferation Kit to allow identification of CLL cells (violet positive) in co-culture with purified NK cells (violet negative). Lysed CLL cells were then identified by uptake of propidium iodide.

Treatment of CLL cells with selinexor in the presence of Q-VD inhibited apoptosis successfully (**Figure 4-3A**, 'no NK' column). Addition of NK cells induced CLL cell lysis (**Figure 4-3A**, '0 nM' row) and NK cell specific lysis of CLL cells was enhanced by pre-treatment of CLL cells with selinexor (**Figure 4-3B**). Furthermore, NK specific lysis was enhanced when CLL cells were pre-treated with LMB (**Figure 4-3C**). In accordance with enhanced NK specific lysis of CLL cells, increased NK cell activation was observed as measured by CD107a and IFNγ expression against selinexor pre-treated CLL cells (**Figure 4-4**).

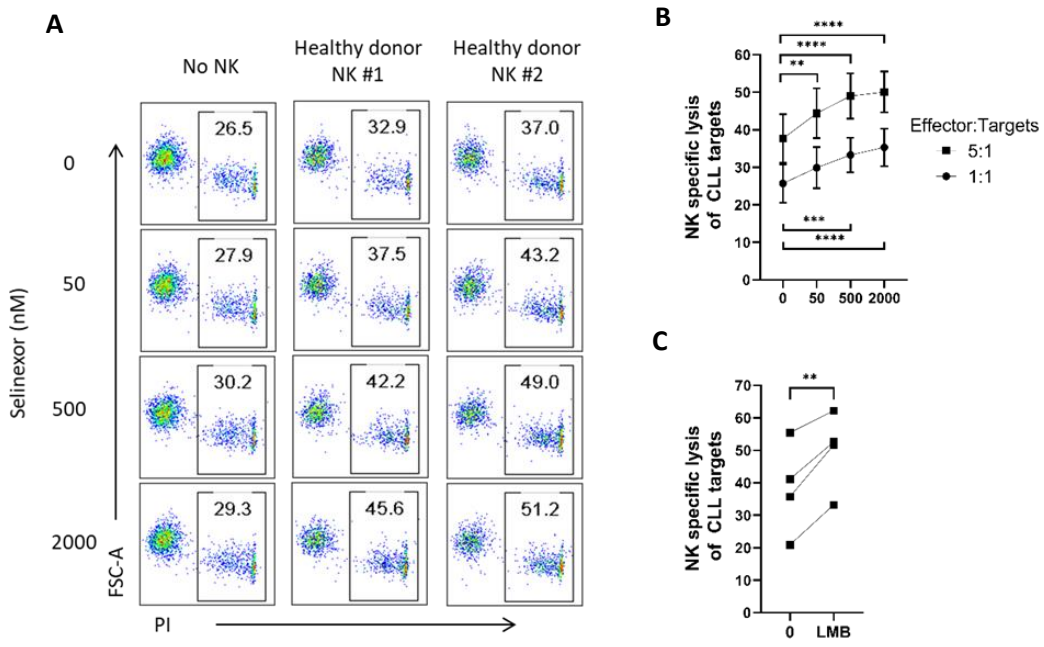


**Figure 4-3: XPO1 inhibitors sensitise CLL cells to NK specific lysis.**

Purified healthy donor NK cells were co-cultured for 4 hrs with CLL cells pre-treated with XPO1 inhibitors (in the presence of 30 µM Q-VD) at effector:target ratios of 5:1 and 1:1. (**A**) Representative flow cytometry plots of the proportion of lysed CLL cells (propidium iodide positive, PI) after CLL cells from one CLL donor were co-cultured with NK from two different healthy donors (E:T = 5:1). Spontaneous lysis of CLL cells was measured at each selinexor concentration (no NK column) and NK cell specific lysis in (**B**) and (**C**) was calculated as $\frac{\%\ CLL\ lysed\ with\ NK - \%\ CLL\ lysed\ without\ NK}{100 - \%\ CLL\ lysed\ without\ NK} * 100$ to account for spontaneous and drug-induced cell death. Shown in (**B**) is mean ± SEM (n=10 of 5 CLL donors and 3 healthy donor NK) and differences in NK specific lysis between the 0 nM control and selinexor concentrations were calculated with repeated-measure one-way ANOVA followed by Dunnett's multiple comparison test: **P<0.01, ****P<0.001. In (**C**), NK specific lysis of 4 CLL donors was assessed using NK cells from 2 healthy donors (E:T = 5:1) and significance in NK specific lysis between control and leptomycin B (LMB, 50 nM) treatment was calculated with paired t test: **P<0.01.

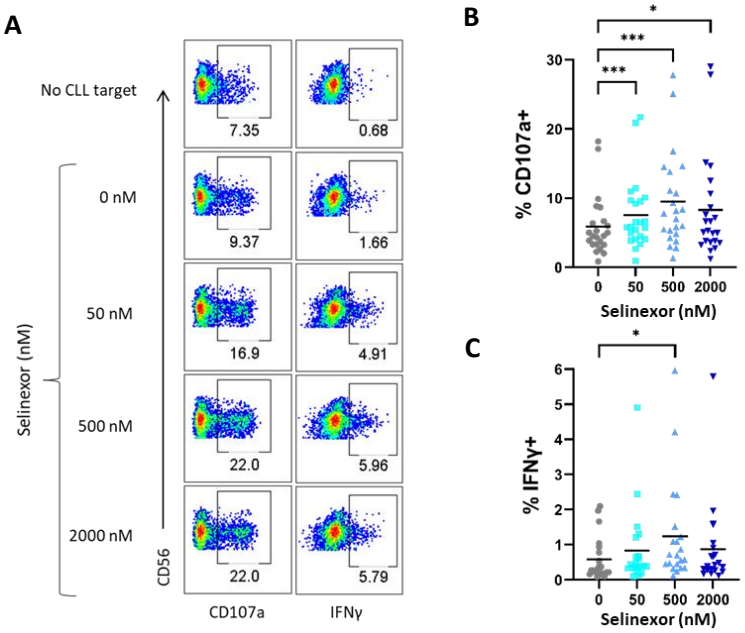


**Figure 4-4: Selinexor pre-treatment of CLL cells enhances NK cell activation.**

CLL cells were pre-treated with selinexor (50-2000 nM) for 24 hours and then co-cultured with healthy donor PBMC for 4 hours. (**A**) CD56+CD3- NK cell activation was measured by expression of CD107a and IFNγ as shown in the flow plots. Numbers represent the percentage of NK cells within gates. (**B-C**) NK activation across multiple CLL donor and healthy donor NK cell co-cultures (n=23 for **B** and n=21 for **C** using 8 CLL donors and 7 healthy donors). Each point represents individual CLL-NK co-cultures with background NK activation accounted for (no CLL target well in **A**). Lines represent means at each selinexor concentration and statistical significance in NK cell activation between the 0 nM control and selinexor concentrations were calculated by repeated-measured one-way ANOVA followed by Tukey's post-hoc test: *P<0.05, ***P<0.005.

## 4.2 Mechanism for increased sensitivity of selinexor-treated CLL cells to NK cell cytotoxicity

In chapter 3, XPO1 inhibition in malignant B cell lines induced downregulation of surface HLA-E, as such CLL cells treated with XPO1 inhibitors were assessed for surface expression of HLA-E by flow cytometry. CLL cells were identified in the PBMC of patients through co-expression of CD19 and CD5 (**Figure 4-5**).

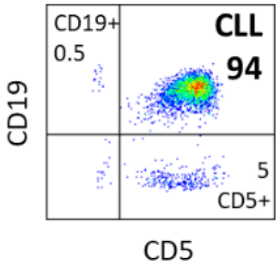


**Figure 4-5: Flow cytometry gating strategy to identify CD5+CD19+ CLL cells.**

Representative example of one CLL patient PBMC stained with antibodies against CD19 and CD5 to identify CD19+CD5+ CLL cells after gating on lymphocytes. CD19+CD5+ cells were gated on to measure NK ligand expression after treatment with XPO1 inhibitors.

On CD19+CD5+ CLL cells, treatment with selinexor downregulated HLA-E surface expression in all samples tested with a mean reduction of 40% at 2000 nM selinexor compared to the untreated control (**Figure 4-6A and B**). CD19 expression and cell morphology, as measured by FSC-A, did not change with increasing concentration of selinexor indicating that XPO1 inhibition specifically modulates HLA-E surface expression. Total HLA expression decreased slightly at high selinexor concentrations (500 nM and 2000 nM), however because the antibody clone W6/32 potentially recognises HLA-E in addition to classical HLA class I molecules (HLA-A/B/C) this may be due to specific HLA-E downregulation (7,493). XPO1 inhibition with LMB also downregulated surface HLA-E expression by 40% and total HLA expression remained unchanged (**Figure 4-6C**).

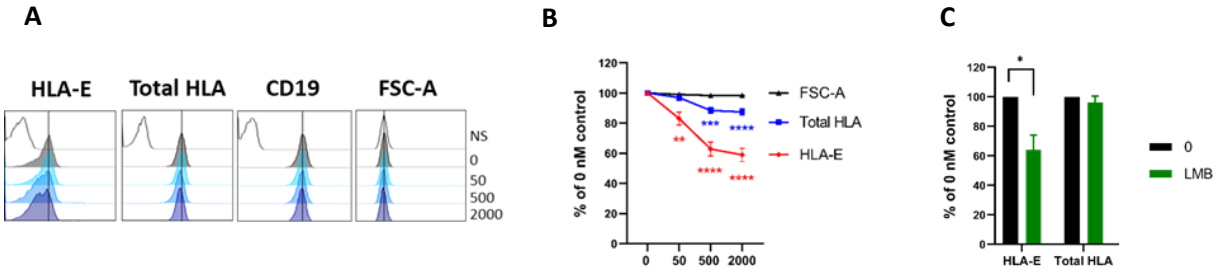


**Figure 4-6: XPO1 inhibitors downregulate HLA-E surface expression on CLL cells.**

(**A**) Histograms of the surface expression of HLA-E, total HLA class I and CD19 on CD19+CD5+ CLL cells after treatment with selinexor for 24 hours (50-2000 nM). Shown is a representative example of one CLL donor. Cell size was measured using the FSC-A parameter. NS = no stain. Black vertical line on each histogram is placed on the peak of the 0 nM control. (**B-C**) Surface expression of HLA-E and total HLA class I on CD19+CD5+ CLL cells after treatment with selinexor (50-2000 nM, **B**) or leptomycin B (50 nM, LMB, **C**) for 24 hrs. Shown is mean expression ± SEM relative to the 0 nM control of 17 CLL patients in **B** and 5 CLL patients in **C**. Asterisks represent significant differences in surface expression to the 0 nM control. This was calculated with repeated-measure one-way ANOVA followed by Dunnett's multiple comparison test for each protein group: **P<0.01, ***P<0.005, **** P<0.001. For (**C**) differences in HLA expression between control and LMB was calculated by paired t-test: *P<0.05.

To determine whether subgroups of CLL patients were differentially sensitised to selinexor-induced HLA-E downregulation, CLL patients were stratified based on *IGHV* mutational status and IgM surface expression, two major prognostic factors (344,494). Patients with unmutated IGHV (U-IGHV) compared to mutated IGHV (M-IGHV) have worse prognosis because of the higher proliferative potential of naïve B cells compared to differentiated B cells (344). High surface expression of IgM, also referred to at the B-cell receptor (BCR), induce more potent survival and proliferative signals (494). IgM surface expression was considered high if the IgM MFI was >50 as in the Chiodin et al., (2022) study. HLA-E downregulation with selinexor was evident in all subgroups of patients and two-way ANOVA interaction analysis did not reveal a difference in CLL subtype response to selinexor, therefore the selinexor-induced HLA-E downregulation is independent of *IGHV* mutational status and surface level of IgM (**Figure 4-7**).

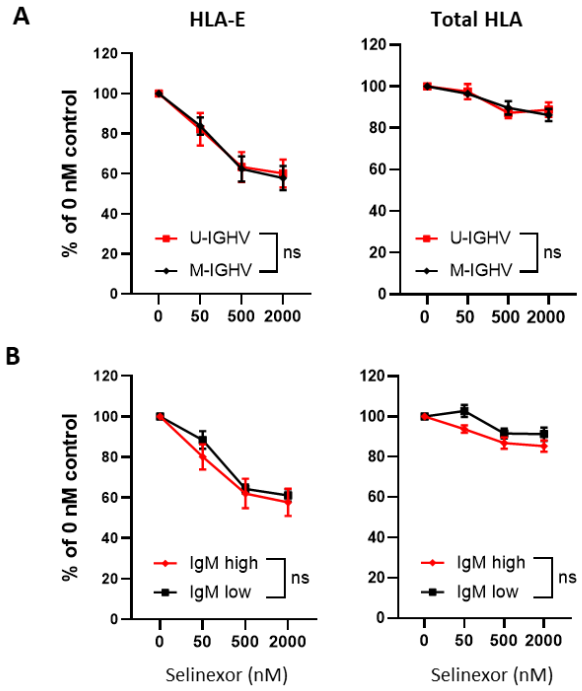


**Figure 4-7: HLA expression on CLL patient cells after *ex vivo* selinexor treatment stratified on IGHV mutational status and IgM surface expression level.**

CLL patient PBMC were treated with selinexor (50-2000 nM) for 24 hrs and HLA-E and total HLA surface expression was assessed on CD5+CD19+ CLL cells. Expression levels were compared between CLL patients with U-*IGHV* (n=9) and M-*IGHV* (n=8) (**A**) and between patients with high surface expression of IgM (>50 MFI, n=11) and low surface expression (<50 MFI, n=6) (**B**). Shown is relative mean expression ± SEM of the untreated control and differences in HLA expression between CLL subtypes were calculated by repeated-measure two-way ANOVA with interaction analysis.

To decipher the duration of selinexor treatment required to decrease the surface expression of HLA-E on CLL cells, HLA-E expression was measured at intervals over a 24-hour period. After 16 hours of treatment with 500 nM selinexor, HLA-E started to become downregulated (13% decrease compared to the 0 hr timepoint) (**Figure 4-8A**). This downregulation continued until the 24-hour timepoint when HLA-E surface expression was decreased by 34% of the 0 hr timepoint. Brefeldin A (BFA) was used as a positive control for downregulating HLA surface expression (9,403). HLA molecules are not completely stable at the plasma membrane and become internalised over time (9). Because BFA inhibits ER-Golgi traffic, this impairs replenishment of HLA molecules at the plasma membrane. Indeed, after 1 hour of BFA treatment, HLA-E surface expression was decreased by 30% and after 24 hours HLA-E expression was decreased by 80% (**Figure 4-8A**). Additionally, total HLA was downregulated by BFA, particularly after 24 hours, but total HLA expression remained stable over the course of the experiment with selinexor as too did CD19 (**Figure 4-8A**). To determine whether HLA-E

downregulation was maintained after selinexor removal from the culture, CLL cells were washed with medium to remove selinexor and replated for 24 and 48 hours and assessed for surface expression of HLA molecules. After 24 and 48 hours without selinexor in the culture, HLA-E expression remained downregulated with no change in expression of total HLA and CD19 (**Figure 4-8**). These data demonstrate that HLA-E takes approximately 16 hours to become downregulated by XPO1 inhibition and remains downregulated after selinexor removal from the culture for at least 48 hours, potentially due to continued disruption to nuclear export.

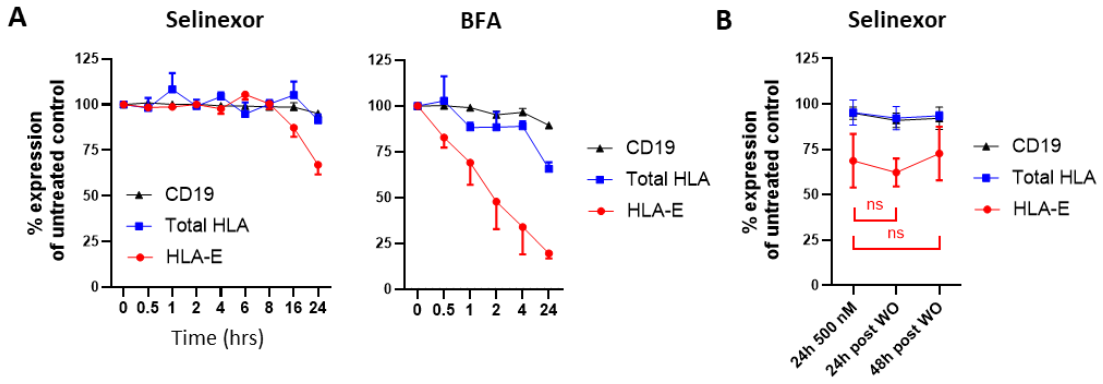


**Figure 4-8: HLA-E is downregulated after 16 hour-selinexor treatment and remains lowly expressed after selinexor removal.**

(**A**) CLL cells were treated with selinexor (500 nM, left) or brefeldin A (BFA, 2 µg/mL, right) for 24 hours and surface expression of HLA-E, total HLA and CD19 was assessed at the timepoints shown during the 24-hour period (n=6). (**B**) CLL cells were treated with selinexor (500 nM) for 24 hours after which selinexor was washed out (WO) from cultures with addition of medium and centrifugation and cells were replated for 24 and 48 hours and assessed for HLA-E, total HLA and CD19 expression (n=4). Shown is mean ± SEM and differences in HLA-E expression between washout timepoints were calculated by repeated-measure two-way ANOVA.

To confirm the specificity of HLA-E downregulation in patient CLL cells after *ex vivo* selinexor treatment, degranulation (CD107a positivity) and IFNγ expression of NKG2A+ NK cells from healthy donor PBMC against selinexor-treated CLL cells was examined. For NK cell degranulation, both NKG2A+ and NKG2A- NK cells were significantly activated by selinexor (**Figure 4-9A and B**). However, the NKG2A+ NK cell population was more sensitive to activation as highlighted by CD107a fold change calculations (**Figure 4-9C**). In terms of IFNγ expression, a similar pattern was observed in that both NKG2A+ and NKG2A- NK cell populations had significantly increased expression of IFNγ with increasing selinexor concentration, however the increase observed in NKG2A+ NK cells was greater than that of NKG2A- NK cells (**Figure 4-10**). The fold change in IFNγ production could not be

calculated due to the low production of IFNγ in the no CLL target controls. When leptomycin B was used an alternative XPO1 inhibitor, it preferentially activated NKG2A+ NK cells compared to NKG2A- NK cells (**Figure 4-11**). Finally, to understand whether degranulating NK cells were also producing IFNγ, NK cells were assessed for expression of both CD107a and IFNγ (**Figure 4-12**). With increasing selinexor concentration and with LMB treatment, IFNγ was only expressed, although only slightly (increase of 1%), by degranulating CD107a+ NK cells as show by a significant difference within the CD107a+IFNγ+ NK cell population and not the IFN single positive population at 500 nM selinexor (blue line compared to purple line, P<0.05, **Figure 4-12**).

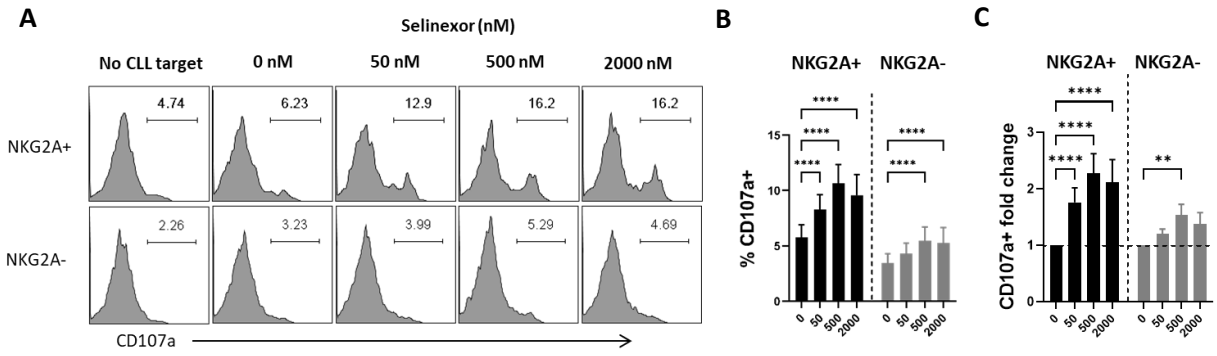


**Figure 4-9: NKG2A+ and NKG2A- NK cell degranulation against patient CLL cells pre-treated with selinexor *ex vivo*.**

Healthy donor NK cells were co-cultured for 4 hrs with selinexor-treated CLL cells and NK cell degranulation in NKG2A+ and NKG2A- NK cells were measured by expression of CD107a as in (**A**). Shown in (**B**) is the summary of NK degranulation in 23 individual co-cultures using 8 CLL donors and 7 healthy donor PBMC. The proportion of CD107a+ NK cells was normalised to the 'no CLL target' control. (**C**) Fold change in expression of CD107a in NKG2A NK cell populations relative to the untreated control. Differences in CD107a expression between the 0 nM control and selinexor concentrations in both NK cell populations were calculated by repeated-measure two-way ANOVA followed by Dunnett's multiple comparison test: **P<0.01, ****P<0.001.

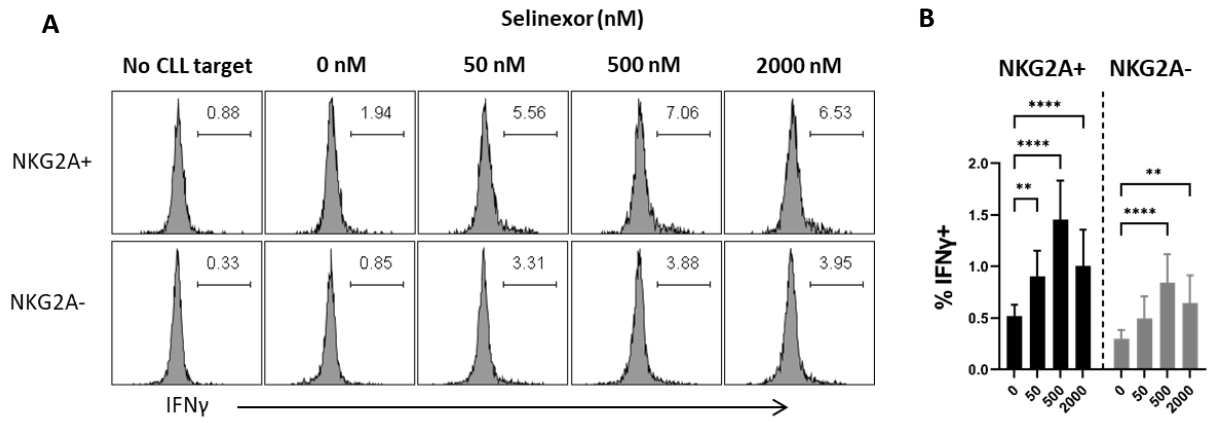


**Figure 4-10: IFNγ production in NKG2A+ and NKG2A- NK cells after co-culture with patient derived CLL cells pre-treated with selinexor *ex vivo*.**

Healthy donor NK cells were co-cultured for 4 hrs with selinexor-treated CLL cells and production of IFNγ in NKG2A+ and NKG2A- NK cells were assessed as in (**A**). (**B**) IFNγ production in 21 individual co-cultures using 8 CLL donors and 7 healthy donor PBMC. The proportion of IFNγ+ NK cells was normalised to the 'no CLL target' control. Differences in IFNγ expression between the 0 nM control and selinexor concentrations in both NK cell populations were as calculated by repeated-measure two-way ANOVA followed by Dunnett's multiple comparison test: **P<0.01, ****P<0.001.

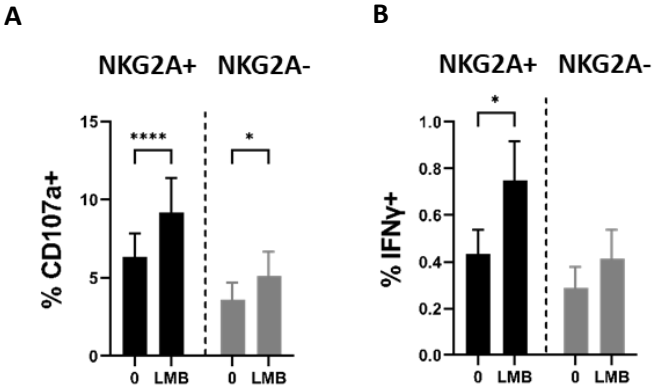


**Figure 4-11: NKG2A+ and NKG2A- NK cell activation against LMB-treated CLL cells.**

Healthy donor NK cells were co-cultured for 4 hrs with LMB-treated CLL cells and NK activation in NKG2A+ and NKG2A- NK cells were assessed by expression of the degranulation surface marker CD107a (**A**) and by production of IFNγ (**B**). Shown is mean ± SEM of 17 individual co-cultures using 7 CLL donors and 5 healthy donor PBMC. Differences in CD107a and IFNγ expression between LMB-treated and untreated controls in NK cell populations were calculated by repeated-measure two-way ANOVA followed by Dunnett's multiple comparison test: *P<0.05, ****P<0.001.

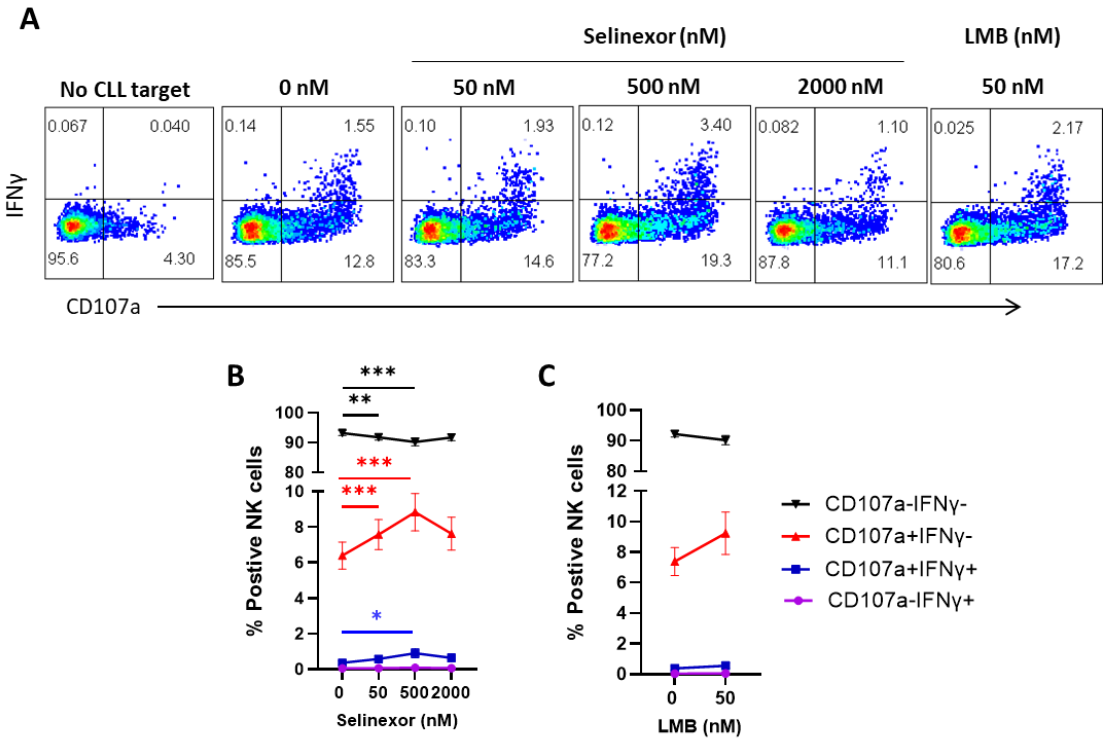


**Figure 4-12: IFNγ is expressed in degranulating CD107a+ NK cells after co-culture with CLL cells pre-treated with XPO1 inhibitors.**

Healthy donor PBMC were co-cultured for 4 hrs with selinexor (50-2000 nM) or leptomycin B (LMB, 50 nM) pre-treated CLL cells (16 to 24-hour treatment) and expression of CD107a and IFNγ was assessed by flow cytometry. (**A**) Gating used to identify CD107a-IFNγ single and double positive cells after gating on CD56+CD3- NK cells. Shown is one representative example when NK cells were co-cultured with no target cells (No CLL target), with untreated CLL cells (0 nM) and with selinexor (50-2000 nM) or LMB (50 nM)-treated cells. (**B-C**) Percent single and double positive NK cells after healthy donor PBMC co-culture with selinexor (**B**, n=21) or LMB (**C**, n=15) pre-treated CLL cells. Shown is mean ± SD and significant differences between SINE-treated samples for each NK cell population were calculated using repeated-measure two-way ANOVA: *P<0.05, **P<0.01, ***P<0.005.

To understand the mechanism for increased activation in the NKG2A- NK cell population against patient CLL cells pre-treated with XPO1 inhibitors, expression of activating NK cell ligands were examined on CLL cells after of selinexor treatment. It is known that CLL cells evade NK cell-mediated immunity through loss of NKG2D ligand expression (49,495) and higher levels of soluble ULBP2 and soluble MIC-A/B are associated with poor treatment-free survival (496). Therefore, it was assessed whether NKG2D ligand expression increased with selinexor treatment which would enhance NKG2D+ NK cell activation. No change in expression of NKG2D ligands ULBP-1, ULBP-2/5/6 and MIC-A/B was observed (**Figure 4-13**). As a result, further major activating ligands were assessed, but similarly, no change in expression was observed for CD54/ICAM-1 and B7-H6 with increasing selinexor

concentration (**Figure 4-14**). Finally, as NK cells also destroy cancer target cells through engaging death receptors, expression of FAS, DR4 and DR5 were assessed on CLL patient cells post selinexor treatment (**Figure 4-15**). No change in FAS expression was observed with increasing selinexor concentration. For DR4, a small but significant increase in expression was recorded at 2000 nM selinexor. However, at all concentrations of selinexor DR5 expression increased, but not in a concentration-dependent manner (**Figure 4-15**).

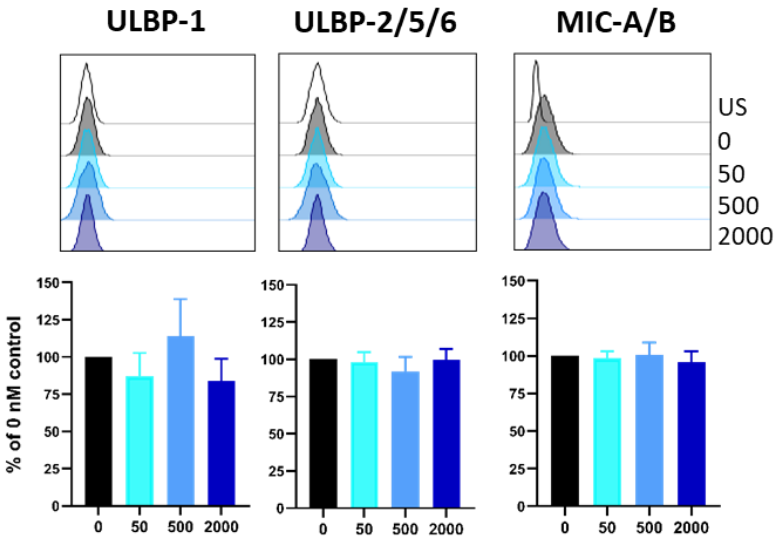


**Figure 4-13: NKG2D ligand expression on CLL cells treated with selinexor.**

CD19+CD5+ CLL cells were assessed for NKG2D ligands expression post selinexor treatment. Shown is a representative example of one CLL donor and below graphs display mean ± SEM of at least 4 CLL patients.

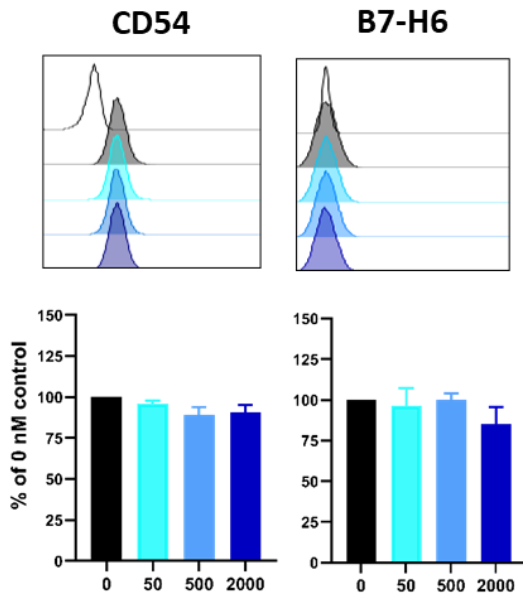


**Figure 4-14: Expression of NK cell activating ligands on CLL cells treated with selinexor.**

CD19+CD5+ CLL cells were assessed for expression of NK cell activating ligands CD54 and B7-H6 after 24-hour treatment with selinexor (50-2000 nM). Shown is a representative example of one CLL donor and below graphs displaying mean ± SEM of at least 4 CLL patients.

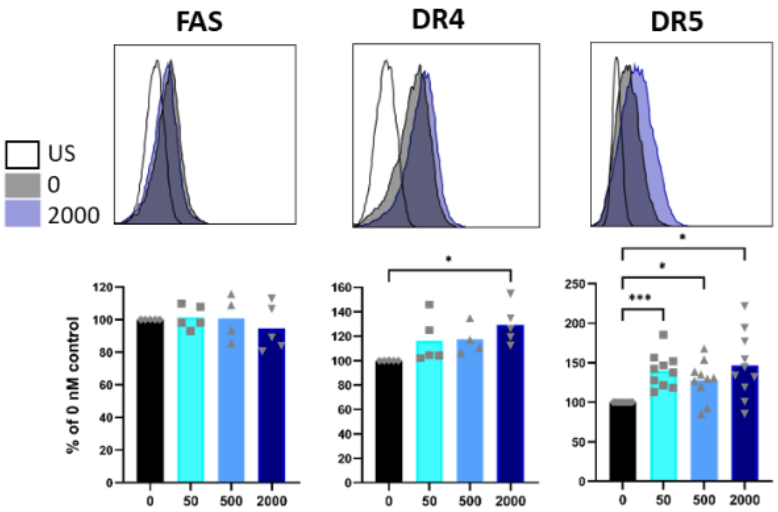


**Figure 4-15: Selinexor increases the expression of death receptor 5 on CLL cells.**

Expression of FAS, DR4 and DR5 on CD19+CD5+ CLL cells treated with selinexor for 24 hours. Expression histograms of a representative CLL donor treated with DMSO (0 nM) or 2000 nM selinexor (top row). US = unstained. Bottom row is the mean expression relative to the 0 nM control of at least 4 CLL donor PBMC. Each point represents one CLL donor. Significant differences in expression between selinexor concentrations were calculated with repeated-measure one-way ANOVA followed by Tukey's post-hoc test: *P<0.05, ***P<0.005.

As a result of increased DR5 expression on CLL cells post selinexor treatment, it was hypothesised that TRAIL blockade would reverse the enhanced NK specific lysis seen with selinexor. Anti-TRAIL antibodies were added to CLL-NK co-cultures and NK specific lysis of CLL targets was assessed. Through inhibiting TRAIL engagement with death receptors, NK specific lysis of CLL targets in DMSO-treated samples (0 nM) was approximately halved compared to controls (**Figure 4-16**, black bars). In selinexor samples, TRAIL blockade completely reversed NK specific lysis to levels comparable to the anti-TRAIL, 0 nM sample (**Figure 4-16**). This highlights the importance of death receptor-mediated killing of CLL cells and indicates that TRAIL blockade counteracts the selinexor-induced decrease in HLA-E expression. Overall this suggests that in the absence of an important NK receptor:ligand interaction (TRAIL:DR4/5), NKG2A modulation of NK cell function is impaired.

To assess the contribution of TRAIL to impair NKG2A+ NK cell activation with selinexor, a LAMP assay was performed. In the presence of anti-TRAIL blocking antibodies, NKG2A+ NK cell activation was diminished slightly (2.5%), but significantly, demonstrating that TRAIL engagement with DR5 facilitates an NK cell activating response, perhaps through prolonged, more productive NK-cancer cell interactions. The downregulation of HLA-E by selinexor was still capable of activating NKG2A+ NK cells, albeit to a lesser extent with anti-TRAIL antibodies (**Figure 4-17**). Overall, the anti-TRAIL antibody experiments demonstrate that XPO1 inhibition with selinexor in primary CLL cells promotes NK cytotoxicity via two mechanisms, enhanced death receptor signalling and enhanced degranulation.

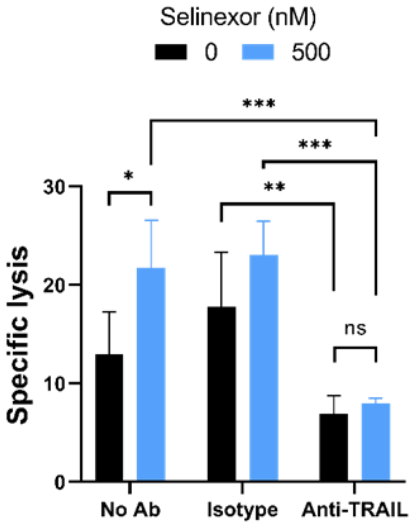


**Figure 4-16: TRAIL blockade protects CLL cells from NK cell specific lysis with selinexor.**

CLL cells were treated with 500 nM selinexor for 24 hours. Isolated NK cells were incubated with 10 µg/mL anti-TRAIL antibody or IgG2a isotype control for 20 minutes before being co-cultured with CLL cells for 4 hours at an E:T = 1:1. Shown is mean ± SEM (n=6) and significant differences in NK specific lysis between treatments were calculated with repeated-measure two-way ANOVA followed by Tukey's post-hoc test: *P<0.05, **P<0.01, *** P<0.005.

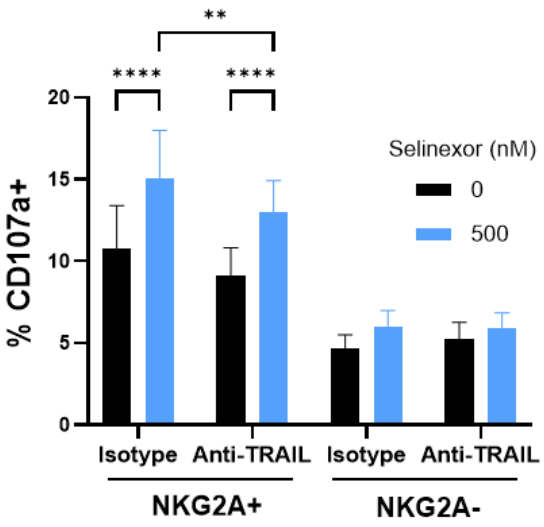


**Figure 4-17: TRAIL blockade slightly impairs NKG2A+ NK cell degranulation with selinexor.**

CLL cells were treated with 500 nM selinexor or DMSO control for 24 hours. Healthy donor PBMC were incubated with 10 µg/mL anti-TRAIL antibody or IgG2a isotype control for 20 minutes before being co-cultured with CLL cells for 4 hours at an E:T = 1:1. Shown is mean ± SEM (n=8) expression of the activation marker CD107a expressed on NKG2A+ and NKG2A- NK cells and significant differences in NK cell activation between treatment groups were calculated with repeated-measure two-way ANOVA followed by Tukey's post-hoc test: **P<0.01, **** P<0.001.

## 4.3 Combining XPO1 inhibition with approved treatments for CLL

Through the expression of CD16a, NK cells contribute to the efficacy of anti-CD20 (mAb) therapy via ADCC (489). It was shown in follicular lymphoma and non-Hodgkin lymphoma that the valine-allele of CD16a (V158), which provides higher affinity for the Fc region of antibodies (150), correlates with better response to and overall survival of rituximab therapy (261,262). This indicates that NK cells play an important role in anti-CD20 mAb therapy. Therefore, it was assessed whether selinexor could potentiate NK cell activation in combination with anti-CD20 mAbs against primary CLL cells in a similar manner to B-cell lymphoma cell lines in section 3.6.

First, it was determined whether selinexor modulates CD20 expression on the surface of CLL cells. After 24-hour treatment with selinexor (50-2000 nM), CD20 expression remained stably expressed at the plasma membrane (**Figure 4-18**). Next NK cell activation assays were performed to assess the effect of selinexor plus anti-CD20 mAbs rituximab and obinutuzumab on ADCC. To avoid unwanted NK cell activation against healthy B cells among healthy donor PBMC, unbound anti-CD20 mAbs were removed from CLL cells before addition of healthy donor PBMC. NK cell activation was then compared between NKG2A+ and NKG2A- NK cells to determine whether selinexor-induced HLA-E downregulation impacted ADCC. XPO1 inhibition combined with anti-CD20 mAbs further activated NKG2A+ NK cells compared to single agent treatments in contrast to NKG2A- NK activation (**Figure 4-19**). These data confirm previous findings with cell lines that XPO1 inhibition downregulates HLA-E surface expression which enhances the activation of NKG2A+ NK cells in the presence of direct targeting mAbs.

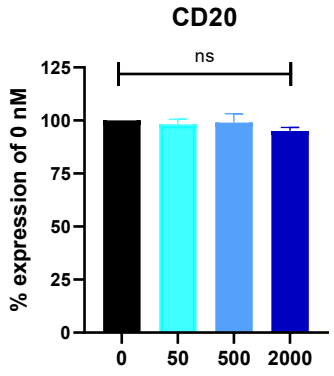


**Figure 4-18: CD20 is stably expressed on CLL cells after selinexor treatment.**

Percent expression of CD20 relative to the DMSO (0 nM) control on CD19+CD5+ CLL cells after 24-hour treatment with selinexor (50-2000 nM). Shown is mean ± SEM of 5 CLL donors and differences in CD20 expression between selinexor concentrations were calculated by repeated-measure one-way ANOVA.

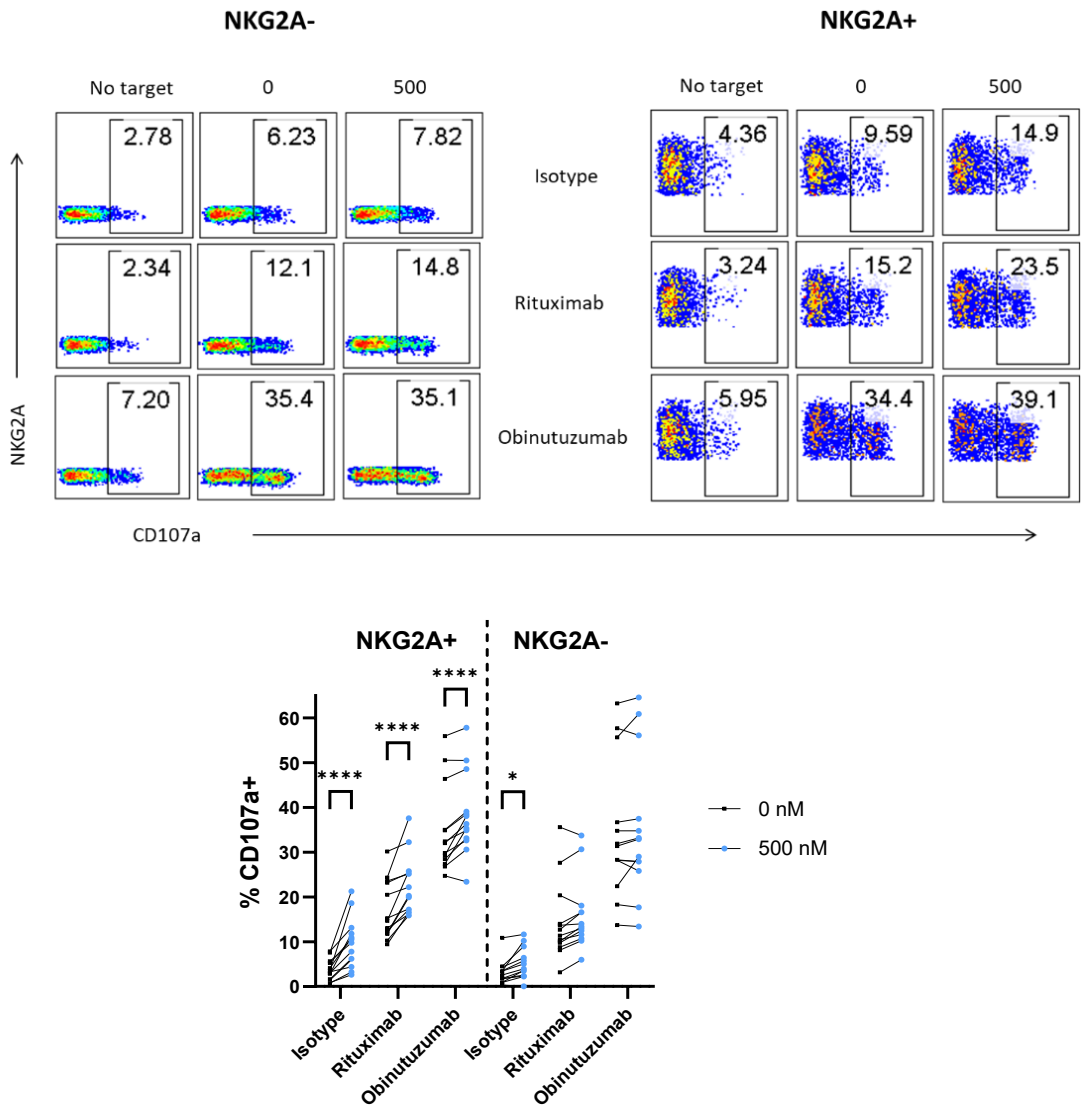


**Figure 4-19: Selinexor enhances NK cell activation in the presence anti-CD20 mAbs.**

CLL cells were treated with 500 nM selinexor for 24 hours after which they were incubated with 0.1 µg/mL anti-CD20 mAbs rituximab or obinutuzumab. Cetuximab was used as the isotype control. mAbs were washed off CLL cells after 20 minutes and healthy donor PBMC were added to CLL cells at an E:T = 5:1 for 4 hours. NK cell activation in the NKG2A+ and NKG2A- NK cell populations was assessed via expression of CD107a. Shown above is a representative example of NK cell activation in different treatment groups. Below is the percentage of NK cells positive for CD107a with background activation in no target controls taken into account (n=13). Significant differences in NK cell activation between treatments were assessed by repeated-measure two-way ANOVA followed by Sidak's post-hoc test: *P<0.05, ****P<0.01.

To assess whether enhanced ADCC of NKG2A+ NK cells with XPO1 inhibitors was specific to targeting CD20 or a general effect, selinexor was combined with daratumumab, an anti-CD38 mAb approved for the treatment of patients with multiple myeloma. Again, CD38 expression was assessed on CLL cells post selinexor treatment and no difference in expression was observed (**Figure 4-20**). NK cells express CD38, therefore to avoid NK cell fratricide (263) unbound daratumumab was removed from CLL cultures before addition of healthy donor PBMC. Because not all CLL donor cells express CD38, patients positive and negative for CD38 were separated. For CD38+ CLL donors, XPO1 inhibition combined with daratumumab almost doubled the activation of NKG2A+ NK cells compared to single agent treatments (**Figure 4-21**). As for the NKG2A- NK cell population, no additive effect was seen for the combined treatment. When CD38- CLL cells were used as targets, the effect of daratumumab was lost, but the enhanced NK cell activation with selinexor remained, with significance observed for NKG2A+ NK cells only. These experiments demonstrate that through downregulating HLA-E with XPO1 inhibitors, ADCC can be potentiated independent of the target antigen.

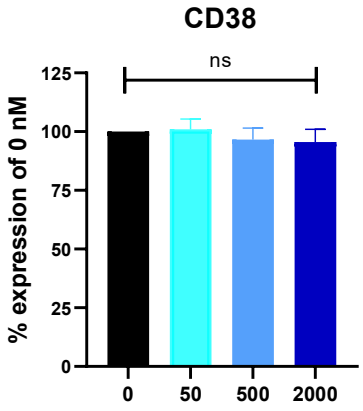


**Figure 4-20: CD38 is stably expressed on CLL cells treated with selinexor.**

Percent expression of CD38 relative to the DMSO (0 nM) control on CD19+CD5+ CLL cells after 24-hour treatment with selinexor (50-2000 nM). Shown is mean ± SEM of 4 CLL donors and differences in CD38 expression between selinexor concentrations were calculated by repeated-measure one-way ANOVA.

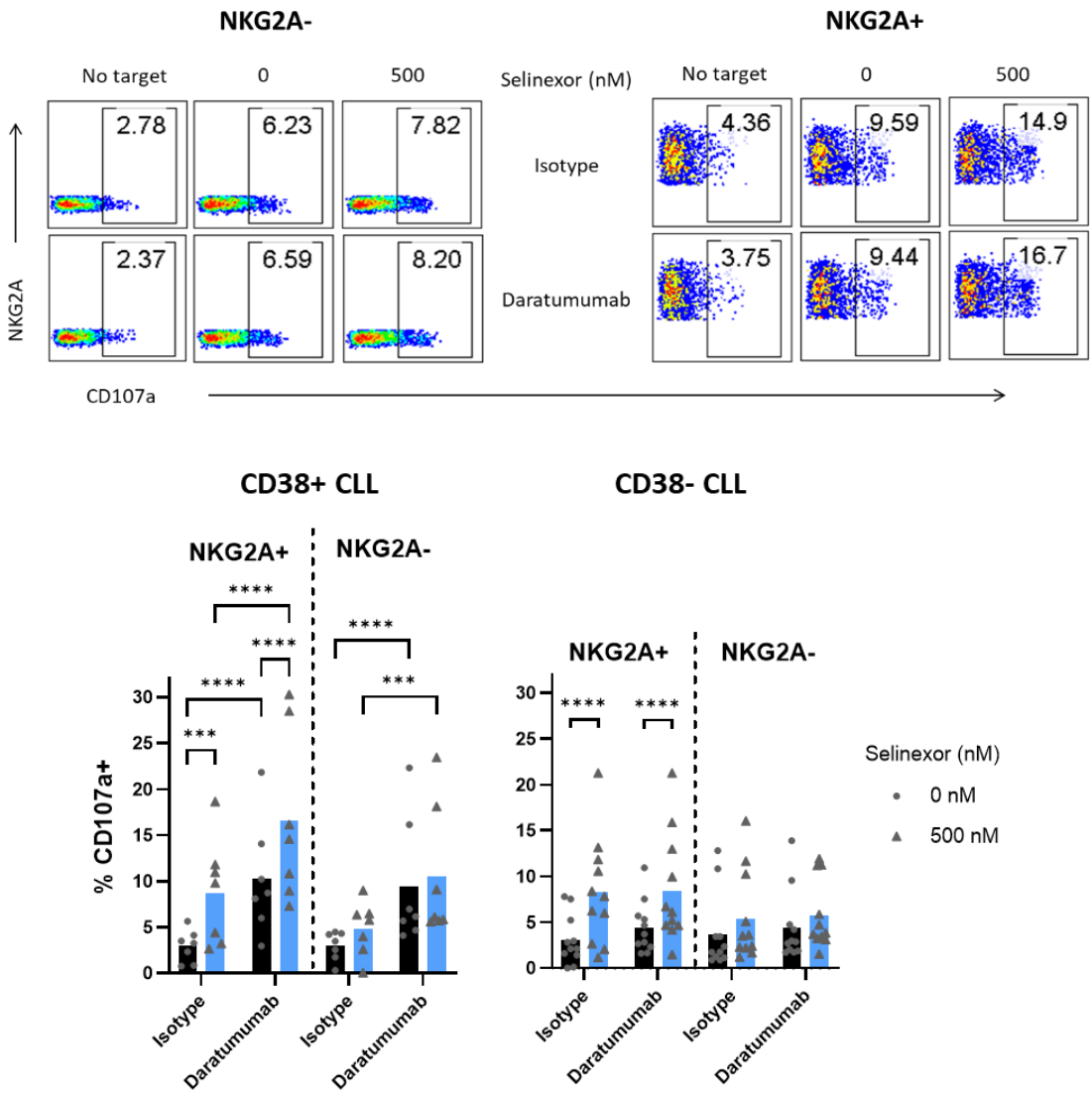


**Figure 4-21: Selinexor enhances NK cell activation in the presence of the anti-CD38 mAb daratumumab.**

CLL cells were treated with 500 nM selinexor for 24 hours after which they were incubated with 0.1 µg/mL anti-CD38 mAb daratumumab. Cetuximab was used as the isotype control. Unbound daratumumab was removed from CLL cultures after 20 minutes and healthy donor PBMC were added to CLL cells at an E:T = 5:1 for 4 hours. Shown above is a representative example of NK cell activation in different treatment groups. Below is the mean percentage of NKG2A+ and NKG2A- NK cells positive for CD107a with background activation in no target controls taken into account against CLL target cells positive for CD38 (n=7) and negative for CD38 (n=11). Each point represents an individual co-culture. Significant differences in NK cell activation between treatments were assessed by repeated-measure two-way ANOVA followed by Sidak's post-hoc test: ***P<0.005, ****P<0.01.

Selinexor is being clinically evaluated in CLL in combination with the bruton's tyrosine kinase inhibitor (BTKi) ibrutinib (NCT02303392). As previous experiments used selinexor as a single agent, it was assessed whether selinexor retained its NK sensitising effect on CLL cells in the presence of ibrutinib and the next-generation BTKi acalabrutinib. As single agents, BTKi did not downregulate or increase the surface expression of HLA-E or total HLA proteins (**Figure 4-22**). However, in combination with selinexor, HLA-E expression decreased to a similar level to single agent selinexor treatment (**Figure 4-22**). Total HLA expression did not change across all treatments.

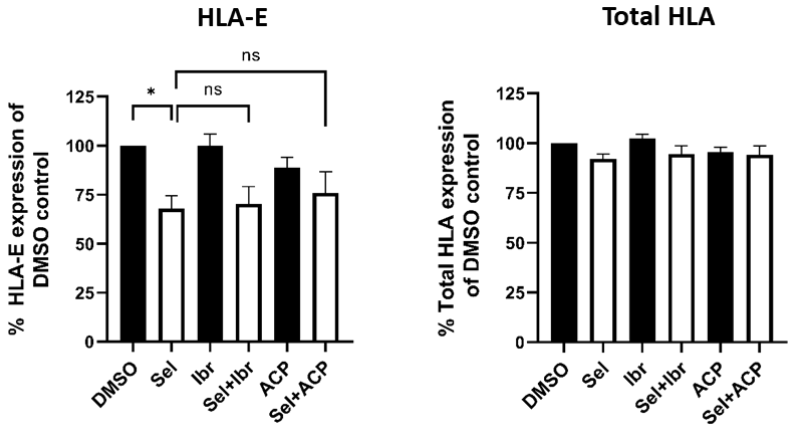


**Figure 4-22: XPO1 inhibition induces HLA-E downregulation in the presence of BTK inhibitors.**

Expression of HLA-E (clone 3D12) and total HLA (clone W6/32) on CD19+CD5+ CLL cells after treatment with 500 nM selinexor (sel) and 1 µM BTKi ibrutinib (Ibr) or acalabrutinib (ACP). CLL cells were incubated with drug combinations as indicated for 24 hours. Graphs represent mean ± SEM of 5 CLL donors. Significant differences in expression between treatments were calculated by repeated measure one-way ANOVA followed by Tukey's post-hoc test: *P<0.05.

To dissect whether selinexor plus BTKi sensitised CLL cells to NK cell lysis, purified NK cells were co-cultured with pre-treated CLL cells and used in the NK specific lysis assay as previously described. BTKi treatment alone did not sensitise CLL cells to NK specific lysis (**Figure 4-23**). When BTKi were used in combination with selinexor, CLL cells were sensitised to NK-mediated killing at equivalent magnitude to selinexor single agent treatment, in line with retained HLA-E downregulation by selinexor in the presence of BTKi (**Figure 4-23**).

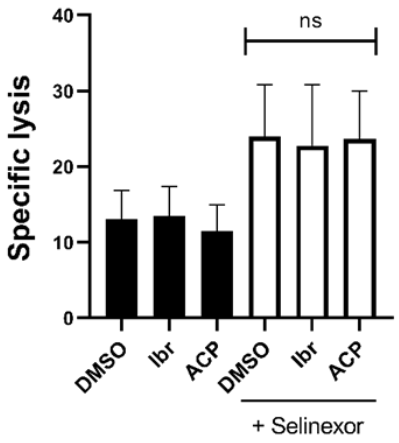


**Figure 4-23: Selinexor sensitises CLL cells to NK specific lysis in the presence of BTK inhibitors.**

CLL cells were treated with 500 nM selinexor and 1 µM BTKi ibrutinib (Ibr) or acalabrutinib (ACP) in the presence of the apoptotic inhibitor Q-VD. CLL cells were incubated with drug combinations as indicated for 24 hours. After treatment, purified NK cells were co-cultured with CLL cells (E:T=1:1) for 4 hours and CLL cell death was measured by uptake of propidium iodide. Drug-induced cell death was accounted for in each treatment. Graphs represent mean ± SEM (n=4). Differences in expression between treatments were calculated by repeated measure one-way ANOVA: $P<0.05$.

*Ex vivo* treatment of CLL cells with selinexor and BTKi preceded co-culture with healthy donor PBMC/NK in the experiments described previously. It is well recognised that BTKi have off-target effects by inhibiting interleukin-2 inducible tyrosine kinase (ITK) (497), an enzyme important for NK cell function (498). As a result, ibrutinib treatment of NK cells reduces their ADCC capacity and impairs their proliferation (499). Therefore, NK cell activation against CLL pre-treated targets was assessed when drug combinations were added to the CLL-NK 4-hour co-culture. In accordance with the literature, ibrutinib monotherapy impaired NK cell activation, whilst acalabrutinib impaired NK cell activation to a lesser extent (**Figure 4-24**). When selinexor was used alongside BTKi, selinexor had no effect on NK cell activation in combination with ibrutinib, however selinexor partially rescued NK cell function in combination with acalabrutinib (**Figure 4-24**). This highlights the potent inhibitory off-target effect of ibrutinib on NK cell function that HLA-E downregulation with selinexor cannot recover. It also suggests that next generation BTKi would be more efficacious in combination with selinexor in CLL. This experiment also illustrates that 4-hour selinexor treatment of NK cells during co-culture does not impair their enhanced activation.

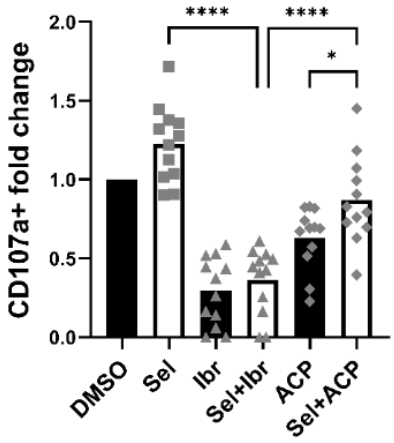


**Figure 4-24: The second generation BTK inhibitor acalabrutinib does not impair increased NK cell activation with selinexor.**

NK cell activation as measured by fold change in CD107a expression when healthy donor PBMC were co-cultured with CLL cells pre-treated for 24 hrs with selinexor (500 nM) and BTK inhibitors Ibrutinib (Ibr, 1 µM) and Acalabrutinib (ACP, 1 µM). During 4-hour co-culture, selinexor and BTK inhibitors were re-added to assess NK cell function by the anti-cancer agents. Shown is the mean ± SEM (n=12 of 4 CLL donors and 5 healthy donor PBMC) and significant differences in NK cell activation between treatments were assessed by repeated-measure one-ANOVA followed by Tukey's post-hoc test: *P<0.05, ****P<0.001.

## 4.4 Lymph node microenvironmental support

Within patients, CLL cells transit through secondary lymphoid organs where they encounter microenvironments that promote cell survival, proliferation and facilitate drug resistance (500). Within these environments, little is known on CLL cell sensitivity to NK cell activation and to selinexor treatment. As such, to model microenvironmental support and investigate selinexor sensitivity and NK cell function, CLL cells were incubated with IL-4 and CD40L, well recognised supportive molecules found in lymph nodes (501).

Initially, it was checked whether IL-4 and CD40L alone or in combination impact HLA-E and total HLA expression on CLL cells. CD40L and the combination of IL-4 and CD40L, but not IL-4 alone, significantly increased the expression of HLA-E on the surface of CLL cells (**Figure 4-25**). Total HLA expression followed a similar pattern to HLA-E, but to a lesser extent, most likely because of the binding of the W6/32 clone (anti-HLA-A/B/C) to HLA-E (502,503). As a result of increased HLA-E with IL-4 and CD40L, it was assessed whether selinexor retained its ability to downregulate HLA-E in the presence of lymph node-associated signals. Selinexor was able to downregulate HLA-E on CLL cells

incubated with IL-4 and CD40L in a dose-dependent manner (**Figure 4-26**). Baseline levels of HLA-E on CLL cells were achieved at 500-2000 nM selinexor in the presence of IL-4 + CD40L because no significant differences compared to the untreated control were observed. In addition to measuring HLA expression on CLL cells immersed in a lymph node-associated microenvironment, expression of death receptors DR4 and DR5 were also measured. Unlike HLA-E, DR4 and DR5 expression did not significantly increase (or decrease) in the presence of IL-4 and CD40L (**Figure 4-26**). However, as shown previously without environmental support signals, selinexor enhanced the expression of DR5 on CLL cells even in the presence of IL-4 and CD40L (**Figure 4-26**). Overall, the lymph node-associated signals IL-4 + CD40L enhance the expression of HLA-E on CLL cells and XPO1 inhibition with selinexor is able to overcome this increase while also enhancing DR5 expression.

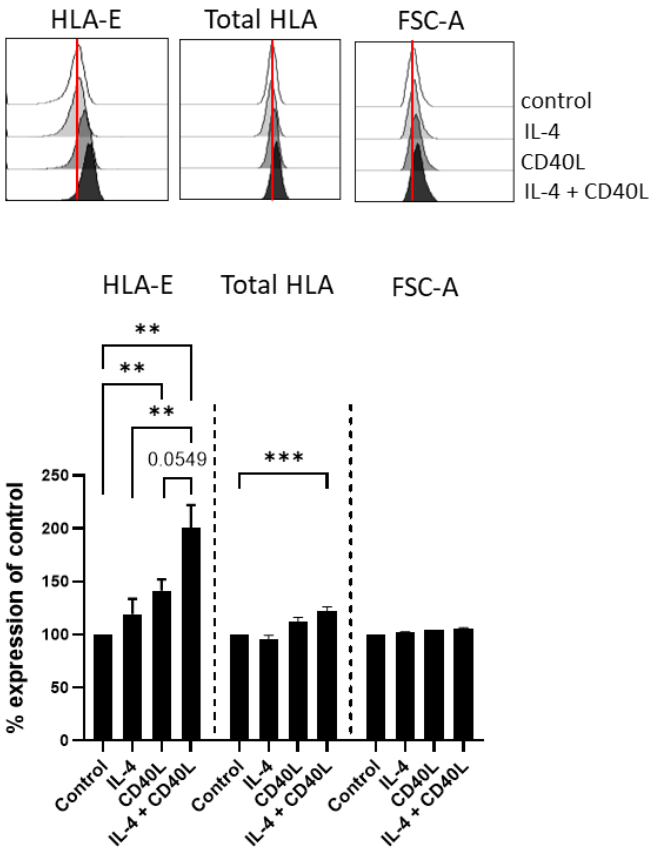


**Figure 4-25: Lymph node-associated signals IL-4 and CD40L increase HLA-E expression on CLL cells.**

Expression of HLA-E and total HLA proteins on CLL cells incubated with lymph node support molecules IL-4 (10 ng/mL) and CD40L (300 ng/mL) alone and in combination for 24 hours. Shown above, HLA expression on a representative CLL donor post microenvironmental support incubation. FSC-A shown as an approximate of cell morphology. Red lines positioned at the peak of the untreated control histograms. Below is the percent expression and percent FSC-A relative to the untreated control using CLL cells from 15 individual donors. Significant differences in expression between conditions were calculated using repeated-measure two-way ANOVA followed by Tukey's post-hoc test: *P<0.05, **P<0.01, ***P<0.005.

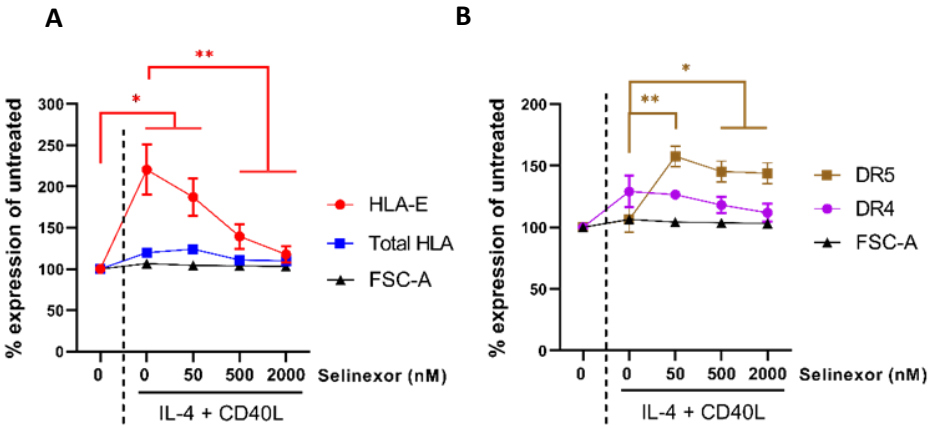


**Figure 4-26: Selinexor reduces HLA-E expression on CLL cells incubated with IL-4 + CD40L.**

CLL cells from 12 donors were treated with selinexor (50-2000 nM) for 24 hours in the presence of IL-4 (10 ng/mL) and CD40L (300 ng/mL). IL-4 and CD40L were added 1 hour before addition of selinexor. HLA (**A**) and death receptor expression (**B**) was then assessed by flow cytometry and expression relative to the untreated control was calculated. FSC-A was measured to compare cell morphology across treatments. Differences in expression between treatments compared to the 0 nM (IL-4+CD40L) control were calculated by repeated-measure two-way ANOVA followed by Tukey's post-hoc test: *P<0.05, **P<0.01.

As a result of enhanced HLA-E expression on CLL cells incubated with IL-4 + CD40L, it was assessed whether this had a functional consequence on NK cells and whether XPO1 inhibition could abrogate this. The leading hypothesis was that increased HLA-E expression inhibits NKG2A+ NK cell activation and selinexor treatment rescues NKG2A+ NK cell function. CLL cells were treated as before with selinexor (500 nM) in the presence of IL-4 and CD40L for 24 hours and the next day NKG2A+ and NKG2A- NK cell activation was assessed in terms of degranulation (CD107a expression) (**Figure 4-27**) and IFNγ production (**Figure 4-28**). IL-4 and CD40L led to decreased degranulation and decreased IFNγ production in NKG2A+ NK cells, but not NKG2A- NK cells. When selinexor was added to CLL cells with microenvironmental support, NKG2A+ NK cell activation was rescued (**Figure 4-27** and **Figure 4-28**). For NKG2A- NK cells, the level of activation was unaffected by IL-4 + CD40L, but when selinexor was added to IL-4 + CD40L cultures, this increased NKG2A- NK cell activation rescued (**Figure 4-27** and **Figure 4-28**), most likely due to increased DR5 expression (**Figure 4-26**). Additionally, NK cell activation against CLL cells treated with selinexor in the presence of IL4 and CD40L surpassed the activation in the untreated control group (**Figure 4-27** and **Figure 4-28**). This highlights the importance of enhanced DR5 expression on CLL cells with selinexor because although HLA-E

expression recovered to baseline levels with 500 nM selinexor in the presence of IL-4 + CD40L (**Figure 4-26**), NKG2A+ NK cells not only recovered their activation capacity but surpassed baseline levels.

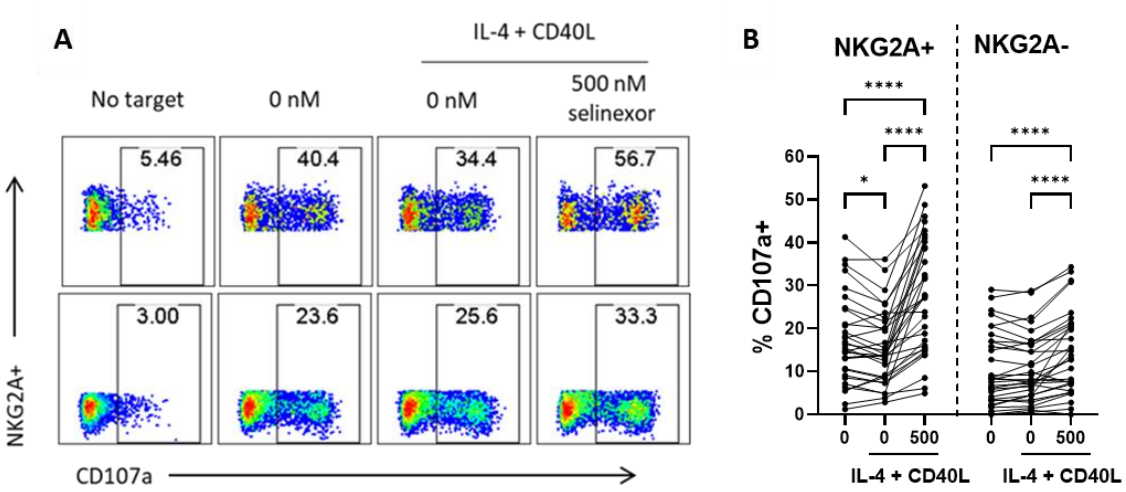


**Figure 4-27: IL-4 + CD40L protect CLL cells from on NK cell degranulation, which is reversed by selinexor treatment.**

CLL cells were treated with 500 nM selinexor in the presence of IL-4 (10 ng/mL) and CD40L (300 ng/mL) for 24 hours. Microenvironmental support molecules were added 1 hour before selinexor. CLL cells were then co-cultured with healthy donor PBMC for 4 hours and NKG2A+ and NKG2A- NK cell degranulation was assessed by CD107a expression. (**A**) Example of one healthy donor NK degranulation in the NKG2A+ and NKG2A- NK cell populations against one CLL donor. Background NK activation (No target samples) was taken away from co-culture samples. (**B**) Percentage of CD107a+ NK cells in the NKG2A+ and NKG2A- NK cell populations. Each point represents an individual co-culture (N = 32) using 10 CLL donors and 8 healthy donor PBMC. Significant differences in NK cell activation between treatment groups were calculated with repeated-measure two-way ANOVA followed by Tukey's post-hoc test: *P<0.05, ****P<0.001.

**B**

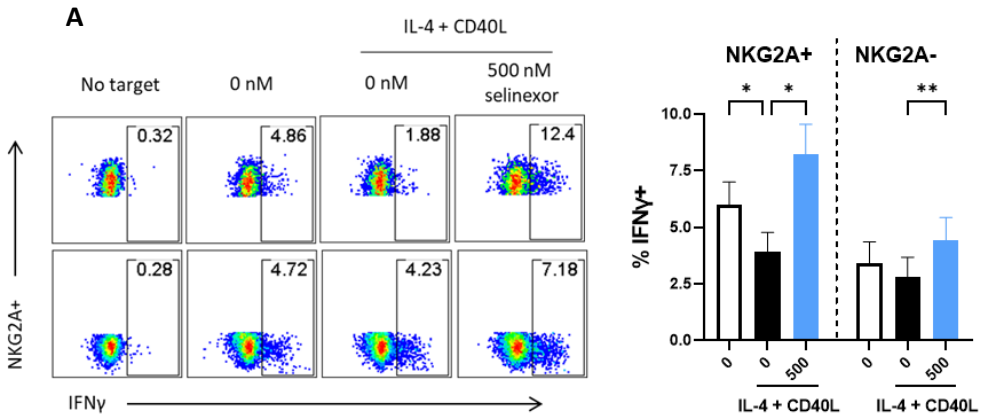


**Figure 4-28: IL-4 + CD40L dampens IFNγ production by NK cells, which is reversed by selinexor treatment.**

CLL cells were treated with 500 nM selinexor in the presence of IL-4 (10 ng/mL) and CD40L (300 ng/mL) for 24 hours. Microenvironmental support molecules were added 1 hour before selinexor. CLL cells were then co-cultured with healthy donor PBMC for 4 hours and production of IFNγ in NKG2A+ and NKG2A- NK cells was assessed by flow cytometry. (**A**) Example of IFNγ production by NKG2A+ and NKG2A- NK cells after co-culture with CLL cells. Background IFNγ production (No target samples) in each NK population was taken away from co-culture samples. (**B**) Percentage of IFNγ+ NK cells in the NKG2A+ and NKG2A- NK cell populations (N = 9) using 4 CLL donors and 4 healthy donor PBMC. Significant differences in IFNγ production between treatments were calculated with repeated-measure two-way ANOVA followed by Tukey's post-hoc test: *P<0.05, **P<0.01.

To determine whether the increase in HLA-E expression seen on CLL cells incubated *ex vivo* with lymph node-associated signals also occurs *in vivo*, CD5+CD19+ cells within CLL patient PBMC were subdivided into populations based on CXCR4 and CD5 expression to identify CLL cells that have recently egressed from the lymph nodes. This was based on previous reports that found that activated, CLL cells from lymph nodes increase expression of CD5 and downregulate CXCR4 to allow entry into the circulation (504,505). CXCR4 is a chemokine receptor that recognises CXCL12 which is found at high levels in the lymph nodes which is required for B cell entry (506). Therefore, CLL cells that have recently egressed from the lymph nodes can be identified as having low expression of CXCR4 and high expression of CD5 (CXCR4lo CD5hi) in the circulation. In this setting, it can be asked, *in vivo*, does the lymph node microenvironment enhance HLA-E expression? In this experiment, to maintain consistency in cell numbers between CLL cell populations, and in accordance with previous publications, approximately 5% of CXCR4lo CD5hi cells, 5% of CXCR4hi CD5lo cells and 5% of CLL cells with intermediate expression of CXCR4 and CD5 were gated on and assessed for expression of HLA proteins (**Figure 4-29**). In the CXCR4lo CD5hi CLL cell population, HLA-E expression was significantly higher compared to CXCR4hi CD5lo cells and intermediate cells (**Figure 4-29 and Figure 4-30**). In accordance with the *ex vivo* data simulating the lymph node microenvironment, CLL cells in patient

PBMC that have recently left the lymph node express higher levels of HLA-E compared to CLL cells that have been in the circulation for longer. This indicates that the lymph node provides a microenvironment in which malignant B cells may evade NK-mediated immunity and suggests that selinexor treatment could sensitise these cells to NK cell anti-tumour functions.

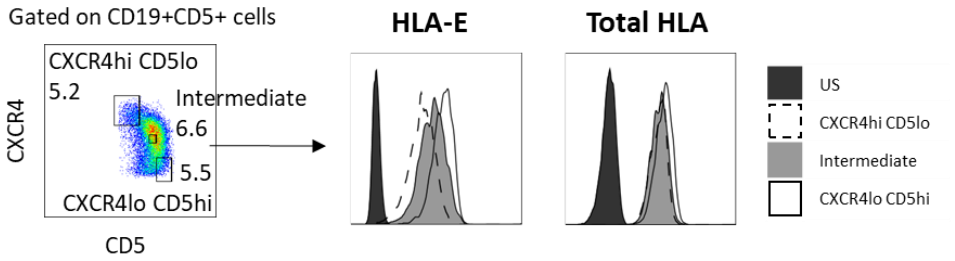


**Figure 4-29: Gating strategy to measure HLA expression on CLL cell populations based on CXCR4 and CD5 expression.**

To identify CLL cells that have recently left the lymph nodes in patient PBMC, CD19+CD5+ cells were examined for expression of CXCR4 and CD5. CLL cells that have recently entered the circulation from lymph nodes are identified as CXCR4lo CD5hi. Expression of HLA-E and total HLA proteins was measured on these cells alongside controls of CXCR4hi CD5lo cells and CLL cells with intermediate expression of CXCR4 and CD5. Number on left flow plot shows the percentage of cells within gates. US = unstained.

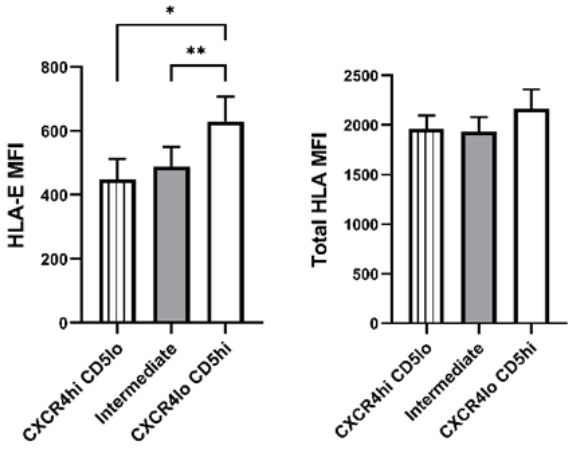


**Figure 4-30: CXCR4lowCD5hi CLL cells have increased HLA-E expression.**

HLA-E and total HLA protein expression as measured by geometric mean fluorescence intensity (MFI) on CLL cell populations subdivided into groups based on expression level of CXCR4 and CD5. Expression of HLA-E and HLA proteins was compared between CLL cells that have recently entered the circulation from lymph nodes (CXCR4lo CD5hi) to control of CXCR4hi CD5lo CLL cells and CLL cells with intermediate expression of CXCR4 and CD5. Shown is mean ± SEM (n=11 CLL donors) and significant differences in HLA expression between CLL cell populations were calculated with repeated-measure one-way ANOVA followed by Tukey's post-hoc test: *P<0.05, **P<0.01.

## 4.5 HLA-E expression on healthy immune cell populations treated with selinexor

In addition to measuring HLA-E expression on primary CLL cells, it was assessed whether selinexor affects HLA-E expression on B cells, T cells, NK cells and monocytes derived from healthy donors to determine whether selinexor specifically impacts cancerous cells. PBMC were treated with selinexor for 24 hours and B cells, T cells, NK cells and monocytes were identified with antibodies against CD19, CD3, CD56 and CD14, respectively. Consistent with decreased HLA-E surface expression on malignant B cells, HLA-E expression decreased on healthy donor B lymphocytes, perhaps reflecting the higher expression of HLA-E on B cells compared to other lymphocyte populations (23) (**Figure 4-31**). T cells and NK cells only slightly downregulated HLA-E at the plasma membrane with increasing selinexor concentration. However, like healthy B cells, HLA-E expression on monocytes was reduced by selinexor treatment. As for total HLA expression, a slight reduction in surface expression with selinexor was recorded on B cells and monocytes compared to NK cells and T cells (**Figure 4-31**).

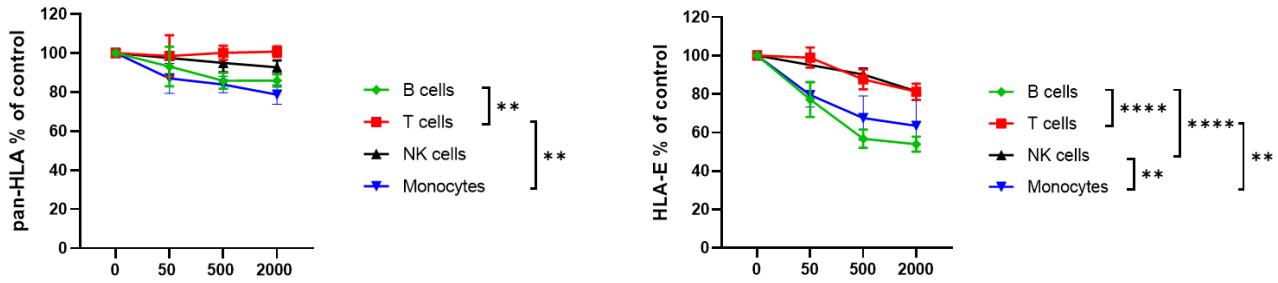


**Figure 4-31: Selinexor decreases HLA-E surface expression on healthy donor B cells and monocytes.**

CLL patient PBMC were treated with 50, 500 or 2000 nM selinexor in the presence of Q-VD for 24 hours. Percent expression of pan-HLA (left) and HLA-E (right) relative to the 0 nM control in healthy donor CD19+ B cells (n=9), CD3+ T cells (n=9), CD3-CD56+ NK cells (n=6) and CD14+ monocytes (n=3) after treatment with selinexor (50-2000 nM). Two-way ANOVA followed by post-hoc analysis comparing protein expression level changes with selinexor concentration between immune cell populations. **P<0.01, ****P<0.001.

## 4.6 Autologous NK cell activation with selinexor

Until now, activation of healthy donor NK cells has been examined against patient CLL cells treated *ex vivo* with selinexor which mimics adoptive transfer conditions. To assess whether patient NK cells will be affected by XPO1 inhibition, CLL donors with low a percentage of circulating CD19+CD5+ CLL cells were used for assessing autologous NK cell activation in the presence of selinexor. Because it is well established that CLL cells are highly suppressive towards NK cells and that NK cells from patients are highly dysfunctional (48,374,507), rituximab was also added to cultures in order to stimulate an NK cell immune response (49). Against self-CLL cells, patient NK cells were activated by the addition of rituximab, but in the presence of selinexor, patient NK cells did not become further activated, nor did their activation without rituximab (**Figure 4-32**). In fact, NK cell activation decreased with increasing concentration of selinexor, indicating that 24-hour XPO1 inhibition impairs intrinsic NK cell functions. Interestingly, at 50 nM selinexor, only NKG2A- NK cell activation was impaired which suggests that the downregulation of HLA-E on CLL cells by selinexor may induce a response by patient NKG2A+ NK cells at low selinexor concentrations (**Figure 4-32**). Overall, these data demonstrate that to capitalise on the NK-sensitising effect of SINE compounds, selinexor may best combine with an adoptive transfer approach.

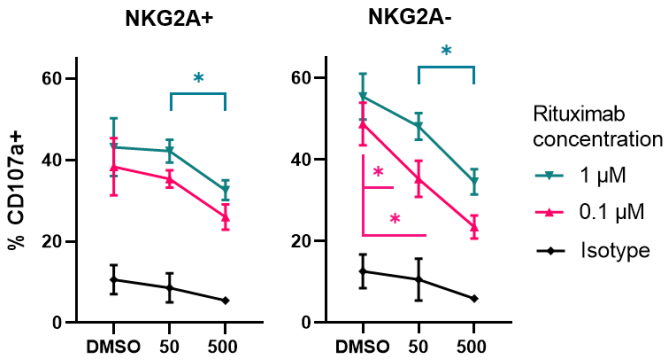


**Figure 4-32: Selinexor does not enhance autologous NK cell activation against CLL cells.**

CLL patient donors with low percentage of circulating CD19+CD5+ CLL cells (<60%) were treated with selinexor (50-500 nM) for 24 hours in the presence of 30 µM Q-VD and 1 ng/mL IL-15. The next day rituximab (anti-CD20) was added to CLL patient PBMC at the given concentrations for 4 hours after which NK cell activation as measured by CD107a expression was assessed in NKG2A+ and NKG2A- NK cells. Cetuximab (anti-EGFR) was used as an isotype control. Each point represents the mean of each treatment group ± SEM of 3 CLL donors. Significant differences in NK cell activation between treatments were calculated with repeated-measure two-way ANOVA: *P<0.05.

## 4.7 Discussion

### 4.7.1 XPO1 inhibition downregulates HLA-E and increases the surface expression of DR5 on CLL cells

Using CLL patient PBMC as a patient-derived malignant B cell model, selinexor activated an NK cell immune response by downregulating the inhibitory NK cell ligand HLA-E, mirroring the results obtained with B-cell lymphoma cell lines (**Figure 4-3 and Figure 4-6**). This then reflected in increased activation of NKG2A+ NK cells although, NKG2A- NK cells were also activated slightly with SINE compounds (**Figure 4-9**). Subsequent death receptor expression analysis demonstrated that XPO1 inhibition enhanced DR5 expression (**Figure 4-15**) and following TRAIL blockade in co-culture experiments, NK specific lysis of CLL targets was inhibited (**Figure 4-16**). In mouse models of B-cell lymphoma, TRAIL-death receptor interactions have been shown to be important in inhibiting spontaneous lymphoid tumour generation (228) and death receptor deficiency promotes lymphoma aggression (508), therefore SINE modulation of DR5 may be important for improving NK cell function against malignant B cells *in vivo*. The mechanism for DR5 upregulation on CLL cells with XPO1 inhibitors remains to be determined, but reports have shown that DR5 expression is regulated by p53 activation (509,510), by epigenetic mechanisms (511) and by ER stress (402,403), any of which XPO1 inhibitors could be modulating in CLL cells.

Interestingly, TRAIL blockade completely abolished NK-mediated lysis of CLL cells and selinexor treatment did not sensitise CLL cells to NK cells in the presence of anti-TRAIL antibodies (**Figure 4-16**). This implies that for HLA-E downregulation to influence NK cell activation against CLL cells, there is a requirement for sufficient activating signals. It was recently shown that TRAIL engagement to DR4/5 facilitates IL-15 signalling-induced granzyme B production, degranulation and IFNγ production alongside inducing apoptotic signals in target cells (137,138). Although TRAIL has limited capacity to signal with its small intracellular domain (twenty amino acids long, UniProt: TNFRSF10A), TRAIL-DR4/5 interactions may enable prolonged NK-cancer cell interactions allowing NKG2A to fine tune the NK cell immune response. Importantly, the effects of TRAIL are usually measured post 18 hours (133), and in these experiments a 4-hour co-culture timepoint was assessed, therefore the protection induced by anti-TRAIL mAbs must be related to early degranulation events modulated by NKG2A. The downregulation of HLA-E will allow for more potent activating signals derived from TRAIL to enhance the degranulation of NKG2A+ NK cells. Thus, in the presence of TRAIL blocking antibodies, selinexor-induced downregulation of HLA-E is unable to modulate NKG2A+ NK cell function, resulting in weak NK cell degranulation and poor killing capacity. activating signals are removed as with TRAIL blockade, dampening of inhibitory NKG2A signalling with selinexor will weakly activate NK cells resulting in poor cytotoxic capabilities.

In the presence of anti-TRAIL antibodies, NKG2A+ NK cells were still more activated against CLL cells with selinexor (**Figure 4-17**), but counterintuitively their ability to lyse CLL cells was completely diminished (**Figure 4-16**). In a study by Wurzer et al., (2021), CLL cells were shown to be resistant to granzyme B-mediated NK cell death by fast reorganisation of the cytoskeleton to impede immunological synapse formation. In another study investigating mechanisms of NK serial killing, NK cells quickly switched from granzyme-mediated killing to death receptor-mediated killing (133). Considering both these research studies, the abolishment of NK cytotoxicity in parallel to enhanced NK cell activation with selinexor and anti-TRAIL antibodies perhaps reflects CLL cell resistance to granzyme B-mediated cell death and the inability of NK cells to switch to death-receptor mediated killing resulting in incomplete caspase activation and CLL cell death.

The primary response by NK cells to SINE-treated CLL cells was shown to be degranulation (**Figure 4-12**), although this may reflect a short co-culture timepoint of 4 hours or the strength of stimulus (513), and CLL cells are known to be suppressive to NK cells (374). Another reason may reflect the maturation status of healthy donor NK cells between donors. It was shown in mice that immature NK cells preferentially degranulate and mature human CD57+ NK cells produce more IFNγ compared to CD57- NK cells (84). Therefore, in the experiments performed here, donor NK cell maturation status may have limited the amount of IFNγ detected in assays (514). Measuring CD57 expression in LAMP assays may address the differences in low IFNγ production and high degranulation after co-culture with SINE-treated CLL cells.

In the LAMP experiment, it would be interesting to compare NKG2A+TRAIL+ NK cell activation against single positive populations like in the Carlsten *et al.,* (2019) study with bortezomib to determine the individual contribution of DR5 upregulation and HLA-E downregulation with selinexor. It would be hypothesised that double positive (TRAIL+NKG2A+) NK cells would be more activated against selinexor-treated CLL cells compared to single positive populations, and double negative populations would not be activated by XPO1 inhibition. This knowledge could then be applied to strategies combining CAR NK cells with small molecules, such that CARs are designed against receptors which become upregulated after small molecule treatment. This has been shown for nutlin-3a which enhanced PVR expression on neuroblastoma cells leading to enhanced *in vitro* and *in vivo* cytotoxic capacities of DNAM-1 CAR NK cells (325,326). From this work designing an anti-CD19 CAR NK cell positive for both TRAIL and NKG2A may enhance CAR function against selinexor-treated CLL cells.

### 4.7.2 XPO1 inhibitors potentiate ADCC by anti-CD20 and anti-CD38 mAbs

In selinexor co-cultures with mAbs, the enhanced activating signals derived from CD16a and the reduced inhibitory signals derived from NKG2A resulted in further activation of NKG2A+ NK cells compared to single agent treatments (**Figure 4-19** and **Figure 4-21**). The fine-tuning of the NK cell

immune response by selinexor described above with NKG2A and TRAIL seems to be true for activating signals derived from CD16a also. The expression of CD38 and CD20 did not change with selinexor treatment (**Figure 4-18** and **Figure 4-20**) and enhanced ADCC was only observed in the NKG2A+ NK cell population (**Figure 4-19** and **Figure 4-21**). This shows that increased DR5 expression by selinexor does not contribute towards enhancing ADCC as no increase in NKG2A- NK cell activation was observed with anti-CD20 or anti-CD38 mAbs. The activating signals derived from TRAIL may therefore be masked by the strong activating signals derived from CD16a and hence there is no additive effect. Indeed, CD16a activation alone is sufficient to activate NK cells without addition of further co-stimulation (184). Alternatively, CD16a perhaps induced strong activation and facilitated a high affinity immunological synapse to allow for sufficient release of granzyme B to enter and lyse CLL cells without the need for death-receptor mediated cell death.

In addition to promoting NKG2A+ NK cell ADCC against CLL cells using anti-CD20 mAbs, XPO1 inhibition promoted ADCC using daratumumab, an anti-CD38 mAb approved for multiple myeloma. This shows that XPO1 inhibition is not specific for improving ADCC of anti-CD20 mAbs as neither CD20 nor CD38 expression increased with XPO1 inhibition and only the NKG2A+ NK cell population was further activated by combined selinexor-mAb treatment. This further illustrates the mechanism of HLA-E downregulation by XPO1 inhibition in promoting mAb ADCC and indeed NKG2A on NK cells can impede ADCC (265,266), therefore by modulating NKG2A:HLA-E interactions with selinexor ADCC by NKG2A+ NK cells can be increased.

### 4.7.3 Lymph node-derived signals IL-4 and CD40L protect CLL cells from NK cell activation

CLL cells transit through the body via secondary lymphoid organs where they are immersed in a microenvironment rich in molecules capable of supporting cancer cell survival, proliferation, and drug resistance (501). Data presented here demonstrate for the first time that the lymph node additionally confers CLL cells protection from NK cells via upregulation of HLA-E (**Figure 4-25**, **Figure 4-27** and **Figure 4-28**). The mechanism behind enhanced HLA-E expression was not explored, but upregulation depends mainly on CD40L and is further upregulated in combination with IL-4. This is in accordance with anti-CD40 antibodies upregulating the mouse HLA-E homologue Qa-$1^b$ on mouse splenocytes (34). It could be speculated that the promotion of cell division in the lymph node by IL-4 and CD40L increases the abundance of HLA-E stabilising peptides and indeed NF-κB, which is downstream of CD40, can bind *HLA-G* (515) and *HLA-B* (516) genes which serve as HLA-E stabilising peptides (26,199). Additionally, the interplay of transcription factors downstream of CD40 and IL-4 receptors may induce *HLA-E* gene expression which could be mediated via STAT-1. IL-4 signalling has been recorded to induce low levels of STAT1 activation (517) and NF-κB induction (383) by CD40 signalling may induce STAT1 expression via the secretion of interferons including IFNγ and TNFα as observed in transformed 721 B cell lines (518) and breast cancer cells (519), respectively.

In the context of B cell activation and maturation, HLA-E upregulation could be similar to that observed with activated T cells in which HLA-E upregulation confers protection from NK-mediated destruction (28,520). Moreover, viral infection induces Qa-$1^b$ expression on B lymphocytes which inhibits NK cell control of cytotoxic T lymphocytes resulting in reduced viral burden (27). Therefore, HLA-E:NKG2A interactions have been reported between B cells and NK cells during inflammation and these interactions may play important roles in B cell malignancies, particularly in secondary lymphoid organs.

### 4.7.4 Second generation BTK inhibitors do not impair enhanced NK cell function with XPO1 inhibition

Enhanced HLA-E expression on CLL cells by *ex vivo* incubation with IL-4 and CD40L was confirmed *in vivo* by measuring HLA-E expression on CXCR4lo CD5hi CLL cells which identifies those cells that have recently left the lymph nodes. It will be interesting to further validate these findings by examining HLA-E expression on CLL cells from ibrutinib-treated patients. This is because BTKi treatment promotes CLL cell egress from the lymph nodes due to downregulation of CXCR4 expression (521). Therefore, it could be hypothesised that CLL cells from ibrutinib-treated patient PBMC will have higher levels of surface HLA-E than ibrutinib-naïve patients. As selinexor is in clinical trials for CLL in combination with ibrutinib, by promoting CLL cell egress from an NK-suppressive environment selinexor treatment may further potentiate the NK cell immune response against CLL cells by downregulating HLA-E. However, as shown in this study and in previous reports (499,522), BTKi impede NK cell function through off-target inhibition of ITK, and hence the selinexor-sensitising effect was lost in **Figure 4-24**. Using a next-generation BTKi such as acalabrutinib, zanubrutinib or orelabrutinib in combination with selinexor may promote improved responses in CLL patients as acalabrutinib only showed partial NK inhibition in line with previous reports (328,522). Use of orelabrutinib combined with rituximab improved B-cell lymphoma regression in mouse models and mice treated with the combination had greater NK activation compared to single agent treatments (329). Whether the same *in vivo* effect is seen with selinexor remains to be determined.

### 4.7.5 XPO1 inhibition did not enhance autologous NK cell function against CLL cells

In an autologous setting, selinexor did not sensitise CLL cells to patient NK cells. At low selinexor concentrations only NKG2A+ NK cells retained their ADCC capacity highlighting that XPO1 inhibition may provide some benefit towards ADCC via modulation to the NKG2A:HLA-E inhibitory axis. On encountering selinexor for 24 hours (**Figure 4-32**), NK cells show slight impairment in activation compared to incubation at 4 hours as observed in the BTKi LAMP experiment (**Figure 4-24**). This reflects the fact that nuclear export is a physiologically important process that all cell types rely on. XPO1 is known to potentiate STAT signalling (38) which are important signal transducers downstream

of cytokines and crucial for NK cell function (523). Therefore, XPO1 blockade may impede NK cell signalling resulting in impaired NK cell activation. Crucially XPO1 blockade may impair signalling downstream of activating receptors such as NKG2D which warrant investigations that may shed light on which cancers, through their differential expression of activating receptor ligands, will be most sensitised to NK cell cytotoxicity via XPO1 inhibition. But it is questionable as to whether a simple, 2D culture system best represents how selinexor directly effects NK cell function. IL-2 is able to enhance the survival of NK via upregulation of BCL-2 (524). Therefore, using IL-2 as an alternative to IL-15 in the autologous experiment may improve NK cell function with selinexor. XPO1 inhibition was also shown to inhibit T cell function *in vitro* through impairment of TCR signalling (459), but *in vivo* T cell activation was enhanced with XPO1 inhibitors (406,525).

Furthermore, other forms of microenvironmental support exist that may confer CLL cell resistance to NK cell activation which XPO1 inhibition may interfere with including CLL cell interactions with T follicular helper cells and the stimulation of the BCR (501). A murine model will enable investigations into how XPO1 inhibition modulates the NK cell immune response in secondary lymphoid organs and in the tumour microenvironment. Additionally, investigating NK cell function with XPO1 inhibitors in human lymph node models may be possible using 3D models of CLL patient PBMC (491).

*In vivo* models will also enable investigation into immune cell crosstalk in the presence of XPO1 inhibition. Selinexor was shown to downregulate HLA-E on healthy CD14+ cells and healthy B cells. NKG2A blockade showed transient depletion of healthy monocytes and B cells in mice and HLA-E downregulation on these populations by selinexor may induce the same depleting effect (526). But the lack of ligands for activating NK cell receptors on healthy cell populations may mitigate the potential consequence of HLA-E downregulation by selinexor as expanded NK cells spared healthy B cells within the PBMC of CLL patients, but lysed malignant B cells (527).

The duration of selinexor incubation required to induce HLA-E downregulation was calculated to be at least 16 hours for CLL cells, but HLA-E was further downregulated after 24 hours (**Figure 4-8**). When selinexor was washed out of cultures, HLA-E remained downregulated after 48 hours (**Figure 4-8**) in accordance with XPO1 still being occupied by selinexor after 96 hours in cancer cell lines (528). As such, the lack of autologous NK cell activation by selinexor may be due to insufficient HLA-E downregulation on CLL cells in parallel to intrinsic impairment of NK cell function. It could be speculated that *in vivo*, selinexor occupancy in malignant B cells for at least 96 hours will continue to drive HLA-E downregulation so that new, infiltrating NK cells into tumours will drive an immune response against these cells.

Regardless, the autologous experiment also indicates that to capitalise on the immunomodulatory effect of selinexor an allogeneic approach may be required, such as the adoptive transfer of NK/CAR NK cells. Patients with CLL may particularly benefit from allogeneic NK cell therapy given that

autologous NK cell numbers in patient lymph nodes are low (529). The autologous experiment also indicates that selinexor treatment should precede adoptive transfer of NK cells rather than concurrent treatment. This was shown for selinexor-CAR T cell combination therapy *in vitro* (459) and in human lymphoma mouse models (460) in which concurrent treatment had no effect on tumour regression, but sequential treatment (selinexor followed by CAR T cells) promoted efficient tumour clearance. Therefore, chapter 5 sought to investigate the potential of selinexor to potentiate the function of expanded, allogeneic NK cells and anti-CD19 CAR NK cells against B-cell lymphomas.

# Chapter 5 *In vitro* analysis of expanded NK cell and CAR NK cell therapies combined with XPO1 inhibition

## 5.1 Receptor expression on NK cell lines and primary IL-2 expanded NK cells

An advantage of using NK cells in adoptive transfer therapy settings is their improved safety profile compared to T cells, with a lack of graft versus host disease and no evidence of cytokine release syndrome in B cell malignancies (305). Another advantage is that allogeneic NK cells from a single source can be used in multiple patients. This reduces the time from intention to treat to administration of the cellular therapy as an off-the-shelf product can be used. Allogeneic NK cells are derived from multiple sources including cell lines (NK-92 and NKL cells) and primary tissues (peripheral blood, umbilical cord blood and induce pluripotent stem cells) and the effect of selinexor on allogeneic NK cell therapy is unknown. Therefore, the function of NK cell lines and activated and expanded peripheral blood NK cells were assessed when co-cultured with cancer cells pre-treated with selinexor.

First, because XPO1 inhibition sensitises malignant B cells to NK cells via the HLA-E:NKG2A axis, NK cell lines NK-92 and NKL and primary expanded NK cells were assessed for expression of NKG2A. To expand NK cells from healthy donors, NK cells were isolated with magnetic bead separation and cultured for up to 4 weeks in NK MACS medium (Miltenyi) with the addition of human serum and 500 IU/mL IL-2. During the course of the expansion, primary NK cells were assessed on their expansion capacity (**Figure 5-1**) and for expression of NKG2A among other activating and inhibitory receptors as well as on NK-92 and NKL cell lines.

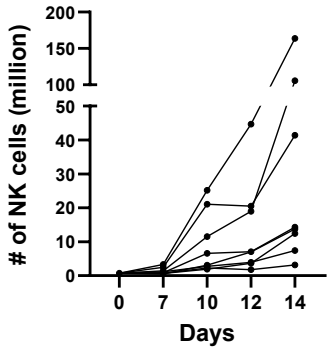


**Figure 5-1: Expansion of primary NK cells expanded with 500 IU/mL IL-2.**

NK cells were isolated from healthy donor PBMC and expanded for two weeks in NK MACS medium supplemented with human serum and 500 IU/mL IL-2. Fresh medium and IL-2 was added every 2-3 days. Each point represents the number of NK cells on that day and each line represents an individual donor (n=8).

The panel of activating receptors assessed in this thesis showed differences in expression between cell lines and primary NK cells and between resting NK cells and expanded NK cells (**Figure 5-2**). CD16a is lowly expressed on NK-92 and NKL cells and is highly expressed on primary NK, however during NK expansion CD16a expression decreased slightly. NKp30, NKp44 and NKp46 increased greatly on expanded NK cells compared to resting NK. NKp30 and NKp44 were expressed more highly on NK-92 compared to NKL and NKp46 was expressed at comparable levels between NK cell lines. The inhibitory receptor CD96 was expressed lowly at comparable levels between cell lines and primary NK cells.

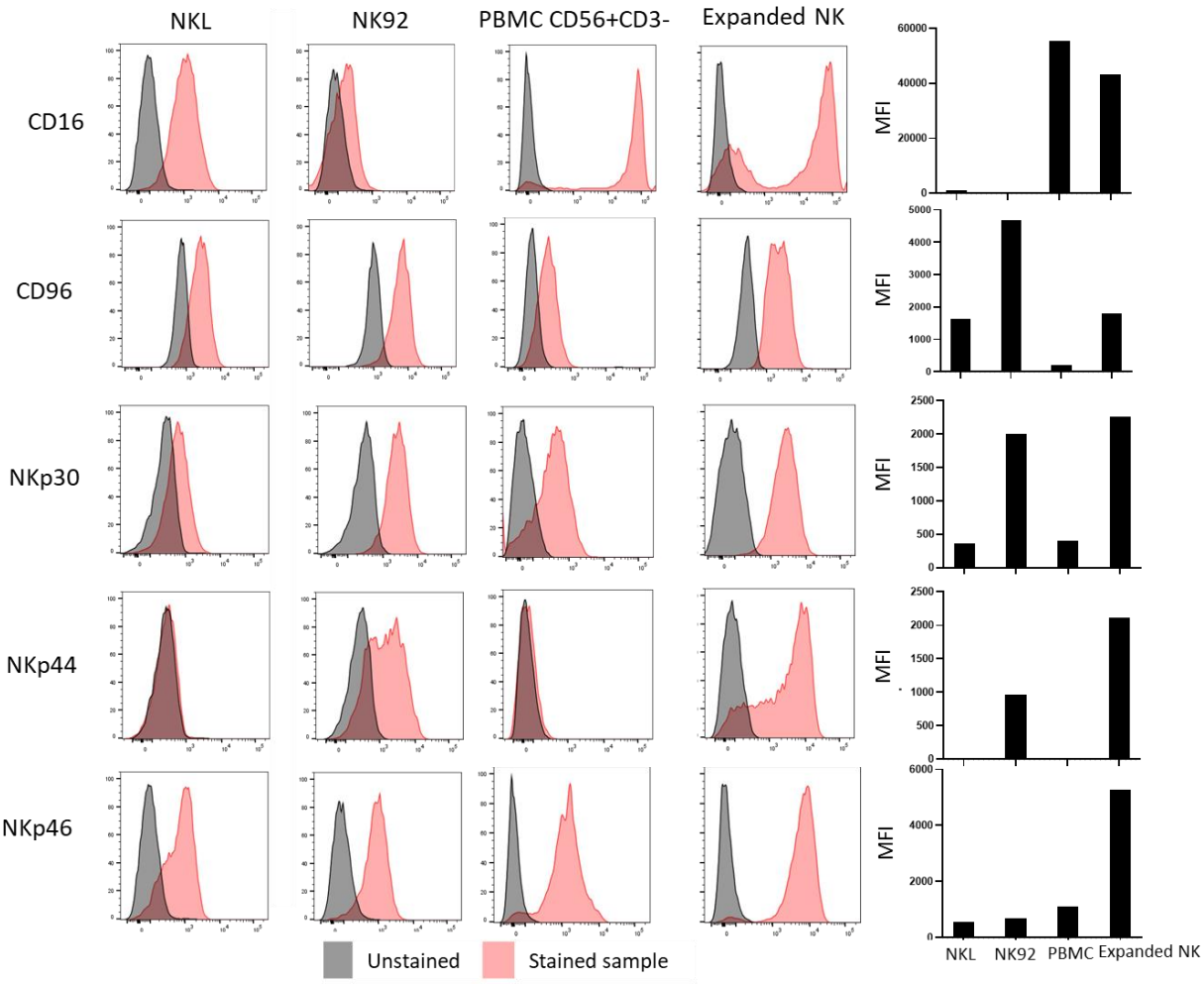


**Figure 5-2: Expression of activating receptors and the inhibitory receptor CD96 on NK cell lines and primary NK cells.**

NK cell lines NKL and NK-92 and resting primary NK cells within PBMC (PBMC CD56+CD3-) and 14-day IL-2 expanded NK cells were assessed for surface expression of the activating NK cell receptors CD16, NKp30, NKp44 and NKp46 and the inhibitory receptor CD96. Shown are the histograms of stained and unstained samples followed by the MFI relative to the unstained controls for each receptor and each cell population from a single experiment.

Next, the expression of NKG2x receptors (NKG2A, NKG2C and NKG2D) on NK cell lines and primary NK cells was assessed. NKG2D was not expressed by NK-92 cells and was lowly expressed on all other cell types (**Figure 5-3**). In accordance with data on cytomegalovirus negative donors, NKG2C is lowly expressed on circulating NK cells (193) and expression can vary considerably between donors (530). Additionally, NKG2C is lowly expressed on IL-2 and IL-15 expanded NK cells (531), however NKG2C expression has been reported on NKL cells (532), therefore a repeat is required to confirm whether the NKG2C antibody stain worked. For NKG2A, NK-92 showed the lowest level of expression and resting NK cells showed two clear populations, one negative for NKG2A (60%) and one positive (30%).

During expansion, NKG2A became upregulated on almost all NK cells. NKL cells expressed high levels of NKG2A, but not as high as compared to expanded NK cells.

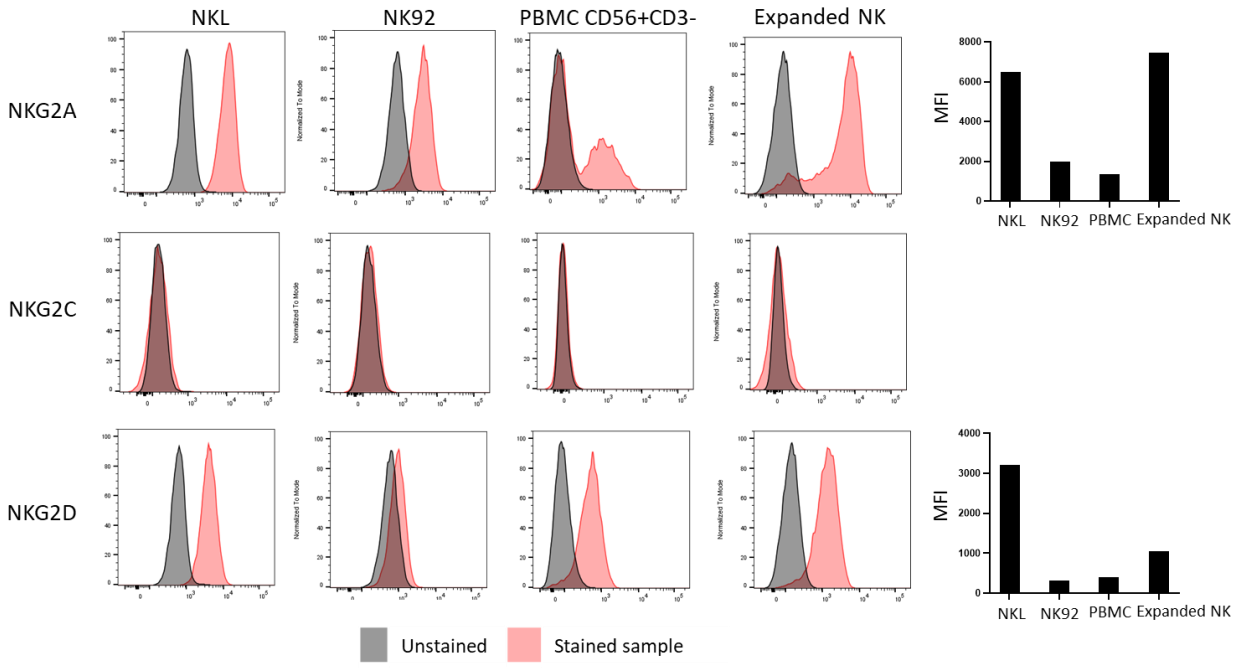


**Figure 5-3: Expression of NKG2x receptors on NK cell lines and primary NK cells.**

NK cell lines NKL and NK-92 and resting primary NK cells within PBMC (PBMC CD56+CD3-) and 14-day IL-2 expanded NK cells were assessed for surface expression of NKG2A, NKG2C and NKG2D. Shown are the histograms of stained and unstained samples followed by the MFI relative to the unstained controls for each receptor and each cell population from a single experiment.

## 5.2 Cytotoxicity of NK cell lines and primary IL-2 expanded NK cells against B cell lymphoma cells treated with XPO1 inhibitors

Given that NKG2A is expressed by NKL and NK-92 cell lines, these cells were assessed for cytotoxicity towards selinexor-treated lymphoma cells, with the hypothesis that selinexor-induced HLA-E downregulation would lead to increased NK cytotoxicity by NKL and NK-92 cells. With increasing selinexor concentration, no increase in NK specific lysis was observed for NK-92 or NKL cell lines (**Figure 5-4**). NKL cells were completely unable to lyse Raji and Ramos cells at the 24-hour timepoint, whereas NK-92 cells possessed cytotoxic capabilities, however this killing ability was not enhanced by XPO1 inhibition.

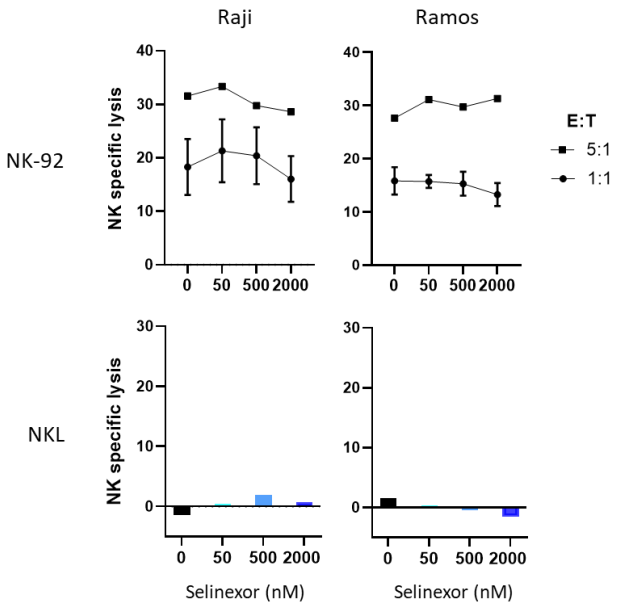


**Figure 5-4: XPO1 inhibition does not enhance NK-92 and NKL cytotoxicity of B cell lymphoma cells.**

NK-92 and NKL cells were co-cultured for 24 hours (E:T = 1:1 and 5:1) with Raji and Ramos cells that were pre-treated with selinexor (50, 500, 2000 nM) for 24 hours. After lysed CFSE+ Raji and Ramos cells were measured using propidium iodide staining and NK specific lysis was calculated as *(% target lysis - % spontaneous lysis) * 100 / (100 - % spontaneous lysis).* Shown is the mean ± SEM for NK-92 cells (n=2) and the mean for NKL cells.

Selinexor treatment did not sensitise Raji and Ramos cells to lysis by NK-92 or NKL cells, therefore it was investigated whether NKG2A was functional on NK-92 and NKL cells. To do this NK cell lines were co-cultured with Raji and Ramos cells in the absence and presence of anti-NKG2A blocking antibodies. For both NK cell lines, the presence of anti-NKG2A antibodies did not enhance NK cytotoxicity against either Raji or Ramos cells (**Figure 5-5**). NKL cells were poorly cytotoxic towards lymphoma cells, NKL cells were modestly cytotoxic towards Raji, but more cytotoxic towards Ramos. As for expanded, primary NK cells, these were highly cytotoxic towards Ramos and moderately cytotoxic towards Raji. However, in contrast to NK cell lines, increasing selinexor concentration enhanced expanded NK cell lysis, likewise with anti-NKG2A antibodies in the co-culture (**Figure 5-5**). Therefore, these data suggest that NKG2A is dysfunctional on NK-92 and NKL cell lines and this may explain the lack of enhanced cytotoxicity when co-cultured with selinexor-treated lymphoma cells which have decreased HLA-E surface expression.

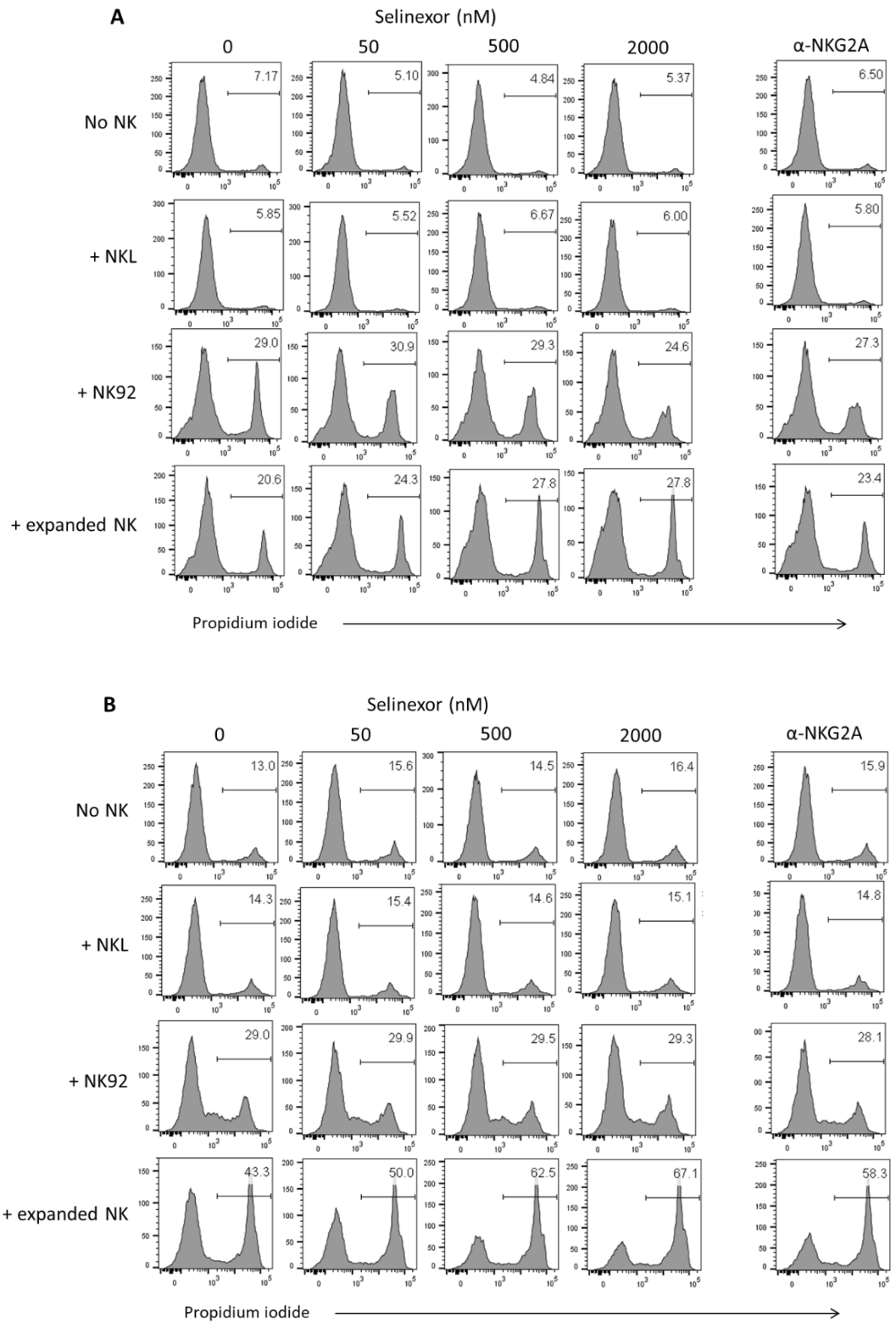


**Figure 5-5: Anti-NKG2A blocking antibodies do not promote NK-92 and NKL cytotoxicity.**

Cytotoxicity of NK cell lines NK-92 and NKL and primary IL-2 expanded NK cells when co-cultured with Raji (**A**) and Ramos (**B**) cells in the presence of anti-NKG2A antibodies (10 µg/mL). NK specific lysis of selinexor-treated (50, 500, 2000 nM) lymphoma cells is also shown. NK cells and cancer cells were co-cultured at an E:T of 5:1 for 24 hours after which lysed cancer cells were measured using propidium iodide staining by flow cytometry. Shown is one experiment with one donor and numbers on histograms represent the proportion of lysed cells gated on CFSE-stained cancer cells.

To combine XPO1 inhibition with adoptive NK cell therapies, primary NK cells may therefore be beneficial compared with NK cell lines. As such, to confirm that selinexor sensitises lymphoma cells to expanded NK cell lysis, further NK donors were tested for expression of NKG2A during expansion and for their ability to lyse selinexor-treated lymphoma targets. As shown in **Figure 5-6**, approximately 50% of day 0 NK cells isolated from PBMC expressed NKG2A. At day 7 most NK cells expressed NKG2A and at day 14, almost 100% of NK cells expressed NKG2A in all donors tested. To establish the reason for high NKG2A expression on all expanded NK cells in the population, day 0 NK cells were labelled with CFSE and the rate of CFSE dilution was assessed on NKG2A+ and NKG2A- NK cells over time. At day 7, proliferation was observed only in the NKG2A+ NK cell population and this was reflected in an increase in the proportion of NKG2A+ cells, suggesting that during NK proliferation NKG2A becomes upregulated (**Figure 5-7**). After two weeks, few NKG2A- NK cells remained and these mostly showed signs of proliferation with no upregulation of NKG2A. During co-culture experiments with selinexor-treated lymphoma cells, in accordance with high NKG2A expression after 14-day expansion, expanded NK cells were highly cytotoxic towards selinexor-treated lymphoma cell lines, even at a low effector:target ratio of 1:10 (**Figure 5-8**). This held true for the next generation XPO1 inhibitor eltanexor which also induced XPO1 degradation (**Figure 5-9A**), specific downregulation of HLA-E (**Figure 5-9B**) and sensitised Raji and Ramos cells to lysis by 14-day, IL-2 expanded NK cells (**Figure 5-9C**), illustrating a class effect of XPO1 inhibitors in sensitising B-cell lymphoma cells to expanded NK cell cytotoxicity.

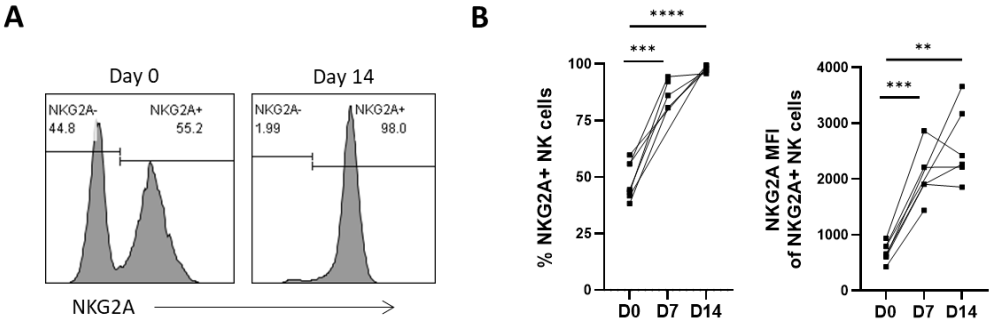


**Figure 5-6: NKG2A expression on IL-2 expanded NK cells.**

NKG2A expression on primary NK cells after isolation on day 0 (D0) and after 7-day (D7) and 14-day (D14) expansion with 500 IU/mL IL-2. (**A**) Representative histogram of NKG2A expression on D0 and D14 pure NK cells. Numbers on histograms represent the percentage within horizontal gates. (**B**) Percentage (left) of NK cells expressing NKG2A within the D0, D7 and D14 NK cell population. NKG2A MFI (right) when gated on NKG2A+ NK cells within the D0, D7 and D14 population. Each line represents individual matched donors. Paired sample t-test: ****P<0.001, ***P<0.005, **P<0.01.

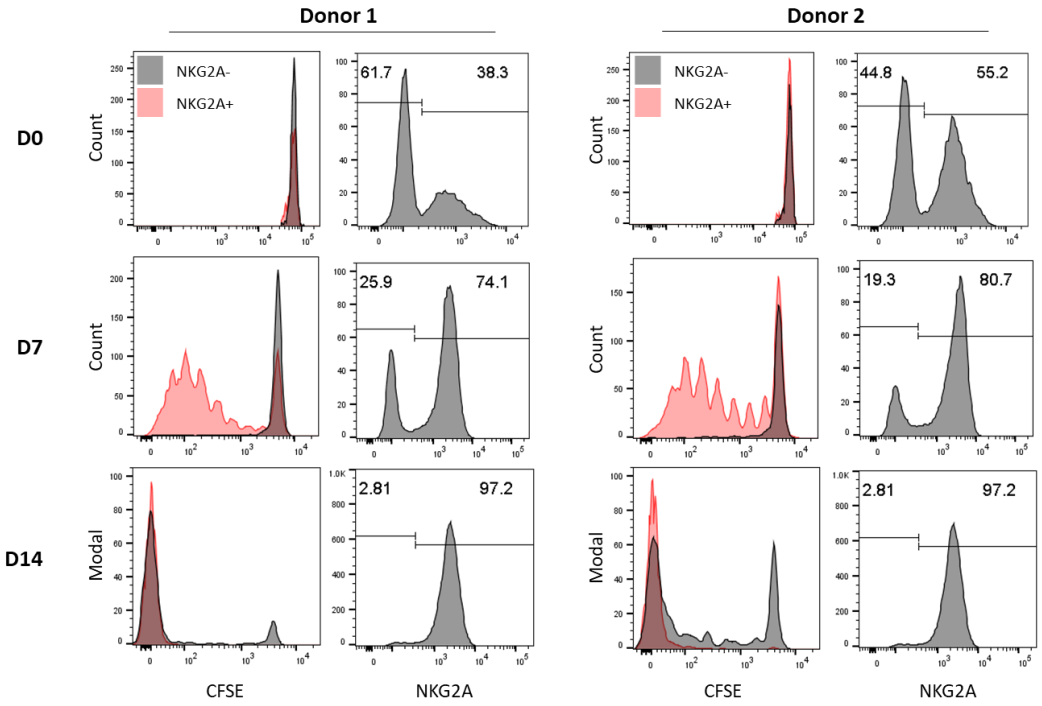


**Figure 5-7: Proliferation of NKG2A+ and NKG2A- NK cells during 14-day expansion.**

NK cells were isolated from healthy donor PBMC on day 0 (D0) and labelled with CFSE. During 14-day expansion, CFSE dilution was measured in NKG2A+ and NKG2A- NK cell populations on day 7 (D7) and day 14 (D14). Shown is one experiment using NK cells from two different donors and the proportion of NKG2A- and NKG2A+ NK cells within the CD56+CD3- NK cell population is displayed. For D0 and D7, cell count is displayed on the y-axis for CFSE dilution histograms, and for D14 the modal is shown because of low NKG2A- NK cell numbers.

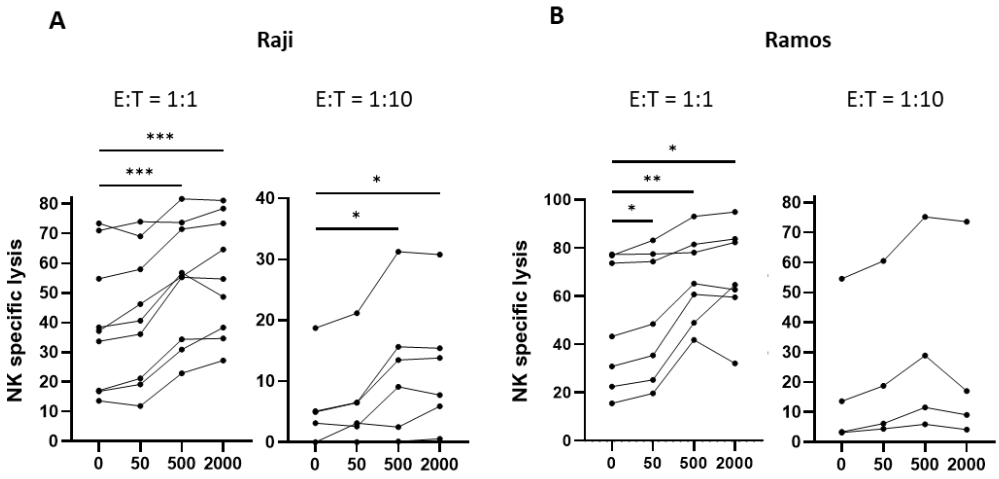


**Figure 5-8: XPO1 inhibition enhances expanded NK cell cytotoxicity of B cell lymphoma cells.**

Raji (**A**) and Ramos (**B**) cells were pre-treated with selinexor (50-2000 nM) for 24 hours in the presence of QVD followed by co-culture with IL-2 expanded NK cells (14-21 days) for 24 hours at E:T ratios of 1:1 and 1:10. Each line represents an individual donor NK cells and differences in NK specific lysis between control and treatment groups were calculated with repeated-measure one-way ANOVA followed by Dunnett's post-hoc test: ***P<0.005, **P<0.01, *P<0.05.

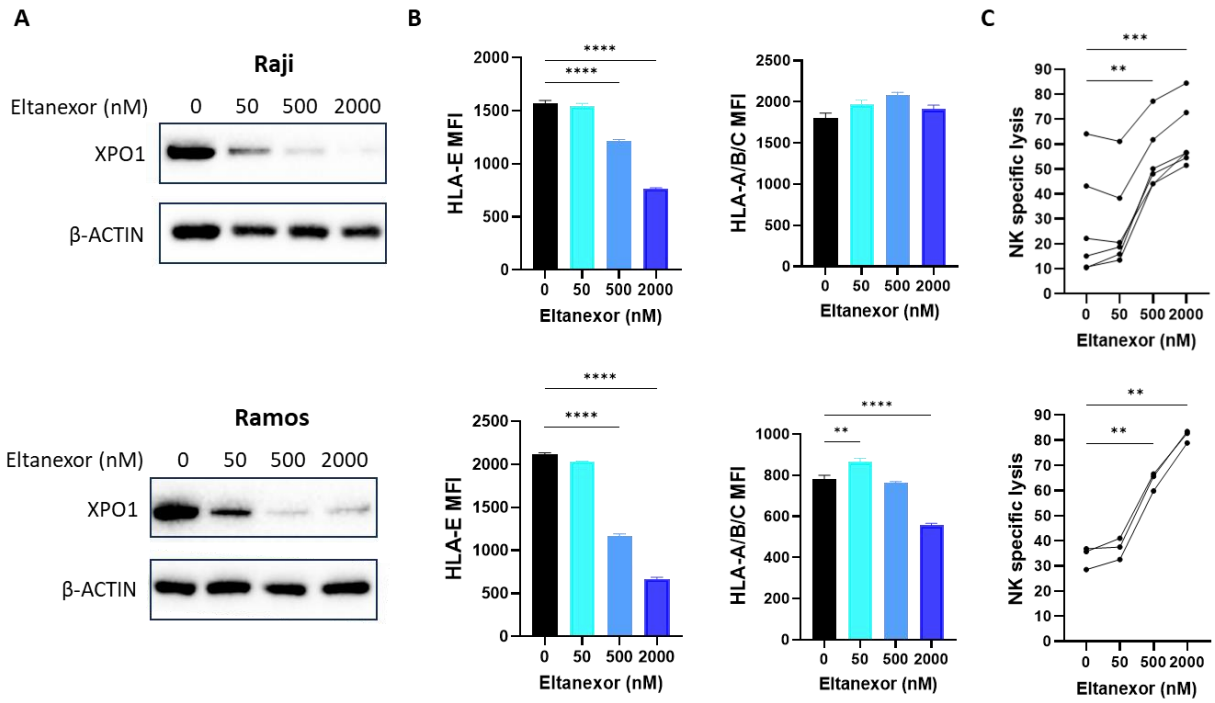


**Figure 5-9: The next generation XPO1 inhibitor eltanexor downregulates HLA-E expression which sensitises B cell lymphoma cells to expanded NK cell cytotoxicity.**

Raji (above) and Ramos (below) were treated with the next generation XPO1 inhibitor eltanexor (50-2000 nM) or DMSO control (0 nM) for 24 hours in the presence of the apoptotic inhibitor Q-VD (30 µM). After, cancer cells were assessed for XPO1 degradation by western blot (**A**), for surface expression of HLA-E and HLA-A/B/C (**B**) and for sensitivity to lysis by 14-day IL-2 expanded NK cells at an E:T = 1:1 (**C**). Shown in **B** is the mean MFI ± SEM of HLA-E and HLA-A/B/C stained with the antibody clones 3D12 and W6/32, respectively (n=3). In **C** each line represents matched, individual expanded NK cell donors (n=6 for Raji, n=3 for Ramos). Significant differences in HLA expression and NK specific lysis between the DMSO control and eltanexor drug concentrations were calculated with ordinary and repeated-measure one-way ANOVA, respectively, followed by Dunnett's post-hoc test: ****P<0.001, **P<0.01.

Because HLA-E downregulation by selinexor sensitised lymphoma cells to expanded NK cell specific lysis, it was assessed whether blocking NKG2A:HLA-E interactions with antibodies against NKG2A would enhance NK cytotoxicity. The widely available clone Z199 was used to block NKG2A because it binds the same region as the clinically tested antibody monalizumab and because Z199 has similar binding kinetics to monalizumab (279). By blocking NKG2A:HLA-E interactions, expanded NK cells more readily lysed lymphoma target cells compared to the DMSO-treated control with an increase in NK specific lysis of 20% for Raji and 12% for Ramos (**Figure 5-10**). The magnitude of increased NK specific lysis induced by anti-NKG2A antibodies was comparable to selinexor treatment. When selinexor and anti-NKG2A antibodies were combined, a slight additive effect was observed for Raji cells, but not for Ramos. Overall these data suggest that by impairing NKG2A:HLA-E interactions

through XPO1 inhibition or antibody blockade promotes the cytotoxicity of IL-2 expanded NK cells that express high levels of NKG2A.

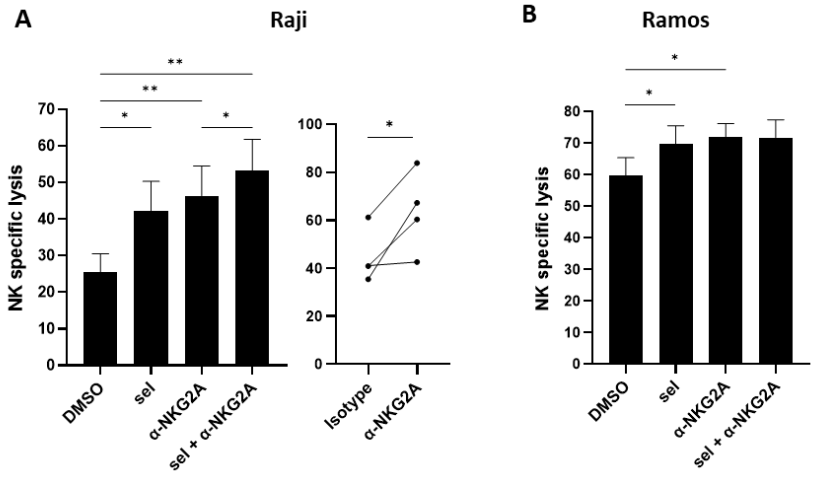


**Figure 5-10: Anti-NKG2A blocking antibodies enhance expanded NK cell cytotoxicity.**

Raji (**A**) and Ramos (**B**) cells were pre-treated with selinexor (500 nM, sel) or DMSO control for 24 hours in the presence of QVD followed by co-culture with IL-2 expanded NK cells (14-21 days) in the absence or presence of NKG2A blocking antibodies (Z199, 10 µg/mL) for 24 hours at an E:T ratio of 1:1. For Raji cells (**A**), the effect of the antibody isotype on NK specific lysis was assessed compared to the anti-NKG2A antibody. Bars represent the mean ± SEM (n=7) and each line represents an individual donor NK cells and differences in NK specific lysis between treatment groups were calculated with repeated-measure one-way ANOVA followed by Tukey's post-hoc test or paired sample t-test: **P<0.01, *P<0.05.

## 5.3 Assessing expanded NK cell cytotoxicity in a 2D lymph node support model

### 5.3.1 IL-4 and CD40L increase HLA-E expression on B cell lymphoma cells, which is reversed by XPO1 inhibition

In chapter 4, primary CLL cells incubated with lymph node-associated molecules IL-4 and CD40L were resistant to NK cell activation via upregulation of HLA-E. Through using selinexor, HLA-E upregulation by IL4 and CD40L was overcome. Like in CLL, T follicular helper cells are present in non-Hodgkin lymphoma (384), thus IL-4 and CD40L were used again to mimic T cell support. It was examined whether IL-4 and CD40L can also enhance HLA-E expression on B-cell lymphoma cell lines and

whether XPO1 inhibition could counteract this. With lymph node support, all B cell lymphoma cell lines tested had increased surface expression of HLA-E (**Figure 5-11**). For total HLA class I expression, a significant increase was also observed with IL-4 and CD40L except for SUDHL4 whilst for CD19 expression, no increase was measured with lymph node support (**Figure 5-11**). Whether inhibiting XPO1 with selinexor could overcome enhanced HLA-E expression was then assessed. On all cell lines selinexor downregulated HLA-E expression in the presence of IL4 + CD40L (**Figure 5-12**). Total HLA class I molecules were only downregulated with selinexor in SUDHL6 cells. Interestingly, CD19 expression was also downregulated by selinexor which may have implications for CD19 directed therapies.

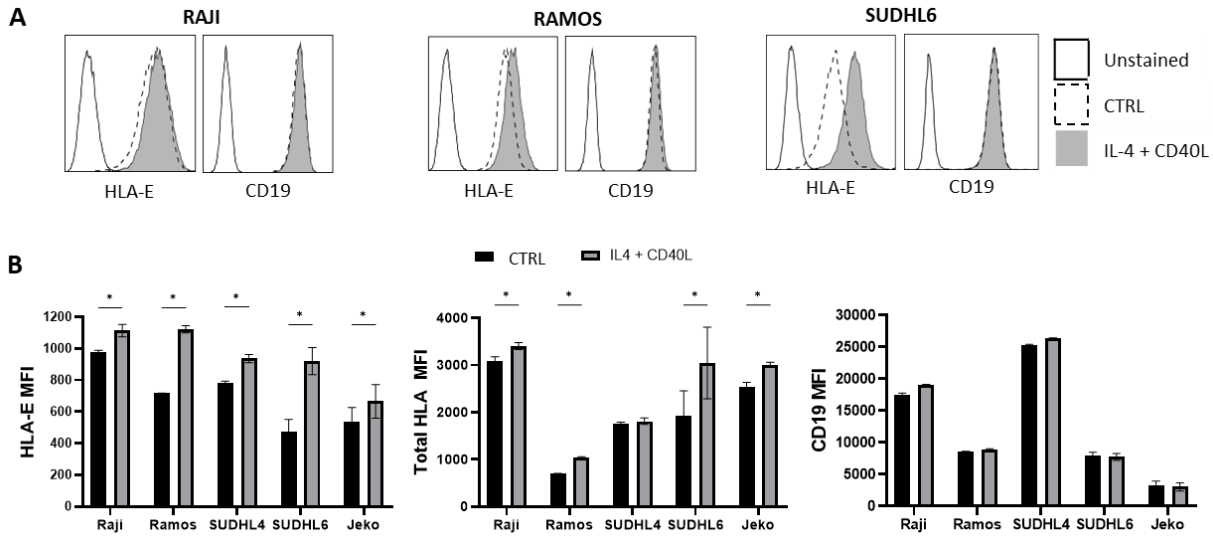


**Figure 5-11: HLA and CD19 expression on lymphoma cell lines incubated with lymph node-associated molecules IL-4 and CD40L.**

Raji (n=3), Ramos (n=3), SUDHL4 (n=3), SUDHL6 (n=4) and JeKo-1 (n=6) cells were incubated with lymph node support molecules IL-4 (10 ng/mL) + CD40L (300 ng/mL) for 24 hours and assessed for expression of HLA-E, total HLA and CD19. (**A**) histograms of HLA-E and CD19 expression on Raji, Ramos and SUDHL6 after 24-hour incubation with IL-4 + CD40L. (**B**) Mean ± SEM for the MFI of HLA-E, total HLA and CD19 on multiple B cell lymphoma cell lines after IL-4 + CD40L incubation. Significant differences in protein expression between control (CTRL) and treatment groups were calculated using paired sample t-test: *P<0.05.

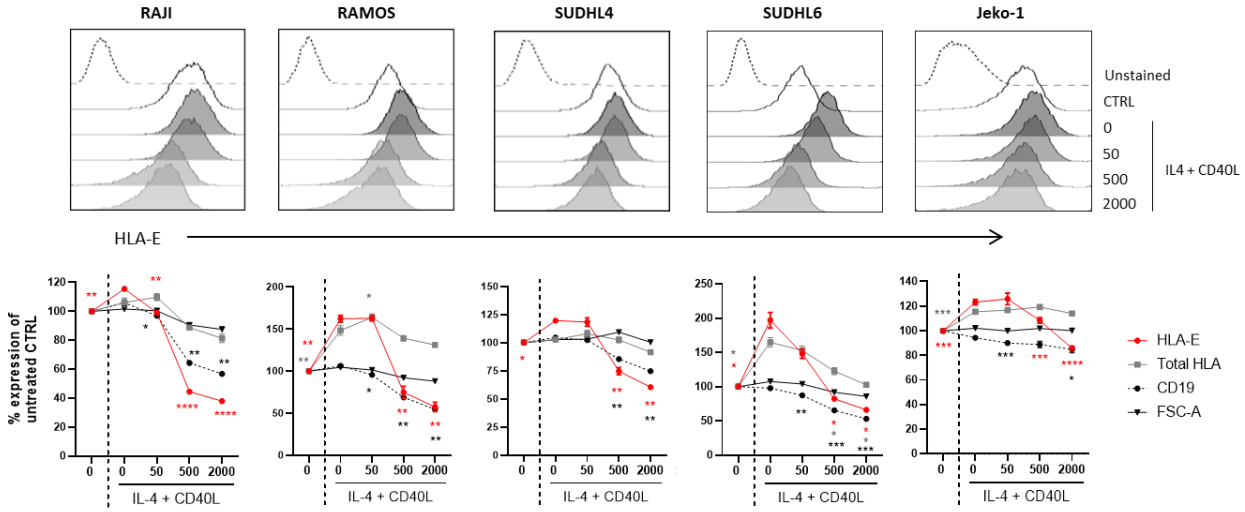


**Figure 5-12: HLA and CD19 expression on lymphoma cell lines treated with selinexor in the presence of IL-4 + CD40L.**

Raji (n=4), Ramos (n=4), SUDHL4 (n=3), SUDHL6 (n=3) and JeKo-1 (n=6) cells were treated with selinexor (50-2000 nM) in the presence of lymph node support molecules IL-4 (10 ng/mL) + CD40L (300 ng/mL) for 24 hours and assessed for expression of HLA-E, total HLA and CD19. Above are representative histograms of HLA-E expression in the different conditions and below are the summaries of the merged replicates. 0 nM control represents DMSO-treated cells in the absence of IL-4 + CD40L. Mean ± SEM expression relative to the untreated control is shown for each protein and cell line and significant differences in protein expression between the IL-4 + CD40L, 0 nM control and treatment groups were calculated using two-way ANOVA followed by Dunnett's post-hoc test: ****P<0.001, ***P<0.005, **P<0.01, *P<0.05.

### 5.3.2 IL-4 and CD40L protects B cell lymphoma cells from NK cell anti-tumour functions, which is reversed by XPO1 inhibition

Because of the increase in HLA-E expression on B-cell lymphoma cells in the presence of lymph node support, it was assessed whether this had functional consequences on expanded NK cell activity. B-cell lymphoma cell lines were co-cultured with expanded NK cells for 24 hours following IL-4 + CD40L incubation. Without NK cells, IL4 + CD40L did not improve or reduce lymphoma cell viability (**Figure 5-13**). However, when co-cultured with expanded NK cells, IL-4 + CD40L conferred protection from NK cells as shown by decreased raw lysis and decreased NK specific lysis (**Figure 5-13**).

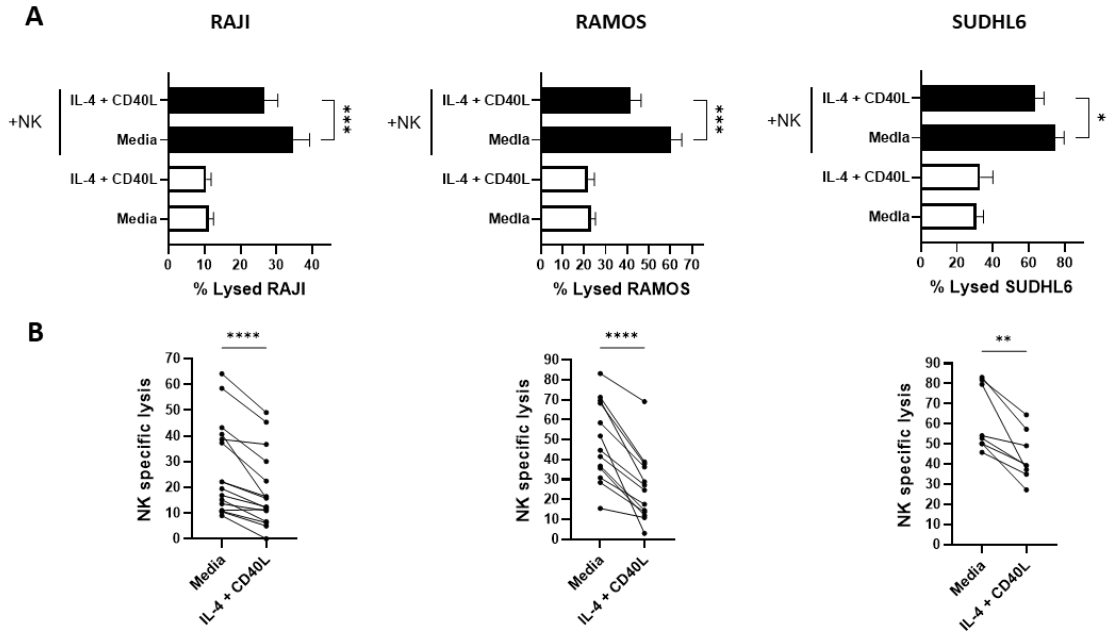


**Figure 5-13: Lymph node-associated molecules IL-4 and CD40L protect B cell lymphoma cells from expanded NK cell cytotoxicity.**

B cell lymphoma cell lines were incubated with IL-4 (10 ng/mL) + CD40L (300 ng/mL) for 24 hours before being co-cultured with IL-2 expanded NK cells (day 14-21) for an additional 24 hours (Z199, 10 ng/mL) or isotype control at an E:T of 1:1. (**A**) Shown is the mean ± SEM of raw lymphoma lysis (propidium iodide positive cancer cells) in cultures with and without NK cells for Raji (n=16), Ramos (n=13) and SUDHL6 (n=8). Significant differences in lymphoma lysis between groups were calculated using repeated-measure one-way ANOVA followed by Tukey's post-hoc test. (**B**) NK specific lysis calculated using the data in (**A**) of lymphoma targets. The difference in NK specific lysis between the two treatment groups was calculated with paired sample t-test: ****P<0.001, ***P<0.005, **P<0.01, *P<0.05.

To determine the contribution of HLA-E to protect lymphoma cells from NK cytotoxicity with IL-4 + CD40L, NKG2A blocking antibodies were added to co-cultures. As shown previously, IL-4 + CD40L protected cell lines from NK cytotoxicity, but in the presence of anti-NKG2A antibodies NK specific lysis was restored (**Figure 5-14**). Against Ramos cells, anti-NKG2A antibodies completely restored NK cell function and against Raji cells blocking antibodies further activated NK cell killing as compared to the isotype control without lymph node support (**Figure 5-14**). For SUDHL6, anti-NKG2A antibodies partially restored NK cell killing, potentially due to high expression of other HLA class I molecules in the presence of IL-4 + CD40L (**Figure 5-11**). In contrast, without lymph node support, anti-NKG2A antibodies failed to enhance NK specific lysis against SUDHL6 cells, perhaps because of the low expression of HLA-E as compared to other cell lines (**Figure 5-11**).

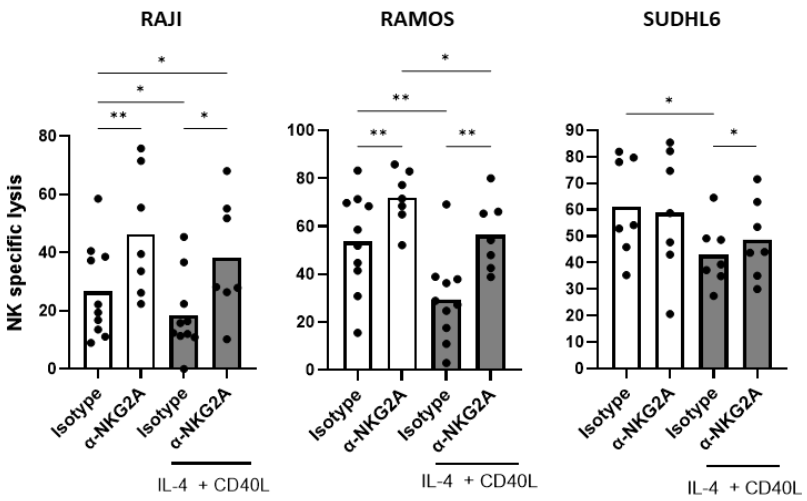


**Figure 5-14: Anti-NKG2A antibodies reverse the NK-protective effect of IL-4 + CD40L in B cell lymphoma cells.**

B cell lymphoma cell lines were incubated with IL-4 (10 ng/mL) + CD40L (300 ng/mL) for 24 hours before being co-cultured with IL-2 expanded NK cells (day 14-21) for an additional 24 hours in the presence of anti-NKG2A antibodies (Z199, 10 ng/mL) or isotype control at an E:T of 1:1. NK specific lysis was then calculated through propidium iodide staining of cancer cells in cultures. Shown is the mean of at least 7 individual donor NK cells and differences in NK specific lysis between treatment groups were calculated with repeated-measure one-way ANOVA followed by Tukey's post-hoc test: **P<0.01, *P<0.05.

Blocking NKG2A:HLA-E interactions reversed protection induced by IL-4 + CD40L, therefore it was hypothesised that downregulation of HLA-E with selinexor would also reverse this protective effect against NK cells. As such, lymphoma cell lines were treated with selinexor in the presence of IL-4 + CD40L lymph node support molecules and expanded NK cell specific lysis against these targets cells was assessed. In a similar fashion to NKG2A blockade with antibodies, killing of Ramos was completely recovered by selinexor and NK specific lysis against Raji cells was further enhanced compared to the no lymph node support control by selinexor (**Figure 5-15**). Likewise, with IL-4 + CD40L NK specific lysis of SUDHL6 cells was only slightly increased by selinexor and without lymph node support selinexor did not sensitise SUDHL6 cells to lysis by NK cells (**Figure 5-15**). This again reflects the fact that HLA-E expression is very low on SUDHL6 at homeostasis and therefore inhibiting NKG2A:HLA-E interactions in this setting does not enhance NK cell function.

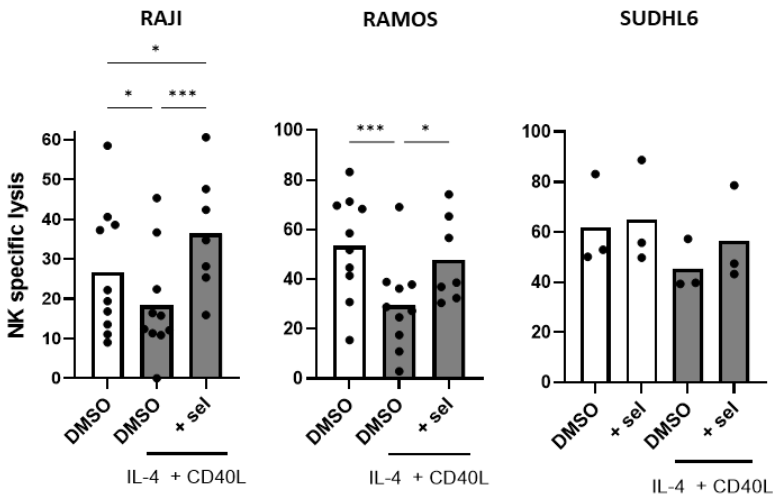


**Figure 5-15: XPO1 inhibition reverses the NK-protective effect of IL-4 + CD40L in B cell lymphoma cells.**

B cell lymphoma cell lines were incubated with IL-4 (10 ng/mL) + CD40L (300 ng/mL) for 24 hours in the presence of 500 nM selinexor (+ sel) before being co-cultured with IL-2 expanded NK cells (day 14-21) for an additional 24 hours at an E:T of 1:1. NK specific lysis was then calculated through propidium iodide staining of cancer cells in cultures. Shown is the mean NK specific lysis of at least 7 individual donor NK cells of Raji and Ramos and 3 donor NK cells for SUDHL6. Significant differences in NK specific lysis between treatment groups were calculated with repeated-measure one-way ANOVA followed by Tukey's post-hoc test: **P<0.01, *P<0.05.

## 5.4 The immunomodulatory effect of XPO1 inhibition in B-cell cell lines with impaired HLA-E expression

Following the result that SUDHL6 was not sensitised to expanded NK specific lysis with XPO1 inhibitors - potentially due to low basal levels of HLA-E surface expression - it was assessed whether this remained true in B lymphoblastoid cell lines with impaired HLA-E expression. The 721 B lymphoblastoid cell line was derived from circulating B cells of a healthy individual and was transformed and immortalised by Epstein-barr virus (533). Subsequent cell lines were descended from the 721 parental cell line including 721.221 which upon exposure to gamma radiation was mutated in *HLA-A/B/C* genes and 721.174 which is deficient in TAP expression (161,534). Consequently, these cells express unstable HLA-E molecules at the plasma membrane with non-canonical peptides presented in the binding groove. This is the result of HLA-A/B/C leader sequences being unavailable to stabilise HLA-E in 721.221 cells and TAP deficient 721.174 cells being unable to load peptides onto HLA-E and other HLA class I proteins. As such sensitisation to NK cell killing by selinexor was examined in these cells.

First, to confirm low expression levels of HLA-E in 721.221 and 721.174 cells and the consequence of selinexor treatment on HLA-E expression, the cell lines were treated with selinexor for 24 hours and the surface expression of HLA-E was measured by flow cytometry (**Figure 5-16**). As expected, 721.221 cells were negative for HLA-A/B/C expression and 721.174 cells expressed HLA-A/B/C at low levels (**Figure 5-16**). For HLA-E, surface expression was very low for 721 cell lines (<600 MFI) and this remained low with selinexor treatment (**Figure 5-17**). Interestingly, the expression of HLA-E on SUDHL6 cells was comparable to 721 cell lines. Because no change in HLA-E expression was observed for 721 cell lines treated with selinexor, western blot for XPO1 expression was assessed to confirm sensitivity of 721 cell lines to selinexor treatment. XPO1 was degraded with selinexor in 721 cell lines and this was associated with increased expression on the tumour suppressor protein p53. Because β-ACTIN was loaded unevenly HLA-E expression was quantitively measured using ImageJ and HLA-E expression is presented on the blot relative to β-ACTIN (**Figure 5-18**). Unlike Raji cells in which no change in HLA-E expression was observed with selinexor, 721.221 had increased HLA-E expression and 721.174 had decreased HLA-E expression. However, these changes are not reflected in surface expression changes due to impaired peptide loading and low stability at the plasma membrane (**Figure 5-17**).

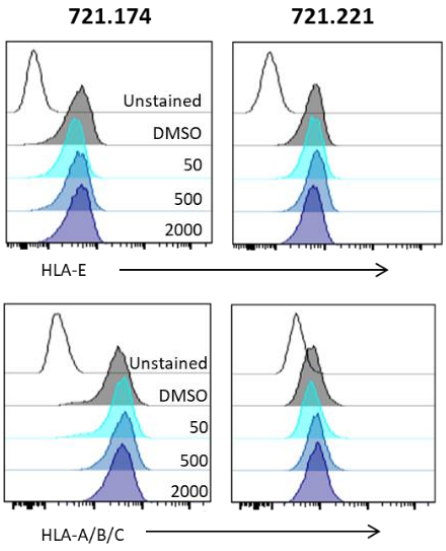


**Figure 5-16: Flow cytometry histograms of HLA proteins on B lymphoblastoid cell lines 721.174 and 721.221.**

721.174 (TAP deficient) and 721.221 (HLA-A/B/C knockout) cell lines with impaired HLA presentation were treated with selinexor (50-2000 nM) or DMSO for 24 hours and assessed for expression of HLA-E and HLA-A/B/C expression. Shown are representative histograms from one experiment.

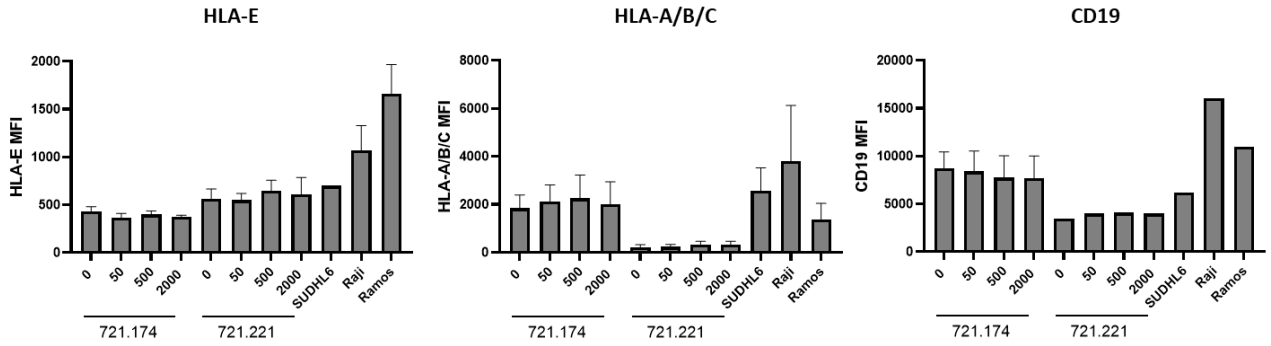


**Figure 5-17: Selinexor does not affect the expression of HLA proteins and CD19 on 721.174 and 721.221 cell lines.**

721.174 (TAP deficient, n=3) and 721.221 (HLA-A/B/C knockout, n=3) cell lines with impaired HLA presentation were treated with selinexor (50-2000 nM) or DMSO (0 nM) for 24 hours and assessed for expression of HLA-E , HLA-A/B/C and CD19 expression. SUDHL6, Raji and Ramos cells were also stained for comparison to 721 cells. Shown is mean + MFI.

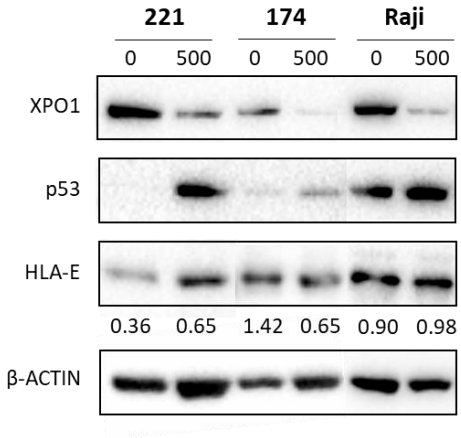


**Figure 5-18: Selinexor degrades XPO1 and induces p53 in 721 cell lines.**

XPO1, p53 and HLA-E protein abundance in 721.221, 721.174 and Raji cells treated with 500 nM selinexor for 24 hours. Numbers on blot represent HLA-E protein abundance relative to the β-ACTIN loading control calculated using ImageJ.

Next, NK functional analysis was performed on selinexor-treated 721 cell lines, with the hypothesis that selinexor does not sensitise cell lines to NK specific lysis due to no change in HLA-E surface expression with XPO1 inhibition. As for cell lines in previous experiments, 721 cell lines were pre-treated with selinexor for 24 hours and co-cultured with expanded NK cells that express high levels of NKG2A. The duration of co-culture was set at 4 hours instead of 24 hours to allow for a window of response because NK cells are highly active against HLA low cells and would lyse all 721 cells in culture at steady state (17). With increasing selinexor concentration, no increase in NK specific lysis was observed (**Figure 5-19**). To ascertain whether HLA-E was functionally engaging with NKG2A on 721 cell lines, NKG2A blocking antibodies were added to co-cultures. NK cytotoxicity did not increase with anti-NKG2A antibodies in 721 co-cultures unlike with Raji cells that express functional HLA-E (**Figure 5-19**). These experiments therefore demonstrate that for selinexor to exert immunomodulatory effects, cancer cells require functional antigen processing and presentation machinery so that HLA-E surface expression can be modulated.

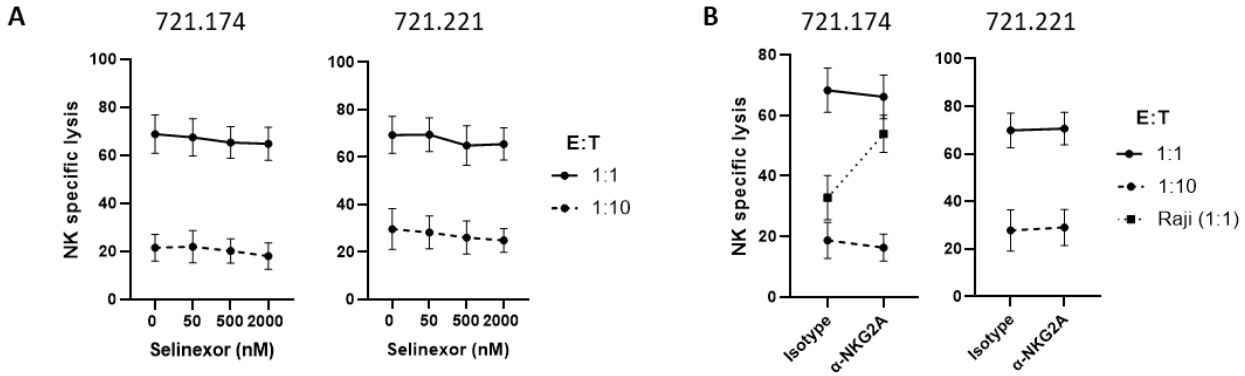


**Figure 5-19: Selinexor or anti-NKG2A mAbs do not sensitise 721 cell lines to NK cell cytotoxicity.**

(**A**) 721 cell lines were pre-treated with selinexor (50-2000 nM) for 24 hours in the presence of Q-VD followed co-culture with expanded NK cells (day 14-21, E:T = 1:1 and 1:10, N =5) for 4 hours and 721 cell death was measured using propidium iodide. (**B**) 721 cell lines and Raji were co-cultured with expanded NK cells (n=5) for 4 hours in the presence anti-NKG2A antibodies (10 µg/mL) at the E:T ratios displayed. Shown is mean ± SEM of NK specific lysis.

## 5.5 The effect of a pro-inflammatory tumour microenvironment on B-cell lymphoma cell sensitivity to expanded NK cells

### 5.5.1 IFNγ production by expanded NK cells co-cultured with selinexor-treated B-cell lymphoma cells

Tumours with high infiltration of immune cells are referred to as immunologically 'hot' tumours. Within these tumours, IFNγ is present which has pro-inflammatory properties such as skewing Th1 immunity, recruitment of DCs, priming NK cells and increasing the expression of HLA class I molecules, including HLA-E, to increase antigen presentation to T cells (535). As such, IFNγ is widely used in 2D culture models to mimic a pro-inflammatory tumour microenvironment (TME) (145,536–538).

One source of IFNγ is NK cells which upon activation increase their production of IFNγ and secrete this into the microenvironment (142). Therefore, to determine whether expanded NK cells increase IFNγ production upon encountering lymphoma cell lines pre-treated with selinexor and contribute towards inducing a pro-inflammatory TME, the abundance of IFNγ was assessed using flow cytometry and ELISA from expanded NK-cancer co-cultures. As measured by flow cytometry, IFNγ expression by expanded NK cells increased after co-culture with selinexor-treated RAJI cells (**Figure 5-20**). The dose-dependent increase in IFNγ expression was variable across donors. For ELISA experiments, an increase in IFNγ abundance was observed in 50 nM co-cultures compared to the untreated control (**Figure 5-20**). At 500 nM, the abundance of IFNγ returned to 0 nM levels for 3 out of 4 donors, with the other having a decreased quantity of IFNγ compared to the 0 nM control. As such, this suggests that there is a difference in expanded NK cell production and secretion of IFNγ, perhaps reflecting the viability of target cells in co-cultures. For example, at higher selinexor concentrations, NK-mediated lysis of cancer targets is enhanced which then may limit the stimulus required for NK cells to secrete IFNγ.

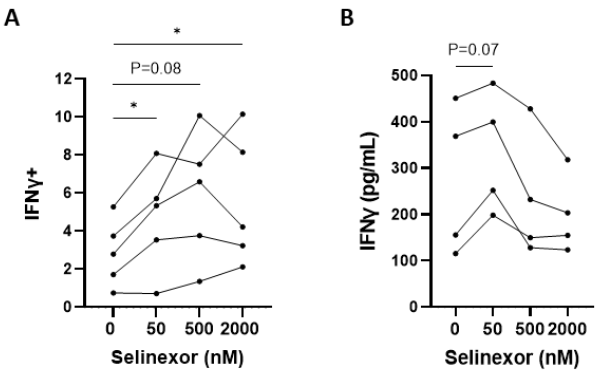


**Figure 5-20: IFNγ production and secretion by expanded NK cells co-culture with selinexor-treated B cell lymphoma cells.**

Expanded NK cells (D14-21) were co-cultured with Raji cells pre-treated with selinexor (50-2000 nM) for 4 hours at E:T = 1:1 and assessed for intracellular expression of IFNγ by flow cytometry (**A**). Shown is the percentage of CD56+CD3- NK cells positive for IFNγ with baseline IFNγ (no targets in culture) taken away from co-culture (n=5). Alternatively, NK-Raji co-cultures lasted 24 hours at E:T = 1:1 (100,000 NK: 100,000 Raji, n=4) after which supernatants were assessed for abundance of IFNγ by ELISA (**B**). For both graphs lines represent individual donor NK cells and significant differences between IFNγ expression/abundance between treatment groups and the 0 nM control were calculated with repeated-measure one-way ANOVA: *P<0.05.

### 5.5.2 A pro-inflammatory TME modelled by IFNγ induces the expression of HLA-E on B cell lymphoma cells

IFNγ is known to enhance the expression of HLA-E through the activation of STAT1 signalling (36). Upon IFNγ binding to the IFNγ receptor, JAK kinases become activated leading to the phosphorylation and dimerisation of STAT1 which induces nuclear import and activation of target genes, including HLA-E and STAT1 autoregulation (36). Interestingly, XPO1 interacts with dephosphorylated STAT1 to promote its nuclear export and therefore enable the propagation of IFNγ signalling (38). As such, selinexor may inhibit continued IFNγ signalling through nuclear retention of dephosphorylated STAT1. Therefore, it was investigated whether, firstly, IFNγ within the supernatant of expanded NK-cancer cell co-cultures can enhance HLA-E expression and secondly, whether selinexor can impair HLA-E upregulation in this setting (**Figure 5-21**). All supernatants from co-cultures greatly enhanced HLA-E surface expression (**Figure 5-22**). This increase was comparable to the increase observed using recombinant IFNγ. For HLA-A/B/C, a slight increase in surface expression was observed with co-culture supernatants and with recombinant IFNγ (**Figure 5-22**). In the presence of selinexor, HLA-E expression was downregulated in a dose-dependent manner for supernatant co-cultures and for recombinant IFNγ, HLA-E was downregulated by selinexor (**Figure 5-22**). However, selinexor did not affect total class I HLA expression on Ramos and only slightly downregulated these proteins on SUDHL6. Therefore, NK-cancer co-culture supernatants is able to enhance HLA-E expression on B-cell lymphoma cell lines and this increase is counteracted by XPO1 inhibition. Similarly, by using recombinant IFNγ HLA-E expression was increased on cell lines to a similar extent as co-culture supernatants and this increase was again impaired by selinexor.

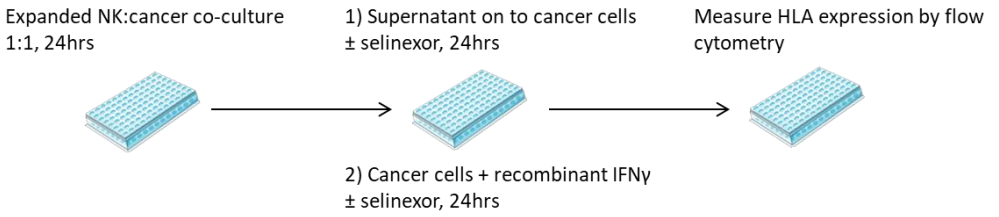


**Figure 5-21: Workflow to examine HLA expression on cancer cells that were resuspended in expanded NK:cancer cell co-culture supernatant.**

Expanded NK cells were co-cultured with B-cell lymphoma cells at an E:T = 1:1 (200,000:200,000) for 24 hours and the supernatants from these co-cultures were added to cancer cells. Selinexor (50-2000 nM) was then added to cancer cultures for an additional 24 hours. Human recombinant IFNγ (10 ng/mL) ± selinexor (500 nM) was added to cancer cells as a control for HLA expression changes.

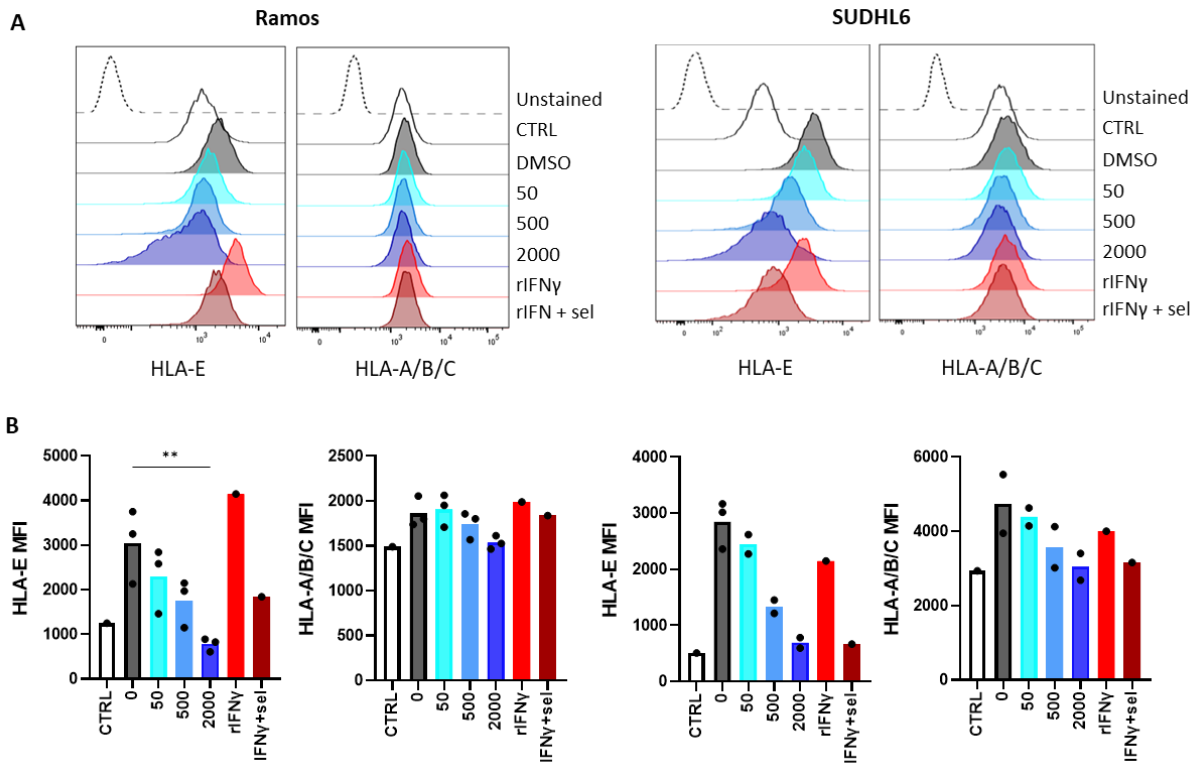


**Figure 5-22: NK-cancer cell co-culture supernatants enhance HLA-E expression, which is reversed by XPO1 inhibition.**

Expanded NK cells were co-cultured with Ramos and SUDHL6 cells at an E:T = 1:1 (200,000:200,000) for 24 hours and the supernatants from these co-cultures were used to resuspend Ramos and SUDHL6, respectively. To the resuspended Ramos and SUDHL6 cells, selinexor (50-2000 nM) was added for an additional 24 hours or DMSO as a control (0 nM). Recombinant IFNγ (10 ng/mL) ± selinexor (500 nM) was also added to cells as a control for increased HLA expression. (**A**) Representative example of HLA-E and HLA-A/B/C expression on Ramos and SUDHL6 from co-culture supernatants from one donor NK cells. Control (CTRL) represents basal expression of HLA molecules on cell lines without resuspension with co-culture supernatants or IFNγ or selinexor treatment. (**B**) Mean MFI of HLA-E and HLA-A/B/C from co-culture supernatants from 2-3 individual donor NK cells. For Ramos, significant differences in HLA expression between treatment groups were calculated using one-way ANOVA followed by Dunnett's post-hoc test: *P<0.05.

### 5.5.3 Mechanism for HLA-E downregulation with XPO1 inhibitors in the presence of IFNγ

To decipher the mechanism behind selinexor impeding IFNγ-induced HLA-E upregulation on B-cell lymphoma cell lines, western blot analysis of STAT1 phosphorylation was performed. The hypothesis was that selinexor inhibits STAT1 phosphorylation in the presence of IFNγ leading to decreased expression of HLA-E and total STAT1. Indeed, IFNγ induced STAT1 phosphorylation (pSTAT1) which correlated with increased total STAT1 (tSTAT1) and increased HLA-E expression on Raji, Ramos and SUDHL6 (**Figure 5-23**). When XPO1 function was inhibited by selinexor, pSTAT, tSTAT1 and HLA-E expression levels decreased in accordance with selinexor inhibiting IFNγ signalling by nuclear retention of STAT1 (**Figure 5-23**). Interestingly, in 721 cell lines with impaired antigen processing and presentation machinery, IFNγ signalling also increased HLA-E expression, however this did not translate into increased expression of HLA-E at the plasma membrane (**Figure 5-24**). This is because although there is increased abundance of HLA-E inside 721 cells, HLA-E fails to become stabilised and fails to exit the ER because no HLA-E binding peptides (HLA-A/B/C leader sequences) are present in 721.221 cells and because TAP deficiency in 721.174 cells results in no peptide loading on HLA-E.

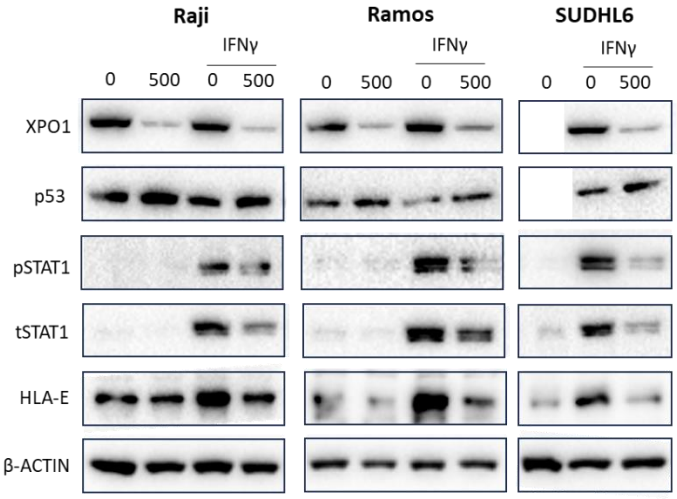


**Figure 5-23: Selinexor impairs IFNγ signalling in B-cell lymphoma cell lines.**

Raji, Ramos and SUDHL6 cell lines were incubated with IFNγ (10 ng/mL) in the absence and presence of selinexor (500 nM) or DMSO (0 nM) for 24 hours and expression of XPO1, p53, phosphorylated STAT1 (pSTAT1), total STAT1 (tSTAT1) and HLA-E were assessed by western blot. Shown is one blot from two independent experiments. The blots of XPO1 and p53 for the 0 nM sample of SUDHL6 are missing due to the limited number of wells on the gel at the time of the experiment.

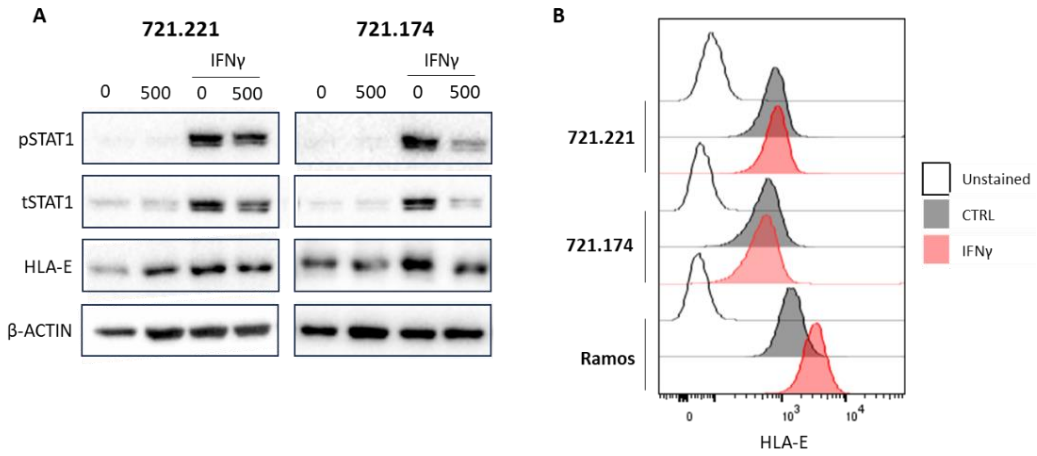


**Figure 5-24: IFNγ signalling is functional in 721 cell lines but does not induce HLA-E expression.**

(**A**) 721.221 and 721.174 cell lines were incubated with IFNγ (10 ng/mL) in the absence and presence of selinexor (500 nM) or DMSO (0 nM) for 24 hours and expression of phosphorylated STAT1 (pSTAT1), total STAT1 (tSTAT1) and HLA-E were assessed by western blot. (**B**) Surface expression of HLA-E on 721 cell lines incubated with 10 ng/mL IFNγ for 24 hours measured by flow cytometry. Ramos cells were used as a control for increased HLA-E expression with IFNγ.

Another method to compare total HLA-E and surface HLA-E expression in the presence of IFNγ and selinexor is through intracellular and surface flow cytometry staining of B-cell lymphoma cells. The advantage of this method is improved quantification of HLA-E expression compared to western blot. To measure total levels of HLA-E, B-cell lymphoma cell lines were permeabilised which allows 3D12 antibodies to stain extracellular and intracellular HLA-E. Antibody staining with whole, intact cells enables surface expression levels to be measured. As expected, in permeabilised cells HLA-E staining intensity was far greater than intact cells, illustrating that HLA-E is trapped in the ER in accordance with previous reports (9) (**Figure 5-25**). This was not the case with the W6/32 antibody which showed similar staining intensity in permeabilised and intact cells, showing that HLA-A/B/C-binding peptides are in abundance to stabilise and export HLA-A/B/C proteins to the plasma membrane (**Figure 5-25**). Of note, in 721.221 which are knock-out for HLA-A/B/C, HLA-E expression in permeabilised cells was higher than Ramos, but at the surface Ramos had higher HLA-E expression (**Figure 5-26**). This confirms that the majority of HLA-E in 721.221 cannot escape the ER because of the absence of leader peptides from HLA-A/B/C proteins, whereas some HLA-E molecules in Ramos can translocate from the ER to the plasma membrane.

Incubating cell lines with IFNγ ± selinexor, IFNγ alone enhanced 3D12 staining intensity in permeabilised and intact cells and XPO1 inhibition decreased HLA-E expression in both staining conditions (**Figure 5-25**). Employing this method to cell lines without incubation with IFNγ showed that only surface HLA-E expression was downregulated by selinexor, which co-insides with results in

chapter 3 where, at steady state, XPO1 inhibition affected surface HLA-E expression due to reduced availability of peptides to stabilise HLA-E and enable ER exit. In the case of IFNγ, selinexor inhibits HLA-E transcription through STAT1 nuclear accumulation alongside reducing the peptide pool to impede HLA-E transport to the plasma membrane, acting via two mechanisms to downregulate surface HLA-E expression. For W6/32 staining intensity, with IFNγ this increased in permeabilised and intact cells (**Figure 5-25**). Interestingly, however, selinexor did not decrease W6/32 staining intensity in the presence of IFNγ. As such, in a pro-inflammatory TME with high levels of IFNγ, selinexor can disrupt HLA-E expression but high classical class I HLA protein expression is maintained.

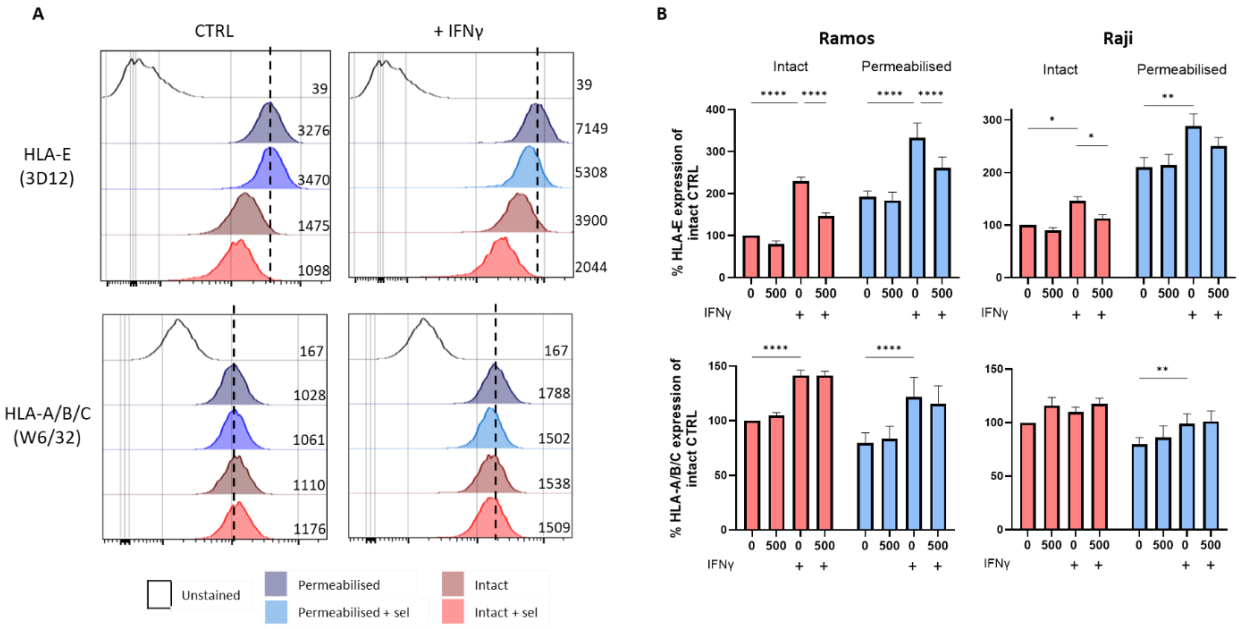


**Figure 5-25: Selinexor impairs total HLA-E expression in the presence of IFNγ.**

Raji and Ramos cells were treated with selinexor (sel, 500 nM) or DMSO (0 nM) for 24 hours in the presence or absence of IFNγ (10 ng/mL) followed by staining with antibodies against HLA-E (clone 3D12) and HLA-A/B/C (clone W6/32) when cells were permeabilised (intracellular and extracellular expression) or left intact (surface expression). (**A**) Representative histograms of 3D12 and W6/32 staining intensities of Ramos cells from one experiment. Numbers on histograms depict the MFI and vertical dashed lines represent the histogram peak in the permeabilised, untreated sample. (**B**) Mean expression ± SEM relative to the DMSO-treated (0 nM) control in the absence of IFNγ in intact and permeabilised Ramos (n=6) and Raji cells (n=5). Significant differences in HLA expression between treatment groups for intact and permeabilised cells were calculated with two-way ANOVA followed by Tukey's post-hoc test: ****P<0.001, **P<0.01, *P<0.05.

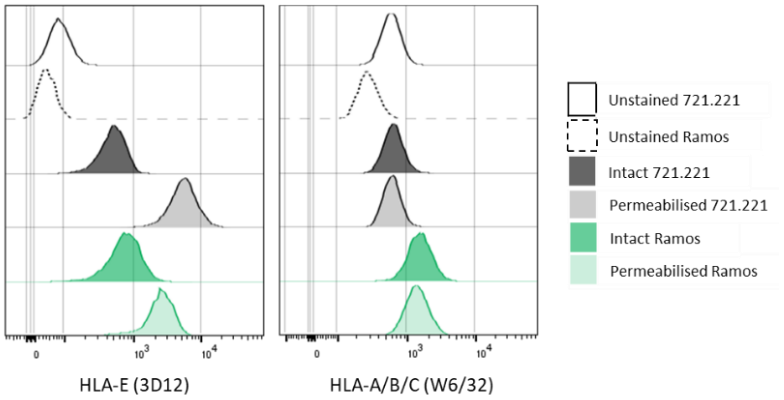


**Figure 5-26: HLA-E is trapped internally in 721.221 cells.**

Flow cytometry histograms of 721.221 and Ramos cells when stained with antibodies against HLA-E (clone 3D12) and HLA-A/B/C (clone W6/32) in permeabilisation (intracellular and extracellular expression) and 'intact' (surface expression) conditions.

### 5.5.4 IFNγ protects B cell lymphoma cells from NK cell anti-tumour functions via HLA-E:NKG2A interactions that is overcome by XPO1 inhibition

With NK cell adoptive transfer in patients with 'hot' tumours, allogeneic NK cells will transit to the TME where they will encounter tumour cells submersed in an environment with high levels of IFNγ and therefore high HLA-E expression. Equally, in 'cold' tumours allogeneic NK cells upon activation will secrete IFNγ which will promote HLA-E expression on tumours, initiating a feedback loop to dampen NK cell-mediated immunity via NKG2A. In the previous sections, it was shown that NK-cancer co-culture supernatants and recombinant IFNγ increase HLA-E expression which selinexor was able to counteract. As such, whether these have functional consequences on allogeneic NK cell function was investigated. B-cell lymphoma cell lines were treated with selinexor in the presence of recombinant IFNγ for 24 hours followed by co-culture with expanded, allogeneic NK cells ± anti-NKG2A monoclonal antibodies. Across all cell lines (Ramos, Raji and SUDHL6) IFNγ protected cancer cells from NK cytotoxicity (**Figure 5-27**). For Raji and Ramos, blocking NKG2A fully restored NK cytotoxicity, demonstrating that the increase in HLA-E by IFNγ protects lymphoma cell lines from NK. For SUDHL6, NKG2A blockade only partially restored NK cytotoxicity, most likely due to the large increase in classical HLA class I proteins when incubated with IFNγ as shown in **Figure 5-22**. When lymphoma cells were treated with selinexor, NK cytotoxicity was also completely restored for Ramos and Raji cells and only partially restored for SUDHL6 (**Figure 5-27**). Again, this demonstrates that the IFNγ-induced HLA-E upregulation protects lymphoma cells from NK cytotoxicity which can be reversed through selinexor-induced HLA-E downregulation. There was no clear benefit of combining selinexor with NKG2A blockade, besides for Raji at an E:T of 1:10, because NKG2A receptor signalling

was blocked by either HLA-E downregulation on tumour cells or by inhibiting NKG2A:HLA-E interaction with monoclonal antibodies (**Figure 5-27**). Together, these data demonstrate that IFNγ protects B-cell lymphoma cells from NK cytotoxicity via upregulation of HLA-E. This protection can be reversed through the use of antibodies against NKG2A or by using XPO1 inhibitors to inhibit NKG2A:HLA-E interactions.

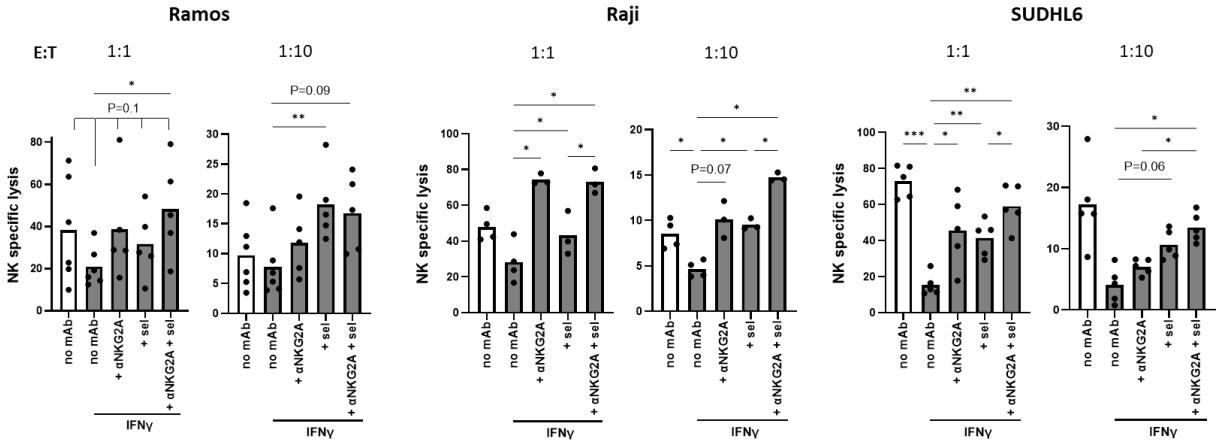


**Figure 5-27: IFNγ protects B-cell lymphoma cells from expanded NK cell lysis via HLA-E:NKG2A interactions.**

Ramos, Raji and SUDHL6 cells were treated with 500 nM selinexor in the presence of IFNγ (10 ng/mL) for 24 hours and co-cultured with expanded NK cells (day 14-21) ± anti-NKG2A monoclonal antibodies (Z199, 10 µg/mL) for a further 24 hours at an E:T ratio of 1:1 or 1:10. Propidium iodide was used to measure cancer-specific cell death in co-cultures by flow cytometry. Shown is mean NK specific lysis of target cells with dots representing individual donor NK cells (at least 3 individual donors). Significant differences in NK specific lysis between treatment groups was calculated by repeated-measure/mixed effects one-way ANOVA depending on whether groups contained equal numbers of donors, followed by Tukey's post-hoc test: ***P<0.005, **P<0.01, *P<0.05.

To demonstrate that IFNγ-induced HLA-E upregulation was responsible for producing protective effects in B-cell cell lines, LAMP experiments were performed to compare the activation of NKG2A+ and NKG2A- NK cells expanded over 5 days. Day 5 expanded NK cells were used to ensure that NKG2A- NK cells remained in the expanded NK cell population (**Figure 5-6**). The degranulation ability and the production of IFNγ was diminished in the NKG2A+ NK cell population and not the NKG2A- NK cell population when day 5 expanded NK cells were co-cultured with Raji cells that were pre-incubated with IFNγ (**Figure 5-28**). Selinexor treatment in the presence of IFNγ rescued NKG2A+ NK cell activation whilst no change in the activation of NKG2A- NK cells was observed (**Figure 5-28**).

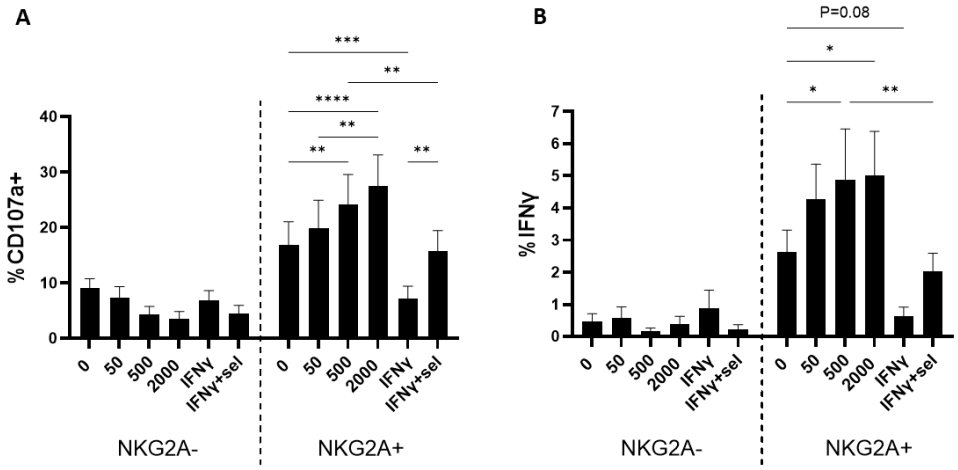


**Figure 5-28: IFNγ impairs NKG2A+ NK cell activation, which is overcome by XPO1 inhibition.**

Raji cells were treated with selinexor (0-2000 nM) in the presence and absence of recombinant IFNγ (10 ng/mL, sel = 500 nM) for 24 hours before co-culture with day 5, IL-2 (500 IU/mL) expanded NK cells for 4 hours. Degranulation (**A**) as measured by CD107a positivity and IFNγ production (**B**) was measured on NKG2A+ and NKG2A- NK cells (CD56+CD3-) by flow cytometry. Shown is mean ± SEM of CD107+ and IFNγ+ cells accounting for background activation in no target cultures (n=6 individual NK cell donors). Significant differences in activation between treatments groups were calculated using repeated measure one-way ANOVA followed by Tukey's post-hoc test: ****P<0.001, ***P<0.005, **P<0.01, *P<0.05.

To further support that IFNγ-induced HLA-E upregulation protect malignant B cells from NK cytotoxicity, 721.221 and 721.174 cells with functional IFNγ signalling but impaired HLA-E upregulation (**Figure 5-24**) were assessed for sensitivity to NK specific lysis. Indeed, IFNγ did not protect 721 cell lines from expanded NK cytotoxicity, illustrating that functional antigen processing and presentation machinery, including HLA-E expression, is required for IFNγ-induced protection from NK cells (**Figure 5-29**).

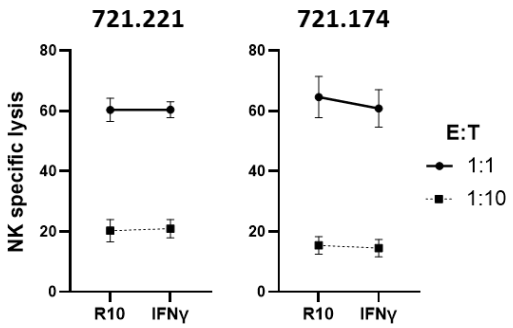


**Figure 5-29: IFNγ does not protect 721 cell lines from expanded NK cell cytotoxicity.**

721.221 and 721.174 cells were incubated with IFNγ (10 ng/mL) for 24 hours followed by co-culture with expanded NK cells (day 14-21) for an additional 4 hours at an E:T ratio of 1:1 or 1:10. Propidium iodide was used to measure 721-specific cell death in co-cultures by flow cytometry. Shown is mean ± SEM using expanded NK cells from 5 individual donors.

## 5.6 Investigating selinexor-expanded NK cell treatment approaches for future *in vivo* studies

As currently demonstrated in this chapter, XPO1 inhibition with selinexor sensitises B-cell lymphoma cells to NK specific lysis via disruption of the NKG2A:HLA-E inhibitory axis. The question remains of how to administer both treatments in patients, either sequentially or concurrently. In previous experiments sequential administration was mimicked such that cells were treated with selinexor first and then expanded NK cells were co-cultured with cancer cells. Concurrent administration entails the administration of both treatments at the same time and the applicability of this approach was explored next. Lymphoma cells were either co-cultured with expanded NK cells in the presence of selinexor (concurrent treatment, 24h sel co-culture), pre-treated for 24 hours with selinexor and co-cultured with expanded NK cells in the absence of XPO1 inhibition (sequential, 24h PT), or pre-treated with selinexor for 24 hours and co-cultured with NK cells in the presence of selinexor (sequential combined with concurrent, 24h PT + 24h sel co-culture). Differences in NK cytotoxicity were then compared between treatment approaches at each selinexor concentration. Firstly, concurrent treatment resulted in a slight decrease in NK cytotoxicity at high selinexor concentrations when compared to the untreated control (**Figure 5-30**). When this method was compared to the sequential approach, NK cytotoxicity was much lower in the concurrent samples at high selinexor concentrations. When the two administration methods were combined into a sequential + concurrent approach resembling scenarios where selinexor would be given followed by adoptive transfer of NK cells with further selinexor doses, NK cytotoxicity was only slightly impaired compared

to the sequential approach (**Figure 5-30**). When selinexor was added to co-cultures, NK cell viability decreased, highlighting the indiscriminatory toxic effect of XPO1 inhibition (**Figure 5-30**). Interestingly, although not significant, sequential + concurrent treatment induced higher NK cell death than concurrent treatment which perhaps reflects combined activation-induced cell death and selinexor-induced cell death which correlates with increased NK specific lysis of lymphoma cells in the sequential + concurrent treatment groups. Ultimately, this experiment illustrates that to maximise adoptive NK cell transfer approaches with selinexor, a sequential approach may be required to avoid allogeneic NK cell death and to allow the prior sensitisation of lymphoma cells to NK cells via HLA-E downregulation.

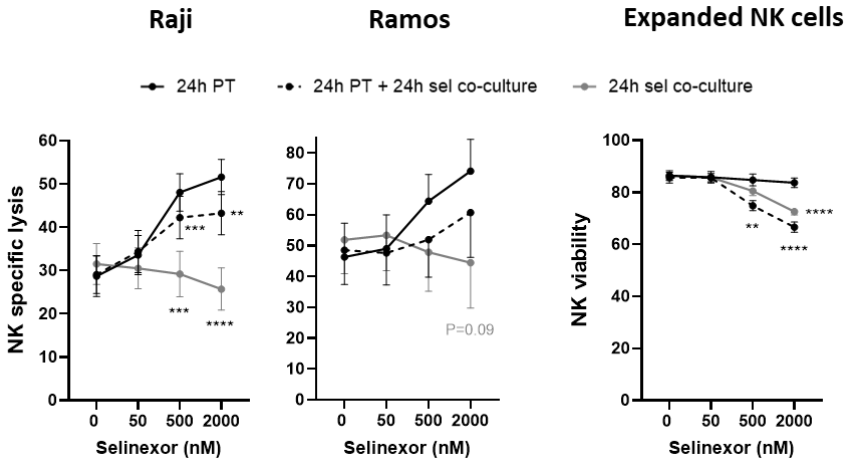


**Figure 5-30: Sequential vs concurrent selinexor-expanded NK cell treatments *in vitro*.**

CellTrace-labelled Raji and Ramos cells were pre-treated (PT) with selinexor (50-2000 nM) for 24 hours in the presence of Q-VD followed by co-culture with expanded NK cells for an additional 24 hours at an E:T = 1:1. During the co-culture selinexor was added to co-cultures to the corresponding pre-treated concentrations (24h PT + 24h sel co-culture), or DMSO was added (24h PT) or lymphoma cells not pre-treated with selinexor were co-cultured with expanded NK cells in the presence of selinexor (50-2000 nM, 24h sel co-culture). After the co-culture, propidium iodide was added to enable calculation of NK specific lysis of cancer targets (left and middle) and to allow NK viability to be measured (right). Shown is mean NK specific lysis and NK viability ± SEM using expanded NK cells from individual donor (Raji N = 6, Ramos N = 4, NK viability = 6). Significant differences in NK specific lysis and NK viability between the three administration methods for each selinexor concentration were calculated using repeated-measure two-way ANOVA followed by Dunnett's post-hoc test: ****P<0.001, ***P<0.005, **P<0.01.

Nod-SCID-gamma chain deficient (NSG) mice are frequently used to study the function of human NK cells and Stadel et al., (2022) employed the NSG model to investigate selinexor combined with CAR T cell therapy against Raji cells as used throughout this thesis. As portrayed in section 5.2, B-cell lymphoma cell lines were not sensitised by selinexor to NK cell lines NK-92 and NKL cells, therefore a primary NK cell adoptive transfer technique is required. Before *in vivo* experiments can be performed, a selinexor toxicity test was performed in NSG mice. NSG mice were administered a moderate selinexor dose (10 mg/kg) which was administered by oral gavage twice a week for two weeks in line with clinical practises (525). As a means to measure drug toxicity, mice were weighed every two to three days with a terminal endpoint of 15% weight loss of the original weight before the first selinexor dose. Both mice treated with selinexor lost weight after each dose of selinexor (**Figure 5-31**). After the third dose on day 7, one selinexor-treated mouse lost 14% of its original weight after two days, at which point mice were weight every day (**Figure 5-31**). However, during the course of the experiment until day 16 that mouse recovered to its original weight. Vehicle-treated mice were unaffected by the oral gavage procedure and maintained the same weight throughout the experiment, highlighting that the weight loss observed in the selinexor-treated mice was due to the activity of the compound inhibiting XPO1 function, demonstrating the correct preparation of the drug and weight loss is known to occur in mice treated with selinexor (407,525).

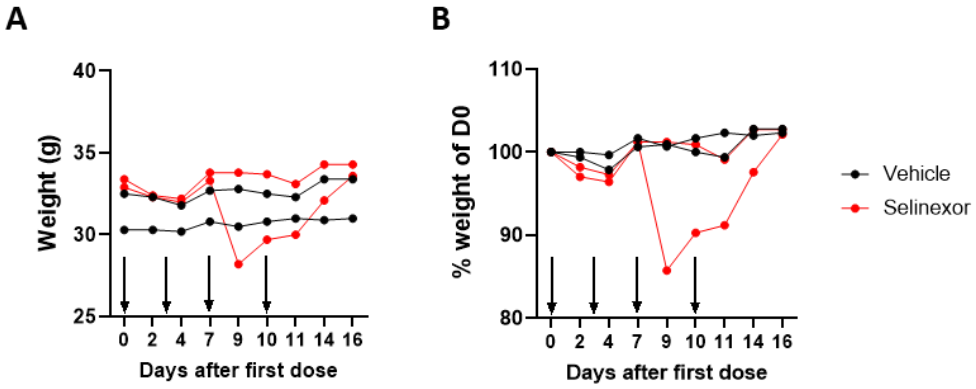


**Figure 5-31: Toxicity of twice weekly selinexor in NSG mice administered for two weeks.**

NSG mice were administered 10 mg/kg of selinexor (n=2) or vehicle control (0.6% Plasdone PVP K-29/32 and 0.6% Poloxamer Pluronic F-68 in water, n=2) by oral gavage twice a week for two weeks as demonstrated by the arrows on the X-axis. Shown is raw weight (**A**) and relative weight to the weight at day 0 before the first dose (**B**) over time for 16 days. Every day fresh food pellets were soaked in water and provided in cages to aid food intake.

Finally, to time selinexor administration and the adoptive transfer of expanding NK cells (day 14-21 of expansion) to measure tumour control, information on the growth kinetics of B-cell lymphoma cell lines in NSG mice are required. Raji cells were used as the model cell line because of the promising *in vitro* data on sequential vs concurrent selinexor treatment (**Figure 5-30**) and for its well characterised *in vivo* use, particularly with selinexor (460). After subcutaneous injection of Raji into NSG mice, it took 14 days before tumours became apparent (**Figure 5-32**). Once visible, tumours grew quickly, reaching the terminal endpoint after 9 days. Tumour growth in both mice mirrored each other, highlighting that Raji growth kinetics are comparable between mice. In conclusion, the Raji growth kinetics, selinexor toxicity/dosing schedule and two-week NK cell expansion accurately align to enable an *in vivo* experiment to be performed in the future.

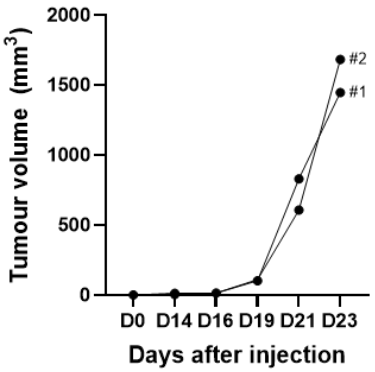


**Figure 5-32: Raji tumour growth kinetics in NSG mice.**

Two NSG mice were injected subcutaneously with $5x10^6$ Raji cells in 100 µL. Tumour size was measured over time and the volume was calculated as 0.5*width*length*length. The terminal endpoint was set at a tumour diameter of 12 mm or tumour volume of 1500 $mm^3$, whichever came first. Shown is tumour volume ($mm^3$) of each mouse over the course of 23 days.

## 5.7 Examining CAR NK cell function against selinexor-treated B-cell lymphoma cells

### 5.7.1 Generation of anti-CD19 CAR NK cells

Besides adoptive transfer of expanded, allogeneic NK cells into B-cell lymphoma and CLL patients, primary, allogeneic NK cells modified with a CAR construct targeting a tumour antigen can be used to promote the efficacy of adoptive transfer therapy approaches. Targeting the CD19 receptor on malignant B cells is a promising strategy because of the high expression of CD19 on B cells. Indeed, anti-CD19 CAR T cell therapy is approved by NICE for the treatment of B cell malignancies (539).

Additionally, due to their improved safety profile, anti-CD19 CAR NK cells are undergoing clinical investigation in B cell malignancies, which have demonstrated encouraging survival data and excellent safety profiles (305). Combinations of CAR T cells with other drugs is an area of intense research (367) and whether CAR NK cell approaches can be improved through combinations with anti-cancer therapies including small molecules and monoclonal antibodies will be deduced over time. As a proof-of-concept, it was investigated here whether XPO1 inhibition with selinexor can enhance anti-CD19 CAR NK cell function *in vitro,* as shown for expanded NK cells.

First, to generate anti-CD19 CAR NK cells from primary NK cells, the FMC63-41BB-CD3ζ second generation CAR construct encoding the small chain variable fragment of the anti-CD19 antibody clone FMC63 attached to the CD8 transmembrane domain and intracellular activation domains 4-1BB and CD3ζ was transfected into the packaging cell line 293FT together with the third-generation lentiviral packaging system (pMDLg/pRRE, RSV-rev and VSV-G). CAR constructs using the FMC63 mouse antibody clone are used in the manufacture of CAR T cells in the clinic (361) and the FMC63 CAR and VSV-G lentiviruses have been used for the generation of CAR NK cells (540–542). The concentration of plasmids used to transfect 293FT cells is found in chapter 2 (**Table 2-1**). Whilst 293FT cells produced lentivirus vectors carrying the FMC63-41BB-CD3ζ construct, NK cells were isolated from healthy donor PBMC and expanded for 2-4 days before being transduced for 24 hours with fresh, filtered 293FT supernatant containing lentiviruses in the presence of the transduction enhancer Vecotfusin-1 (Miltenyi). NK cells were then washed to remove Vectofusin-1 and 72 hours after transduction CAR NK cell transduction efficacy and cytotoxicity was assessed (**Figure 5-33**).

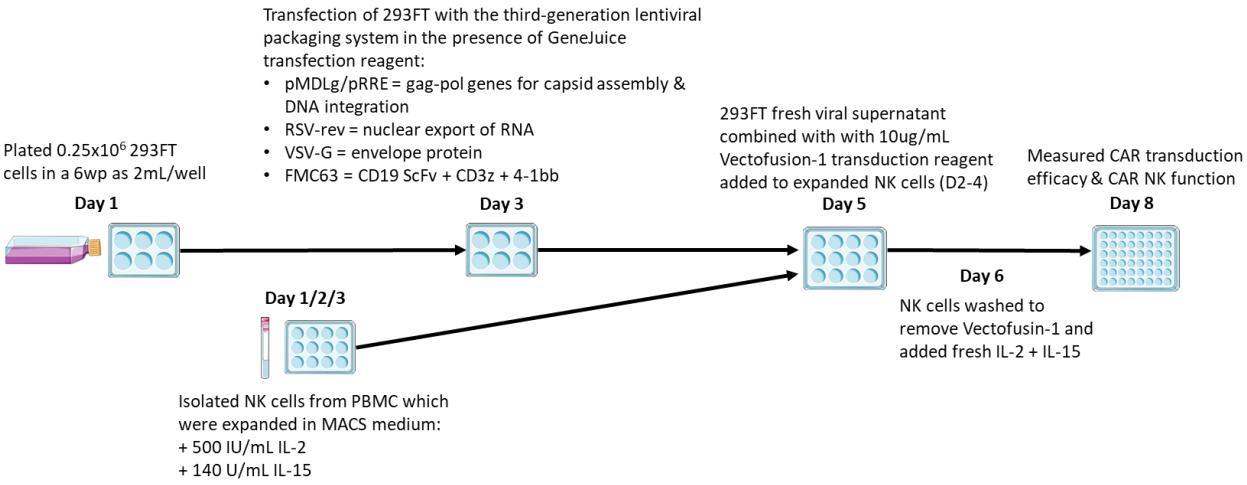


**Figure 5-33: Generation of anti-CD19 CAR NK cells using lentivirus transduction.**

Lentivirus vectors containing the FMC63-41BB-CD3ζ construct were produced in 293FT cells in antibiotic-free medium using the transfection reagent GeneJuice (1:20 dilution). The constructs used to generate lentivirus were pMDLg/pRRE, RSV-rev and VDV-G and the concentrations of which can be found in results section X. 48 hours after transfection, fresh, filtered 293FT supernatants containing lentiviruses were put on expanded NK cells (day 2-4) along with the transduction reagent Vectofusin-1 (10 µg/mL) for 24 hours in a 48 or 96 well plate format depending on the number of NK cells being transduced. After, NK cells were washed to remove Vectofusin-1 by removal of ~90% of the medium and fresh medium was added containing 500 IU/mL IL-2 and 140 U/mL IL-15. 48 hours later CAR transduction efficacy was measured by flow cytometry using recombinant CD19-FITC and CAR NK cell function was assessed against CD19+ B-cell lymphoma cell lines. Untransduced NK cells were produced following the same protocol using supernatant from 293FT cells that were not transfected with DNA constructs.

To optimise the number of NK cells required for transduction, NK cell numbers ranging from 25,000 to 1x10$^6$ NK cells were transduced with lentivirus vectors. 25,000-0.4x10$^6$ NK cells were transduced in 96 well plates while >0.4x10$^6$ NK cells were transduced in 24 well plates. As assessed with the FITC-labelled recombinant CD19 protein using flow cytometry, the lower the number of NK cells transduced the greater the transduction efficacy (**Figure 5-34**).

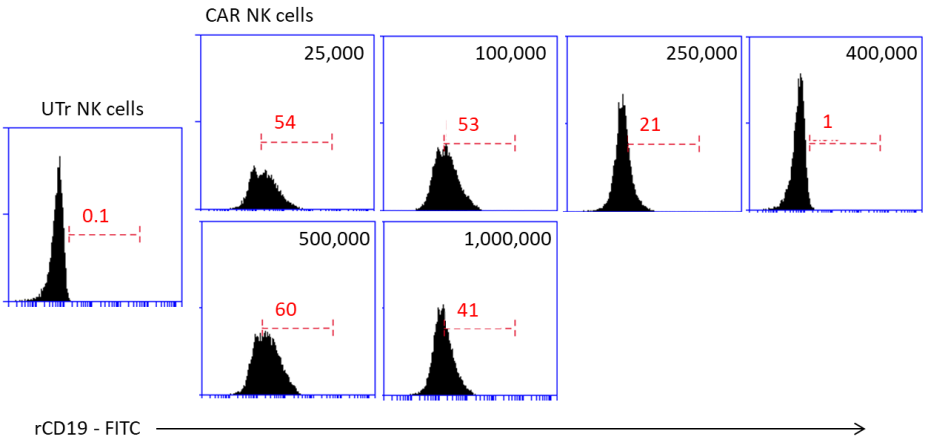


**Figure 5-34: Optimisation of NK cell numbers required for transduction.**

25,000-1x10$^6$ NK cells expanded over 3 days were transduced for 24 hours with second generation FMC63 CAR constructs using lentiviral transduction. NK numbers >0.4x10$^6$ were transduced in 24 well plates (bottom) and <0.4x10$^6$ were transduced in 96 well plates (top). Shown is CAR expression histograms after staining with FITC-labelled recombinant CD19 (rCD19). Black numbers on plots represent the number of NK cells used for transduction and the red numbers show the proportion of CAR+ NK cells. The gate was drawn based on the untransduced (UTr) control.

Next, it was determined how stable the CAR construct was on NK cells which is important for using these in functional assays and for *in vivo* experiments. After generating CAR NK cells with high transduction efficacy (61% positive on day 3 post transduction), the CAR construct was lost when cells were stained on day 7 post transduction (**Figure 5-35**). In CAR NK cells with low transduction efficacy (8-12% positive on day 3 post transduction), on day 5 the CAR construct was lost (**Figure 5-35**). Therefore, CAR NK cells at day 3 post transduction were used in functional assays. As such, the maximum number of 1x10$^6$ NK cells was used for transduction to ensure sufficient numbers of CAR NK cells for functional analysis. To measure CAR expression across multiple donors using 1x10$^6$ NK cells for transduction, twelve healthy donor NK cells were transduced and CAR expression was measured with FITC-labelled recombinant CD19 on day 3 post transduction. All donors were transduced successfully with mean CAR expression 21.2% (range 3% - 61.9%) (**Figure 5-36**).

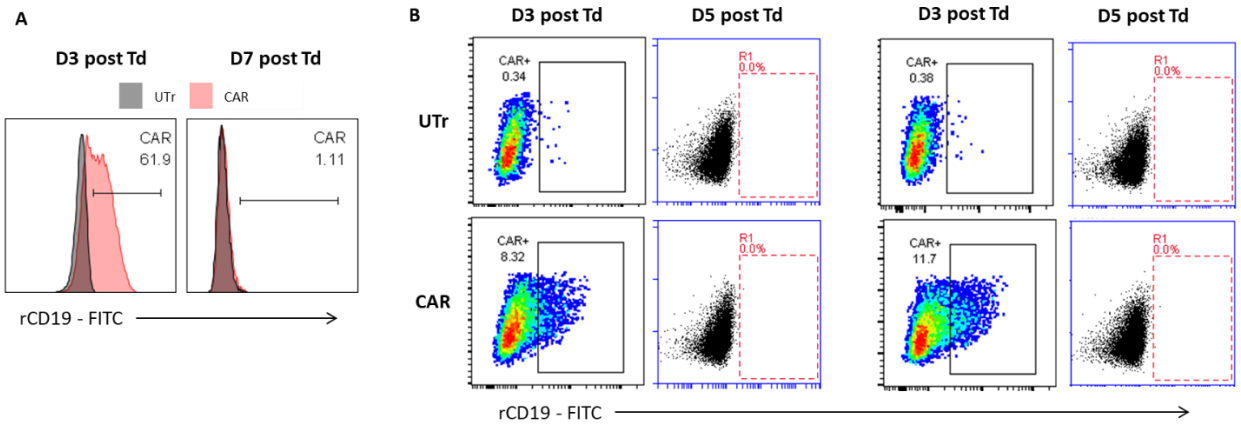


**Figure 5-35: Anti-CD19 CAR expression is unstable on NK cells.**

CAR NK cells were generated with high transduction (Td) efficacy as previously described and stained with FITC-labelled recombinant CD19 (rCD19) on day 3 (D3) and day 7 (D7) post Td (**A**). Shown are histograms of untransduced (UTr) and CAR NK cells at D3 and D7, and the horizontal gate was drawn based on the UTr control, with the numbers on plots representing the percentage positive for CAR. Two more donors with low Td efficacy were stained with rCD19 on D3 and D5 (**B**). Shown are dot plots and dots within gates are positive for CAR expression with the number representing the proportion of cells. The gates were drawn based on the UTr control for each donor.

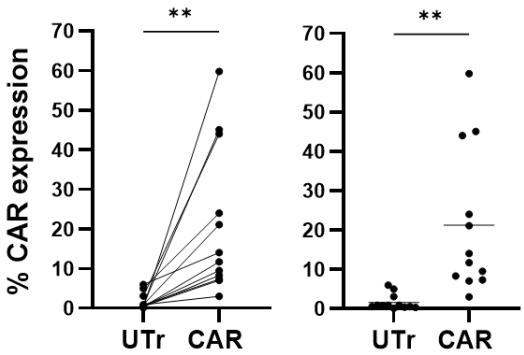


**Figure 5-36: Anti-CD19 CAR transduction efficacy in primary NK cells.**

1x10$^6$ primary NK cells from isolated from PBMC and expanded for 2-4 days were transduced with supernatants from 293FT cells transfected with lentivirus plasmid constructs and the FMC63-41BB-CD3ζ CAR construct. Untransduced NK cells (UTr) were plated in supernatants from 293FT cells that were not transfected with plasmids. On day 3 post transduction, cells were stained with FITC-labelled recombinant CD19 to assess CAR transduction efficacy by flow cytometry. Shown is percentage of CAR positive NK cells of 12 individual donors with each line representing matched donor transduction efficacy (left) and on the right is portrayed the mean transduction efficacy across samples. The difference in CAR expression between untransduced and transduced NK cells was calculated with paired-sample t-test: **P<0.01.

### 5.7.2 Selinexor promotes anti-CD19 CAR NK cell function

NK cells were successfully transduced to express the anti-CD19 CAR construct, but whether the CAR was functional on NK cells was assessed here. To determine whether the CAR construct promoted NK cell cytotoxicity CAR NK cells were co-cultured with CD19+ Raji cells and NK specific lysis was compared to the untransduced control (UTr). Raji cells were chosen as targets for their high expression of CD19 compared to other cell lines (543). The E:T ratio between UTr NK-Raji and CAR NK-Raji co-cultures was kept the same to avoid bias in lysis data because UTr NK cells, as shown in previous chapters, possess cytotoxic capabilities, for example if UTr co-cultures contained more NK cells compared to CAR co-cultures then information on CAR activity would be lost. This is also true for CAR co-cultures containing more NK cells than UTr co-cultures, because in this setting the increased lysis of targets could be either due to CAR expression or more total NK cells in co-cultures. When CAR NK cells and UTr NK cells were co-cultured with Raji at an E:T of 1:3, the proportion of lysed Raji cells within CAR NK co-cultures was greater than that of UTr co-cultures which demonstrates functional CAR expression on NK cells to promote NK cytotoxicity (**Figure 5-37**).

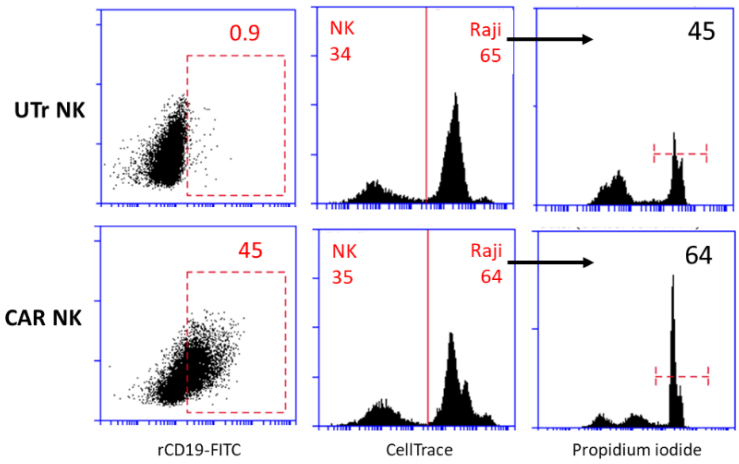


**Figure 5-37: XPO1 inhibition promotes anti-CD19 CAR NK cell cytotoxicity.**

Representative example of anti-CD19 CAR NK cell cytotoxicity against CD19+ Raji cells. Untransduced NK cells (UTr NK) and anti-CD19 CAR NK cells were co-cultured with CellTrace-labelled Raji cells at the same E:T ratio (~1:3) for 4 hours after which cancer cell death was measured via propidium iodide staining. Numbers on plots represent the percentage of cells within gates.

Next, it was investigated whether anti-CD19 CAR NK cell cytotoxicity could be enhanced by selinexor pre-treatment of B-cell lymphoma cells via downregulation of HLA-E. In experiments with expanded NK cells, NK cells were expanded for 14-21 days at which point NKG2A expression was expressed highly on all NK cells. Because CAR NK cells had to be used in functional assays on day 3 post transduction, corresponding to day 5-7 of NK cell expansion, not all NK cells, and therefore not all CAR NK cells, will expression NKG2A. When CAR NK cells were stained with FITC-labelled rCD19 and anti-NKG2A antibodies, the anti-CD19 CAR was expressed on NKG2A+ and NKG2A- NK cells, but crucially a subset of NKG2A+ NK cells expressed the CAR construct (**Figure 5-38**). Considering this, selinexor-treated Raji cells were co-cultured with anti-CD19 CAR NK cells for 4 hours and NK specific lysis was measured. For all seven donors, CAR expression enhanced NK cell function compared to the UTr controls (**Figure 5-39**). With XPO1 inhibition, CAR NK cell cytotoxicity was enhanced in a dose-dependent manner and anti-NKG2A blocking antibodies also enhanced CAR NK cell cytotoxicity (**Figure 5-39**). This demonstrates that the inhibitory NKG2A:HLA-E axis can be disrupted to promote CAR NK cell function.

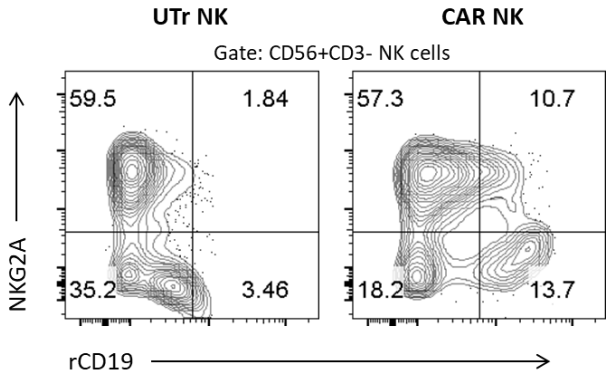


**Figure 5-38: CAR expression on NKG2A+ and NKG2A- NK cells.**

Anti-CD19 CAR NK cells and untransduced (UTr) NK cells 3 days post transduction were stained with FITC-labelled recombinant (rCD19) and anti-NKG2A antibodies. Shown are flow cytometry plots of CD56+CD3- NK cells from one donor demonstrating CAR expression on NKG2A+ and NKG2A- NK cell populations. Numbers on plots demonstrate the percentage of cells within quadrant gates.

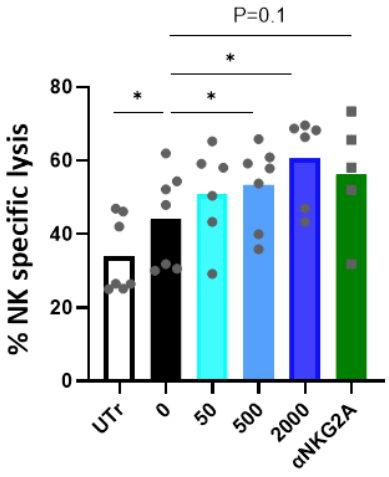


**Figure 5-39: Selinexor and anti-NKG2A mAbs promote anti-CD19 CAR NK cell cytotoxicity.**

CellTrace-labelled Raji cells were treated with selinexor (50-2000 nM) or DMSO control (0 nM) for 24 hours in the presence of Q-VD (30 µM) after which they were co-cultured with untransduced (UTr) or anti-CD19 CAR NK cells at an E:T = 1:1 for 4 hours in the presence or absence of anti-NKG2A antibodies (Z199, 10 µg/mL). Propidium iodide was used to measure Raji cell death in co-cultures and NK specific lysis was calculated taking into account drug-induced cell death. Each dot represents an individual donor NK cells (N of at least 5) and shown is the mean NK specific lysis of each group with significant differences in the mean of each group compared to the 0 nM CAR NK cell group were calculated with one-ANOVA followed by Tukey's post-hoc test: *P<0.05.

The mean increase in NK specific lysis of CAR NK cells between 0 nM and 500 nM co-cultures was 9%, whereas for expanded NK cells in **Figure 5-10** was 18%. This may reflect CD19 expression on tumour targets treated with selinexor, as such CD19 expression was measured on tumour cells post-selinexor treatment. For Raji and Ramos cells, CD19 expression decreased with 500 nM selinexor and at different concentrations of selinexor CD19 expression on primary CLL cells decreased compared to the untreated control (**Figure 5-40**).

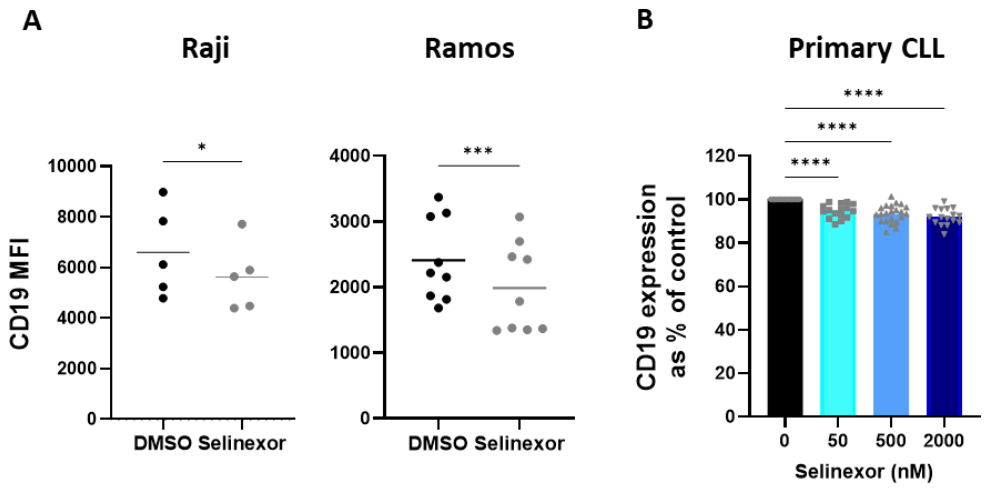


**Figure 5-40: Selinexor downregulates CD19 surface expression.**

Raji and Ramos cells were treated with 500 nM selinexor for 24 hours and CD19 surface expression was assessed by flow cytometry. Shown is MFI of cell lines with each point representing an individual treatment across 3 independent experiments and differences in CD19 MFI means were calculated with paired sample t-test: ***P<0.005, *P<0.05 (**A**). Primary CLL PBMC were treated with selinexor (50-2000 nM) for 24 hours and CD19 expression was assessed on CD19+CD5+ CLL cells by flow cytometry. Shown is mean expression relative to the untreated control of 23 individual CLL patients and significant differences in CD19 expression of treatment groups compared to the 0 nM control were calculated with one-way ANOVA followed by Dunnett's post-hoc test: ****P<0.001.

As shown previously, IFNγ protected B-cell lymphoma cells from expanded NK cells (**Figure 5-27** and **Figure 5-28**). Whether this occurred with anti-CD19 CAR NK cells was investigated. In the presence of IFNγ, CAR NK cytotoxicity was greatly impaired (reduction of 14%), reducing levels of killing to that comparable to the UTr control (Mean NK specific lysis of UTr = 18% and CAR = 19%) (**Figure 5-41**). Selinexor treatment of Raji recovered NK specific lysis of CAR NK cells back to levels observed for the untreated control and interestingly, although slight, selinexor regained the enhanced NK cytotoxicity of CAR NK cells compared to UTr NK cells (difference of 4.5%, without IFNγ difference = 10%) (**Figure 5-41**). This experiment therefore demonstrates that IFNγ is able to protect B-cell lymphoma cells from CAR NK cell cytotoxicity and XPO1 inhibition is able to overcome this.

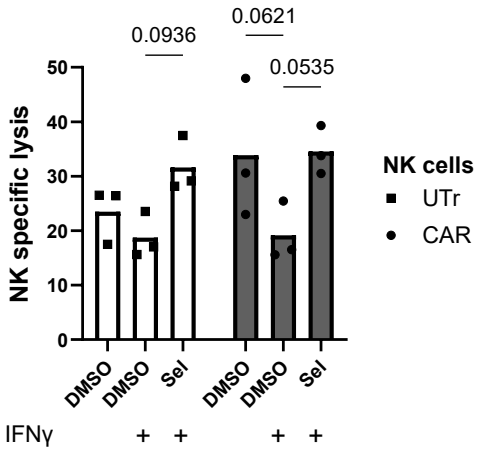


**Figure 5-41: IFNγ protects Raji cells from anti-CD19 CAR NK cell cytotoxicity, which is reversed by selinexor.**

Raji cells were treated with selinexor (500 nM, sel) in the presence of IFNγ (10 ng/mL) for 24 hours after which Raji was co-cultured with untransduced (UTr) or anti-CD19 CAR NK cells (CAR) for 4 hours at an E:T = 1:1. Propidium iodide was used to identify lysed Raji cells in co-cultures and NK specific lysis was calculated. Shown is the mean NK specific lysis of 3 donors and significant differences in NK specific lysis between treatment groups and NK cells were calculated using repeated-measure two-way ANOVA followed by Tukey's post-hoc test.

Finally, because IFNγ decreased CAR NK cell cytotoxicity, the contribution of NKG2A to impair CAR NK cell activation was assessed with the LAMP assay. As expected, CAR NK cells are generally more activated than UTr NK cells across all conditions (**Figure 5-42A**). IFNγ greatly reduced the degranulation of NKG2A+ NK cell populations and selinexor was able to recover NKG2A+ NK cell activation (**Figure 5-42A**). In the absence of IFNγ, increased NKG2A+ NK cell activation was observed within both UTr and CAR NK cell populations with increased selinexor concentration (**Figure 5-42** and **Figure 5-42A**) in accordance with enhanced CAR NK cytotoxicity reported in **Figure 5-39**. Next the contribution of NKG2A signalling in CAR+ NK cells to increase NK activation with selinexor in the absence and presence of IFNγ was investigated. To do this, NKG2A- and NKG2A+ NK cells were gated upon within CAR NK cell co-cultures in CAR- and CAR+ NK cells (**Figure 5-42B**). Firstly, it can be noted that NKG2A+ NK cells are enriched in the CAR- NK cell population (**Figure 5-42B**). In the absence of IFNγ, only NKG2A+CAR- NK cells become increasingly activated with increased concentration of selinexor (**Figure 5-42C**). NKG2A+CAR+ NK cells only become more activated with selinexor in the presence of IFNγ, perhaps reflecting that only high levels of HLA-E can induce sufficient signalling by NKG2A to dampen activating signals from the CAR (**Figure 5-42C**). Overall, although only conducted with one donor, these preliminary data suggest that, at baseline, NKG2A+CAR- NK cells within the CAR NK cell population contribute to enhanced NK activation and cytotoxicity with selinexor. Only in

settings with high HLA-E expression, such as in a pro-inflammatory TME with IFNγ, does XPO1 inhibition promote NKG2A+CAR+ NK cell activation.

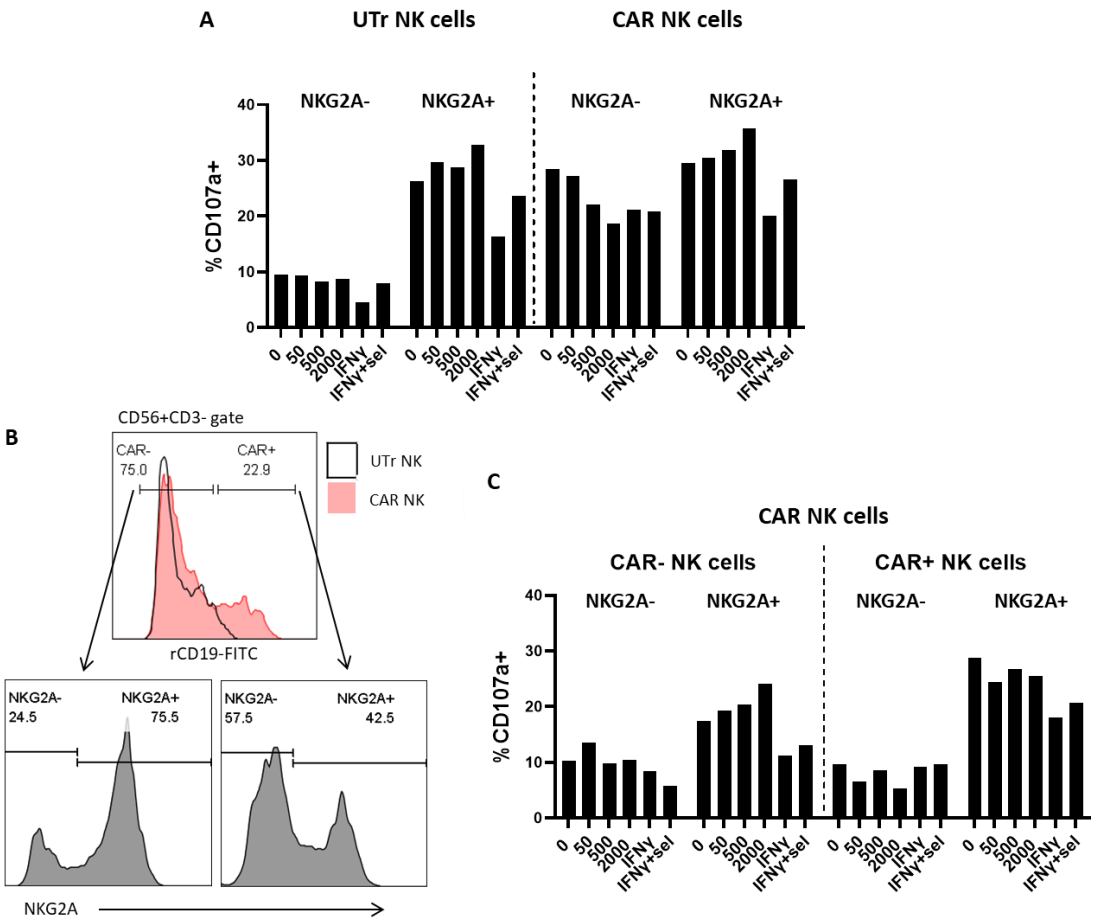


**Figure 5-42: NKG2A+/- CAR NK cell activation against Raji cells incubated with IFNγ ± selinexor.**

Raji cells were treated with selinexor (50-2000 nM) in the absence and presence of IFNγ (10 ng/mL, sel = 500 nM) for 24 hours followed by co-culture with anti-CD19 CAR NK cells or untransduced (UTr) NK cells for 4 hours at an E:T = 1:1. NK cell activation within NKG2A- and NKG2A+ populations was measured as the percentage of CD107a positive cells within UTr and CAR NK cell co-cultures (**A**). CAR NK transduction efficacy measured using FITC-labelled recombinant CD19 (rCD19) and the percentage of NKG2A- and NKG2A+ NK cells within CAR- and CAR+ gates which were drawn based on the UTr control (**B**). Within CAR NK co-cultures, NKG2A- and NKG2A+ NK cells within CAR positive and CAR negative gates as shown in (**B**) were assessed for activation using CD107a (**C**). Shown is an experiment using NK cells from one donor.

## 5.8 The effect of XPO1 inhibition in malignant B cells on T cell, CAR T cell and macrophage activation

### 5.8.1 XPO1 inhibition sensitises malignant B cells to CAR T cell lysis

In contrast to CAR NK cells, CAR T cells are approved for the treatment of B-cell malignancies, with four clinically approved anti-CD19 CAR T cell therapies for relapsed and refractory B-cell lymphomas and leukaemia (361). CAR T cells are generated autologously which results in a period of time (~ one month) between apheresis and CAR T cell adoptive transfer. As such, a bridging therapy is required to maintain a patient's condition before receiving CAR T cell infusion and one of these being investigated is selinexor (462).

Studies investigating selinexor-CAR T cell combination therapy have demonstrated improved tumour regression in pre-clinical models of B-cell lymphoma (460) and in small scale, early phase clinical trials using anti-BCMA CAR T cells to treat multiple myeloma (461,462). When selinexor and anti-CD19 CAR T cells were combined *in vitro*, selinexor enhanced the cytotoxicity of anti-CD19 CAR T cells (459). However, the mechanism for enhanced lysis is unknown. It was therefore investigated whether HLA-E reduction by selinexor could modulate CAR T cell activity given that NKG2A has previously been reported on CAR T cells (214). CAR T cells were gifted by Nurdan Askoy (Cancer Sciences, University of Southampton) which were generated with the FMC63 anti-CD19 scFv construct using lentiviral vector transduction. Flow cytometry staining with the anti-FMC63 idiotype antibody showed that the CAR construct was expressed by 10-14% of CD3+ T lymphocytes (**Figure 5-43**). When these CAR T cells were co-cultured with CD19+ Raji cells, in accordance with previous studies (459), selinexor sensitised Raji to CAR T cell lysis (**Figure 5-44**). At an effector:target (E:T) ratio of 1:1, anti-CD19 CAR T cell lysis of Raji cells increased with increasing concentration of selinexor (**Figure 5-44**). This trend was apparent at the 5:1 E:T, however significance between selinexor and DMSO samples was not achieved. Interestingly, UTr CAR T cell cytotoxicity was not enhanced by selinexor.

To determine whether NKG2A may contribute to enhanced cytotoxicity of CAR T cells with selinexor, NKG2A expression was measured on CAR T cells. NKG2A was not expressed on CAR+ T cells, but it was expressed on a small proportion (~1-5%) of CAR negative T cells (**Figure 5-45**). As such, the enhanced cytotoxicity of anti-CD19 CAR T cells cannot be explained by reduced NKG2A signalling and NKG2A expression on CAR negative T cells does not promote their cytotoxicity against selinexor-treated Raji cells with downregulated HLA-E surface expression.

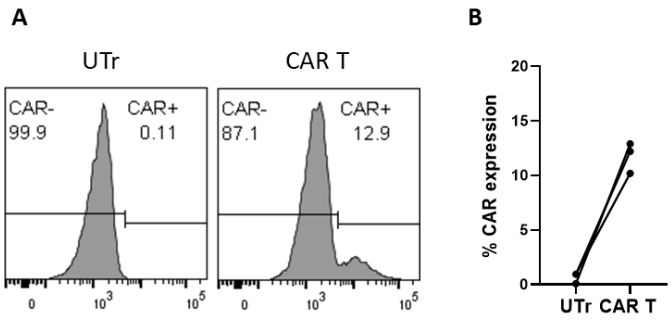


**Figure 5-43: CAR T cell transduction efficacy.**

(**A**) T cells were stained with anti-FMC63 idiotype antibodies followed by secondary antibody staining using anti-human IgG-APC. Representative donor displaying the CD3+ lymphocyte CAR histogram gate in untransduced (UTr) and CAR T cells. Numbers on histograms represent the percentage of cells within gates. (**B**) Percentage of T cells positive for CAR expression. Each line represents matched UTr and CAR T cells from a single donor (n=3).

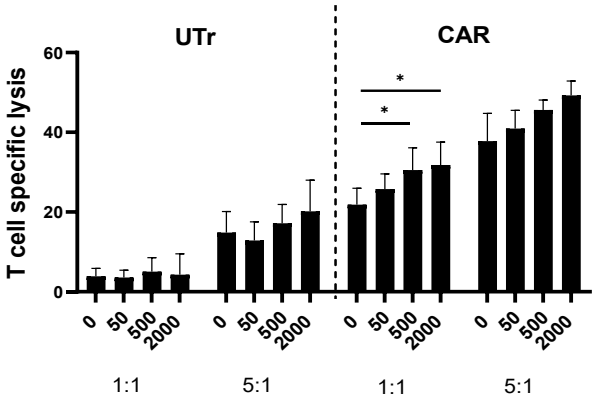


**Figure 5-44: Selinexor promotes CAR T cell lysis of Raji cells.**

Raji cells were treated with selinexor or DMSO (0 nM) for 24 hours and co-cultured with anti-CD19 CAR T cells or untransduced T cells (UTr) for a further 24 hours at an effector:target ratio of 1:1 and 5:1. Propidium iodide was used to identify the proportion of lysed CFSE positive Raji cells in co-cultures. T cell specific lysis was then calculated to account for selinexor-induced apoptosis which is displayed on the graph as mean ± SEM using T cells from three healthy donors. Significant differences in T cell specific lysis between selinexor and DMSO samples were calculated using repeated-measure two-way ANOVA followed by Dunnett's post-hoc test: *P<0.05.

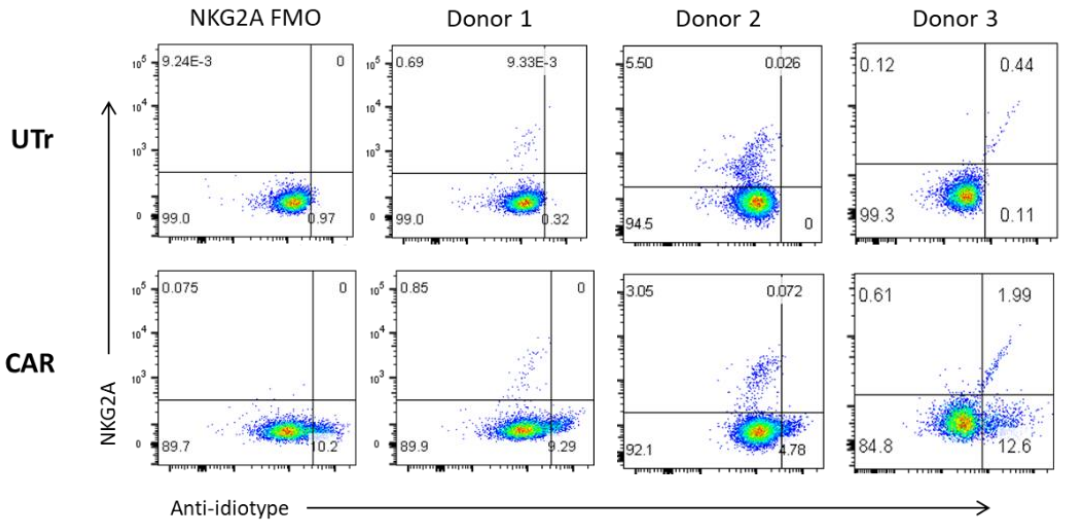


**Figure 5-45: NKG2A expression on anti-CD19 CAR T cells.**

Anti-CD19 CAR T cells and untransduced T cells (UTr) were stained with antibodies against NKG2A and unlabelled FMC63 idiotype (anti-idiotype). To detect bound anti-idiotype, an APC-labelled anti-human IgG secondary antibody was used. For donor 3, the anti-NKG2A antibody used was recombinant human IgG1 as such the secondary antibody also recognised the NKG2A antibody as well as the anti-idiotype. For donors 1 and 2, an anti-NKG2A antibody raised in mouse was used. Numbers on flow cytometry plots represent the percentage of cells within gates. The anti-idiotype gate was drawn based on the UTr control and the NKG2A gate was drawn based on the NKG2A FMO (fluorescent minus one).

### 5.8.2 NKG2A expression on stimulated T cells

NKG2A was demonstrated to be lowly expressed on T cells after 1-week of culture during CAR T cell generation. However, in patients who received CAR T cells, 28-days post infusion NKG2A became upregulated (214). Additionally, NKG2A was shown to be upregulated on murine T cells after two-three rounds of stimulation with rest periods between stimulations (210). Therefore, in order to investigate how NKG2A expression may impact CAR T cell function, T cells were stimulated two to three times with T cell TransAct™ (a polymer matrix containing recombinant CD3 and CD28 agonists, added as 1:100 dilution, Miltenyi) with rest periods in-between stimulations and examined for expression of NKG2A. Over the course of two stimulations, NKG2A expression did not increase on UTr T cells or CAR T cells (**Figure 5-46**). To confirm activation of T cells with TransAct™, T cells were also stained for expression of CD137 (4-1bb), CD25, CD69 and PD-1 (**Figure 5-47**). After 3-day stimulation with TransAct™ (D3, D10 and D17) all activation markers were highly expressed on T cells. After removing TransAct™ from the media and allowing T cells to rest for 4 days in the presence of IL-7 and IL-15 cytokines, expression of CD137 was lost. For CD25 and PD-1, the rest period induced their downregulation to an intermediate phenotype, but CD69 was stably expressed by T cells even after the rest periods demonstrating the differential expression kinetics of activation markers on T cells. As for NKG2A, three rounds of stimulation failed to induce its expression (**Figure 5-47**). Overall, these data illustrate that XPO1 inhibition by selinexor sensitises B-cell lymphoma cells to anti-CD19 CAR T cell lysis independent of NKG2A and ways to upregulate NKG2A on T cells are required to study whether HLA-E:NKG2A interactions can be modulated to promote CAR T cell function.

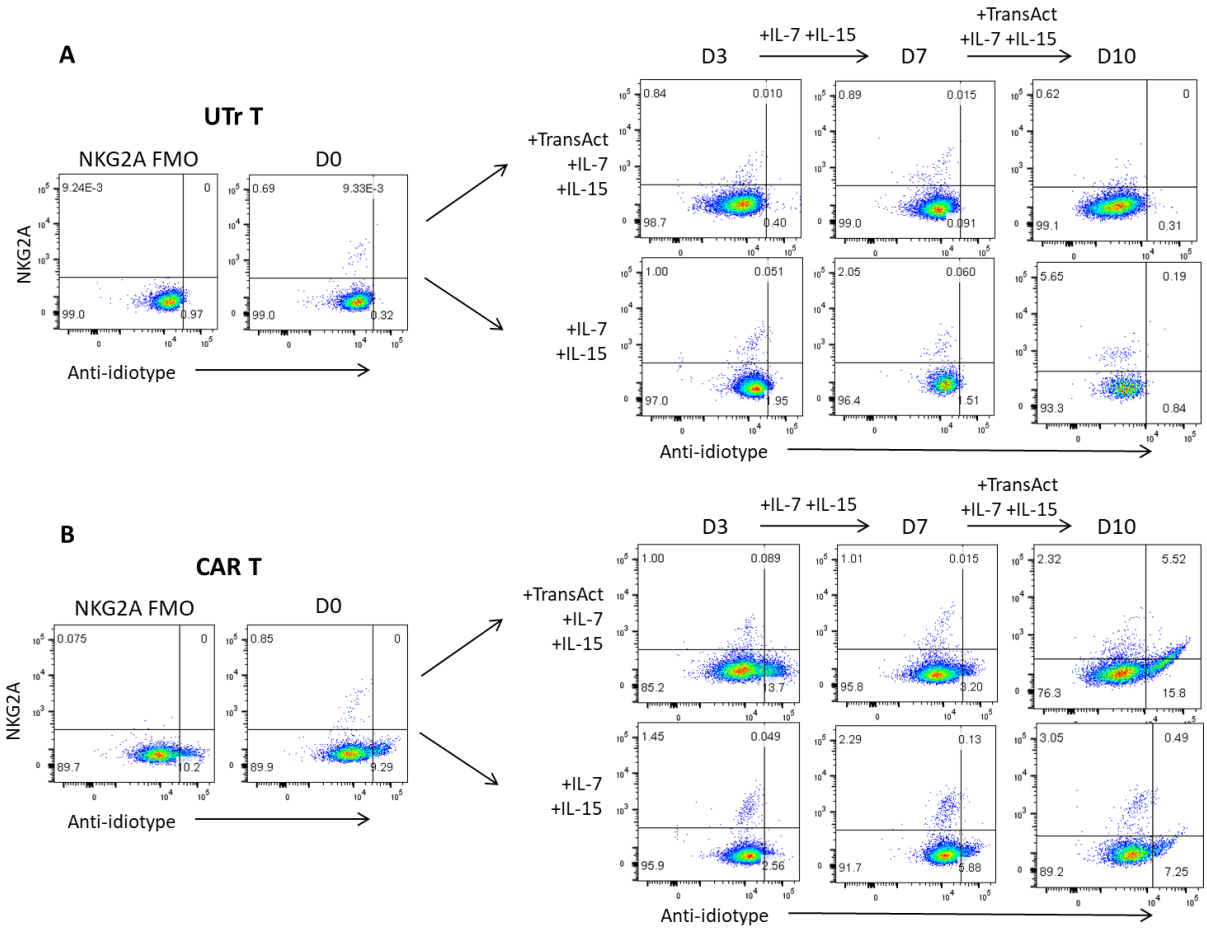


**Figure 5-46: NKG2A expression on T cells after multiple rounds of stimulation.**

Untransduced T cells (UTr, A) and anti-CD19 CAR T cells (B) were cultured with IL-7 (500 U/mL) + IL-15 (290 U/mL) for 10 days and stimulated twice with TransAct™ (1:100 dilution, Miltenyi) on day 0 (D0) and day 7 (D7) for 3 days at which point cells were washed and replated with cytokines for 4 days. As a control, T cells were left unstimulated but cytokines were replenished on the appropriate days. Shown are flow cytometry plots of NKG2A against anti-idiotype CAR staining on D0, D3, D7 and D10. NKG2A gates were drawn based on the NKG2A FMO (fluorescence minus one) control and anti-idiotype gates were drawn based on the UTr control.

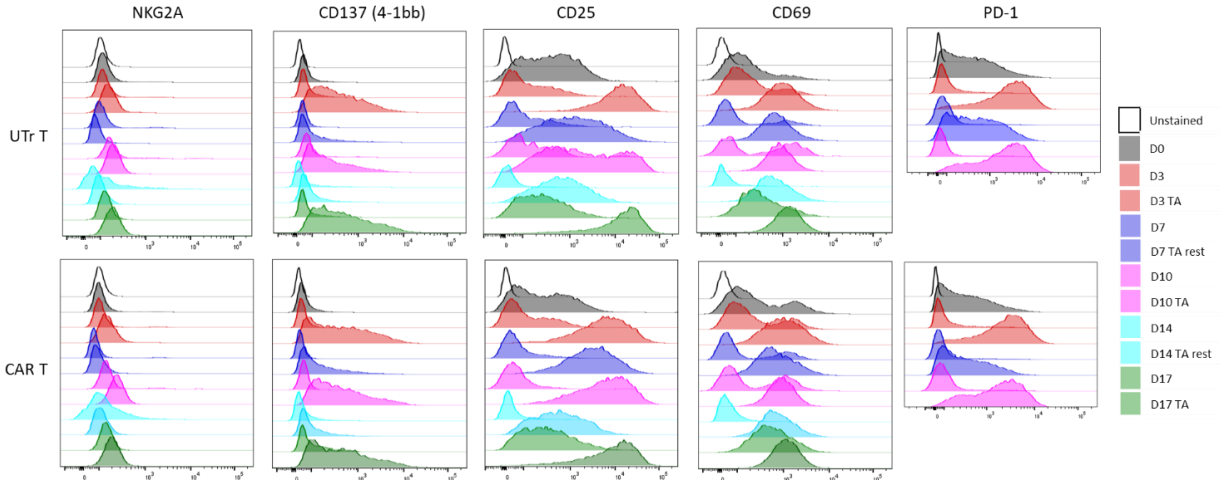


**Figure 5-47: Expression of activation markers on T cells after repeated rounds of stimulation.**

Untransduced T cells (UTr) and anti-CD19 CAR T cells were cultured with IL-7 (500 U/mL) + IL-15 (290 U/mL) for 17 days and stimulated three times with TransAct™ (1:100 dilution, TA) on day 0 (D0), day 7 (D7) and day 14 (D14) for 3 days at which point cells were washed and replated with cytokines for 4 days described here as a rest period. As a control, T cells were left unstimulated but cytokines were replenished on the appropriate days. Shown are flow cytometry histograms of one experiment (of two repeats) of NKG2A and activation markers CD137, CD25, CD69 and PD-1 gated on CD3+ lymphocytes. The figure legend is colour coded by day and ordered top to bottom to reflect the order of histograms.

### 5.8.3 Macrophage phagocytosis of malignant B-cells is enhanced by selinexor

Recently it was shown that HLA-E is also a ligand for LILRB1 and LILRB2 receptors (34). LILRB1/2 are expressed by multiple cell types including NK cells and macrophages, with particularly important functions in regulating macrophage phagocytosis (287). The ITIM domains of LILRB1/2 transduce inhibitory signals into macrophages to impair phagocytosis (544). Therefore, it was hypothesised that downregulation of HLA-E by selinexor would enhance macrophage phagocytosis. To assess this, macrophages were generated from circulating monocytes using macrophage-colony stimulating factor (M-CSF) and co-cultured with selinexor-treated Raji cells that were labelled with CellTrace™. Phagocytosis was calculated as the percentage of CD14+CellTrace+ cells (**Figure 5-48**). Raji cells were incubated with Q-VD during selinexor treatment to inhibit selinexor-induced apoptosis. After treatment with selinexor macrophage phagocytosis was slightly enhanced (**Figure 5-49**). To ascertain whether HLA-E is important in regulating macrophage phagocytosis, Raji cells were incubated with IFNγ to induce high levels of HLA-E and macrophage phagocytosis was subsequently assessed. IFNγ-induced HLA-E expression had no impact on macrophage phagocytosis, however selinexor still maintained its ability enhance to the phagocytosis of Raji cells in the presence of IFNγ (**Figure 5-50**). Overall, these experiments suggest that selinexor sensitises B-cell lymphoma cells to macrophage phagocytosis.

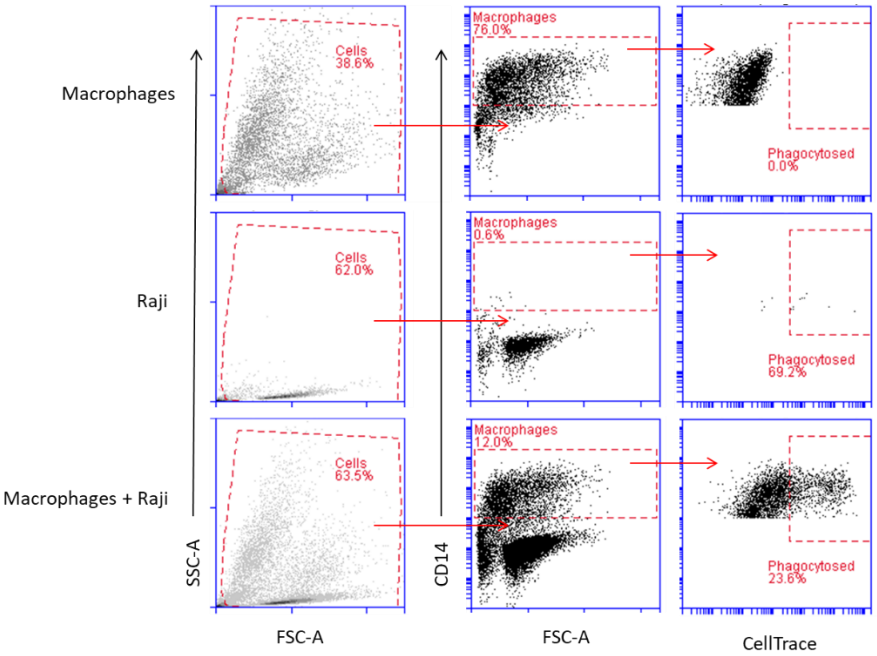


**Figure 5-48: Gating strategy to measure macrophage phagocytosis.**

To measure phagocytosis, cells within cultures were gated with SSC vs FSC and monocyte-derived macrophages were identified with CD14. Raji cells were labelled with CellTrace™ before co-culture to enable identification of target cells engulfed by macrophages. The CD14 positive gate was drawn based on the Raji-only control (middle) and the phagocytosis gate was drawn based on the no target, macrophage-only control (top). The complete co-culture gating is shown at the bottom.

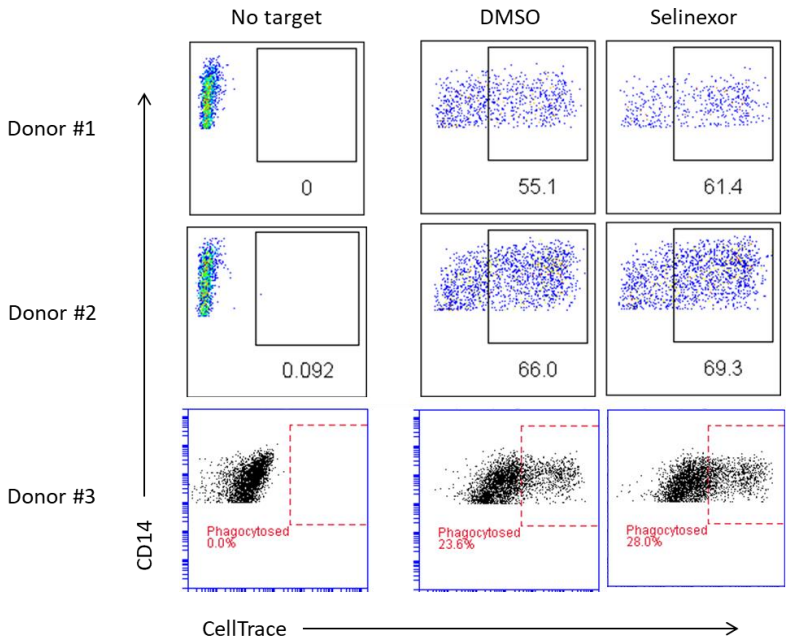


**Figure 5-49: Selinexor enhances macrophage phagocytosis or Raji cells.**

Raji cells were pre-labelled with CellTrace™ and treated with selinexor (500 nM) for 24 hours or DMSO control in the presence of Q-VD to inhibit drug-induced apoptosis. Raji cells were then co-cultured with monocyte-derived macrophages at an E:T = 1:1 for 2 hours after which phagocytosis was measured by flow cytometry as the percentage of CellTrace™ positive cells within the CD14+ macrophage gate. Shown is an experiment using macrophages derived from three donors.

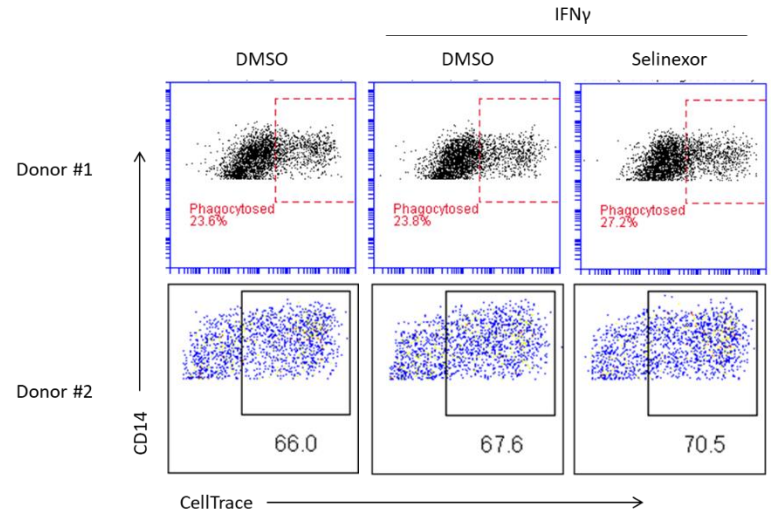


**Figure 5-50: Macrophage phagocytosis of Raji cells pre-treated with IFNγ.**

Raji cells were pre-labelled with CellTrace™ and treated with selinexor (500 nM) or DMSO control ± IFNγ (10 ng/mL) for 24 hours in the presence of Q-VD to inhibit drug-induced apoptosis. Raji cells were then co-cultured with monocyte-derived macrophages at an E:T = 1:1 for 2 hours after which phagocytosis was measured by flow cytometry as the percentage of CellTrace™ positive cells within the CD14+ macrophage gate. Shown is an experiment using macrophages derived from two donors.

## 5.9 Discussion

### 5.9.1 XPO1 inhibition sensitises malignant B cells to primary, expanded NK cells but not NKL or NK-92 cell lines

NK cell adoptive transfer therapies under clinical investigation source NK cells from cell lines such as NKL and NK-92 and from primary sources such as peripheral blood and umbilical cord blood, all of which have their advantages and disadvantages (545,546). As shown in this chapter, NKL, NK-92 and expanded NK cells derived from peripheral blood NK have different receptor expression profiles, with the expression data shown here equal to that reported by Gunesch et al., (2019). Of note, NKG2C was not expressed on primary NK cells, thus the modulation of HLA-E by XPO1 inhibition will specifically impact NKG2A signalling and not NKG2C. The differences in receptor expression may impact the efficacy of combination therapy approaches with small molecules or monoclonal antibodies (mAbs) targeting checkpoint receptors or mAbs used to induce ADCC (**Figure 5-2 and Figure 5-3**). For example, although CD16 was lowly expressed by NK cell lines, rituximab only induced ADCC by primary NK cells (532) demonstrating that CD16 expression on NKL and NK-92 is inactive. This is similar for NKG2A on NK cell lines which was lowly expressed on NKL and NK-92 compared to expanded NK cells and NKG2A blockade experiments failed to increase NKL and NK-92 cytotoxicity (**Figure 5-5**). Therefore, NKG2A appears to be dysfunctional on NKL and NK-92 cells, either NKG2A fails to engage with HLA-E to induce inhibitory signalling or NKG2A is constitutively activated. The latter seems most plausible because NK cell lines were much less cytotoxic compared to primary NK cells (**Figure 5-5**), although this could reflect low expression of activating receptors on NK cells lines (**Figure 5-2**). Moreover, published articles investigating NKG2A function on NK92 and NKL cell lines genetically disrupt NKG2A as opposed to using antibody blockade approaches to promote NKL and NK-92 cytotoxicity (243,547). These data also confirm that XPO1 inhibition impairs HLA-E:NKG2A interactions because selinexor did not promote NK cell lines cytotoxicity (**Figure 5-4 and Figure 5-5**). As such, future selinexor-NK cell adoptive transfer combinations should use primary expanded NK cells.

To ensure sufficient numbers of NK cells for adoptive transfer, NK cells derived from blood products are expanded of which there are multiple techniques being tested clinically (545). A feeder-free method was used here using IL-2 to proliferate NK cells, chosen for its potential for wider applications because of the negation of feeder cells (546). This expansion method was shown to enhance NKG2A expression rapidly over 5-7 days, most likely due to proliferation inducing NKG2A expression than NKG2A+ NK cells out competing NKG2A- NK cells (**Figure 5-6**). NKG2A becomes expressed because it maintains the proliferative capacity of NK cells (82) and multiple NK expansion protocols upregulate NKG2A (243,311,548,549). When expanded NK cells were co-cultured with

selinexor-treated or eltanexor-treated B-cell lymphoma cells, cytotoxicity was greatly enhanced (**Figure 5-8** and **Figure 5-9**) potentially due to the increased dependence on NKG2A signalling in expanded NK cells compared to resting NK cells as shown by higher and homogenous NKG2A expression on expanded NK cells (**Figure 5-3 and Figure 5-6**). Indeed, NKG2A knockout approaches with CRISPR and siRNA have shown enhanced effector functions against tumour cells (315,317,480,550,551). Whether XPO1 inhibition promotes the activation and cytotoxicity of NK cells expanded using other expansion protocols remains to be determined, however, all reported expansion methods to date induce NKG2A expression suggesting that selinexor will enhance the function of NK cells expanded using any expansion protocol (243,311,548,549).

### 5.9.2 Functional HLA-E expression is required for the immunomodulatory activity of selinexor

721 cell lines were used throughout the chapter to demonstrate that the immunogenic effect of selinexor was HLA-E-dependent. They were also used specifically for their B-cell properties similar to malignant B cells used in experiments as opposed to using cell lines derived from different cell types. Although 721.221 and 721.174 cell lines are not complete knockouts of HLA-E, the expression of HLA-E is very low (**Figure 5-17**), and the peptides presented by HLA-E on these cells are unconventional. This is because 721.221 is knockout for HLA-A/B/C for which the leader sequence peptides are presented by HLA-E and 721.174 is deficient in TAP, the transporter protein which loads peptides on to HLA molecules. As such, HLA-E expression is severely impaired, and it is unable to engage NKG2A on NK cells as demonstrated in NKG2A blockade experiments in which anti-NKG2A mAbs did not enhance expanded NK cell cytotoxicity against 721 cell lines (**Figure 5-19B**). In a similar manner, XPO1 inhibition did not sensitise 721 cell lines to NK cell cytotoxicity (**Figure 5-19A**). This was because, firstly, NKG2A is not engaging with HLA-E on 721 cells, therefore modulating this interaction with selinexor did not induce a response by NK cells. It was shown recently that peptides derived from HLA class I leader sequences engage NKG2A on NK cells and other protein-derived peptides inhibited HLA-E:NKG2A interaction (34). Secondly, HLA-E was not further downregulated due to already impaired peptide processing and presentation in 721 cells (**Figure 5-16 and Figure 5-17**). In section 3.4.3, it was illustrated that selinexor-induced HLA-E downregulation was because of impaired trafficking of HLA-E to the plasma membrane, reducing the rate of HLA-E recovery at the surface, most likely because of reduced peptide stabilisation and transport of HLA-E out of the endoplasmic reticulum (ER) which is the main limiting factor of HLA-E surface expression (9). Hence, XPO1 inhibition has no consequence on HLA-E expression in 721 cells and therefore no impact on NK cell function because HLA-E peptide loading, and ER exit is severely dysfunctional in 721 cells. **Figure 5-26** demonstrates in 721.221 cells that the majority of HLA-E molecules are trapped in the ER and are unable to reach the plasma membrane. This is consistent with HLA-E being a sensor of functional antigen processing and presentation machinery as functional HLA-E surface expression is dependent

on all proteins within the peptide loading complex (34). It will be interesting to determine whether re-expressing TAP in 721.174 or re-introducing HLA class I proteins in 721.221 would enhance HLA-E expression to facilitate the immunomodulatory properties of XPO1 inhibitors.

To further establish that selinexor selectively inhibits the HLA-E:NKG2A interaction to promote NK cell function, NKG2A signalling could be assessed. Upon engagement with HLA-E, NKG2A recruits SHP-1 and SHP-2 phosphatases to turn off activating signals (192), and the activation of SHP-1 and SHP-2 can be measured with western blotting against phosphorylated proteins (314). It would be expected that XPO1 inhibition in cancer cells results in reduced SHP-1/-2 phosphorylation in NK cells due to lack of NKG2A stimulation, but as inhibitory KIR also signal via SHP-1/-2 it will be difficult to precisely determine that NKG2A signalling is reduced (167,168). To adequately transduce inhibitory signals, NKG2A forms clusters on NK cells which can be visualised with confocal microscopy (208,552,553). Using expanded NK cells with high NKG2A expression co-cultured with B-cell lymphoma cells, it will be interesting to investigate cluster formation and downstream NKG2A signalling in the presence of selinexor.

### 5.9.3 Increased HLA-E expression by the lymph node support molecules IL-4+CD40L protect B-cell lymphoma cells from NK cell cytotoxicity, which is reversed by selinexor

Here, IL-4+CD40L was shown to protect CLL cells from NKG2A activation (section 4.4) and B-cell lymphoma cells from NK-mediated lysis (**Figure 5-13**). The mechanism was shown to be via HLA-E upregulation because NKG2A blockade and selinexor treatment fully recovered the lysis ability of NK cells (**Figure 5-14**). Similar to experiments with IFNγ using 721 cell lines with impaired HLA expression, 721 cell lines could be incubated with IL-4 and CD40L to demonstrate that IL-4 and CD40L do not confer any resistance to NK cell-mediated lysis in the absence of functional HLA-E presentation (**Figure 5-29**). IL-4 and CD40L induce the expression of anti-apoptotic BCL2 family of proteins which may play a role in conferring intrinsic resistance to NK cell lysis (378,383).

Modulation of the NKG2A:HLA-E axis in SUDHL6 with antibodies or selinexor only partially recovered NK specific lysis, which perhaps reflects the large increase in HLA-A/B/C expression with IL-4+CD40L (**Figure 5-11**). Using HLA class I blocking mAbs or anti-KIR antibodies such as lirilumab in combination with anti-NKG2A mAbs would help to resolve this assumption. Additionally, without IL-4+CD40L incubation, SUDHL6 was not sensitised to expanded NK cells by selinexor or anti-NKG2A mAbs (**Figure 5-14 and Figure 5-15**). This is most likely due to the low levels of HLA-E at the surface of SUDHL6 which was comparable to 721.221 cells which have impaired HLA-E surface expression (**Figure 5-17**). The major difference between 721.221 cells and SUDHL6 is that SUDHL6 has functional HLA class I expression (**Figure 5-17**), which therefore further confirms that the modulation of HLA-E:NKG2A interactions is important for the immunomodulatory activity of XPO1 inhibitors.

It is difficult to correlate HLA-E expression increases with protection from NK cells because firstly the ability of HLA-E to engage NKG2A depends on the peptides loaded onto HLA-E which may differ for cell lines (25), secondly because there is variation in NK cell donor activity dependent on receptor expression, time of donation and individual donor NK cell education and finally, because NKG2A:HLA-E exhibits inhibitory/activating saturation kinetics (17,208). This is evidenced by the very small increase in HLA-E expression on Raji which consequently leads to a large reduction in NK specific lysis (**Figure 5-12 and Figure 5-13**).

The HLA-E-inducible effect of IL-4 and CD40L differed across cell lines which may reflect the differential expression of the IL-4 receptor and CD40 (**Figure 5-12**). It will be interesting to determine whether different concentrations of IL-4 and CD40L result in the corresponding changes in HLA-E expression. Additionally, experiments using cells negative for CD40 such as T cells and NK cells and other immune cells positive for CD40 such as macrophages and measuring their response to lymph node support molecules will affirm the link between CD40 signalling and HLA-E expression. The potential mechanism behind the increase in HLA-E expression with IL4 and CD40L was not explored, but through western blot or qPCR analysis of HLA-E will determine whether total or surface protein levels increase.

Increased HLA-E expression with CD40L and IL-4 on B cells will most likely occur in germinal centers where maturing B cells are in close contact with T follicular helper cells which provide CD40L support (554). The exact mechanism for upregulation of HLA-E with CD40L and IL-4 remains to be determined, however these data reveal that CD40 signalling has a more potent effect on HLA-E upregulation (555). This is in accordance with data showing that anti-CD40 antibodies to stimulate CD40 signalling in murine splenocytes enhances Qa-$1^b$ expression (34). NKG2A+ NK cells have been reported within the lymph nodes, suggesting that HLA-E upregulation by IL-4 and CD40L may protect B cells undergoing somatic hypermutation from NK cell destruction (478). Whether other molecules in germinal centers contribute to HLA-E upregulation awaits exploration such as BAFF interactions and TLR agonism (384). Human 3D models of lymph nodes using CLL patient PBMC have been designed to enable drug screens (491). In this 3D model it will be interesting to test HLA-E expression changes on CLL cells and the ability of NK cells, both autologous and allogenic, to lyse CLL cells in this setting.

### 5.9.4 IFNγ protects B-cell lymphoma cells from NK cytotoxicity via the NKG2A:HLA-E axis, which is overcome by XPO1 inhibition

When NK cells are adoptively transferred into patients, NK cells may encounter a pro-inflammatory tumour microenvironment (TME) enriched in IFNγ and it has been shown that NK cell function becomes rapidly impaired upon entry into the TME (245,535). It was illustrated here that IFNγ can protect malignant B cells from NK cytotoxicity which is in accordance with other reports that IFNγ protects tumour cells from NK-mediated lysis via engagement with NKG2A using the same concentration of IFNγ used in this thesis (22,536,537). It would have been interesting to perform an IFNγ dose response experiment to measure HLA-E increases at the plasma membrane and correlate this with NK cell activation/cytotoxicity since IFNγ tumour concentration has been shown to be lower (lung cancer ~ 0.4-0.05 ng/mL) (556) than those used in the experiments here (10 ng/mL).

It is well known that IFNγ induces HLA-E expression via STAT1 activation (36) and STAT1 is dephosphorylated in the nucleus and recycled to the cytoplasm by XPO1 to enable continued IFNγ signalling (38). In **Figure 5-23**, selinexor was shown to inhibit chronic IFNγ signalling via decreased STAT1 phosphorylation and therefore decreased expression of total STAT1 and HLA-E. To confirm nuclear retention of STAT1 by selinexor, western blot of STAT1 in segregated cytosolic and nuclear fractions could be performed with the hypothesis that STAT1 is enriched in the nuclear compartment after selinexor treatment.

Expanded NK cells are more highly activated with increasing concentrations of selinexor, producing more IFNγ as illustrated by flow cytometry (**Figure 5-20A**). This enhanced production of IFNγ was not exactly replicated in ELISA experiments (**Figure 5-20B**). At 50 nM selinexor, more IFNγ was measured in co-culture supernatants compared to the untreated control, however at higher concentrations of selinexor IFNγ abundance decreased, even though IFNγ production, degranulation and NK specific lysis continued to increase with increasing concentration of selinexor. This perhaps reflects the differences in the dynamics of IFNγ production and secretion compared to perforin and granzyme which follow different secretory pathways (142). The enhanced NK cell cytotoxicity at high selinexor concentrations may reduce the stimulus required to release IFNγ as one study demonstrated that IFNγ secretion was dependent on successful binding to target cells (557) and another showed that NKG2D signalling promoted IFNγ secretion (244). It must be noted however, that the ELISA experiment was only performed with four donors, so more robust analyses need to be performed before conclusions can be made.

As well as recombinant IFNγ inducing HLA-E expression in B-cell lymphoma cells, supernatants from NK-cancer co-cultures induced HLA-E expression on cell lines (**Figure 5-22**). Whether this is due to the presence of IFNγ in the supernatants remains to be deduced, but IFNγ is produced by NK cells upon recognition of cancer targets (**Figure 5-20**). Blocking IFNγ binding to its receptor in supernatants by

antibody blockade or using cancer cell lines knockout for IFNγR would confirm this. Through the use of selinexor to activate IFNγ production by NK cells one can imagine an HLA-E expression feedback loop arising. XPO1 inhibition will enhance NK cell activation, leading to increased IFNγ in the TME resulting in increased expression of HLA-E on tumours cells and subsequent NK cell inhibition via NKG2A signalling. However, as this chapter has shown, XPO1 inhibition impairs IFNγ-induced HLA-E upregulation via STAT1 inhibition, as such selinexor may allow for a prolonged NK cell immune response in a pro-inflammatory TME. Interestingly, HLA-E was upregulated on the DLBCL cell line SUDHL6 the most by IFNγ (**Figure 5-22**) and IL-4+CD40L (**Figure 5-11**) and RNA-seq analysis of 33 tumour types reported that DLBCL samples expressed HLA-E the highest, perhaps reflecting the ability of DLBCL cells to respond to microenvironmental stimuli (243).

HLA-E flow cytometry staining of permeabilised and intact cells further demonstrates that XPO1 inhibition impedes HLA-E plasma membrane trafficking and does not affect total HLA-E protein expression in the absence of IFNγ (**Figure 5-25**), confirming data from western blot assays and acid strip experiments in chapter 3. In permeabilised cells HLA-E expression was maintained with selinexor treatment, but with intact cells, HLA-E staining intensity decreased signifying decreased surface levels of HLA-E. A limitation with the experimental procedure is the concomitant cell surface and intracellular staining which does not truly reflect intracellular levels of HLA-E. An alternative method would be to saturate surface HLA-E with unlabelled antibody followed by intracellular staining with fluorescently labelled antibody to collect a true measure of intracellular HLA-E abundance.

No intrinsic protection is conferred by IFNγ because when 721 cell lines were incubated with IFNγ, which are responsive to IFNγ as shown by increased phosphorylated STAT1 (**Figure 5-24**), no protection was provided from NK cytotoxicity (**Figure 5-29**). This highlights that no intrinsic factors are induced by IFNγ that desensitise cells from apoptosis. Hence, an external factor modulating the interaction with, and activation of, NK cells is involved in conferring protection, and this thesis indicates that increased HLA-E expression is responsible.

In experiments where selinexor and anti-NKG2A antibodies were combined, additive effects on NK cell cytotoxicity were observed for SUDHL6 and Raji cells (**Figure 5-10 and Figure 5-27**). It was expected that the combination treatment would not further enhance NK cell cytotoxicity due to complete NKG2A inhibition with antibodies. This observation could be explained by the VL9 peptides presented by HLA-E which have been shown to modulate monalizumab and Z199 (anti-NKG2A mAb clone used in this thesis) ability to block NKG2A:HLA-E interactions (279). For example, when the HLA-C leader peptide is presented by HLA-E, Z199 more effectively blocked HLA-E:NKG2A interactions compared to when HLA-A or HLA-B leader sequences were presented (279). This resulted in more effective NK-mediated lysis of targets cells expressing HLA-E presenting HLA-C

peptides with monalizumab. Considering the additive observations with selinexor and anti-NKG2A antibodies, perhaps Raji cells present HLA-B-derived peptides in which the Z199 anti-NKG2A mAb is not fully effective, enabling the downregulation of HLA-E by selinexor to further promote NK-mediated lysis of Raji. Additionally, of the 16 classical VL9 peptides that stabilise HLA-E, only six produce functional complexes with HLA-E and these have shown differential engagement with NKG2A, consequently inducing varying inhibitory effects in NK cells (23). This may also contribute to the additive effects recorded with selinexor plus anti-NKG2A mAbs. Another potential reason for the observed additive effect of selinexor-anti-NKG2A combination treatment is the internalisation of anti-NKG2A antibodies. 40% of the anti-NKG2A antibody BMS986315 was internalised after 20 hours (558), but whether the antibody clone Z199 used here is internalised remains to be determined. Naturally, NKG2A is continuously turned over at the plasma membrane, even in the absence of HLA-E engagement (552). Taken together, it is likely that Z199 is internalised enabling new NKG2A molecules to engage with HLA-E on target cells, but in the presence of selinexor this inhibition is reduced resulting in combined effects of anti-NKG2A-selinexor treatment.

Moreover, the additive effect observed here could also be explained by a recent paper illustrating that genetic ablation of NKG2A by CRISPR-Cas9 is more effective at promoting expanded NK cell function than NKG2A antibodies, both *in vitro* and *in vivo* (314). This finding may also reflect that anti-NKG2A mAb efficacy is dependent on the VL9 peptides presented by HLA-E (279). In the perspective of this thesis, through introducing downregulation of HLA-E with selinexor and blocking NKG2A function with mAbs, the accumulative effective is to promote NK cell function towards that observed with complete genetic ablation of NKG2A (314,317,480).

Growing evidence suggests that HLA-E is capable of presenting non-canonical peptides, for example peptides derived from HSP60 (24). Interestingly, HSP60 is upregulated in JeKo-1 cells after XPO1 inhibition (485) and HSP60-derived peptides presented on HLA-E are known to abrogate interactions with NKG2A (279). Whether HSP60 is upregulated with Raji and Ramos cells after selinexor treatment remains to be determined. In the meantime, it is interesting to speculate that the selinexor-anti-NKG2A mAb additive effect may also be explained by the induction of HSP60-derived peptides on HLA-E.

An alternative approach to targeting NKG2A with mAbs is to target HLA-E. Through targeting HLA-E the ADCC capability of NK cells can be exploited as demonstrated in a recent publication (280). Additionally, antibodies can be raised against HLA-E specifically presenting VL9 peptides that interact with NKG2A and this will spare any HLA-E:NKG2C interactions that activate NK cells via presentation of non-canonical peptides (281).

It will be important to consider the effect of IFNγ on NK cell function because IFNγ can activate NK cells via STAT1 leading to enhanced cytotoxicity (559). Moreover, IFNγ is important in impeding

tumour growth (560,561) and IFNγ-producing NK cells are crucial for remodelling the TME to promote anti-tumour immune responses (141), therefore it will be important to consider the general effect on the immune system when disrupting IFNγ signalling with SINEs. Experiments should be conducted investigating the combined effect of IFNγ on tumour cells and NK cells in the presence and absence of selinexor. The SHP-1 phosphatase activated by NKG2A is known to inhibit IFNγ signalling by reversing the effects of JAK1/2 kinases (562,563), as such through reducing HLA-E:NKG2A engagement with selinexor SHP-1 repression of IFNγ signalling in NK cells may be impaired allowing the positive effects of IFNγ to perpetuate in NK cells. However, it has been reported that chronic STAT1 phosphorylation in NK cells can impair NK cell cytotoxicity and mutation of the phosphorylation site in STAT1 delayed leukaemia onset in mouse models (564). Therefore, the effect of XPO1 inhibition on IFNγ signalling in NK cells needs dissecting to understand whether XPO1 inhibition in the context of IFNγ signalling is productive or repressive of NK cell function. Additionally, in this context it will be important to understand how metabolism is affected by XPO1 inhibition in NK cells since it is known that XPO1 inhibition can disrupt metabolic-associated gene expression and reduce oxygen consumption rate in tumour cells (472–474). In the TME, oxidative stress in NK cells impairs glucose metabolism which inhibits NK cell anti-tumour functions (565), as such the disruption to metabolic processes induced by XPO1 inhibition in NK cells requires investigation, which may explain impaired NK cell activity in primary CLL autologous assays.

Alongside increasing the expression of HLA-E, total HLA class I molecules were also upregulated by IFNγ however, in contrast to HLA-E, selinexor did not impede the IFNγ-induced HLA-A/B/C upregulation (**Figure 5-25**). This may be attributable to the mechanism for increasing HLA-A/B/C expression by IFNγ compared to HLA-E where STAT1 directly binds to *HLA-E* enhancer regions. IFNγ induces the expression of IRF-1 and NLRC5 via STAT1 and these transcription factors then bind to the promoter of classical HLA class I genes to potentiate their transcription (566–568). XPO1 is not known to translocate IRF-1 out of the nucleus and therefore selinexor will not impede IRF-1-induced expression of HLA class I genes. Furthermore, there is evidence that XPO1 exports NLRC5 (569), as such through using selinexor the increased abundance of NLRC5 from IFNγ signalling will remain in the nucleus and enable continued transcription of HLA class I genes, hence the maintained high expression of HLA-A/B/C (**Figure 5-25**). This ultimately will have consequences for T cell anti-tumour functions in that selinexor will not impede the IFNγ-induced activation of T cells via HLA class I upregulation.

### 5.9.5 Future *in vivo* experiments

Selinexor pre-treatment followed by selinexor addition to cancer-NK co-cultures (sequential + concurrent) resulted in enhanced lysis ability of NK cells, but not to the same extent as selinexor pre-treatment only (sequential treatment) (**Figure 5-30**). This suggests that HLA-E downregulation requires at least 16 hours of selinexor pre-treatment (**Figure 4-8**). Therefore, in the scenario of sequential + concurrent treatment, lymphoma cells are sensitised to NK cell activation which occurs rapidly (<4 hours, **Figure 5-28**), but as time progresses NK cells begin to apoptose (**Figure 5-30**) reducing the NK specific lysis observed in wells compared to sequential treatment. Alternatively, as well as NK cell viability affecting NK specific lysis of the population, XPO1 inhibition may impair NK cell activation. This was reported in Lapalombella et al., (2012) in which ADCC by NK cells was decreased in the presence of selinexor, although not significantly. The mechanism behind this remains to be resolved.

XPO1 inhibition has been reported to impair TCR signalling *in vitro*, however *in vivo* T cell function was maintained (525). Additionally, NK cell numbers in selinexor-treated mice were unaffected (406), and in some cancer models NK numbers were reported to increase (407). This suggests that although NK cell viability was affected by XPO1 inhibition *in vitro* (**Figure 5-30**), in tissue environments where selinexor concentrations may be less compared to 2D culture models and where NK cells will be surrounded by supportive cytokines, XPO1 inhibition may not impact NK cell viability or function. This warrants *in vivo* investigations, particularly in humanised mouse models because previous studies have utilised mice with intact murine immune systems.

From the data presented in section 5.6, a sufficient window exists to study tumour regression of Raji in NSG mice treated with selinexor and NK cell immunotherapy. On day 0 Raji cells can be subcutaneously injected into mice followed by the isolation of NK cells from human PBMC so that after 14 days tumours will be visible (**Figure 5-14**) and NK cells expanded sufficiently to enable intravenous injection of approximately 1-5x$10^6$ NK cells per mouse on subsequent days (**Figure 5-1**). At day 14 once tumours are visible, the first dose of selinexor can be administered and depending on the nature of the experiment, expanded NK cells can be administered on the same day (concomitant) or on the following days either proceeding days of selinexor treatment (sequential) or on the same days as selinexor treatment (sequential + concomitant). Tumour growth and the survival of mice can be measured along with obtaining information on NK cell infiltration/function into tumours and HLA-E expression on Raji cell. These data will affirm whether the effects observed *in vitro* are consistent *in vivo*, adding value to the translatability of selinexor and adoptive NK cell transfer combination therapy approaches.

The *in vivo* potential of combining expanded NK cells with NKG2A:HLA-E inhibition is exemplified by the increased survival of mice co-injected intratumourally with monalizumab and expanded NK cells

in multiple murine cancer models (570). HLA-E:NKG2A interactions also play a crucial role in metastasis. The importance of HLA-E to metastasis is evidenced by increased HLA-E expression on circulating tumour cells compared to metastatic and primary lesions and this increase protects circulating tumour cells from NKG2A+ NK cell-mediated destruction during transit to the metastatic niche (237). Therefore, it will be interesting to determine whether XPO1 inhibition also downregulates HLA-E on solid tumours and whether this could protect from metastasis in intravenous injection metastasis models.

### 5.9.6 XPO1 inhibition and IFNγ modulate the function of anti-CD19 CAR NK cells

In order for *in vivo* experiments to be conducted using CAR NK cells, the first challenge will be to stabilise CAR expression on NK cells (**Figure 5-35**). Although *in vitro* experiments were conducted whilst the CAR was expressed on day 3 post transduction, there will be insufficient CAR NK cell numbers to perform *in vivo* experiments. As such, the CAR requires stabilisation on NK cells which will enable expansion of CAR NK cells *in vitro* before adoptive transfer into mice. There are multiple approaches that may improve CAR stabilisation. First, CAR+ NK cells could be sorted by FACS to obtain pure CAR cultures. This would then determine whether CAR expression is downregulated on NK cells or whether CAR- NK cells outcompete CAR+ NK cells during expansion. Second, irradiated CD19+ targets could be used during expansion to activate and induce proliferation of CAR+ NK cells. Irradiation of CD19+ targets will be required to inhibit their proliferation in cultures. The issue with this technique is that untransduced NK cells will also be activated by cancer targets and this expansion approach introduces a feeder cell. Additionally, CD19+ targets are suspension cells which would make it difficult to separate NK cells from targets cells for downstream applications. Producing an adherent CD19+ cell could avert the suspension target cell problem. Finally, the most realistic and promising approach is to replace the VSV-G lentivirus coat with a baboon-associated lentivirus (BaLV). NK cells are naturally resistant to VSV-G coated lentiviruses and these lentiviruses are widely used for CAR T cell generation (571). The BaLV targets ASCT1/2 receptors for cell entry and these are highly expressed on NK cells as opposed to VSV-G binding LDL receptors (572). As such, NK cell transduction efficacy is massively improved and the stability of CAR expression enhanced (571,572).

Achieving CAR NK cells with stable CAR expression will also allow for NKG2A upregulation on CAR NK cells during two-week expansion. In the CAR NK cell experiments performed here, NK cells were expanded for 5-7 days from initial isolation resulting in a CAR NK cell population with NKG2A+ and NKG2A- NK cells (**Figure 5-38**). As such the full potential of selinexor-CAR NK cell combination may not have been realised (**Figure 5-42**). However, from the one-donor LAMP experiment, it could be argued that selinexor only promotes CAR-NKG2A+ NK cells because the activating signals from the CAR may outcompete the negative NKG2A signalling, resulting in no additional NK activation when HLA-E is downregulated (**Figure 5-42**). Nevertheless, in settings with high HLA-E expression such as

with IFNγ, NKG2A signalling becomes relevant in CAR+ NK cells as NK cell activation was diminished and HLA-E downregulation by selinexor was shown to promote CAR+NKG2A+ NK cell activation (**Figure 5-42**), both of which aligned with the effects on CAR NK cell cytotoxicity (**Figure 5-41**).

The transduction efficacy obtained in this thesis is comparable to that achieved in other studies generating CAR NK cells with VSV-G lentiviruses (541,573). In those studies, *in vitro* experiments were also performed on day 3 post transduction, suggesting stability problems of CAR NK cells used by those research groups. As well as changing the virus coat, the transduction enhancer and NK cell source have also been demonstrated to contribute to transduction efficacy and stability of CAR expression (546). Higher transduction efficacy and increased stability of CAR expression was obtained using cord blood NK cells and NK cell lines compared to peripheral blood NK cells (573,574). Hence, for future CAR NK cell generation the BaLV could be used or a different source of NK cells. Using NK cell lines would be ill-advised since NKG2A is not functionally expressed on NK-92 or NKL cells as selinexor or anti-NKG2A antibodies did not sensitise malignant B cells to NK cell lines (**Figure 5-3** and **Figure 5-4**).

In terms of the CAR construct, changing the CAR to target a different tumour antigen may be warranted since CD19 was downregulated by selinexor and this may impede anti-CD19 CAR NK cell efficacy (**Figure 5-40**). This is indicative of the experiment which demonstrated that NK cell activation with increasing selinexor concentration was driven by CAR-NKG2A+ NK cells rather than CAR+ NK cells, albeit this was performed using only one donor (**Figure 5-42**). A more rational approach may be to target CD20 because CD20 expression was not affected by XPO1 inhibition (**Figure 4-18**). The mechanism behind CD19 downregulation with selinexor remains to be determined, but a recent paper deduced by a CRISPR screen the potential activators and repressors of CD19 expression in malignant B cells and the function and/or expression of these proteins may be effected by selinexor (575).

A proof-of-concept study demonstrated the potential of combining small molecules with NK cell immunotherapy. Nutlin-3a, an MDM2 inhibitor, enhanced the expression of DNAM-1 ligands PVR and Nectin-2 on neuroblastoma cells which promoted the activity of DNAM-1-expressing CAR NK cells (325,326). These studies demonstrated that modulation of NK cell ligands by small molecules could be targeted by CAR NK cell therapy approaches. Although selinexor did not enhance CD19 expression, identifying a target molecule which becomes enhanced at the plasma membrane by selinexor may improve CAR NK cell activation alongside impairing inhibitory signalling by NKG2A.

As well as selinexor promoting CAR NK cell function, NKG2A blockade was also shown to enhance CAR NK cell cytotoxicity against Raji cells (**Figure 5-39**). This is in accordance with recent publications investigating receptors that limit CAR NK cell activation. NKG2A was shown to drive inhibition of anti-BCMA CAR NK cells that target multiple myeloma cells, particularly in settings of high HLA-E

expression such as with IFNγ as reported in **Figure 5-41** (323). Additionally, anti-CD33 CAR NK cells showed enhanced function against AML cells when NKG2A was genetically knocked out (324,576). As such these publications and this thesis demonstrate the importance of NKG2A to impede CAR NK cell functions which can be overcome by inhibiting NKG2A-HLA-E interactions.

### 5.9.7 Future studies investigating the consequences of selinexor-induced HLA-E downregulation on macrophage and NKG2A+ T cell function

Macrophages play important roles in phagocytosis and antigen presentation to T cells and are the most abundant immune cell type in DLBCL (467). Selinexor has been shown to modulate macrophage polarisation and viability. Jiménez et al., (2020) reported that XPO1 inhibition can regulate macrophage polarisation from M2-like pro-tumour macrophages to M1-like anti-tumour macrophages. Additionally, selinexor can specifically deplete lymphoma-associated macrophages in murine models of cancer which improved mouse survival (456). In this chapter, XPO1 inhibition was shown to also modulate macrophage phagocytosis by sensitising Raji cells to increased phagocytosis (**Figure 5-49**). The mechanism remains to be deduced, but the IFNγ-induced HLA-E expression was unable to impair macrophage phagocytosis despite recent evidence that HLA-E is a ligand for the inhibitory macrophage receptors LILRB1/2 (**Figure 5-50**) (34). This may be because HLA-E was maximally inhibiting phagocytosis therefore any further increase in HLA-E expression did not impact phagocytosis, but downregulation by selinexor potentially could induce phagocytosis. Further experiments with increased numbers of donors and different lymphoma cell lines will confirm whether selinexor sensitises B-cell lymphoma cells to phagocytosis and the use of anti-HLA-E antibodies will provide insight into whether disrupting HLA-E:LILRB1/2 interactions promotes phagocytosis.

In accordance with our CAR T cell findings, XPO1 inhibition has been shown to sensitise B cell lymphoma and leukaemia cell lines to anti-CD19 CAR T cells (459). The mechanism described was decreased expression of PD-1, LAG-3 and TIM-3 exhaustion markers on CAR T cells after co-culture with SINE-treated malignant B cell lines, but exactly why this occurs was not explored. Therefore, the mechanism behind improved CAR T cell function with selinexor remains to be confirmed. Regardless, pre-clinical studies have also demonstrated improved anti-tumour immunity when anti-CD19 CAR T cells are combined with selinexor (460). NKG2A is specifically expressed on CD8+ T cells (577), therefore future flow cytometry experiments using T cells should include anti-CD4 and anti-CD8 antibodies to discriminate between these two T cell populations, especially given that CAR T cells are a heterogeneous population (209). Therefore, it will be important to express NKG2A on CD8+ cytotoxic T cells in order to study how XPO1 inhibition directly affects CD8+ T cell activation and CD8+ T cell-mediated lysis of targets.

During the course of CAR T cell treatment in DLBCL patients, NKG2A becomes upregulated as soon as 28 days post infusion (214). This reflects the fact that after repeated rounds of stimulation NKG2A becomes upregulated on murine T cells (210). In **Figure 5-46** repeated stimulation of human circulating T cells failed to induce NKG2A, perhaps reflecting the differences between murine and human checkpoint receptor expression. The failure to induce NKG2A on T cells may be due to incorrect cytokines (IL-7 and IL-15) in the culture. IL-15 alone (577), IL-12 (211,578) and TGFβ (579) have been reported to induce NKG2A expression, therefore to study NKG2A function on T cells with selinexor, T cells should be stimulated and expanded with IL-12, IL-15 or TGFβ. Besides CAR T cells, it will be particularly important to study NKG2A function on T cells because it is becoming increasingly evident that NKG2A identifies tumour-specific T cells (194,213,275) and recently NKG2A was shown to be involved in resistance to anti-PD1 and anti-LAG3 therapy (211). Therefore by abrogating NKG2A signalling a potent anti-tumour T cell immune response may be induced and T cell resistance to antibody blockade may be negated (43,278). In this context, it will be interesting to examine how XPO1 inhibition modulates NKG2A+ T cell function via downregulation of HLA.

# Chapter 6 The NK cell immunomodulatory effect of XPO1 inhibition in multiple myeloma cell lines

## 6.1 HLA-E expression on multiple myeloma cell lines treated with selinexor

Selinexor is also approved for the treatment of relapsed/refractory multiple myeloma as well as DLBCL, therefore it was investigated whether multiple myeloma cells respond similarly to XPO1 inhibition in terms of activating an NK cell immune response. Selinexor induced the degradation of XPO1 and induce apoptosis as shown by appearance of cPARP in the multiple myeloma cell line MM1S (**Figure 6-1**). Total HLA-E protein levels remained constant across selinexor concentrations (**Figure 6-1**). With Q-VD, the absence of cPARP indicates successful inhibition of selinexor-induced apoptosis which will permit robust analysis of NK cell cytotoxicity experiments measuring NK specific lysis of multiple myeloma cells.

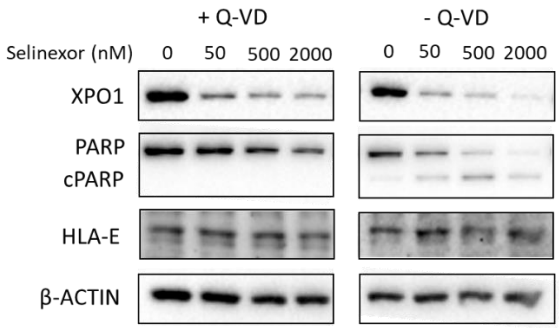


**Figure 6-1: Total HLA-E expression and PARP cleavage in MM.1S cells treated with selinexor in the presence of the apoptotic inhibitor Q-VD.**

Western blot analysis of HLA-E protein expression in MM1S cell treated with selinexor (50-2000 nM) or DMSO (0 nM) for 24 hours in the presence and absence of the apoptotic inhibitor Q-VD (30 μM). Apoptotic signalling leads to caspase-dependent PARP cleavage (cPARP, lower molecular weight) and therefore cPARP abundance correlates with apoptosis in cells. Shown is one western blot experiments from two and β-ACTIN was used as a loading control.

Next surface expression levels of HLA-E were assessed after XPO1 inhibition in multiple multiple myeloma cell lines. HLA-E was downregulated on three of the six cell lines (MM1S, OPM2 and U266) whilst total HLA expression (HLA-A/B/C) did not change with XPO1 inhibition (**Figure 6-2**). For AMO, JJN3 and L363 cell lines surface HLA-E expression level did not change with XPO1 inhibition, perhaps due to the low basal level of HLA-E on these cell lines.

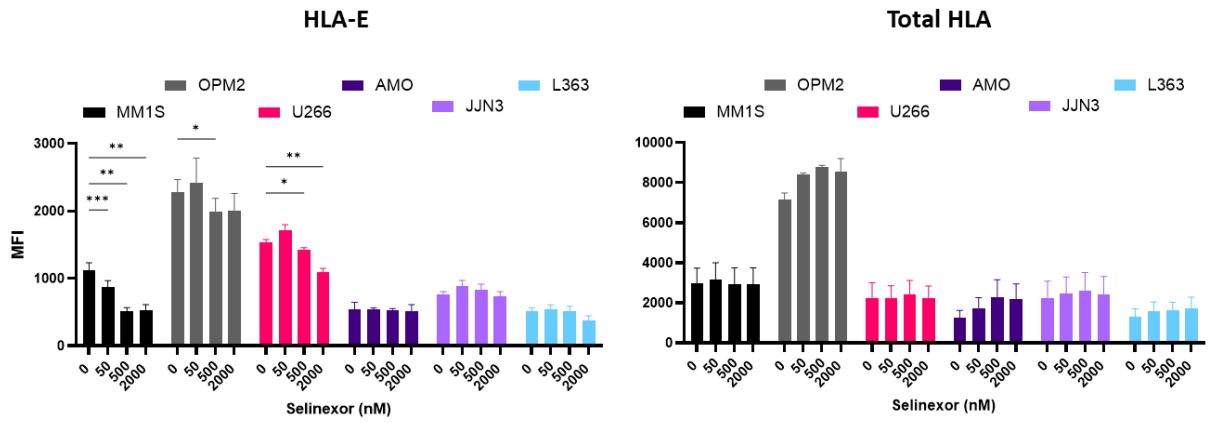


**Figure 6-2: Selinexor downregulates HLA-E on multiple myeloma cells with high basal levels of HLA-E.**

Multiple myeloma cell lines MM1S, OPM2, U266, AMO, JJN3 and L363 were treated with selinexor (50-2000 nM) or DMSO control (0 nM) for 24 hours and the surface expression of HLA-E (using the 3D12 antibody clone) and total HLA class I (using the W6/32 antibody clone) was assessed by flow cytometry. Shown is the mean MFI of samples ± SEM for at least 3 replicates performed over individual experiments and significant differences in surface expression of HLA proteins between the untreated control and selinexor treatments were calculated with two-way ANOVA followed by Dunnett's post-hoc test: ***P<0.001, **P<0.01, *P<0.05.

## 6.2 NK cell function against multiple myeloma cells treated with selinexor

Next, because HLA-E was downregulated on MM1S cells with XPO1 inhibition, the sensitivity of MM1S cells to resting NKG2A+ NK cells after treatment with selinexor was assessed. MM1S cells were treated with selinexor for 24 hours and then co-cultured with healthy donor PBMC and the activation of NKG2A positive (NKG2A+) and negative (NKG2A-) CD56+CD3- NK cell populations was assessed by flow cytometry staining of CD107a. With selinexor MM1S cells were sensitised to NKG2A+ NK cell activation due to the selinexor-induced HLA-E downregulation (**Figure 6-3A**). When selinexor-treated MM1S cells were co-cultured with purified NK cells, NK cell cytotoxicity was enhanced compared to DMSO control (**Figure 6-3B**). Finally, given that NKG2A is highly expressed on

14-day, IL-2 expanded NK cells, selinexor-treated MM1S cells were co-cultured with expanded NK cells and NK cell cytotoxicity was assessed. Indeed, expanded NK cells were highly cytotoxic towards selinexor-treated MM1S cells in a dose-dependent manner (**Figure 6-3C**).

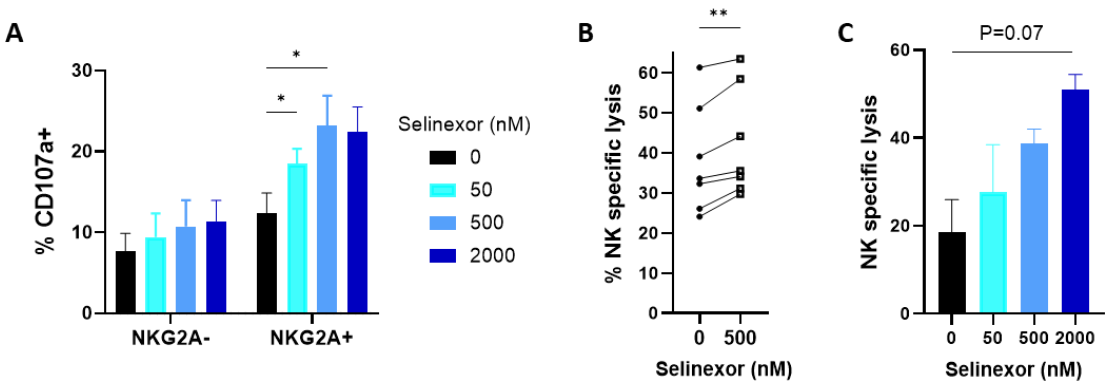


**Figure 6-3: Selinexor sensitises MM1S cells to NKG2A+ NK cell activation and cytotoxicity.**

MM1S cells were treated for 24 hours with the indicated concentrations of selinexor in the presence of the apoptotic inhibitory Q-VD and then co-cultured for four hours with PBMC to assess NKG2A+ NK cell activation (**A**), co-cultured with purified NK cells to examine NK specific lysis (**B**) or co-cultured with 14-day, IL-2 expanded NK cells with upregulated NKG2A expression to assess NK cytotoxicity (**C**). NK cell activation in **A** was measured as percentage of CD107a+ cells within the CD56+CD3-NKG2A+/- NK cell populations. Shown is mean ± SEM of one experiment using NK cells from three individual donors. Significant differences in NK cell activation within NKG2A NK cell populations between DMSO and selinexor treatments were calculated with repeated-measure two-way ANOVA followed by Dunnett's post-hoc test: *P<0.05. NK specific lysis in **B and C** was calculated as *(% target lysis - % spontaneous lysis) * 100 / (100 - % spontaneous lysis).* MM1S cells were pre-labelled with CellTrace™ to allow identification within co-cultures and lysis was measured using propidium iodide staining. Each line matches DMSO and selinexor-treated wells of the same NK cell donor (n=7, **B**). A significant difference in NK specific lysis between DMSO and selinexor-treated was calculated with paired sample t-test: **P<0.01. Shown in **C** is mean NK specific lysis ± SEM of three individual donor NK cell expansions and significant differences in NK specific lysis between DMSO and selinexor treatments were calculated with repeated-measure one-way ANOVA followed by Dunnett's post-hoc test.

## 6.3 IFNγ treatment of multiple myeloma cells and the effects on HLA-E expression and NK cell function

### 6.3.1 The effect of IFNγ and XPO1 inhibition on the expression of HLA-E in multiple myeloma cell lines

As shown in **Figure 6-2**, basal levels of HLA-E are very low on L363, AMO and JJN3 cell lines which potentially effected the HLA-E downregulation by selinexor as seen with 721 and SUDHL6 cell lines (**Figure 5-17**) in earlier chapters. IFNγ is an important cytokine in the bone marrow for bone remodelling by osteoclasts (580) and IFNγ production by T cells and NK cells is essential for conferring protection from multiple myeloma in mice (581). As such myeloma cells of the bone marrow will be immersed in an IFNγ-rich microenvironment and recombinant IFNγ (rIFNγ) is frequently used to model the pro-inflammatory multiple myeloma microenvironment *in vitro* (314,582–584). Additionally, multiple myeloma cells injected into mice have higher HLA-E expression compared to pre-infusion, suggesting that ways to increase HLA-E expression on multiple myeloma cells will better reflect an *in vivo* environment (585). Therefore, it was assessed whether rIFNγ induces HLA-E expression on L363 multiple myeloma cells with low HLA-E expression and whether XPO1 inhibition can counteract this. L363 cells were incubated with 10 ng/mL rIFNγ in the presence and absence of selinexor for 24 hours and the surface expression of HLA-E and HLA-A/B/C was measured by flow cytometry. With IFNγ, HLA-E and HLA-A/B/C expression increased on L363 cells (**Figure 6-4**). However, when L363 cells were treated with selinexor, only HLA-E surface expression was reduced, highlighting an HLA-E specific effect of XPO1 inhibition (**Figure 6-4**).

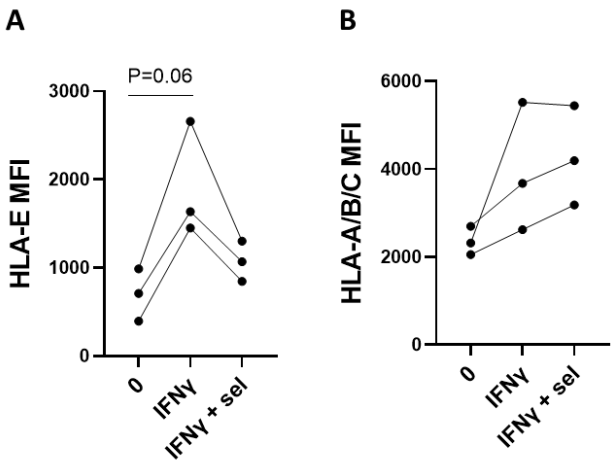


**Figure 6-4: IFNγ enhances HLA-E expression on L363 cells, which is overcome by selinexor.**

L363 multiple myeloma cells were incubated with recombinant IFNγ (10 ng/mL) in the absence and presence of selinexor (sel, 500 nM) for 24 hours. Cells were then surface stained with antibodies against HLA-E (clone 3D12, **A**) and HLA-A/B/C (clone W6/32, **B**) and the MFI was measured by flow cytometry. The experiment was run across three separate experiments and matched samples from the same experiments are joined by lines.

To determine the mechanism of HLA-E downregulation by selinexor in the presence of IFNγ in L363 cells, surface and internal HLA-E expression was assessed to ascertain whether surface levels or total HLA-E levels change with XPO1 inhibition (**Figure 6-5**). Following IFNγ incubation surface levels and total levels of HLA-E and HLA-A/B/C increased (**Figure 6-5**). In the absence of IFNγ, although not significant, XPO1 inhibition slightly reduced surface HLA-E expression whilst total HLA-E levels remained constant and HLA-A/B/C expression was not affected by XPO1 inhibition. XPO1 inhibition in conjunction with IFNγ incubation resulted in impaired HLA-E upregulation by IFNγ, however the IFNγ-induced increase in HLA-A/B/C was unaffected by XPO1 inhibition (**Figure 6-5**). These data demonstrate that IFNγ induces the expression of HLA class I molecules in L363 multiple myeloma cells, but XPO1 inhibition selectively impairs HLA-E upregulation with IFNγ and this may have implications on NK cell functions.

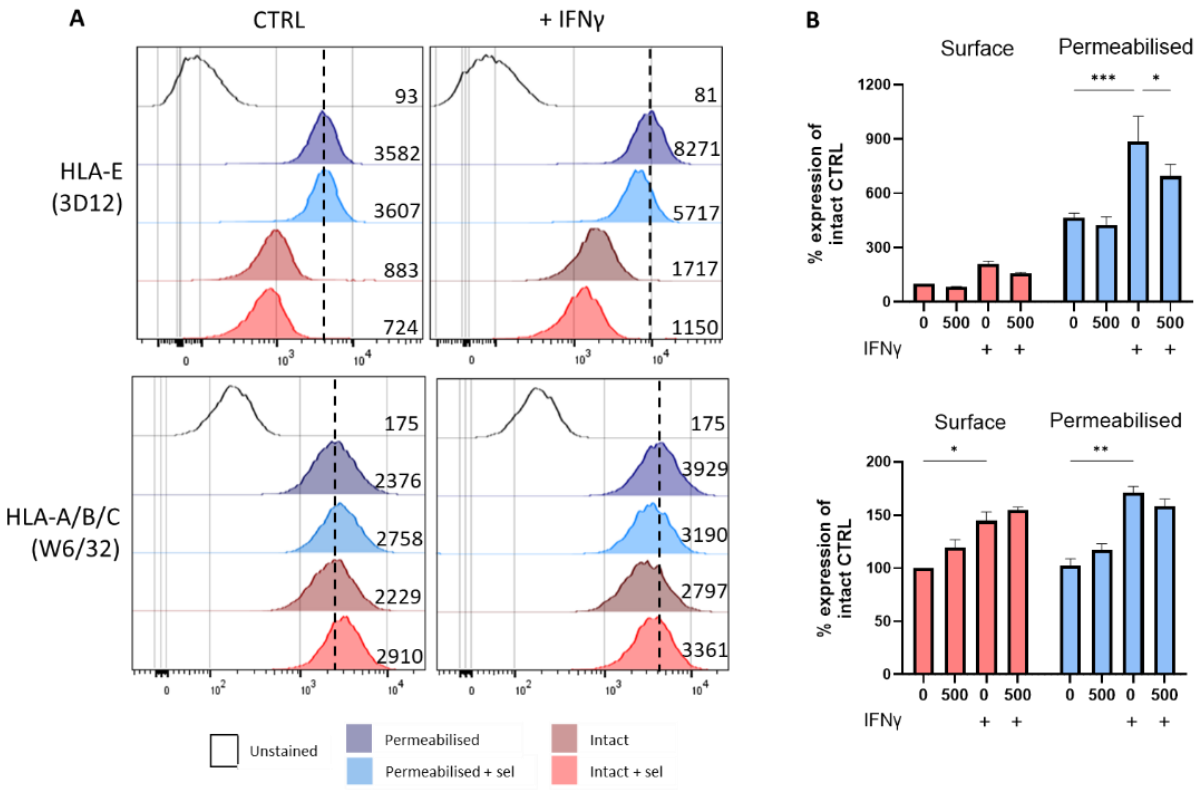


**Figure 6-5: Surface and total expression levels of HLA-E in L363 cells treated with selinexor in the presence of IFNγ.**

L363 cells were treated with selinexor (sel, 500 nM) or DMSO (0 nM) for 24 hours in the presence or absence of IFNγ (10 ng/mL) followed by staining with antibodies against HLA-E (clone 3D12) and HLA-A/B/C (clone W6/32) when cells were permeabilised (intracellular and extracellular expression) or left intact (surface expression). (**A**) Representative histograms of 3D12 and W6/32 staining intensities of L363 cells from one experiment. Numbers on histograms depict the MFI and vertical dashed lines represent the histogram peak in the permeabilised, untreated sample. (**B**) Mean expression ± SEM relative to the DMSO-treated (0 nM) control in the absence of IFNγ in intact and permeabilised L363 cells (n=3). Significant differences in HLA expression between treatment groups for intact and permeabilised cells were calculated with two-way ANOVA followed by Tukey's post-hoc test: ***P<0.005, **P<0.01, *P<0.05.

As shown in section 5.5, XPO1 inhibition impaired STAT1 phosphorylation in B-cell lymphoma cells by IFNγ. Whether this is replicated in L363 multiple myeloma cells was assessed by western blot. IFNγ incubation led to a large increase in STAT1 phosphorylation (pSTAT1) and subsequently an increase in HLA-E expression (**Figure 6-6**). When selinexor was added to cultures pSTAT1 levels decreased as well as total STAT1 (tSTAT1) because STAT1 autoregulates its transcription (39) and this correlated with a downregulation of HLA-E (**Figure 6-6**). Therefore, in a similar mechanism as with B-cell lymphoma, XPO1 inhibition impairs the IFNγ-induced HLA-E upregulation via disruption to STAT1 signalling.

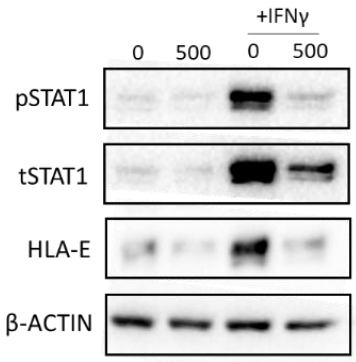


**Figure 6-6: Selinexor impairs IFNγ signalling in L363 cells.**

Western blot analysis of HLA-E protein expression in L363 cells treated with selinexor (500 nM) or DMSO (0 nM) for 24 hours in the presence and absence of IFNγ (10 ng/mL) and the apoptotic inhibitor Q-VD (30 μM). Apoptotic signalling leads to caspase-dependent PARP cleavage (cPARP, lower molecular weight) and therefore cPARP abundance correlates with apoptosis in cells. Shown is one representative experiment of two repeats and β-ACTIN was used as a loading control.

### 6.3.2 Expanded NK cell function against multiple myeloma cells incubated with IFNγ in the presence of XPO1 inhibitors

To explore how NK cell anti-tumour functions against L363 multiple myeloma cells are impacted by IFNγ and XPO1 inhibitors, the cytotoxicity of IL-2 expanded NK cells against L363 cells was assessed, with the hypothesis that the IFNγ-induced HLA-E upregulation would protect L363 cells from NK-mediated lysis and this would be reversed by XPO1 inhibition. As hypothesised, IFNγ protected L363 cells from NK cytotoxicity and this was reversed by XPO1 inhibition with selinexor, even at a low E:T ratio of 1:10 (**Figure 6-7A and B**). To illustrate the importance of HLA-E:NKG2A interactions in contributing to the IFNγ-induced protection in L363 cells, anti-NKG2A monoclonal antibodies were added to NK-L363 co-cultures. Similar to XPO1 inhibition, NKG2A blockade with antibodies completely reversed the protection conferred by IFNγ incubation (**Figure 6-7A**). Combined selinexor and anti-NKG2A treatment resulted in no additional benefit to NK cytotoxicity compared to monotherapy (**Figure 6-7A**). Albeit the sample number was small for anti-NKG2A experiments and further repeats are required to confirm this observation.

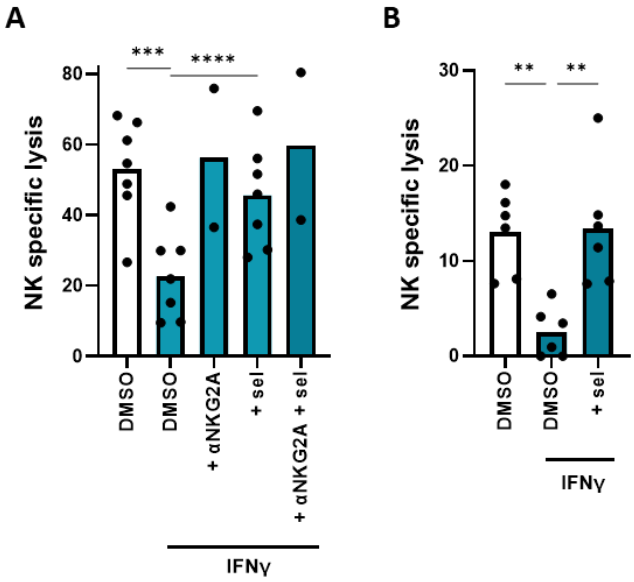


**Figure 6-7: IFNγ protects L363 cells from expanded NK cell cytotoxicity, which is reversed by selinexor.**

L363 multiple myeloma cells were pre-labelled with CellTrace™ and treated with selinexor (500 nM, sel) in the presence of IFNγ (10 ng/mL) and the apoptotic inhibitor Q-VD (30 µM) for 24 hours. L363 cells were subsequently co-cultured with day-14, IL-2 expanded NK cells for a further 24 hours at an E:T ratio of 1:1 (**A**) or 1:10 (**B**) in the absence or presence of anti-NKG2A monoclonal antibodies (αNKG2A, clone Z199). The proportion of lysed L363 cells in co-cultures was measured by propidium iodide staining and NK specific lysis calculated as *(% target lysis - % spontaneous lysis) * 100 / (100 - % spontaneous lysis).* Each point represents an individual NK cell donor (n=6 and n=2 for **A** and n=6 for **B**) and bars show the mean NK specific lysis for each treatment and differences in NK specific lysis between treatment groups and the IFNγ DMSO control were calculated by one-way ANOVA followed by Tukey's post-hoc test: ****P<0.001, ***P<0.005, **P<0.01.

### 6.3.3 The effect of XPO1 inhibition on the expression of receptors targeted by monoclonal antibody therapy and CAR immune cells in multiple myeloma

Immunotherapy treatments for patients with multiple myeloma include anti-CD38 monoclonal antibody (mAb) therapy using daratumumab and CAR T cell therapy against the B-cell maturation antigen (BCMA) (305). Although NK cells also express CD38 leading to NK cell fratricide with daratumumab, NK cells are important in anti-CD38 mAb efficacy (263). Additionally, CAR NK cells targeting CD38 and BCMA are undergoing pre-clinical investigation to determine the effectiveness of CAR NK cell approaches in multiple myeloma (313,322). As such, it was explored whether XPO1 inhibition modulates the expression of these antigens to determine the potential of combining selinexor with immunotherapy approaches that promote NK cell function. XPO1 inhibition had a minimal effect on CD38 expression for most cell lines tested, but interestingly selinexor treatment of

AMO enhanced CD38 expression (**Figure 6-8A**). U266, JJN3 and L363 cells were virtually negative for CD38. BCMA was lowly expressed on cell lines and XPO1 inhibition had a limited effect on BCMA expression, although it could be argued that BCMA decreased on MM1S, L363 and U266 cells, however the variation across samples was very large and was not statistically significant (**Figure 6-8B**). Therefore, when planning ADCC experiments with daratumumab and designing CAR NK cells against BCMA the target cells used in assays should be carefully considered.

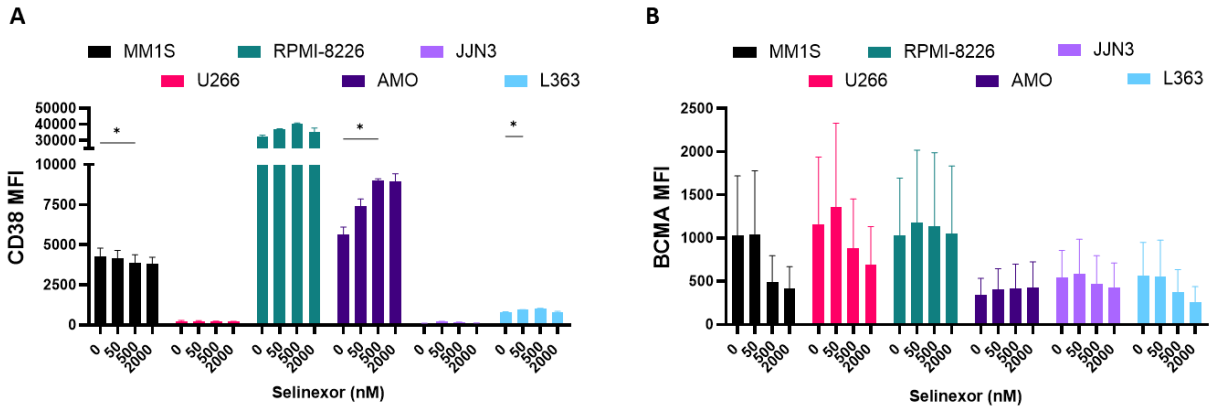


**Figure 6-8: CD38 and BCMA expression on selinexor-treated multiple myeloma cell lines.**

Multiple myeloma cell lines were treated with selinexor (50-2000 nM) or DMSO for 24 hours and assessed for expression of CD38 (**A**) and BCMA (**B**) by flow cytometry. Shown is mean MFI ± SEM of three separate experiments and significant differences in expression of CD38 and BCMA between DMSO and selinexor samples were calculated with one-way ANOVA followed by Tukey's post-hoc test: *P<0.05.

## 6.4 Discussion

### 6.4.1 HLA-E downregulation by XPO1 inhibition on multiple myeloma cell lines

Similar to XPO1 inhibition in B-cell lymphoma cell lines, multiple myeloma cell lines also specifically downregulate surface HLA-E expression (**Figure 6-2**) and as illustrated with MM1S cells, become sensitised to NKG2A+ NK cell activation and to expanded NK cell cytotoxicity (**Figure 6-3**). The importance of NK cells in multiple myeloma is highlighted by multiple studies. An expansion of adaptive NK cells in patients who received autologous stem cell transplantation had a lower risk of relapse (586). Within patients, NK cells present with an exhausted phenotype (238) and newly diagnosed patients with higher NK cell activity have improved survival (587). Recently, it was reported that multiple myeloma patients with impaired NK cell adhesion and limited cytotoxic capacity have worse prognosis (385). These studies demonstrate the critical functions of NK cells against multiple myeloma cells and interestingly, with selinexor it was demonstrated that NK cell infiltration into the bone marrow of myeloma patients was a potential marker of response indicating that NK cells may positively contribute to the selinexor-induced myeloma regression in patients (463). Strategies to enhance NK cell function in multiple myeloma patients are being explored including NK cell engagers and adoptive transfer approaches using allogeneic and CAR NK cells which could be combined with selinexor to promote optimal tumour regression (588).

Besides the MM1S cell line, it can be hypothesised that enhanced NK cell activation with XPO1 inhibitors will be observed for OPM2 and U226 cell lines because these also downregulated HLA-E after XPO1 inhibition (**Figure 6-2**). For AMO, JJN3 and L363 cell lines HLA-E downregulation was not induced by selinexor treatment, perhaps due to the low basal levels of HLA-E (**Figure 6-2**), similar to that of 721 cell lines and SUDHL6 (**Figure 5-17**). As can be seen for L363 cells in **Figure 6-5**, HLA-E is mainly expressed internally because there was a great disparity between the MFI of HLA-E in permeabilised and intact cells. As such, HLA-E trafficking at homeostasis may be impaired in L363, AMO and JJN3 cells, perhaps due to limited HLA-E binding peptide availability as HLA-A/B/C expression was also low in these cell lines (**Figure 6-2**). Hence through using selinexor to inhibit XPO1, HLA-E was unable to be further downregulated at the plasma membrane.

### 6.4.2 HLA-E downregulation on multiple myeloma cell lines by XPO1 inhibition in the presence of IFNγ

IFNγ is routinely used to mimic the pro-inflammatory TME and induce the surface expression of HLA-E on multiple myeloma cells (314,585,589). In the myeloma cell lines tested here, HLA-E was greatly upregulated in a STAT1-dependent manner which XPO1 inhibition was able to disrupt via inhibition of STAT1 nuclear export (38) (**Figure 6-4**, **Figure 6-5** and **Figure 6-6**). The importance of the IFNγ-induced HLA-E upregulation in protecting L363 cells from expanded NK cells was demonstrated with anti-NKG2A antibodies which recovered NK cell cytotoxicity (**Figure 6-7**). The activation of STAT1 by IFNγ in multiple myeloma has been long understood (584), but the consequence on NK cell function has only recently been revealed, in accordance with the findings here, illustrating that multiple myeloma cells are resistant to NK cell functions via HLA-E:NKG2A interactions (536,583). HLA-E and IFNγ signalling via STAT1 were top hits during an in-depth analysis into the mechanisms of resistance to NK cells in multiple myeloma (144). Following these revelations, functional analyses using CRISPR deletion of IFNγ signalling components (*IFNGR2, JAK1/2* and *STAT1*) and *HLA-E* sensitised myeloma cells to NK cell cytotoxicity. This research article clearly demonstrates the inhibitory consequences of IFNγ signalling in myeloma cells on NK cell function and suggest that pharmacologically perturbing IFNγ signalling will sensitise cells to NK cell activation. The data produced here indicate that XPO1 may be a good target to perturb the IFNγ-induced resistance to NK cells in multiple myeloma.

Replicating a pro-inflammatory microenvironment in myeloma cells with IFNγ better recapitulates the *in vivo* environment as when human myeloma cells are intravenously injected into mice and transit to the bone marrow, HLA-E is more highly expressed compared to cells *in vitro* (585). In humans, HLA-E is more highly expressed on plasma cells from myeloma patients compared to healthy controls and during progressive disease HLA-E becomes upregulated (323). IFNγ production by NK cells is crucial to exert cytotoxic effects against myeloma cells (581) and interestingly, IFNγ signalling in patient myeloma cells has been associated with response to selinexor, thus suggesting an on-going immune response within the bone marrow with XPO1 inhibition (590). The data presented in this thesis may provide an explanation for increased IFNγ signalling due to increased production of IFNγ by NKG2A+ immune cells via HLA-E downregulation with selinexor. The data collected here also add to recent data showing that important myeloma microenvironment factors PGE2, lactate and hypoxia also protect myeloma cells, including L363, from NK cells, although the mechanism of this inhibition remains to be determined (591). It will be interesting to examine whether XPO1 inhibition in myeloma cells can counteract these inhibitory stimuli. Collectively, these findings on the immunomodulatory effects of microenvironmental stimuli highlight the importance of modelling tissue environments to increase understanding of the regulatory molecules involved in immunosuppression/activation which will ultimately enable the design of improved anti-cancer therapies.

### 6.4.3 Future experiments investigating the immunomodulatory effect of XPO1 inhibition in multiple myeloma cells and the consequences for NK cell immunotherapy combinations

To confirm whether the NK cell sensitising effect of XPO1 inhibition in multiple myeloma is physiologically relevant, it will be important to perform the experiments outlined here using patient-derived cells. High HLA-E expression in multiple myeloma patients has been associated with worse progression free survival (50), demonstrating that HLA-E:NKG2A interactions may be important for myeloma cell survival and therefore targeting this pathway in patients may improve response to approved therapies and improve survival. As selinexor modulates this inhibitory interaction and CD16 expression is maintained on NK cells during expansion (**Figure 5-2**) it will be interesting to determine whether XPO1 inhibition promotes the effect of NK-stimulating immunotherapy such as CAR NK cells and monoclonal antibodies such as daratumumab (anti-CD38 mAb) both in the laboratory and in clinical trials. A recent study by Reddy et al., (2023) demonstrated by RNA sequencing that selinexor increases the immunogenicity of patient myeloma cells by increased CD38 and SLAMF7 expression. Whether this has functional consequences on NK cell activation and specifically NKG2A+ NK cell activation will be of interest to explore.

Alongside modulating HLA-E expression, XPO1 inhibition increased the expression of CD38 on L363 and AMO cells (**Figure 6-8**) and as a result may potentiate ADCC by Daratumumab. HDACs have also been shown to increase CD38 expression on myeloma cells and potentiate ADCC by daratumumab (592). Therefore, it will be interesting to determine whether XPO1 inhibitors can augment ADCC with daratumumab and elotuzumab (anti-SLAMF7). Why CD38 expression on MM1S cells did not increase with XPO1 inhibition remains to be explored, but for U266, JJN3 and L363 CD38 expression was not expressed at homeostasis (**Figure 6-8**). With daratumumab it has to be considered that CD38 is also expressed by NK cells which leads to NK cell fratricide (263). Strategies are underway investigating mechanisms to circumvent CD38 expression on NK cells including daratumumab combination therapy with adoptive transfer of CD38(low) NK cells or NK cells with CD38 blocked by daratumumab $F(ab)_2$ fragments (263,322,593,594). Interestingly, expansion of NK cells has been shown to augment daratumumab *in vitro* against primary myeloma samples (595) and *in vivo* (311,594), therefore selinexor may potentiate ADDC of expanded NK cells with daratumumab. Besides targeting CD38, SLAMF7 is a target of mAb immunotherapy (elotuzumab) for multiple myeloma and how the expression of this receptor changes with XPO1 inhibition should be examined to assess the potential of combining selinexor with elotuzumab.

In terms of BCMA expression, this remained stably expressed on myeloma cell lines except for on MM1S and U266 cells, but further replicates are required to enable more robust analyses and conclusions to be drawn (**Figure 6-8**). BCMA is an approved target of CAR T cell therapy in multiple myeloma (361), however relapse is a common problem with median progression free survival of 5-27

months across studies (361). As such, novel combinations are being assessed including combinations with small molecules (367), such as selinexor. Anti-BCMA CAR T cells have been combined with selinexor in two patients with relapsed/refractory extramedullary multiple myeloma (NCT05201118). Patients were treated with selinexor followed by lymphodepletion and CAR T cell adoptive transfer with further doses of selinexor (462). To date this treatment has induced deep, durable responses in both patients and it would be interesting to determine whether HLA-E:NKG2A interactions contribute to this since NKG2A is upregulated on CAR T cells 28 days post infusion (214). This early clinical trial data demonstrates the potential of combining CAR T cells with selinexor in multiple myeloma and the data presented in this chapter indicate that XPO1 inhibition may enhance the efficacy of CAR NK cells, especially given that HLA-E:NKG2A interactions have been shown to drive multiple myeloma resistance to anti-BCMA CAR NK cells (323).

# Chapter 7 Discussion

In summary, the work outlined in this thesis demonstrated that XPO1 inhibition with the clinically approved, first-in-class XPO1 inhibitor selinexor promotes NK cell function against malignant B cells and multiple myeloma cells via disruption of NKG2A:HLA-E interactions. This remained true for microenvironments that stimulate HLA-E expression on cancer cells such as mimicking the pro-inflammatory tumour microenvironment with IFNγ and, revealed for the first time here, with the lymph node-associated molecules IL-4 and CD40L. These findings are in accordance with high HLA-E expression on multiple tumour types (46,243,372), most likely due to inflammatory signalling within the TME (34). Modulating NKG2A:HLA-E interactions within the TME is a focus of intense research with the NKG2A blocking mAb monalizumab in phase III clinical trials in combination with durvalumab for advanced non-small cell lung cancer (NCT05221840) and for head and neck squamous cell carcinoma in combination with cetuximab (NCT04590963) (276,277).

Modulation of immune cell functions by small molecules in addition to their intrinsic anti-cancer toxicities is becoming increasingly evident (388) and these present an opportunity for tailored immunotherapy combinations (367). One mechanism for which anti-cancer agents can promote immune cell function is via inhibition of HLA-E:NKG2A interactions. For example, the proteasome inhibitor bortezomib (403) and CREB inhibitors (583) downregulate HLA-E expression on tumour cells. Moreover, the tyrosine kinase inhibitor dasatinib downregulates NKG2A on AML patient NK cells (405). This research project has added to this literature by illustrating that XPO1 inhibitors possess NK cell immunmodulatory activity via downregulation of HLA-E expression on B-cell lymphoma and multiple myeloma cell lines (596) and on primary CLL cells (597).

The mechanism by which selinexor downregulates HLA-E expression was due to impaired intracellular trafficking to the plasma membrane (**Figure 7-1**). HLA-E has fast internalisation kinetics due to unstable peptide presentation at the plasma membrane and due to its cytoplasmic tail which more readily recruits clathrin to mediate endocytosis (9). Hence, in the presence of XPO1 inhibitors, it is hypothesised that impaired global protein translation rates reduce the HLA-E-peptide binding pool which is required to stimulate egress of HLA-E from the endoplasmic reticulum to the plasma membrane (**Figure 7-1**). As such, the slow trafficking of HLA-E to the plasma membrane with XPO1 inhibitors reduces total HLA-E surface levels and indeed disruption of the peptide pool via proteasome inhibition with bortezomib selectively decreases HLA-E surface expression (403).

Blocking NKG2A:HLA-E interactions may be particularly important for tumours immersed in an environment that promotes HLA-E expression such as the lymph nodes and in a pro-inflammatory environment rich in IFNγ. Indeed infiltrating NK cells become rapidly dysfunctional upon tumour

entry (245), and intra-tumoral injection of NK cells and anti-NKG2A mAbs have been shown to promote tumour regression in mice (570). In an inflammatory setting, IFNγ induces HLA-E protein expression via STAT1 phosphorylation (36) and XPO1 supports chronic IFNγ signalling through the export of de-phosphorylated STAT1 (38). Within the cytoplasm, STAT1 is then able to be phosphorylated again by JAK1/2 to re-initiate nuclear import and *HLA-E* transcription. Therefore, SINE compounds inhibit the IFNγ-induced HLA-E expression via nuclear retention of unphosphorylated STAT1 (**Figure 7-1**). This mechanism of HLA-E downregulation by selinexor in combination with reduced intracellular transport of HLA-E to the plasma membrane significantly reduces the surface expression of HLA-E (**Figure 7-1**). As a consequence, NKG2A signalling in NK cells is reduced leading to enhanced NKG2A+ NK cell activation and increased NK cell-mediated killing of cancer target cells.

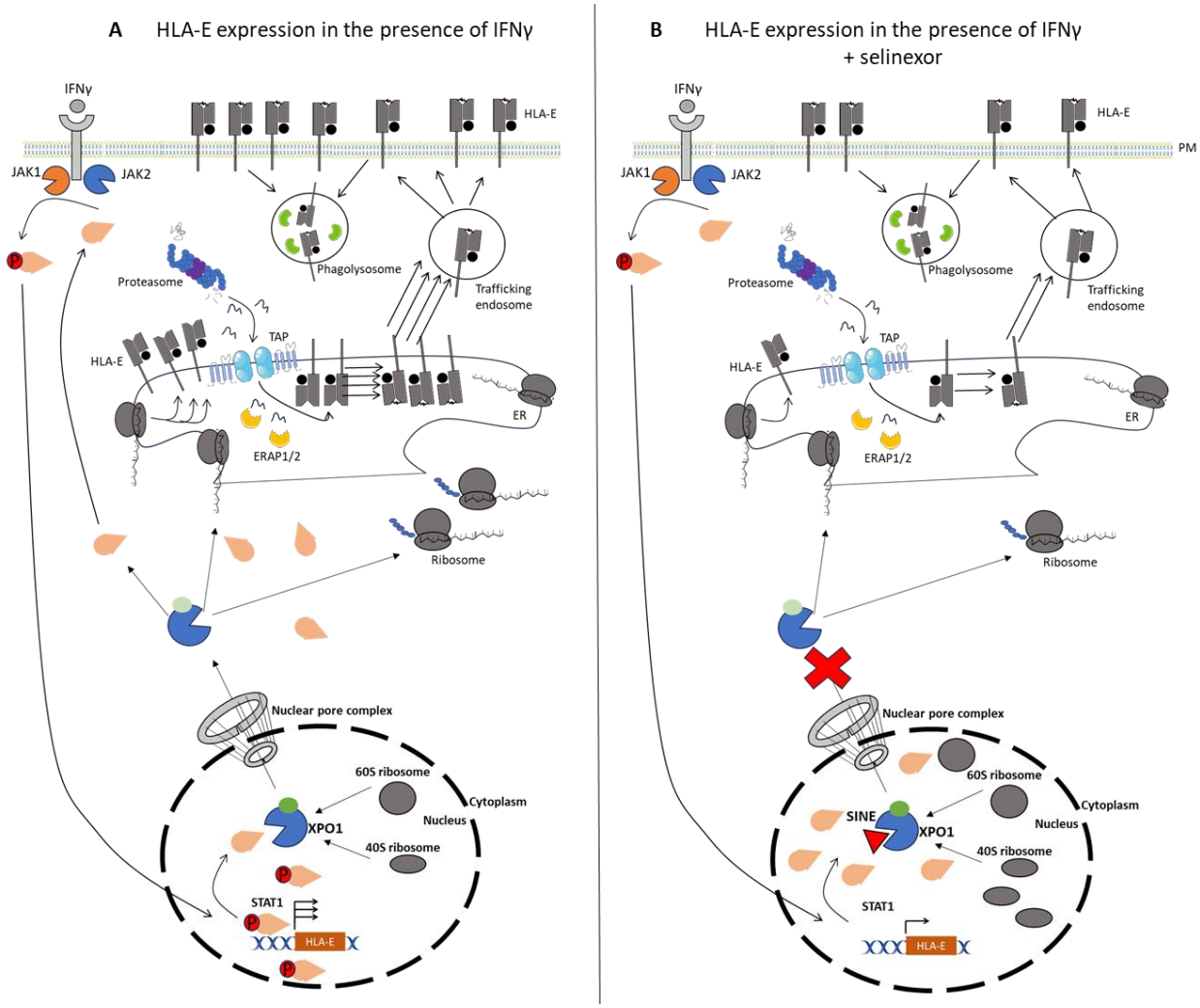


**Figure 7-1: Mechanism for HLA-E downregulation by SINE compounds.**

**(A)** *HLA-E* expression is controlled transcriptionally by phosphorylated STAT1 (pSTAT1) and is translated in the endoplasmic reticulum (ER) where HLA-E is loaded with peptides to stimulate ER egress to the plasma membrane (PM). The instability of the HLA-E-peptide loaded complex at the PM and the intracellular tail of HLA-E induces rapid internalisation. IFNγ in the TME induces the expression of HLA-E by activating STAT1 via phosphorylation by JAK1 and JAK2 kinases. p-STAT1 binds to an enhancer region of *HLA-E* to stimulate its transcription and thus increasing total and surface levels of the HLA-E protein. STAT1 is then dephosphorylated in the nucleus and exported to the cytoplasm to re-initiate the IFNγ-STAT1 phosphorylation signalling cascade. In the presence of selective inhibitors of nuclear export, for example selinexor (**B**), the rate of HLA-E recovery at the plasma membrane is diminished potentially due to inefficient peptide loading in the ER because of the reduced peptide pool. SINE compounds also inhibit the export of STAT1 out of the nucleus and therefore inhibit chronic IFNγ signalling resulting in decreased transcription of *HLA-E* and hence reduced levels of the HLA-E protein. This in combination with reduced plasma membrane trafficking of HLA-E reduces the surface expression of HLA-E.

As a result of increased NKG2A+ NK cell activation by SINE compounds, when selinexor was combined with direct targeting monoclonal antibodies (mAbs), ADCC was enhanced in the NKG2A+ NK cell population (**Figure 7-2**). There is a high infiltration of NK cells in DLBCL patient tumours (467) and NKG2A:HLA-E interactions may be important in DLBCL since *HLA-E* and *Klrc1* gene expression are highly correlated in patient tumours (243). Additionally, patients with CLL possess dysfunctional NK cells and high HLA-E expression may contribute to this (48,372,373) therefore, the use of selinexor combined with ADCC-inducing mAbs may improve tumour regression in patients by stimulating patient NK cells. Selinexor is in multiple clinical trials with the anti-CD20 mAb rituximab for the treatment of DLBCL and with daratumumab and elotuzumab for the treatment of multiple myeloma (**Table 1-2**). Therefore, it will be interesting to determine whether these mAbs combine with selinexor to enhance NKG2A+ NK cell anti-tumour functions in patients and improve tumour regression. NK cell infiltration (463) and IFNγ signalling (590) in the bone marrow is associated with response to selinexor in multiple myeloma, therefore unleashing NK cell anti-tumour functions further with mAbs may induce significant myeloma regression in patients. However, this thesis illustrated that *in vitro* selinexor treatment of autologous CLL patient NK cells impaired ADCC, therefore adoptive transfer approaches with selinexor may be a more effective approach at promoting tumour regression.

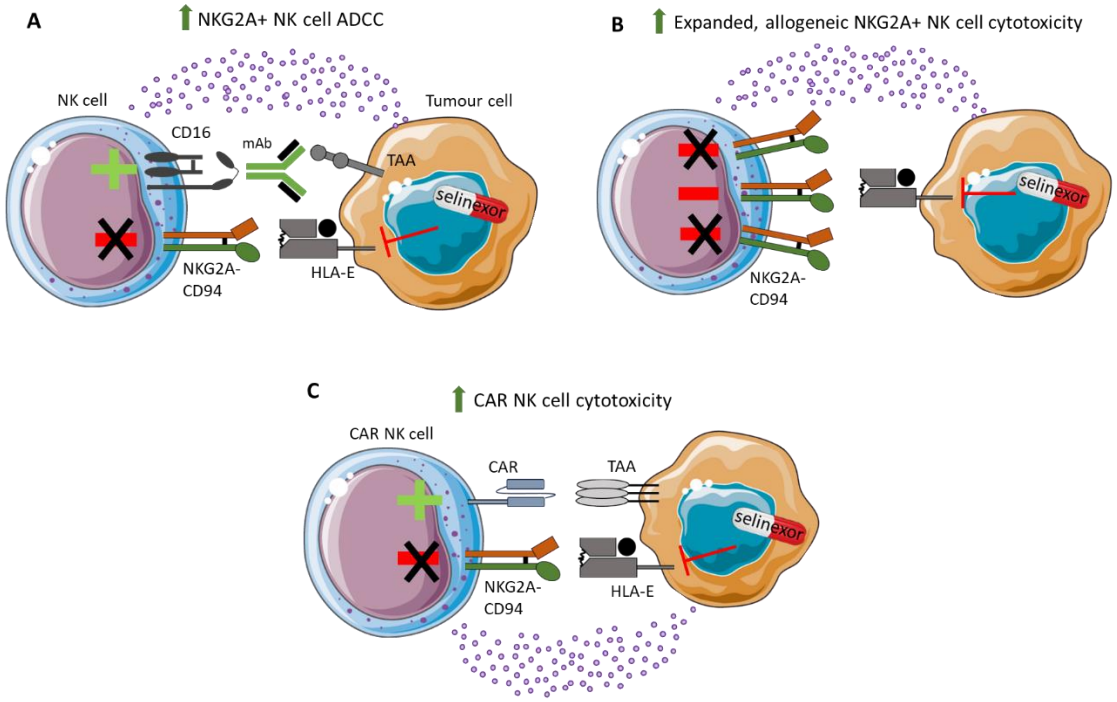


**Figure 7-2: The NK-stimulating immunotherapies promoted by XPO1 inhibition.**

Through the downregulation of HLA-E by XPO1 inhibitors such as selinexor ADCC is enhanced in NKG2A+ NK cells (**A**), the cytotoxicity of expanded, allogeneic NK cells with upregulated NKG2A are increased (**B**) and CAR NK cell function is potentiated (**C**). TAA = tumour-associated antigen.

Adoptive transfer of allogeneic and CAR NK cells show high potential for the treat haematological malignancies. A recent phase I/II clinical trial demonstrated that anti-CD19 CAR NK cells in CLL and DLBCL had a great safety profile with no evidence of cytokine release syndrome or graft-versus-host disease and a 68% 1-year overall survival was achieved (305). As shown here and by other research studies (43,243,480), NKG2A is greatly upregulated on expanded NK cells and these are used to generate CAR NK cells. Therefore, modulation of the NKG2A:HLA-E axis may enhance the efficacy of adoptive transfer and CAR NK cell approaches, and strategies may include the use of XPO1 inhibitors or anti-NKG2A antibodies. Indeed, selinexor and anti-NKG2A mAbs were able to enhance the function of allogeneic, IL-2 expanded NK cells and anti-CD19 CAR NK cells (**Figure 7-2**). This is in accordance with data showing that anti-NKG2A antibodies promote expanded NK cell cytotoxicity (551) and augment the activation of anti-CD33 (576) and anti-BCMA CAR NK cells (323). Additionally, approaches to impede NKG2A expression such as genetic ablation via siRNAs or CRISPR-Cas9 (314,317,480,548,550) or protein expression blockers may improve adoptive NK cell therapy efficacy (243). Pre-clinical experiments are warranted to examine sequential selinexor and adoptive NK cell therapy strategies similar to those conducted in B-cell lymphoma mouse models which investigated

anti-CD19 CAR T in combination with selinexor (460) and similar to phase I/II clinical trials assessing selinexor and anti-BCMA CAR T cell therapy to treat patients with multiple myeloma (461,462).

Recently it was shown that genetic ablation of NKG2A was more effective at promoting NK cell immune responses compared to NKG2A antibody blockade (314). This thesis also demonstrated that complete abrogation of NKG2A:HLA-E interactions by anti-NKG2A mAbs and XPO1 inhibition further promotes NK cell cytotoxicity compared to monotherapy treatments. This observation was potentially due to the differential presentation of peptides by HLA-E which are known modulate the efficacy of NKG2A mAbs (279). Therefore further modulation of HLA-E:NKG2A interactions was required to potently activate NK cells as shown by selinexor treatment.

## 7.1 Limitations of study and future work

The data presented in this thesis indicate that selinexor and adoptive NK cells would most effectively be combined sequentially. Concurrent treatment led to no enhanced killing by expanded NK cells, perhaps due to intrinsic toxicity of selinexor in NK cells, impairment of activating receptor expression and signalling, reduced STAT function, or negative effects on metabolism. These are the main limitations of the presented work. How XPO1 specifically effects NK cell function and how this can be reverted e.g. using cytokine treatment or targeting of specific activating receptors needs exploring. XPO1 is lowly expressed in healthy NK cells compared to NK cell lines (598), thus using primary NK cells will be important to understand how XPO1 inhibition disrupts NK cell functions. NK cancer cell lines can be sensitive or resistant to apoptosis with selinexor (598), therefore using cells lines resistant to apoptosis will help to understand how XPO1 inhibition disrupts NK cell cytotoxic functions.

Another limitation of the study is the lack of identifying the activating signal induced by XPO1 inhibition that is allowing for reduced NKG2A signalling to activate NK cells. Recognizing this, through antibodies against activating receptors in LAMP assays, may identify receptor-ligand interactions that will sensitise cancer cells to selinexor-induced HLA-E downregulation.

Another limitation of the study is the absence of killing assays with sorted NKG2A+ and NKG2A- NK cells, that would have confirmed enhanced cytotoxicity of NKG2A+ NK cells with XPO1 inhibition. It would also have been insightful to conduct NKG2A genetic ablation studies, with the hypothesis that genetic ablation in NK cells eliminates enhanced activation with XPO1 inhibition, similar to the studies conducted with NK-92 and NKL cell lines. Furthermore, the reverse experiment could have been performed through ablation of HLA-E expression in cancer cell lines and assessing the impact on selinexor sensitivity.

In contrast to targeting NKG2A, approaches to specifically target HLA-E may be preferred. This is because HLA-E is highly expressed on tumours (46,243) and HLA-E targetting offers the opportunity to induce ADCC and ADCP in addition to inhibition of NKG2A checkpoint signalling via the IgG1 isotype. Indeed anti-HLA-E mAbs have been identified which potentiate NK cell and macrophage anti-tumour functions (280,281). In this setting, selinexor treatment may hinder anti-HLA-E antibody approaches. Additionally, XPO1 inhibition potentially downregulates CD19 expression on B-cell lymphoma cell lines, but not in CLL, which may have implications for anti-CD19 immunotherapy approaches and approaches targeting other receptors in combination with selinexor require exploration. These highlight the importance of understanding the immunomodulatory effect of small molecules on target proteins to enable the design of potent combination therapy strategies.

## 7.2 Conclusion

The modulation of the inhibitory NKG2A:HLA-E axis by XPO1 inhibitors described in this thesis leads to the sensitisation of malignant B cells and multiple myeloma cells to NK cell anti-tumour functions. As a consequence, selinexor-treated cancer cells are more vulnerable to NK-stimulating immunotherapies such as direct targeting mAbs, expanded, allogeneic NK cells and anti-CD19 CAR NK cells (**Figure 7-2**). This thesis highlights the importance of understanding how small molecules impact the immunogenicity of tumours in addition to their intrinsic toxicity, so that tailored combination therapies can be designed with the aim to induce potent anti-tumour immune responses and cancer cell apoptosis in patients. Pre-clinical studies will shed light on the potential of selinexor and NK-stimulating immunotherapies to promote tumour regression *in vivo* and in the future NK cell immunotherapy approaches may enhance the efficacy of selinexor treatment for patients with B cell malignancies and multiple myeloma.

# List of References


1. Colmenero P, Zhang AL, Qian T, Lu L, Cantor H, Söderström K, et al. Qa-1b-Dependent Modulation of Dendritic Cell and NK Cell Cross-Talk In Vivo. J Immunol. 2007 Oct 1;179(7):4608–15.

2. Aguilar-Hernandez MM, Blunt MD, Dobson R, Yeomans A, Thirdborough S, Larrayoz M, et al. IL-4 enhances expression and function of surface IgM in CLL cells. Blood. 2016 Jun 16;127(24):3015–25.

3. Klein U, Dalla-Favera R. Germinal centres: role in B-cell physiology and malignancy. Nat Rev Immunol 2008 81. 2008 Jan;8(1):22–33.

4. Bournazos S, Gupta A, Ravetch J V. The role of IgG Fc receptors in antibody-dependent enhancement. Nat Rev Immunol 2020 2010. 2020 Aug 11;20(10):633–43.

5. Meyer S, Leusen JHW, Boross P. Regulation of complement and modulation of its activity in monoclonal antibody therapy of cancer. https://doi.org/104161/mabs29670. 2014 Sep 1;6(5):1133–44.

6. Moretta L, Pietra G, Romagnani C, Manzini C, Mingari MC. The emerging role of HLA-E-restricted CD8+ T lymphocytes in the adaptive immune response to pathogens and tumors. Vol. 2010, Journal of Biomedicine and Biotechnology. Wiley; 2010.

7. Braud V, Jones EY, McMichael A. The human major histocompatibility complex class Ib molecule HLA-E binds signal sequence-derived peptides with primary anchor residues at positions 2 and 9. Eur J Immunol. 1997;27(5):1164–9.

8. Vitiello A, Potter TA, Sherman LA. The Role of β 2 -Microglobulin in Peptide Binding by Class I Molecules. Science (80- ). 1990 Dec 7;250(4986):1423–6.

9. He W, Gea-Mallorquí E, Colin-York H, Fritzsche M, Gillespie GM, Brackenridge S, et al. Intracellular trafficking of HLA-E and its regulation. J Exp Med. 2023 Aug 7;220(8).

10. Reich Z, Altman JD, Boniface JJ, Lyons DS, Kozono H, Ogg G, et al. Stability of empty and peptide-loaded class II major histocompatibility complex molecules at neutral and endosomal pH: Comparison to class I proteins. Proc Natl Acad Sci U S A. 1997 Mar 18;94(6):2495–500.

11. Carey BS, Poulton KV, Poles A. Factors affecting HLA expression: A review. Vol. 46, International Journal of Immunogenetics. Int J Immunogenet; 2019. p. 307–20.

12. Le Gall S, Erdtmann L, Benichou S, Berlioz-Torrent C, Liu L, Benarous R, et al. Nef interacts with the μ subunit of clathrin adaptor complexes and reveals a cryptic sorting signal in MHC I molecules. Immunity. 1998;8(4):483–95.

13. O'Callaghan CA, Tormo J, Willcox BE, Braud VM, Jakobsen BK, Stuart DI, et al. Structural features impose tight peptide binding specificity in the nonclassical MHC molecule HLA-E. Mol Cell. 1998;1(4):531–41.

14. Strong RK, Holmes MA, Li P, Braun L, Lee N, Geraghty DE. HLA-E allelic variants. Correlating differential expression, peptide affinities, crystal structures, and thermal stabilities. J Biol Chem. 2003 Feb 14;278(7):5082–90.

15. Braud VM, Allan DSJ, O'Callaghan CA, Soderstrom K, D'Andrea A, Ogg GS, et al. HLA-E binds to natural killer cell receptors CD94/NKG2A, B and C. Nature. 1998 Feb 19;391(6669):795–9.

16. Apps R, Meng Z, Prete GQ Del, Lifson JD, Zhou M, Carrington M. Relative expression levels of the HLA class-I proteins in normal and HIV-infected cells. J Immunol. 2015 Apr 15;194(8):3594.

17. Cassidy SA, Cheent KS, Khakoo SI. Effects of peptide on NK cell-mediated MHC I recognition. Front Immunol. 2014;5(MAR):133.

18. Nguyen AT, Szeto C, Gras S. The pockets guide to HLA class I molecules. Vol. 49, Biochemical Society Transactions. Portland Press Ltd; 2021. p. 2319–31.

19. Lee N, Llano M, Carretero M, Akiko-Ishitani, Navarro F, López-Botet M, et al. HLA-E is a major ligand for the natural killer inhibitory receptor CD94/NKG2A. Proc Natl Acad Sci U S A. 1998 Apr 28;95(9):5199–204.

20. Johnson AE, Van Waes MA. The translocon: a dynamic gateway at the ER membrane. Annu Rev Cell Dev Biol. 1999;15:799–842.

21. Bland FA, Lemberg MK, McMichael AJ, Martoglio B, Braud VM. Requirement of the proteasome for the trimming of signal peptide-derived epitopes presented by the nonclassical major histocompatibility complex class I molecule HLA-E. J Biol Chem. 2003 Sep 5;278(36):33747–52.

22. lo Monaco E, Tremante E, Cerboni C, Melucci E, Sibilio L, Zingoni A, et al. Human leukocyte antigen E contributes to protect tumor cells from lysis by natural killer cells. Neoplasia. 2011;13(9):822–30.

23. Lin Z, Bashirova AA, Viard M, Garner L, Quastel M, Beiersdorfer M, et al. HLA class I signal peptide polymorphism determines the level of CD94/NKG2–HLA-E-mediated regulation of

effector cell responses. Nat Immunol. 2023 Jul 1;24(7):1087.

24. Michaëlsson J, Teixeira de Matos CT, Achour A, Lanier LL, Kärre K, Söderström K. A signal peptide derived from hsp60 binds HLA-E and interferes with CD94/NKG2A recognition. J Exp Med. 2002 Dec 2;196(11):1403–14.

25. Ruibal P, Derksen I, van Wolfswinkel M, Voogd L, Franken KLMC, El Hebieshy AF, et al. Thermal-exchange HLA-E multimers reveal specificity in HLA-E and NKG2A/CD94 complex interactions. Immunology. 2023 Mar 1;168(3):526–37.

26. Huisman BD, Guan N, Rückert T, Garner L, Singh NK, McMichael AJ, et al. High-throughput characterization of HLA-E-presented CD94/NKG2x ligands reveals peptides which modulate NK cell activation. Nat Commun. 2023 Dec 1;14(1).

27. Xu HC, Huang J, Pandyra AA, Lang E, Zhuang Y, Thöns C, et al. Lymphocytes Negatively Regulate NK Cell Activity via Qa-1b following Viral Infection. Cell Rep. 2017 Nov 28;21(9):2528–40.

28. Lu L, Ikizawa K, Hu D, Werneck MBF, Wucherpfennig KW, Cantor H. Regulation of Activated CD4+ T Cells by NK Cells via the Qa-1–NKG2A Inhibitory Pathway. Immunity. 2007 May 25;26(5):593–604.

29. Takao S, Ishikawa T, Yamashita K, Uchiyama T. The Rapid Induction of HLA-E Is Essential for the Survival of Antigen-Activated Naive CD4 T Cells from Attack by NK Cells. J Immunol. 2010 Nov 15;185(10):6031–40.

30. Zhou Z, Zhang C, Zhang J, Tian Z. Macrophages help NK cells to attack tumor cells by stimulatory NKG2D ligand but protect themselves from NK killing by inhibitory ligand Qa-1. PLoS One. 2012 May 18;7(5).

31. McMurtrey C, Harriff MJ, Swarbrick GM, Duncan A, Cansler M, Null M, et al. T cell recognition of Mycobacterium tuberculosis peptides presented by HLA-E derived from infected human cells. PLoS One. 2017 Nov 1;12(11).

32. García P, Llano M, De Heredia AB, Willberg CB, Caparrós E, Aparicio P, et al. Human T cell receptor-mediated recognition of HLA-E. Eur J Immunol. 2002;32(4):936–44.

33. Walters LC, Rozbesky D, Harlos K, Quastel M, Sun H, Springer S, et al. Primary and secondary functions of HLA-E are determined by stability and conformation of the peptide-bound complexes. Cell Rep. 2022 Jun 14;39(11).

34. Middelburg J, Ghaffari S, Schoufour TAW, Sluijter M, Schaap G, Göynük B, et al. The MHC-E

peptide ligands for checkpoint CD94/NKG2A are governed by inflammatory signals, whereas LILRB1/2 receptors are peptide indifferent. Cell Rep. 2023 Dec 26;42(12):113516.

35. Morandi F, Airoldi I, Pistoia V. IL-27 driven upregulation of surface HLA-E expression on monocytes inhibits IFN-γ release by autologous NK cells. J Immunol Res. 2014;2014.

36. Gustafson KS, Ginder GD. Interferon-γ induction of the human leukocyte antigen-E gene is mediated through binding of a complex containing STAT1α to a distinct interferon-γ-responsive element. J Biol Chem. 1996 Aug 16;271(33):20035–46.

37. ten Hoeve J, de Jesus Ibarra-Sanchez M, Fu Y, Zhu W, Tremblay M, David M, et al. Identification of a Nuclear Stat1 Protein Tyrosine Phosphatase. Mol Cell Biol. 2002 Aug 1;22(16):5662–8.

38. McBride KM, McDonald C, Reich NC. Nuclear export signal located within theDNA-binding domain of the STAT1transcription factor. EMBO J. 2000 Nov 11;19(22):6196.

39. Yuasa K, Hijikata T. Distal regulatory element of the STAT1 gene potentially mediates positive feedback control of STAT1 expression. Genes to Cells. 2016 Jan 1;21(1):25–40.

40. Morrow AN, Schmeisser H, Tsuno T, Zoon KC. A Novel Role for IFN-Stimulated Gene Factor 3II in IFN-γ Signaling and Induction of Antiviral Activity in Human Cells. J Immunol. 2011 Feb 1;186(3):1685–93.

41. Hanahan D, Weinberg RA. Hallmarks of cancer: the next generation. Cell. 2011 Mar 4;144(5):646–74.

42. Seliger B, Barbara Seliger C. Molecular mechanisms of HLA class I-mediated immune evasion of human tumors and their role in resistance to immunotherapies. HLA. 2016 Nov 1;88(5):213–20.

43. André P, Denis C, Soulas C, Bourbon-Caillet C, Lopez J, Arnoux T, et al. Anti-NKG2A mAb Is a Checkpoint Inhibitor that Promotes Anti-tumor Immunity by Unleashing Both T and NK Cells. Cell. 2018 Dec 13;175(7):1731-1743.e13.

44. Palmisano GL, Contardi E, Morabito A, Gargaglione V, Ferrara GB, Pistillo MP. HLA-E surface expression is independent of the availability of HLA class I signal sequence-derived peptides in human tumor cell lines. Hum Immunol. 2005 Jan;66(1):1–12.

45. Andersson E, Poschke I, Villabona L, Carlson JW, Lundqvist A, Kiessling R, et al. Non-classical HLA-class I expression in serous ovarian carcinoma: Correlation with the HLA-genotype, tumor infiltrating immune cells and prognosis. Oncoimmunology. 2016;5(1):e1052213.

46. Borst L, van der Burg SH, van Hall T. The NKG2A-HLA-E axis as a novel checkpoint in the tumor microenvironment. Clin Cancer Res. 2021 Nov 1;26(21):5549–56.

47. Dubrot J, Du PP, Lane-Reticker SK, Kessler EA, Muscato AJ, Mehta A, et al. In vivo CRISPR screens reveal the landscape of immune evasion pathways across cancer. Nat Immunol. 2022 Sep 23;23(10):1495–506.

48. McWilliams EM, Mele JM, Cheney C, Timmerman EA, Fiazuddin F, Strattan EJ, et al. Therapeutic CD94/NKG2A blockade improves natural killer cell dysfunction in chronic lymphocytic leukemia. Oncoimmunology. 2016 Oct 2;5(10).

49. Veuillen C, Aurran-Schleinitz T, Castellano R, Rey J, Mallet F, Orlanducci F, et al. Primary B-CLL resistance to NK cell cytotoxicity can be overcome in vitro and in vivo by priming NK cells and monoclonal antibody therapy. J Clin Immunol. 2012 Jun;32(3):632–46.

50. Lagana A, Ruan DF, Melnekoff D, Leshchenko V, Perumal D, Rahman A, et al. Increased HLA-E Expression Correlates with Early Relapse in Multiple Myeloma. Blood. 2018 Nov 29;132(Supplement 1):59–59.

51. Yang Y, Liu Z, Wang H, Zhang G. HLA-E Binding Peptide as a Potential Therapeutic Candidate for High-Risk Multiple Myeloma. Front Oncol. 2021 Jun 9;11:2127.

52. Nguyen S, V B, N D, M K, JP V, P D, et al. HLA-E upregulation on IFN-gamma-activated AML blasts impairs CD94/NKG2A-dependent NK cytolysis after haplo-mismatched hematopoietic SCT. Bone Marrow Transplant. 2009;43(9):693–9.

53. Seliger B, Jasinski-Bergner S, Quandt D, Stoehr C, Bukur J, Wach S, et al. HLA-E expression and its clinical relevance in human renal cell carcinoma. Oncotarget. 2016 Oct 10;7(41):67360.

54. Hrbac T, Kopkova A, Siegl F, Vecera M, Ruckova M, Kazda T, et al. HLA-E and HLA-F Are Overexpressed in Glioblastoma and HLA-E Increased After Exposure to Ionizing Radiation. Cancer Genomics Proteomics. 2022;19(2):151.

55. Chen H, Song Y, Deng C, Xu Y, Xu H, Zhu X, et al. Comprehensive analysis of immune infiltration and gene expression for predicting survival in patients with sarcomas. Aging (Albany NY). 2021 Jan 1;13(2):2168.

56. Yazdi MT, Riet S van, van Schadewijk A, Fiocco M, van Hall T, Taube C, et al. The positive prognostic effect of stromal CD8+ tumor-infiltrating T cells is restrained by the expression of HLA-E in non-small cell lung carcinoma. Oncotarget. 2016;7(3):3477–88.

57. Salomé B, Sfakianos JP, Ranti D, Daza J, Bieber C, Charap A, et al. NKG2A and HLA-E define an

alternative immune checkpoint axis in bladder cancer. Cancer Cell. 2022 Sep;40(9):1027-1043.e9.

58. Reusing SB, Manser AR, Groeneveld-Krentz S, Rebmann V, Horn PA, Meisel R, et al. HLA-E expression constitutes a novel determinant for ALL disease monitoring following hematopoietic stem cell transplantation. Bone Marrow Transplant 2021 567. 2021 Mar 3;56(7):1723–7.

59. Ulbrecht M, Couturier A, Martinozzi S, Pla M, Srivastava R, Peterson PA, et al. Cell surface expression of HLA-E: Interaction with human β2-microglobulin and allelic differences. Eur J Immunol. 1999;29(2):537–47.

60. Wagner B, Dührsen U, Hüttmann A, Nückel H, Michita RT, Rohn H, et al. Genetic Variants of the NKG2C/HLA-E Receptor-Ligand Axis Are Determinants of Progression-Free Survival and Therapy Outcome in Aggressive B-Cell Lymphoma. Cancers (Basel). 2020 Nov 1;12(11):1–12.

61. Hirankarn N, Kimkong I, Mutirangura A. HLA-E polymorphism in patients with nasopharyngeal carcinoma. Tissue Antigens. 2004 Nov 1;64(5):588–92.

62. Zheng H, Lu R, Xie S, Wen X, Wang H, Gao X, et al. Human leukocyte antigen-E alleles and expression in patients with serous ovarian cancer. Cancer Sci. 2015 May 1;106(5):522–8.

63. Ruiz-Lorente I, Gimeno L, López-Abad A, López Cubillana P, Fernández Aparicio T, Asensio Egea LJ, et al. Differential Role of NKG2A/HLA-E Interaction in the Outcomes of Bladder Cancer Patients Treated with M. bovis BCG or Other Therapies. Biomedicines. 2025 Jan 1;13(1).

64. Hallner A, Bernson E, Hussein BA, Sander FE, Brune M, Aurelius J, et al. The HLA-B 221 dimorphism impacts on NK cell education and clinical outcome of immunotherapy in acute myeloid leukemia. Blood. 2019 Mar 28;133(13):1479–88.

65. Hosseini E, Minagar A, Ghasemzadeh M, Arabkhazaeli A, Ghasemzadeh A. HLA-E*01:01 + HLA-E*01:01 genotype confers less susceptibility to COVID-19, while HLA-E*01:03 + HLA-E*01:03 genotype is associated with more severe disease. Hum Immunol. 2023 Apr 1;84(4):263–71.

66. Faget D V., Ren Q, Stewart SA. Unmasking senescence: context-dependent effects of SASP in cancer. Vol. 19, Nature Reviews Cancer. Nature Publishing Group; 2019. p. 439–53.

67. Antonangeli F, Zingoni A, Soriani A, Santoni A. Senescent cells: Living or dying is a matter of NK cells. J Leukoc Biol. 2019 May 27;105(6):1275–83.

68. Pereira BI, Devine OP, Vukmanovic-Stejic M, Chambers ES, Subramanian P, Patel N, et al.

Senescent cells evade immune clearance via HLA-E-mediated NK and CD8+ T cell inhibition. Nat Commun. 2019 Dec 1;10(1):1–13.

69. Yang X, Man K, Ng KT-P. IDDF2022-ABS-0267 HLA-E/NKG2A hampers tumor surveillance of natural killer cells induced by TLR4-mediated hepatic senescence. Gut. 2022 Sep 1;71(Suppl 2):A28–9.

70. Abel AM, Yang C, Thakar MS, Malarkannan S. Natural killer cells: Development, maturation, and clinical utilization. Front Immunol. 2018 Aug 13;9(AUG):1869.

71. Doyle EH, Aloman C, El-Shamy A, Eng F, Rahman A, Klepper AL, et al. A subset of liver resident natural killer cells is expanded in hepatitis C-infected patients with better liver function. Sci Rep. 2021 Jan 15;11(1):1–13.

72. Bi J, Wang X. Molecular Regulation of NK Cell Maturation. Front Immunol. 2020 Aug 11;11:1945.

73. Iizuka K, Chaplin DD, Wang Y, Wu Q, Pegg LE, Yokoyama WM, et al. Requirement for membrane lymphotoxin in natural killer cell development. Proc Natl Acad Sci U S A. 1999 May 25;96(11):6336–40.

74. Wu Q, Sun Y, Wang J, Lin X, Wang Y, Pegg LE, et al. Signal Via Lymphotoxin-βR on Bone Marrow Stromal Cells Is Required for an Early Checkpoint of NK Cell Development. J Immunol. 2001 Feb 1;166(3):1684–9.

75. Tang PMK, Zhou S, Meng XM, Wang QM, Li CJ, Lian GY, et al. Smad3 promotes cancer progression by inhibiting E4BP4-mediated NK cell development. Nat Commun. 2017 Mar 6;8(1):1–15.

76. Marcoe JP, Lim JR, Schaubert KL, Fodil-Cornu N, Matka M, McCubbrey AL, et al. TGF-β is responsible for NK cell immaturity during ontogeny and increased susceptibility to infection during mouse infancy. Nat Immunol. 2012 Sep;13(9):843–50.

77. Male V, Nisoli I, Kostrzewski T, Allan DSJ, Carlyle JR, Lord GM, et al. The transcription factor E4bp4/Nfil3 controls commitment to the NK lineage and directly regulates Eomes and Id2 expression. J Exp Med. 2014;211(4):635–42.

78. Gascoyne DM, Long E, Veiga-Fernandes H, de Boer J, Williams O, Seddon B, et al. The basic leucine zipper transcription factor E4BP4 is essential for natural killer cell development. Nat Immunol. 2009;10(10):1118–24.

79. Nagler A, Lanier LL, Cwirla S, Phillips JH. Comparative studies of human FcRIII-positive and

negative natural killer cells. J Immunol. 1989;143(10):3183–91.

80. Jacobs R, Hintzen G, Kemper A, Beul K, Kempf S, Behrens G, et al. CD56bright cells differ in their KIR repertoire and cytotoxic features from CD56dim NK cells. Eur J Immunol. 2001;31(10):3121–6.

81. Björkström NK, Riese P, Heuts F, Andersson S, Fauriat C, Ivarsson MA, et al. Expression patterns of NKG2A, KIR, and CD57 define a process of CD56dim NK-cell differentiation uncoupled from NK-cell education. Blood. 2010 Nov 11;116(19):3853–64.

82. Kaulfuss M, Mietz J, Fabri A, vom Berg J, Münz C, Chijioke O. The NK cell checkpoint NKG2A maintains expansion capacity of human NK cells. Sci Rep. 2023 Dec 1;13(1).

83. Rettman P, Willem C, David G, Riou R, Legrand N, Esbelin J, et al. New insights on the natural killer cell repertoire from a thorough analysis of cord blood cells. J Leukoc Biol. 2016 Sep 1;100(3):471–9.

84. Lopez-Vergès S, Milush JM, Pandey S, York VA, Arakawa-Hoyt J, Pircher H, et al. CD57 defines a functionally distinct population of mature NK cells in the human CD56dimCD16+ NK-cell subset. Blood. 2010 Nov 11;116(19):3865–74.

85. Farag SS, Caligiuri MA. Human natural killer cell development and biology. Blood Rev. 2006 May 1;20(3):123–37.

86. Hashemi E, Malarkannan S. Tissue-Resident NK Cells: Development, Maturation, and Clinical Relevance. Cancers (Basel). 2020 Jun 1;12(6):1–23.

87. Sun JC, Beilke JN, Lanier LL. Adaptive immune features of natural killer cells. Nat 2009 4577229. 2009 Jan 11;457(7229):557–61.

88. Nabekura T, Lanier LL. Tracking the fate of antigen-specific versus cytokine-activated natural killer cells after cytomegalovirus infection. J Exp Med. 2016 Nov 14;213(12):2745–58.

89. Lopez-Vergès S, Milush JM, Schwartz BS, Pando MJ, Jarjoura J, York VA, et al. Expansion of a unique CD57$^{+}$NKG2Chi natural killer cell subset during acute human cytomegalovirus infection. Proc Natl Acad Sci U S A. 2011 Sep 6;108(36):14725–32.

90. Foley B, Cooley S, Verneris MR, Pitt M, Curtsinger J, Luo X, et al. Cytomegalovirus reactivation after allogeneic transplantation promotes a lasting increase in educated NKG2C+ natural killer cells with potent function. Blood. 2012 Mar 15;119(11):2665–74.

91. Nabekura T, Deborah EA, Tahara S, Arai Y, Love PE, Kako K, et al. Themis2 regulates natural killer cell memory function and formation. Nat Commun. 2023 Nov 8;14(1):1–17.

92. Lau CM, Adams NM, Geary CD, Weizman O El, Rapp M, Pritykin Y, et al. Epigenetic control of innate and adaptive immune memory. Nat Immunol. 2018 Aug 6;19(9):963–72.

93. Rückert T, Lareau CA, Mashreghi MF, Ludwig LS, Romagnani C. Clonal expansion and epigenetic inheritance of long-lasting NK cell memory. Nat Immunol. 2022 Oct 26;23(11):1551–63.

94. Rebuffet L, Melsen JE, Escalière B, Basurto-Lozada D, Bhandoola A, Björkström NK, et al. High-dimensional single-cell analysis of human natural killer cell heterogeneity. Nat Immunol. 2024 Jul 2;25(8):1474–88.

95. He Y, Tian Z. NK cell education via nonclassical MHC and non-MHC ligands. Cell Mol Immunol 2016 144. 2016 Jun 6;14(4):321–30.

96. Kim S, Poursine-Laurent J, Truscott SM, Lybarger L, Song YJ, Yang L, et al. Licensing of natural killer cells by host major histocompatibility complex class I molecules. Nature. 2005 Aug 4;436(7051):709–13.

97. Raulet DH, Vance RE. Self-tolerance of natural killer cells. Vol. 6, Nature Reviews Immunology. Nat Rev Immunol; 2006. p. 520–31.

98. Joncker NT, Fernandez NC, Treiner E, Vivier E, Raulet DH. NK Cell Responsiveness Is Tuned Commensurate with the Number of Inhibitory Receptors for Self-MHC Class I: The Rheostat Model. J Immunol. 2009 Apr 15;182(8):4572–80.

99. Liao NS, Bix M, Zijlstra M, Jaenisch R, Raulet D. MHC class I deficiency: Susceptibility to natural killer (NK) cells and impaired NK activity. Science (80- ). 1991;253(5016):199–202.

100. Höglund P, Öhlén C, Carbone E, Franksson L, Ljunggren HG, Latour A, et al. Recognition of β2-microglobulin-negative (β2m-) T-cell blasts by natural killer cells from normal but not from β2m- mice: Nonresponsiveness controlled by β2m- bone marrow in chimeric mice. Proc Natl Acad Sci U S A. 1991 Nov 15;88(22):10332–6.

101. Zhang X, Feng J, Chen S, Yang H, Dong Z. Synergized regulation of NK cell education by NKG2A and specific Ly49 family members. Nat Commun 2019 101. 2019 Nov 1;10(1):1–12.

102. Shreeve N, Depierreux D, Hawkes D, Traherne JA, Sovio U, Huhn O, et al. The CD94/NKG2A inhibitory receptor educates uterine NK cells to optimize pregnancy outcomes in humans and mice. Immunity. 2021 Jun 8;54(6):1231-1244.e4.

103. Bern MD, Beckman DL, Ebihara T, Taffner SM, Poursine-Laurent J, White JM, et al. Immunoreceptor tyrosine-based inhibitory motif–dependent functions of an MHC class I-

specific NK cell receptor. Proc Natl Acad Sci U S A. 2017 Oct 3;114(40):E8440–7.

104. Viant C, Fenis A, Chicanne G, Payrastre B, Ugolini S, Vivier E. SHP-1-mediated inhibitory signals promote responsiveness and anti-tumour functions of natural killer cells. Nat Commun. 2014;5.

105. Wu Z, Park S, Lau CM, Zhong Y, Sheppard S, Sun JC, et al. Dynamic variability in SHP-1 abundance determines natural killer cell responsiveness. Sci Signal. 2021 Nov 9;14(708).

106. Ardolino M, Azimi CS, Iannello A, Trevino TN, Horan L, Zhang L, et al. Cytokine therapy reverses NK cell anergy in MHC-deficient tumors. J Clin Invest. 2014 Nov 3;124(11):4781–94.

107. Bern MD, Parikh BA, Yang L, Beckman DL, Poursine-Laurent J, Yokoyama WM. Inducible down-regulation of MHC class I results in natural killer cell tolerance. J Exp Med. 2019 Jan 7;216(1):99–116.

108. Lanier LL. Evolutionary struggles between NK cells and viruses. Nat Rev Immunol. 2008 Apr;8(4):259–68.

109. Kim S, Iizuka K, Aguila HL, Weissman IL, Yokoyama WM. In vivo natural killer cell activities revealed by natural killer cell-deficient mice. Proc Natl Acad Sci U S A. 2000 Mar 14;97(6):2731–6.

110. Raulet DH, Guerra N. Oncogenic stress sensed by the immune system: role of natural killer cell receptors. Nat Rev Immunol. 2009 Aug;9(8):568–80.

111. French AR, Yokoyama WM. Natural killer cells and viral infections. Curr Opin Immunol. 2003 Feb 1;15(1):45–51.

112. Algarra I, Cabrera T, Garrido F. The HLA crossroad in tumor immunology. Hum Immunol. 2000 Jan 1;61(1):65–73.

113. Blunt MD, Khakoo SI. Activating killer cell immunoglobulin-like receptors: Detection, function and therapeutic use. Int J Immunogenet. 2020 Feb 1;47(1):1–12.

114. Orange JS. Formation and function of the lytic NK-cell immunological synapse. Vol. 8, Nature Reviews Immunology. Nature Publishing Group; 2008. p. 713–25.

115. Friedman D, Simmonds P, Hale A, Bere L, Hodson NW, White MRH, et al. Natural killer cell immune synapse formation and cytotoxicity are controlled by tension of the target interface. J Cell Sci. 2021 Apr 4;134(7).

116. Paul S, Lal G. The molecular mechanism of natural killer cells function and its importance in

cancer immunotherapy. Front Immunol. 2017 Sep 13;8(SEP):1124.

117. Yu T-K, Caudell EG, Smid C, Grimm EA. IL-2 Activation of NK Cells: Involvement of MKK1/2/ERK But Not p38 Kinase Pathway. J Immunol. 2000 Jun 15;164(12):6244–51.

118. Hsu HT, Mace EM, Carisey AF, Viswanath DI, Christakou AE, Wiklund M, et al. NK cells converge lytic granules to promote cytotoxicity and prevent bystander killing. J Cell Biol. 2016 Dec 12;215(6):875.

119. Yang X, Stennicke HR, Wang B, Green DR, Jänicke RU, Srinivasan A, et al. Granzyme B Mimics Apical Caspases. J Biol Chem. 1998 Dec 18;273(51):34278–83.

120. Sutton VR, Davis JE, Cancilla M, Johnstone RW, Ruefli AA, Sedelies K, et al. Initiation of Apoptosis by Granzyme B Requires Direct Cleavage of Bid, but Not Direct Granzyme B–Mediated Caspase Activation. J Exp Med. 2000 Nov 11;192(10):1403.

121. Julien O, Wells JA. Caspases and their substrates. Vol. 24, Cell Death and Differentiation. Nature Publishing Group; 2017. p. 1380–9.

122. Cohnen A, Chiang SC, Stojanovic A, Schmidt H, Claus M, Saftig P, et al. Surface CD107a/LAMP-1 protects natural killer cells from degranulation-associated damage. Blood. 2013 Aug 22;122(8):1411–8.

123. Li Y, Orange JS. Degranulation enhances presynaptic membrane packing, which protects NK cells from perforin-mediated autolysis. PLoS Biol. 2021 Aug 1;19(8).

124. Bird CH, Christensen ME, Mangan MSJ, Prakash MD, Sedelies KA, Smyth MJ, et al. The granzyme B-Serpinb9 axis controls the fate of lymphocytes after lysosomal stress. Cell Death Differ. 2014 Jan 31;21(6):876–87.

125. Masilamani M, Nguyen C, Kabat J, Borrego F, Coligan JE. CD94/NKG2A Inhibits NK Cell Activation by Disrupting the Actin Network at the Immunological Synapse. J Immunol. 2006 Sep 15;177(6):3590–6.

126. Stebbins CC, Watzl C, Billadeau DD, Leibson PJ, Burshtyn DN, Long EO. Vav1 dephosphorylation by the tyrosine phosphatase SHP-1 as a mechanism for inhibition of cellular cytotoxicity. Mol Cell Biol. 2003 Sep;23(17):6291–9.

127. Borhis G, Ahmed PS, Mbiribindi B, Naiyer MM, Davis DM, Purbhoo MA, et al. A Peptide Antagonist Disrupts NK Cell Inhibitory Synapse Formation. J Immunol. 2013 Mar 15;190(6):2924–30.

128. Tomaz D, Pereira PM, Guerra N, Dyson J, Gould K, Henriques R. Nanoscale Colocalization of NK

Cell Activating and Inhibitory Receptors Controls Signal Integration. Front Immunol. 2022 Jun 1;13:868496.

129. Köhler K, Xiong S, Brzostek J, Mehrabi M, Eissmann P, Harrison A, et al. Matched sizes of activating and inhibitory receptor ligand pairs are required for optimal signal integration by human natural killer cells. PLoS One. 2010;5(11):15374.

130. Brzostek J, Chai JG, Gebhardt F, Busch DH, Zhao R, Van Der Merwe PA, et al. Ligand dimensions are important in controlling NK-cell responses. Eur J Immunol. 2010;40(7):2050–9.

131. Inoue H, Miyaji M, Kosugi A, Nagafuku M, Okazaki T, Mimori T, et al. Lipid rafts as the signaling scaffold for NK cell activation: Tyrosine phosphorylation and association of LAT with phosphatidylinositol 3-kinase and phospholipase C-γ following CD2 stimulation. Eur J Immunol. 2002;32(8):2188–98.

132. Wilson NS, Dixit V, Ashkenazi A. Death receptor signal transducers: nodes of coordination in immune signaling networks. Nat Immunol. 2009;10(4):348–55.

133. Prager I, Liesche C, Van Ooijen H, Urlaub D, Verron Q, Sandström N, et al. NK cells switch from granzyme B to death receptor-mediated cytotoxicity during serial killing. J Exp Med. 2019 Sep 1;216(9):2113–27.

134. Gwalani LA, Orange JS. Single degranulations in Natural Killer cells can mediate target cell killing. J Immunol. 2018 May 1;200(9):3231.

135. Ramírez-Labrada A, Pesini C, Santiago L, Hidalgo S, Calvo-Pérez A, Oñate C, et al. All About (NK Cell-Mediated) Death in Two Acts and an Unexpected Encore: Initiation, Execution and Activation of Adaptive Immunity. Front Immunol. 2022 May 16;13.

136. Sato K, Hida S, Takayanagi H, Yokochi T, Kayagaki N, Takeda K, et al. Antiviral response by natural killer cells through TRAIL gene induction by IFN-α/β. Eur J Immunol. 2001;31(11):3138–46.

137. Höfle J, Trenkner T, Kleist N, Schwane V, Vollmers S, Barcelona B, et al. Engagement of TRAIL triggers degranulation and IFNγ production in human natural killer cells. EMBO Rep. 2022 Aug 3;23(8).

138. Alves LC, Berger MD, Koutsandreas T, Kirschke N, Lauer C, Spörri R, et al. Non-apoptotic TRAIL function modulates NK cell activity during viral infection. EMBO Rep. 2020 Jan 7;21(1):e48789.

139. Sciumè G, Mikami Y, Jankovic D, Nagashima H, Villarino A V., Morrison T, et al. Rapid Enhancer Remodeling and Transcription Factor Repurposing Enable High Magnitude Gene Induction

upon Acute Activation of NK Cells. Immunity. 2020 Oct 13;53(4):745-758.e4.

140. Vivier E, Raulet DH, Moretta A, Caligiuri MA, Zitvogel L, Lanier LL, et al. Innate or adaptive immunity? The example of natural killer cells. Science (80- ). 2011 Jan 7;331(6013):44–9.

141. Bonavita E, Bromley CP, Jonsson G, Guerra N, Davis DM, Correspondence SZ. Antagonistic Inflammatory Phenotypes Dictate Tumor Fate and Response to Immune Checkpoint Blockade. Immunity. 2020;53:1215–29.

142. Reefman E, Kay JG, Wood SM, Offenhäuser C, Brown DL, Roy S, et al. Cytokine Secretion Is Distinct from Secretion of Cytotoxic Granules in NK Cells. J Immunol. 2010 May 1;184(9):4852–62.

143. Böttcher JP, Bonavita E, Chakravarty P, Blees H, Cabeza-Cabrerizo M, Sammicheli S, et al. NK Cells Stimulate Recruitment of cDC1 into the Tumor Microenvironment Promoting Cancer Immune Control. Cell. 2018 Feb 22;172(5):1022-1037.e14.

144. Dufva O, Gandolfi S, Huuhtanen J, Dashevsky O, Duàn H, Saeed K, et al. Single-cell functional genomics reveals determinants of sensitivity and resistance to natural killer cells in blood cancers. Immunity. 2023 Dec 12;56(12):2816-2835.e13.

145. Zheng H, Guan X, Meng X, Tong Y, Wang Y, Xie S, et al. IFN-γ in ovarian tumor microenvironment upregulates HLA-E expression and predicts a poor prognosis. J Ovarian Res. 2023 Dec 1;16(1):1–9.

146. Nielsen N, Ødum N, Ursø B, Lanier LL, Spee P. Cytotoxicity of CD56 bright NK cells towards autologous activated CD4 + T cells is mediated through NKG2D, LFA-1 and TRAIL and dampened via CD94/NKG2A. PLoS One. 2012 Feb 22;7(2).

147. Xu HC, Grusdat M, Pandyra AA, Polz R, Huang J, Sharma P, et al. Type I Interferon Protects Antiviral CD8+ T Cells from NK Cell Cytotoxicity. Immunity. 2014 Jun 19;40(6):949–60.

148. Xu HC, Huang J, Pandyra AA, Lang E, Zhuang Y, Thöns C, et al. Lymphocytes Negatively Regulate NK Cell Activity via Qa-1b following Viral Infection. Cell Rep. 2017 Nov 28;21(9):2528–40.

149. Lanier LL, Ruitenberg JJ, Phillips JH. Functional and biochemical analysis of CD16 antigen on natural killer cells and granulocytes. J Immunol. 1988;141(10):3478–85.

150. Wu J, Edberg JC, Redecha PB, Bansal V, Guyre PM, Coleman K, et al. A novel polymorphism of FcγRIIIa (CD16) alters receptor function and predisposes to autoimmune disease. J Clin Invest. 1997 Sep 1;100(5):1059–70.

151. Bruhns P, Iannascoli B, England P, Mancardi DA, Fernandez N, Jorieux S, et al. Specificity and affinity of human Fcγ receptors and their polymorphic variants for human IgG subclasses. Blood. 2009 Apr 16;113(16):3716–25.

152. Turaj AH, Hussain K, Cox KL, Rose-Zerilli MJJ, Testa J, Dahal LN, et al. Antibody Tumor Targeting Is Enhanced by CD27 Agonists through Myeloid Recruitment. Cancer Cell. 2017 Dec 11;32(6):777-791.e6.

153. Freud AG, Mundy-Bosse BL, Yu J, Caligiuri MA. The Broad Spectrum of Human Natural Killer Cell Diversity. Immunity. 2017 Nov 21;47(5):820–33.

154. Björkström NK, Lindgren T, Stoltz M, Fauriat C, Braun M, Evander M, et al. Rapid expansion and long-term persistence of elevated NK cell numbers in humans infected with hantavirus. J Exp Med. 2011 Jan 17;208(1):13–21.

155. Kamimura Y, Lanier LL. Homeostatic control of memory cell progenitors in the natural killer cell lineage. Cell Rep. 2015 Jan 13;10(2):280–91.

156. Lee J, Zhang T, Hwang I, Kim A, Nitschke L, Kim MJ, et al. Epigenetic Modification and Antibody-Dependent Expansion of Memory-like NK Cells in Human Cytomegalovirus-Infected Individuals. Immunity. 2015 Mar 17;42(3):431–42.

157. Romee R, Rosario M, Berrien-Elliott MM, Wagner JA, Jewell BA, Schappe T, et al. Cytokine-induced memory-like natural killer cells exhibit enhanced responses against myeloid leukemia. Sci Transl Med. 2016 Sep 21;8(357).

158. Gang M, Wong P, Berrien-Elliott MM, Fehniger TA. Memory-like natural killer cells for cancer immunotherapy. Semin Hematol. 2020 Oct 1;57(4):185.

159. Horowitz A, Strauss-Albee DM, Leipold M, Kubo J, Nemat-Gorgani N, Dogan OC, et al. Genetic and environmental determinants of human NK cell diversity revealed by mass cytometry. Sci Transl Med. 2013 Oct 10;5(208):208ra145.

160. Whitehead AS, Colten HR, Chang CC, Demars R. Localization of the human MHC-linked complement genes between HLA-B and HLA-DR by using HLA mutant cell lines. J Immunol. 1985 Jan 1;134(1):641–3.

161. Paulsson KM, Wang P, Anderson PO, Chen S, Pettersson RF, Li S. Distinct differences in association of MHC class I with endoplasmic reticulum proteins in wild-type, and beta 2-microglobulin- and TAP-deficient cell lines. Int Immunol. 2001;13(8):1063–73.

162. Hilton HG, Parham P. Missing or altered self: human NK cell receptors that recognize HLA-C.

Immunogenet 2017 698. 2017 Jul 10;69(8):567–79.

163. Saunders PM, Vivian JP, O'Connor GM, Sullivan LC, Pymm P, Rossjohn J, et al. A bird's eye view of NK cell receptor interactions with their MHC class I ligands. Immunol Rev. 2015 Sep 1;267(1):148–66.

164. Boyington JC, Brooks AG, Sun PD. Structure of killer cell immunoglobulin-like receptors and their recognition of the class I MHC molecules. Immunol Rev. 2001;181:66–78.

165. Cassidy S, Mukherjee S, Myint TM, Mbiribindi B, North H, Traherne J, et al. Peptide selectivity discriminates NK cells from KIR2DL2- and KIR2DL3-positive individuals. Eur J Immunol. 2015 Feb 1;45(2):492–500.

166. Sivori S, Della Chiesa M, Carlomagno S, Quatrini L, Munari E, Vacca P, et al. Inhibitory Receptors and Checkpoints in Human NK Cells, Implications for the Immunotherapy of Cancer. Front Immunol. 2020 Sep 3;11:2156.

167. Burshtyn DN, Scharenberg AM, Wagtmann N, Rajagopalan S, Berrada K, Yi T, et al. Recruitment of tyrosine phosphatase HCP by the killer cell inhibitory receptor. Immunity. 1996 Jan 1;4(1):77–85.

168. Olcese L, Lang P, Vély F, Cambiaggi A, Marguet D, Bléry M, et al. Human and mouse killer-cell inhibitory receptors recruit PTP1C and PTP1D protein tyrosine phosphatases. J Immunol. 1996 Jun 15;156(12):4531–4.

169. Lanier LL, Cortiss BC, Wu J, Leong C, Phillips JH. Immunoreceptor DAP12 bearing a tyrosine-based activation motif is involved in activating NK cells. Nature. 1998 Feb 12;391(6668):703–7.

170. Garcia-Beltran WF, Hölzemer A, Martrus G, Chung AW, Pacheco Y, Simoneau CR, et al. Open conformers of HLA-F are high-affinity ligands of the activating NK-cell receptor KIR3DS1. Nat Immunol 2016 179. 2016 Jul 25;17(9):1067–74.

171. Blunt MD, Fisher H, Schittenhelm RB, Mbiribindi B, Fulton R, Khan S, et al. The nuclear export protein XPO1 provides a peptide ligand for natural killer cells. Sci Adv. 2024 Aug 23;10(34):eado6566.

172. Blunt MD, Vallejo Pulido A, Fisher JG, Graham L V., Doyle ADP, Fulton R, et al. KIR2DS2 Expression Identifies NK Cells With Enhanced Anticancer Activity. J Immunol. 2022 Jul 15;209(2):379–90.

173. Rettman P, Blunt MD, Fulton RJ, Vallejo AF, Bastidas-Legarda LY, España-Serrano L, et al.

Peptide: MHC-based DNA vaccination strategy to activate natural killer cells by targeting killer cell immunoglobulin-like receptors. J Immunother cancer. 2021 May 20;9(5).

174. Naiyer MM, Cassidy SA, Magri A, Cowton V, Chen K, Mansour S, et al. KIR2DS2 recognizes conserved peptides derived from viral helicases in the context of HLA-C. Sci Immunol. 2017 Sep 15;2(15).

175. David G, Djaoud Z, Willem C, Legrand N, Rettman P, Gagne K, et al. Large Spectrum of HLA-C Recognition by Killer Ig–like Receptor (KIR)2DL2 and KIR2DL3 and Restricted C1 Specificity of KIR2DS2: Dominant Impact of KIR2DL2/KIR2DS2 on KIR2D NK Cell Repertoire Formation. J Immunol. 2013 Nov 1;191(9):4778–88.

176. Blunt MD, Rettman P, Bastidas-Legarda LY, Fulton R, Capizzuto V, Naiyer MM, et al. A novel antibody combination to identify KIR2DS2 $^{high}$ natural killer cells in KIR2DL3/L2/S2 heterozygous donors. HLA. 2019 Jan 1;93(1):32–5.

177. Graham L V., Fisher JG, Doyle ADP, Sale B, Del Rio L, French AJE, et al. KIR2DS2+ NK cells in cancer patients demonstrate high activation in response to tumour-targeting antibodies. Front Oncol. 2024 Sep 2;14:1404051.

178. Sekine T, Marin D, Cao K, Li L, Mehta P, Shaim H, et al. Specific combinations of donor and recipient KIR-HLA genotypes predict for large differences in outcome after cord blood transplantation. Blood. 2016 Jul 14;128(2):297–312.

179. Siebert N, Jensen C, Troschke-Meurer S, Zumpe M, Jüttner M, Ehlert K, et al. Neuroblastoma patients with high-affinity FCGR2A, -3A and stimulatory KIR 2DS2 treated by long-term infusion of anti-GD2 antibody ch14.18/CHO show higher ADCC levels and improved event-free survival. Oncoimmunology. 2016 Nov 1;5(11).

180. Quatrini L, Vacca P, Tumino N, Besi F, Di Pace AL, Scordamaglia F, et al. Glucocorticoids and the cytokines IL-12, IL-15, and IL-18 present in the tumor microenvironment induce PD-1 expression on human natural killer cells. J Allergy Clin Immunol. 2021 Jan 1;147(1):349–60.

181. De Louche CD, Roghanian A. Human inhibitory leukocyte Ig-like receptors: from immunotolerance to immunotherapy. JCI insight. 2022 Jan 25;7(2).

182. Chen H, Chen Y, Deng M, John S, Gui X, Kansagra A, et al. Antagonistic anti-LILRB1 monoclonal antibody regulates antitumor functions of natural killer cells. J Immunother Cancer. 2020 Aug 1;8(2):e000515.

183. Vivier E, Morin P, O'Brien C, Druker B, Schlossman SF, Anderson P. Tyrosine phosphorylation of the Fc gamma RIII(CD16): zeta complex in human natural killer cells. Induction by antibody-

dependent cytotoxicity but not by natural killing. J Immunol. 1991;146(1):206–10.

184. Bryceson YT, March ME, Ljunggren HG, Long EO. Synergy among receptors on resting NK cells for the activation of natural cytotoxicity and cytokine secretion. Blood. 2006 Jan 1;107(1):159–66.

185. Long EO, Sik Kim H, Liu D, Peterson ME, Rajagopalan S. Controlling natural killer cell responses: Integration of signals for activation and inhibition. Vol. 31, Annual Review of Immunology. Annual Reviews; 2013. p. 227–58.

186. Barrow AD, Martin CJ, Colonna M. The Natural Cytotoxicity Receptors in Health and Disease. Front Immunol. 2019;10(MAY):909.

187. Tahara-Hanaoka S, Shibuya K, Onoda Y, Zhang H, Yamazaki S, Miyamoto A, et al. Functional characterization of DNAM-1 (CD226) interaction with its ligands PVR (CD155) and nectin-2 (PRR-2/CD112). Int Immunol. 2004 Apr;16(4):533–8.

188. Cifaldi L, Doria M, Cotugno N, Zicari S, Cancrini C, Palma P, et al. DNAM-1 activating receptor and its ligands: How do viruses affect the NK cell-mediated immune surveillance during the various phases of infection? Vol. 20, International Journal of Molecular Sciences. Multidisciplinary Digital Publishing Institute; 2019. p. 3715.

189. Billadeau DD, Upshaw JL, Schoon RA, Dick CJ, Leibson PJ. NKG2D-DAP10 triggers human NK cell-mediated killing via a Syk-independent regulatory pathway. Nat Immunol. 2003 May 11;4(6):557–64.

190. Wu J, Song Y, Bakker ABH, Bauer S, Spies T, Lanier LL, et al. An activating immunoreceptor complex formed by NKG2D and DAP10. Science (80- ). 1999 Jul 30;285(5428):730–2.

191. Guerra N, Tan YX, Joncker NT, Choy A, Gallardo F, Xiong N, et al. NKG2D-Deficient Mice Are Defective in Tumor Surveillance in Models of Spontaneous Malignancy. Immunity. 2008 Apr 11;28(4):571–80.

192. Le Dréan E, Vély F, Olcese L, Cambiaggi A, Guia S, Krystal G, et al. Inhibition of antigen-induced T cell response and antibody-induced NK cell cytotoxicity by NKG2A: Association of NKG2A with SHP-1 and SHP-2 protein-tyrosine phosphatases. Eur J Immunol. 1998;28(1):264–76.

193. Gumá M, Angulo A, Vilches C, Gómez-Lozano N, Malats N, López-Botet M. Imprint of human cytomegalovirus infection on the NK cell receptor repertoire. Blood. 2004 Dec 1;104(12):3664–71.

194. Kaiser BK, Barahmand-pour F, Paulsene W, Medley S, Geraghty DE, Strong RK. Interactions

between NKG2x immunoreceptors and HLA-E ligands display overlapping affinities and thermodynamics. J Immunol. 2005 Mar 1;174(5):2878–84.

195. Kaiser BK, Pizarro JC, Kerns J, Strong RK. Structural basis for NKG2A/CD94 recognition of HLA-E. Proc Natl Acad Sci U S A. 2008 May 6;105(18):6696–701.

196. Vance RE, Kraft JR, Altman JD, Jensen PE, Raulet DH. Mouse CD94/NKG2A is a natural killer cell receptor for the nonclassical major histocompatibility complex (MHC) class I molecule Qa-1(b). J Exp Med. 1998 Nov 16;188(10):1841–8.

197. Lauterbach N, Wieten L, Popeijus HE, Voorter CEM, Tilanus MGJ. HLA-E regulates NKG2C+ natural killer cell function through presentation of a restricted peptide repertoire. Hum Immunol. 2015;76(8):578–86.

198. Ulbrecht M, Modrow S, Srivastava R, Peterson PA, Weiss EH. Interaction of HLA-E with peptides and the peptide transporter in vitro: implications for its function in antigen presentation. J Immunol. 1998;160(9):4375–85.

199. Braud VM, Allan DSJ, Wilson D, McMichael AJ. TAP- and tapasin-dependent HLA-E surface expression correlates with the binding of an MHC class I leader peptide. Curr Biol. 1998 Jan 1;8(1):1–10.

200. Llano M, Lee N, Navarro F, García P, Albar JP, Geraghty DE, et al. HLA-E-bound peptides influence recognition by inhibitory and triggering CD94/NKG2 receptors: Preferential response to an HLA-G-derived nonamer. Eur J Immunol. 1998;28(9):2854–63.

201. Hammer Q, Dunst J, Christ W, Picarazzi F, Wendorff M, Momayyezi P, et al. SARS-CoV-2 Nsp13 encodes for an HLA-E-stabilizing peptide that abrogates inhibition of NKG2A-expressing NK cells. Cell Rep. 2022 Mar 8;38(10):110503.

202. Nattermann J, Nischalke HD, Hofmeister V, Kupfer B, Ahlenstiel G, Feldmann G, et al. HIV-1 infection leads to increased HLA-E expression resulting in impaired function of natural killer cells. Antivir Ther. 2005;10(1):95–107.

203. Hammer Q, Rückert T, Borst EM, Dunst J, Haubner A, Durek P, et al. Peptide-specific recognition of human cytomegalovirus strains controls adaptive natural killer cells article. Nat Immunol. 2018 Apr 9;19(5):453–63.

204. Heatley SL, Pietra G, Lin J, Widjaja JML, Harpur CM, Lester S, et al. Polymorphism in Human Cytomegalovirus UL40 Impacts on Recognition of Human Leukocyte Antigen-E (HLA-E) by Natural Killer Cells. J Biol Chem. 2013 Mar 22;288(12):8679–90.

205. Paterson RL, La Manna MP, De Souza VA, Walker A, Gibbs-Howe D, Kulkarni R, et al. An HLA-E-targeted TCR bispecific molecule redirects T cell immunity against Mycobacterium tuberculosis. Proc Natl Acad Sci U S A. 2024 May 5;121(19).

206. Gunturi A, Berg RE, Forman J. Preferential Survival of CD8 T and NK Cells Expressing High Levels of CD94. J Immunol. 2003 Feb 15;170(4):1737–45.

207. Rouas-Freiss N, Marchal RE, Kirszenbaum M, Dausset J, Carosella ED. The α1 domain of HLA-G1 and HLA-G2 inhibits cytotoxicity induced by natural killer cells: Is HLA-G the public ligand for natural killer cell inhibitory receptors? Proc Natl Acad Sci U S A. 1997 May 13;94(10):5249–54.

208. Cheent KS, Jamil KM, Cassidy S, Liu M, Mbiribindi B, Mulder A, et al. Synergistic inhibition of natural killer cells by the nonsignaling molecule CD94. Proc Natl Acad Sci U S A. 2013 Oct 15;110(42):16981–6.

209. Jabri B, Selby JM, Negulescu H, Lee L, Roberts AI, Beavis A, et al. TCR specificity dictates CD94/NKG2A expression by human CTL. Immunity. 2002 Oct 1;17(4):487–99.

210. Borst L, Sluijter M, Sturm G, Charoentong P, Santegoets SJ, van Gulijk M, et al. NKG2A is a late immune checkpoint on CD8 T cells and marks repeated stimulation and cell division. Int J cancer. 2022 Feb 15;150(4):688–704.

211. Andrews LP, Butler SC, Cui J, Cillo AR, Cardello C, Liu C, et al. LAG-3 and PD-1 synergize on CD8+ T cells to drive T cell exhaustion and hinder autocrine IFN-γ-dependent anti-tumor immunity. Cell. 2024 Aug 8;187(16):4355-4372.e22.

212. Braud VM, Aldemir H, Breart B, Ferlin WG. Expression of CD94-NKG2A inhibitory receptor is restricted to a subset of CD8+ T cells. Trends Immunol. 2003 Apr 1;24(4):162–4.

213. Chen X, Lin Y, Yue S, Yang Y, Wang X, Pan Z, et al. Differential expression of inhibitory receptor NKG2A distinguishes disease-specific exhausted CD8+ T cells. MedComm. 2022 Mar 1;3(1).

214. Good CR, Aznar MA, Kuramitsu S, Samareh P, Agarwal S, Donahue G, et al. An NK-like CAR T cell transition in CAR T cell dysfunction. Cell. 2021 Dec 9;184(25):6081-6100.e26.

215. Jiang Y, Chen O, Cui C, Zhao B, Han X, Zhang Z, et al. KIR3DS1/L1 and HLA-Bw4-80I are associated with HIV disease progression among HIV typical progressors and long-term nonprogressors. BMC Infect Dis. 2013 Sep 2;13(1):1–11.

216. Littera R, Chessa L, Deidda S, Angioni G, Campagna M, Lai S, et al. Natural killer-cell immunoglobulin-like receptors trigger differences in immune response to SARS-CoV-2

infection. PLoS One. 2021 Aug 1;16(8 August).

217. Zhang R, Xu J, Hong K, Yuan L, Peng H, Tang H, et al. Increased NKG2A found in cytotoxic natural killer subset in HIV-1 patients with advanced clinical status. AIDS. 2007 Dec;21(SUPPL. 8).

218. Cohen GB, Gandhi RT, Davis DM, Mandelboim O, Chen BK, Strominger JL, et al. The Selective Downregulation of Class I Major Histocompatibility Complex Proteins by HIV-1 Protects HIV-Infected Cells from NK Cells. Immunity. 1999 Jun 1;10(6):661–71.

219. Romero-Martín L, Duran-Castells C, Olivella M, Rosás-Umbert M, Ruiz-Riol M, Sanchez J, et al. Disruption of the HLA-E/NKG2X axis is associated with uncontrolled HIV infections. Front Immunol. 2022 Nov 18;13.

220. Nattermann J, Nischalke HD, Hofmeister V, Ahlenstiel G, Zimmermann H, Leifeld L, et al. The HLA-A2 restricted T cell epitope HCV core 35-44 stabilizes HLA-E expression and inhibits cytolysis mediated by natural killer cells. Am J Pathol. 2005;166(2):443–53.

221. Zhang C, Wang X mei, Li S ran, Twelkmeyer T, Wang W hong, Zhang S yuan, et al. NKG2A is a NK cell exhaustion checkpoint for HCV persistence. Nat Commun 2019 101. 2019 Apr 3;10(1):1–11.

222. Gonçalves MAG, Le Discorde M, Simões RT, Rabreau M, Soares EG, Donadi EA, et al. Classical and non-classical HLA molecules and p16(INK4a) expression in precursors lesions and invasive cervical cancer. Eur J Obstet Gynecol Reprod Biol. 2008;141(1):70–4.

223. Yaqinuddin A, Kashir J. Innate immunity in COVID-19 patients mediated by NKG2A receptors, and potential treatment using Monalizumab, Cholroquine, and antiviral agents. Med Hypotheses. 2020 Jul 1;140:109777.

224. Zheng M, Gao Y, Wang G, Song G, Liu S, Sun D, et al. Functional exhaustion of antiviral lymphocytes in COVID-19 patients. Cell Mol Immunol 2020 175. 2020 Mar 19;17(5):533–5.

225. Maucourant C, Filipovic I, Ponzetta A, Aleman S, Cornillet M, Hertwig L, et al. Natural killer cell immunotypes related to COVID-19 disease severity. Sci Immunol. 2020;5(50).

226. Brooks CR, Elliott T, Parham P, Khakoo SI. The Inhibitory Receptor NKG2A Determines Lysis of Vaccinia Virus-Infected Autologous Targets by NK Cells. J Immunol. 2006 Jan 15;176(2):1141–7.

227. Smyth MJ, Thia KYT, Street SEA, MacGregor D, Godfrey DI, Trapani JA. Perforin-mediated cytotoxicity is critical for surveillance of spontaneous lymphoma. J Exp Med. 2000 Sep

4;192(5):755–60.

228. Zerafa N, Westwood JA, Cretney E, Mitchell S, Waring P, Iezzi M, et al. Cutting Edge: TRAIL Deficiency Accelerates Hematological Malignancies. J Immunol. 2005 Nov 1;175(9):5586–90.

229. van den Broek MF, Kägi D, Zinkernagel RM, Hengartner H. Perforin dependence of natural killer cell-mediated tumor control in vivo. Eur J Immunol. 1995;25(12):3514–6.

230. Imai K, Matsuyama S, Miyake S, Suga K, Nakachi K. Natural cytotoxic activity of peripheral-blood lymphocytes and cancer incidence: An 11-year follow-up study of a general population. Lancet. 2000 Nov 25;356(9244):1795–9.

231. Henriksen JR, Donskov F, Waldstrøm M, Jakobsen A, Hjortkjaer M, Petersen CB, et al. Favorable prognostic impact of Natural Killer cells and T cells in high-grade serous ovarian carcinoma. Acta Oncol (Madr). 2020 Jun 2;59(6):652–9.

232. Villegas FR, Coca S, Villarrubia VG, Jiménez R, Chillón MJ, Jareño J, et al. Prognostic significance of tumor infiltrating natural killer cells subset CD57 in patients with squamous cell lung cancer. Lung Cancer. 2002;35(1):23–8.

233. Lee S byul, Cha J, Kim I kyung, Yoon JC, Lee HJ, Park SW, et al. A high-throughput assay of NK cell activity in whole blood and its clinical application. Biochem Biophys Res Commun. 2014 Mar 14;445(3):584–90.

234. Huntington ND, Cursons J, Rautela J. The cancer–natural killer cell immunity cycle. Vol. 20, Nature Reviews Cancer. Nature Research; 2020. p. 437–54.

235. Sun Y, Yao Z, Zhao Z, Xiao H, Xia M, Zhu X, et al. Natural killer cells inhibit metastasis of ovarian carcinoma cells and show therapeutic effects in a murine model of ovarian cancer. Exp Ther Med. 2018 Aug 1;16(2):1071–8.

236. Liu X, Zuo F, Song J, Tang L, Wang X, Liu X, et al. Immune checkpoints HLA-E:CD94-NKG2A and HLA-C:KIR2DL1 complementarily shield circulating tumor cells from NK-mediated immune surveillance. Vol. 10, Cell Discovery. 2024. p. 1–5.

237. Liu X, Song J, Zhang H, Liu X, Zuo F, Zhao Y, et al. Immune checkpoint HLA-E:CD94-NKG2A mediates evasion of circulating tumor cells from NK cell surveillance. Cancer Cell. 2023 Feb 13;41(2):272–87.

238. D'Souza C, Keam SP, Yeang HXA, Neeson M, Richardson K, Hsu AK, et al. Myeloma natural killer cells are exhausted and have impaired regulation of activation. Haematologica. 2021 Sep 1;106(9):2522.

239. Matsuzaki H, Kagimoto T, Oda T, Kawano F, Takatsuki K. Natural Killer Activity and Antibody-Dependent Cell-Mediated Cytotoxicity in Multiple Myeloma. Jpn J Clin Oncol. 1985 Dec 1;15(4):611–7.

240. Szudy-Szczyrek A, Ahern S, Kozioł M, Majowicz D, Szczyrek M, Krawczyk J, et al. Therapeutic Potential of Innate Lymphoid Cells for Multiple Myeloma Therapy. Cancers 2021, Vol 13, Page 4806. 2021 Sep 26;13(19):4806.

241. Ulvmoen A, Greiff V, Bechensteen AG, Inngjerdingen M. NKG2A discriminates natural killer cells with a suppressed phenotype in pediatric acute leukemia. J Leukoc Biol. 2024 Jan 19;115(2):334–43.

242. Wang WT, Zhu HY, Wu YJ, Xia Y, Wu JZ, Wu W, et al. Elevated absolute NK cell counts in peripheral blood predict good prognosis in chronic lymphocytic leukemia. J Cancer Res Clin Oncol. 2018 Mar 1;144(3):449–57.

243. Kamiya T, Seow SV, Wong D, Robinson M, Campana D. Blocking expression of inhibitory receptor NKG2A overcomes tumor resistance to NK cells. J Clin Invest. 2019 May 1;129(5):2094–106.

244. Paul S, Kulkarni N, Shilpi N, Lal G. Intratumoral natural killer cells show reduced effector and cytolytic properties and control the differentiation of effector Th1 cells. Oncoimmunology. 2016 Dec 1;5(12).

245. Dean I, Lee CYC, Tuong ZK, Li Z, Tibbitt CA, Willis C, et al. Rapid functional impairment of natural killer cells following tumor entry limits anti-tumor immunity. Nat Commun. 2024 Jan 24;15(1):1–18.

246. Sheffer M, Lowry E, Beelen N, Borah M, Amara SNA, Mader CC, et al. Genome-scale screens identify factors regulating tumor cell responses to natural killer cells. Nat Genet. 2021 Jul 12;53(8):1196–206.

247. Almalte Z, Samarani S, Iannello A, Debbeche O, Duval M, Infante-Rivard C, et al. Novel associations between activating killer-cell immunoglobulin-like receptor genes and childhood leukemia. Blood. 2011 Aug 4;118(5):1323–8.

248. Bachanova V, Weisdorf DJ, Wang T, Marsh SGE, Trachtenberg E, Haagenson MD, et al. Donor KIR B Genotype Improves Progression-Free Survival of Non-Hodgkin Lymphoma Patients Receiving Unrelated Donor Transplantation. Biol Blood Marrow Transplant. 2016 Sep 1;22(9):1602–7.

249. Alomar SY, Alkhuriji A, Trayhyrn P, Alhetheel A, Al-jurayyan A, Mansour L. Association of the

genetic diversity of killer cell immunoglobulin-like receptor genes and HLA-C ligand in Saudi women with breast cancer. Immunogenetics. 2017 Feb 1;69(2):69–76.

250. Wiśniewski A, Jankowska R, Passowicz-Muszyńska E, Wiśniewska E, Majorczyk E, Nowak I, et al. KIR2DL2/S2 and HLA-C C1C1 genotype is associated with better response to treatment and prolonged survival of patients with non-small cell lung cancer in a Polish Caucasian population. Hum Immunol. 2012 Sep;73(9):927–31.

251. Cariani E, Pilli M, Zerbini A, Rota C, Olivani A, Zanelli P, et al. HLA and killer immunoglobulin-like receptor genes as outcome predictors of hepatitis C virus-related hepatocellular carcinoma. Clin Cancer Res. 2013 Oct 1;19(19):5465–73.

252. Beksac K, Beksac M, Dalva K, Karaagaoglu E, Tirnaksiz MB. Impact of "Killer Immunoglobulin-Like Receptor /Ligand" Genotypes on Outcome following Surgery among Patients with Colorectal Cancer: Activating KIRs Are Associated with Long-Term Disease Free Survival. PLoS One. 2015 Jul 16;10(7).

253. Gras Navarro A, Kmiecik J, Leiss L, Zelkowski M, Engelsen A, Bruserud Ø, et al. NK Cells with KIR2DS2 Immunogenotype Have a Functional Activation Advantage To Efficiently Kill Glioblastoma and Prolong Animal Survival. J Immunol. 2014 Dec 15;193(12):6192–206.

254. Wang W, Erbe A, JA H, ZS M, PM S. NK Cell-Mediated Antibody-Dependent Cellular Cytotoxicity in Cancer Immunotherapy. Front Immunol. 2015;6(JUL).

255. Scott SD. Rituximab: A new therapeutic monoclonal antibody for non-Hodgkin's lymphoma. Vol. 6, Cancer Practice. Cancer Pract; 1998. p. 195–7.

256. Vidarsson G, Dekkers G, Rispens T. IgG subclasses and allotypes: From structure to effector functions. Front Immunol. 2014;5(OCT).

257. Oflazoglu E, Audoly LP. Evolution of anti-CD20 monoclonal antibody therapeutics in oncology. MAbs. 2010 Jan;2(1):14.

258. Mössner E, Brünker P, Moser S, Püntener U, Schmidt C, Herter S, et al. Increasing the efficacy of CD20 antibody therapy through the engineering of a new type II anti-CD20 antibody with enhanced direct and immune effector cell - mediated B-cell cytotoxicity. Blood. 2010 Jun 3;115(22):4393–402.

259. Goede V, Fischer K, Busch R, Engelke A, Eichhorst B, Wendtner CM, et al. Obinutuzumab plus Chlorambucil in Patients with CLL and Coexisting Conditions. N Engl J Med. 2014 Mar 20;370(12):1101–10.

260. Klanova M, Oestergaard MZ, Trneny M, Hiddemann W, Marcus R, Sehn LH, et al. Prognostic impact of natural killer cell count in follicular lymphoma and diffuse large b-cell lymphoma patients treated with immunochemotherapy. Clin Cancer Res. 2019 Aug 1;25(15):4632–43.

261. Cartron G, Dacheux L, Salles G, Solal-Celigny P, Bardos P, Colombat P, et al. Therapeutic activity of humanized anti-CD20 monoclonal antibody and polymorphism in IgG Fc receptor FcγrIIIa gene. Blood. 2002 Feb 1;99(3):754–8.

262. Weng WK, Levy R. Two immunoglobulin G fragment C receptor polymorphisms independently predict response to rituximab in patients with follicular lymphoma. J Clin Oncol. 2003 Nov 1;21(21):3940–7.

263. Wang Y, Zhang Y, Hughes T, Zhang J, Caligiuri MA, Benson DM, et al. Fratricide of NK Cells in Daratumumab Therapy for Multiple Myeloma Overcome by Ex Vivo-Expanded Autologous NK Cells. Clin Cancer Res. 2018 Aug 15;24(16):4006–17.

264. Casneuf T, Xu XS, Adams HC, Axel AE, Chiu C, Khan I, et al. Effects of daratumumab on natural killer cells and impact on clinical outcomes in relapsed or refractory multiple myeloma. Blood Adv. 2017 Oct 24;1(23):2105–14.

265. Beelen NA, Ehlers FAI, Bos GMJ, Wieten L. Inhibitory receptors for HLA class I as immune checkpoints for natural killer cell-mediated antibody-dependent cellular cytotoxicity in cancer immunotherapy. Vol. 72, Cancer Immunology, Immunotherapy. Cancer Immunol Immunother; 2023. p. 797–804.

266. Palmieri G, Tullio V, Zingoni A, Piccoli M, Frati L, Lopez-Botet M, et al. CD94/NKG2-A Inhibitory Complex Blocks CD16-Triggered Syk and Extracellular Regulated Kinase Activation, Leading to Cytotoxic Function of Human NK Cells. J Immunol. 1999 Jun 15;162(12):7181–8.

267. Borgerding A, Hasenkamp J, Engelke M, Burkhart N, Trümper L, Wienands J, et al. B-lymphoma cells escape rituximab-triggered elimination by NK cells through increased HLA class I expression. Exp Hematol. 2010 Mar 1;38(3):213–21.

268. Britstol Myers Squibb. U.S. Food and Drug Administration Approves First LAG-3-Blocking Antibody Combination, Opdualag™ (nivolumab and relatlimab-rmbw), as Treatment for Patients with Unresectable or Metastatic Melanoma [Internet]. news.bms.com. 2022 [cited 2023 Feb 9]. Available from: https://www.biospace.com/article/releases/u-s-food-and-drug-administration-approves-first-lag-3-blocking-antibody-combination-opdualag-nivolumab-and-relatlimab-rmbw-as-treatment-for-patients-with-unresectable-or-metastatic-melanoma/?s=74

269. Benson DM, Bakan CE, Mishra A, Hofmeister CC, Efebera Y, Becknell B, et al. The PD-1/PD-L1 axis modulates the natural killer cell versus multiple myeloma effect: a therapeutic target for CT-011, a novel monoclonal anti-PD-1 antibody. Blood. 2010 Sep 30;116(13):2286–94.

270. Dong W, Wu X, Ma S, Wang Y, Nalin AP, Zhu Z, et al. The mechanism of anti-PD-L1 antibody efficacy against PD-L1 negative tumors identifies NK cells expressing PD-L1 as a cytolytic effector. Cancer Discov. 2019 Oct 1;9(10):1422.

271. Lu T, Ma R, Mansour AG, Bustillos C, Li Z, Li Z, et al. Preclinical Evaluation of Off-The-Shelf PD-L1+ Human Natural Killer Cells Secreting IL15 to Treat Non-Small Cell Lung Cancer. Cancer Immunol Res. 2024 Jun 4;12(6):731–43.

272. Zhang Q, Bi J, Zheng X, Chen Y, Wang H, Wu W, et al. Blockade of the checkpoint receptor TIGIT prevents NK cell exhaustion and elicits potent anti-tumor immunity. Nat Immunol. 2018 Jun 18;19(7):723–32.

273. Hasan MF, Campbell AR, Croom-Perez TJ, Oyer JL, Dieffenthaller TA, Robles-Carrillo LD, et al. Knockout of the inhibitory receptor TIGIT enhances the antitumor response of ex vivo expanded NK cells and prevents fratricide with therapeutic Fc-active TIGIT antibodies. J Immunother Cancer. 2023 Dec 1;11(12):e007502.

274. Hasan MF, Croom-Perez TJ, Oyer JL, Dieffenthaller TA, Robles-Carrillo LD, Eloriaga JE, et al. TIGIT Expression on Activated NK Cells Correlates with Greater Anti-Tumor Activity but Promotes Functional Decline upon Lung Cancer Exposure: Implications for Adoptive Cell Therapy and TIGIT-Targeted Therapies. Cancers (Basel). 2023 May 1;15(10):2712.

275. Cazzetta V, Bruni E, Terzoli S, Carenza C, Franzese S, Piazza R, et al. NKG2A expression identifies a subset of human Vδ2 T cells exerting the highest antitumor effector functions. Cell Rep. 2021 Oct 19;37(3):109871.

276. Cohen RB, Bauman JR, Salas S, Colevas AD, Even C, Cupissol D, et al. Combination of monalizumab and cetuximab in recurrent or metastatic head and neck cancer patients previously treated with platinum-based chemotherapy and PD-(L)1 inhibitors. J Clin Oncol. 2020 May 25;38(15_suppl):6516–6516.

277. Fayette J, Lefebvre G, Posner MR, Bauman J, Salas S, Even C, et al. Results of a phase II study evaluating monalizumab in combination with cetuximab in previously treated recurrent or metastatic squamous cell carcinoma of the head and neck (R/M SCCHN). Ann Oncol. 2018 Oct 1;29:viii374.

278. van Montfoort N, Borst L, Korrer MJ, Sluijter M, Marijt KA, Santegoets SJ, et al. NKG2A

Blockade Potentiates CD8 T Cell Immunity Induced by Cancer Vaccines. Cell. 2018 Dec 13;175(7):1744-1755.e15.

279. Battin C, Kaufmann G, Leitner J, Tobias J, Wiedermann U, Rölle A, et al. NKG2A-checkpoint inhibition and its blockade critically depends on peptides presented by its ligand HLA-E. Immunology. 2022 Aug 6;166(4).

280. Hwang JK, Marston DJ, Wrapp D, Li D, Tuyishime M, Brackenridge S, et al. A high affinity monoclonal antibody against HLA-E-VL9 enhances natural killer cell anti-tumor killing. bioRxiv Immunol. 2024 Jul 11;2024.07.08.602401.

281. Li D, Brackenridge S, Walters LC, Swanson O, Harlos K, Rozbesky D, et al. Mouse and human antibodies bind HLA-E-leader peptide complexes and enhance NK cell cytotoxicity. Commun Biol. 2022 Nov 20;5(1).

282. Gornalusse GG, Hirata RK, Funk SE, Riolobos L, Lopes VS, Manske G, et al. HLA-E-expressing pluripotent stem cells escape allogeneic responses and lysis by NK cells. Nat Biotechnol 2017 358. 2017 May 15;35(8):765–72.

283. Li W, Zhu X, Xu Y, Chen J, Zhang H, Yang Z, et al. Simultaneous editing of TCR, HLA-I/II and HLA-E resulted in enhanced universal CAR-T resistance to allo-rejection. Front Immunol. 2022 Dec 2;13:7242.

284. Guo Y, Xu B, Wu Z, Bo J, Tong C, Chen D, et al. Mutant B2M-HLA-E and B2M-HLA-G fusion proteins protects universal chimeric antigen receptor-modified T cells from allogeneic NK cell-mediated lysis. Eur J Immunol. 2021 Oct 1;51(10):2513–21.

285. Jo S, Das S, Williams A, Chretien AS, Pagliardini T, Le Roy A, et al. Endowing universal CAR T-cell with immune-evasive properties using TALEN-gene editing. Nat Commun. 2022 Jun 30;13(1):1–16.

286. Sætersmoen M, Kotchetkov IS, Torralba-Raga L, Mansilla-Soto J, Sohlberg E, Krokeide SZ, et al. Targeting HLA-E Positive Cancers with a Novel NKG2A/C Switch Receptor. bioRxiv. 2023 Dec 15;2023.12.14.571754.

287. Redondo-García S, Barritt C, Papagregoriou C, Yeboah M, Frendeus B, Cragg MS, et al. Human leukocyte immunoglobulin-like receptors in health and disease. Front Immunol. 2023;14.

288. Pasero C, Gravis G, Guerin M, Granjeaud S, Thomassin-Piana J, Rocchi P, et al. Inherent and tumor-driven immune tolerance in the prostate microenvironment impairs natural killer cell antitumor activity. Cancer Res. 2016 Apr 15;76(8):2153–65.

289. Sun H, Sun C. The Rise of NK Cell Checkpoints as Promising Therapeutic Targets in Cancer Immunotherapy. Front Immunol. 2019;10(OCT).

290. Kohrt HE, Thielens A, Marabelle A, Sagiv-Barfi I, Sola C, Chanuc F, et al. Anti-KIR antibody enhancement of anti-lymphoma activity of natural killer cells as monotherapy and in combination with anti-CD20 antibodies. Blood. 2014 Jan 1;123(5):678.

291. Sönmez C, Wölfer J, Holling M, Brokinkel B, Stummer W, Wiendl H, et al. Blockade of inhibitory killer cell immunoglobulin-like receptors and IL-2 triggering reverses the functional hypoactivity of tumor-derived NK-cells in glioblastomas. Sci Reports 2022 121. 2022 Apr 26;12(1):1–11.

292. Vey N, Chretien A, Dumas P, Recher C, Gastaud L, Lioure B, et al. Randomized Phase 2 Trial of Lirilumab as maintenance Treatment in Acute Myeloid Leukemia: Results of the EFFIKIR Trial. medRxiv. 2024 Aug 23;2024.08.23.24312477.

293. Melero I, Hervas-Stubbs S, Glennie M, Pardoll DM, Chen L. Immunostimulatory monoclonal antibodies for cancer therapy. Nat Rev Cancer 2007 72. 2007 Feb;7(2):95–106.

294. Turaj AH, Cox KL, Penfold CA, French RR, Mockridge CI, Willoughby JE, et al. Augmentation of CD134 (OX40)-dependent NK anti-tumour activity is dependent on antibody cross-linking. Sci Rep. 2018 Dec 1;8(1).

295. Heckel F, Turaj AH, Fisher H, Chan HTC, Marshall MJE, Dadas O, et al. Agonistic CD27 antibody potency is determined by epitope-dependent receptor clustering augmented through Fc-engineering. Commun Biol. 2022 Dec 1;5(1).

296. Gauthier L, Morel A, Anceriz N, Rossi B, Blanchard-Alvarez A, Grondin G, et al. Multifunctional Natural Killer Cell Engagers Targeting NKp46 Trigger Protective Tumor Immunity. Cell. 2019 Jun 13;177(7):1701-1713.e16.

297. Colomar-Carando N, Gauthier L, Merli P, Loiacono F, Canevali P, Falco M, et al. Exploiting Natural Killer Cell Engagers to Control Pediatric B-cell Precursor Acute Lymphoblastic Leukemia. Cancer Immunol Res. 2022 Jan 25;10(3).

298. Demaria O, Gauthier L, Debroas G, Vivier E. Natural killer cell engagers in cancer immunotherapy: Next generation of immuno-oncology treatments. Eur J Immunol. 2021 Aug 1;51(8):1934–42.

299. Reusing SB, Vallera DA, Manser AR, Vatrin T, Bhatia S, Felices M, et al. CD16xCD33 Bispecific Killer Cell Engager (BiKE) as potential immunotherapeutic in pediatric patients with AML and biphenotypic ALL. Cancer Immunol Immunother. 2021 Dec 1;70(12):3701–8.

300. Felices M, Kodal B, Hinderlie P, Kaminski MF, Cooley S, Weisdorf DJ, et al. Novel CD19-targeted TriKE restores NK cell function and proliferative capacity in CLL. Blood Adv. 2019 Mar 26;3(6):897–907.

301. Shimasaki N, Coustan-Smith E, Kamiya T, Campana D. Expanded and armed natural killer cells for cancer treatment. Cytotherapy. 2016 Nov 1;18(11):1422–34.

302. Morris EC, Neelapu SS, Giavridis T, Sadelain M. Cytokine release syndrome and associated neurotoxicity in cancer immunotherapy. Nat Rev Immunol 2021 222. 2021 May 17;22(2):85–96.

303. Liu E, Marin D, Banerjee P, Macapinlac HA, Thompson P, Basar R, et al. Use of CAR-Transduced Natural Killer Cells in CD19-Positive Lymphoid Tumors. N Engl J Med. 2020 Feb 6;382(6):545–53.

304. Valeri A, García-Ortiz A, Castellano E, Córdoba L, Maroto-Martín E, Encinas J, et al. Overcoming tumor resistance mechanisms in CAR-NK cell therapy. Front Immunol. 2022;13:953849.

305. Marin D, Li Y, Basar R, Rafei H, Daher M, Dou J, et al. Safety, efficacy and determinants of response of allogeneic CD19-specific CAR-NK cells in CD19+ B cell tumors: a phase 1/2 trial. Nat Med. 2024 Jan 18;30(3):772–84.

306. Miller JS, Soignier Y, Panoskaltsis-Mortari A, McNearney SA, Yun GH, Fautsch SK, et al. Successful adoptive transfer and in vivo expansion of human haploidentical NK cells in patients with cancer. Blood. 2005 Apr 15;105(8):3051–7.

307. Garg TK, Szmania SM, Khan JA, Hoering A, Malbrough PA, Moreno-Bost A, et al. Highly activated and expanded natural killer cells for multiple myeloma immunotherapy. Haematologica. 2012;97(9):1348–56.

308. Calvo T, Reina-Ortiz C, Giraldos D, Gascón M, Woods D, Asenjo J, et al. Expanded and activated allogeneic NK cells are cytotoxic against B-chronic lymphocytic leukemia (B-CLL) cells with sporadic cases of resistance. Sci Reports 2020 101. 2020 Nov 10;10(1):1–14.

309. Shanley M, Daher M, Dou J, Li S, Basar R, Rafei H, et al. Interleukin-21 engineering enhances NK cell activity against glioblastoma via CEBPD. Cancer Cell. 2024 Aug 12;42(8):1450-1466.e11.

310. Zhang C, Kadu S, Xiao Y, Johnson O, Kelly A, O'Connor RS, et al. Sequential Exposure to IL21 and IL15 During Human Natural Killer Cell Expansion Optimizes Yield and Function. Cancer Immunol Res. 2023 Nov 1;11(11):1524–37.

311. Thangaraj JL, Ahn SY, Jung SH, Vo MC, Chu TH, Thi Phan MT, et al. Expanded natural killer cells augment the antimyeloma effect of daratumumab, bortezomib, and dexamethasone in a mouse model. Cell Mol Immunol. 2021 Jul 1;18(7):1652–61.

312. Zhao XY, Jiang Q, Jiang H, Hu LJ, Zhao T, Yu XX, et al. Expanded clinical-grade membrane-bound IL-21/4-1BBL NK cell products exhibit activity against acute myeloid leukemia in vivo. Eur J Immunol. 2020 Sep 1;50(9):1374–85.

313. Leivas A, Valeri A, Córdoba L, García-Ortiz A, Ortiz A, Sánchez-Vega L, et al. NKG2D-CAR-transduced natural killer cells efficiently target multiple myeloma. Blood Cancer J 2021 118. 2021 Aug 14;11(8):1–11.

314. Gong Y, Germeraad WTV, Zhang X, Wu N, Li B, Janssen L, et al. NKG2A genetic deletion promotes human primary NK cell anti-tumor responses better than an anti-NKG2A monoclonal antibody. Mol Ther. 2024;0(0).

315. Figueiredo C, Seltsam A, Blasczyk R. Permanent silencing of NKG2A expression for cell-based therapeutics. J Mol Med (Berl). 2009 Feb;87(2):199–210.

316. Furutani E, Su S, Smith A, Berg M, Childs R. siRNA Inactivation of the Inhibitory Receptor NKG2A Augments the Anti-Tumor Effects of Adoptively Transferred NK Cells In Tumor-Bearing Hosts. Blood. 2010 Nov 19;116(21):1015.

317. Mac Donald A, Guipouy D, Lemieux W, Harvey M, Bordeleau LJ, Guay D, et al. KLRC1 knockout overcomes HLA-E-mediated inhibition and improves NK cell antitumor activity against solid tumors. Front Immunol. 2023 Aug 21;14:1231916.

318. Berrien-Elliott M, Romee R, Wagner JA, Becker-Hapak M, Neal C, Schappe T, et al. NKG2A Represents an Important Immune Checkpoint for Human Cytokine-Induced Memory-like NK Cells in Patients with AML. Blood. 2017;130(Supplement 1):167.

319. Bednarski JJ, Zimmerman C, Berrien-Elliott MM, Foltz JA, Becker-Hapak M, Neal CC, et al. Donor memory-like NK cells persist and induce remissions in pediatric patients with relapsed AML after transplant. Blood. 2022 Mar 17;139(11):1670–83.

320. Dezfouli AB, Yazdi M, Pockley AG, Khosravi M, Kobold S, Wagner E, et al. NK Cells Armed with Chimeric Antigen Receptors (CAR): Roadblocks to Successful Development. Cells. 2021 Dec 1;10(12).

321. Baghery Saghchy Khorasani A, Yousefi AM, Bashash D. CAR NK cell therapy in hematologic malignancies and solid tumors; obstacles and strategies to overcome the challenges. Int Immunopharmacol. 2022 Sep 1;110.

322. Cichocki F, Bjordahl R, Goodridge JP, Mahmood S, Gaidarova S, Abujarour R, et al. Quadruple gene-engineered natural killer cells enable multi-antigen targeting for durable antitumor activity against multiple myeloma. Nat Commun 2022 131. 2022 Nov 29;13(1):1–15.

323. Encinas J, García-Ortiz A, Maroto-Martín E, Castellano E, Oliva R, Fernández RA, et al. S256: HLA-E/NKG2A CHECKPOINT DRIVES MULTIPLE MYELOMA RESISTANCE TO CAR-NK THERAPY. HemaSphere. 2023 Aug 8;7(Suppl):e16745e9.

324. Albinger N, Pfeifer R, Nitsche M, Mertlitz S, Campe J, Stein K, et al. Primary CD33-targeting CAR-NK cells for the treatment of acute myeloid leukemia. Blood Cancer J. 2022 Apr 1;12(4).

325. Focaccetti C, Benvenuto M, Pighi C, Vitelli A, Napolitano F, Cotugno N, et al. DNAM-1-chimeric receptor-engineered NK cells, combined with Nutlin-3a, more effectively fight neuroblastoma cells in vitro: a proof-of-concept study. Front Immunol. 2022 Jul 28;13.

326. Veneziani I, Infante P, Ferretti E, Melaiu O, Battistelli C, Lucarini V, et al. Nutlin-3a Enhances Natural Killer Cell-Mediated Killing of Neuroblastoma by Restoring p53-Dependent Expression of Ligands for NKG2D and DNAM-1 Receptors. Cancer Immunol Res. 2021 Feb 1;9(2):170–83.

327. Yano M, Sharpe C, Lance JR, Ravikrishnan J, Zapolnik K, Mo X, et al. Evaluation of allogeneic and autologous membrane-bound IL-21-expanded NK cells for chronic lymphocytic leukemia therapy. Blood Adv. 2022 Oct 25;6(20):5641–54.

328. Rajasekaran N, Sadaram M, Hebb J, Sagiv-Barfi I, Ambulkar S, Rajapaksa A, et al. Three BTK-Specific Inhibitors, in Contrast to Ibrutinib, Do Not Antagonize Rituximab-Dependent NK-Cell Mediated Cytotoxicity. Blood. 2014 Dec 6;124(21):3118–3118.

329. Yu H, Wang X, Li J, Ye Y, Wang D, Fang W, et al. Addition of BTK inhibitor orelabrutinib to rituximab improved anti-tumor effects in B cell lymphoma. Mol Ther - Oncolytics. 2021 Jun 25;21:158–70.

330. Alaggio R, Amador C, Anagnostopoulos I, Attygalle AD, Araujo IB de O, Berti E, et al. The 5th edition of the World Health Organization Classification of Haematolymphoid Tumours: Lymphoid Neoplasms. Vol. 36, Leukemia. Nature Publishing Group; 2022. p. 1720–48.

331. Küppers R. Mechanisms of B-cell lymphoma pathogenesis. Vol. 5, Nature Reviews Cancer. Nature Publishing Group; 2005. p. 251–62.

332. Seifert M, Scholtysik R, Küppers R. Origin and pathogenesis of B cell lymphomas. Methods Mol Biol. 2013;971:1–25.

333. Thandra KC, Barsouk A, Saginala K, Padala SA, Barsouk A, Rawla P. Epidemiology of Non-

Hodgkin's Lymphoma. Vol. 9, Medical sciences (Basel, Switzerland). Multidisciplinary Digital Publishing Institute (MDPI); 2021.

334. Mlynarczyk C, Fontán L, Melnick A. Germinal center-derived lymphomas: The darkest side of humoral immunity. Vol. 288, Immunological Reviews. Wiley-Blackwell; 2019. p. 214–39.

335. Taub R, Kirsch I, Morton C, Lenoir G, Swan D, Tronick S, et al. Translocation of the c-myc gene into the immunoglobulin heavy chain locus in human Burkitt lymphoma and murine plasmacytoma cells. Proc Natl Acad Sci U S A. 1982;79(24 I):7837–41.

336. Dalla-Favera R, Bregni M, Erikson J, Patterson D, Gallo RC, Croce CM. Human c-myc onc gene is located on the region of chromosome 8 that is translocated in Burkitt lymphoma cells. Proc Natl Acad Sci U S A. 1982;79(24 I):7824–7.

337. Kelly K, Cochran BH, Stiles CD, Leder P. Cell-specific regulation of the c-myc gene by lymphocyte mitogens and platelet-derived growth factor. Cell. 1983 Dec 1;35(3 PART 2):603–10.

338. Hafner A, Bulyk ML, Jambhekar A, Lahav G. The multiple mechanisms that regulate p53 activity and cell fate. Vol. 20, Nature Reviews Molecular Cell Biology. Nature Publishing Group; 2019. p. 199–210.

339. Bolen CR, Klanova M, Trnény M, Sehn LH, He J, Tong J, et al. Prognostic impact of somatic mutations in diffuse large B-cell lymphoma and relationship to cell-of-origin: data from the phase III GOYA study. Haematologica. 2020 Sep 9;105(9):2298.

340. Huang JZ, Sanger WG, Greiner TC, Staudt LM, Weisenburger DD, Pickering DL, et al. The t(14;18) defines a unique subset of diffuse large B-cell lymphoma with a germinal center B-cell gene expression profile. Blood. 2002 Apr 1;99(7):2285–90.

341. Challa-Malladi M, Lieu YK, Califano O, Holmes AB, Bhagat G, Murty V V., et al. Combined Genetic Inactivation of β2-Microglobulin and CD58 Reveals Frequent Escape from Immune Recognition in Diffuse Large B Cell Lymphoma. Cancer Cell. 2011 Dec 13;20(6):728–40.

342. Hu S, Xu-Monette ZY, Tzankov A, Green T, Wu L, Balasubramanyam A, et al. MYC/BCL2 protein coexpression contributes to the inferior survival of activated B-cell subtype of diffuse large B-cell lymphoma and demonstrates high-risk gene expression signatures: a report from The International DLBCL Rituximab-CHOP Consortium Program. Blood. 2013 May 16;121(20):4021–31.

343. Matutes E, Owusu-Ankomah K, Morilla R, Garcia Marco J, A Houlihan A, Que TH, et al. The immunological profile of B-cell disorders and proposal of a scoring system for the diagnosis of

CLL - PubMed. Leukemia,. 1994;8(10):1640–5.

344. Hamblin TJ, Davis Z, Gardiner A, Oscier DG, Stevenson FK. Unmutated Ig VH Genes Are Associated With a More Aggressive Form of Chronic Lymphocytic Leukemia. Blood. 1999 Sep 15;94(6):1848–54.

345. Crombie J, Davids MS. IGHV mutational status testing in chronic lymphocytic leukemia. Am J Hematol. 2017 Dec 1;92(12):1393–7.

346. Damle RN, Wasil T, Fais F, Ghiotto F, Valetto A, Allen SL, et al. Ig V Gene Mutation Status and CD38 Expression As Novel Prognostic Indicators in Chronic Lymphocytic Leukemia. Blood. 1999 Sep 15;94(6):1840–7.

347. Sigmund AM, Kittai AS. Richter's Transformation. Vol. 24, Current Oncology Reports. Springer; 2022. p. 1081–90.

348. D'Avola A, Drennan S, Tracy I, Henderson I, Chiecchio L, Larrayoz M, et al. Surface IgM expression and function are associated with clinical behavior, genetic abnormalities, and DNA methylation in CLL. Blood. 2016 Aug 11;128(6):816–26.

349. Bulian P, Shanafelt TD, Fegan C, Zucchetto A, Cro L, Nučkel H, et al. CD49d Is the Strongest Flow Cytometry–Based Predictor of Overall Survival in Chronic Lymphocytic Leukemia. J Clin Oncol. 2014 Mar 20;32(9):897.

350. Gattei V, Bulian P, Del Principe MI, Zucchetto A, Maurillo L, Buccisano F, et al. Relevance of CD49d protein expression as overall survival and progressive disease prognosticator in chronic lymphocytic leukemia. Blood. 2008 Jan 15;111(2):865–73.

351. Ibrahim S, Keating M, Do KA, O'Brien S, Huh YO, Jilani I, et al. CD38 expression as an important prognostic factor in B-cell chronic lymphocytic leukemia. Blood. 2001 Jul 1;98(1):181–6.

352. Till KJ, Lin K, Zuzel M, Cawley JC. The chemokine receptor CCR7 and alpha4 integrin are important for migration of chronic lymphocytic leukemia cells into lymph nodes. Blood. 2002 Apr 15;99(8):2977–84.

353. Dal Bo M, Tissino E, Benedetti D, Caldana C, Bomben R, Del Poeta G, et al. Microenvironmental Interactions in Chronic Lymphocytic Leukemia: The Master Role of CD49d. Semin Hematol. 2014 Jul 1;51(3):168–76.

354. Schweighoffer E, Tybulewicz VL. Signalling for B cell survival. Curr Opin Cell Biol. 2018 Apr 1;51:8–14.

355. Burger JA, Barr PM, Robak T, Owen C, Ghia P, Tedeschi A, et al. Long-term efficacy and safety

of first-line ibrutinib treatment for patients with CLL/SLL: 5 years of follow-up from the phase 3 RESONATE-2 study. Leukemia. 2020 Oct 18;34(3):787–98.

356. Munir T, Brown JR, O'Brien S, Barrientos JC, Barr PM, Reddy NM, et al. Final analysis from RESONATE: Up to six years of follow-up on ibrutinib in patients with previously treated chronic lymphocytic leukemia or small lymphocytic lymphoma. Am J Hematol. 2019 Dec 1;94(12):1353–63.

357. Kapoor I, Bodo J, Hill BT, Hsi ED, Almasan A. Targeting BCL-2 in B-cell malignancies and overcoming therapeutic resistance. Cell Death Dis 2020 1111. 2020 Nov 2;11(11):1–11.

358. Parikh SA, Gale RP, Kay NE. Chronic lymphocytic leukemia in 2020: a surfeit of riches? Leuk 2020 348. 2020 May 11;34(8):1979–83.

359. Golay J, Da Roit F, Bologna L, Ferrara C, Leusen JH, Rambaldi A, et al. Glycoengineered CD20 antibody obinutuzumab activates neutrophils and mediates phagocytosis through CD16B more efficiently than rituximab. Blood. 2013 Nov 14;122(20):3482–91.

360. Capuano C, Pighi C, Molfetta R, Paolini R, Battella S, Palmieri G, et al. Obinutuzumab-mediated high-affinity ligation of FcγRIIIA/CD16 primes NK cells for IFNγ production. Oncoimmunology. 2017 Mar 4;6(3).

361. Cappell KM, Kochenderfer JN. Long-term outcomes following CAR T cell therapy: what we know so far. Vol. 20, Nature Reviews Clinical Oncology. Nature Publishing Group; 2023. p. 359–71.

362. Sehn LH, Salles G. Diffuse Large B-Cell Lymphoma. Longo DL, editor. N Engl J Med. 2021 Mar 4;384(9):842–58.

363. Harrysson S, Eloranta S, Ekberg S, Enblad G, El-Galaly TC, Sander B, et al. Outcomes of relapsed/refractory diffuse large B-cell lymphoma and influence of chimaeric antigen receptor T trial eligibility criteria in second line—A population-based study of 736 patients. Br J Haematol. 2022 Jul 1;198(2):267–77.

364. Locke FL, Miklos DB, Jacobson CA, Perales M-A, Kersten M-J, Oluwole OO, et al. Axicabtagene Ciloleucel as Second-Line Therapy for Large B-Cell Lymphoma. N Engl J Med. 2022 Feb 17;386(7):640–54.

365. Abrisqueta P, Delgado J, Alcoceba M, Oliveira AC, Loscertales J, Hernández-Rivas JA, et al. Clinical outcome and prognostic factors of patients with Richter syndrome: real-world study of the Spanish Chronic Lymphocytic Leukemia Study Group (GELLC). Br J Haematol. 2020 Sep 1;190(6):854–63.

366. Hampel PJ, Rabe KG, Call TG, Ding W, Leis JF, Chanan-Khan AA, et al. Clinical outcomes in patients with chronic lymphocytic leukemia with disease progression on ibrutinib. Blood Cancer J. 2022 Sep 1;12(9):1–6.

367. Uslu U, Castelli S, June CH. CAR T cell combination therapies to treat cancer. Cancer Cell. 2024 Jul 16;

368. Richter J. Like a bridge over troubled water: keeping the myeloma down en route to CAR-T. Vol. 14, Blood Cancer Journal. Nature Publishing Group; 2024. p. 1–2.

369. Palmer S, Hanson CA, Zent CS, Porrata LF, LaPlant B, Geyer SM, et al. Prognostic importance of T and NK-cells in a consecutive series of newly diagnosed patients with chronic lymphocytic leukaemia. Br J Haematol. 2008 Jun;141(5):607–14.

370. Kay N, Zarling J. Impaired Natural Killer Activity in Patients With Chronic Lymphocytic Leukemia Is Associated With a Deficiency of Azurophilic Cytoplasmic Granules in Putative NK Cells. Blood. 1984 Feb 1;63(2):305–9.

371. Maki G, Hayes GM, Naji A, Tyler T, Carosella ED, Rouas-Freiss N, et al. NK resistance of tumor cells from multiple myeloma and chronic lymphocytic leukemia patients: implication of HLA-G. Leukemia. 2008;22(5):998–1006.

372. McWilliams E, Mele JM, Fiazuddin F, Cheney C, Muthusamy N, Awan FT. Targeting the Tumor Evasion Interaction of NKG2A and Its Ligand HLA-E Increases Natural-Killer Cell Activity in Chronic Lymphocytic Leukemia. Blood. 2015 Dec 3;126(23):1289–1289.

373. Parry HM, Stevens T, Oldreive C, Zadran B, McSkeane T, Rudzki Z, et al. NK cell function is markedly impaired in patients with chronic lymphocytic leukaemia but is preserved in patients with small lymphocytic lymphoma. Oncotarget. 2016;7(42):68513–26.

374. Hofland T, Endstra S, Gomes CKP, De Boer R, De Weerdt I, Bobkov V, et al. Natural Killer Cell Hypo-responsiveness in Chronic Lymphocytic Leukemia can be Circumvented in Vitro by Adequate Activating Signaling. HemaSphere. 2019 Dec 1;3(6).

375. Huergo-Zapico L, Acebes-Huerta A, Gonzalez-Rodriguez AP, Contesti J, Gonzalez-Garcia E, Payer AR, et al. Expansion of NK Cells and Reduction of NKG2D Expression in Chronic Lymphocytic Leukemia. Correlation with Progressive Disease. PLoS One. 2014 Oct 6;9(10):9–144.

376. Azoulay T, Slouzky I, Karmona M, Filatov M, Hayun M, Ofran Y, et al. Compromised activity of natural killer cells in diffuse large b-cell lymphoma is related to lymphoma-induced modification of their surface receptor expression. Cancer Immunol Immunother. 2022 Sep 1;

377. MacFarlane AW, Jillab M, Smith MR, Alpaugh RK, Cole ME, Litwin S, et al. NK cell dysfunction in chronic lymphocytic leukemia is associated with loss of the mature cells expressing inhibitory killer cell Ig-like receptors. Oncoimmunology. 2017 Jul 3;6(7).

378. Bojarczuk K, Sasi BK, Gobessi S, Innocenti I, Pozzato G, Laurenti L, et al. BCR signaling inhibitors differ in their ability to overcome Mcl-1-mediated resistance of CLL B cells to ABT-199. Blood. 2016 Jun 23;127(25):3192–201.

379. De Totero D, Reato G, Mauro F, Cignetti A, Ferrini S, Guarini A, et al. IL4 production and increased CD30 expression by a unique CD8+ T-cell subset in B-cell chronic lymphocytic leukaemia. Br J Haematol. 1999;104(3):589–99.

380. Pascutti MF, Jak M, Tromp JM, Derks IAM, Remmerswaal EBM, Thijssen R, et al. IL-21 and CD40L signals from autologous T cells can induce antigen-independent proliferation of CLL cells. Blood. 2013;122(17):3010–9.

381. Rossmann ED, Lewin N, Jeddi-Tehrani M, Österborg A, Mellstedt H. Intracellular T cell cytokines in patients with B cell chronic lymphocytic leukaemia (B-CLL). Eur J Haematol. 2002;68(5):299–306.

382. Blunt MD, Dobson R, Smith LD, Strefford JC, Conley PB, Pandey A, et al. Regulation of B-Cell Receptor Signalling By the Tumour Microenvironment in Chronic Lymphocytic Leukemia (CLL) and Its Impact on Adhesion and miRNA Expression. Blood. 2016 Dec 2;128(22):351.

383. Lee HH, Dadgostar H, Cheng Q, Shu J, Cheng G. NF-κB-mediated up-regulation of Bcl-x and Bfl-1/A1 is required for CD40 survival signaling in B lymphocytes. Proc Natl Acad Sci U S A. 1999 Aug 3;96(16):9136–41.

384. Graham L V., Khakoo SI, Blunt MD. NK Cells in the Lymph Nodes and Their Role in Anti-Tumour Immunity. Biomed 2024. 2024 Jul 25;12(8):1667.

385. Blanquart E, Ekren R, Rigaud B, Joubert MV, Baylot virginie, Daunes H, et al. NK cells with adhesion defects and reduced cytotoxic functions are associated with a poor prognosis in Multiple Myeloma. Blood J. 2024 Jun 14;144(12):1271–83.

386. Pérez-Andrés M, Almeida J, Martín-Ayuso M, Moro MJ, Martín-Nuñez G, Galende J, et al. Clonal plasma cells from monoclonal gammopathy of undetermined significance, multiple myeloma and plasma cell leukemia show different expression profiles of molecules involved in the interaction with the immunological bone marrow microenvironment. Leuk 2005 193. 2005 Jan 27;19(3):449–55.

387. Holt D, Ma X, Kundu N, Fulton A. Prostaglandin E 2 (PGE 2) suppresses natural killer cell

function primarily through the PGE 2 receptor EP4. Cancer Immunol Immunother. 2011 Nov 17;60(11):1577–86.

388. Offringa R, Kötzner L, Huck B, Urbahns K. The expanding role for small molecules in immuno-oncology. Nat Rev Drug Discov 2022 2111. 2022 Aug 18;21(11):821–40.

389. Galluzzi L, Humeau J, Buqué A, Zitvogel L, Kroemer G. Immunostimulation with chemotherapy in the era of immune checkpoint inhibitors. Nat Rev Clin Oncol 2020 1712. 2020 Aug 5;17(12):725–41.

390. Schlicher L, Green LG, Romagnani A, Renner F. Small molecule inhibitors for cancer immunotherapy and associated biomarkers – the current status. Front Immunol. 2023 Oct 31;14:1297175.

391. Pan R, Ryan J, Pan D, Wucherpfennig KW, Letai A. Augmenting NK cell-based immunotherapy by targeting mitochondrial apoptosis. Cell. 2022 Apr 28;185(9):1521-1538.e18.

392. Afolabi LO, Bi J, Li X, Adeshakin AO, Adeshakin FO, Wu H, et al. Synergistic Tumor Cytolysis by NK Cells in Combination With a Pan-HDAC Inhibitor, Panobinostat. Front Immunol. 2021 Aug 31;12:3577.

393. Osman MS, Burshtyn DN, Kane KP. Activating Ly-49 receptors regulate LFA-1-mediated adhesion by NK cells. J Immunol. 2007 Feb 1;178(3):1261–7.

394. Driouk L, Gicobi JK, Kamihara Y, Rutherford K, Dranoff G, Ritz J, et al. Chimeric Antigen Receptor T Cells Targeting NKG2D-Ligands Show Robust Efficacy Against Acute Myeloid Leukemia and T-Cell Acute Lymphoblastic Leukemia. Front Immunol. 2020 Dec 15;11:580328.

395. Chu Y, Yahr A, Huang B, Ayello J, Barth M, S. Cairo M. Romidepsin alone or in combination with anti-CD20 chimeric antigen receptor expanded natural killer cells targeting Burkitt lymphoma in vitro and in immunodeficient mice. Oncoimmunology. 2017 Sep 2;6(9).

396. Xu Y, Li S, Wang Y, Liu J, Mao X, Xing H, et al. Induced CD20 Expression on B-Cell Malignant Cells Heightened the Cytotoxic Activity of Chimeric Antigen Receptor Engineered T Cells. Hum Gene Ther. 2019 Apr 4;30(4):497–510.

397. Brignone C, Bradley KE, Kisselev AF, Grossman SR. A post-ubiquitination role for MDM2 and hHR23A in the p53 degradation pathway. Oncogene. 2004 Apr 5;23(23):4121–9.

398. Vassilev LT, Vu BT, Graves B, Carvajal D, Podlaski F, Filipovic Z, et al. In Vivo Activation of the p53 Pathway by Small-Molecule Antagonists of MDM2. Science (80- ). 2004 Feb 6;303(5659):844–8.

399. Chen J, Liu X, Zeng Z, Li J, Luo Y, Sun W, et al. Immunomodulation of NK Cells by Ionizing Radiation. Front Oncol. 2020 Jun 16;10:874.

400. Michelin S, Gallegos CE, Dubner D, Favier B, Carosella ED. Ionizing radiation modulates the surface expression of human leukocyte antigen-G in a human melanoma cell line. Hum Immunol. 2009 Dec;70(12):1010–5.

401. Acebes-Huerta A, Huergo-Zapico L, Gonzalez-Rodriguez AP, Fernandez-Guizan A, Payer AR, López-Soto A, et al. Lenalidomide Induces Immunomodulation in Chronic Lymphocytic Leukemia and Enhances Antitumor Immune Responses Mediated by NK and CD4 T Cells. Biomed Res Int. 2014;2014.

402. Hallett WHD, Ames E, Motarjemi M, Barao I, Shanker A, Tamang DL, et al. Sensitization of tumor cells to NK cell-mediated killing by proteasome inhibition. J Immunol. 2008 Jan 1;180(1):163–70.

403. Carlsten M, Namazi A, Reger R, Levy E, Berg M, St. Hilaire C, et al. Bortezomib sensitizes multiple myeloma to NK cells via ER-stress-induced suppression of HLA-E and upregulation of DR5. Oncoimmunology. 2019 Feb 1;8(2):e1534664–e1534664.

404. Yun HD, Schirm DK, Felices M, Miller JS, Eckfeldt CE. Dinaciclib enhances natural killer cell cytotoxicity against acute myelogenous leukemia. Blood Adv. 2019 Aug 27;3(16):2448–52.

405. Chang MC, Cheng HI, Hsu K, Hsu YN, Kao CW, Chang YF, et al. NKG2A Down-Regulation by Dasatinib Enhances Natural Killer Cytotoxicity and Accelerates Effective Treatment Responses in Patients With Chronic Myeloid Leukemia. Front Immunol. 2019;9(JAN).

406. Farren MR, Hennessey RC, Shakya R, Elnaggar O, Young G, Kendra K, et al. The exportin-1 inhibitor selinexor exerts superior antitumor activity when combined with T-Cell checkpoint inhibitors. Mol Cancer Ther. 2017 Mar 1;16(3):417–27.

407. Farren MR, Shakya R, Hennessey R, Mace T, Yang J, Elnaggar O, et al. Selinexor, a selective inhibitor of nuclear export (SINE), shows enhanced activity in combination with PD-1/PD-L1 blockade in syngeneic murine models of colon cancer and melanoma. J Immunother Cancer. 2015 Dec;3(S2):P355.

408. Reddy Sudalagunta P, Renatino-Canevarolo R, Meads MB, Noyes D, Achille A, Silva M, et al. Selinexor Disrupts Epigenetic Programing and Modulates Immunogenicity in Multiple Myeloma. Blood. 2023 Nov 2;142(Supplement 1):3301–3301.

409. Azizian NG, Azizian NG, Li Y, Li Y. XPO1-dependent nuclear export as a target for cancer therapy. J Hematol Oncol 2020 131. 2020 Jun 1;13(1):1–9.

410. Yang Y, Guo L, Chen L, Gong B, Jia D, Sun Q. Nuclear transport proteins: structure, function, and disease relevance. Signal Transduct Target Ther. 2023 Dec 1;8(1).

411. Fornerod M, Ohno M, Yoshida M, Mattaj I. CRM1 is an export receptor for leucine-rich nuclear export signals. Cell. 1997 Sep 19;90(6):1051–60.

412. Crochiere M, Kashyap T, Kalid O, Shechter S, Klebanov B, Senapedis W, et al. Deciphering mechanisms of drug sensitivity and resistance to Selective Inhibitor of Nuclear Export (SINE) compounds. BMC Cancer. 2015 Nov 17;15(1):910.

413. Ferreira BI, Cautain B, Grenho I, Link W. Small Molecule Inhibitors of CRM1. Vol. 11, Frontiers in Pharmacology. Frontiers Media S.A.; 2020. p. 518989.

414. Walker JS, Hing ZA, Harrington B, Baumhardt J, Ozer HG, Lehman A, et al. Recurrent XPO1 mutations alter pathogenesis of chronic lymphocytic leukemia. J Hematol Oncol. 2021 Dec 1;14(1).

415. Rose AS, Bradley AR, Valasatava Y, Duarte JM, Prlic A, Rose PW. NGL viewer: web-based molecular graphics for large complexes. Bioinformatics. 2018 Nov 1;34(21):3755–8.

416. Senapedis WT, Baloglu E, Landesman Y. Clinical translation of nuclear export inhibitors in cancer. Vol. 27, Seminars in Cancer Biology. Academic Press; 2014. p. 74–86.

417. Santiago A, Li D, Zhao LY, Godsey A, Liao D. p53 SUMOylation promotes its nuclear export by facilitating its release from the nuclear export receptor CRM1. Mol Biol Cell. 2013 Sep 1;24(17):2739–52.

418. Yoshimura M, Ishizawa J, Ruvolo V, Dilip A, Quintás-Cardama A, Mcdonnell TJ, et al. Induction of p53-mediated transcription and apoptosis by exportin-1 (XPO1) inhibition in mantle cell lymphoma. Cancer Sci. 2014;105(7):795–801.

419. Zhang K, Wang M, Tamayo AT, Shacham S, Kauffman M, Lee J, et al. Novel selective inhibitors of nuclear export CRM1 antagonists for therapy in mantle cell lymphoma. Exp Hematol. 2013 Jan 1;41(1):67-78.e4.

420. Köhler A, Hurt E. Exporting RNA from the nucleus to the cytoplasm. Vol. 8, Nature Reviews Molecular Cell Biology. Nature Publishing Group; 2007. p. 761–73.

421. Liu Y, Azizian NG, Dou Y, Pham L V., Li Y. Simultaneous targeting of XPO1 and BCL2 as an effective treatment strategy for double-hit lymphoma. J Hematol Oncol. 2019 Nov 21;12(1).

422. Kashyap T, Argueta C, Aboukameel A, Unger TJ, Klebanov B, Mohammad RM, et al. Selinexor, a Selective Inhibitor of Nuclear Export (SINE) compound, acts through NF-κB deactivation and

combines with proteasome inhibitors to synergistically induce tumor cell death. Oncotarget. 2016;7(48):78883–95.

423. Camus V, Miloudi H, Taly A, Sola B, Jardin F. XPO1 in B cell hematological malignancies: from recurrent somatic mutations to targeted therapy. Vol. 10, Journal of Hematology and Oncology. BioMed Central Ltd.; 2017. p. 1–13.

424. Cosson A, Chapiro E, Bougacha N, Lambert J, Herbi L, Cung HA, et al. Gain in the short arm of chromosome 2 (2p+) induces gene overexpression and drug resistance in chronic lymphocytic leukemia: analysis of the central role of XPO1. Leukemia. 2017 Jul 1;31(7):1625–9.

425. García-Santisteban I, Arregi I, Alonso-Mariño M, Urbaneja MA, Garcia-Vallejo JJ, Bañuelos S, et al. A cellular reporter to evaluate CRM1 nuclear export activity: functional analysis of the cancer-related mutant E571K. Cell Mol Life Sci. 2016 Jun 16;73(24):4685–99.

426. Miloudi H, Bohers É, Guillonneau F, Taly A, Gibouin VC, Viailly PJ, et al. XPO1E571K Mutation Modifies Exportin 1 Localisation and Interactome in B-Cell Lymphoma. Cancers (Basel). 2020 Oct 1;12(10):1–20.

427. Taylor J, Sendino M, Gorelick AN, Pastore A, Chang MT, Penson A V., et al. Altered nuclear export signal recognition as a driver of oncogenesis. Cancer Discov. 2019 Oct 1;9(10):1452–67.

428. Kolijn PM, Späth F, Khouja M, Hengeveld PJ, van der Straten L, Darzentas N, et al. Genetic drivers in the natural history of chronic lymphocytic leukemia development as early as 16 years before diagnosis. Blood. 2023 Oct 19;142(16):1399–403.

429. Xu Z, Pan B, Miao Y, Li Y, Qin S, Liang J, et al. Prognostic value and therapeutic targeting of XPO1 in chronic lymphocytic leukemia. Clin Exp Med. 2023 Oct 1;23(6):2651–62.

430. Wang AY, Liu H. The past, present, and future of CRM1/XPO1 inhibitors. Vol. 6, Stem Cell Investigation. AME Publishing Company; 2019.

431. Marullo R, Rutherford SC, Revuelta M V., Zamponi N, Culijkovic B, Kotlov N, et al. XPO1 Enables Adaptive Regulation of mRNA Export Required for Genotoxic Stress Tolerance in Cancer Cells. Cancer Res. 2024 Jan 2;84(1).

432. Birnbaum DJB, Finetti P, Birnbaum D, Mamessier E, Bertucci F. XPO1 expression is a poor-prognosis marker in pancreatic adenocarcinoma. J Clin Med. 2019 Apr 30;8(5):596.

433. Chen L, Huang Y, Zhou L, Lian Y, Wang J, Chen D, et al. Prognostic roles of the transcriptional expression of exportins in hepatocellular carcinoma. Biosci Rep. 2019 Aug 19;39(8).

434. Turner JG, Kashyap T, Dawson JL, Gomez J, Bauer AA, Grant S, et al. XPO1 inhibitor

combination therapy with bortezomib or carfilzomib induces nuclear localization of IkBa and overcomes acquired proteasome inhibitor resistance in human multiple myeloma. Oncotarget. 2016;7(48):78896–909.

435. Reddy A, Zhang J, Davis NS, Moffitt AB, Love CL, Waldrop A, et al. Genetic and Functional Drivers of Diffuse Large B Cell Lymphoma. Cell. 2017 Oct 10;171(2):481.

436. Gandhi UH, Senapedis W, Baloglu E, Unger TJ, Chari A, Vogl D, et al. Clinical Implications of Targeting XPO1-mediated Nuclear Export in Multiple Myeloma. Vol. 18, Clinical Lymphoma, Myeloma and Leukemia. Elsevier Inc.; 2018. p. 335–45.

437. Abeykoon JP, Paludo J, Nowakowski KE, Stenson MJ, King RL, Wellik LE, et al. The effect of CRM1 inhibition on human non-Hodgkin lymphoma cells. Blood Cancer J 2019 93. 2019 Feb 26;9(3):1–4.

438. Lapalombella R, Sun Q, Williams K, Tangeman L, Jha S, Zhong Y, et al. Selective inhibitors of nuclear export show that CRM1/XPO1 is a target in chronic lymphocytic leukemia. Blood. 2012 Nov 29;120(23):4621–34.

439. Roberts BJ, Hamelehle KL, Sebolt JS, Leopold WR. In vivo and in vitro anticancer activity of the structurally novel and highly potent antibiotic CI-940 and its hydroxy analog (PD 114,721). Cancer Chemother Pharmacol. 1986 Mar;16(2):95–101.

440. Newlands ES, Rustin GJS, Brampton MH. Phase I trial of elactocin. Br J Cancer. 1996;74(4):648–9.

441. Mutka SC, Yang WQ, Dong SD, Ward SL, Craig DA, Timmermans PBMWM, et al. Identification of nuclear export inhibitors with potent anticancer activity in vivo. Cancer Res. 2009 Jan 15;69(2):510–7.

442. Kudo N, Matsumori N, Taoka H, Fujiwara D, Schreiner EP, Wolff B, et al. Leptomycin B inactivates CRM1/exportin 1 by covalent modification at a cysteine residue in the central conserved region. Proc Natl Acad Sci U S A. 1999 Aug 3;96(16):9112–7.

443. Sun Q, Carrasco YP, Hu Y, Guo X, Mirzaei H, MacMillan J, et al. Nuclear export inhibition through covalent conjugation and hydrolysis of Leptomycin B by CRM1. Proc Natl Acad Sci U S A. 2013 Jan 22;110(4):1303–8.

444. Etchin J, Sanda T, Mansour MR, Kentsis A, Montero J, Le BT, et al. KPT-330 inhibitor of CRM1 (XPO1)-mediated nuclear export has selective anti-leukaemic activity in preclinical models of T-cell acute lymphoblastic leukaemia and acute myeloid leukaemia. Br J Haematol. 2013 Apr;161(1):117–27.

445. Tai YT, Landesman Y, Acharya C, Calle Y, Zhong MY, Cea M, et al. CRM1 inhibition induces tumor cell cytotoxicity and impairs osteoclastogenesis in multiple myeloma: Molecular mechanisms and therapeutic implications. Leukemia. 2014;28(1):155–65.

446. Sun Q, Chen X, Zhou Q, Burstein E, Yang S, Jia D. Inhibiting cancer cell hallmark features through nuclear export inhibition. Vol. 1, Signal Transduction and Targeted Therapy. Springer Nature; 2016. p. 16010.

447. Parikh K, Cang S, Sekhri A, Liu D. Selective inhibitors of nuclear export (SINE)-A novel class of anti-cancer agents. J Hematol Oncol. 2014;7(1).

448. Stephens DM, Huang Y, Ruppert AS, Walker JS, Canfield D, Cempre CB, et al. Selinexor Combined with Ibrutinib Demonstrates Tolerability and Safety in Advanced B-Cell Malignancies: A Phase I Study. Clin Cancer Res. 2022 Jun 23;OF1–6.

449. Hing ZA, Mantel R, Beckwith KA, Guinn D, Williams E, Smith LL, et al. Selinexor is effective in acquired resistance to ibrutinib and synergizes with ibrutinib in chronic lymphocytic leukemia. Blood. 2015;125(20):3128–32.

450. Liu Y, Yang R, Feng H, Du Y, Yang B, Zhang M, et al. Adverse events reporting of XPO1 inhibitor - selinexor: a real-word analysis from FAERS database. Sci Rep. 2024 May 28;14(1):1–8.

451. Hing ZA, Fung HYJ, Ranganathan P, Mitchell S, El-Gamal D, Woyach JA, et al. Next-generation XPO1 inhibitor shows improved efficacy and in vivo tolerability in hematological malignancies. Leukemia. 2016 Dec 1;30(12):2364–72.

452. Kotlov N, Bagaev A, Revuelta M V., Phillip JM, Cacciapuoti MT, Antysheva Z, et al. Clinical and Biological Subtypes of B-cell Lymphoma Revealed by Microenvironmental Signatures. Cancer Discov. 2021;11(6):1468–89.

453. Zhao L, Luo B, Wang L, Chen W, Jiang M, Zhang N. Pan-cancer analysis reveals the roles of XPO1 in predicting prognosis and tumorigenesis. Transl Cancer Res. 2021 Nov 1;10(11):4664–79.

454. Arruga F, Gyau BB, Iannello A, Deaglio S, Vitale N, Vaisitti T. Immune Response Dysfunction in Chronic Lymphocytic Leukemia: Dissecting Molecular Mechanisms and Microenvironmental Conditions. Int J Mol Sci. 2020 Mar 1;21(5).

455. Jiménez I, Carabia J, Bobillo S, Palacio C, Abrisqueta P, Pagès C, et al. Repolarization of tumor infiltrating macrophages and increased survival in mouse primary CNS lymphomas after XPO1 and BTK inhibition. J Neurooncol. 2020 Aug 1;149(1):13–25.

456. Kady N, Wang C, Wolfe A, Maine I, Abdelrahman S, Murga-Zamalloa CA, et al. Xpo-1 Antagonism Impairs CSF-1R Expression and Depletes Lymphoma-Associated Macrophages in T-Cell Lymphomas. Blood. 2023 Nov 2;142(Supplement 1):1647–1647.

457. Baron S, Rashal T, Vaisman D, Elhasid R, Shukrun R. Selinexor, a selective inhibitor of nuclear export, inhibits human neutrophil extracellular trap formation in vitro. Front Pharmacol. 2022 Nov 24;13.

458. Martini S, Figini M, Croce A, Frigerio B, Pennati M, Gianni AM, et al. Selinexor Sensitizes TRAIL-R2-Positive TNBC Cells to the Activity of TRAIL-R2xCD3 Bispecific Antibody. Cells. 2020 Oct 2;9(10).

459. Wang S, Sellner L, Wang L, Sauer T, Neuber B, Gong W, et al. Combining selective inhibitors of nuclear export (SINEs) with chimeric antigen receptor (CAR) T cells for CD19-positive malignancies. Oncol Rep. 2021 Jun 23;46(2):170.

460. Stadel R, Liu R, Landesman Y, Wald D, Hosahalli Vasanna S, de Lima MJG. Sequential Administration of Selinexor then CD19 CAR-T Cells Exhibits Enhanced Efficacy in a Mouse Model of Human Non-Hodgkin's Lymphoma. Blood. 2022 Nov 15;140(Supplement 1):7413–4.

461. Zhang Y, Zong X, LI J, Jia S, Geng H, Zeng L, et al. PB2289: PRELIMINARY DATA FROM A FIRST-IN HUMAN PHASE II STUDY OF SEQUENTIAL USE OF SELINEXOR AND CD19 CHIMERIC ANTIGEN RECEPTOR MODIFIED T-CELL THERAPY (CART19) IN PATIENTS WITH RELAPSED OR REFRACTORY B-CELL NON-HODGKIN LYMPHOMA. HemaSphere. 2023 Aug 8;7(Suppl):e42135d7.

462. Wang D, Fu H, Que Y, Ruan H, Xu M, Long X, et al. A novel two-step administration of XPO-1 inhibitor may enhance the effect of anti-BCMA CAR-T in relapsed/refractory extramedullary multiple myeloma. J Transl Med. 2023 Dec 1;21(1):1–10.

463. Hu F, Chen XQ, Li XP, Lu YX, Chen SL, Wang DW, et al. Drug resistance biomarker ABCC4 of selinexor and immune feature in multiple myeloma. Int Immunopharmacol. 2022 Jul 1;108:108722.

464. Keoni CLI, Brown TL. Inhibition of apoptosis and efficacy of pan caspase inhibitor, Q-VD-OPh, in models of human disease. Vol. 8, Journal of Cell Death. SAGE Publications; 2015. p. 1–7.

465. Alter G, Malenfant JM, Altfeld M. CD107a as a functional marker for the identification of natural killer cell activity. J Immunol Methods. 2004 Nov 1;294(1–2):15–22.

466. Oslowski CM, Urano F. Measuring ER stress and the unfolded protein response using mammalian tissue culture system. In: Methods in Enzymology. Academic Press Inc.; 2011. p.

71–92.

467. Serna L, Azcoaga P, Brahmachary M, Caffarel MM, Braza MS. Diffuse large B-cell lymphoma microenvironment displays a predominant macrophage infiltrate marked by a strong inflammatory signature. Front Immunol. 2023 May 2;14:1048567.

468. Takao S, Ishikawa T, Uchiyama T. The Expression Level of HLA-E on Activated T Cells Determines Their Fate When Activated NK Cells Were Nearby Present. Blood. 2008 Nov 16;112(11):1529–1529.

469. Dinavahi SS, Chen YC, Punnath K, Berg A, Herlyn M, Foroutan M, et al. Targeting WEE1/AKT restores p53-dependent NK cell activation to induce immune checkpoint blockade responses in 'cold' melanoma. Cancer Immunol Res. 2022 Jun 6;10(6):757.

470. Chollat-Namy M, Ben Safta-Saadoun T, Haferssas D, Meurice G, Chouaib S, Thiery J. The pharmalogical reactivation of p53 function improves breast tumor cell lysis by granzyme B and NK cells through induction of autophagy. Cell Death Dis. 2019 Sep 20;10(10):1–20.

471. Belkahla S, Brualla JM, Fayd'herbe de Maudave A, Falvo P, Allende-Vega N, Constantinides M, et al. The metabolism of cells regulates their sensitivity to NK cells depending on p53 status. Sci Rep. 2022 Feb 25;12(1):1–13.

472. Jiang J, Wang Y, Liu D, Wang X, Zhu Y, Tong J, et al. Selinexor Synergistically Promotes the Antileukemia Activity of Venetoclax in Acute Myeloid Leukemia by Inhibiting Glycolytic Function and Downregulating the Expression of DNA Replication Genes. ImmunoTargets Ther. 2023;12:135.

473. Spampinato M, Zuppelli T, Dulcamare I, Longhitano L, Sambataro D, Santisi A, et al. Enhanced Antitumor Activity by the Combination of Dasatinib and Selinexor in Chronic Myeloid Leukemia. Pharmaceuticals. 2024 Jul 5;17(7):894.

474. Moore SA, Landes JR, Simonette RA, He Q, Doan HQ, Rady PL, et al. Selinexor targets expression of metabolic genes in Merkel cell carcinoma cells. Vol. 316, Archives of Dermatological Research. 2024.

475. Reiners KS, Topolar D, Henke A, Simhadri VR, Kessler J, Sauer M, et al. Soluble ligands for NK cell receptors promote evasion of chronic lymphocytic leukemia cells from NK cell anti-tumor activity. Blood. 2013 May 2;121(18):3658–65.

476. Sen Santara S, Lee DJ, Crespo Â, Hu JJ, Walker C, Ma X, et al. The NK cell receptor NKp46 recognizes ecto-calreticulin on ER-stressed cells. Nature. 2023 Apr 13;616(7956):348–56.

477. Minute L, Teijeira A, Sanchez-Paulete AR, Ochoa MC, Alvarez M, Otano I, et al. Cellular cytotoxicity is a form of immunogenic cell death. J Immunother Cancer. 2020 Mar 1;8(1):e000325.

478. Enqvist M, Jacobs B, Junlén HR, Schaffer M, Melén CM, Friberg D, et al. Systemic and Intra-Nodal Activation of NK Cells After Rituximab Monotherapy for Follicular Lymphoma. Front Immunol. 2019 Sep 12;10:473494.

479. Upchurch-Ange KC, Oter G, Gimlin S, Weidanz DW, Weidanz J. Characterization of a novel therapeutic antibody targeting peptide/HLA-E. J Immunol. 2023 May 1;210(1_Supplement):146.02-146.02.

480. Bexte T, Alzubi J, Reindl LM, Wendel P, Schubert R, Salzmann-Manrique E, et al. CRISPR-Cas9 based gene editing of the immune checkpoint NKG2A enhances NK cell mediated cytotoxicity against multiple myeloma. Oncoimmunology. 2022;11(1).

481. Biber G, Sabag B, Raiff A, Ben-Shmuel A, Puthenveetil A, Benichou JIC, et al. Modulation of intrinsic inhibitory checkpoints using nano-carriers to unleash NK cell activity. EMBO Mol Med. 2022 Jan 11;14(1).

482. Ben-Shmuel A, Biber G, Sabag B, Barda-Saad M. Modulation of the intracellular inhibitory checkpoint SHP-1 enhances the antitumor activity of engineered NK cells. Vol. 18, Cellular and Molecular Immunology. Nature Publishing Group; 2021. p. 1314–6.

483. Bernard PL, Delconte R, Pastor S, Laletin V, Costa Da Silva C, Goubard A, et al. Targeting CISH enhances natural cytotoxicity receptor signaling and reduces NK cell exhaustion to improve solid tumor immunity. J Immunother Cancer. 2022 May 1;10(5):e004244.

484. Wahba A, Rath BH, O'Neill JW, Camphausen K, Tofilon PJ. The XPO1 inhibitor selinexor inhibits translation and enhances the radiosensitivity of glioblastoma cells grown in vitro and in vivo. Mol Cancer Ther. 2018 Aug 1;17(8):1717–26.

485. Tabe Y, Kojima K, Yamamoto S, Sekihara K, Matsushita H, Davis RE, et al. Ribosomal biogenesis and translational flux inhibition by the selective inhibitor of nuclear export (sine) XPO1 antagonist KPT-185. PLoS One. 2015 Sep 4;10(9).

486. Li S, Fu J, Walker CJ, Yang J, Bhutani D, Chakraborty R, et al. Dual targeting of protein translation and nuclear protein export results in enhanced antimyeloma effects. Blood Adv. 2023 Jun 27;7(12):2926–37.

487. Ong G, Ragetli R, Mnich K, Doble BW, Kammouni W, Logue SE. IRE1 signaling increases PERK expression during chronic ER stress. Cell Death Dis. 2024 Apr 18;15(4):1–11.

488. Enqvist M, Nilsonne G, Hammarfjord O, Wallin RPA, Björkström NK, Björnstedt M, et al. Selenite Induces Posttranscriptional Blockade of HLA-E Expression and Sensitizes Tumor Cells to CD94/NKG2A-Positive NK Cells. J Immunol. 2011 Oct 1;187(7):3546–54.

489. Bowles JA, Wang S-Y, Link BK, Allan B, Beuerlein G, Campbell M-A, et al. Anti-CD20 monoclonal antibody with enhanced affinity for CD16 activates NK cells at lower concentrations and more effectively than rituximab. Blood. 2006 Oct 15;108(8):2648.

490. Eitler J, Rackwitz W, Wotschel N, Gudipati V, Murali Shankar N, Sidorenkova A, et al. CAR-mediated targeting of NK cells overcomes tumor immune escape caused by ICAM-1 downregulation. J Immunother cancer. 2024 Feb 27;12(2).

491. Haselager M V., Van Driel BF, Perelaer E, De Rooij D, Lashgari D, Loos R, et al. In Vitro 3D Spheroid Culture System Displays Sustained T Cell-dependent CLL Proliferation and Survival. HemaSphere. 2023 Sep 23;7(9):E938.

492. Daher M, Rezvani K. Next generation natural killer cells for cancer immunotherapy: the promise of genetic engineering. Vol. 51, Current Opinion in Immunology. Elsevier Ltd; 2018. p. 146–53.

493. Sensi M, Pietra G, Molla A, Nicolini G, Vegetti C, Bersani I, et al. Peptides with dual binding specificity for HLA-A2 and HLA-E are encoded by alternatively spliced isoforms of the antioxidant enzyme peroxiredoxin 5. Int Immunol. 2009 Mar 1;21(3):257–68.

494. Chiodin G, Drennan S, Martino EA, Ondrisova L, Henderson I, del Rio L, et al. High surface IgM levels associate with shorter response to ibrutinib and BTK bypass in patients with CLL. Blood Adv. 2022 Sep 27;6(18):5494–504.

495. Hilpert J, Grosse-Hovest L, Grünebach F, Buechele C, Nuebling T, Raum T, et al. Comprehensive analysis of NKG2D ligand expression and release in leukemia: implications for NKG2D-mediated NK cell responses. J Immunol. 2012 Aug 1;189(3):1360–71.

496. Nückel H, Switala M, Sellmann L, Horn PA, Dürig J, Dührsen U, et al. The prognostic significance of soluble NKG2D ligands in B-cell chronic lymphocytic leukemia. Leukemia. 2010 Jun;24(6):1152–9.

497. Dubovsky JA, Beckwith KA, Natarajan G, Woyach JA, Jaglowski S, Zhong Y, et al. Ibrutinib is an irreversible molecular inhibitor of ITK driving a Th1-selective pressure in T lymphocytes. Blood. 2013;122(15):2539–49.

498. Khurana D, Arneson LN, Schoon RA, Dick CJ, Leibson PJ. Differential regulation of human NK cell-mediated cytotoxicity by the tyrosine kinase Itk. J Immunol. 2007 Mar 15;178(6):3575–82.

499. Kohrt HE, Sagiv-Barfi I, Rafiq S, Herman SEM, Butchar JP, Cheney C, et al. Ibrutinib antagonizes rituximab-dependent NK cell-mediated cytotoxicity. Blood. 2014 Mar 20;123(12):1957–60.

500. Kipps TJ, Stevenson FK, Wu CJ, Croce CM, Packham G, Wierda WG, et al. Chronic lymphocytic leukaemia. Nat Rev Dis Prim 2017 31. 2017 Jan 19;3(1):1–22.

501. Stevenson FK, Forconi F, Kipps TJ. Exploring the pathways to chronic lymphocytic leukemia. Blood. 2021 Sep 9;138(10):827–35.

502. Tremante E, Lo Monaco E, Ingegnere T, Sampaoli C, Fraioli R, Giacomini P. Monoclonal antibodies to HLA-E bind epitopes carried by unfolded β2m-free heavy chains. Eur J Immunol. 2015 Aug 1;45(8):2356–64.

503. Brackenridge S, John N, Früh K, Borrow P, McMichael AJ. The antibodies 3D12 and 4D12 recognise distinct epitopes and conformations of HLA-E. Front Immunol. 2024 Mar 20;15:1329032.

504. Calissano C, Damle RN, Marsilio S, Yan XJ, Yancopoulos S, Hayes G, et al. Intraclonal complexity in chronic lymphocytic leukemia: Fractions enriched in recently born/divided and older/quiescent cells. Mol Med. 2011 Sep 23;17(11):1374–82.

505. Kluckova K, Clear AJ, D'Avola A, Rassenti LZ, Kipps TJ, Gribben JG, et al. B-cell Receptor Signaling Induced Metabolic Alterations in Chronic Lymphocytic Leukemia Can Be Partially Bypassed by TP53 Abnormalities. HemaSphere. 2022 Jun 13;6(6):E722.

506. Okada T, Ngo VN, Ekland EH, Förster R, Lipp M, Littman DR, et al. Chemokine requirements for b cell entry to lymph nodes and Peyer's patches. J Exp Med. 2002 Jul 1;196(1):65–75.

507. Yano M, Byrd JC, Muthusamy N. Natural Killer Cells in Chronic Lymphocytic Leukemia: Functional Impairment and Therapeutic Potential. Cancers (Basel). 2022 Nov 24;14(23):5787.

508. Finnberg N, Klein-Szanto AJP, El-Deiry WS. TRAIL-R deficiency in mice promotes susceptibility to chronic inflammation and tumorigenesis. J Clin Invest. 2008 Jan 2;118(1):111–23.

509. Wu GS, Burns TF, McDonald ER, Jiang W, Meng R, Krantz ID, et al. KILLER/DR5 is a DNA damage-inducible p53-regulated death receptor gene. Vol. 17, Nature Genetics. Nat Genet; 1997. p. 141–3.

510. Hori T, Kondo T, Kanamori M, Tabuchi Y, Ogawa R, Zhao QL, et al. Nutlin-3 enhances tumor necrosis factor-related apoptosis-inducing ligand (TRAIL)-induced apoptosis through up-regulation of death receptor 5 (DR5) in human sarcoma HOS cells and human colon cancer HCT116 cells. Cancer Lett. 2010 Jan 1;287(1):98–108.

511. Min K jin, Woo SM, Shahriyar SA, Kwon TK. Elucidation for modulation of death receptor (DR) 5 to strengthen apoptotic signals in cancer cells. Vol. 42, Archives of Pharmacal Research. Springer; 2019. p. 88–100.

512. Wurzer H, Filali L, Hoffmann C, Krecke M, Biolato AM, Mastio J, et al. Intrinsic Resistance of Chronic Lymphocytic Leukemia Cells to NK Cell-Mediated Lysis Can Be Overcome In Vitro by Pharmacological Inhibition of Cdc42-Induced Actin Cytoskeleton Remodeling. Front Immunol. 2021 May 24;12:619069.

513. Kurago ZB, Lutz CT, Smith KD, Colonna M. NK Cell Natural Cytotoxicity and IFN-γ Production Are Not Always Coordinately Regulated: Engagement of DX9 KIR+ NK Cells by HLA-B7 Variants and Target Cells. J Immunol. 1998 Feb 15;160(4):1573–80.

514. Vahlne G, Becker S, Brodin P, Johansson MH. IFN-γ production and degranulation are differentially regulated in response to stimulation in murine natural killer cells. Scand J Immunol. 2008 Jan 1;67(1):1–11.

515. Langat DK, Morales PJ, Omwandho CO, Fazleabas AT. Polymorphisms in the Paan-AG promoter influence NF-kappaB binding and transcriptional activity. Immunogenetics. 2007 May;59(5):359–66.

516. Johnson DR, Pober JS. HLA class I heavy-chain gene promoter elements mediating synergy between tumor necrosis factor and interferons. Mol Cell Biol. 1994 Feb 1;14(2):1322–32.

517. Wang IM, Lin H, Goldman SJ, Kobayashi M. STAT-1 is activated by IL-4 and IL-13 in multiple cell types. Mol Immunol. 2004 Jul;41(9):873–84.

518. Najjar I, Baran-Marszak F, Le Clorennec C, Laguillier C, Schischmanoff O, Youlyouz-Marfak I, et al. Latent Membrane Protein 1 Regulates STAT1 through NF-κB-Dependent Interferon Secretion in Epstein-Barr Virus-Immortalized B Cells. J Virol. 2005 Apr 15;79(8):4936–43.

519. Dejardin E, Deregowski V, Greimers R, Cai Z, Chouaib S, Merville MP, et al. Regulation of major histocompatibility complex class I expression by NF-κB-related proteins in breast cancer cells. Oncogene. 1998 Jul 1;16(25):3299–307.

520. Takao S, Ishikawa T, Yamashita K, Uchiyama T. The Rapid Induction of HLA-E Is Essential for the Survival of Antigen-Activated Naive CD4 T Cells from Attack by NK Cells. J Immunol. 2010 Nov 15;185(10):6031–40.

521. Woyach JA, Smucker K, Smith LL, Lozanski A, Zhong Y, Ruppert AS, et al. Prolonged lymphocytosis during ibrutinib therapy is associated with distinct molecular characteristics and does not indicate a suboptimal response to therapy. Blood. 2014 Mar 20;123(12):1810–7.

522. Flinsenberg TWH, Tromedjo CC, Hu N, Liu Y, Guo Y, Thia KYT, et al. Differential effects of BTK inhibitors ibrutinib and zanubrutinib on NK-cell effector function in patients with mantle cell lymphoma. Haematologica. 2020 Feb 1;105(2):e76–9.

523. Gotthardt D, Putz EM, Straka E, Kudweis P, Biaggio M, Poli V, et al. Loss of STAT3 in murine NK cells enhances NK cell–dependent tumor surveillance. Blood. 2014 Oct 9;124(15):2370–9.

524. Armant M, Delespesse G, Sarfati M. IL-2 and IL-7 but not IL-12 protect natural killer cells from death by apoptosis and up-regulate bcl-2 expression. Immunology. 1995;85(2):331–7.

525. Tyler PM, Servos MM, De Vries RC, Klebanov B, Kashyap T, Sacham S, et al. Clinical dosing regimen of selinexor maintains normal immune homeostasis and T-cell effector function in Mice: Implications for combination with immunotherapy. Mol Cancer Ther. 2017 Mar 1;16(3):428–39.

526. Ruggeri L, Urbani E, André P, Mancusi A, Tosti A, Topini F, et al. Effects of anti-NKG2A antibody administration on leukemia and normal hematopoietic cells. Haematologica. 2016 Apr 30;101(5):626–33.

527. Sánchez-Martínez D, Azaceta G, Muntasell A, Aguiló N, Núñez D, Gálvez EM, et al. Human NK cells activated by EBV+ lymphoblastoid cells overcome anti-apoptotic mechanisms of drug resistance in haematological cancer cells. Oncoimmunology. 2015;4(3):1–13.

528. Crochiere ML, Baloglu E, Klebanov B, Donovan S, Alamo D del, Lee M, et al. A method for quantification of exportin-1 (XPO1) occupancy by Selective Inhibitor of Nuclear Export (SINE) compounds. Oncotarget. 2016 Dec 7;7(2):1863–77.

529. De Weerdt I, Hofland T, De Boer R, Dobber JA, Dubois J, Van Nieuwenhuize D, et al. Distinct immune composition in lymph node and peripheral blood of CLL patients is reshaped during venetoclax treatment. Blood Adv. 2019 Sep 10;3(17):2642–52.

530. Liu LL, Béziat V, Oei VYS, Pfefferle A, Schaffer M, Lehmann S, et al. Ex vivo expanded adaptive NK cells effectively kill primary acute lymphoblastic leukemia cells. Cancer Immunol Res. 2017 Aug 1;5(8):654–65.

531. Murad S, Michen S, Becker A, Füssel M, Schackert G, Tonn T, et al. NKG2C+ NK Cells for Immunotherapy of Glioblastoma Multiforme. Int J Mol Sci. 2022 May 1;23(10).

532. Gunesch JT, Angelo LS, Mahapatra S, Deering RP, Kowalko JE, Sleiman P, et al. Genome-wide analyses and functional profiling of human NK cell lines. Mol Immunol. 2019 Nov 1;115:64.

533. Neitzel H. A routine method for the establishment of permanent growing lymphoblastoid cell

lines. Hum Genet. 1986 Aug;73(4):320–6.

534. Kavathas P, Bach FH, DeMars R. Gamma ray-induced loss of expression of HLA and glyoxalase I alleles in lymphoblastoid cells. Proc Natl Acad Sci U S A. 1980;77(7):4251–5.

535. Gocher AM, Workman CJ, Vignali DAA. Interferon-γ: teammate or opponent in the tumour microenvironment? Vol. 22, Nature Reviews Immunology. Nature Publishing Group; 2022. p. 158–72.

536. Hofman T, Ng SW, Garcés-Lázaro I, Heigwer F, Boutros M, Cerwenka A. IFNγ mediates the resistance of tumor cells to distinct NK cell subsets. J Immunother Cancer. 2024 Jul 1;12(7):e009410.

537. Malmberg K-J, Levitsky V, Norell H, Matos CT de, Carlsten M, Schedvins K, et al. IFN-γ protects short-term ovarian carcinoma cell lines from CTL lysis via a CD94/NKG2A-dependent mechanism. J Clin Invest. 2002 Nov 15;110(10):1515–23.

538. Ismael A, Robinette A, Dona K, Kudalkar R, Manning V, Galloway J, et al. CREB1 Promotes Immune Escape of Multiple Myeloma Cells By Inducing HLA-E. Blood. 2023 Nov 2;142(Supplement 1):1930.

539. Mahase E. NICE recommends new CAR-T treatment for lymphoma for some patients on NHS. BMJ. 2021 Jan 20;372:n184.

540. Egli L, Kaulfuss M, Mietz J, Picozzi A, Verhoeyen E, Münz C, et al. CAR T cells outperform CAR NK cells in CAR-mediated effector functions in head-to-head comparison. Exp Hematol Oncol. 2024 Dec 1;13(1):1–18.

541. Gang M, Marin ND, Wong P, Neal CC, Marsala L, Foster M, et al. CAR-modified memory-like NK cells exhibit potent responses to NK-resistant lymphomas. Blood. 2020 Nov 12;136(20):2308–18.

542. Müller S, Bexte T, Gebel V, Kalensee F, Stolzenberg E, Hartmann J, et al. High Cytotoxic Efficiency of Lentivirally and Alpharetrovirally Engineered CD19-Specific Chimeric Antigen Receptor Natural Killer Cells Against Acute Lymphoblastic Leukemia. Front Immunol. 2020 Jan 24;10:3123.

543. Malik-Chaudhry HK, Prabhakar K, Ugamraj HS, Boudreau AA, Buelow B, Dang K, et al. TNB-486 induces potent tumor cell cytotoxicity coupled with low cytokine release in preclinical models of B-NHL. MAbs. 2021 Jan 1;13(1).

544. Colonna M, Nakajima H, Navarro F, López-Botet M. A novel family of Ig-like receptors for HLA

class I molecules that modulate function of lymphoid and myeloid cells. J Leukoc Biol. 1999;66(3):375–81.

545. Maia A, Tarannum M, Lérias JR, Piccinelli S, Borrego LM, Maeurer M, et al. Building a Better Defense: Expanding and Improving Natural Killer Cells for Adoptive Cell Therapy. Vol. 13, Cells. Multidisciplinary Digital Publishing Institute; 2024. p. 451.

546. Gong Y, Klein Wolterink RGJ, Wang J, Bos GMJ, Germeraad WTV. Chimeric antigen receptor natural killer (CAR-NK) cell design and engineering for cancer therapy. J Hematol Oncol. 2021 Dec 1;14(1).

547. Huang RS, Shih HA, Lai MC, Chang YJ, Lin S. Enhanced NK-92 Cytotoxicity by CRISPR Genome Engineering Using Cas9 Ribonucleoproteins. Front Immunol. 2020 May 22;11:1008.

548. Mohammadian Gol T, Kim M, Sinn R, Ureña-Bailén G, Stegmeyer S, Gratz PG, et al. CRISPR-Cas9-Based Gene Knockout of Immune Checkpoints in Expanded NK Cells. Int J Mol Sci. 2023 Nov 1;24(22):16065.

549. Cooley S, McCullar V, Wangen R, Bergemann TL, Spellman S, Weisdorf DJ, et al. KIR reconstitution is altered by T cells in the graft and correlates with clinical outcomes after unrelated donor transplantation. Blood. 2005 Dec 15;106(13):4370–6.

550. Berrien-Elliott MM, Pamela W, Neal C, Wagner JA, Becker-Hapak M, Schappe T, et al. Primary Human NK Cell Gene-Editing Reveals a Critical Role for NKG2A in Cytokine-Induced Memory-like NK Cell Responses. Blood. 2019 Nov 13;134(Supplement_1):3237.

551. Croom-Perez TJ, Robles-Carrillo LD, Dieffenthaller TA, Copik AJ. Abstract 2819: Suppression of NKG2A mediated inhibition in ex vivo expanded natural killer cells increases their cytotoxicity. Cancer Res. 2022 Jun 15;82(12_Supplement):2819–2819.

552. Borrego F, Kabat J, Sanni TB, Coligan JE. NK Cell CD94/NKG2A Inhibitory Receptors Are Internalized and Recycle Independently of Inhibitory Signaling Processes. J Immunol. 2002 Dec 1;169(11):6102–11.

553. Sanni TB, Masilamani M, Kabat J, Coligan JE, Borrego F. Exclusion of Lipid Rafts and Decreased Mobility of CD94/NKG2A Receptors at the Inhibitory NK Cell Synapse. Mol Biol Cell. 2004 Jul;15(7):3210.

554. Crotty S. T Follicular Helper Cell Differentiation, Function, and Roles in Disease. Immunity. 2014 Oct 16;41(4):529–42.

555. Hiroi M, Ohmori Y. Transcriptional Synergism between NF-κB and STAT1. J Oral Biosci. 2005

Jan 1;47(3):230–42.

556. Song M, Ping Y, Zhang K, Yang L, Li F, Zhang C, et al. Low-dose IFNg induces tumor cell stemness in tumor microenvironment of non–small cell lung cancer. Cancer Res. 2019;79(14):3737–48.

557. Jewett A, Gan XH, Lebow LT, Bonavida B. Differential secretion of TNF-α and IFN-γ by human peripheral blood-derived NK subsets and association with functional maturation. J Clin Immunol. 1996;16(1):46–54.

558. Harlow E, Lane D. Anti-NKG2A antibodies and uses thereof. Cold Spring Harb Protoc. 2020 Nov 14;(2):pdb.prot4277.

559. Paolini R, Bernardini G, Molfetta R, Santoni A. NK cells and interferons. Cytokine Growth Factor Rev. 2015 Apr 1;26(2):113–20.

560. Kaplan DH, Shankaran V, Dighe AS, Stockert E, Aguet M, Old LJ, et al. Demonstration of an interferon γ-dependent tumor surveillance system in immunocompetent mice. Proc Natl Acad Sci U S A. 1998 Jun 23;95(13):7556–61.

561. Shankaran V, Ikeda H, Bruce AT, White JM, Swanson PE, Old LJ, et al. IFNγ, and lymphocytes prevent primary tumour development and shape tumour immunogenicity. Nature. 2001 Apr 26;410(6832):1107–11.

562. Wei Q, Luo S Bin, He G. Mechanism study of tyrosine phosphatase shp-1 in inhibiting hepatocellular carcinoma progression by regulating the SHP2/GM-CSF pathway in TAMs. Sci Rep. 2024 Apr 21;14(1):1–9.

563. Wu C, Sun M, Liu L, Zhou GW. The function of the protein tyrosine phosphatase SHP-1 in cancer. Gene. 2003 Mar 13;306(1–2):1–12.

564. Putz EM, Gotthardt D, Hoermann G, Csiszar A, Wirth S, Berger A, et al. CDK8-Mediated STAT1-S727 Phosphorylation Restrains NK Cell Cytotoxicity and Tumor Surveillance. Cell Rep. 2013 Aug 15;4(3):437–44.

565. Poznanski SM, Singh K, Ritchie TM, Aguiar JA, Fan IY, Portillo AL, et al. Metabolic flexibility determines human NK cell functional fate in the tumor microenvironment. Cell Metab. 2021 Jun 1;33(6):1205-1220.e5.

566. Forero A, Ozarkar S, Li H, Lee CH, Hemann EA, Nadjsombati MS, et al. Differential Activation of the Transcription Factor IRF1 Underlies the Distinct Immune Responses Elicited by Type I and Type III Interferons. Immunity. 2019 Sep 17;51(3):451-464.e6.

567. Chang CH, Hammer J, Loh JE, Fodor WL, Flavell RA. The activation of major histocompatibility complex class I genes by interferon regulatory factor-1 (IRF-1). Immunogenetics. 1992 Apr;35(6):378–84.

568. Kang YH, Biswas A, Field M, Snapper SB. STAT1 signaling shields T cells from NK cell-mediated cytotoxicity. Nat Commun. 2019 Feb 22;10(1):1–13.

569. Meissner TB, Li A, Liu YJ, Gagnon E, Kobayashi KS. The nucleotide-binding domain of NLRC5 is critical for nuclear import and transactivation activity. Biochem Biophys Res Commun. 2012 Feb 24;418(4):786–91.

570. Melero I, Ochoa MC, Molina C, Sanchez-Gregorio S, Garasa S, Luri-Rey C, et al. Intratumoral co-injection of NK cells and NKG2A-neutralizing monoclonal antibodies. EMBO Mol Med. 2023 Nov 8;15(11).

571. Colamartino ABL, Lemieux W, Bifsha P, Nicoletti S, Chakravarti N, Sanz J, et al. Efficient and Robust NK-Cell Transduction With Baboon Envelope Pseudotyped Lentivector. Front Immunol. 2019 Dec 16;10:483230.

572. Bari R, Granzin M, Tsang KS, Roy A, Krueger W, Orentas R, et al. A distinct subset of highly proliferative and lentiviral vector (LV)-transducible NK cells define a readily engineered subset for adoptive cellular therapy. Front Immunol. 2019 Aug 22;10(AUG):471032.

573. Wen W, Chen X, Shen XY, Li HY, Zhang F, Fang FQ, et al. Enhancing cord blood stem cell-derived NK cell growth and differentiation through hyperosmosis. Stem Cell Res Ther. 2023 Dec 1;14(1):1–14.

574. Liu E, Tong Y, Dotti G, Shaim H, Savoldo B, Mukherjee M, et al. Cord blood NK cells engineered to express IL-15 and a CD19-targeted CAR show long-term persistence and potent antitumor activity. Leukemia. 2018 Feb 1;32(2):520–31.

575. Witkowski MT, Lee S, Wang E, Lee AK, Talbot A, Ma C, et al. NUDT21 limits CD19 levels through alternative mRNA polyadenylation in B cell acute lymphoblastic leukemia. Nat Immunol. 2022 Sep 22;23(10):1424–32.

576. Albinger N, Bexte T, Al-Ajami A, Wendel P, Buchinger L, Gessner A, et al. P1354: CRISPR/CAS9 GENE EDITING OF IMMUNE CHECKPOINT RECEPTOR NKG2A IMPROVES THE ANTI-LEUKEMIC EFFICACY OF PRIMARY CD33-TARGETING CAR-NK CELLS. HemaSphere. 2023 Aug 8;7(Suppl):e71265f8.

577. Mingari MC, Ponte M, Bertone S, Schiavetti F, Vitale C, Bellomo R, et al. HLA class I-specific inhibitory receptors in human T lymphocytes: Interleukin 15-induced expression of

CD94/NKG2A in superantigen- or alloantigen-activated CD8+ T cells. Proc Natl Acad Sci U S A. 1998 Feb 3;95(3):1172–7.

578. Sáez-Borderías A, Romo N, Magri G, Gumá M, Angulo A, López-Botet M. IL-12-dependent inducible expression of the CD94/NKG2A inhibitory receptor regulates CD94/NKG2C+ NK cell function. J Immunol. 2009 Jan 15;182(2):829–36.

579. Bertone S, Schiavetti F, Bellomo R, Vitale C, Ponte M, Moretta L, et al. Transforming growth factor-β-induced expression of CD94/NKG2A inhibitory receptors in human T lymphocytes. Eur J Immunol. 1999;29(1):23–9.

580. Takayanagi H, Ogasawara K, Hida S, Chiba T, Murata S, Sato K, et al. T-cell-mediated regulation of osteoclastogenesis by signalling cross-talk between RANKL and IFN-γ. Nature. 2000 Nov 30;408(6812):600–5.

581. Guillerey C, De Andrade LF, Vuckovic S, Miles K, Ngiow SF, Yong MCR, et al. Immunosurveillance and therapy of multiple myeloma are CD226 dependent. J Clin Invest. 2015 May 1;125(5):2077–89.

582. Tognarelli S, Wirsching S, Von Metzler I, Rais B, Jacobs B, Serve H, et al. Enhancing the activation and releasing the brakes: A double hit strategy to improve NK cell cytotoxicity against multiple myeloma. Front Immunol. 2018 Nov 27;9(NOV):2743.

583. Ismael A, Robinette AJ, Huric L, Schuetz J, Dona K, Benson D, et al. CREB1 promotes expression of immune checkpoint HLA-E leading to immune escape in multiple myeloma. Leukemia. 2024 Jun 20;1–10.

584. Zhao M, Flynt FL, Hong M, Chen H, Gilbert CA, Briley NT, et al. MHC class II transactivator (CIITA) expression is upregulated in multiple myeloma cells by IFN-gamma. Mol Immunol. 2007 Apr;44(11):2923–32.

585. Sarkar S, Michel Van Gelder ·, Noort W, Xu Y, Kasper ·, Rouschop MA, et al. Optimal selection of natural killer cells to kill myeloma: the role of HLA-E and NKG2A. Cancer Immunol Immunother. 2015;3:951–63.

586. Merino AM, Mehta RS, Luo X, Kim H, De For T, Janakiram M, et al. Early Adaptive Natural Killer Cell Expansion Is Associated with Decreased Relapse After Autologous Transplantation for Multiple Myeloma. Transplant Cell Ther. 2021 Apr 1;27(4):310.e1-310.e6.

587. Jurisic V, Srdic T, Konjevic G, Markovic O, Colovic M. Clinical stage-depending decrease of NK cell activity in multiple myeloma patients. Med Oncol. 2007 Sep 24;24(3):312–7.

588. Clara JA, Childs RW. Harnessing natural killer cells for the treatment of multiple myeloma. Semin Oncol. 2022 Feb 1;49(1):69–85.

589. Mahaweni NM, Ehlers FAI, Sarkar S, Janssen JWH, Tilanus MGJ, Bos GMJ, et al. NKG2A Expression Is Not per se Detrimental for the Anti-Multiple Myeloma Activity of Activated Natural Killer Cells in an In Vitro System Mimicking the Tumor Microenvironment. Front Immunol. 2018 Jun 22;9(JUN).

590. Restrepo P, Bhalla S, Ghodke-Puranik Y, Aleman A, Leshchenko V, Melnekoff DT, et al. A Three-Gene Signature Predicts Response to Selinexor in Multiple Myeloma. JCO Precis Oncol. 2022 Jun 15;6(6):e2200147.

591. Mahaweni NM, Bos GMJ, Mitsiades CS, Tilanus MGJ, Wieten L. Daratumumab augments alloreactive natural killer cell cytotoxicity towards CD38+ multiple myeloma cell lines in a biochemical context mimicking tumour microenvironment conditions. Cancer Immunol Immunother. 2018 Jun 1;67(6):861–72.

592. García-Guerrero E, Götz R, Doose S, Sauer M, Rodríguez-Gil A, Nerreter T, et al. Upregulation of CD38 expression on multiple myeloma cells by novel HDAC6 inhibitors is a class effect and augments the efficacy of daratumumab. Leukemia. 2021 Jan 1;35(1):201–14.

593. Hoerster K, Uhrberg M, Wiek C, Horn PA, Hanenberg H, Heinrichs S. HLA Class I Knockout Converts Allogeneic Primary NK Cells Into Suitable Effectors for “Off-the-Shelf” Immunotherapy. Front Immunol. 2021 Jan 29;11:3557.

594. Cherkasova E, Espinoza L, Kotecha R, Reger RN, Berg M, Aue G, et al. Treatment of Ex Vivo Expanded NK Cells with Daratumumab F(ab’)2 Fragments Protects Adoptively Transferred NK Cells from Daratumumab-Mediated Killing and Augments Daratumumab-Induced Antibody Dependent Cellular Toxicity (ADCC) of Myeloma. Blood. 2015 Dec 3;126(23):4244–4244.

595. Reina-Ortiz C, Constantinides M, Fayd-Herbe-de-Maudave A, Présumey J, Hernandez J, Cartron G, et al. Expanded NK cells from umbilical cord blood and adult peripheral blood combined with daratumumab are effective against tumor cells from multiple myeloma patients. Oncoimmunology. 2020;10(1).

596. Fisher JG, Walker CJ, Doyle AD, Johnson PW, Forconi F, Cragg MS, et al. Selinexor Enhances NK Cell Activation Against Malignant B Cells via Downregulation of HLA-E. Front Oncol. 2021;11(December):1–12.

597. Fisher JG, Doyle ADP, Graham L V., Sonar S, Sale B, Henderson I, et al. XPO1 inhibition sensitises CLL cells to NK cell mediated cytotoxicity and overcomes HLA-E expression.

Leukemia. 2023 Oct 1;37(10):2036–49.

598. Wang Y, Chen J, Gao Y, Chai KXY, Hong JH, Wang P, et al. CDK4/6 inhibition augments anti-tumor efficacy of XPO1 inhibitor selinexor in natural killer/T-cell lymphoma. Cancer Lett. 2024 Aug 10;597:217080.